U.S. Department
of Commerce

Volume 92
Number 2
April 1994

Fishery Bulletin

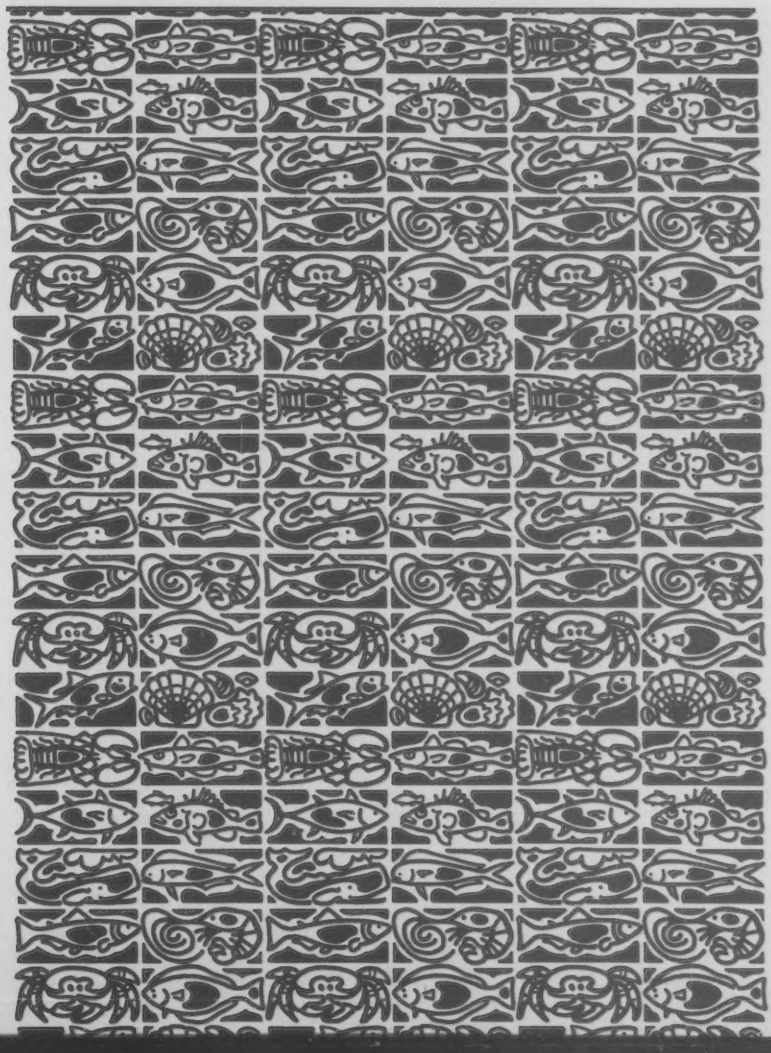

U.S. Department of Commerce
Ronald H. Brown
Secretary

National Oceanic and Atmospheric Administration
D. James Baker
Under Secretary for
Oceans and Atmosphere

National Marine Fisheries Service
Rolland A. Schmitten
Assistant Administrator
for Fisheries

Fishery Bulletin

Scientific Editor
Dr. Ronald W. Hardy
Northwest Fisheries Science Center
National Marine Fisheries Service, NOAA
2725 Montlake Boulevard East
Seattle, Washington 98112-2097

Editorial Committee
Dr. Andrew E. Dizon National Marine Fisheries Service
Dr. Linda L. Jones National Marine Fisheries Service
Dr. Richard D. Methot National Marine Fisheries Service
Dr. Theodore W. Pietsch University of Washington
Dr. Joseph E. Powers National Marine Fisheries Service
Dr. Tim D. Smith National Marine Fisheries Service

Managing Editor
Sharyn Matriotti
National Marine Fisheries Service
Scientific Publications Office
7600 Sand Point Way NE, BIN C15700
Seattle, Washington 98115-0070

The *Fishery Bulletin* (ISSN 0090-0656) is published quarterly by the Scientific Publications Office, National Marine Fisheries Service, NOAA, 7600 Sand Point Way NE, BIN C15700, Seattle, WA 98115-0070. Second class postage is paid in Seattle, Wash., and additional offices. POSTMASTER send address changes for subscriptions to Fishery Bulletin, Superintendent of Documents, Attn: Chief, Mail List Branch, Mail Stop SSOM, Washington, DC 20402-9373.

Although the contents have not been copyrighted and may be reprinted entirely, reference to source is appreciated.

The Secretary of Commerce has determined that the publication of this periodical is necessary in the transaction of the public business required by law of this Department. Use of funds for printing of this periodical has been approved by the Director of the Office of Management and Budget.

For sale by the Superintendent of Documents, U.S. Government Printing Office, Washington, DC 20402. Subscription price per year: $27.00 domestic and $33.75 foreign. Cost per single issue: $13.00 domestic and $16.25 foreign. **See back page for order form.**

The *Fishery Bulletin* carries original research reports and technical notes on investigations in fishery science, engineering, and economics. The Bulletin of the United States Fish Commission was begun in 1881; it became the Bulletin of the Bureau of Fisheries in 1904 and the Fishery Bulletin of the Fish and Wildlife Service in 1941. Separates were issued as documents through volume 46; the last document was No. 1103. Beginning with volume 47 in 1931 and continuing through volume 62 in 1963, each separate appeared as a numbered bulletin. A new system began in 1963 with volume 63 in which papers are bound together in a single issue of the bulletin. Beginning with volume 70, number 1, January 1972, the *Fishery Bulletin* became a periodical, issued quarterly. In this form, it is available by subscription from the Superintendent of Documents, U.S. Government Printing Office, Washington, DC 20402. It is also available free in limited numbers to libraries, research institutions, State and Federal agencies, and in exchange for other scientific publications.

U.S. Department
of Commerce
Seattle, Washington

Volume 92
Number 2
April 1994

Fishery Bulletin

Contents

iii **Errata**

207 **Blood, Deborah M., Ann C. Matarese, and Mary M. Yoklavich**
Embryonic development of walleye pollock, *Theragra chalcogramma*, from Shelikof Strait, Gulf of Alaksa

223 **Brodeur, Richard D., and William C. Rugen**
Diel vertical distribution of ichthyoplankton in the northern Gulf of Alaska

236 **Clark, Malcolm R., and Dianne M. Tracey**
Changes in a population of orange roughy, *Hoplostethus atlanticus*, with commercial exploitation on the Challenger Plateau, New Zealand

254 **Daniel, Louis B., III, and John E. Graves**
Morphometric and genetic identification of eggs of spring-spawning sciaenids in lower Chesapeake Bay

262 **Ditty, James G., Richard F. Shaw, and Joseph S. Cope**
A re-description of Atlantic spadefish larvae, *Chaetodipterus faber* (family: Ephippidae), and their distribution, abundance, and seasonal occurrence in the northern Gulf of Mexico

275 **Ditty, James G., Richard F. Shaw, Churchill B. Grimes, and Joseph S. Cope**
Larval development, distribution, and abundance of common dolphin, *Coryphaena hippurus*, and pompano dolphin, *C. equiselis* (family: Coryphaenidae), in the northern Gulf of Mexico

292 **Kastelle, Craig R., Daniel K. Kimura, Ahmad E. Nevissi, and Donald R. Gunderson**
Using Pb-210/Ra-226 disequilibria for sablefish, *Anoplopoma fimbria*, age validation

302 **Moltschaniwskyj, Natalie A., and Peter J. Doherty**
Distribution and abundance of two juvenile tropical *Photololigo* species (Cephalopoda: Loliginidae) in the central Great Barrier Reef Lagoon

313 **Murie, Debra J., Daryl C. Parkyn, Bruce G. Clapp, and Geoffrey G. Krause**
Observations on the distribution and activities of rockfish, *Sebastes* spp., in Saanich Inlet, British Columbia, from the *Pisces IV* submersible

324 **Perrin, William F., Gary D. Schnell, Daniel J. Hough, James W. Gilpatrick Jr., and Jerry V. Kashiwada**
Reexamination of geographic variation in cranial morphology of the pantropical spotted dolphin, *Stenella attenuata*, in the eastern Pacific

347 **Powell, Eric N., John M. Klinck, Eileen E. Hofmann, and Sammy M. Ray**
Modeling oyster populations. IV: Rates of mortality, population crashes, and management

374 **Prager, Michael H.**
A suite of extensions to a nonequilibrium surplus-production model

390 **Stoner, Allan W., and Megan Davis**
Experimental outplanting of juvenile queen conch, *Strombus gigas*: comparison of wild and hatchery-reared stocks

412 **Taylor, David M., Paul G. O'Keefe, and Charles Fitzpatrick**
A snow crab, *Chionoecetes opilio* (Decapoda, Majidae), fishery collapse in Newfoundland

420 **Warlen, Stanley M.**
Spawning time and recruitment dynamics of larval Atlantic menhaden, *Brevoortia tyrannus*, into a North Carolina estuary

434 **Reilly, Stephen B., and Paul C. Fiedler**
Interannual variability of dolphin habitats in the eastern tropical Pacific. I: Research vessel surveys, 1986–1990

451 **Fiedler, Paul C., and Stephen B. Reilly**
Interannual variability of dolphin habitats in the eastern tropical Pacific. II: Effects on abundances estimated from tuna vessel sightings, 1975–1990

Notes

464 **Aurioles-Gamboa, David, Maria Isabel Castro-González, and Ricardo Pérez-Flores**
Annual mass strandings of pelagic red crabs, *Pleuroncodes planipes* (Crustacea: Anomura: Galatheidae), in Bahia Magdalena, Baja California Sur, Mexico

471 **Ennevor, Bridget C.**
Mass marking coho salmon, *Oncorhynchus kisutch*, fry with lanthanum and cerium

474 **Hazin, Fabio H. V., Clara E. Boeckman, Elizabeth C. Leal, Rosangela P. T. Lessa, Kohei Kihara, and Kazuyuki Otsuka**
Distribution and relative abundance of the blue shark, *Prionace glauca*, in the southwestern equatorial Atlantic Ocean

Errata

(1)

Bigelow, Keith A.

Age and growth of the oceanic squid *Onychoteuthis borealijaponica* in the North Pacific
Fish. Bull. 92(1):13-25

Figure 5 should read as shown below.

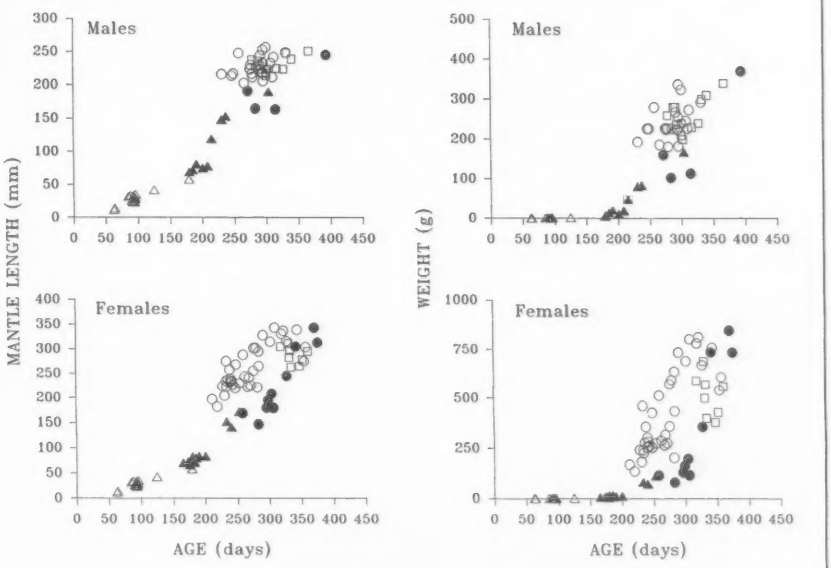

Figure 5

Relation between age (determined by number of increments within statoliths) and mantle length (mm) and weight (g) for male and female *Onychoteuthis borealijaponica*. Western North Pacific 1990 (open circles), central North Pacific 1990 (closed circles), central North Pacific 1991 (closed triangles = juveniles-subadults, open triangles = unknown sex), and eastern North Pacific 1990 (open squares).

(2)

Perryman, Wayne L., and Morgan S. Lynn

Examination of stock and school structure of striped dolphin (*Stenella coeruleoalba*) in the eastern Pacific from aerial photogrammetry
Fish. Bull. 92(1):122-131

Figures 3, 4, and 7, and Tables 1, 2, and 3 show an incorrectly typeset species name for striped dolphin. The correct name should read striped dolphin, *Stenella coeruleoalba*.

The National Marine Fisheries Service (NMFS) does not approve, recommend, or endorse any proprietary product or proprietary material mentioned in this publication. No references shall be made to NMFS, or to this publication furnished by NMFS, in any advertising or sales promotion which would indicate or imply that NMFS approves, recommends or endorses any proprietary product or proprietary material mentioned herein, or which has as its purpose an intent to cause directly or indirectly the advertised product to be used or purchased because of this NMFS publication.

Embryonic development of walleye pollock, *Theragra chalcogramma*, from Shelikof Strait, Gulf of Alaska*

Deborah M. Blood
Ann C. Matarese
Mary M. Yoklavich**
Alaska Fisheries Science Center, National Marine Fisheries Service, NOAA
7600 Sand Point Way N.E., Seattle, WA 98115-0070

Abstract.— Eggs of walleye pollock, *Theragra chalcogramma*, from Shelikof Strait, Alaska, were reared at three temperatures: 3.8°, 5.7°, and 7.7°C. Development was divided into 21 stages. A piecewise regression model with midpoints of each stage describes the relation between time to each stage of development and temperature. Preserved eggs of each stage are described, illustrated, and photographed. Midpoint of hatch was 393 hours at 3.8°C, 303 hours at 5.7°C, and 234 hours at 7.7°C. Mean length of larvae at hatch increased linearly with temperature.

We compared rate of development, time to 50% hatch, and morphological development with other studies of walleye pollock eggs. Rate of development and time to 50% hatch were similar among populations of eastern North Pacific walleye pollock. Western North Pacific walleye pollock required longer incubation times than eastern North Pacific walleye pollock. Morphological development of Shelikof Strait eggs differs from development of western North Pacific walleye pollock eggs: optic vesicles, myomeres, eye lenses, heart, and otic capsules appear earlier than in Shelikof Strait eggs, and eye pigment appears later. The differences in development may be exacerbated by the condition of the eggs in which they were examined (e.g. preserved vs. live). Developmental differences between stocks are discussed with the conclusion that model components for egg mortality and spawning biomass must be based on specimens collected in the area of interest.

Walleye pollock, *Theragra chalcogramma*, is the most abundant member of the family Gadidae in the subarctic Pacific Ocean and Bering Sea, supporting the largest single-species commercial fishery in the world (Megrey, 1991). In the Gulf of Alaska, Shelikof Strait is the principal spawning area (Kendall and Picquelle, 1990) and has been the site of intensive research to understand processes leading to recruitment variability of walleye pollock (Schumacher and Kendall, 1991).

Age determination of fertilized eggs is a basis for investigating biotic and abiotic impacts on the earliest life-history stage and thus for understanding interannual variability in walleye pollock recruitment. Age of walleye pollock eggs has been crucial to several studies. Egg mortality and spawning biomass are estimated by modeling age-specific egg abundance over time (Picquelle and Megrey, 1993; Bates[1]). Patterns in horizontal or vertical distribution and abundance of walleye pollock eggs in the western Gulf of Alaska have been described by grouping developmental stages into broad age groups (Kendall and Kim, 1989; Kendall and Picquelle, 1990).

Egg age is an independent variable in the models used to estimate egg production and mortality. Therefore, increasing the accuracy in measuring egg ages should improve estimates of these values. In past studies, walleye pollock eggs have been incubated in the laboratory to develop temperature-specific equations that estimate duration of development or age of the eggs, to describe morphological development, to observe effects of light on egg buoyancy and hatching rate, and to obtain larvae for experiments (Table 1). Although these incubation studies provide pertinent data on ontogeny of walleye pollock, none can be used with accuracy to determine age of eggs

[1] Bates, R. D. 1987. Estimation of egg production, spawner biomass, and egg mortality for walleye pollock, *Theragra chalcogramma*, in Shelikof Strait from ichthyoplankton surveys during 1981. U.S. Dep. Commer., NOAA, Nat. Mar. Fish. Serv., Northwest Alaska Fish. Cent., 7600 Sand Point Way N.E., Bin C15700, Bldg. 4, Seattle, WA 98115-0070. Proc. Rep. 87-20, 192 p.

* Contribution 0148 of the Fisheries Oceanography Coordinated Investigations, NOAA, Seattle.

** Present address: Southwest Fisheries Science Center, Pacific Fisheries Environmental group, National Marine Fisheries Service, NOAA, P.O. Box 831, Monterey, CA 93942

Manuscript accepted 3 November 1993
Fishery Bulletin 92: 207–222 (1994)

Table 1

Summary of *Theragra chalcogramma* egg incubation studies.

Reference	Temperature (°C)	Source and region	Stages[1]	Regression equation	Morphological description	Illustrations	Photographs
Gorbunova, 1954	3.4, 8.2 (means)	western Pacific Ocean	None	No	Yes	Yes	No
Yusa, 1954	6.0–7.0	Ishikari Bay, Japan	27[2]	No	Yes	Yes	Yes
Hamai et al., 1971	2.4–2.5, 6.5–6.7, 9.9–10.1, (means)	Funka Bay, Japan	4	Stage-specific equation to predict age (d) at any stage	No	No	No
Hamai et al., 1974	5.0 (mean)	Funka Bay, Japan	6	No	No	No	No
Matarese 1983, unpubl.[3]	5.0	N. Gulf of Alaska	21	Stage-specific equation to predict age (h) at any stage[4]	No	No	No
Haynes and Ignell, 1983	2.0, 5.0, 6.0, 8.0, 11.0	Stephens Passage, SE Alaska	7	General equation to predict age (h) at any stage	No	No	No
Nakatani and Maeda, 1984	–1.0, 0.0, 2.0, 4.0, 7.0, 10.0, 13.0	Funka Bay, Japan	5	To 50% hatch	No	No	No
Paul, 1984, unpubl.[5]	5.0	N. Gulf of Alaska	21	No	No	No	No
Bailey and Stehr, 1986	5.6, 8.5	Puget Sound, Washington	None	No	No	No	No
Olla and Davis, 1993	6.0	Shelikof Strait, Alaska	None	No	No	No	No

[1] Prior to hatch.
[2] Reported as intervals of time.
[3] A. C. Matarese, Alaska Fisheries Science Center, National Marine Fisheries Service, 7600 Sand Point Way NE., Seattle, WA 98115.
[4] In Bates 1987 (Footnote 1).
[5] A. J. Paul, University of Alaska Fairbanks, Institute of Marine Science, Seward Marine Center Lab, P.O. Box 730, Seward, AK 99664.

from Shelikof Strait. Eggs need to be obtained from the study area and incubated at a range of temperatures occurring in the area. Categorizing the continuous process of egg development into a large number of stages should increase the precision of the egg-age estimate.

The first objective of our study was to incubate Shelikof Strait walleye pollock eggs at the mean water temperature for Shelikof Strait, bracketing that temperature to include upper and lower extremes. Egg development times were used to produce a stage duration table and a regression model to estimate egg age based on water temperature and developmental stage. Morphological development is described for 21 developmental stages. These descriptions are accompanied by illustrations and photographs to facilitate identification of body structures and stage hallmarks.

The second objective was to compare our rates of egg development to other walleye pollock incubation studies. Morphological development is included in this comparison.

Methods

Incubation

Adult walleye pollock were collected with a rope trawl off Cape Kekurnoi (57°42.5'N, 155°16.2'W) in Shelikof Strait, Alaska, on 7 April 1989 from the NOAA research vessel *Miller Freeman*. Eggs from one female and milt from three or four males were hand stripped into glass petri dishes, gently mixed, and left undisturbed for one minute. Eggs were then rinsed, transferred to 3°C (surface water temperature) seawater in glass jars (3.8 L), and held two hours. Floating eggs with a perivitelline space were assumed to be fertilized (Blaxter, 1969; Alderdice, 1988). Viable eggs were poured into eighteen 0.5-L jars filled with 3°C seawater. Eggs were not counted but apportioned similarly among the jars at a concentration of about one egg/mL. Six capped jars were held in each of three water bath incubators onboard the *Miller Freeman*. Initial incubation temperatures were set to include the range of temperatures in the area. Mean water temperature at depths of 150–200 m in Shelikof Strait, where most eggs are found (March–May) (Kendall and Kim, 1989), is 5°C; extremes of 3.6° and 5.9°C have been reported (Reed and Schumacher, 1989). Incubators were sealed to minimize light and movement and placed in separate refrigerators adjusted to 3°, 5°, and 7°C. One-half of the water in the jars was replaced every day with seawater of the same temperature. Eggs were preserved in phosphate buffered formalin (5%)[2] or Stockard's solution[3] (Velsen, 1980). Stockard's solution cleared the chorion and darkened embryonic tissue, easing examination of embryonic development. Phosphate buffered formalin did not darken embryonic tissue as much as Stockard's solution, yielding better definition of some structures like somites and otic capsules. Live, newly hatched larvae were measured (standard length in millimeters) and preserved (5% buffered formalin). Detailed examination and morphological description of embryos were completed after eggs were returned to the laboratory.

During the first 24 hours after fertilization, eggs were sampled at 2–3 hour intervals. After 24 hours, intervals were increased to about 6 hours. When an interval was less or greater than 6 hours, the subsequent sampling time was adjusted to return to the original 6–hour schedule. Data were not recorded for three sampling times late in development because intervals were inadvertently extended to 12 hours (236, 258, and 282 hours).

At each interval, 10 to 50 eggs were sampled from one jar per incubator; only one jar was sampled to ensure there would be enough eggs and larvae left to sample near the end of the incubation period. Jars were sampled in rotation throughout the duration of the experiment until no eggs remained. When eggs began to hatch, all jars were checked and newly hatched larvae were removed in addition to eggs scheduled to be sampled. Dead eggs were removed from the designated sample jar at each interval. Water bath temperatures were recorded for every sampling interval. Frequent opening of refrigerators during the initial short sampling intervals increased temperatures in the refrigerators despite thermostat adjustments. Water bath temperatures stabilized after 48 hours to 3.8°, 5.7°, and 7.7°C.

Morphological descriptions

Eggs were examined with the aid of a dissecting microscope (6–50× magnification) and described according to a 21-stage scheme adapted from Naplin and Obenchain (1980) (Table 2). Morphological terms follow Trinkaus (1951) with one exception: the term "blastodisc," in this paper, includes the germinal area from the time of cytoplasm polarization until embryonic shield formation (Markle and

Table 2

Stages of embryonic development of *Theragra chalcogramma* (adapted from Naplin and Obenchain, 1980).

Stage	Developmental stage
1	Precell
2	2 cell
3	4 cell
4	8 cell
5	16 cell
6	32+ cell
7	Blastodermal cap
8	Early germ ring
9	Germ ring 1/4 down yolk
10	Germ ring 1/2 down yolk
11	Germ ring 3/4 down yolk
12	Late germ ring
13	Early middle (blastopore closure)
14	Middle middle (appearance of pigment)
15	Late middle (tail bud thickens)
16	Early late (tail bud lifts from yolk)
17	Tail 5/8 around yolk
18	Tail 3/4 around yolk
19	Tail 7/8 around yolk
20	Full circle around yolk
21	Tail 1-1/8 around yolk

[2] 50 mL 37% formaldehyde, 4.0 g sodium phosphate monobasic, 6.5 g sodium phosphate dibasic, made up to 1 L with distilled water.

[3] 50 mL 37% formaldehyde, 40 mL glacial acetic acid, 60 mL glycerin, and 850 mL distilled water.

Waiwood, 1985, in part). Eggs preserved in Stockard's solution were photographed with a Nikon F2 camera fitted with a PB6 200-mm bellows extension and a 24-mm 1:2.8 reverse-mounted lens. This configuration produced a 47× magnification. Reflected light was supplied by two synchronized flash units. Other photographs (stages 5 and 6) were taken with a single-lens reflex adapter (0.32×) on a Wild M-8 dissecting microscope with transmitted light. At 50×, the phototube and adapter increased magnification to 66×.

Analysis

Endpoint, midpoint, and duration of stage (in hours) were estimated for eggs incubated at each temperature. For stages 1–20, stage endpoint was determined by the presence of two stages during a sampling time; if stages n and n+1 were present, the time at which the eggs were sampled was considered a transition and therefore the endpoint for stage n. If there was no transition, the endpoint for stage n was the midpoint between the last sampling time during which stage-n eggs were present and the first time stage-n+1 eggs were observed. Duration and midpoint of stage n were determined as

$$\text{Duration Stage } n = \text{Endpoint Stage } (n) - \text{Endpoint Stage } (n-1);$$

$$\text{Midpoint Stage } n = \text{Endpoint Stage } (n-1) + \frac{\text{Duration Stage } n}{2}.$$

Endpoint of stage 21 was the sampling interval when the last embryo had hatched. With the midpoints and time of 50% hatch, a piece-wise least-squares linear regression model (SAS, 1985) was derived to estimate age (hours) of eggs at a specific stage incubated at any temperature within the limits of this experiment.

Differences in mean lengths of larvae hatched from the three temperature groups were analyzed by a Student-Newman-Keuls test. Lengths of larvae hatching at stages 20 and 21 were analyzed by a two-way analysis of variance (ANOVA) by using stage and temperature.

We chose five representative developmental stages and compared time to midpoint of each stage among incubation studies. Comparison with Hamai et al. (1971, 1974) was possible for only three stages. We grouped data on time to 50% hatch into western and eastern North Pacific studies and performed a log-transformed analysis of covariance to test for differences in time to 50% hatch between these two areas with incubation temperature as the covariate.

Results

Incubation rates

Temperatures of the three water baths increased at the beginning of sampling (Fig. 1). Temperature spikes that occurred after 288 hours in the 5.7°C jars and after 396 hours in the 3.8°C jars, were associated with the appearance of large numbers of larvae; water baths may have warmed when refrigerators were opened frequently to measure larvae.

Eggs developed at similar rates among incubation temperatures for the first 36 hours through stage 6 (Fig. 2). After stage 6, at about 36 hours, when temperatures had stabilized, development rates began to diverge. Duration of stages 7–21 was variable (Table 3). Usually the duration of a stage was longer at cooler temperatures. However, this was not always the case, and stages 12 and 20 required similar amounts of time regardless of temperature. At all temperatures, hatching began during stage 20; the percentage of eggs hatched by the beginning of stage 21 was 35% at 3.8°, 40% at 5.7°, and 8.1% at 7.7°C. Four larvae from the 7.7°C group hatched after 192 hours; another 18 hours elapsed before other larvae hatched at this temperature. These early larvae were not included in this analysis because we assumed that the hiatus in hatching times indicated that early hatching was anomalous, i.e. hatching may have been mechanically induced. After hatching began, time required for 50% hatch decreased as temperature increased: 48, 36, and 24 hours at 3.8°, 5.7°, and 7.7°C. The elapsed time between hatching of the first and last larvae was 72 hours at 3.8°C and 60 hours at both 5.7° and 7.7°C.

Eggs developed normally at 5.7° and 7.7°C; however, curvature of the spine was observed in some late-stage embryos incubated at 3.8°C. These abnormal eggs hatched, but most larvae were not measured because of curvature. Mean length at hatch of all larvae increased with incubation temperature: 4.15 (SD 0.380, n=100), 4.29 (SD 0.272, n=192), and 4.55 mm (SD 0.303, n=84) at 3.8°, 5.7°, and 7.7°C (Fig. 3). Mean lengths of larvae from the three temperature groups were significantly different (P<0.05). In addition, larval lengths increased as the hatching period progressed at all temperatures. Length of larvae hatching at stages 20 and 21 was significantly different at all temperatures (P<0.01); larvae that hatched at stage 21 were 9–13% longer than larvae that hatched at stage 20.

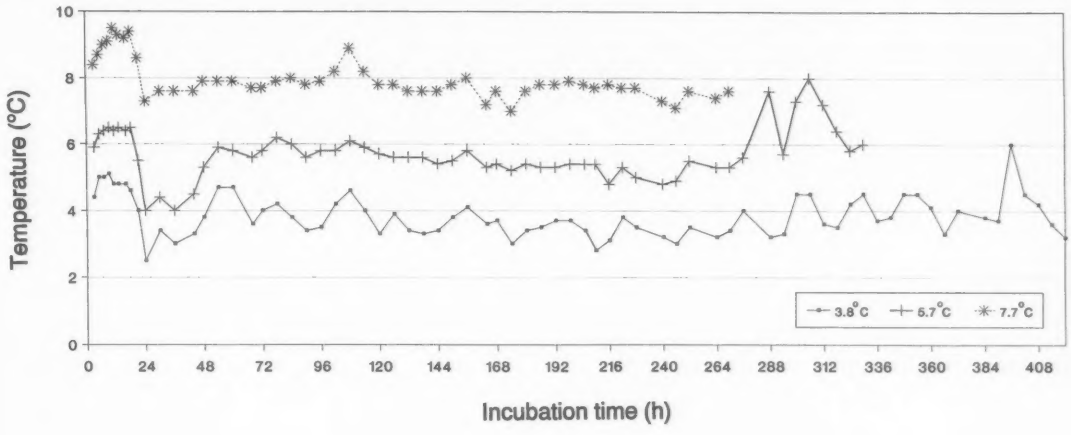

Figure 1
Temperatures recorded in water baths during incubation of *Theragra chalcogramma* eggs.

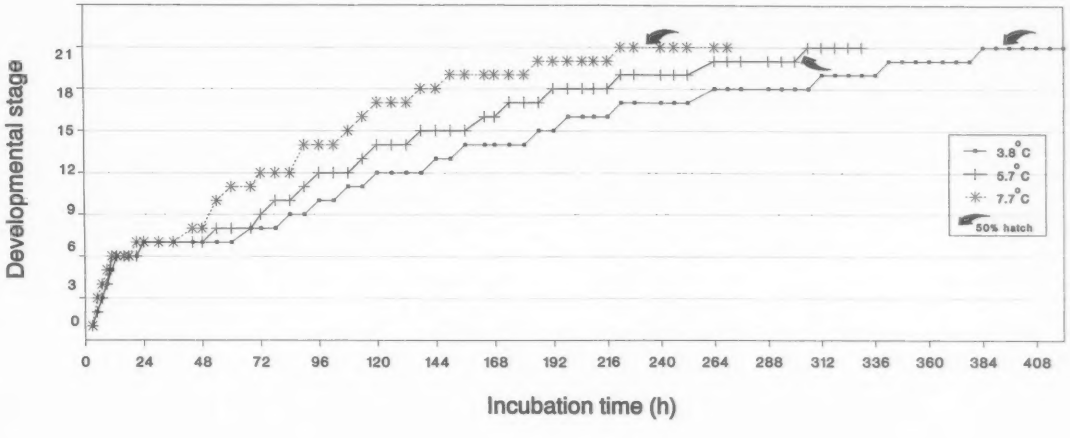

Figure 2
Development of *Theragra chalcogramma* eggs incubated at 3.8°, 5.7°, and 7.7°C. Points represent occurrence of stages at scheduled sampling times.

The piece-wise regression model (SAS, 1985) has two separate components and is discontinuous between stages 6 and 7 (Fig. 4). This type of model was necessary because of the rapid divergence of developmental rates at all temperatures after stage 6; it was not possible to fit one equation to the entire incubation time. The two components are described by the following equations:

component 1: stages 1–6

$$\text{Age} = 3.27 - 0.13\,(\text{stage})\,(\text{temperature}) + 0.47\,(\text{stage}^2);$$

component 2: stages 7–21

$$\text{Age} = 17.82 + 7.05(\text{stage}) - 0.656\,(\text{stage})\,(\text{temperature}) + 0.043(\text{stage}^3) - 0.0032\,(\text{temperature})\,(\text{stage}^3),$$

Table 3

Endpoint, midpoint, and duration in hours (h) of stage of development of *Theragra chalcogramma* eggs incubated at 3.8°, 5.7°, and 7.7°C.

	3.8°C			5.7°C			7.7°C		
Stage	Endpoint (h)	Midpoint (h)	Duration (h)	Endpoint (h)	Midpoint (h)	Duration (h)	Endpoint (h)	Midpoint (h)	Duration (h)
1	4.00	2.00	4.00	4.00	2.00	4.00	3.50	1.75	3.50
2	6.00	5.00	2.00	6.00	5.00	2.00	4.00	3.75	0.50
3	8.00	7.00	2.00	7.00	6.50	1.00	5.00	4.50	1.00
4	10.25	9.12	2.25	9.00	8.00	2.00	7.00	6.00	2.00
5	12.50	11.37	2.25	10.25	9.62	1.25	10.25	8.62	3.25
6	22.50	17.50	10.00	22.50	16.37	12.25	19.50	14.87	9.25
7	64.00	43.25	41.50	51.00	36.75	28.50	40.00	29.75	20.50
8	78.00	71.00	14.00	68.00	59.50	17.00	48.00	44.00	8.00
9	90.00	84.00	12.00	75.00	71.50	7.00	54.00	51.00	6.00
10	105.00	97.50	15.00	87.00	81.00	12.00	57.00	55.50	3.00
11	120.00	112.50	15.00	93.00	90.00	6.00	68.00	62.50	11.00
12	138.00	129.00	18.00	108.00	100.50	15.00	84.00	76.00	16.00
13	153.00	145.50	15.00	114.00	111.00	6.00	87.00	85.50	3.00
14	180.00	166.50	27.00	135.00	124.50	21.00	102.00	94.50	15.00
15	195.00	187.50	15.00	164.00	149.50	29.00	111.00	106.50	9.00
16	219.00	207.00	24.00	174.00	169.00	10.00	117.00	114.00	6.00
17	252.00	235.50	33.00	189.00	181.50	15.00	132.00	124.50	15.00
18	312.00	282.00	60.00	219.00	204.00	30.00	144.00	138.00	12.00
19	336.00	324.00	24.00	258.00	238.50	39.00	180.00	162.00	36.00
20	378.00	357.00	42.00	300.00	279.00	42.00	219.00	199.50	39.00
21	414.00	393.00[1]	36.00	330.00	303.00[1]	30.00	270.00	234.00[1]	51.00

[1] 50% hatch.

where age of the egg is expressed in hours. The value of R^2 is 0.96 for component 1 and 0.99 for component 2.

We compared our rates of egg development to other walleye pollock incubation studies in the 5–7°C range (Table 4). There was a significant difference between regression equations of incubation time to 50% hatch and temperature for western versus eastern North Pacific studies ($P<0.01$), but the slopes were not different ($P=0.18$). Based on the 95% confidence interval about the parameter estimates, time to 50% hatch of western North Pacific walleye pollock tended to be 1.2 to 1.3 times longer on average than that of the eastern North Pacific fish at a specific temperature.

Morphological descriptions

Walleye pollock eggs are pelagic and have a smooth, clear chorion and homogeneous yolk. No oil globules are present. Preserved eggs range from 1.2 to 1.8 mm in diameter, although most are 1.35–1.45 mm (Matarese et al., 1989). Appearance of the egg varies with type of preservative. There was little or no shrinkage of yolk material in Stockard's solution, whereas yolk of formalin-preserved eggs decreased in volume and the yolk membrane frequently collapsed. This effect of formalin preservation was helpful in determining how much of the tail had lifted away from the yolk in late-stage embryos.

Development of walleye pollock eggs and embryos, from fertilization to just before hatching, was divided into the following 21 stages (Table 2):

Precell (stage 1) Cytoplasm at the animal pole forms a blastodisc; bands of cytoplasm extend from below the equator to the blastodisc (Fig. 5A), which is without distinct margins (Fig. 6A). When intact, the yolk membrane almost touches the inner wall of the chorion. The perivitelline space is most visible over the blastodisc.

2 cells (stage 2) The first cell division of the blastodisc is in the horizontal plane. Cell material may not be equally divided (Figs. 5B and 6B).

4 cells (stage 3) The second cleavage is perpendicular to, and in the same plane as, the first. Cells are roughly equal in size and form a square (Figs. 5C and 6C).

8 cells (stage 4) The third cleavage is perpendicular to the second cleavage (parallel to first cleavage). Each cell divides in half in the horizontal

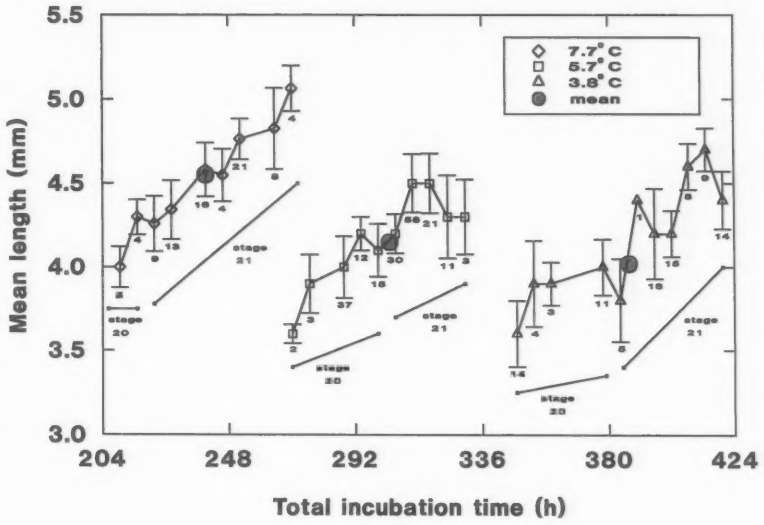

Figure 3

Mean hatch lengths at each sampling interval during the hatching period of *Theragra chalcogramma* larvae incubated at 3.8°, 5.7°, and 7.7°C. Stage of development at hatch is also shown. Shaded circle indicates overall mean length for each temperature. Vertical bars are standard deviations; numbers indicate sample size.

plane. Cells form a rectangle with the four cells in the center smaller than those at the corners of the rectangle (Figs. 5D and 6D).

16 cells (stage 5) The fourth cleavage is perpendicular to the third; this is the last stage in which cell division is restricted to the horizontal plane. Most eggs have a square or rectangular block of cells with four cells on each side; all cells are in contact with yolk through this stage (Figs. 5E and 6E).

32 cells (stage 6) Initially, the single layer of cells has a flat, irregular square or rectangular shape. Cell division continues in horizontal and vertical planes, transforming the blastodisc into a hollow cap of cells on the yolk resembling a raspberry (Figs. 5F and 6F). Cells increase in number but the size of the blastodisc remains constant. The perivitelline space widens between yolk and chorion.

Blastodermal cap (stage 7) The blastodisc progresses through two steps: at first, cell size decreases from continued cleavage; cell material appears granular and the blastodisc resembles a flattened dome on the yolk surface. Then, the base of the cell mass sinks below the yolk surface; the periblast extends beyond the equator of the blastodisc, giving the appearance of a "flying saucer" in lateral view (Figs. 5G and 6G).

Early germ ring (stage 8) The center of the blastodisc flattens and the periphery (germ ring) thickens in preparation to overgrow the yolk (epiboly). The blastocoel, visible on one side of the blastodisc, appears grainy and pale (Fig. 5H). The margin between blastocoel and blastodisc is indistinct (Fig. 6H).

Germ ring 1/4 around yolk (stage 9) The blastodisc, now the embryonic shield, expands as the germ ring begins to overgrow the yolk. The margin of the future anterior end of the embryo is slightly curved and sharply defined. Cell material covering the blastocoel appears less grainy than in the previous stage. After preservation, this thin cellular layer appears concave in lateral view. The germ ring margin is thin and flattened, extending 1/4 around yolk (Figs. 5I and 6I).

Germ ring 1/2 around yolk (stage 10) The germ ring envelopes half the yolk and the anterior margin of the embryonic shield is sharply curved and thick (Figs. 5J and 6J). The beginning of neural development is visible; a neural keel extends from the anterior margin of the embryonic shield to 2/3 its length (Fig. 5K).

Germ ring 3/4 around yolk (stage 11) Head and upper body region begin to differentiate but no distinct brain lobes are apparent. Optic vesicles develop. Prospective head and body mesoderm outlines the hour-glass shape of the developing embryo (Fig. 7A). The notochord is visible ventrally. The germ ring has progressed 3/4 down the yolk (Fig. 6K).

Late germ ring (stage 12) Myomere differentiation begins; separate myomeres are not visible. The midbody expands dorsoventrally; prospective head and body mesoderm forms a narrow outline of the embryo. The blastopore is open and the germ ring envelopes more than 7/8 of the yolk (Figs. 7B and 8A).

Early middle stage (stage 13) The blastopore is closed. The notochord and 7–12 incomplete myomeres are visible. Tail margin is indistinct and

flat; the medial portion of the tail bud is thicker (Figs. 7C and 8B). The body of the embryo appears flattened. Although not distinguishable in preserved specimens, Kupffer's vesicle is visible in the live egg.

Middle middle stage (stage 14) Embryos have 14–16 myomeres. Differentiation begins in eyes and mid- and hindbrain. Forebrain very small and underdeveloped. The tail bud margin is defined but still flattened (Fig. 8C). The entire length of the body is thicker. Small melanophores are scattered along the dorsum between the hindbrain and 4/5 of body length (Fig. 7D).

Late middle stage (stage 15) About 20–25 myomeres are visible. Eye lenses are formed. The liver appears as a slight bulge in the body wall, and the gut area is delineated. The tail bud is thick and appears lifted from the yolk surface with the margin attached (Fig. 7E). Pigment is darker than in the previous stage and dendritic, extending from midbrain to tip of tail bud and confined mostly to the dorsum. Nares, mid- and hindbrain, and pectoral bud anlagen are visible dorsally (Fig. 8D).

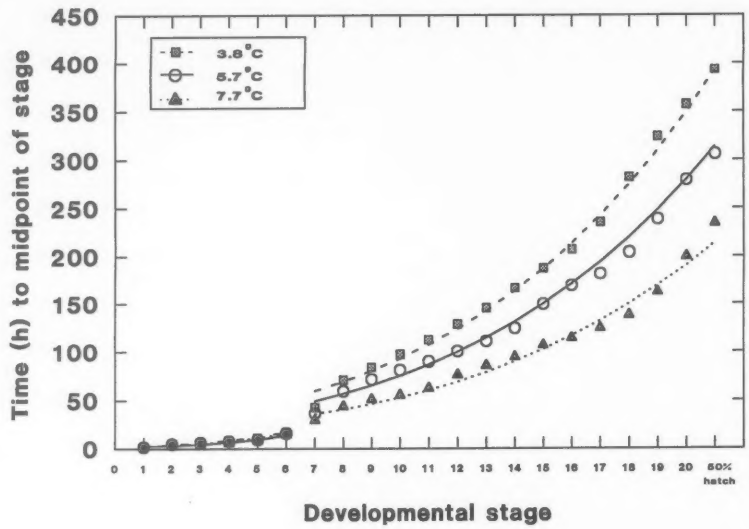

Figure 4

Time (h) to midpoint of stage of *Theragra chalcogramma* eggs incubated at 3.8°, 5.7°, and 7.7°C. Fitted lines are results of regression model; symbols are observed values.

Early late stage (stage 16) Heart tissue begins to expand when the embryo has about 24–36 myomeres. Forebrain differentiates from midbrain. The tail bud lifts from the yolk surface (Figs. 7F and 8E) and pigment forms two parallel rows dorsoposteriorly.

Tail 5/8 around yolk (stage 17) The embryo has 27–36 myomeres. More of the tail lifts from the

Table 4

Comparison of time (h) to estimated midpoint of five developmental milestones of *Theragra chalcogramma* embryos incubated at 5–7°C.

	Eastern North Pacific incubation studies				Western North Pacific incubation studies			
Stage	Matarese, 1983, unpubl.[1] (5.0°C)	Paul, 1984, unpubl.[2] (5.0°C)	Haynes and Ignell, 1983[3] (6.0°C)	This study (5.7°C)	Hamai et al., 1971[4] (6.5–6.7°C)	Yusa, 1954 (6.0–7.0°C)	Nakatani and Maeda, 1984[5] (7.0°C)	Hamai et al., 1974 (5.0°C)
Blastodermal cap	37.5	39.5	35	36.8		28.5	31	
Blastopore closure	114	118	105	108	100	102	148	139
Tail 3/4	211.7	217	161	204		234	192	
Tail full circle	274.5	264	250	279	250	270	216	330
50% hatch	349	320	285	303	345	288+	298	411

[1] A. C. Matarese, Alaska Fisheries Science Center, National Marine Fisheries Service, 7600 Sand Point Way N.E., Seattle, WA 98115.
[2] A. J. Paul, University of Alaska Fairbanks, Institue of Marine Science, Seward Marine Center Lab, P.O. Box 730, Seward, AK 99664.
[3] Values except for hatch estimated from Table 3 in Haynes and Ignell (1983). 50% hatch from Table 7.
[4] Values except for hatch estimated from Fig. 3 in Hamai et al. (1971).
[5] Values except for hatch estimated from Fig. 5 in Nakatani and Maeda (1984).

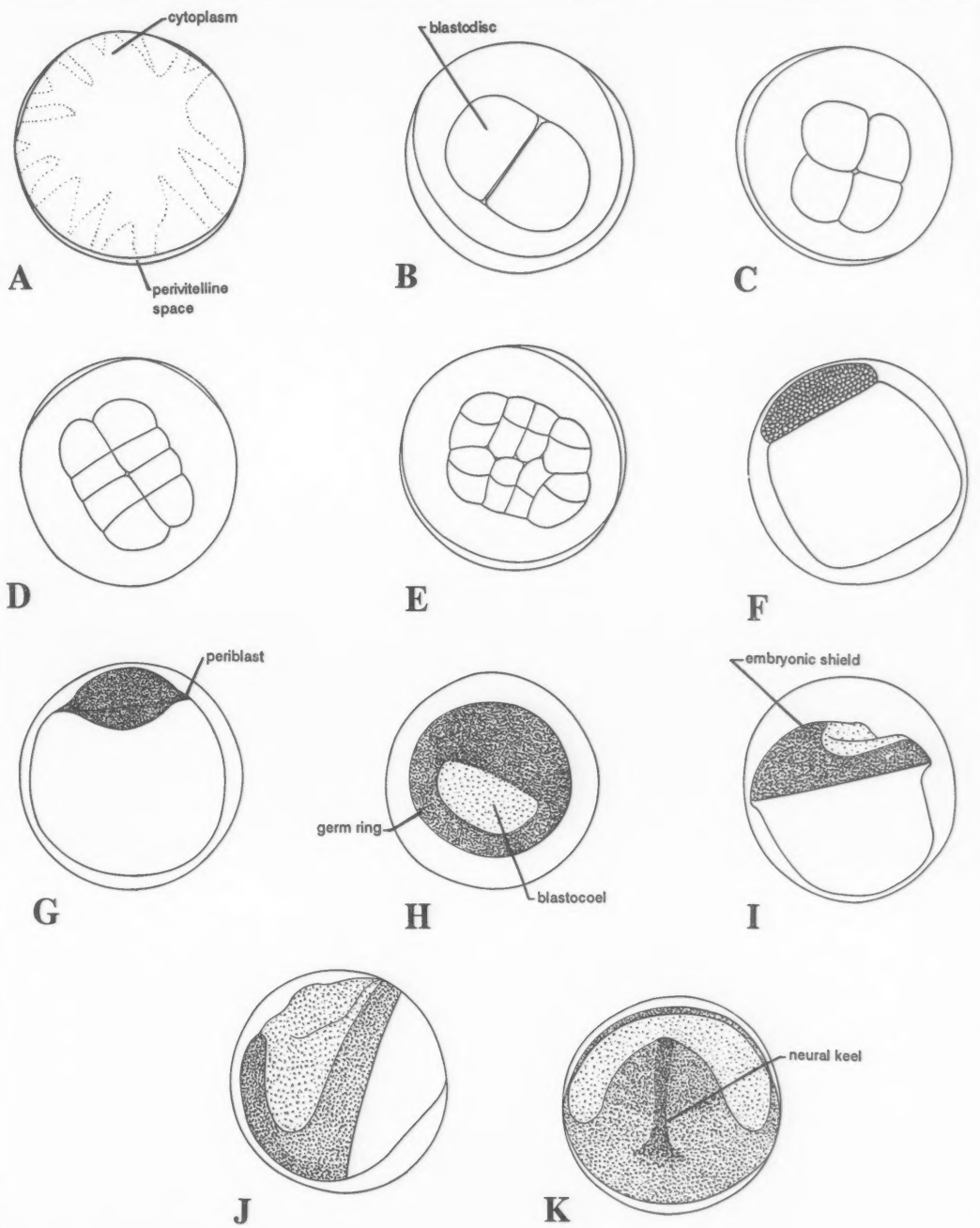

Figure 5

Illustrations of preserved *Theragra chalcogramma* eggs. (**A**) Stage 1 (precell); (**B**) Stage 2 (2 cell); (**C**) Stage 3 (4 cell); (**D**) Stage 4 (8 cell); (**E**) Stage 5 (16 cell); (**F**) Stage 6 (32 cell); (**G**) Stage 7 (blastodermal cap); (**H**) Stage 8 (early germ ring); (**I**) Stage 9 (germ ring 1/4, lateral view); (**J**) Stage 10 (germ ring 1/2, lateral view); (**K**) Stage 10 (dorsal view).

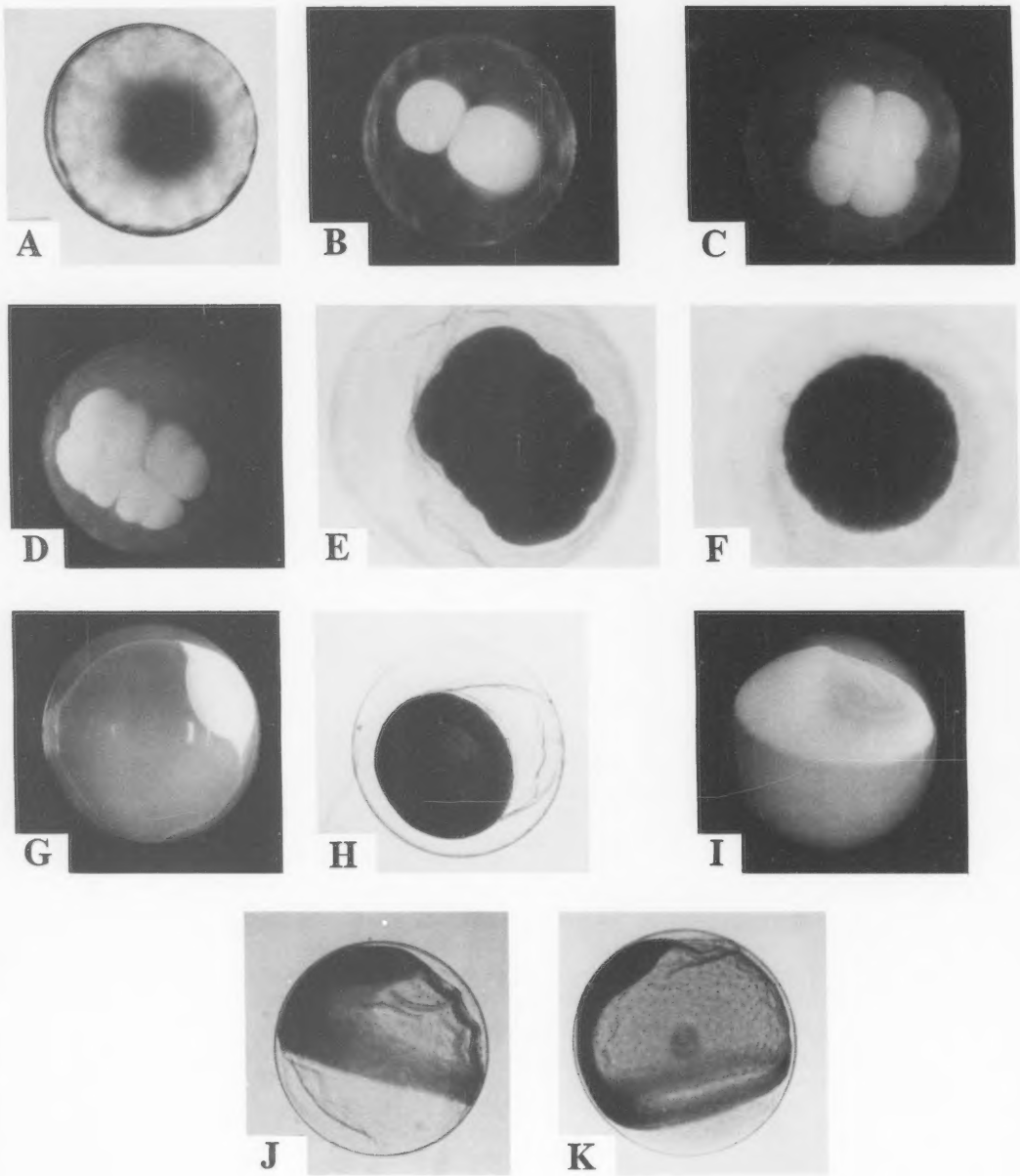

Figure 6

Photographs of preserved *Theragra chalcogramma* eggs. (**A**) Stage 1 (precell); (**B**) Stage 2 (2 cell); (**C**) Stage 3 (4 cell); (**D**) Stage 4 (8 cell); (**E**) Stage 5 (16 cell); (**F**) Stage 6 (32 cell); (**G**) Stage 7 (blastodermal cap); (**H**) Stage 8 (early germ ring); (**I**) Stage 9 (germ ring 1/4); (**J**) Stage 10 (germ ring 1/2); (**K**) Stage 11 (germ ring 3/4).

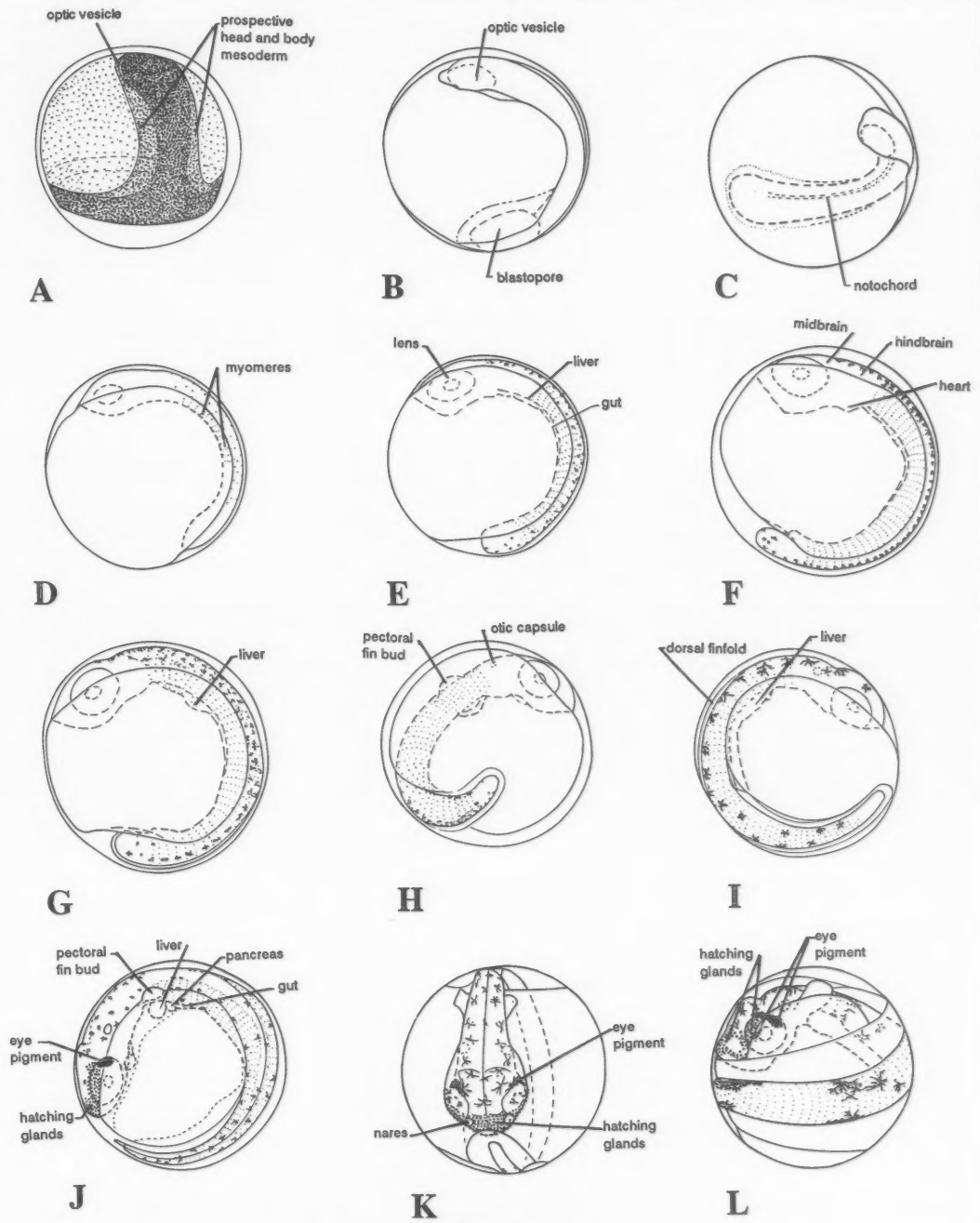

Figure 7

Illustrations of preserved *Theragra chalcogramma* eggs. (**A**) Stage 11 (germ ring 3/4); (**B**) Stage 12 (blastopore almost closed); (**C**) Stage 13 (early middle); (**D**) Stage 14 (middle middle); (**E**) Stage 15 (late middle); (**F**) Stage 16 (early late); (**G**) Stage 17 (tail 5/8 circle); (**H**) Stage 18 (tail 3/4 circle); (**I**) Stage 19 (tail 7/8 circle); (**J**) Stage 20 (tail full circle, lateral view); (**K**) Stage 20 (dorsal view); (**L**) Stage 21 (tail 1-1/8 circle).

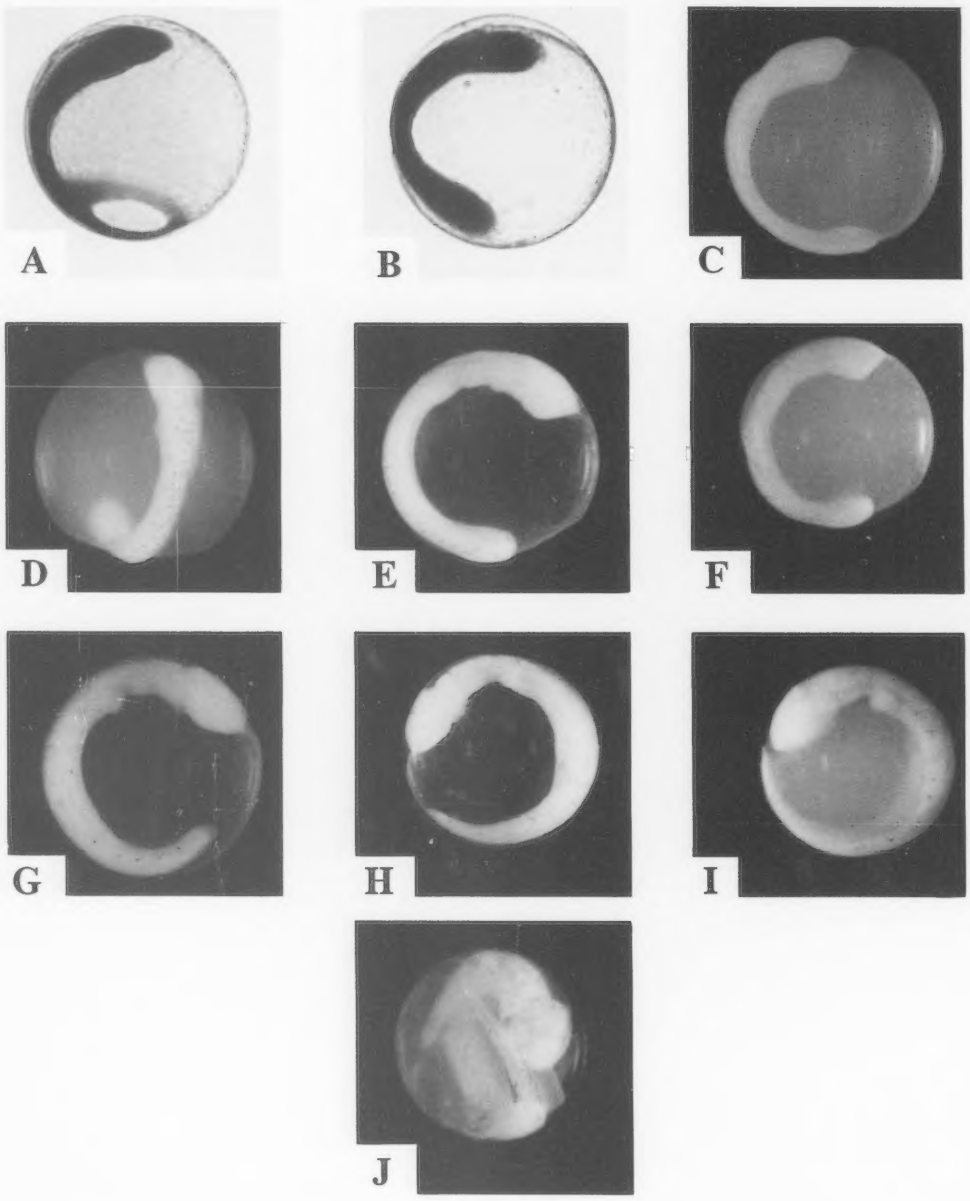

Figure 8

Photographs of preserved *Theragra chalcogramma* eggs. (**A**) Stage 12 (blastopore almost closed); (**B**) Stage 13 (early middle); (**C**) Stage 14 (middle middle); (**D**) Stage 15 (late middle); (**E**) Stage 16 (early late); (**F**) Stage 17 (tail 5/8 circle); (**G**) Stage 18 (tail 3/4 circle); (**H**) Stage 19 (tail 7/8 circle); (**I**) Stage 20 (tail full circle); (**J**) Stage 21 (tail 1-1/8 circle).

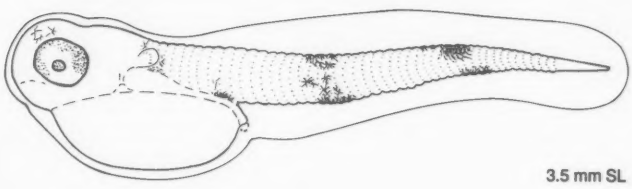

Figure 9
Illustration of preserved *Theragra chalcogramma* yolk-sac larva (Matarese et al., 1989).

yolk surface (Fig. 8F). The dorsal finfold is formed on the posterior 1/3 of the body and pigment on the head extends at least to the posterior margin of the eye (Fig. 7G). The liver is prominent and the heart is beating in the live egg.

Tail 3/4 around yolk (stage 18) The embryo has 36–41 myomeres. The tip of the tail is tapered and curves away from the longitudinal axis of the embryo (Fig. 7H). The dorsal finfold extends to midbody and pectoral fin buds are prominent. Otic capsules are formed. Large stellate melanophores are scattered over the dorsum, extending just to the midlateral surface; posterior to the anus, two rows of melanophores are seen dorsally and a few are found along the ventral midline (Fig. 8G). The tip of the tail is unpigmented.

Tail 7/8 around yolk (stage 19) When the embryo has 44–48 myomeres, the dorsal finfold extends anteriorly 2/3 body length, inserting just posterior to the pectoral fin buds and centered over the liver (Figs. 7I and 8H). Pigment on the head extends to the middle of the eye. At midbody, pigment is scattered on either side of the dorsal midline, extending to just above the lateral midline. Postanal pigment migrates toward the dorsal and ventral midlines.

Tail full circle around yolk (stage 20) The embryo has 48–49 myomeres and the pancreas is visible adjacent to the liver (Fig. 7J). The embryo now encircles the yolk and the tail tip may reach from near the snout to as far back as the posterior margin of the eye (Fig. 8I). Hatching glands, similar to those of other teleosts (Yamagami, 1988), are discernible on the surface of the snout and may extend over the dorsal surface of the eye (Figs. 7J and 7K). The posterior portion of the eye is pigmented. Postanal pigment migrates and begins to form the postanal bars found in yolk-sac larvae (Matarese et al., 1989) (Fig. 9).

Tail 1 1/8 times around yolk (stage 21) The embryo has 49–50 myomeres and the tail tip elongates, extending beyond the posterior margin of the eye (Fig. 8J). The urinary bladder is visible posterior to the anus (1/3 body length; not shown on figure) and the dorsal finfold extends to midbrain. Head pigment extends to the anterior margin of the eye (Fig. 7L). The dorsal half of the eye is pigmented. Most body pigment coalesces to three areas: dorsally, on gut; a bar at 1/2 body length; and a bar at 3/4 body length. In the postanal bars, most pigment is along dorsal and ventral midlines; some pigment extends onto the lateral body. Pigment is scattered on the preanal body.

Discussion

Time from first hatch to 50% hatch was inversely related to temperature. Hatch times reflected the effects of temperature described by Yamagami (1988), who demonstrated that the hatching enzyme secreted by the embryo solubilizes the chorion more rapidly at higher temperatures. The first larvae to hatch were stage 20. Early hatching may have been an artifact of rearing conditions. However, hatching glands were present at this stage, which, with the appearance of eye pigment, may correspond to a level of development that would enable these larvae to survive. Early hatching may occur naturally with some frequency. Within batches of walleye pollock larvae from Puget Sound that had been incubated in the laboratory, larvae hatching early grew to an equivalent size as larvae hatching later (larvae hatched on day 1 were the same length at day 3 as larvae hatched on day 3). Those early hatched larvae also began to feed at the same time as larvae hatched later.[4]

Rate of development and time to 50% hatch were similar among studies of walleye pollock from the eastern North Pacific, specifically the Gulf of Alaska (Matarese, unpubl. data; Haynes and Ignell, 1983; and this study; Paul[5]). From data on time (days) to 50% hatch for all temperatures reported in all incubation studies (Fig. 10), incubation times of western North Pacific walleye pollock are longer than eastern North Pacific walleye pollock.

This finding appears to conflict with Haynes and Ignell's (1983) comparison with Yusa's (1954) study in which they report similar rates of development

[4] Olla, B. Mark O. Hatfield Marine Science Center, Oregon State University, 2030 Marine Science Drive, Newport, OR 97365-5297. Pers. commun. 18 August 1992.

[5] Paul, A. J. University of Alaska Fairbanks, Institute of Marine Science, Seward Marine Center Lab, P.O. Box 730, Seward, AK 99664. Unpubl. data.

for eastern and western stocks. However, their comparison was made with midpoints of stages calculated from a regression model instead of observed midpoints. Also, Yusa (1954) reported a temperature range of 6–7°C instead of a mean; our interpretation of Haynes and Ignell's (1983) classification and calculation of Yusa's (1954) data suggests incubation temperatures were always above 6.5°C (see their Table 6 and our Table 4). Finally, Haynes and Ignell (1983) monitored midpoints of stages more closely than midpoint of hatch and did not specifically refer to 50% hatch.[6] We assumed the values reported as observed midpoints of hatch (their Table 7) were close to 50% hatch. Yusa's (1954) study could not be compared with ours with regard to time to 50% hatch.

Time of hatch is often a result of how eggs are treated during incubation and may vary with different batches.[7] However, walleye pollock eggs from Japanese waters are larger than those from the Gulf of Alaska (mean=1.4–1.6 mm and 1.3–1.4 mm, respectively; Bailey and Stehr, 1986). At similar temperatures, larger eggs take longer to develop (Pepin, 1991). The difference in incubation time emphasizes the need to collect data from fish specific to the area of interest. This will reduce the sources of variation in development time for laboratory-reared eggs; failure to identify and improve these sources would compromise the usefulness of models predicting egg age based on water temperature.

Development is a continuous process. The sampling intervals and arbitrary designation of stage endpoints break development into subjective units. Using the 21-stage scheme, we did not see a clear decrease in each stage duration with an increase in temperature. However, this will not affect the usefulness of our results. When stages are grouped to encompass a greater degree of morphological development, as in Haynes and Ignell (1983) and Picquelle and Megrey (1993), development time is inversely related to temperature. A greater number of stages within a group increases the accuracy of prediction of egg age. A large number of stages also allows others greater flexibility in grouping those stages.

Our regression model predicts temperature-specific development time for purposes of computing rates of egg production and egg mortality. There is no biological basis upon which the regression is predicated because stages that are assigned to the eggs are arbitrary; stages are ordinal data that are based on morphological criteria without consideration for development time. An alternative method to estimate development time from temperature is to fit a separate regression for each stage. The disadvantage of this alternative method is that many parameters are fitted with few data points.

Two studies describing morphological development, Gorbunova (1954) and Yusa (1954), have been published. Gorbunova (1954) was not comparable to our study. We compared our descriptions of morphological development with Yusa (1954). We assigned stages to descriptions of hourly morphological devel-

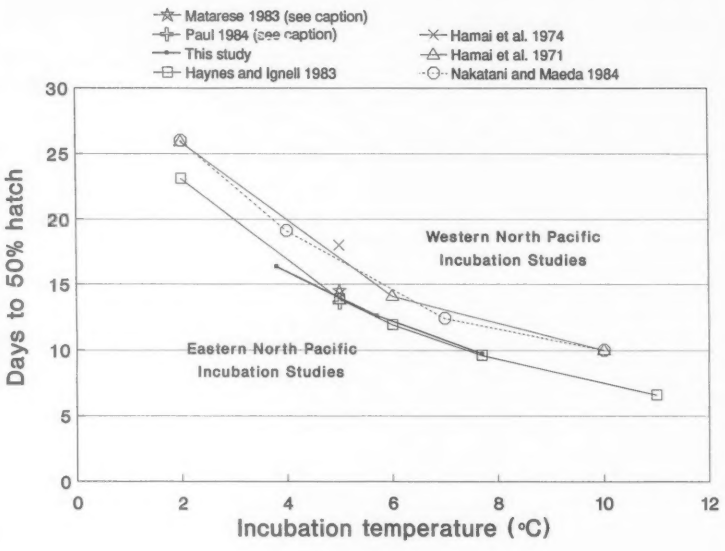

Figure 10

Days to 50% hatch for *Theragra chalcogramma* eggs at various temperatures of incubation. (A. C. Matarese, unpubl. data, Alaska Fisheries Science Center, National Marine Fisheries Service, 7600 Sand Point Way N.E., Seattle, WA 98115. A. J. Paul, unpubl. data, University of Alaska Fairbanks, Institute of Marine Science, Seward Marine Center Lab, P.O. Box 730, Seward, AK 99664.)

[6] Haynes, E., National Marine Fisheries Service, Auke Bay Laboratory, 11305 Glacier Highway, Juneau, AK 99801-8626. Pers. commun. April 1991.

[7] Paul, A. J., University of Alaska Fairbanks, Institute of Marine Science, Box 730, Seward, AK 99664. Pers. commun. 17 March 1992.

opment of walleye pollock embryos incubated at 6.0–7.0°C (Yusa, 1954) for comparison with morphological characteristics of eggs reared at 5.7°C in this study. We used hallmarks of each stage (e.g. number of cells, germ ring advancement, number of myomeres, tail growth around yolk) to distribute Yusa's (1954) descriptions into 21 stages. Yusa's (1954) descriptions were similar to ours up to stage 11. Beginning with stage 11, Yusa (1954) described the development of some structures occurring one or more stages earlier than this study: myomeres and nares were sighted one stage earlier; brain differentiation and eye lenses, two stages earlier; the heart, three stages earlier; and the otic capsules, five stages earlier (Table 5). Otoliths sighted by Yusa (1954) were not visible in our specimens. Conversely, eye pigment was observed in our study one stage earlier than that observed by Yusa (1954). Other structures appeared at the same stage in each study: optic vesicles, Kupffer's vesicle, liver, gut, and pectoral-fin anlagen. Also, after stage 13, similar numbers of myomeres were visible at like stages in both studies as was the beating of the heart.

Differences between the two studies may be the result of egg condition when examined: Yusa (1954) described live eggs, whereas most of our descriptions were of preserved eggs. Formalin preservation may obscure myomeres or destroy structures such as embryonic otoliths (McMahon and Tash, 1979). Stockard's solution darkens embryonic tissue and obscures fine details. Also, morphological development may differ between western and eastern North Pacific walleye pollock, further emphasizing the need to restrict data collection to specific areas of interest to increase accuracy of interpretation.

Acknowledgments

We thank the following people whose combined efforts helped us accomplish our research and produce this paper: William Rugen assisted with shipboard experiments; Kevin Bailey, Gail Theilacker, and Steve Porter helped us interpret the morphology of late-stage eggs and yolk-sac larvae; Trish Brown provided statistical analyses; Morgan Busby photographed the eggs; and Beverly Vinter illustrated eggs and helped interpret many morphological structures. We thank Art Kendall, A. J. Paul, Kevin Bailey, Susan Picquelle, and Bori Olla for preliminary reviews of the manuscript. Gail Theilacker and Richard Brodeur helped refine later versions. We also thank the members of FOCI who assisted with field collections.

Literature cited

Alderdice, D. F.
1988. Osmotic and ionic regulation in teleost eggs and larvae. *In* W. S. Hoar and D. J. Randall (eds.), Fish physiology, Vol. XI, Part A, p.163–251. Academic Press, Inc., San Diego.

Table 5

Descriptions of morphological development of *Theragra chalcogramma* embryos at comparable stages by Yusa (1954) and this study.

Stage	Yusa (6.0–7.0°C)	This study (5.7°C)
11	medullary plate and optic vesicles visible	optic vesicles visible
12	5–7 myomeres; 3 sections of brain visible	myomeres begin to differentiate
13	9–13 myomeres; heart, otic capsules, otoliths, eye lenses, and Kupffer's vesicle visible	7–12 myomeres; Kupffer's vesicle visible
14	16–17 myomeres; nares and pigment along dorsum visible	14–16 myomeres; pigment along dorsum visible; mid- and hindbrain differentiation
15	18–30 myomeres; liver, gut, and pectoral anlagen visible; 3 sections of brain formed	20–25 myomeres; eye lens, nares, pectoral anlagen, liver, and gut visible
16	35 myomeres	24–36 myomeres; heart visible; 3 sections of brain formed
17	37 myomeres; heart beating	27–36 myomeres; heart beating
18	40 myomeres	36–41 myomeres; otic capsules visible
19		44–48 myomeres
20		48–49 myomeres; eye pigment appears
21	eye pigment appears	

Bailey, K. M., and C. L. Stehr.
1986. Laboratory studies on the early life history of the walleye pollock, *Theragra chalcogramma* (Pallas). J. Exp. Mar. Biol. Ecol. 99:233–246.

Blaxter, J. H. S.
1969. Development: eggs and larvae. *In* W. S. Hoar and D. J. Randall (eds.), Fish physiology, Vol. III, p.177–252. Academic Press, New York.

Gorbunova, N. N.
1954. Reproduction and development of the walleye pollock, *Theragra chalcogramma* (Pallas). Tr. Inst. Okeanol. Akad. Nauk. SSSR 11:132–195. (In Russian, transl. by S. Pearson, 1972, Natl. Mar. Mammal Lab., NMFS, 7600 Sand Point Way N.E., Seattle, WA 98115–0070.)

Hamai, I., K. Kyushin, and T. Kinoshita.
1971. Effect of temperature on the body form and mortality in the development and early larval stages of the Alaska pollock, *Theragra chalcogramma* (Pallas). Bull. Fac. Fish. Hokkaido Univ. 22:11–29.

Hamai, I., K. Kyushin, and T. Kinoshita.
1974. On the early larval growth, survival, and variation of body form in the walleye pollock, *Theragra chalcogramma* (Pallas), in rearing experiment feeding the different diets. Bull. Fac. Fish. Hokkaido Univ. 25:20–35.

Haynes, E. B., and S. E. Ignell.
1983. Effect of temperature on rate of embryonic development of walleye pollock, *Theragra chalcogramma*. Fish. Bull. 81:890–894.

Kendall, A. W., Jr., and S. Kim.
1989. Buoyancy of walleye pollock (*Theragra chalcogramma*) eggs in relation to water properties and movement in Shelikof Strait, Gulf of Alaska. *In* R. J. Beamish and G. A. McFarlane (eds.), Effects of ocean variability on recruitment and an evaluation of parameters used in stock assessment models, p.169–180. Can. Spec. Publ. Fish. Aquat. Sci. 108.

Kendall, A. W., Jr., and S. J. Picquelle.
1990. Egg and larval distributions of walleye pollock *Theragra chalcogramma* in Shelikof Strait, Gulf of Alaska. Fish. Bull. 88:133–154.

Markle, D. F., and K. G. Waiwood.
1985. Fertilization failure in gadids: aspects of its measurement. J. Northw. Atl. Fish. Sci. 6:87–93.

Matarese, A. C., A. W. Kendall Jr., D. M. Blood, and B. M. Vinter.
1989. Laboratory guide to early life history stages of Northeast Pacific fishes. U.S. Dep. Commer., NOAA Tech. Rep. NMFS 80, 652 p.

McMahon, T. E., and J. C. Tash.
1979. Effects of formalin (buffered and unbuffered) and hydrochloric acid on fish otoliths. Copeia 1979:155–156.

Megrey, B. A.
1991. Population dynamics and management of walleye pollock (*Theragra chalcogramma*) in the Gulf of Alaska, 1976–1986. Fish. Res. 11:321–354.

Nakatani, T., and T. Maeda.
1984. Thermal effect on the development of walleye pollock eggs and their upward speed to the surface. Bull. Jpn. Soc. Sci. Fish. 50:937–942.

Naplin, N. A., and C. L. Obenchain.
1980. A description of eggs and larvae of the snake eel, *Pisodonophis cruentifer* (Ophichthidae). Bull. Mar. Sci. 30:413–423.

Olla, B. L., and M. W. Davis.
1993. The influence of light on egg buoyancy and hatching rate of the walleye pollock, *Theragra chalcogramma* (Pallas). J. Fish. Biol. 42:693–698.

Pepin, P.
1991. Effect of temperature and size on development, mortality, and survival rates of the pelagic early life history stages of marine fish. Can. J. Fish. Aquat. Sci. 48:503–518.

Picquelle, S. J., and B. A. Megrey.
1993. A preliminary spawning biomass estimate of walleye pollock, *Theragra chalcogramma,* in the Shelikof Strait, Alaska, based on the annual egg production method. Bull. Mar. Sci. 53:728–749.

Reed, R. K., and J. D. Schumacher.
1989. Transport and physical properties in central Shelikof Strait, Alaska. Cont. Shelf Res. 9:261–268.

SAS Institute, Inc.
1985. SAS® user's guide: basics, version-5 edition. SAS Institute, Inc., Cary, NC, 1290 p.

Schumacher, J. D., and A. W. Kendall Jr.
1991. Some interactions between young walleye pollock and their environment in the western Gulf of Alaska. Calif. Coop. Oceanic Fish. Invest. Rep. 32:22–40.

Trinkaus, J. P.
1951. A study of the mechanism of epiboly in the egg of *Fundulus heteroclitus*. J. Exp. Zool. 118:269–319.

Velsen, F. P. J.
1980. Embryonic development in eggs of sockeye salmon, *Oncorhynchus nerka*. Can. Spec. Pub. Fish. Aquat. Sci. 49, 19 p.

Yamagami, K.
1988. Mechanisms of hatching in fish. *In* W. S. Hoar and D. J. Randall (eds.), Fish physiology, Vol. XI, Part A, p. 447–499. Academic Press, Inc., San Diego.

Yusa, T.
1954. On the normal development of the fish, *Theragra chalcogramma* (Pallas), Alaska pollock. Bull. Hokkaido Reg. Fish. Res. Lab. 10:1–15.

Diel vertical distribution of ichthyoplankton in the northern Gulf of Alaska*

Richard D. Brodeur
William C. Rugen

Alaska Fisheries Science Center, National Marine Fisheries Service, NOAA
7600 Sand Point Way NE, Seattle, WA 98115

Abstract.—The diel vertical distribution patterns of several abundant ichthyoplankton taxa were examined from depth-stratified tows off Kodiak Island in the western Gulf of Alaska during 1986 and 1987. Most larvae were found in the upper 45 m of the water column throughout the diel period but were concentrated in higher densities near the surface (0–15 m) in daylight hours and at greater depths at night. Four of the five dominant taxa examined in detail showed significantly greater weighted mean depths during the night than during the day. This pattern was the opposite to that previously reported for the numerically dominant taxa (*Theragra chalcogramma*) in this area. Since there was no clear relation between the diel vertical distribution of these taxa and the vertical distribution of water temperature and density or copepod nauplii prey, we hypothesize that this reverse migration is either a strategy to minimize spatial overlap with predators that follow a normal diel migration pattern or one to optimize light levels for feeding.

Planktonic eggs and larvae of marine fishes exist in three dimensions in the open ocean. Unfortunately, traditional ichthyoplankton surveys, which use non-closing sampling gear, provide information only on two dimensions, integrating the vertical indirectly into the horizontal dimensions. It is well known that vertical current shear can be substantial over short distances and that light, temperature, hydrostatic pressure and food show much stronger gradients in the vertical relative to the horizontal dimensions in the water column (Laprise and Dodson, 1993). Thus, a larva can often change not only its geographic position, but also its immediate environment by altering its vertical position in the water column.

Diel vertical migration is well documented for larval, juvenile, and adult life history stages of marine fishes (see review by Neilson and Perry, 1990). The adaptive significance of these migrations is presently in dispute, but it has been attributed to position maintenance, bioenergetic optimization, thermoregulation, and predator avoidance (Kerfoot, 1985; Lampert, 1989). In addition, the degree of migration and amplitude of depths over which a species vertically migrates often changes during ontogenetic development (Brewer and Kleppel, 1986; de Lafontaine and Gascon, 1989).

Knowledge of vertical distribution patterns of marine fish larvae is crucial not only in understanding ecological processes but also has practical implications in the assessment of abundance. Sampling just the upper depths of a species range can lead to substantial underestimates of abundance, whereas sampling the entire water column for surface-dwelling taxa may waste limited ship time. Despite the importance of the larval phase in recruitment of marine fishes, relatively little is known about larval vertical distribution patterns off the continental shelf in the North Pacific Ocean. With the exception of walleye pollock, *Theragra chalcogramma*, which has been fairly well studied through much of its geographic range (Kamba, 1977; Kendall et al., 1987; Pritchett and Haldorson, 1989; Kendall et al.[1]), the only comprehensive studies on vertical distribution of coastal ichthyoplankton in the northeast Pacific Ocean are from the California Current region (Ahlstrom, 1959; Boehlert et al., 1985; Brewer and Kleppel, 1986; Lenarz et al., 1991). This paper presents information on the vertical distribution of five abundant ichthyoplankton taxa (other than walleye pollock) collected in the

Manuscript accepted 18 October 1993
Fishery Bulletin 92:223–235 (1994)

*Contribution No. 0181 of the Fisheries Oceanography Coordinated Investigations.

coastal waters of Alaska during spring and examines diel differences in these patterns in relation to environmental and biotic factors.

Materials and methods

Samples examined were collected from two cruises of the NOAA ship *Miller Freeman* in the area southwest of Kodiak Island in the northern Gulf of Alaska (Fig. 1). During May 1986 and 1987, 22 depth-stratified tows were made with a 1-m^2 Multiple Opening/Closing Net and Environmental Sensing System (MOCNESS) (Wiebe et al., 1976) equipped with 153-µm mesh. The net was towed obliquely and nets were opened sequentially at the desired depth strata. The primary purpose of the sampling was to collect information on the vertical distribution of walleye pollock larvae, which are generally found in the upper 50 m (Kendall et al.[1]), and their prey. Therefore, the emphasis during the sampling was on the upper part of the water column. The nets sampled the following nominal depths: 0–15, 15–30, 30–45, 45–60, 60–80, 80–100, and >100 m. Maximum sampling depth varied (range 150–252 m) depending on the depth of the water column at a particular station. There were eight depth strata sampled at most stations but the cutoff depth between the seventh and eighth net was variable. Therefore, we pooled the catches from these two nets into a single depth stratum (>100 m) for analysis. The actual sampling depths are given in Table 1. More complete station and catch information is given in Siefert et al.[2,3]

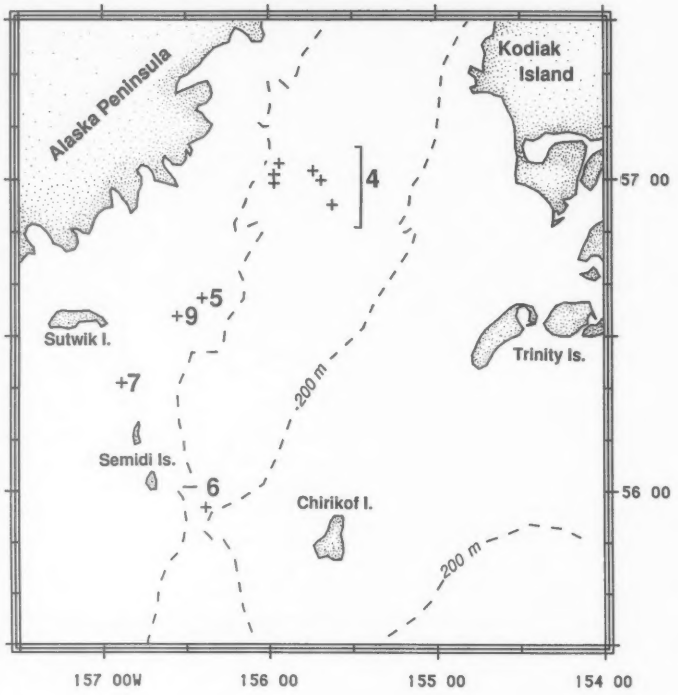

Figure 1
Location of MOCNESS sampling series in Shelikof Strait used to determine vertical distribution of larvae in 1986 and 1987.

The 22 tows were grouped into five collection series (Table 1) based upon date and location of sampling (see Kendall et al.[1]) and included two complete diel series. The first diel series (Series 4) attempted to sample the same body of water over a four day period during 1986 by following a radar-tracked drifter drogued at 35 m (Incze et al., 1990). The second diel series (Series 9) sampled the same location on three successive days during 1987. Other collections (Series 5, 6, and 7) were taken at various times of the day but in the same general area as these two series (Fig. 1, Table 1).

Retrieved nets were thoroughly washed and contents were preserved in 5% buffered formalin. Samples were sorted to the lowest possible taxon and life history stage at the Polish Sorting Center in Szczecin, Poland. The volume filtered was estimated from a mechanical flowmeter mounted on the MOCNESS frame and abundances were converted to number per 1000 m^3. Up to 50 preserved larvae of each taxon from each net were measured to the nearest 0.1 mm standard length. Net depth, temperature, and

[1] Kendall, A. W., Jr., L. S. Incze, P. B. Ortner, S. R. Cummings, and P. K. Brown. In review. The vertical distribution of eggs and larvae of walleye pollock (*Theragra chalcogramma*) in Shelikof Strait, Gulf of Alaska. Submitted to Fish. Bull.

[2] Siefert, D. L. W., L. S. Incze, and P. B. Ortner. 1988. Vertical distribution of zooplankton, including ichthyoplankton, in Shelikof Strait, Alaska: data from Fisheries Oceanography Coordinated Investigations (FOCI) cruise in May 1986. NWAFC Processed Rep. 88-28, 232 p.

[3] Siefert, D. L. W., L. S. Incze, and P. B. Ortner. 1990. Vertical distribution of zooplankton, including ichthyoplankton, in Shelikof Strait, Alaska: data from Fisheries Oceanography Coordinated Investigations (FOCI) cruise in May 1987. NWAFC Processed Rep. 90-05, 129 p.

Table 1

Station and tow data for collection subset used in the diel series ordered by time of day.

Series	Tow	Year	Date	Bottom depth (m)	Local time	Time period	Net depths (m) 1	2	3	4	5	6	7
4	5	1986	10 May	293	0745	Dawn	2–15	15–30	29–45	46–58	59–78	79–99	101–229
4	1	1986	8 May	220	0746	Dawn	1–15	15–31	35–45	45–61	61–80	80–100	101–200
9	4	1987	23 May	201	0747	Dawn	0–15	15–30	30–45	45–60	60–80	80–100	100–150
9	8	1987	24 May	190	0800	Dawn	0–15	15–30	30–45	45–60	60–80	80–100	100–150
6	2	1986	15 May	223	0940	Day	2–14	15–29	30–44	45–60	61–80	80–100	100–175
5	1	1986	13 May	210	1010	Day	2–15	16–30	30–45	45–61	61–80	80–100	101–152
4	6	1986	10 May	296	1341	Day	2–14		30–45			77–99	99–214
5	2	1986	13 May	210	1351	Day	2–14	15–29	30–44	45–59	59–78	80–99	100–176
4	2	1986	8 May	227	1356	Day	2–14	15–30	30–47			79–99	99–200
9	5	1987	23 May	179	1422	Day	0–15	15–30	30–45	45–60	60–80	80–100	100–150
9	9	1987	24 May	190	1543	Day	0–15	15–30	30–45	45–60	60–80	80–100	100–150
7	2	1986	18 May	123	1911	Dusk	2–15	15–30	30–45	45–59	60–79	80–100	
4	3	1986	9 May	235	2006	Dusk	2–13	13–28	29–45	46–59	60–79		100–200
4	7	1986	11 May	293	2011	Dusk	3–14	14–30	31–44	43–59	60–78	78–97	98–252
9	6	1987	24 May	179	2107	Dusk	0–15	15–30	30–45	45–60	60–80	80–100	100–150
9	10	1987	25 May	196	2122	Dusk	0–15	15–30	30–45	45–60	60–80	80–100	100–150
5	3	1986	14 May	210	2200	Night	2–14	14–30	30–45	46–60	60–80	81–101	100–163
7	1	1986	17 May	126	2416	Night	1–15	16–30	31–45	45–59	60–80	80–99	
4	4	1986	9 May	242	0135	Night	2–15	15–30	30–58		59–80	80–100	100–202
9	11	1987	25 May	198	0218	Night	0–15	15–30	30–45	45–60	60–80	80–100	100–150
9	7	1987	24 May	195	0219	Night	0–15	15–30	30–45	45–60	60–80	80–100	100–150
6	1	1986	15 May	229	0353	Night	2–15	15–29	30–44	45–60	60–80	80–100	100–172

salinity were measured continuously in real time during the tow and stored for later analysis.

To examine diel variations in density and size of larvae with depth, collections from the 22 tows were grouped into one of four time periods (hours): dawn (0530–0830), day (0830–1830), dusk (1830–2130), and night (2130–0530). Diel-depth variation in density of eggs and larvae at each depth was examined by using a two-way ANOVA on log-transformed data. The log (X+1) transformation was used to achieve homogeneous variances (Bartlett's Test, all P>0.05). In addition, a weighted mean depth of occurrence of eggs or larvae of the dominant species for each time interval was calculated as follows:

$$\overline{D}_t = \frac{\sum_{i=1}^{n_t}\sum_{j=1}^{7} N_{ijt} D_{ijt}}{\sum_{i=1}^{n_t}\sum_{j=1}^{7} N_{ijt}},$$

where n_t = number of tows in time interval t,
N_{ijt} = number of larvae in net j in tow i in time interval t,
D_{ijt} = midpoint depth of net j in tow i in time interval t with a variance equal to

$$Var(\overline{D}_t) = \frac{n_t}{\left(\sum_{i=1}^{n_t} N_{it}\right)^2 (n_t - 1)} \sum_{i=1}^{n_t} N_{it}^2 (\overline{D}_{it} - \overline{D}_t)^2,$$

where N_{it} = number of larvae in tow i in time interval t.

Differences in the weighted mean depths over the four time periods were tested with ANOVA, and Tukey multiple-comparison tests were conducted when significant differences were observed. Untransformed larval lengths for the three most abundant species were entered as dependent variables in two-way ANOVAs, with time of day and depth as factors.

Results

Species composition

Eggs and larvae of species other than walleye pollock were found in 134 of the 145 samples collected

during the 1986 and 1987 cruises. Flathead sole (*Hippoglossoides elassodon*) eggs were the only pelagic eggs other than walleye pollock collected and were found in 28.4% of the samples. This species had a mean density of 62.99 eggs/1000 m^3 (SD=179.66) and comprised 74.9% of the total egg abundance in the 22 tows.

A total of 33 larval taxa were identified but only a few taxa occurred in more than 10% of the samples (Table 2). Larvae other than walleye pollock occurred in 92.4% of the collections but made up only 26.3% of the overall total abundance of larvae (total mean density=143.61 larvae/1000 m^3; SD=257.03). Larvae of three taxa (*H. elassodon*, *Ammodytes hexapterus*, and *Bathymaster* spp.[4]) were found at sufficient densities to enable examination of their vertical abundance and length distribution patterns in detail for the four time periods. Two other species (*Gadus macrocephalus* and *Pleuronectes bilineatus*) were found at relatively high densities during day and night but at low densities during the twilight periods; hence, these taxa were examined only for day-night differences.

Vertical distribution

The distribution of *H. elassodon* eggs showed little variation in weighted mean depth by time of day (F=3.10, P>0.05); the highest abundances were

[4] Larvae of three *Bathymaster* species known to occur in the study area are presently not identifiable to species. Based on the abundance and distribution patterns of the adults, most of the larvae present in our collections are probably *B. signatus*. (A. Matarese, Alaska Fisheries Science Center, Seattle, WA 98115. Pers. commun. 1992).

Table 2

Summary of all larvae including walleye pollock collected in the 1986–87 vertical distribution study.

Scientific name	Common name	Percent occurrence (n=145)	Mean density (no./1000m^3)	Length range (mm)
Osmerus mordax	rainbow smelt	0.69	0.25	21
Leuroglossus schmidti	northern smoothtongue	0.69	0.02	9–15
Stenobrachius leucopsarus	northern lampfish	4.14	3.05	4–7
Protomyctophum thompsoni	bigeye lanternfish	0.69	0.04	10
Myctophidae	unidentified myctophid	0.69	0.06	3
Gadus macrocephalus	Pacific cod	15.86	27.51	3–11
Theragra chalcogramma	walleye pollock	93.79	402.71	3–8
Gadidae	unidentified gadid	2.76	0.36	4
Sebastes spp.	unidentified rockfish	1.38	0.17	4–5
Hexagrammos decagrammus	kelp greenling	1.38	0.05	8–11
Dasycottus setiger	spinyhead sculpin	0.69	0.07	8
Gymnocanthus spp.	unidentified sculpin	0.69	0.07	7–8
Hemilepidotus hemilepidotus	red Irish lord	1.38	0.13	11–13
Icelinus spp.	unidentified sculpin	7.59	0.65	4–5
Malacocottus zonurus	darkfin sculpin	0.69	0.05	6–7
Radulinus asprellus	slim sculpin	1.38	0.10	4–5
Ruscarius meanyi	Puget Sound sculpin	0.69	0.04	4
Agonidae	unidentified poacher	10.34	0.84	5–10
Nectoliparis pelagicus	tadpole sculpin	0.69	0.07	4–8
Cyclopteridae	unidentified snailfish	2.07	0.19	4–5
Bathymaster spp.	unidentified ronquil	13.10	30.67	4–7
Anoplarchus spp.	unidentified prickleback	2.07	0.26	8–10
Lumpenella longirostris	longsnout prickleback	1.38	0.05	10–11
Lumpenus maculatus	daubed shanny	6.21	0.64	12–23
Poroclinus rothrocki	whitebarred prickleback	4.83	0.97	10–15
Cryptacanthodes aleutensis	dwarf wrymouth	1.38	0.19	14
Pholis spp.	unidentified gunnel	0.69	0.04	13–17
Zaprora silenus	prowfish	3.45	0.40	12–14
Ammodytes hexapterus	Pacific sand lance	40.69	12.76	6–19
Hippoglossoides elassodon	flathead sole	17.93	59.81	4–19
Pleuronectes bilineatus	rock sole	13.10	3.71	3–10
Pleuronectes vetulus	English sole	0.69	0.13	8
Psettichthys melanostictus	sand sole	0.69	0.14	4–5
Pleuronectidae	unidentified flounder	0.69	0.10	4

found in the surface layer (0–15 m) during all four time periods (Fig. 2). Although there were significant (P=0.005) differences in density by depth strata, neither the diel density differences alone (P=0.838) nor the interaction between time and depth (P=0.996) was significant.

The majority of larvae, excluding pollock larvae, from all collections combined were collected from the upper three depth strata (Fig. 3). The maximum density overall occurred at the second depth stratum (15–30 m), below which larval density declined with depth. However, this overall vertical distribution pattern was apparently confounded by higher larval densities found during the night when the larvae were mainly caught in the 15–30 m stratum; during the other three time periods the highest densities were in surface waters (Fig. 4). The weighted mean depth of larvae overall was significantly (P<0.05) greater at night than during the other three time periods (Table 3) and the interaction between time and depth was marginally significant (P=0.05; Table 4), suggesting that there were diel differences in overall larval depth distribution.

Four of the five most abundant larval taxa showed the greatest weighted mean depths (Table 3) and the lowest surface densities (Fig. 4) at night. This general pattern was also evident in the two time periods examined for the fifth species, *G. macrocephalus*, but the diel differences were not significant (Table 3). Only *A. hexapterus* and *G. macrocephalus* showed significant diel differences in larval density, with highest densities occurring at night (Table 4). None of the dominant taxa, however, showed a significant interaction between time and depth strata.

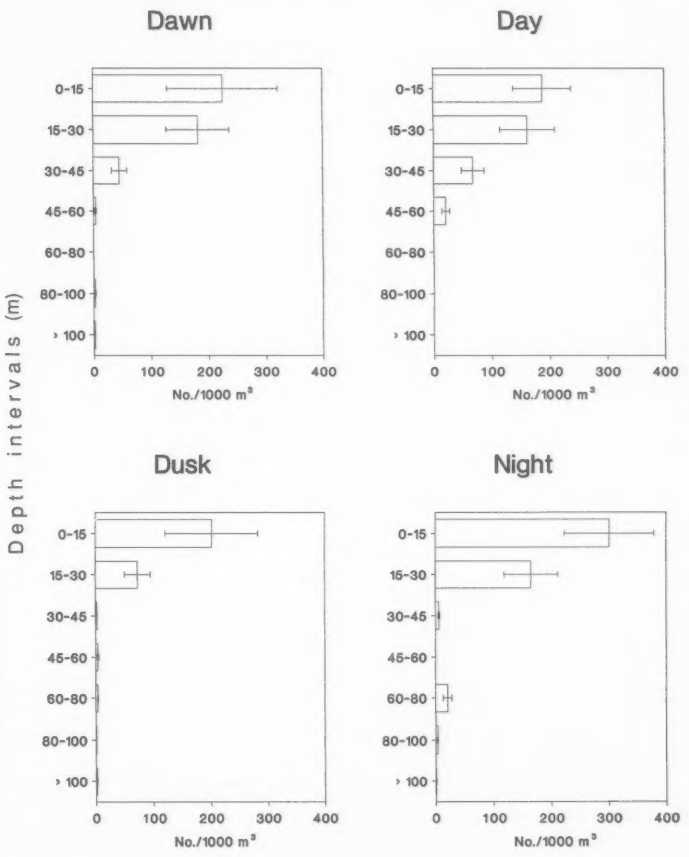

Figure 2

Diel vertical distribution of *Hippoglossoides elassodon* eggs. Bars are mean abundances per 1000 m^3 at each depth interval and error bars are ± one standard deviation about the mean abundance.

Length distributions

The distribution of larval lengths by time of day and depth showed no consistent pattern among the three most abundant species (Fig. 5). Although time and time-depth interactions were significant (all P<0.03) factors in explaining the variation in mean length of *H. elassodon* and *Bathymaster* spp., none of the factors was significant for *A. hexapterus*. Examining only the strata where more than two lengths were available, we found that the smallest larvae of both *Bathymaster* spp. and *A. hexapterus* were caught in the surface stratum at night but in deeper strata during daylight hours (Fig. 5). However, *H. elassodon* showed an increase in mean length with depth during daylight hours and the reverse pattern at night (Fig. 5). *Hippoglossoides elassodon* was the only taxon to show a significant difference in length distributions between night and day collections (Kolmogorov-Smirnov Test; Z=3.881; P=0.001). Although the lack of larger larvae in daytime collections might suggest some daytime gear avoidance by this species

(Fig. 6), there were few small larvae caught at night, which cannot be explained by gear avoidance. Since the majority (>95%) of these lengths were from larvae collected from the same location (Series 9), sampling variability cannot be invoked as an explanation for this pattern.

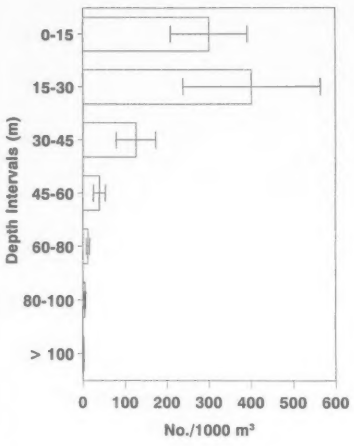

Figure 3

Vertical distribution of all larvae excluding walleye pollock (*Theragra chalcogramma*) combined over all time periods. Bars are mean abundances per 1000 m^3 at each depth interval and error bars are ± one standard deviation about the mean abundance.

Discussion

Our results indicate that the vast majority (>99%) of pelagic eggs and larvae (excluding walleye pollock) are distributed in the upper 100 m of the water column during the spring months. Therefore, sampling to this depth should be sufficient to characterize the horizontal distribution patterns of these species. Of the common taxa we examined, all but *H. elassodon* have demersal eggs (Matarese et al., 1989). The transit time to surface waters following hatching from demersal eggs is apparently of such short duration that even newly hatched larvae were rarely collected below 100 m. However, this does not appear to be the case for walleye pollock, which spawn at depths greater than 200 m in Shelikof Strait, with mean depths of eggs and yolk-sac larvae generally greater than 100 m (Kendall and Kim, 1989; Kendall et al.[1]).

The diel vertical distribution pattern that we observed for several taxa is not the pattern typically observed for most ichthyoplankton and for zooplankton in general. The more common pattern, termed a 'Type I' migration (Neilson and Perry, 1990), involves a nocturnal ascent into surface waters and is undertaken by larvae of a diversity of fish species.

Table 3

Weighted mean depths (m) and standard deviations of the mean depths (in parentheses) for each taxon and for all larvae excluding walleye pollock by time of day and overall depth for all times combined. Also given are the results of the ANOVAs testing for diel differences in weighted mean depth and the significant ($P < 0.05$) Tukey multiple-comparison tests between time periods.

Dawn	Day	Dusk	Night	Overall	*F*-value	Tukey test
All Larvae (excluding walleye pollock)						
16.59 (2.72)	17.46 (1.52)	15.45 (2.25)	25.74 (1.52)	21.75 (1.87)	33.17***	Night>Day=Dawn=Dusk
Hippoglossoides elassodon						
14.82 (0.63)	16.94 (2.73)	10.80 (0.42)	20.10 (0.05)	18.06 (1.33)	31.89***	Night>Day=Dawn>Dusk
Ammodytes hexapterus						
31.21(11.45)	27.67 (4.59)	22.67 (2.38)	37.51 (4.45)	32.85 (3.39)	6.05**	Night>Dusk=Day
***Bathymaster* spp.**						
8.21 (0.11)	11.25 (0.08)	11.28 (1.08)	37.95 (2.84)	18.12 (6.05)	441.48***	Night>Dusk=Day>Dawn
Pleuronectes bilineatus						
—	19.75 (1.83)	—	30.73 (1.63)	25.47 (4.64)	128.36***	Night>Day
Gadus macrocephalus						
—	20.36(10.35)	—	24.92 (0.12)	22.12 (6.56)	1.14 n.s.	

*** $P<0.001$.
** $P<0.01$;
n.s. $P>0.05$.

However, the reverse pattern ('Type II' migration), although less frequently documented, has been observed for larvae of several fish species, including many of the taxa we examined. For example, Boehlert et al. (1985) observed larval *G. macrocephalus* at lower depths at night than during the day off the Oregon coast. Walline[5] found that *Bathymaster* spp. in the Bering Sea generally migrated downward at night. Larvae of *A. hexapterus* collected in bays around Kodiak Island were concentrated from 10 to 30 m during the day but were found at lower depths at night (Rogers et al.[6]), and larvae of a congener (*A. personatus*) collected off Japan also exhibited reverse migration (Yamashita et al., 1985). Rogers et al.[6] and Pritchett and Haldorson (1989) found that rock sole (*P. bilineatus*), as well as larvae of several other taxa, showed reverse diel migrations during the spring.

We believe that sampling bias could not have resulted in the observed reverse distributions. Eggs of *H. elassodon*, as expected, showed no differences by time of day in our study and walleye pollock larvae in these same collections exhibited a normal diel migration pattern (Type I), occurring mainly in the 30–45 m range during daytime and above 30 m at night (Kendall et al.[1]; see also Kendall et al., 1987). Net avoidance, although suggested by the higher night catches overall as well as the larger mean size of larvae collected at night, is not a plausible explanation for the observed diel pattern. Light-aided daytime avoidance would be expected to influence the catch of larvae in the surface strata more than those in deeper strata, thus leading to underestimates of near-surface daytime abundances and the magnitude of reverse migration.

The prevalence of the reverse diel migration pattern in our study suggests an adaptive role for this behavior. Temperature gradients are relatively minor (<1°C) over the upper 50–60 m where most of the migration occurs (Fig. 7), and the majority of the larvae appear to be above the seasonal thermocline at all times of the day. Thus, we see no possibility of temperature-mediated energetic advantage related to migration at any time of the day. Similarly, observed density gradients are not pronounced (<0.5 σ_t units) within this surface layer (Fig. 7; Kendall et al.[1]) and there appears to be no physical mechanism that would aggregate either

Table 4

Results of two-way ANOVAs testing for differences in density of larvae by depth and time of day.

Source of variation	df	Sum of squares	Mean square	*F*-ratio	*P*-value
All larvae (excluding walleye pollock)					
Time	3	14.60	4.86	9.85	0.00
Depth	6	51.63	8.61	17.40	0.00
Time × depth	18	14.11	0.78	1.58	0.05
Error	4868	2406.73	0.49		
Hippoglossoides elassodon					
Time	3	4.97	1.66	0.48	0.69
Depth	6	93.59	15.60	4.54	0.00
Time × depth	18	15.49	0.86	0.25	0.99
Error	116	398.59	3.44		
Ammodytes hexapterus					
Time	3	55.08	18.36	11.70	0.00
Depth	6	94.13	15.69	9.99	0.00
Time × depth	18	34.27	1.90	1.21	0.26
Error	116	182.03	1.57		
***Bathymaster* spp.**					
Time	3	8.84	2.95	1.24	0.30
Depth	6	44.33	7.39	3.10	0.01
Time × depth	18	21.35	1.19	0.49	0.96
Error	116	276.73	2.39		
Pleuronectes bilineatus					
Time	1	1.68	1.68	1.35	0.25
Depth	6	19.01	3.17	2.55	0.03
Time × depth	6	3.47	0.58	0.47	0.83
Error	69	85.78	1.24		
Gadus macrocephalus					
Time	1	9.12	9.12	4.09	0.05
Depth	6	22.46	3.74	1.68	0.14
Time × depth	6	7.06	1.18	0.53	0.79
Error	69	153.81	2.23		

[5] Walline, P. D. 1981. Hatching dates of walleye pollock (*Theragra chalcogramma*) and vertical distribution of ichthyoplankton from the eastern Bering Sea, June–July 1979. NWAFC Processed Rep. 81-05, 22 p.

[6] Rogers, D. E., D. J. Rabin, B. J. Rogers, K. J. Garrison, and M. E. Wangerin. 1979. Seasonal composition and food web relationships of marine organisms in the nearshore zone of Kodiak Island including ichthyoplankton, meroplankton (shellfish), zooplankton and fish. Univ. Washington, Fish. Res. Inst. Rep. FRI-UW-7925, 291 p.

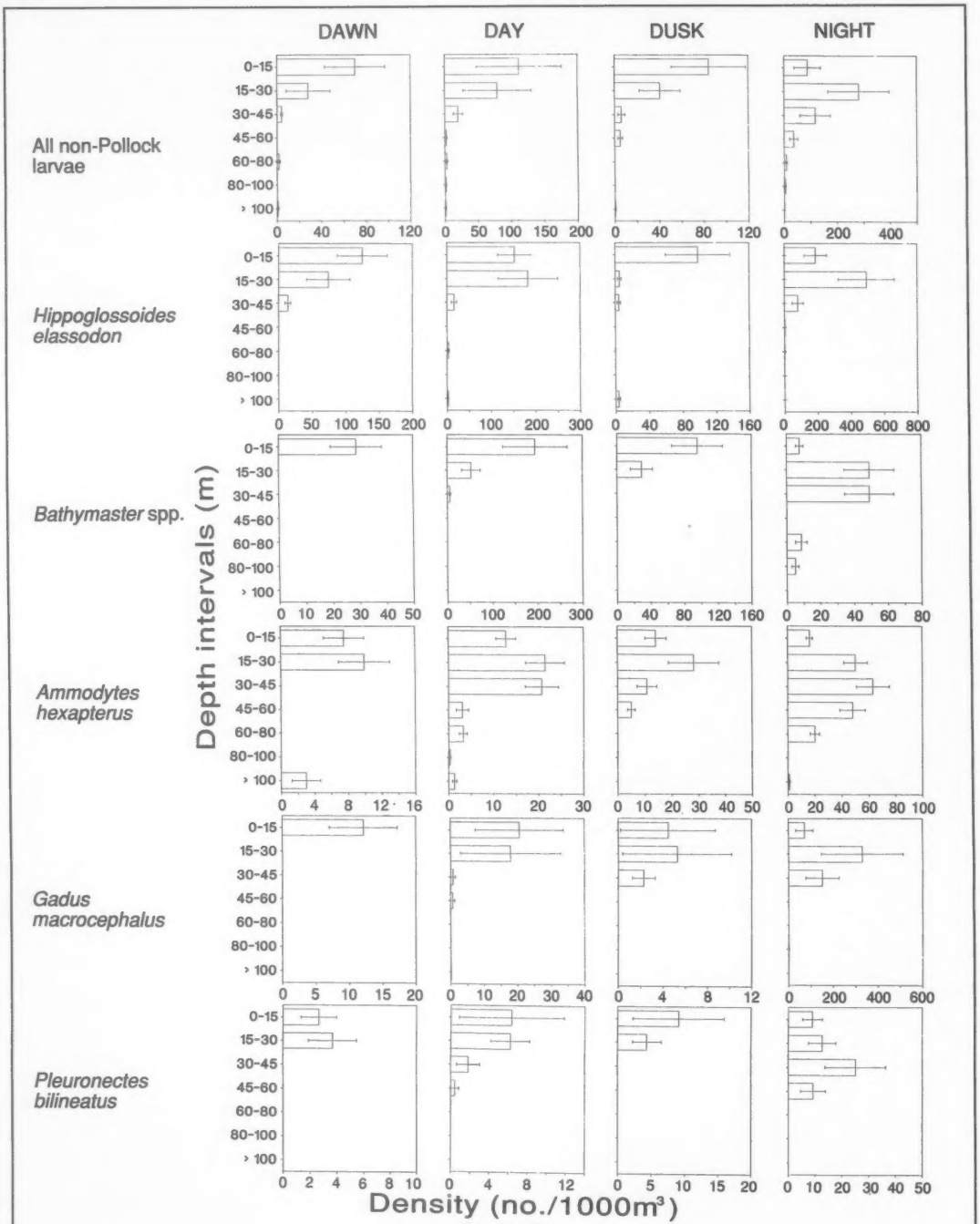

Figure 4

Diel changes in the vertical distribution of all larvae (excluding walleye pollock), and *Hippoglossoides elassodon*, *Bathymaster* spp., *Ammodytes hexapterus*, *Gadus macrocephalus*, and *Pleuronectes bilineatus* larvae. Bars are mean abundances per 1000 m^3 at each depth interval and error bars are ± one standard deviation about the mean abundance.

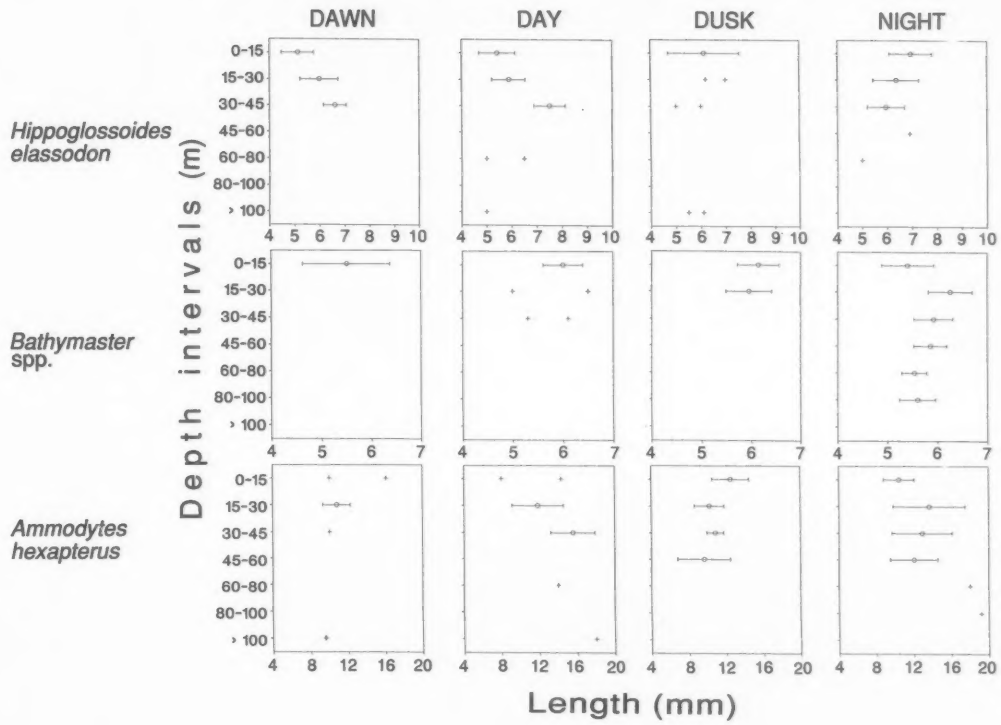

Figure 5

Diel vertical distribution of larval lengths of *Hippoglossoides elassodon*, *Bathymaster* spp., and *Ammodytes hexapterus*. Circles are mean length at each depth interval and error bars are ± one standard deviation about the mean length. The plus signs indicate actual lengths measured when less than three lengths were available from a particular depth stratum.

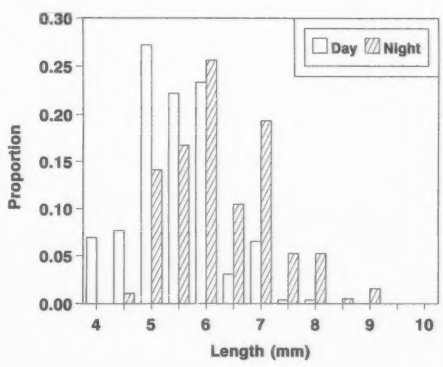

Figure 6

Day versus night proportional length distributions of *Hippoglossoides elassodon* larvae.

larvae or their prey at certain depths or inhibit them from migrating to different depths.

The fact that walleye pollock larvae, which are the dominant fish larvae in this area representing 70–80% of the larvae present in Shelikof Strait in the spring (Rugen[7]; this study), show a normal migration pattern (Kendall et al., 1987) suggests one potential explanation for reverse migration patterns of other larvae. If other larvae feed on the same microzooplankton prey as larval walleye pollock and these prey resources were limiting, then the presence of these other larvae in surface waters at different times of the day than those of walleye pollock would reduce competition with the numerically dominant taxon. Copepod nauplii, an important

[7] Rugen, W. C. 1990. Spatial and temporal distribution of larval fish in the Western Gulf of Alaska, with emphasis on the period of peak abundance of walleye pollock (*Theragra chalcogramma*) larvae. NWAFC Processed Rep. 90-01, 162 p.

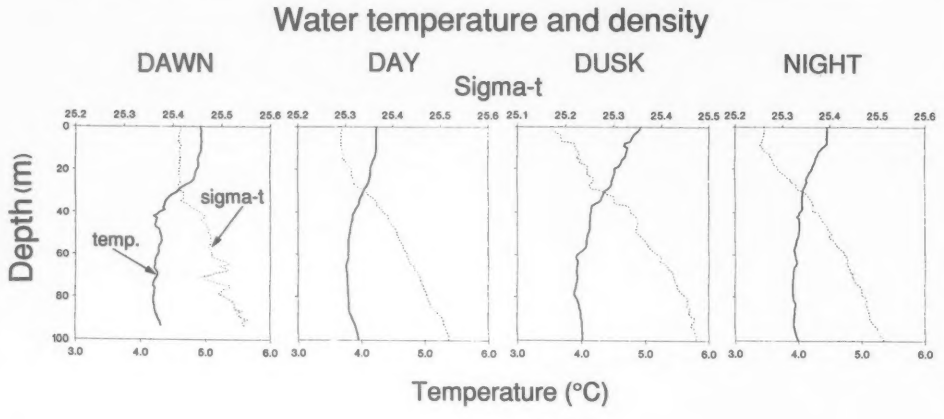

Figure 7

Diel vertical profiles of temperature and density (σ_t). Data are means of at least four casts within each time interval and were collected at 1 m depth intervals.

component of the diet of many larval fishes including walleye pollock (Kendall et al., 1987), were the most abundant microzooplankton category found in Shelikof Strait, mostly in the upper 30 m during May 1986 and 1987 (Incze and Ainaire[8]). During diel Series 4, copepod nauplii had overall mean depths between 20 and 34 m but showed no obvious diel pattern in depth distribution (Kendall et al.[1]). Although feeding at a different time of day from walleye pollock might reduce interference competition (i.e. behavioral interactions) with the dominant species, it is highly unlikely, based on typical larval fish and copepod naupliar densities, that prey resources could ever be depleted by larval fish (Cushing, 1983; MacKenzie et al., 1990). Moreover, if food were limiting, then it would be advantageous for all larvae to stay in the layer of maximum food concentration throughout the diel period to maximize total intake. Thus, we do not see a trophic benefit accruing from a reverse migration pattern for these larvae.

If feeding by these larvae is periodic and dependent on some minimum light level, then the vertical distribution pattern can be partially explained by larval feeding response. Assuming light levels were limiting feeding at depths below 30 m, then it would be necessary for larvae to ascend to a shallower depth during the daytime when light is at a maximum. Following the cessation of feeding at dusk, larvae would be expected to become inactive and passively sink to deeper levels at night. Such a mechanism has been postulated for Japanese sand lance (*A. personatus*) by Yamashita et al. (1985) who demonstrated a nocturnal cessation of feeding in this species. Although we lack data on the diel feeding chronology of any of the taxa examined here, it is possible that feeding occurs mainly in the crepuscular periods, with a temporary cessation of ingestion occuring during midday as observed in the field for larval walleye pollock (Canino and Bailey[9]). The shallowest mean depth occurs at either dawn or dusk for the three common species that were examined over the four time periods with slightly greater depths occurring during midday. If larvae were not feeding during the middle of the day, it would be advantageous to cease swimming altogether and sink through the water column to avoid being sensed by mechanoreceptive or visual predators. Following a particular isolume would produce a similar daytime pattern but could not account for the deeper distribution at night that we observed. Larval walleye pollock in the laboratory have been shown to avoid high light levels (Olla and Davis, 1990) but they also require relatively low light levels to initiate feeding (Paul, 1983). Unfortunately, we have no data available on the light levels necessary for feeding in the taxa we examined with which we can evaluate this hypothesis.

[8] Incze, L. S., and T. Ainaire. In review. Zooplankton of Shelikof Strait, Alaska. I. Micro-zooplankton prey of larval pollock, *Theragra chalcogramma*. Submitted to Fish. Bull.

[9] Canino, M. F., and K. M. Bailey. In review. Gastric evacuation of walleye pollock, *Theragra chalcogramma* (Pallas), larvae in response to feeding. Submitted to Journal of Fish Biology.

A potential disadvantage to a diurnal ascent is increased susceptibility to visually feeding planktivorous fishes. However, acoustic and trawl survey data suggest that epipelagic fish predators are rare during the spring in this area and the majority of the nekton biomass is found in midwater or near the bottom (Brodeur et al., 1991), well below the depth of most larvae. On the other hand, euphausiids, which are possibly the major invertebrate predator on walleye pollock yolk-sac larvae, undergo a nocturnal ascent to surface water and descend to greater depths during the day in Shelikof Strait (Bailey et al., 1993). If euphausiids were also predators on non-pollock larvae and feed only in the surface layer above the nightime depths of these larvae, then a distinct advantage would be conferred upon individuals adopting a reverse diel migration pattern, as has been postulated for copepods (Ohman et al., 1983; Ohman, 1990). Based on field and experimental results, it has become increasingly apparent that predators can alter the diel vertical distribution patterns of invertebrate prey (Ohman et al., 1983; Gliwicz, 1986; Bollens and Frost, 1989; Levy, 1990; Neill, 1990; Frost and Bollens, 1992), but evidence for this effect on larval fish as prey is presently lacking.

Although a variation in depth by time of day was apparent for all species and consistent among species, it was not substantial enough to be statistically significant in all cases (e.g. *G . macrocephalus*). This may be due in part to the lack of resolution of our sampling intervals. The smallest average migration that we could detect is ~15 m; thus, diel vertical migrations less than that were not likely to be detected. Although a daily ambit of 30 m is not exceptional for larger larvae, it may be excessive for newly hatched individuals. For a study specifically examining the diel vertical distribution of the species considered here, we recommend sampling with a multiple net system every 5 m over the upper 40 m of the water column. Some bias may have also resulted from combining tows from different years, weeks, or geographic areas into our four time periods, which was necessitated by the relatively low occurrence rate and densities of these taxa. However, the remarkably strong and consistent diel differences among the different taxa, despite this introduced sampling variability, lend credence to our findings.

If there was differential migration by size classes of larvae, this condition might also obscure some of our results. The vertical distribution of larval lengths of the dominant species did not show any consistent patterns by time of day. The mean length by depth varied significantly for *H. elassodon*; smaller larvae were found at greater depths during the daytime and at the surface at night. This cannot be explained by visual gear avoidance alone since the nighttime pattern would then be expected to be random rather than exhibit the increasing mean length with depth that we observed. A possible explanation for this pattern might be that larger larvae may migrate a greater distance than smaller larvae, a pattern frequently observed in other fish larvae (Neilson and Perry, 1990). It is also possible that the migration of different size classes is asynchronous (Pearre, 1979). However, the available size ranges of the dominant species in our data was not extensive enough to examine diel migration patterns of different size classes. Moreover, caution should be exercised in examining larval length data in multiple net systems. Since larvae shrink upon death (Theilacker, 1980; Hay, 1981) and the likelihood of death may be related to time in net, we may assume that larvae caught in the first (deepest) net may have undergone more shrinkage than those in the last (surface) net.

In conclusion, this study shows that all the common larvae exhibit a reverse vertical migration pattern, opposite to that of the overall dominant species, walleye pollock. In Auke Bay, an inland embayment in Southeast Alaska (58°22' N) on the eastern side of the Gulf of Alaska, Haldorson et al. (1993) found a Type I migration for the numerically dominant osmerid larvae in their sampling and a Type II migration for the five next most abundant taxa (*T. chalcogramma*, *H. elassodon*, *P. bilineatus*, *Leuroglossus schmidti*, and Agonidae). These authors attribute this diel-depth distribution pattern to temperature preferences by each species, although their vertical temperature gradients were more pronounced than what we observed in our study. Since most abiotic variables (other than light intensity) and food resources varied little over the depths through which much of the migration occurred in Shelikof Strait, we hypothesize that the reverse migration pattern that we documented was either a predator-avoidance mechanism or else an optimization of light levels for feeding. The prevalence of reverse migration in this and other studies suggests that it may be more common than previously suspected, especially in higher latitude ecosystems, and the factors contributing to this phenomenon merit further investigation.

Acknowledgments

The MOCNESS tow collections used in this study were made available by Lew Incze (Bigelow Laboratory) and Peter Ortner (Atlantic Oceanographic

and Meteorological Laboratories, NOAA). Field assistance was provided by Shailer Cummings (AOML) and the crew of the NOAA ship *Miller Freeman*. Susan Picquelle and Patricia Brown (Alaska Fisheries Science Center) assisted in statistical analysis. Art Kendall, Gary Stauffer, Jeff Napp, Bori Olla, Susan Sogard, and Michael Davis (AFSC), R. Ian Perry (Pacific Biological Station), Steven Bollens (Woods Hole Oceanographic Institution), and two anonymous reviewers provided valuable comments on earlier versions of the manuscript.

Literature cited

Ahlstrom, E. H.
1959. Vertical distribution of pelagic fish eggs and larvae off California and Baja California. U.S. Fish. Wild. Serv., Fish. Bull. 60:107–146.

Bailey, K. M., R. D. Brodeur, N. Merati, and M. M. Yoklavich.
1993. Predation on walleye pollock (*Theragra chalcogramma*) eggs and yolk-sac larvae by pelagic crustacean invertebrates in the western Gulf of Alaska. Fish. Oceanog. 2:30–39.

Boehlert, G. W., D. M. Gadomski, and B. C. Mundy.
1985. Vertical distribution of ichthyoplankton off the Oregon coast in spring and summer months. Fish. Bull. 83:611–621.

Bollens, S. M., and B. W. Frost.
1989. Predator-induced diel vertical migration in a planktonic copepod. J. Plankton Res. 11:1047–1065.

Brewer, G. D., and G. S. Kleppel.
1986. Diel vertical distribution of fish larvae and their prey in nearshore waters of southern California. Mar. Ecol. Prog. Ser. 27:217–226.

Brodeur, R. D., K. M. Bailey, and S. Kim.
1991. Cannibalism on eggs by walleye pollock *Theragra chalcogramma* in Shelikof Strait, Gulf of Alaska. Mar. Ecol. Prog. Ser. 71:207–218.

Cushing, D. H.
1983. Are fish larvae too dilute to affect the density of their food organisms? J. Plankton Res. 847–854.

de Lafontaine, Y., and D. Gascon.
1989. Ontogenetic variation in the vertical distribution of eggs and larvae of Atlantic mackerel (*Scomber scombrus*). Rapp. P.-v. Réun. Cons. int. Explor. Mer 191:137–145.

Frost, B. W., and S. M. Bollens.
1992. Variability of diel vertical migration in the marine planktonic copepod *Pseudocalanus newmani* in relation to its predators. Can. J. Fish. Aquat. Sci. 49:1137–1141.

Gliwicz, M. Z.
1986. Predation and the evolution of vertical migration in zooplankton. Nature 320:746–748.

Haldorson, L., M. Prichett, A. J. Paul, and D. Ziemann.
1993. Vertical distribution and migration of fish larvae in a Northeast Pacific bay. Mar. Ecol. Prog. Ser. 101:67–80.

Hay, D. E.
1981. Effects of capture and fixation on gut contents and body size of Pacific herring larvae. Rapp. P.-v. Réun. Cons. int. Explor. Mer 178:395–400.

Incze, L. S., P. B. Ortner, and J. D. Schumacher.
1990. Microzooplankton, vertical mixing and advection in a larval fish patch. J. Plankton Res. 12:365–379.

Kamba, M.
1977. Feeding habits and vertical distribution of walleye pollock, *Theragra chalcogramma* (Pallas), in early life stage in Uchiura Bay, Hokkaido. Res. Inst. N. Pac. Fish., Hokkaido Univ., Spec. Vol., p. 175–197.

Kendall, A. W., Jr., and S. Kim.
1989. Buoyancy of walleye pollock (*Theragra chalcogramma*) eggs in relation to water properties and movement in Shelikof Strait, Gulf of Alaska. *In* R. J. Beamish and G. A. McFarlane (eds.), Effects of ocean variability on recruitment and evaluation of parameters used in stock assessment models, p. 169–180. Can. Spec. Pub. Fish. Aquat. Sci. 108.

Kendall, A. W., Jr., M. E. Clarke, M. M. Yoklavich, and G. W. Boehlert.
1987. Distribution, feeding, and growth of larval walleye pollock, *Theragra chalcogramma*, in Shelikof Strait, Gulf of Alaska. Fish. Bull. 85:499–521.

Kerfoot, W. C.
1985. Adaptive value of vertical migration: comments on the predation hypothesis and some alternatives. Contrib. Mar. Sci. 27:91–113.

Lampert, W. H.
1989. The adaptive significance of diel vertical migration of zooplankton. Funct. Ecol. 3:21–27.

Laprise, R., and J. J. Dodson.
1993. Nature of environmental variability experienced by benthic and pelagic animals in the St. Lawrence Estuary, Canada. Mar. Ecol. Prog. Ser. 94:129–139.

Lenarz, W. H., R. J. Larson, and S. Ralston.
1991. Depth distributions of late larvae and pelagic juveniles of some fishes of the California Current. Calif. Coop. Oceanic Fish. Invest. Rep. 32:41–46.

Levy, D. A.
1990. Reciprocal diel vertical migration behavior in planktivores and zooplankton in British Columbia lakes. Can. J. Fish. Aquat. Sci. 47:1755–1764.

MacKenzie, B. R., W. C. Leggett, and R. H. Peters.
1990. Estimating larval fish ingestion rates: can laboratory derived values be reliably extrapolated to the field? Mar. Ecol. Prog. Ser. 67:209–225.

Matarese, A. C., A. W. Kendall Jr., D. M. Blood, and B. M. Vinter.
1989. Laboratory guide to early life history stages of Northeast Pacific fishes. U.S. Dep. Commer., NOAA Tech. Rep. NMFS 80, 652 p.

Neill, W. E.
1990. Induced vertical migration in copepods as a defence against invertebrate predation. Nature 345:524–526.

Neilson, J. D., and R. I. Perry.
1990. Diel vertical migrations of marine fishes: an obligate or facultative process? Adv. Mar. Biol. 26:115–168.

Ohman, M. D.
1990. The demographic benefits of diel vertical migration by zooplankton. Ecol. Monogr. 60:257–281.

Ohman, M. D., B. W. Frost, and E. B. Cohen.
1983. Reverse diel vertical migration: an escape from invertebrate predators. Science 220:1404–1407.

Olla, B. L., and M. W. Davis.
1990. Effects of physical factors on the vertical distribution of larval walleye pollock *Theragra chalcogramma* under controlled laboratory conditions. Mar. Ecol. Prog. Ser. 63:105–112.

Paul, A. J.
1983. Light, temperature, nauplii concentrations, and prey capture by first feeding pollock larvae *Theragra chalcogramma*. Mar. Ecol. Prog. Ser. 13:175–179.

Pearre, S.
1979. Problems in the detection and interpretation of vertical migration. J. Plankton Res. 1:29–44.

Pritchett, M., and L. Haldorson.
1989. Depth distribution and vertical migration of larval walleye pollock (*Theragra chalcogramma*). *In* Proceedings of the international symposium on the biology and management of walleye pollock, November 14–16, 1988, Anchorage, Alaska, p. 173–183. Alaska Sea Grant Rep. 89-1, Univ. Alaska, Fairbanks.

Theilacker, G. H.
1980. Changes in body measurements of larval northern anchovy, *Engraulis mordax*, and other fishes due to handling and preservation. Fish. Bull. 78:685–692.

Wiebe, P. D., K. H. Burt, S. H. Boyd, and A. W. Morton.
1976. A multiple opening/closing net and environmental sensing system for zooplankton. J. Mar. Res. 34:313–326.

Yamashita, Y., D. Kitagawa, and T. Aoyama.
1985. Diel vertical migration and feeding rhythm of the larvae of the Japanese sand-eel *Ammodytes personatus*. Bull. Japan. Soc. Sci. Fish. 51:1–5.

Changes in a population of orange roughy, *Hoplostethus atlanticus*, with commercial exploitation on the Challenger Plateau, New Zealand

Malcolm R. Clark
Dianne M. Tracey
MAF Fisheries Greta Point, P.O. Box 297
295 Evans Bay Parade, Wellington, New Zealand

Abstract.—The commercial fishery for orange roughy on the Challenger Plateau developed in 1981, increased markedly throughout the mid-1980s, and then declined rapidly by 1990. Data from research trawl surveys and commercial fishing returns over the period are examined, and changes in the population are described.

The distribution of orange roughy changed over the period examined; there was a contraction of the areas of high density and apparent fishing-out of aggregations on relatively flat bottom. Aggregations are now largely confined to pinnacles. Biomass of orange roughy, measured by bottom trawl survey indices and commercial catch per unit of effort, declined substantially and is currently estimated to be about 20% of virgin levels. Most other incidental species in the trawl surveys have also declined in abundance, and there are no indications of 'species replacement.'

Data on size, reproductive stage, size at maturity, and feeding have also been examined. Size structure of the population has not changed over time. Time of spawning (July) and the pattern of gonad development have been consistent over the years. Diet composition has also remained similar; dominant prey groups are natant decapod crustaceans and small fish.

It is suggested that biological changes have not been apparent because orange roughy are a long-lived, slow-growing species, with low productivity. There could be a long response time to fishing pressure, yet orange roughy populations can be quickly reduced to low levels by commercial fishing.

Manuscript accepted 4 November 1993
Fishery Bulletin 92:236–253 (1994)

Orange roughy (*Hoplostethus atlanticus* Collett) has a worldwide distribution on the continental slope at depths of 700 to 1,500 m. However, it is fished commercially only off New Zealand, Australia, and in the northeastern Atlantic Ocean. The New Zealand fishery is the most established, having started in 1978; the others date from 1988 and 1991, respectively. Orange roughy is one of the most valuable commercial species in New Zealand waters, with annual landings of 40–50,000 metric tons (t) and export earnings of NZ $100–150 million (Robertson, 1991).

The New Zealand fishery for orange roughy occurs in a number of areas (Fig. 1), including the Challenger Plateau, a broad submarine plateau off the west coast of New Zealand. The commercial fishery on the Plateau developed in late 1981 and rapidly expanded into one of the most important orange roughy fisheries in New Zealand waters, with annual catches up to approximately 16,000 t (Table 1). The fishery operates primarily during winter (June–August), when the fish form large spawning aggregations at depths of 850–900 m (Clark, 1991a).

The fishery has been managed by a Total Allowable Catch (TAC) system since 1982. Tracey et al. (1990) and Clark (1991a) discussed details of this management regime. Initially, catches were limited to 7,000 t by the TAC for all areas of the New Zealand Exclusive Economic Zone (EEZ), outside the established fishing grounds on the east coast. A TAC of 4,950 t was set for 1983–84 and 1984–85 (October–September fishing year) on the Challenger Plateau and west coast of the South Island. This was raised to 6,190 t specifically for the Challenger fishery in 1985–86 based on biomass estimates from a trawl survey in winter 1984. The quota was raised to 10,000 t in 1986–87, and further to 12,000 t in 1987–88, in order to assess the effects of heavier fishing on the population dynamics of orange roughy ("adaptive management"). In the following fishing year only 8,200 t of quota were allocated, the rest withheld because of signs that the orange roughy population was declining rapidly. During 1989–90 the TAC was reduced to 2,500 t after new stock assessments showed the population was overexploited and had declined to low levels (Clark and Francis, 1990). The TAC was further reduced for 1990–91 to promote rebuilding of the population.

These changes occurred against a background of increasing infor-

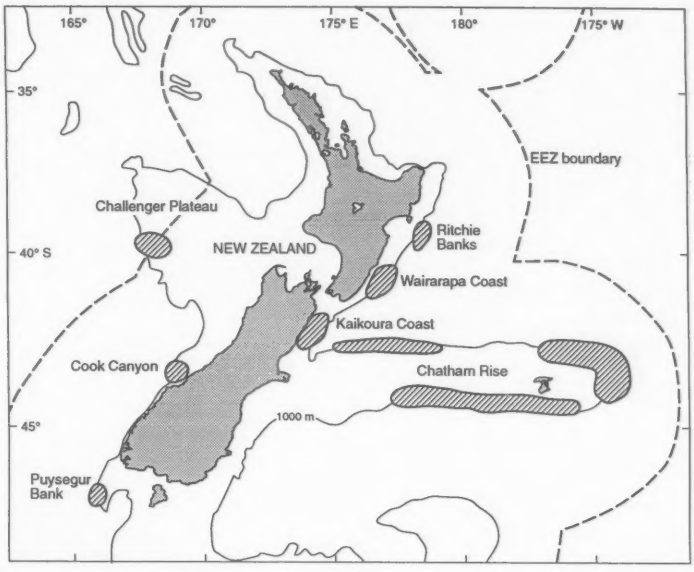

Figure 1

Map of New Zealand and offshore waters of the Exclusive Economic Zone (EEZ), showing the location of the Challenger Plateau and other major fishing areas for orange roughy (*Hoplostethus atlanticus*).

Table 1

Reported catches (t) of orange roughy (*Hoplostethus atlanticus*) from the Challenger Plateau (ORH 7A and outside EEZ) (from Clark 1992; total estimated catch includes allowance for research survey catches and a correction for 15–30% under-estimation of true catch in reported catch figures because of burst trawls, fish discards, and incorrect official conversion factor).

Fishing year (Oct–Sept)	Total reported catch	Total estimated catch	TAC
1980/81	33	43	
1981/82	4,248	5,522	
1982/83	11,839	15,409	
1983/84	9,527	12,514	4,950
1984/85	5,117	6,707	4,950
1985/86	7,753	10,251	6,190
1986/87	11,492	15,750	10,000
1987/88	12,181	15,830	12,000
1988/89	10,241	12,627	12,000[1]
1989/90	4,309	5,171	2,500
1990/91	1,357	1,560	1,900

[1] 8,219 t allocated.

mation on orange roughy. It has only recently been realized that orange roughy is very slow-growing and long-lived. Mace et al. (1990) recorded a growth rate of about three cm per year for the first four years of life (validated ages), and an estimated age at maturity of 24 years and maximum age over 50 years. They estimated natural mortality to be low (less than 0·1 yr^{-1}) and concluded that sustainable yields of orange roughy would be relatively low and show slow recovery from over-fishing. Recent estimates of the maximum age of orange roughy from Australian waters approach 150 years (Fenton et al., 1991).

Quotas for orange roughy harvest from New Zealand have been reduced in recent years on the basis of information which suggests much lower productivity than originally assumed. However, the Challenger Plateau population had already declined markedly and provides some insight into the effects of heavy fishing pressure on orange roughy population dynamics.

There is an extensive literature on general responses of fish populations to exploitation, covering lake ecosystems (e.g. Regier and Loftus, 1972; Spangler et al., 1977), coral reef fisheries (e.g. Russ and Alcala, 1989), and relatively shallow-water marine environments (e.g. Hempel, 1978; Pauly, 1979; Grosslein et al. 1980). There have been few studies on deep-water or long-lived species such as orange roughy. The closest is probably Pacific ocean perch (*Sebastes alutus*) which is found at depths to 600 m in the North Pacific Ocean and has a maximum age of 90 years (e.g. Gunderson, 1977; Leaman, 1991).

There are a number of general population responses to exploitation, which include

1 Decline in abundance of fished species.
2 Contraction of distribution or areas of high density.
3 Change in age structure or size structure, or both, with fewer old, large fish and the population dominated by new recruits.
4 Increase in growth rate of individuals, with a decrease in age for a given length.
5 Lower age at maturity or size at maturity, or both.

6 Possible change in species composition over time ('species replacement').

Such responses are often observed in short-lived, fast-growing species (e.g. Pauly, 1979; Grosslein et al., 1980). Some have also been noted with *Sebastes alutus* (Gunderson, 1977; Leaman, 1991), but it is not clear whether these changes would occur in such a long-lived species as orange roughy, or over what time period such changes would become apparent. Orange roughy on the Challenger Plateau have been exploited for only 10 years, and hence it seems unlikely that marked changes in biological characteristics could occur over such a relatively short time period in relation to the longevity of the species. Therefore, we might expect to observe changes in biomass and distribution, as well as age and size structure of the population, but not changes in growth rate or reproductive potential.

In this paper, we summarize some of the available data on distribution, abundance, and biology of orange roughy on the Challenger Plateau, primarily over the period 1984–90. This period covers the early years of the developing fishery, to maximum levels of exploitation, and subsequent decline of the population. We describe the reduction in size and distribution of the stock and investigate associated changes in size structure, aspects of reproduction, and feeding.

Methods

Research trawl surveys

Trawl surveys have been carried out in the winter (June–July) of each year from 1984 to 1990. The vessel used, area covered, intensity of trawling, and survey design differed between years, and all are not directly comparable (Table 2). Surveys from 1987 to 1989 were treated as fully comparable, but only selected data have been used from other surveys: distribution from 1984 and 1990, and biology (size, reproductive, and feeding data) from 1984, 1985, 1986, and 1990.

The general survey design was two–phase stratified random (after Francis, 1984). The survey area was divided into a number of strata based on depth and certain bottom features (e.g. pinnacles). General stratification is shown in Figure 2. The depth range covered was 800 to 1,200 m. New, random station positions within strata were selected each year, except in strata 10 and 11 on pinnacles where a random tow direction was adjusted to avoid untrawlable ground, and these trawls were repeated each year. A similar net design and gear set up was used for each survey. Tow length was standardized where possible at 1.5 nautical miles (nmi). Trawling speed was 3.0–3.5 knots.

Biomass indices were calculated by the area swept method as described by Francis (1981). Biomass and its standard error were calculated from the following formulae:

$$B = \sum (X_i a_i) / cb$$

and

$$S_B = \sqrt{\sum s_i^2 a_i^2 / c^2 b^2} \ ,$$

where B is biomass (t), X_i is the mean catch rate (kg·km^{-1}) in stratum i, a_i is the area of stratum i (km^2), b is the width swept by the gear (defined as doorspread (m) by MAF Fisheries), c is the catchability coefficient (an estimate of the proportion of fish available to be caught by the net), S_B is the standard error of the biomass, s_i is the standard error of X_i.

The catchability coefficient was assigned a value of 0.27, which represents the wingend spread divided by the doorspread, because orange roughy form schools which are not believed to be herded substantially by doors or sweeps.[1]

Approximate 95% confidence limits (CL) were calculated as

$$CL = B \pm 2S_B .$$

[1] Orange Roughy Working Group, MAF Fisheries, Greta Point, P.O. Box 297, Wellington, New Zealand, pers. commun. 1991.

Table 2

Trawl surveys carried out on the Challenger Plateau for orange roughy (*Hoplostethus atlanticus*).

Vessel	Year	Date	Area (km^2)	Number of trawls	Survey design
Arrow	1984	3/7–18/7	11,956	118	2 phase SRTS[1]
Arrow	1985	4/7–20/7	209	16	1 phase SRTS
Arrow	1986	4/7–17/7	94	10	transect grid
Amaltal Explorer	1987	18/6–13/7	8,270	129	2 phase SRTS
Amaltal Explorer	1988	4/7–24/7	8,270	85	2 phase SRTS
Amaltal Explorer	1989	8/7–30/7	8,270	160	2 phase SRTS
Will Watch	1990	7/7–29/7	8,270	141	2 phase SRTS

[1] Stratified random trawl survey.

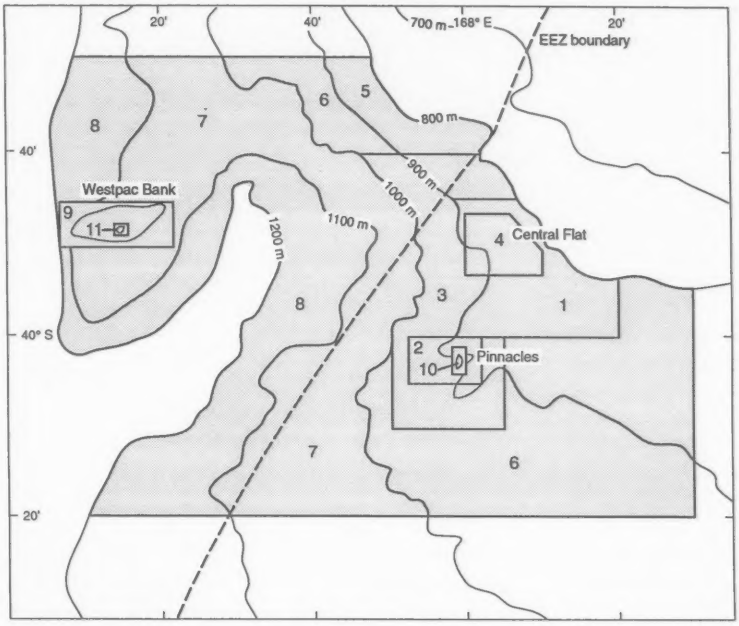

Figure 2

The Challenger Plateau survey area, showing bathymetry (depth contour in m) and details of survey stratification.

The coefficient of variation (CV) is a measure of the precision of the biomass estimate, and was calculated by

$$CV = S_B / B \times 100.$$

Stock reduction analysis

A stock reduction technique was used to estimate virgin biomass based on the method of Francis (1990, 1992). This incorporated a complete catch history for the stock, a time series of abundance indices, and life history parameters used in a deterministic age–structured population model (see Clark, 1992). The latter were the von Bertalanffy growth parameters (L_∞=39.5 cm, k=0.059·yr^{-1}, t_0 = –0.3 yr), natural mortality=0.04·yr^{-1}, weight-length parameters (a=0.0963, b=2.68), age at maturity (24 yr), age at entry to the fishery (24 yr), and Beverton-Holt recruitment steepness of 0.75.

Five sets of abundance indices were used from trawl surveys between 1984 and 1990, and commercial catch per unit of effort (CPUE) data (unstandardized mean catch per tow by monthly groupings):

1 CPUE in winter months (June–September) from 1983 to 1989. This covered the period of development of the fishery through to maximum exploitation. It is felt that the fishery was not constrained much by the TAC over this time.
2 CPUE in winter months from 1983 to 1991. This includes data from 1990 and 1991, following a substantial reduction in TAC and effort.
3 CPUE in non-winter months from 1983 to 1991.
4 Trawl survey indices from 1987 to 1989. These surveys covered the same area, had the same design, and used the same vessel.
5 Trawl survey indices from 1984 and 1987 to 1990. This series incorporated data from a smaller area surveyed in 1984 and from the 1990 survey, both of which used a different vessel from 1987 to 89.

The maximum likelihood method was used to estimate virgin biomass. Ninety-five percent confidence intervals were estimated by using bootstrapping techniques with the coefficient of variation fixed at 20%. The best estimate of virgin biomass was then used in an age-structured model (detailed in Francis, 1992) to estimate current biomass.

Biological data

Standard procedure during trawl surveys was to take a random sample of about 200 fish from each tow. These were measured (standard length rounded down to the nearest whole cm [standard MAF Fisheries procedure]) and sexed. Twenty of these fish were randomly selected, their otoliths extracted, and more detailed data collected: standard length (rounded down to the nearest whole mm), weight (rounded down to the nearest gm), sex, stage of gonad maturity (see below), gonad weight (rounded down to the nearest gm), fullness of stomach, state of digestion of contents, and stomach contents (to species level where possible).

Size Length-frequency distributions have been constructed to represent the total population where possible. In the years 1984 and 1987–90, data have

been scaled by percentage sampled to represent each catch and further scaled by stratum biomass to approximate the population. Samples in 1985 and 1986 were scaled to represent solely the catch, as survey design was inadequate for biomass estimation.

Length-frequency data are difficult to compare statistically and, for the purposes of this study, have not been attempted. However, to enable a general comparison, a single distribution was constructed combining length-frequency data from all years weighted by the number of tows each year. This distribution is plotted together with those from each year separately.

Mean size by sex was calculated separately for three main regions of spawning within the survey area (strata 1, 4; 10; 9, 11) as it was unlikely these areas had been fished equally (see later 'Commercial Fishery' section). The sample sizes used in calculating the standard error were number of tows, not number of fish. Orange roughy can associate in size groups; between-tow variance was greater than within-tow variance. Variance is represented by ±2.0 standard errors for all years except 1986, when ±2.2 standard errors was arbitrarily used because there were only 10 trawls.

Reproduction Macroscopic staging of reproductive condition followed Pankhurst et al. (1987):

Stage	Female	Male
1	Immature/resting	Immature/resting
2	Early maturation	Early maturation
3	Maturation	Maturation
4	Ripe	Ripe/running ripe
5	Running ripe	Spent
6	Spent	—

Relative frequency of gonad stages was examined. Analyses were based on the samples taken. They were not scaled in any way, as there were no apparent differences between the length frequencies of the samples and the distribution of the total population. Only data from females are presented, as their macroscopic gonad stages can be determined more accurately than those from males.

Size at maturity was determined from samples taken over the total survey area using a 'probit analysis' approach (after Pearson and Hartley, 1976). It was assumed that length at maturity is normally distributed in the population. The regression part of the analysis was repeated 10 times to ensure convergence of the estimate.[2] A standard linear regression analysis was carried out on results to investigate trends over time by using the SAS statistical package (SAS, 1988).

Feeding Data on frequency of occurrence were available from all surveys. Frequency of occurrence was defined as the number of stomachs in which a food item occurs, expressed as a proportion of the total number of stomachs containing food. Only stomachs with part-full or full classifications, and with fresh or partly digested contents, were included in analyses.

Commercial fishing data

Data on the catch and position of each tow and the start and finish times have been collected since 1980. However, catch and effort information is difficult to standardize and interpret for orange roughy. Fish can be highly aggregated at various times of the year, and 'windows' or escape panels in the net are frequently used to reduce catch size and minimise damage to nets. Fishing performance varies with experience of skipper and crew, and technology has advanced considerably in recent years (in particular, development of Global Positioning System navigation, which enabled improved accuracy when fishing pinnacles). Fishing logbooks often do not have accurate information on length of tow on the bottom. Fishing for orange roughy on the Challenger Plateau occurs on a variety of bottom terrain: on flat bottom, in troughs and steep slope, and on the tops and sides of pinnacles. In each case, the effective fishing time and fishing technique differ greatly, and they are almost separate types of fisheries. In order to gain an indication of trends in catch rates, data were examined on the basis of mean catch per tow for two size classes of vessel (20–60 m, generally domestic fresh fish boats; and 60–90 m, domestic factory trawlers). Catch per unit of effort (CPUE) values were similar for both classes, and so data here are combined. Monthly data were amalgamated into two time periods: first, 'winter' (June, July, August) which covers the spawning period; second, 'out of season' (all other months). This division represents two distinct phases of orange roughy distribution, as well as differences in the mode of fishing (Clark, 1992). The former period is characterized by the formation of relatively stable, dense aggregations of fish, whereas in the latter period the orange roughy are more dispersed and widely distributed (Clark, 1991a). Fishing in winter generally involves shorter tows, often with smaller nets, than does out-of-season fishing.

[2] Francis, C., MAF Fisheries, pers. commun. 1991.

In the following text, three colloquial area names have been used. These are given below with specific strata numbers (see Fig. 2):

Central Flat	strata 1, 4
Pinnacles	stratum 10
Westpac Bank	strata 9, 11

Results

Distribution

Trawl surveys The distribution of orange roughy in the survey area changed substantially between years (Fig. 3). In 1984 high catch rates were observed across much of the Central Flat area. (No trawls were made on the Pinnacles although heavy marks were observed on the echosounder; the survey did not cover the Westpac Bank area.) In 1987 fish were still widely distributed in the Central Flat; there were two main schools and further concentrations around the Pinnacles and the Westpac Bank. In 1988 there was a marked contraction in the area of high catch rates; a single small aggregation was observed on the Central Flat, and by 1989 there were no aggregations in the Central Flat region. High catch rates still occurred on the Pinnacles and Westpac Bank in 1989, and these actually increased in 1990, after the TAC and fishing effort were greatly reduced.

Commercial fishery The commercial fishery has been centered mainly inside the EEZ, targeting aggregations of orange roughy on the Central Flat and Pinnacles. Distribution of effort (number of tows) and catch between these two areas has changed over time (Table 3). In the period 1982–87, over 80% of the catch from the two areas was taken from the Central Flat with over 75% of the number of tows. In 1988 there was a marked increase in the proportion of catch and effort on the Pinnacles, and a corresponding reduction on the Central Flat. This shift continued in 1989 and 1990, during which the Pinnacles accounted for 65–70% of the catch. These changes reflect the change in distribution observed in the research trawl surveys.

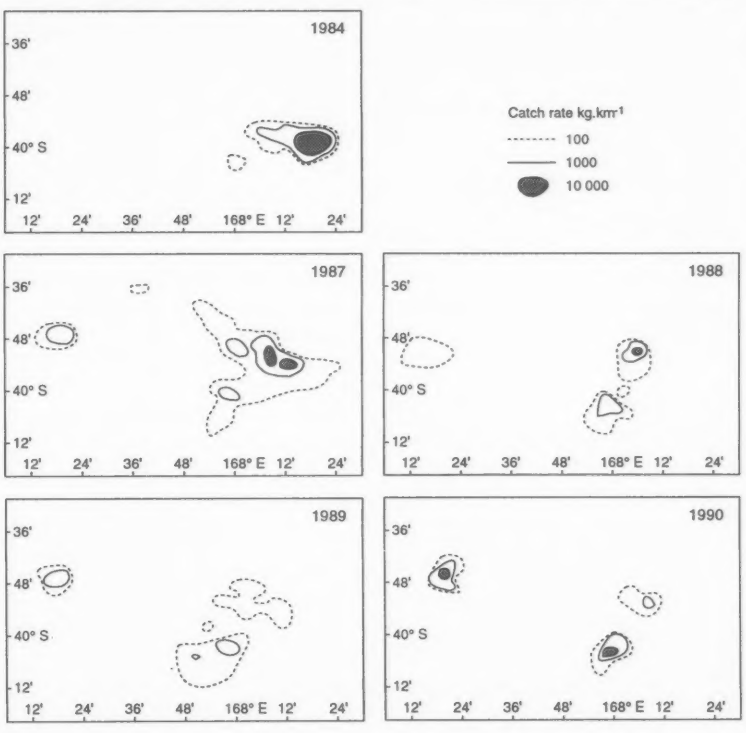

Figure 3
Contours of trawl survey catch rates (kg·km^{-1}) of orange roughy (*Hoplostethus atlanticus*) in 1984 and 1987–90.

Relative abundance

Trawl surveys Biomass indices (estimates of relative biomass) from trawl surveys in 1987, 1988, and 1989 are given in Table 4. The indices indicate a marked decline in biomass over the period. The distribution of biomass among strata changed over the years 1987–90 (Table 5). In 1987 and 1988 over 60% of the biomass was in the Central Flat area, but only 30% in 1989 and 1990. Over this period, there was an increase in the proportion on the Pinnacles, especially between 1989 and 1990. Biomass levels in the surrounding areas have fluctuated but were particularly high in 1989. The proportion of biomass on the Westpac Bank has remained comparatively constant.

Commercial fishery Mean catch per tow for all New Zealand vessels in the fishery from 1983 to 1991 is given in Table 6. Catch rates in winter, when the fish are aggregated for spawning, are generally higher than in other months. Although aggregations occur at other times, presumably for feeding, they are not as large or as stable as in winter. Catch rates in both periods declined steadily from 1983 to 1989 to between about 15% and 20% of original levels. The trend is slightly different in the two periods; winter catch rates declined more sharply to 1988, whereas in the other months the largest decrease was between 1983 and 1984. Catch rates increased in 1990, following a reduction of the TAC, when there were less vessels and fewer trawls on the grounds.

Individual trawl catch rates for orange roughy can be highly variable, consisting of 'hits' and 'misses.' Therefore it is not useful to describe the variance around these mean catch rates, beyond commenting that there is wide variation. It should be stressed that the changes in catch rates presented here may give an indication of changes in stock size but should be treated with caution. Difficulties in interpretation of such data for orange roughy are described in the 'Methods' section, and the form of relationship between mean catch per tow and stock abundance is uncertain.

Stock reduction results

Abundance indices used in, and estimates of virgin biomass from, the stock reduction analyses are given in Table 7. Point estimates of B_0 range from 95,000 t to 278,000 t. The best fits of data to the model (those with the lowest CV) are from the winter CPUE series. Results from trawl survey data have higher CVs but confirm that an estimate of the order of 100,000 t is reasonable.

The 1987–89 trawl survey series gave the lowest virgin biomass estimate. It was not considered reliable because there were only three indices, and high fishing mortality rates were required to support the catch history. A maximum F of 1.0 is regarded as realistic for orange roughy (Francis et al., 1992). This constrains the virgin biomass to a minimum value of 94,000 t.

The estimate from non-winter CPUE is comparatively high. It has a large CV and is based on relatively low numbers of trawls (because most fishing effort is in winter). Such a biomass level would also

Table 3

Distribution of commercial catch (% of total catch taken in the two areas) and effort (% of number of tows) for orange roughy (*Hoplostethus atlanticus*) for the Central Flat and Pinnacles (winter period, June to August).

	Central Flat		Pinnacles	
Year	% catch	% tows	% catch	% tows
1982	97.2	95.6	2.8	4.4
1983	97.0	94.7	3.0	5.3
1984	95.2	93.6	4.8	6.4
1985	87.7	78.0	12.3	22.0
1986	87.3	83.2	12.7	16.8
1987	84.4	77.3	15.6	22.7
1988	52.9	56.0	47.1	44.0
1989	34.0	43.3	66.0	56.7
1990	30.2	45.0	69.8	55.0

Table 4

Biomass indices (t) of orange roughy (*Hoplostethus atlanticus*) from trawl surveys, conducted from 1987 to 1989. (CV = coefficient of variation.)

Year	Biomass (t)	CV
1987	78,661	26
1988	30,946	27
1989	11,746	11

Table 5

Comparison of biomass estimates (t) of orange roughy (*Hoplostethus atlanticus*) by region from 1987 to 1990.

	1987		1988		1989		1990	
Region	Biomass (t)	%	Biomass (t)	%	Biomass (t)	%	Biomass (t)	%
Central Flat	56,636	72.0	21,051	68.0	3,275	27.9	4,228	30.8
Pinnacles	7,794	9.9	5,215	16.9	2,821	24.0	5,508	40.1
Surrounding background	10,717	13.6	2,878	9.3	5,088	43.3	3,208	23.3
Westpac Bank	3,514	4.5	1,802	5.8	563	4.8	794	5.8
Total	78,661	100.0	30,946	100.0	11,747	100.0	13,738	100.0

Table 6

Catch per unit of effort (mean catch (t) per trawl) of orange roughy (*Hoplostethus atlanticus*) for New Zealand fishing vessels.

Calendar year	Winter		Other months	
	CPUE	No. trawls	CPUE	No. trawls
1983	16.2	222	9.2	307
1984	15.3	54	5.2	515
1985	13.3	87	4.6	530
1986	10.5	512	3.3	486
1987	10.2	681	2.4	255
1988	5.9	1,269	2.7	99
1989	3.7	1,094	1.3	81
1990	6.6	325	7.3	25
1991	4.1	264	0.1	4

suggest low values of F in recent years, which seems unlikely given the substantial effort in the fishery yet catches being less than the TAC.

There is considerable uncertainty in all the data sets. However, assuming a virgin biomass of 110,000 t (as an approximation of the trawl survey and winter CPUE values), the decline in mid-year biomass of the population was rapid and the level in 1991 was about 20% of the virgin level (Table 8).

Other species

Biomass indices of the 12 main bycatch species caught in the trawl surveys from 1987 to 1989 are presented in Table 9. The coefficients of variation of these mean values range from 11% to 69% and differ between years and species, which limits their comparability.

However, there were no strong indications of increasing abundance of any species relative to abundance in 1987. There was little apparent change in abundance of ribaldo (*Mora moro*), leafscaled gulper shark (*Centrophorus squamosus*), widenosed chimaera (*Rhinochimaera pacifica*), spiky oreo (*Neocyttus rhomboidalis*), Owston's spiny dogfish (*Centroscymnus owstoni*), or white rattail (*Trachyrinchus* sp.). Declining abundance was suggested for big scaled brown slickhead (*Alepocephalus* sp.), basketwork eel (*Diastobranchus capensis*), Johnson's cod (*Halargyreus johnsoni*), smallscaled brown slickhead (*Alepocephalus australis*), shovelnosed spiny dogfish (*Deania calcea*), and seal shark (*Dalatias licha*). The biomass of species relative to orange roughy has generally increased for all species except seal shark. This change is strongest for ribaldo, Owston's dogfish, widenosed chimaera, leafscaled gulper shark, and white rattail.

Size structure

Length-frequency distributions of orange roughy from the entire survey area were similar in all years with no marked differences from the overall weighted length frequency (Fig. 4). There was a strong unimodal distribution with the peak at 32–33 cm standard length. Fish ranged in standard length from 9 cm to 44 cm.

Sex ratios varied between years, but were generally about 1 : 1. However, females always dominated the size distribution above about 35 cm. The mean

Table 7

Summary of biomass indices for orange roughy (*Hoplostethus atlanticus*) used in stock reduction analyses, and estimates of virgin biomass (B_0) (mean and 95% confidence interval), and coefficients of variation (CV).

Year	CPUE (winter)	CPUE (winter)	CPUE (other months)	Trawl survey (full area)	Trawl survey (reduced area)
1983	16.2	16.2	9.2		
1984	15.3	15.3	5.2		143,500
1985	13.3	13.3	4.6		
1986	10.5	10.5	3.3		
1987	10.2	10.2	2.4	78,600	75.000
1988	5.9	5.9	2.7	30.900	28,900
1989	3.7	3.7	1.3	11,700	11,000
1990		6.6	7.3		12,900
1991		4.1	0.1		
Parameter estimates					
B_0 (t)	100,000	122,000	278,000	83,000	95,000
B_0 (95% CI)	94,000–156,000	94,000–224,000	216,000–500,000	94,000–181,000	94,000–194,000
CV (%)	8	22	76	27	37

Table 8

Estimated biomass values by year (mid-year biomass, rounded to nearest 100 t) for orange roughy (*Hoplostethus atlanticus*).

Year	Biomass (t)	Year	Biomass (t)
1980	110,000	1986	67,000
1981	110,000	1987	54,900
1982	107,000	1988	40,500
1983	96,500	1989	28,400
1984	83,200	1990	22,300
1985	74,600	1991	21,400

size of females was significantly greater than that of males (t–test, $P<0.05$). Size data were also examined by the following subareas: Central Flat, Pinnacles, and Westpac Bank. Length frequencies by sex were generally similar to those for the total survey area and are not presented here. However, the distributions were approximately normal in shape and could be described by their means and standard errors to provide a simpler comparison between areas and between years (Fig. 5). There were no apparent differences between years or between areas (t–test, $P<0.05$), and no consistent trend in size over time.

Reproduction

All trawl surveys occurred during the months of June–July. There was considerable variation evident in the overall proportions of fish of different reproductive stage between years and areas (Table 10). To a large extent this reflected the timing of the survey (e.g. 1987 was earlier than the others) and showed a high proportion of maturing fish. However, in all years the majority of fish sampled were mature and were involved in that year's spawning (stages 3–6).

The Central Flat and Pinnacle regions were typically dominated by mature fish in or near spawning condition. In 1987 on the Westpac Bank there was a high proportion of fish that were in very early stages of maturation and hence unlikely to spawn in that year. From 1988 to 1990 the proportion of actively spawning fish increased. However, levels of nonspawning fish have consistently been higher here than in the Central Flat and Pinnacle areas.

Timing of spawning

The progression of gonad stages appeared consistent between years for which data spanning several weeks in July exist (Fig. 6). A pattern of maturing fish declining to low levels was observed early in

Table 9

Biomass (t) of the main bycatch species in the trawl surveys, their proportion of that year's orange roughy (*Hoplostethus atlanticus*) biomass (ref ORH), and their proportion of their biomass in 1987 (ref 1987).

	1987				1988				1989			
	Biomass	(CV)	Ref 1987	Ref ORH	Biomass	(CV)	Ref 1987	Ref ORH	Biomass	(CV)	Ref 1987	Ref ORH
Ribaldo	295	(14)	1.0	0.004	378	(16)	1.3	0.012	317	(11)	1.1	0.027
Owston's dogfish	567	(32)	1.0	0.007	358	(31)	0.6	0.011	400	(20)	0.7	0.034
Leafscaled gulper shark	160	(32)	1.0	0.002	167	(52)	1.0	0.005	208	(40)	1.3	0.018
Spiky oreo	75	(38)	1.0	0.001	156	(36)	2.1	0.005	68	(28)	0.9	0.006
Bigscaled brown slickhead	1,345	(20)	1.0	0.017	486	(21)	0.4	0.016	314	(20)	0.2	0.026
Basketwork eel	332	(19)	1.0	0.004	153	(37)	0.5	0.005	57	(39)	0.2	0.005
Johnson's cod	145	(17)	1.0	0.002	61	(36)	0.4	0.002	44	(16)	0.3	0.004
White rattail	467	(23)	1.0	0.006	345	(29)	0.7	0.011	610	(17)	1.3	0.052
Smallscaled brown slickhead	1,197	(39)	1.0	0.015	285	(22)	0.2	0.009	610	(13)	0.5	0.052
Widenosed chimaera	274	(21)	1.0	0.003	662	(20)	2.4	0.021	283	(16)	1.0	0.024
Shovelnosed dogfish	277	(23)	1.0	0.003	218	(41)	0.8	0.007	73	(31)	0.3	0.006
Seal shark	467	(32)	1.0	0.006	87	(69)	0.2	0.003	47	(39)	0.1	0.004

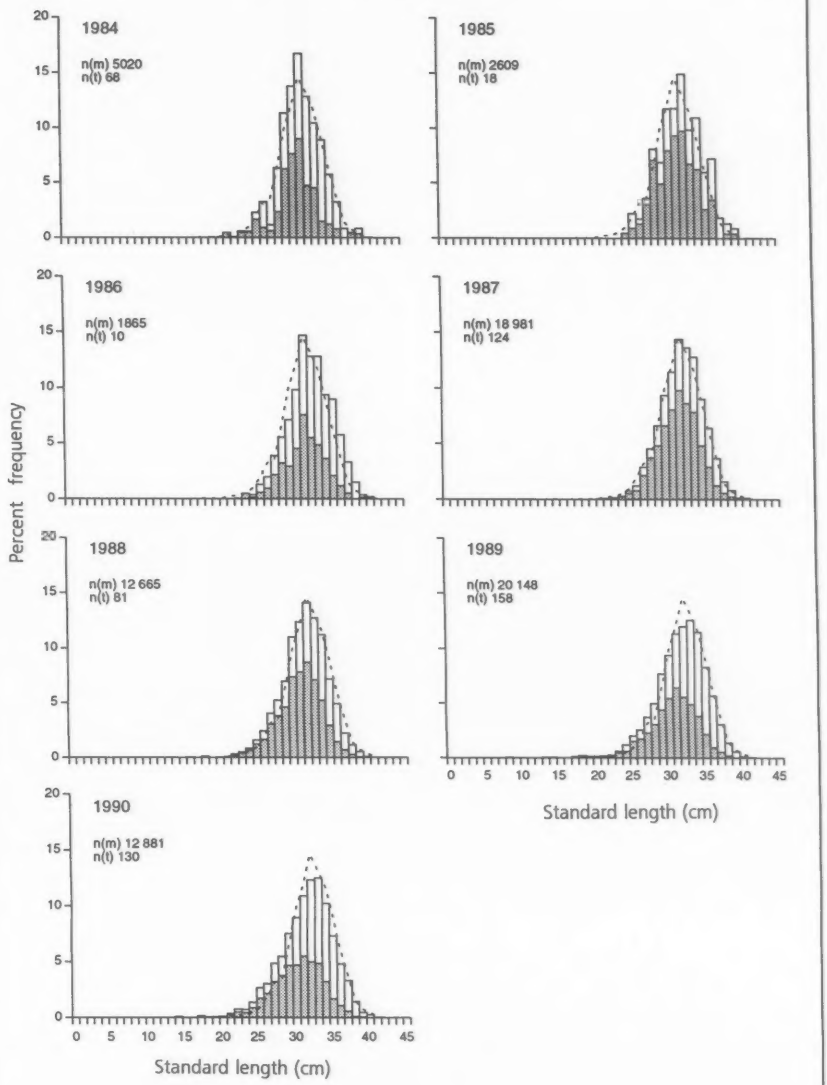

Figure 4

Length-frequency distribution of the orange roughy (*Hoplostethus atlanticus*) population by year (stipple=male, clear=female, dashed line=weighted length frequency for all years combined, $n(m)$=number of fish measured, $n(t)$=number of trawls from which samples were taken, data are scaled by stratum areas to represent total population-size distribution).

July; ripe fish dominated through mid-July; and the proportion of spent fish increased progressively from low levels during the first two weeks in July to peak in the third or fourth week.

Data are insufficient to examine regional variation in this pattern, but there may be some differences between areas; fish appear to spawn slightly later on the Westpac Bank than those on the Central

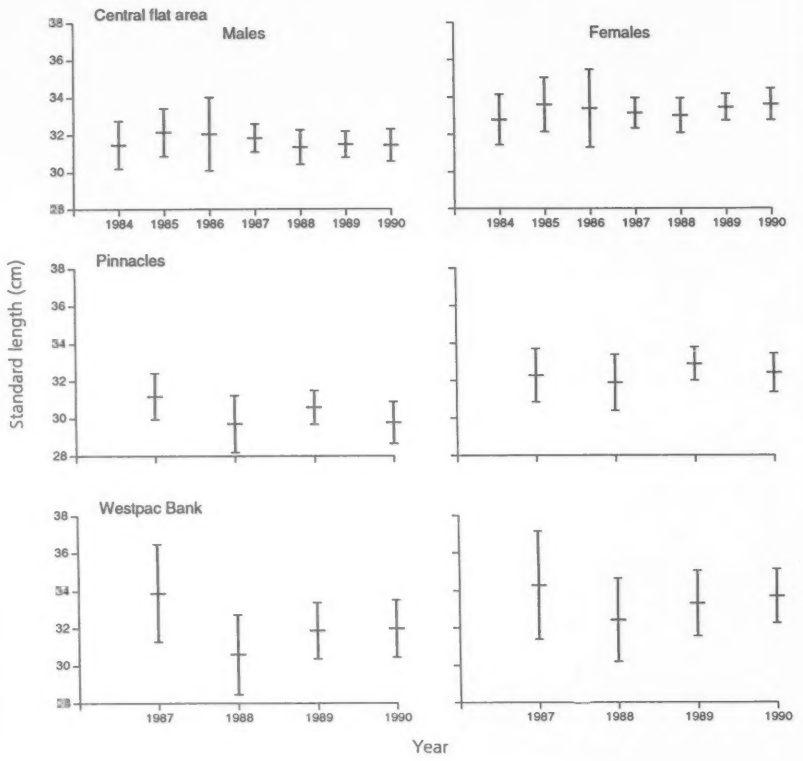

Figure 5

Mean length (±2 standard errors) of orange roughy (*Hoplostethus atlanticus*) by year in the three main spawning areas: Central Flat, Pinnacles, and Westpac Bank.

Flat and Pinnacles. The increase in ripe fish towards the end of the 1990 survey was due largely to sampling the Westpac Bank at this time.

The onset of spawning, defined as the first date on which 20% of fish sampled were spent (after Pankhurst, 1988), has been relatively consistent over the years (Table 11). Actual dates based on females have ranged from 9 July to 16 July.

Size at maturity

Mean lengths at maturity for males and females by year are given in Table 12. There is a significant trend of decreasing mean size for males (linear regression F–test, $P<0.05$), but there is no consistent trend for females.

Feeding

Data on frequency of occurrence of broad taxonomic prey groups from 1984 to 1990 showed the most common prey were natant decapod crustaceans and fish (Table 13).

The main groups that could be identified were macrourids (small species of *Coelorinchus* and *Coryphaenoides*) and myctophids (species of *Lampanyctus* and *Lampanyctodes*). Natant decapod crustacean prey were mainly species in the genera *Pasiphaea*, *Sergestes*, *Oplophorus,* and *Acanthephyra*. Squids and amphipods were also frequent prey.

Discussion

Orange roughy on the Challenger Plateau were overexploited in the late 1980s. Research trawl survey and commercial catch and effort data show similar changes in distribution and abundance. There was a marked contraction in the area of high catch rates,

Table 10

Gonad stage proportions of female orange roughy (*Hoplostethus atlanticus*) by area by year (n = sample size; 1 = immature/resting, 2 = early maturation, 3 = maturation, 4 = ripe, 5 = running ripe, 6 = spent).

	Gonad stage						
Area and year	1	2	3	4	5	6	n
Central Flat							
1987	0	2.8	81.9	14.7	0	0.6	531
1988	0	1.2	3.4	20.3	17.1	58.0	438
1989	0.3	1.2	20.5	46.5	12.4	19.1	591
1990	0.4	2.0	13.3	41.1	10.0	33.2	460
Pinnacles							
1987	0.4	8.5	74.4	15.9	0	0.8	246
1988	0	5.0	9.9	31.5	14.0	39.6	222
1989	0	1.6	17.6	43.4	7.3	30.1	426
1990	0.3	1.6	10.8	34.9	9.0	43.4	378
Westpac Bank							
1987	0	45.6	50.9	0	0	3.5	57
1988	0	33.7	16.3	32.6	2.3	15.1	86
1989	0	21.4	19.1	35.7	9.5	14.3	84
1990	3.9	15.1	17.5	35.9	8.7	18.9	206

Table 11

Date at which 20% of orange roughy (*Hoplostethus atlanticus*) sampled were spent.

Year	Male	Female
1984	13 July	12 July
1985	8 July	9 July
1986	after 16 July	10 July
1987	before 12 July	10 July
1988	10 July	16 July
1989	20 July	15 July
1990	11 July	9 July

Table 12

Mean length (cm) at maturity and two standard errors (SE), of orange roughy (*Hoplostethus atlanticus*) by sex and year.

	Male		Female	
Year	Length	2 SE	Length	2 SE
1984	27.1	0.54	25.7	0.68
1987	24.4	0.80	24.3	1.02
1988	23.2	1.12	22.7	1.56
1989	23.6	1.16	23.4	1.38
1990	22.3	1.10	24.5	1.00

a reduction in the number of spawning schools, and a marked decline in biomass. Stock reduction analyses have estimated virgin biomass to be about 110,000 t. The stock had declined to about 20% of this by 1991, well below the optimal long-term biomass of 30% of virgin levels predicted by computer modelling under an $F_{0.1}$ fishing strategy (Clark, 1992).

It is clear that the Challenger Plateau spawning population declined rapidly and substantially with commercial fishing in the 1980s. However, it is uncertain exactly how much of the change was directly attributable to the fishery. There are no data on size of the stock prior to its exploitation, so the level of any natural fluctuations in population size and distribution is unknown. It is possible that stock size might have decreased in the absence of any fishing, but it seems very unlikely, given the longevity of orange roughy, that such changes would occur as rapidly as we observed. There could also have been a progressive change in the availability of fish in the area covered by the trawl surveys or bulk of the commercial fleet. Adult orange roughy do not necessarily spawn each year (e.g. Bell et al., 1992; authors' unpubl. data) and hence may not migrate to the general spawning area. In the early years of the fishery, large catches were taken over much of the year, but the period of large catches became progressively reduced to the winter months (Clark, 1991a). This suggests that initially there were resident fish on the grounds, with a migratory component which used the area for spawning only. If this latter group had a variable number of spawners each year, this could have affected how well trawl survey or CPUE data reflected true biomass. However, if this occurred, greater variation in abundance indices between years than observed would be expected. There could also have been other spawning grounds that fish from the 'Challenger stock' used. However, there were no indications of this from either commercial or research survey trawling beyond the main grounds. A further alternative explanation for the observed decline in abundance could be a change in vulnerability to the trawl gear, either by fish residing above the bottom in midwater, or by heavy fishing pressure disrupting existing aggregations or preventing their formation. There is no information on the former (although no fish marks were noted on the echosounder above the bottom during the last two research surveys), but the latter is likely to have occurred (Clark and Tracey, 1991). The effects of fishing on school stability could have resulted in a greater decline in catch rates than true abundance, but reduced stability of schools

was not observed prior to 1988, and so does not explain the consistent downward trend in CPUE indices. Hence, although alternative hypotheses cannot be discounted, fishing is most likely to have been the major factor in the observed depletion of the stock.

Most other 'bycatch' species also declined in abundance, although changes were relatively minor compared with that of orange roughy. There was no strong indication of any 'species replacement' of orange roughy. The fishery on the Challenger Plateau targets specifically orange roughy, and other species are not caught in large quantities. In the trawl surveys, orange roughy have generally accounted for over 95% of the biomass. The commercial fishery would probably take even less bycatch than the surveys because it focuses on the aggregations which are usually almost exclusively orange roughy. Intuitively, some compensatory increase in other components of the Challenger Plateau community is to be expected because of the extent of orange roughy depletion, but there is no information on biomass, trophic interactions, and productivity of other fish or invertebrate species. In addition, even if most of the other finfish species have higher fecundity and faster growth rates than orange roughy, there could be a relatively long response time to changes in species dominance.

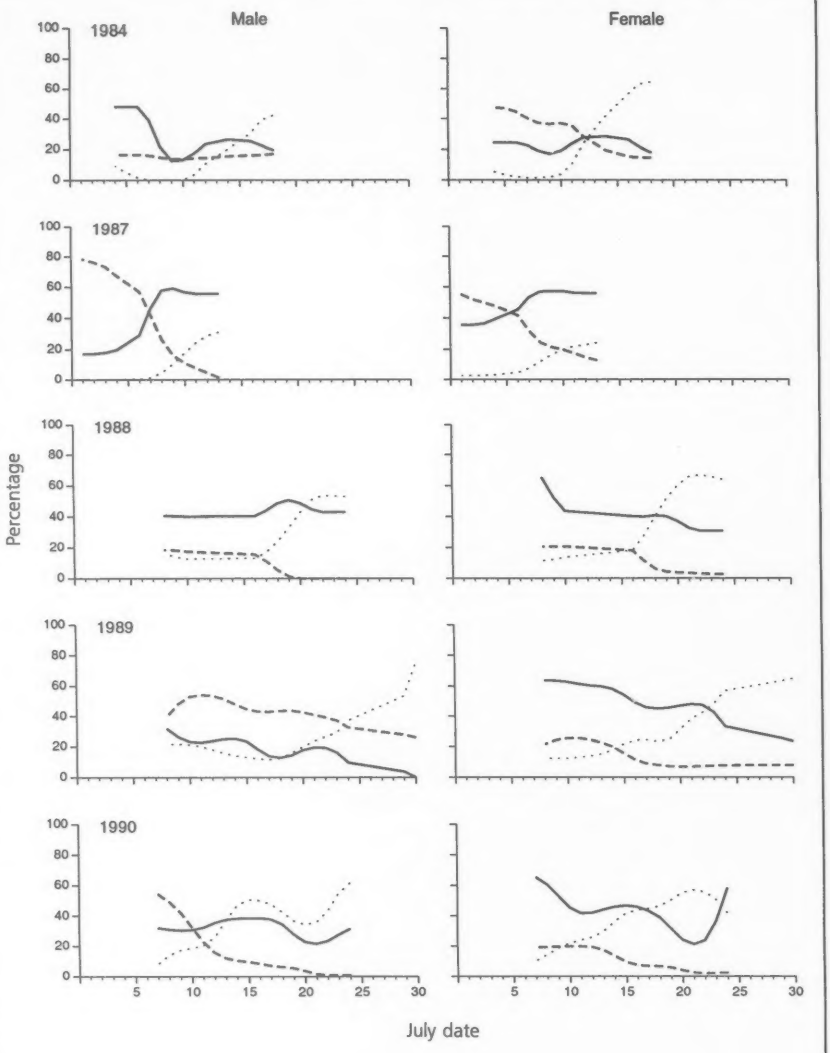

Figure 6

Relative proportions of maturing, ripe, and spent gonads of orange roughy (*Hoplostethus atlanticus*) by day during research surveys in 1984 and 1987–90 (5 day running mean; maturing=dashed line, ripe=solid line, spent=dotted line; maturing=stage-3 male, stage-3 female; ripe=stage-4 male, stages 4 and 5 female; spent=stage-5 male, stage-6 female).

There has been no apparent change in the size structure of the orange roughy population. With heavy exploitation, a truncation of the length frequency distribution and a reduction in the mean size of fish in the population might have been expected, as larger fish were removed and new recruits entered the population. Such changes in size structure of exploited populations are well documented (e.g.

Table 13

Frequency of occurrence of major prey groups of orange roughy (*Hoplostethus atlanticus*) by year.

	1984	1985	1986	1987	1988	1989	1990
Crustacea							
Amphipoda	13.5	7.6	0	6.3	8.0	19.1	5.9
Decapoda/Natantia	53.8	56.1	22.8	44.5	43.0	23.5	34.5
Euphausiacea/Mysidacea	4.3	0.7	13.6	7.7	8.0	2.8	2.3
Crustacean remains/other groups	6.4	5.3	9.1	13.5	9.3	10.0	9.3
Mollusca							
Cephalopoda	14.5	9.1	13.6	10.4	10.6	9.5	7.7
Thaliacea							
Salpidae	—			—	0.3	0.4	0.7
Teleosts	45.7	29.5	40.9	33.1	30.1	36.3	36.6

Smith, 1968; Gulland 1971; Edwards and Bowman, 1979; Grosslein et al., 1980; Rowling, 1990), although none of these studies have dealt with a species as long-lived or slow-growing as orange roughy. The length frequency distribution of spawning orange roughy consists largely of 25–40 cm fish. These sizes are probably fully vulnerable to trawl gear with 100 mm mesh size (legal minimum). Hence, there could be relatively constant fishing mortality across all size groups. There have been no indications of large numbers of new recruits in the length frequency data. This may suggest low levels of recruitment, or at least no entry of any strong year class since 1984 that would reduce mean size.

Interpretation of changes in size structure is also limited by the lack of age data for adult orange roughy. Available ageing data (Mace et al., 1990; MAF Fisheries[3]) for orange roughy suggest a wide range of ages for a given length, and it is possible that age structure may change more rapidly than size structure. Smith et al. (1991) reported a reduction in genetic diversity of orange roughy from several New Zealand areas, including the Challenger Plateau, and suggested this was due to higher mortality of older fish that may remain longer on the spawning grounds than that of younger fish.

Size at maturity showed a significant decline in males, but not in females. It is possible that one sex could be more vulnerable to fishing, but there are no indications of unbalanced sex ratios in commercial catches (authors' unpubl. data). Macroscopic examination of gonads for identification of gonad stage is more reliable in females, where criteria based on colour and size of oocytes are clearer than the presence of milt in male gonads. However, the data may not be representative of true size at maturity in the total population. It is possible that the size at maturity measured here is lower than the true population value because fish that migrate to the spawning grounds are primarily those that are mature, and the relative proportions of immature and mature small fish are not accurately represented.

The apparent lack of change in size at maturity is not surprising in view of the stability of the total population length frequency. An increase in growth rate, with a corresponding reduction in the age at maturity, of individuals in an exploited population is well documented (e.g. Pitt, 1975; Spangler et al., 1977; Borisov, 1978; Hempel, 1978; Leaman, 1991). However, Pitt (plaice, *Hippoglossoides platessoides*, on the Grand Banks) and Leaman (*Sebastes* spp. in the north Pacific Ocean) noted that whereas age at first maturity decreased with exploitation, size at maturity remained the same. Orange roughy are estimated to be about 24 years of age at maturity (Mace et al., 1990), and hence such functional changes in growth rate or maturity may not be obvious after 10 years of fishing, despite a major reduction in population size.

Orange roughy on the Challenger Plateau have consistently spawned in the same general area at the same time of year from 1984 to 1990. The gonad-stage pattern observed in trawl surveys has been similar each year. However, there is evidence of some regional variability in the proportion of fish spawning. The Central Flat and Pinnacles have consistently sustained levels of spawning fish over 90%. On the Westpac Bank this proportion has been lower, and the percentage spawning has progressively increased from 1987 (54%) to 1990 (81%). Reasons for this are not clear. Sample sizes from the Westpac Bank are smaller than those from the other areas but still come from at least six trawls, which should give a representative sample. In 1987 no

[3] MAF Fisheries, unpubl. data, 1993.

actively spawning fish were caught, perhaps because the survey had been taken in June/early July and peak spawning on the Westpac Bank could have occurred slightly later than in the other two areas (Clark, 1991b). Originally it was thought that fish on the Westpac Bank migrated east to the Central Flat and Pinnacles for spawning (Clark and Tracey, 1988). However, in subsequent years ripe and running-ripe fish were found. Nevertheless, in 1987 there was a large proportion of fish that were not spawning that year. It is possible that the Westpac Bank has only developed as a spawning ground since 1987, but if so, whether heavy fishing on the other grounds was a factor is unknown. The biomass index on the Westpac Bank has declined since 1987, so it is unlikely that there has been a major shift of fish from the Central Flat or Pinnacles.

The time of spawning (defined by 20% spent) has consistently been in the second and third weeks of July. Pankhurst (1988) reported that day length was a critical factor in synchronizing the reproductive cycle of orange roughy. The changes in dates of 20% spent between years do not correlate exactly with annual changes in the shortest day, but day length could nevertheless be an important general cue. Gonadal development has remained consistent despite major changes in the size of the population and the spawning school structure. There are indications that heavy fishing pressure may disrupt the stability of schools of orange roughy (Clark and Tracey, 1991). In 1989 when fishing effort was at its peak, a comparatively high proportion of the biomass was in 'background' areas, outside the three main regions of spawning activity. Catch rates in the spawning areas were lower than in other years. It is possible that fishing pressure was affecting the formation of aggregations, but nevertheless reproductive development still occurred normally. However, the success of spawning could have been reduced because the fish were more dispersed.

The diet of orange roughy, and the relative frequency of occurrence of prey groups, were similar over the period examined. Natant decapod crustaceans and fish remains have dominated the diet. This diet composition concurs with other accounts of orange roughy feeding habits in New Zealand waters (e.g. Liwoch and Linkowski 1986; Rosecchi et al., 1988) and is similar to diet composition of orange roughy in the North Atlantic Ocean (e.g. Mauchline and Gordon, 1984; Gordon and Duncan, 1987), Indian Ocean (Kotlyar and Lipskaya, 1981), and off southeastern Australia (Bulman and Koslow, 1992). The trophic effects of the decline in orange roughy biomass are unknown. There is little information on predator–prey relationships within communities containing orange roughy. Published feeding studies and observations from research cruises at different times during the year (authors' unpubl. data) indicate that orange roughy do not prey on eggs or larvae of other fish species. The only published data on predation of orange roughy record them in stomachs of seal shark on the Challenger Plateau (Clark and Tracey, 1988). Sperm whales (*Physeter catodon*) are often observed in orange roughy spawning areas, and although they can dive to depths of over 1000 m. It is uncertain whether they feed on orange roughy.

Orange roughy are slow-growing and long-lived with low productivity, making them highly susceptible to the effects of overfishing. Long-term sustainable yield for the Challenger Plateau stock is estimated at 1.6% of virgin biomass (Clark, 1992). In the early years of a developing fishery catch levels are likely to be high. The schooling behavior of orange roughy for spawning or feeding means that large catches can be taken in a short time, and high catch rates may be maintained despite decreasing biomass. CPUE declined on the Challenger Plateau but not as consistently on the Chatham Rise where the population was also reduced by heavy fishing (Francis et al., 1992), although there was a progressive shortening of the period over which high catch rates occurred (Coburn and Doonan, in press).

In 1986, the TAC on the Challenger Plateau was increased from 6,000 to 10,000 t in order to assess the impact of heavier fishing and to learn more about the productivity of orange roughy. At that stage there was little understanding of stock size, or age and growth characteristics of the species. Hence the intention was to increase catch sufficiently to provide a contrast in abundance indices and give information on the resilience of the stock. However, there were several problems with this 'adaptive management' strategy as applied to Challenger Plateau orange roughy. The first was that it began without good data on the abundance of the stock against which to measure any change. It would have been preferable to have had at least two years of abundance data before increasing fishing pressure. At the time, CPUE had not been examined, and trawl survey results were inadequate to estimate biomass. A new time series of trawl surveys began in 1987, and although the 1988 survey showed a large decrease, with only two survey results we could not be confident about interpreting the differences as a strong decline in stock size. A further difficulty with such management is that with a slow-growing species like orange roughy, potential effects of any changes in spawning stock size on recruitment will not be evident for 20–25

years when the results of that year's spawning recruit to the fishery. Hence, until that time the fishery will be removing only accumulated adult stock and low levels of virgin stock recruitment. A third important feature of adaptive management is the understanding that it can involve high risk to a species like orange roughy. Changes in biomass could occur rapidly and any quota system and industry response must be flexible, so catch levels can be reduced rapidly.

The recovery of orange roughy from heavy fishing may be slow. Their fecundity is low at 20,000–30,000 eggs·kg^{-1} body weight (Pankhurst and Conroy, 1987; Clark and Tracey, 1991). There is no evidence of a marked change in fecundity of Challenger Plateau fish over the period 1987–90 (authors' unpubl. data), but Leaman (1991) reported reduced fecundity in exploited stocks of *Sebastes alutus*, rather than an increase which might have been expected. In addition, Leaman and Beamish (1984) suggested a possible correlation between longevity of a species and the period between strong year classes. Brown et al. (1983) noted that a reduction in population size of several species in the Georges Bank region to low levels (10–20% of peak abundance) was followed by less frequent occurrence of strong year classes.

High vulnerability to fishing and possible slow recovery from over-fishing are important for management of orange roughy fisheries. Data over a comparatively long time period are required to provide a basis for sound management of long-lived species (Leaman, 1991). It is clear with orange roughy on the Challenger Plateau that such species can be overfished in a much shorter time than that required for the desired data collection. Hence, development of an orange roughy fishery needs careful control from the outset. It is important that research occurs in advance of substantial fishing, so that baseline data on distribution, abundance, and biology are collected. The most commonly used techniques for stock assessment of orange roughy (trawl survey, acoustic survey, CPUE analysis) provide relative abundance indices, and therefore require several surveys before absolute biomass can be determined. Results of surveys in other areas, where the relation between survey indices and true biomass has been established, may be useful, but only if gear, bottom type, and fish distribution are similar. Egg production surveys have been carried out in both New Zealand and Australia, and may enable more rapid assessment in some localized areas. 'Adaptive management,' as discussed above, may be appropriate as an aid to estimate biomass by stock reduction methods, but it must be carried out with flexibility in order to change catch levels quickly. If development of the fishery is carefully regulated in the first few years while such data are collected, later management problems such as too many vessels involved in the fishery and the need to quickly and substantially decrease quota levels could be avoided.

Acknowledgments

The authors thank those too numerous to name, who have participated in research cruises over the years which provided the basic data for this study. We also thank Chris Francis and Ian Doonan for statistical advice, Ralph Coburn for some of the commercial data extracts, and Kevin Sullivan and John Annala (all MAF Fisheries) as well as two anonymous journal referees for constructive comments on the manuscript.

Literature cited

Bell, J. D., J. M. Lyle, C. M. Bulman, K. J. Graham, G. M. Newton, and D. C. Smith.
1992. Spatial variation in reproduction, and occurrence of non-reproductive adults, in orange roughy, *Hoplostethus atlanticus* Collett (Trachichthyidae), from southeastern Australia. J. Fish. Biol. 40:107–122.

Borisov, V. M.
1978. The selective effect of fishing on the population structure of species with a long life cycle. J. Ichthyol. 18:896–904.

Brown, B. E., V. C. Anthony, E. D. Anderson, R. C. Hennemuth, and K. Sherman.
1983. The dynamics of pelagic fishery resources off the northeastern coast of the United States under conditions of extreme fishing perturbations. *In* G. D. Sharp and J. Csirke (eds.), Proceedings of the expert consultation to examine changes in abundance and species composition of neritic fish resources. FAO Fish. Rep. 291:465–505.

Bulman, C. M., and J. A. Koslow.
1992. Diet and food composition of a deep-sea fish, orange roughy *Hoplostethus atlanticus* (Pisces: Trachichthyidae), off southeastern Australia. Mar. Ecol. Prog. Ser. 82:115–129.

Clark, M. R.
1991a. Commercial catch statistics for the orange roughy fishery on the Challenger Plateau, 1980–90. N.Z. Fish. Tech. Rep. 27, 11 p.
1991b. Orange roughy fisheries in the mid–Tasman Sea. *In* K. Abel, M. Williams, and P. Smith (eds.), Australian and New Zealand southern trawl fisheries conference. Aust. Bureau of Rural Resources Proc. 10:223–229.

1992. Assessment of the Challenger Plateau (ORH7A) orange roughy fishery for the 1992–93 fishing year. N.Z. Fish. Assess. Res. Doc. 92/6, 13 p. Avail. MAF Fisheries, P.O. Box 297, Wellington, N.Z.

Clark, M. R., and R. I. C. C. Francis.

1990. Revised assessment of the Challenger Plateau (QMA7A) orange roughy fishery for the 1989–90 fishing year. N.Z. Fish. Assess. Res. Doc. 90/1, 17 p. Avail. MAF Fisheries, P.O. Box 297, Wellington, N.Z.

Clark, M. R., and D. M. Tracey.

1988. Report of an orange roughy trawl survey on Challenger Plateau, June–July 1987. N.Z. Fish. Res. Cent. Int. Rep. 86, 87 p. Avail. MAF Fisheries, P.O. Box 297, Wellington, N.Z.

1991. Trawl survey of orange roughy on the Challenger Plateau, July 1990. N.Z. Fish. Tech. Rep. 26, 20 p.

Coburn, R. P., and I. J. Doonan.

In press. Orange roughy fishing on the North East Chatham Rise: a description of the commercial fishery, 1979–1988. N.Z. Fish. Tech. Rep.

Edwards, R. L., and R. E. Bowman.

1979. Food consumed by continental shelf fishes. *In* H. Clepper (ed.), Predator–prey systems in fisheries management, p. 387–405. Sport Fishing Inst., Washington, D.C.

Fenton, G. E., S. A. Short, and D. A. Ritz.

1991. Age determination of orange roughy, *Hoplostethus atlanticus* (Pisces: Trachichthyidae), using 210Pb : 226Ra disequilibria. Mar. Biol. 109:197–202.

Francis, R. I. C. C.

1981. Stratified random trawl surveys of deep-water demersal fish stocks around New Zealand. N.Z. Fish. Res. Div. Occas. Pub. 32, 28 p.

1984. An adaptive strategy for stratified random trawl surveys. N.Z. J. Mar. Freshwater Res. 18:59–71.

1990. A maximum likelihood stock reduction method. N.Z. Fish. Assess. Res. Doc. 90/4, 12 p. Avail. MAF Fisheries, P.O. Box 297, Wellington, N.Z.

1992. Use of risk analysis to assess fishery management strategies: a case study using orange roughy (*Hoplostethus atlanticus*) on the Chatham Rise, New Zealand. Can. J. Fish. Aquat. Sci. 49: 922–930.

Francis, R. I. C. C., D. A. Robertson, M. R. Clark, and R. P. Coburn.

1992. Assessment of the ORH 3B orange roughy fishery for the 1992/93 fishing year. N.Z. Fish. Assess. Res. Doc. 92/4, 45 p. Avail. MAF Fisheries, P.O. Box 297, Wellington, N.Z.

Gordon, J. D. M., and J. A. R. Duncan.

1987. Aspects of the biology of *Hoplostethus atlanticus* and *H. mediterraneus* (Pisces: Berycomorphi) from the slopes of the Rockall Trough and the Porcupine Sea Bight (North-Eastern Atlantic). J. Mar. Biol. Ass. U.K. 67:119–133.

Grosslein, M. D., R. W. Langton, and M. P. Sissenwine.

1980. Recent fluctuations in pelagic fish stocks of the Northwest Atlantic, Georges Bank region, in relation to species interactions. Rapp. P.-v. Réun. Cons. int. Explor. Mer 177:374–404.

Gulland, J. A.

1971. Ecological aspects of fishery research. Adv. Ecol. Res. 7:115–176.

Gunderson, D. R.

1977. Population biology of Pacific ocean perch, *Sebastes alutus*, stocks in the Washington-Queen Charlotte Sound region, and their response to fishing. Fish. Bull. 75:369–403.

Hempel, G.

1978. North Sea fisheries and fish stocks: a review of recent changes. Rapp. P.-v. Réun. Cons. int. Explor. Mer 173:145–167.

Kotlyar, A. N., and N. Y. Lipskaya.

1981. Feeding of *Hoplostethus atlanticus* Collett (Trachichthyidae, Beryciformes). *In* Fishes of the open ocean, p. 89–93. Inst. Oceanology, Academy of Sciences USSR, Moscow.

Leaman, B. M.

1991. Reproductive styles and life history variables relative to exploitation and management of *Sebastes* stocks. Env. Biol. Fish. 30:253–271.

Leaman, B. M., and R. J. Beamish.

1984. Ecological and management implications of longevity in some Northeast Pacific groundfishes. Int. North Pac. Fish. Comm. Bull. 42:85–97.

Liwoch, M., and T. B. Linkowski.

1986. Some biological features of orange roughy *Hoplostethus atlanticus* (Trachichthyidae) from New Zealand waters. Pr. morsk. Inst. ryb. Gdyni 21:27–41.

Mace, P. M., J. M. Fenaughty, R. P. Coburn, and I. J. Doonan.

1990. Growth and productivity of orange roughy (*Hoplostethus atlanticus*) on the north Chatham Rise. N.Z. J. Mar. Freshwater Res. 24:105–119.

Mauchline, J., and J. D. M. Gordon.

1984. Occurrence and feeding of berycomorphid and percomorphid teleost fish in the Rockall Trough. J. Cons. int. Explor. Mer 41:239–247.

Pankhurst, N. W.

1988. Spawning dynamics of orange roughy, *Hoplostethus atlanticus*, in mid-slope waters of New Zealand. Env. Biol. Fish. 21:101–116.

Pankhurst, N. W., and A. M. Conroy.

1987. Size-fecundity relationships in the orange roughy, *Hoplostethus atlanticus*. N.Z. J. Mar. Freshwater Res. 21:295–300.

Pankhurst, N. W., P. J. McMillan, and D. M. Tracey.

1987. Seasonal reproductive cycles in three commercially exploited fishes from the slope waters off New Zealand. J. Fish Biol. 30:193–212.

Pauly, D.

1979. Theory and management of tropical multi-

species stocks. A review, with emphasis on the Southeast Asian demersal fisheries. ICLARM Stud. Rev. 1.

Pearson, E. S., and H. O. Hartley (eds.).
1976. Biometrika tables for statisticians. 2 vols. Cambridge Univ. Press, Cambridge.

Pitt, T. K.
1975. Changes in abundance and certain biological characteriplatessoides.stics of Grand Bank American plaice, *Hippoglossoides platessoides*. J. Fish. Res. Board Can. 32:1383–1398.

Regier, H. A., and K. H. Loftus.
1972. Effects of fisheries exploitation on salmonid communities in oligotrophic lakes. J. Fish. Res. Board Can. 29:959–968.

Robertson, D. A.
1991. The New Zealand orange roughy fishery: an overview. *In* K. Abel, M. Williams, and P. Smith (eds.), Australian and New Zealand southern trawl fisheries conference. Aust. Bureau of Rural Resources Proc. 10:38–48.

Rosecchi, E., D. M. Tracey, and W. R. Webber.
1988. Diet of orange roughy, *Hoplostethus atlanticus* (Pisces: Trachichthyidae) on the Challenger Plateau, New Zealand. Mar. Biol. 99:293–306.

Rowling, K. R.
1990. Changes in the stock composition and abundance of spawning gemfish *Rexea solandri* (Cuvier), Gempylidae, in southeastern Australian waters. Aust. J. Mar. Freshwater Res. 41:145–163.

Russ, G. R., and A. C. Alcala.
1989. Effects of intense fishing pressure on an assemblage of coral reef fishes. Mar. Ecol. Prog. Ser. 56:13–27.

SAS.
1988. SAS/STAT Users Guide, Release 6.03 ed. SAS Institute, Cary, NC.

Smith, P. J., R. I. C. C. Francis, and M. McVeagh.
1991. Loss of genetic diversity due to fishing pressure. Fish. Res. 10:309–316.

Smith, S. H.
1968. Species succession and fishery exploitation in the Great Lakes. J. Fish. Res. Board Can. 25:667–693.

Spangler, G. R., N. R. Payne, J. E. Thorpe, J. M. Byrne, H. A. Regier, and W. J. Christie.
1977. Responses of percids to exploitation. J. Fish. Res. Board Can. 34:1983–1988.

Tracey, D. M., P. J. McMillan, J. H. Armstrong, and D. A. Banks.
1990. Orange roughy trawl survey: Challenger Plateau and west coast South Island, 1983. N.Z. Fish. Tech. Rep. 22, 34 p.

Morphometric and genetic identification of eggs of spring-spawning sciaenids in lower Chesapeake Bay*

Louis B. Daniel III
John E. Graves**
School of Marine Science
Virginia Institute of Marine Science
The College of William and Mary
Gloucester Point, Virginia 23062

Abstract.—Restriction-fragment length polymorphism (RFLP) analysis of mitochondrial mtDNA was used to identify morphologically similar eggs of spring spawning sciaenids in lower Chesapeake Bay. During spring 1990 and 1991, ichthyoplankton surveys were conducted in lower Chesapeake Bay to estimate seasonal egg production and population biomass of black drum, *Pogonias cromis*. Rearing experiments indicated that at least three species of sciaenid (silver perch, *Bairdiella chrysoura*; weakfish, *Cynoscion regalis* and *P. cromis*) were spawning in the survey area during both years. Specific identification of eggs based on previously published ranges of outside egg diameter (OED) were not reliable because of considerable overlap in diameter distributions. However, analysis of weekly OED frequencies revealed the presence of three modes which differed in temporal occurrence, suggesting the products of three species. Genetic typing of eggs using RFLP analysis of mtDNA confirmed the presence of three species, but demonstrated that eggs of certain size classes represented two species. These results illustrate that reliance on previously published ranges of egg diameter for specific identification of spring-spawning sciaenids may overestimate the spawning biomass of black drum in Chesapeake Bay by as much as 50% owing to misidentification of weakfish eggs.

At least five species of the family Sciaenidae (silver perch, *Bairdiella chrysoura*; spotted seatrout, *Cynoscion nebulosus*; weakfish, *C. regalis*; northern kingfish, *Menticirrhus saxatilis*; and black drum, *Pogonias cromis*) are purported to spawn during the spring in lower Chesapeake Bay (Joseph et al., 1964; Lippson and Moran, 1974; Johnson, 1978; Brown, 1981; Olney, 1983; Cowan et al., 1992). The eggs of spring-spawning sciaenids in lower Chesapeake Bay are morphologically similar, ranging in outside egg diameter (OED) from 0.66 to 1.18 mm, and having single or multiple oil globules of varying sizes (Johnson, 1978; Olney, 1983). As a result, specific identification of eggs based on morphological criteria is problematic. Holt et al. (1988) suggested that it may not be possible to determine the specific identity of sciaenid eggs from morphological criteria; Joseph et al. (1964) reported that positive identification could only be achieved with supplemental hatching studies.

Hatching studies have traditionally been used to identify morphologically similar eggs, including those of sciaenids. Joseph et al. (1964) cultured eggs of several sciaenids collected at a single station in southern Chesapeake Bay (16 May 1962) and raised larvae to an identifiable size (5–7 mm). The smallest eggs (0.630–0.777 mm) were found to be *B. chrysoura*, whereas the larger eggs (0.814–1.110 mm) developed into *P. cromis*. Culture of eggs (0.777–0.950 mm) collected during early June produced no *P. cromis* but did result in larvae of *B. chrysoura* and *C. regalis*. In contrast, Olney (1983) suggested that eggs of *P. cromis*, *C. regalis*, *B. chrysoura*, and *Menticirrhus* spp. were included in a size-frequency distribution of morphologically similar eggs collected from May through August in lower Chesapeake Bay, but that identifications based on diameter were ambiguous because of the high degree of overlap in diameter distributions (Table 1). Confounding this problem is the observation that egg size may change with varying salinity or as the spawning season progresses (Johnson, 1978).

Because many species of Sciaenidae in lower Chesapeake Bay spawn concurrently and have morphologically similar eggs, most studies have relied either on previously published egg size distributions or rearing for identification (Holt et al., 1985, 1988; Comyns et

Manuscript accepted 10 November 1993
Fishery Bulletin 92:254–261 (1994)

*Contribution No. 1818 of the Virginia Institute of Marine Science.
**To whom reprint requests and correspondence should be sent.

Table 1

Reported range of outside egg diameter (OED) and study location for spring-spawning sciaenids.

Species	OED (mm)	Location	Author(s)
Bairdiella chrysoura	0.62–0.78	Chesapeake Bay	Joseph et al., 1964
	0.59–0.82	NW Gulf of Mexico	Holt et al., 1988
Cynoscion nebulosus	0.60–0.85	NW Gulf of Mexico	Holt et al., 1988
	0.70–0.85	NW Gulf of Mexico	Fable et al., 1978
Cynoscion regalis	0.68–1.18	Long Island Sound	Merriman and Sclar, 1952
	0.70–1.17	Chesapeake Bay	Pearson, 1929
	0.84–0.96	Delaware Bay	Wisner, 1965
Menticirrhus saxatilis	0.80–0.85	New Jersey	Welsh and Breeder, 1923
Menticirrhus spp.	0.63–0.87	NW Gulf of Mexico	Holt et al., 1988
Pogonias cromis	0.82–1.02	Chesapeake Bay	Joseph et al., 1964
	0.90–1.20	NW Gulf of Mexico	Holt et al., 1988

al., 1991; Saucier and Baltz, 1992; Saucier et al., 1992). However, the misidentifications that can result from overlapping egg-diameter distributions and the time-consuming nature of culture experiments make methods based on other characters desirable.

The application of biochemical genetics has provided an alternative to culture for positive identification of morphologically similar eggs. Electrophoresis of water-soluble proteins (allozyme analysis) has been used to distinguish between larvae and juveniles of morphologically similar species of marine fishes (eg. Morgan, 1975; Smith and Benson, 1980; Graves et al., 1988). Similarly, restriction fragment length polymorphism (RFLP) analysis of mitochondrial DNA has been employed to discriminate between the eggs of three congeneric serranids that could not be unambiguously identified with a single allozyme locus (Graves et al., 1990). More recently, direct sequencing and RFLP analysis of DNA amplified by the polymerase chain reaction (PCR) have been used to identify morphologically similar larvae of invertebrates (Olson et al., 1991; Silberman and Walsh, 1992).

In this paper we report that identification of eggs of sciaenids in lower Chesapeake Bay during spring based on published morphological criteria, rearing experiments, and genetic analysis are inconsistent. These results indicate that it is not possible to identify sciaenid eggs accurately by using diameter as the sole criteria. In addition, we present the results of weekly plots of egg size-frequency distributions and a RFLP analysis of mtDNA to determine the specific composition of eggs of sciaenids that may be present in lower Chesapeake Bay during spring.

Material and methods

Weekly zooplankton surveys of the lower Chesapeake Bay were conducted during April and May 1990 and 1991 to determine the distribution and abundance of eggs of black drum for an estimate of seasonal egg production. Samples of eggs were obtained with an *in situ* silhouette photography system consisting of paired 60-cm diameter, 335-μ nets fitted to a rigid frame (see Olney and Houde, 1993, for a detailed gear description). All deployments were 5-minute, stepped-oblique tows and yielded a standard plankton sample and a replicate film record. Plankton samples were preserved in 5–8% buffered formalin and sciaenid eggs were identified by using the criteria of Lippson and Moran (1974) and measured to the nearest 0.025 mm with a Zeiss Stemi SR stereomicroscope. Ten subsamples of eggs (n=75–100) sorted from preserved plankton samples were remeasured to assess measurement error.

During several cruises in May 1990 and 1991, eggs were collected in an area off the city of Cape Charles, Virginia, with a 0.5-m Hansen net fitted with 202-μ mesh to seed 1-liter Imhoff settling cones for hatching experiments. Eggs were originally separated as Type I (<0.80 mm) and Type II (>0.85 mm) based on the morphological criteria of Joseph et al. (1964). Rearing chambers were returned to the laboratory and held for 3 to 14 days. In these, larvae were periodically sac-

rificed and preserved in 5–8% buffered formalin. Identifications of preserved sciaenid larvae from pigment characters were based on Ditty (1989).

Sciaenid eggs collected in the same area during spring 1991, 1992, and 1993 were sorted from fresh plankton samples. To avoid contamination by the morphologically similar eggs of the cynoglossid *Symphurus plagiusa* and the soleid *Trinectes maculatus* that contain several oil globules and are abundant in lower Chesapeake Bay during the spring, all eggs with >3 oil globules were omitted from the samples. Although eggs of most spring-spawning sciaenids generally possess three or fewer oil globules (usually two) those of *Menticirrhus saxatilis* may contain from 1 to 16 oil globules (Johnson, 1978). After sorting, eggs were measured, placed in scintillation vials with 26 ppt seawater, and frozen at –70°C for genetic analysis. Individual eggs were thawed and remeasured prior to homogenization to assess shrinkage.

Sciaenid eggs were genetically typed by comparing mtDNA restriction fragment patterns of individual eggs with those of known adults. To obtain patterns of known adults, mature female sciaenids (*B.chrysoura*, *C. nebulosus*, *C. regalis*, *M. saxatilis*, and *P. cromis*) were collected by pound net, trawls, and hook and line in April and May 1990 and 1991. Ovarian tissue was excised and frozen at –70°C. MtDNA was purified from ovarian tissue by cesium chloride equilibrium density gradient ultracentrifugation following the protocols of Lansman et al. (1981). To determine a restriction enzyme that unambiguously identified the different sciaenid species, aliquots of mtDNA were individually digested with the following restriction enzymes: *Apa*I, *Ava*I, *Ban*I, *Ban*II, *Hin*dIII used according to manufacturer's instructions. The resulting fragments were separated electrophoretically on 1.0% agarose mini-gels run at 5 V/cm for four hours and visualized with ethidium bromide.

MtDNA-enriched genomic DNA was isolated from individual eggs following the protocols of Graves et al. (1990). Entire DNA samples were digested with a single discriminating restriction endonuclease, separated electrophoretically, and transferred to a nylon filter (Southern transfer) following standard protocols (Sambrook et al., 1989). Filters were hybridized with highly purified black drum mtDNA, nick-translated with biotin-7–dATP, washed, blocked and visualized following the methods of Graves et al. (1990).

Results

A total of 10,803 sciaenid eggs was sorted from samples collected in 1990 and 1991. Outside egg diameter of all specimens ranged from 0.650 to 1.12 mm. Successive blind readings of samples of 75 to 100 eggs were used to assess measurement error. No differences were found in the size-frequency distributions indicating good agreement within the 0.025–mm size classes (two-sample t-test, $P<0.05$, $n=79$).

Qualitative analysis of culture experiments using the two egg types of Joseph et al. (1964) revealed the presence of three species. Cultures containing eggs designated Type I (<0.80 mm) resulted in larvae of *B. chrysoura*, whereas cultures of eggs designated Type II (>0.85 mm) resulted in larvae of *C. regalis* and *P. cromis*.

Analysis of preserved ichthyoplankton samples from 1990 and 1991 revealed the presence of larvae of *B. chrysoura*, *C. regalis*, and *P. cromis*. No early life history stages of other sciaenids were identified; however, yolk-sac larvae could not be identified to species. Because rearing studies and analysis of field-caught plankton samples revealed the presence of more than two species, we could not rely on the criteria of Joseph et al. (1964) for specific identification. We therefore examined weekly frequency of occurrence of all sciaenid eggs during 1990 (Fig. 1) and 1991 (Fig. 2). Based on temporal occurrence and size frequency we identified three modes. The largest eggs (>0.975 mm), Type C, were most abundant during the period 23 April through 9 May. Type-C eggs declined in abundance throughout May in both years. Mid-sized eggs (0.850–0.950 mm), designated Type B, generally appeared later than Types A and C. Type-B eggs did not exceed 5% of the total frequency of sciaenid eggs until 15 May 1990 and 9 May 1991. Type-B eggs increased in abundance from mid-May until the end of sampling. The smallest eggs (<0.850 mm), designated Type A, co-occurred with Type-C eggs; however, they did not exceed 5% of the total sciaenid eggs until 8 May 1990 and 9 May 1991. In 1990, Type-A eggs peaked in abundance on 15 May and gradually declined throughout the sampling period. In 1991, Type-A eggs were most abundant during the last sample on 28 May.

To test the hypothesis that eggs designated Types A, B, and C were separate species assemblages, the mtDNA restriction fragment patterns of known adult sciaenids were compared with those of fresh egg samples separated into Types A, B, and C. Restriction fragment length polymorphism analysis of mtDNA, purified from adult *B. chrysoura*, *C. nebulosus*, *C. regalis*, *Menticirrhus saxatilis*, and *P. cromis*, revealed species-specific restriction fragment patterns for each of the five enzymes. Of the five enzymes, *Hin*dIII showed the greatest differences between species, facilitating visualization with the Southern blotting procedure (Table 2).

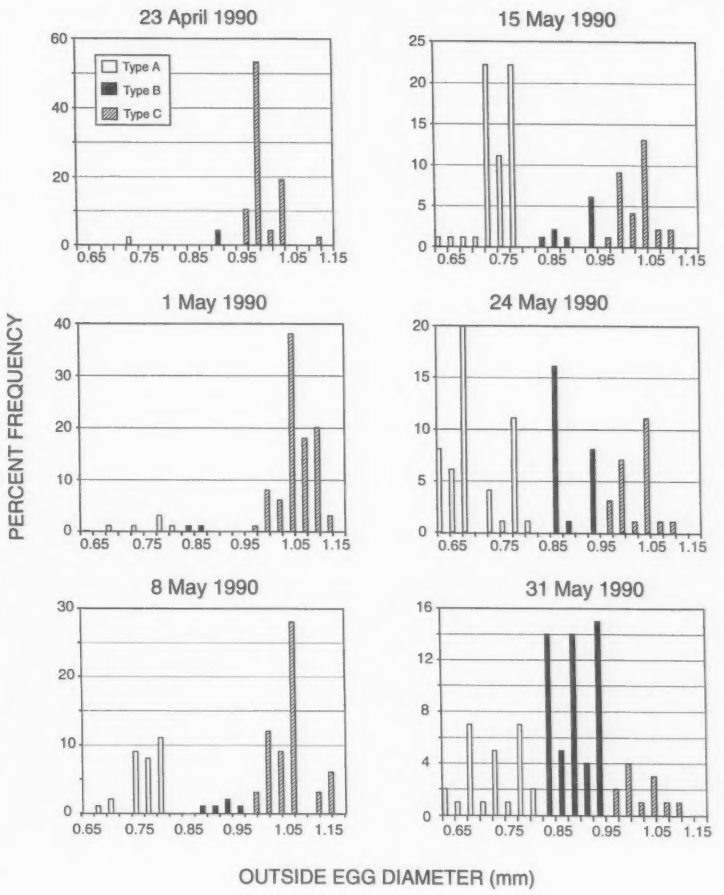

Figure 1

Frequency distributions of outside egg diameters of sciaenid eggs collected over six weeks during spring 1990 in lower Chesapeake Bay.

A total of 62 eggs, representing all sciaenid egg size classes collected in lower Chesapeake Bay, was identified with diagnostic *Hin*dIII restriction fragment patterns. *Bairdiella chrysoura*, *C. regalis*, and *P. cromis* were the only species of sciaenids identified; no other restriction fragment patterns were observed. Genetic identification of eggs designated Type A (<0.850 mm, n=12) resulted in 11 individuals of *B. chrysoura* and one specimen (0.825-mm OED size class) of *C. regalis* (Fig. 3). *Cynoscion regalis* composed the majority of type-B eggs (0.850-0.975 mm, n=18) analyzed, but seven of the 10 largest type-B eggs (0.975-mm OED size class) were identified as black drum. Type-C eggs, those 1.00 mm and larger (n=32), all possessed the restriction fragment pattern diagnostic for *P. cromis*.

Discussion

Identifications of eggs of sciaenids are often based on published diameter distributions or hatching experiments, or both. Results of hatching experiments and genetic analysis in this study indicate that samples of eggs of a single size class may represent the products of two or more species. For example, eggs designated Type I (<0.80 mm) and identified as silver perch by Joseph et al. (1964) were shown with genetic analysis to contain eggs of both weakfish and silver perch. Similarly, eggs designated Type II (>0.85 mm) and identified as black drum by Joseph et al. (1964) were shown with rearing and genetic analysis to contain eggs of both weakfish and black drum.

During the present study, neither hatching experiments nor genetic analysis identified eggs as black drum that were smaller than 0.975 mm OED. While temporally limited, the results of this study suggest that the range in size for eggs of black drum (0.975–1.125 mm) in lower Chesapeake Bay may be more restricted than those previously reported.

The ranges of egg diameter overlapped for silver perch and weakfish. Eggs genetically identified as silver perch ranged in size from 0.650 to 0.825 mm, in agreement with previously reported size ranges for silver perch in the northwestern Gulf of Mexico (0.59–0.82 mm, Holt et al., 1988) and Chesapeake Bay (0.625–0.775 mm, Joseph et al., 1964). Although Holt et al. (1988) identified eggs of silver perch as small as 0.590 mm, no sciaenid eggs smaller than 0.650 mm OED were collected in the present study. Sizes of eggs genetically identified as weakfish were found to range from 0.825 to 0.975 mm in diameter. These values are comparable with those reported by Wisner (1965, 0.84–0.96 mm) but are narrower than

the range (0.68–1.18 mm) given by Merriman and Sclar (1952) for Block Island Sound, New York. While the range in sizes for silver perch and weakfish reported in this study agree with past research, overlaps in these ranges preclude the sole use of egg size for identification.

Neither Joseph et al. (1964), Olney (1983), nor the present study identified eggs of *C. nebulosus* or *M. saxatilis* in samples collected in lower Chesapeake Bay. Fable et al. (1978) described laboratory-spawned eggs of *C. nebulosus* from a single female and reported a mean diameter of 0.77 mm (range 0.70–0.85 mm). Although based upon a limited sample size, Fable et al.'s data indicate that eggs of *C. nebulosus* could be confused with eggs of *B. chrysoura*; however, no eggs in our limited sample of this size range (n=12) were genetically identified as *C. nebulosus*. A possible explanation for the lack of eggs of *C. nebulosus* in the present study may be the tendency for adults to spawn in or around vegetated areas (Brown, 1981). The absence of eggs of *Menticirrhus* spp. in this genetic analysis may be explained by our exclusion of eggs with greater than three oil globules. Additionally, *Menticirrhus saxatilis* reportedly spawns off front beaches and possibly offshore (deSylva et al., 1962); consequently, circulation in the bay may prevent eggs of this species from entering the survey area or they may be transported to areas that were not sampled in our study.

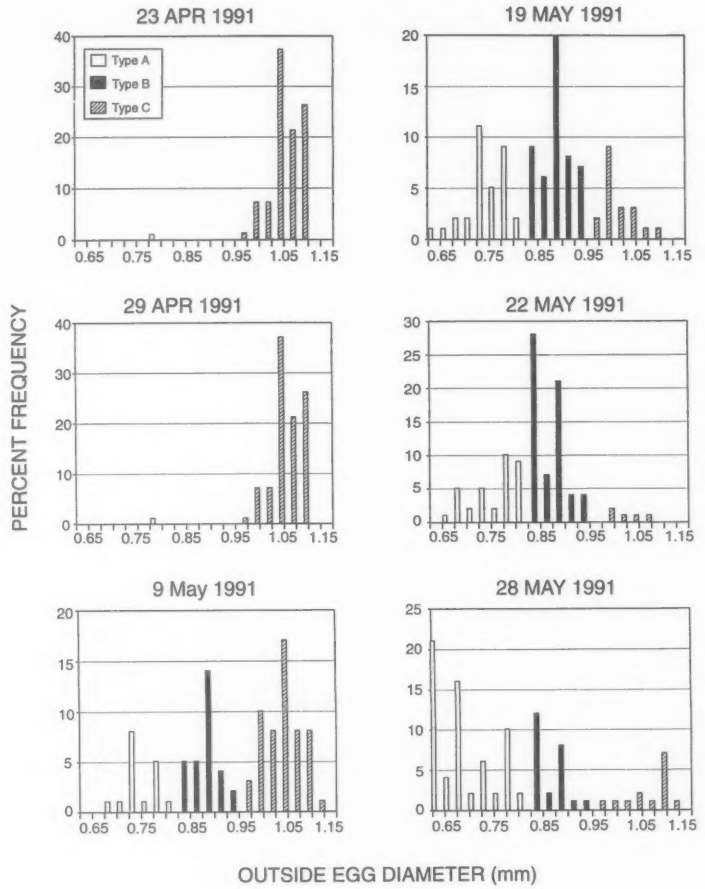

Figure 2

Frequency distributions of outside egg diameters of sciaenid eggs collected over six weeks during spring 1991 in lower Chesapeake Bay.

The identification of species-specific restriction fragment patterns for spring-spawning sciaenids is based on the assumption that there is limited intraspecific variation of the diagnostic restriction fragment patterns. Recent studies of the population genetics of spotted seatrout, black drum, and weakfish (Graves et al., 1992; Gold et al., 1993) indicate that these species exhibit low intraspecific mtDNA variability. Furthermore, no variation of the *Hin*dIII fragment pattern was found in a survey of mtDNA isolated from 25 adult *B. chrysoura* (L. Daniel, unpubl. data). Consequently, the common restriction fragment patterns used to distinguish species in this study were deemed suitable for use in identifications.

Variability in egg-size distributions with changing salinity and over the spawning season were not examined in this study. Consequently, exact size groupings may only be applicable to the particular salinity regime (19–25 ppt) that we sampled. However, samples were taken throughout peak spawning for black drum and silver perch and may encompass the ranges that occur for these species in lower Chesapeake Bay.

Results of our genetic analysis suggest that identifications of eggs of spring-spawning Sciaenidae in

Table 2

Common fragment sizes produced by restriction endonuclease (*Hin*dIII) digestion of mtDNA purified from ovarian tissue of spring spawning sciaenids.

Species	Fragment sizes (Kb)						
Bairdiella chrysoura	5.0	3.9	2.8	1.9	1.7	1.7	1.3
Cynoscion nebulosus	8.5	4.5	3.8[1]				
Cynoscion regalis	5.6	4.3	4.1	2.9			
Menticirrhus saxatilis	5.4	3.2	2.4	2.0	1.9	1.8	
Pogonias cromis	3.3	2.9	2.7	2.5	2.1	1.3	1.0

[1] J. Gold, Texas A&M, College Station, TX, pers. commun. 1993.

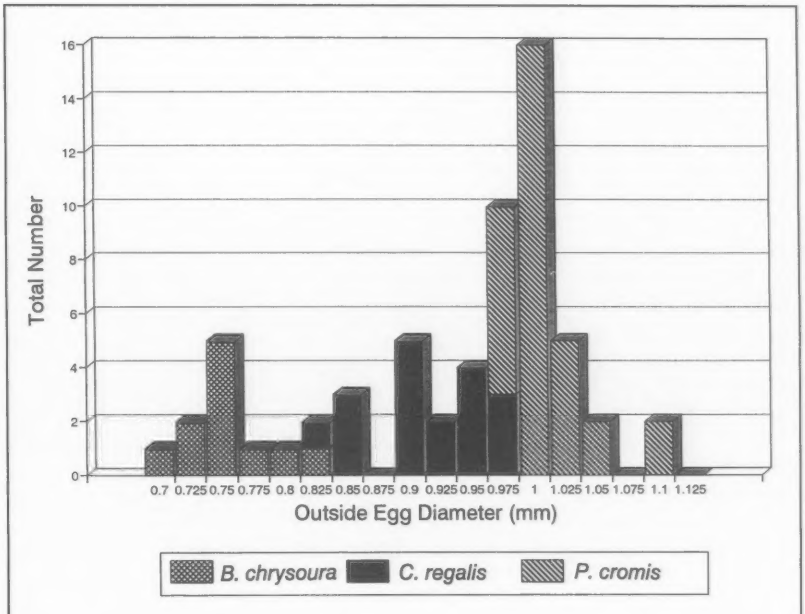

Figure 3

Size distributions of all eggs morphologically typed as sciaenids and identified using genetic techniques.

lower Chesapeake Bay based on OED are subject to error. These findings are particularly timely in light of the increased use of fishery-independent assessments of stock size that require precise estimates of egg abundance (egg production method). Because eggs of black drum and weakfish are spatio-temporally coincident and OEDs overlap, estimates of egg production by black drum in lower Chesapeake Bay may be over-estimated by 50% or greater if identification criteria are based solely on egg size. Likewise, measures of spawning stock biomass will be similarly over-estimated, results that could significantly impact management decisions. Comparable biases in estimates of egg production and spawning stock biomass of weakfish could result from egg misidentifications. However, the more protracted spawning season and greater area of spawning for weakfish in Chesapeake Bay (Olney, 1983) would make these impacts much less severe.

Biochemical techniques are an important tool for the further study of eggs of sciaenids. Genetic analysis has the potential to produce reliable results and permit the storage of samples for later analysis. Additional studies are needed to survey genetic identifications over the entire spawning season and area to determine if egg sizes change over time or are influenced by seasonal changes in hydrography or by age structure of the spawning stock. Finally, the use of genetic techniques, coupled with an extensive examination of morphology could lead to the delineation of other characters that may be useful in separating the eggs of these species.

Acknowledgments

J. McGovern, M. Cavaluzzi, J. Field, C. Baldwin, and K. Kavanaugh kindly assisted with sample collection. P. Crewe patiently processed plankton samples at sea and in the laboratory, and J. McDowell provided valuable technical assistance with mtDNA analyses. J. Olney helped in the design and implementation of the sampling program and provided comments on the manuscript. Additional reviews were provided by J. Musick, J. Cowan, and E. Heist. This study was funded in part by the Virginia Marine Resources Commission under U.S. Fish and Wildlife Contract F-95-R.

Literature cited

Brown, N. J.
1981. Reproductive biology and recreational fishery for spotted seatrout, *Cynoscion nebulosus*, in the Chesapeake Bay area. M.A. thesis, College of William and Mary, Williamsburg, 119 p.

Comyns, B. H., J. Lyczkowski-Shultz, D. L. Nieland, and C. A. Wilson.
1991. Reproduction of red drum, *Sciaenops ocellatus*, in the northcentral Gulf of Mexico: seasonality and spawner biomass. *In* R. D. Hoyt (ed.), Larval fish recruitment and research in the Americas: proceedings of the thirteenth annual larval fish conference, p. 17–26. Dep. Commer., NOAA Tech. Rep. NMFS 95.

Cowan, J. H., R. S. Birdsong, E. D. Houde, J. S Priest, W. C. Sharp, G. B. Mateja.
1992. Enclosure experiments on survival and growth of black drum eggs and larvae in lower Chesapeake Bay. Estuaries 15(3):392–402.

deSylva, D. P., F. A. Kalber Jr., and C. N. Shuster.
1962. Fishes and ecological conditions in the shore zone of the Delaware River estuary, with notes on other species collected in deeper water. Univ. Del. Mar. Lab. Inf. Ser. Publ. 51, 164 p.

Ditty, J. G.
1989. Separating early larvae of sciaenids from the western North Atlantic: a review and comparison of larvae off Louisiana and Atlantic coast of the U.S. Bull. Mar. Sci. 44(3):1083–1105.

Fable, W. A., Jr., T. D. Williams, and C. R. Arnold.
1978. Description of reared eggs and young larvae of the spotted seatrout *Cynoscion nebulosus*. Fish. Bull. 76 (1):65–72.

Gold, J. R., L. R. Richardson, C. Furman, and T. L. King.
1993. Mitochondrial DNA differentiation and population structure in red drum (*Sciaenops ocellatus*) from the Gulf of Mexico and Atlantic Ocean. Mar. Biol. 116(2):175–185.

Graves, J. E., M. A. Simovich, and K. M. Schaefer.
1988. Electrophoretic identification of early juvenile yellowfin tuna, *Thunnus albacares*. Fish. Bull. 86(4):835–838.

Graves, J. E., M. J. Curtis, P. A. Oeth, and R. S. Waples.
1990. Biochemical genetics of southern California basses of the genus *Paralabrax*: specific identification of fresh and ethanol-preserved eggs and early larvae. Fish. Bull. 88:59– 66.

Graves, J. E., J. R. McDowell, and M. L. Jones.
1992. A genetic analysis of weakfish, *Cynoscion regalis*, stock structure along the mid-Atlantic coast. Fish. Bull. 90:469–475.

Holt, G. J., S. A. Holt, and C. R. Arnold.
1985. Diel periodicity of spawning in sciaenids. Mar. Ecol. Prog. Ser. 27:1–7.

Holt, S. A., G. J Holt, and L. Young-Abel.
1988. A procedure for identifying sciaenid eggs. Contr. Mar. Sci. 30:99–108.

Johnson, G. D.
1978. Development of fishes of the mid-Atlantic bight. Vol. IV: Carangidae through Ephippidae. Fish Wildl. Serv., U.S. Dep. Interior, 314 p.

Joseph, E. B., W. H. Massman, and J. J. Norcross.
1964. The pelagic eggs and early larval stages of the black drum from Chesapeake Bay. Copeia 1964:425–434.

Lansman, R. A., J. C. Avise, C. F. Aquadro, J. F. Shapira, and S. W. Daniel.
1981. The use of restriction endonucleases to measure mtDNA sequence relatedness in natural populations. III: techniques and potential applications. J. Mol. Evol. 17:214–226.

Lippson, A. J., and R. L. Moran.
1974. Manual for identification of early developmental stages of fishes of the Potomac River estuary. Maryland Dep. Natl. Resources, Power Plant Sitting Prog. Rep. PPSP-MP-13, 282 p.

Merriman, D. and R. C. Sclar.
1952. The pelagic fish eggs and larvae of Block Island Sound. Bull. Bingham. Oceanogr. Collect. Yale Univ. 13(3):156–219.

Morgan, R. P.
1975. Distinguishing larval white perch and striped bass by electrophoresis. Chesapeake Sci. 16:68–70.

Olney, J. E.
1983. Eggs and early larvae of the bay anchovy, *Anchoa mitchilli*, and the weakfish, *Cynoscion regalis*, in lower Chesapeake Bay with notes on associated ichthyoplankton. Estuaries 6(1):20–35.

Olney, J. E., and E. D. Houde.
1993. Evaluation and use of *in situ* silhouette photography in studies of estuarine zooplankton. Bull. Mar. Sci. 52(2):845–872.

Olson, R. R., J. A. Runstadler, and T. D. Kocher.
1991. Whose larvae? Nature 351:357–358.

Pearson, J. G.
1929. Natural history and conservation of the red drum and other commercial sciaenids on the Texas coast. U.S. Bur. Fish. Bull. 44:129–214.

Sambrook, J., E. F. Fritsch, and T. Maniatis.
1989. Molecular cloning: a laboratory manual, 2nd ed. Cold Spring Harbor Laboratory Press, NY.

Saucier, M. H., and D. M. Baltz.
1992. Spawning site selection by spotted seatrout, *Cynoscion nebulosus*, and black drum, *Pogonias cromis*, in Louisiana. Environ. Biol. Fishes 36:257–272.

Saucier, M. H., D. M. Baltz, and W. A. Roumillat.
1992. Hydrophone identification of spawning sites of spotted seatrout, *Cynoscion nebulosus* (Osteichthys: Sciaenidae) near Charleston, South Carolina. N.E. Gulf Sci. 12(2):141–145.

Silberman, J. D., and P. J. Walsh.
1992. Species identification of spiny lobster phyllosome larvae via ribosomal DNA analysis. Mol. Mar. Biol. Biotech. 1(3):195–205.

Smith, P. J., and P. G. Benson.
1980. Electrophoretic identification of larval and 0-group flounders (*Rhombosolea* spp.) from Wellington Harbor, N.Z. J. Mar. Freshwater Res. 14:401–404.

Welsh, W. W., and C. M. Breeder Jr.
1923. Contribution to life histories of Sciaenidae of the eastern United States coast. U.S. Bur. Fish. Bull. 39:141–201.

Wisner, B. W.
1965. McClane's standard fishing encyclopedia. Holt, Rhinehart and Winston, Inc., New York, NY, 1057 p.

A re-description of Atlantic spadefish larvae, *Chaetodipterus faber* (family: Ephippidae), and their distribution, abundance, and seasonal occurrence in the northern Gulf of Mexico

James G. Ditty
Richard F. Shaw
Joseph S. Cope

Coastal Fisheries Institute, Center for Coastal, Energy, and Environmental Resources
Louisiana State University, Baton Rouge, LA 70803

Abstract.—The Atlantic spadefish *(Chaetodipterus faber)* is the only member of the family Ephippidae in the western Atlantic Ocean and its life history is poorly understood. We redescribe Atlantic spadefish larvae, discuss their relationship to known larvae of other ephippid genera, and discuss the distribution, abundance, and seasonal occurrence of Atlantic spadefish in the northern Gulf of Mexico. Larval Atlantic spadefish are characterized by a small, peak-like, median supraoccipital crest with a single, dorsally directed spine; large preopercle spines, numerous serrate ridges, and other spines on the head; a deep, robust body which becomes laterally compressed; heavy body pigmentation; and early development of specialized spinous scales or "prescales" (at about 5.5-mm standard length [SL]). Transition to juvenile stage begins about 8.0–8.5 mm SL. Developmental morphology and head spination of Atlantic spadefish is similar to that of Pacific spadefish, *Chaetodipterus zonatus*. Sequence of fin completion is pelvics — dorsal and anal soft rays — dorsal spines–pectorals. Overall, ≥85% of Atlantic spadefish larvae were found in waters ≥28.0°C and between 26.7 and 31.3 ppt. Larvae occur primarily in coastal waters, except near the Mississippi River delta, an area with a narrow shelf and rapidly increasing water depths. Delta waters may offer additional habitat suitable to Atlantic spadefish larvae because of lower salinities. Larvae are primarily collected between June and August and in the north-central Gulf of Mexico. Larval Atlantic spadefish are apparently rare in the eastern Gulf off Florida. Catch rates near the Mississippi River delta during August were higher than elsewhere in the north-central Gulf and suggest a possible association with riverine frontal areas which requires further study.

The percoid family Ephippidae is usually considered to comprise five genera and 17 species (Nelson, 1984). The Atlantic spadefish *(Chaetodipterus faber)* is the only member of this family in the western Atlantic Ocean. Rare north of Chesapeake Bay, Atlantic spadefish inhabit coastal waters which extend southward to Brazil (Johnson, 1978). Historically, Atlantic spadefish represented a relatively minor portion of recreational fisheries. Nevertheless, fishing tournaments are currently being used to stimulate interest in their fisheries (Schmied and Burgess, 1987). Ryder (1887) described eggs and yolk-sac larvae of Atlantic spadefish, but Johnson (1978) questioned the identity of these specimens. Larvae ≥2.5 mm standard length (SL) are described and illustrated by Hildebrand and Cable (1938), but this study is insufficient to examine important developmental details and is based on the static rather than dynamic approach to larval description (Berry and Richards, 1973). Finucane et al.[1] illustrated 5.1- and 6.4-mm SL Atlantic spadefish. Johnson (1984) commented on cranial morphology and provided insight on the value of larval characters in resolving the relations among ephippids and their relation to other families. Aspects of juvenile and adult life history are discussed for Atlantic spadefish from South Carolina waters (Hayse, 1990), but the distribution, abundance, and seasonal occurrence of Atlantic spadefish larvae are poorly understood. Our objectives are to redescribe the development of Atlantic spadefish larvae, discuss their relation to known larvae of other ephippid genera, and to describe the distribution, abundance, and seasonal occurrence of Atlantic spadefish larvae in the northern Gulf of Mexico (Gulf).

Materials and methods

The distribution, abundance, and seasonal occurrence of larval Atlan-

[1] Finucane, J. H., L. A. Collins, L. E. Barger, and J. D. McEachran. 1979. Ichthyoplankton/mackerel eggs and larvae. Environmental studies of the south Texas outer continental shelf, 1977. Final Rep. to Bur. Land Manage., Wash., DC, Southeast Fish. Cent., Natl. Mar. Fish. Serv., NOAA, Galveston, TX 77550, 504 p.

Manuscript accepted 19 August 1993
Fishery Bulletin 92:262–274 (1994)

* Contribution No. LSU-CFI-92-7 of Louisiana State University Coastal Fisheries Institute.

tic spadefish were determined from collections taken primarily during Southeast Area Monitoring and Assessment Program (SEAMAP) ichthyoplankton surveys of the Gulf between 1982 and 1986 (SEAMAP[2]). These years represent the first time interval for which a complete set of data were currently available. Latitude 24°30' N was the southern boundary of our study area in the eastern Gulf, a cutoff which approximates the continental shelf break off the southern tip of Florida. Latitude 26°00' N was the southern boundary of the central and western Gulf. These coordinates approximate the U.S. Exclusive Economic Zone (EEZ)/Fishery Conservation Zone (FCZ).

Standard ichthyoplankton survey techniques as outlined by Smith and Richardson (1977) were employed in data collection. Stations sampled by National Marine Fisheries Service (NMFS) vessels were arranged in a systematic grid of about 55–km intervals. NMFS vessels primarily sampled waters >10 m deep. Each cooperating state had its own sampling grid and primarily sampled their coastal waters. Hauls were continuous and made with a 60–cm bongo net (0.333–mm mesh) towed obliquely from within 5 m of the bottom or from a maximum depth of 200 m. A flowmeter was mounted in the mouth of each net to estimate volume of water filtered. Ship speed was about 0.75 m/sec; net retrieval was 20 m/min. At stations <95 m deep, tow retrieval was modified to extend a minimum of 10 minutes in clear water or 5 minutes in turbid water. Tows were made during both day and night depending on when the ship occupied the station. Overall, 1,823 bongo net tows were made between 1982 and 1986. The SEAMAP effort between 1982 and 1984 also involved the collection and processing of 814 neuston samples taken with an unmetered 1×2 m net (0.947–mm mesh) towed at the surface for 10 minutes at each station. SEAMAP sampling during April and May was conducted primarily off the continental shelf; sampling during March, and from June through December, was conducted primarily over the shelf at stations <180 m deep. Additional information on the spatial and temporal coverage of SEAMAP plankton surveys is found in Stuntz et al. (1985), Thompson and Bane (1986, a and b), Thompson et al. (1988), and Sanders et al. (1990). Atlantic spadefish larvae were also obtained from surface-towed 1×2 m neuston net collections (0.947–mm mesh, 71 samples) made by the National Marine Fisheries Service (NMFS, Panama City, Florida) during August 1988. These NMFS collections were associated with riverine/oceanic frontal zones off the Mississippi River delta. Frontal zones near the delta were not sampled during either June or July.

A detailed examination of Atlantic spadefish larvae was made to describe developmental morphology. Body measurements were made on 21 Atlantic spadefish larvae between 1.9 and 12.5 mm (Table 1) and follow Hubbs and Lagler (1958) and Richardson and Laroche (1979). Measurements were made to the nearest 0.1 mm with an ocular micrometer in a dissecting microscope. We follow Leis and Trnski's (1989) criteria for defining length of preopercular spines, body depth, head length, eye diameter, and the eye diameter/head length ratio. We consider notochord length in preflexion and flexion larvae synonymous with SL in postflexion larvae and report all lengths as SL unless otherwise noted. Specimens were field-fixed in 10% formalin and later transferred to 70% ethyl alcohol. Terminology for

[2] SEAMAP. 1983–1987. (plankton). ASCII characters. Data for 1982–1986. Fisheries-independent survey data/National Marine Fisheries Service, Southeast Fisheries Center: Gulf States Marine Fisheries Commission, Ocean Springs, MS (producer).

Table 1

Morphometrics of larval Atlantic spadefish (*Chaetodipterus faber*) from the northern Gulf of Mexico. Measurements are expressed as % standard length (SL) and rounded to the nearest whole number

SL	*N*	Preanal length	Head length	Snout length	Orbit diameter	Body depth pectoral	Prepelvic distance
1.8–2.9	3	42–55	21–31	3–8	13–15	34–44	—
3.0–4.9	3	54–65	35–43	5–7	15–17	50–60	30–36
5.0–6.9	4	60–61	30–42	5–6	15–18	56–63	30–35
7.0–8.9	4	61–64	35–39	7–9	14	55–64	27–37
9.0–10.9	4	59–61	34–35	6–8	13–14	60–65	27–34
11.0–11.9	2	54–56	34–35	7–9	14	60–65	27
12.5	1	60	36	8	14	68	36

location of head spines followed Gregory (1933). One larva was cleared with trypsin then stained with alizarin in each millimeter (mm) length interval to examine small serrate ridges around the orbit (i.e. circumorbital bones), and spines and ridges on the head. We examined spines on the occipital and frontal bones with a scanning electron microscope (SEM), and specialized spinous scales with a compound microscope. Fin rays were counted when first segmented and spines when present. Representative specimens were illustrated with the aid of a camera lucida.

Estimates of larval density (number of larvae/100m^3 of water) and catch (number of larvae/10 tow) were calculated by month. Months were combined across years because not all months were sampled every year (Appendix Table). Densities for stations where larvae were collected (i.e. positive catch stations) were calculated by dividing sum of larvae collected in bongo net tows by total positive catch station volume of water filtered (VWF) and multiplying the result by 100. In addition, an overall (i.e. grand) density estimate was calculated by dividing sum of larvae by total VWF for all stations sampled that month and multiplying the result by 100. Overall density more closely reflects the density of larvae throughout the area by including the total volume of water filtered in calculations. Estimates of larval catch in neuston nets were calculated by dividing sum of larvae by number of positive catch neuston stations or by total number of neuston stations sampled and multiplying the result by 10. Estimates of larval density and catch included stations at long. ≥88°00' W because only one Atlantic spadefish larva was collected east of Mobile Bay, Alabama. Similarly, estimates were calculated only for June through August because May and September had but one positive catch station each.

Temperature and salinity data were gathered from the sea surface. Positive catch station hydrographic data were multiplied by total number of larvae collected at each station to obtain a monthly median and mean. Hydrographic data were also combined across months to obtain an overall (i.e. grand) median and mean. This method gives weight to distribution of larvae rather than to distribution of stations. We used a percent cumulative frequency of ≥85% for defining the relation between distribution of Atlantic spadefish larvae and water temperature, salinity, and station depth. Percent frequency indicates the range of hydrographic conditions most often associated with occurrences of larvae. Proc Univariate was used to calculate median, mean, and percent cumulative frequency statistics (SAS Institute, 1985).

Results

Morphometrics and pigmentation

Early larvae were rotund and deep-bodied; body depth was >50% SL by 3.5 mm and ≥60% by 9 mm (Table 1). Atlantic spadefish became increasingly deep-bodied and laterally compressed after notochord flexion. There were 24 myomeres but these became obscured by pigment in postflexion larvae. The head was large and averaged about 35% SL in larvae >3.0 mm. Head profile became steep and increasingly deeper than long. The mouth was terminal and the upper jaw reached to about mid-eye. Eyes were round and large, ranging from 36 to 43% of head length in larvae >3.5 mm (i.e. about 14–15% SL). The gut was tightly coiled in a single loop and the anus was slightly beyond mid-body (usually 55–60% SL).

Pigment was largely restricted to the anterior-half of the body in early preflexion larvae of Atlantic spadefish. On the head of a 1.8-mm larva, external pigment was scattered over the mid- and hindbrain, nape, opercle, branchiostegal membrane, and along the isthmus and quadrate. Internally, pigment was present along and above the anterior portion of the notochord, and a single median patch was observed on the roof of the mouth. On the abdomen, there was a patch of pigment on the visceral mass immediately anterior to and below the pectoral-fin base. In addition, melanophores were scattered over the pectoral fin base and its finfold and were distributed laterally over the visceral mass and hindgut. A row of about 20–25 small, closely spaced melanophores were visible along the ventral midline of the tail in early larvae. Number of melanophores along the ventral midline of the tail decreased as larvae grew. Melanophores on the nape, opercle, pectoral-fin base, and visceral mass formed a "swath" of pigment over the anterior 55–60% of the body by 2.5–3.0 mm (Fig. 1). By 3.0–3.5 mm, internal melanophores were visible anteriorly on the forebrain and laterally on the midbrain above the eye. Melanophores were also scattered both internally and externally over the hindbrain both anterior to and posterior to the base of the supraoccipital crest. By early postflexion (i.e. 5.0 mm), the head and abdomen were densely pigmented but the posterior portion of the body was sparsely pigmented. Pigmentation increased on the posterior-half of the body as larvae grew, and by 10.0 mm the entire body was pigmented (Fig. 1). Consolidation of pigment into bands began on the head of Atlantic spadefish larvae with one band visible above the eye by 10.0–11.0 mm. This band of pigment was enclosed by indefinite, pale crossbars. The

anterior pale crossbar was situated above the middle of the eye and the posterior crossbar was behind the eye, extending mid-way down the preopercle. Larvae <12.5 mm had only one band of pigment (Fig. 1).

The pelvics were the first fins to have pigment. Pelvic fin buds were pigmented by 4.0 mm; the pelvics were densely pigmented thereafter. Pigment appeared on the pectoral fin along the proximal portion of the rays at about 4.0–4.5 mm. Melanophores were lightly scattered over the pectoral fin in the largest specimen examined (Fig. 1). Melanophores were scattered over the membrane covering the anterior-most dorsal spines by about 6.0 mm and the anal spines by about 8.0 mm. Melanophores were added along the dorsal and anal fins as larvae developed, covering the proximal-third of each soft ray in the largest specimen examined. Pigment was present along the proximal portion of the central rays of the caudal fin by 11.0 mm (Fig. 1).

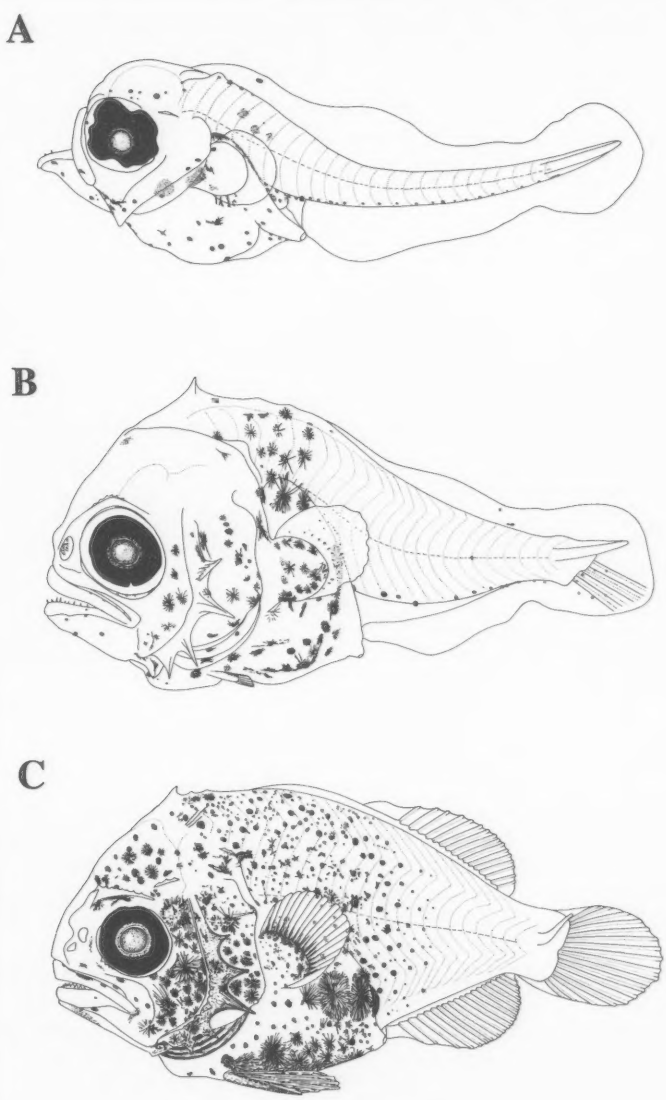

Figure 1

Larval development of Atlantic spadefish, *Chaetodipterus faber,* from the northern Gulf of Mexico. (**A**)1.8 mm; (**B**) 3.5 mm; (**C**) 5.0 mm; (**D**) 7.0 mm; (**E**) 11.6 mm. All measurements are standard length (SL).

Head and body spination

Atlantic spadefish larvae develop two series of preopercular spines, one along the posterior margin of the outer shelf and the other along the inner shelf. Both the outer and inner shelf have dorsal and ventral limbs. Three preopercular spines were present along the outer shelf of a 1.8-mm larva, the largest of which was present at its preopercular angle (Fig. 1). A fourth and a fifth spine were added by 3.5 mm, one dorsal and one ventral to the angle of the preopercle. A sixth preopercular spine, smaller than the others and often difficult to locate, was present by 5.0 mm. This sixth spine was the anterior-most spine along the ventral limb of the exterior shelf and was resorbed by 11.0–12.0 mm in some specimens. One larva we examined had seven preopercular spines along the outer shelf but most had two spines along the dorsal limb, one at the angle, and three along the ventral limb (Fig. 2). Spines along the outer shelf were simple. Two to three spines were also present along the inner shelf of the preopercle by 3.5 mm. Number of spines along the inner shelf increased as larvae grew, resulting in a serrate margin (Fig. 2). A small, poorly developed opercle

spine was forming by 5.0 mm and was difficult to locate on larvae not cleared and stained. A spine also was present along the posterior margin of the interopercle near its junction with the subopercle by 6.0 mm (Fig. 2). The interopercular spine often was hidden by the large spine at the preopercular angle but was more easily located as the preopercular angle spine regressed.

Atlantic spadefish larvae have numerous spines and ridges scattered over the head. A thickened ridge was visible dorsally along the supraoccipital of 2.0-mm larvae. This thickened ridge became a small, peak-like, median supraoccipital crest with a single, dorsally directed spine by 2.5 mm. The supraoccipital spine began to regress by 5.0 mm and was resorbed by 10.0–10.5 mm. A supraorbital ridge was present by 3.5 mm. This ridge became serrate by 4.0 mm. Small serrate ridges were visible along the dorsal margin of both the lacrimal and jugal bones (i.e. first and second suborbitals; Gregory, 1933) and third suborbital bone by 5.0 mm. Spines or spinous ridges were also visible along the fourth and fifth suborbitals, dermosphenotic (i.e. sixth suborbital), posttemporal, pterotic, tabular, and supracleithral bones by 6.0 mm. The ventral margin of the jugal bone near the posterior margin of the maxillary had a single, ventrally directed spine by 7.0 mm (Fig. 2). Individual spines were also scattered over the frontal and occipital bones of young Atlantic spadefish. The bases of these spines were covered by integument so that only a portion of each spine was visible (Fig. 3). All head spines and spinous ridges were present in the largest specimen examined (12.5 mm) but were difficult to locate on larvae not cleared and stained because of heavy body pigment.

Teeth in Atlantic spadefish were placed in an inner and outer band. Teeth first appeared in a single band on the premaxillary and anteriorly on the dentary at about 2.5 mm. Teeth were pointed and closely spaced. A second band of teeth formed along the upper and lower jaws by 4.0 mm; the outer band was slightly larger than the inner band. Teeth were added along the upper and lower jaws as larvae developed (Figs. 1 and 2).

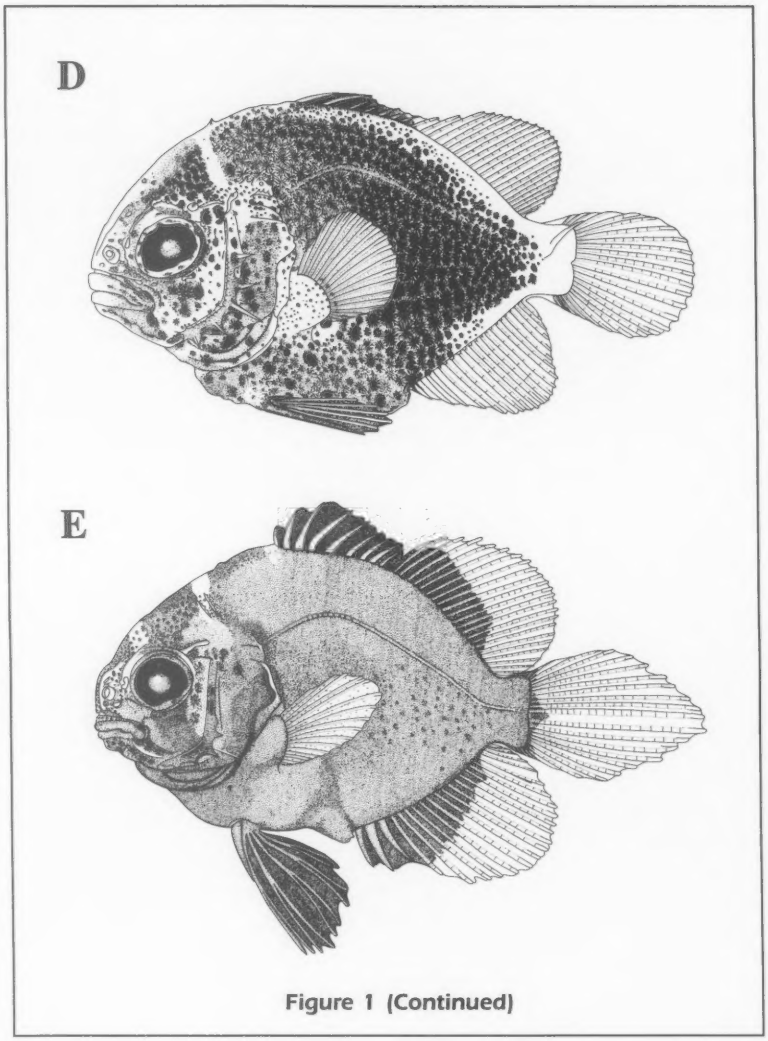

Figure 1 (Continued)

Specialized spinous scales or "pre-scales" began to develop at about 5.5 mm. Pre-scales were characterized by a single, elevated, posteriorly directed spine that was positioned near the center of the scale. Pre-scales developed first on the head and later appeared anteriorly along the lateral midline. Pre-scales were added outward toward the dorsal and ventral midlines and proceeded in a posterior direction, covering the body by 10.0 mm.

The first bones to ossify were the preopercular spines, supraoccipital crest, premaxillary, dentary, and cleithrum. Three predorsal bones (i.e. supra-

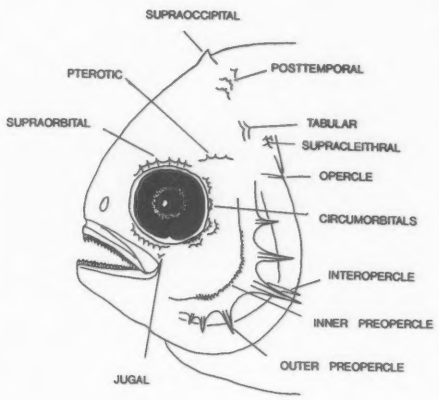

Figure 2

Location of head spines on a 7.0-mm SL larva of Atlantic spadefish, *Chaetodipterus faber*, from the northern Gulf of Mexico.

neurals) were ossifying by 6.0 mm. The anteriormost precaudal vertebrae and dorsal- and anal-fin pterygiophores ossified first; ossification proceeded posteriorly. All caudal bones were ossifying by 8.0 mm. Six branchiostegal rays and 10+14 vertebrae were present in all cleared and stained specimens.

Fin development

A continuous median finfold extended around the body from the nape to the anus of early larvae. Fin ray anlagen began forming obliquely downward in the caudal finfold during flexion (usually 3.5–4.5 mm). Caudal-fin ray development proceeded outward from mid-base as the hypural complex shifted to a terminal position, with the adult complement of 9+8 principal rays attained at about 6.0 mm (Table 2). Development of the dorsal- and anal-fin bases coincided with notochord flexion. Both fin bases and their ray anlagen began to differentiate near mid-fin; development proceeded outward from mid-fin. All dorsal and anal soft rays were present by about 7.0 mm. Soft dorsal and anal fin ray complements were present before their spines (Table 2); dorsal and anal spines developed in an anterior

Figure 3

Scanning electromicrograph of the frontal and occipital spines of a 7.0-mm SL Atlantic spadefish, *Chaetodipterus faber*. Epithelium was partially digested with trypsin to enhance visibility of frontal and occipital spines. Magnification: 140×.

to posterior direction. Pelvic fins were precocious and heavily pigmented. Pelvic buds were visible by 4.0 mm; pelvics had a full complement of elements (I, 5) by 6.0 mm. Pectoral rays began to develop by 5.0 mm and a full complement (17) was present by 8.0 mm. Sequence of fin completion was pelvics – soft dorsal and anal rays – dorsal spines – pectorals. A full complement of elements in all fins by 8.0–8.5 mm marked the beginning of transition to the juvenile stage (Table 2).

Table 2

Fin-ray counts of larval Atlantic spadefish *(Chaetodipterus faber)* from the northern Gulf of Mexico.

Length (mm SL)[1]	Dorsal	Anal	Pectoral	Pelvic	Caudal
4.3	III, Anlagen	8	Anlagen	Anlagen	0–7+7–0
5.0	III, 14	11	7	4	0–6+6–0
6.1	VII, 24	II, 17	13	I, 5	3–9+8–3
7.0	VII, 23	II, 18	16	I, 5	4–9+8–5
8.3	IX, 21	III, 17	17	I, 5	4–9+8–4
9.3	IX, 21	III, 18	17	I, 5	5–9+8–4
10.0	VIII, 23	III, 18	17	I, 5	5–9+8–5

[1] One larva of each length.

Temporal and spatial distribution

Alantic spadefish larvae were collected from May through September primarily in the north-central Gulf. Larvae were usually collected between June and August, density being highest during June and catch highest during August (Table 3). Larval Atlantic spadefish were especially abundant near the Mississippi River delta during August 1988, when 19 of 72 neuston tows (26%) associated with riverine frontal zones collected larvae. During August 1984, however, <5% of neuston tows (n=162) from other areas of the north-central and western Gulf not associated with the delta captured larvae. Only one Atlantic spadefish larva was collected east of Mobile Bay, Alabama (long. 88°00' W). This 4.0-mm specimen was found off Apalachicola Bay (Florida) during August 1984 at a station 13 m deep (Fig. 4). Salinity at this station (34.2 ppt) was the highest recorded with a positive catch during the study. The largest specimen collected in surface-towed nets was 12.5 mm; this observation may indicate that larvae move out of surface waters by this size.

Table 3

Density (number of larvae/100 m^3) and catch (number of larvae/10 neuston tows) of Atlantic spadefish larvae (*Chaetodipterus faber*) from the northern Gulf of Mexico. Months are combined across years (1982–1986, and August 1988). Not all months were sampled each year. Numbers in parentheses are positive catch stations over total stations sampled by month. Monthly density estimates were calculated by dividing sum of larvae by either sum of volume water filtered (VWF) overall, or sum of positive station VWF. Monthly catch estimates were calculated by dividing sum of larvae by number of stations sampled overall or by number of positive catch stations.

Gear	June	July	August
Bongo			
Overall density	0.3[1]	<0.1[2, 3]	<0.1[4, 5]
Positive density	6.2 (19/341)	1.3 (4/134)	1.5 (4/221)
Neuston			
Overall catch	4.0	0.4	17.0
Positive catch	42.6 (19/201)	13.3 (3/92)	131.6 (32/248)

[1] Total VWF – 43,730 m^3, positive catch station VWF – 1,799 m^3, number of larvae collected was 111.
[2] 0.02/100 m^3.
[3] Total VWF – 22,207 m^3, positive catch station VWF – 381 m^3, number of larvae collected was 5.
[4] 0.03/100 m^3.
[5] Total VWF – 35,174 m^3, positive catch station VWF – 796 m^3, number of larvae collected was 12.

Overall, ≥85% of Atlantic spadefish larvae were collected in surface waters ≥28.0°C (median: 28.1°C, mean: 28.7°C, range: 25.0°–32.2°C), at salinities between 26.7 and 31.3 ppt (median: 28.8 ppt, mean: 28.4 ppt, range: 11.8–34.2 ppt), and at station depths <238 m (median: 83 m, mean: 139 m, range: 9–470 m) (Fig. 5). However, distribution of larvae versus station depth was strongly influenced by two very large neuston-net collections of 192 and 64 larvae during August 1985 which represented 40% of all larval Atlantic spadefish taken. These two stations were located in waters near the shelf edge, 50 and 75 km east of the Mississippi River delta (28.1°C, 30.1 ppt, 235 m deep; 27.9°C, 28.1 ppt, 238 m deep, respectively). Other stations had 27 or fewer larvae. Distribution of larvae versus station depth without the two large collections shifted median station depth

shoreward from 83 to 26 m; larvae may, therefore, primarily inhabit coastal waters. This shoreward shift in median station depth was reinforced by distribution of larvae in bongo net tows and by distribution of larvae during June and July (Fig. 4, Table 4). About 86% of all Atlantic spadefish larvae collected in bongo net tows (n=128) were from waters ≤25 m deep. In addition, distribution of larvae during June and July was shoreward of that during August. Similarly, 51% of all stations where larvae were collected (i.e. 41 of 81) were inside 25 m; 64% were inside 50 m. Only 14% of positive catch stations were located beyond the 100 m isobath; most of these stations were near the Mississippi River delta, an area with a narrow shelf and rapidly increasing water depths.

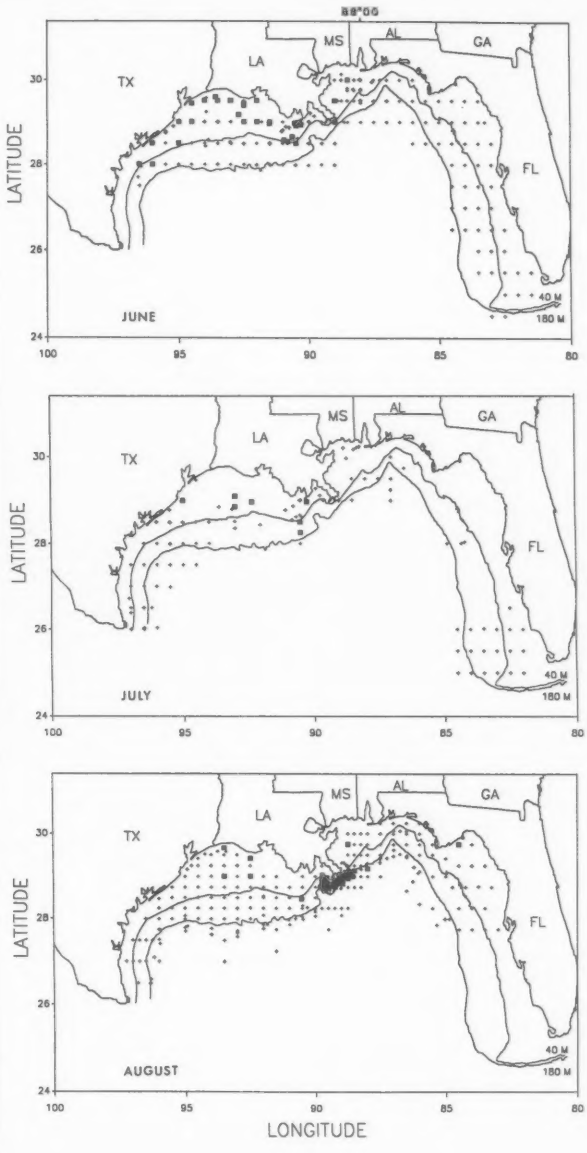

Figure 4

Distribution of Atlantic spadefish larvae (*Chaetodipterus faber*) in the northern Gulf of Mexico by month. Months are combined across years (1982–1986, and August 1988). Not all months sampled each year. Plus (+) signs are total stations sampled and squares are positive catch stations. Distribution of stations are for both bongo and neuston net tows.

Discussion

Our observations on the morphological development of Atlantic spadefish larvae generally agree with Hildebrand and Cable (1938). These authors, however, do not discuss pigment on the roof of the mouth. The presence of a single, median patch of pigment on the roof of the mouth is helpful in identifying early Atlantic spadefish larvae before the supraoccipital crest is clearly visible. Hildebrand and Cable (1938) do not discuss small spines or ridges along the circumorbital bones (i.e. supraorbital, suborbitals, and dermosphenotic) or tabular bone (Fig. 2) but do illustrate serrate ridges above the eye and in the pterotic region (Hildebrand and Cable, 1938, their Figs. 26 and 27). Spination on the circumorbital bones has generally been found only in those larval percoids with cranial ornamentation (Johnson, 1984). Most of these larval percoids also have other specializations, such as spinous scales and an elongate spine at the angle of the preopercle, among other characters (Johnson, 1984). Neither Hildebrand and Cable (1938) nor Johnson (1984) mention the supracleithral spines we found on Atlantic spadefish larvae (Fig. 2) and in larvae of Pacific spadefish, *Chaetodipterus zonatus* (Martinez-Pecero et al., 1990). The "short, hair-like spines on the upper surface of the head" noted by Hildebrand and Cable (1938) on 9.0-mm Atlantic spadefish larvae may be the same spines we found scattered over the frontal and occipital bones (Fig. 3). These frontal and occipital spines are difficult to see under a dissecting microscope because

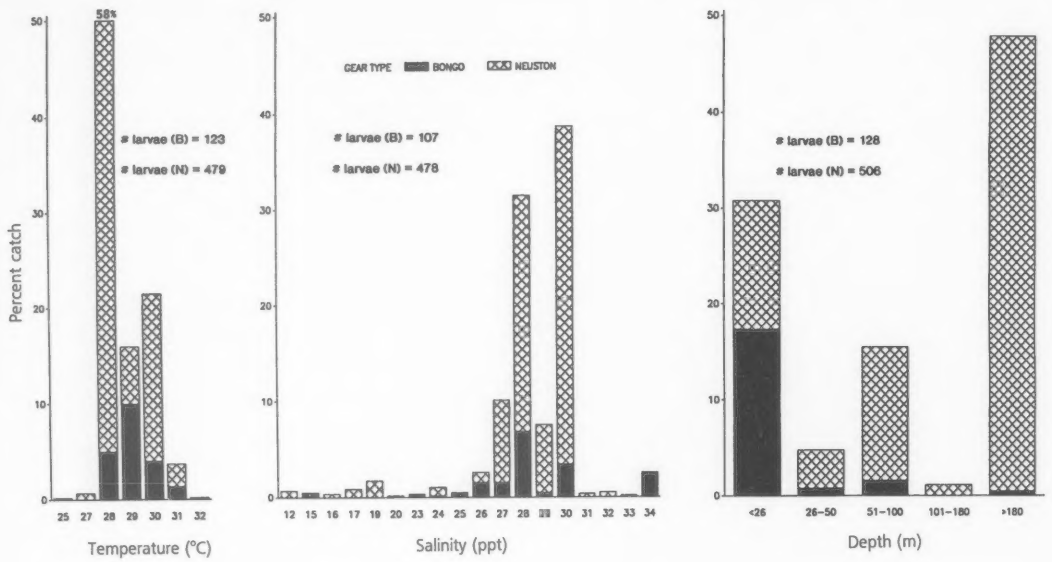

Figure 5

Summary of positive catch station hydrographic data for larval Atlantic spadefish (*Chaetodipterus faber*) from the northern Gulf of Mexico. Percent catch is sum of larvae by interval and gear divided by total number of Atlantic spadefish larvae collected overall. Discrepancies in number of larvae by month among parameters are the result of missing hydrographic data.

Table 4

Summary of hydrographic data by month for Atlantic spadefish (*Chaetodipterus faber*) larvae from the northern Gulf of Mexico. Data are from the surface and for positive catch bongo and neuston net stations only. Station hydrographic data are multiplied by total number of larvae collected at each station to obtain monthly mean and median values.[1] '*N*' is the number of larvae used to obtain mean and median values. Discrepancies in '*N*' by month among parameters resulted from missing hydrographic data.

	Water temperature (°C)				Salinity (ppt)				Station depth (m)			
	N	Mean	Median	Range	*N*	Mean	Median	Range	*N*	Mean	Median	Range
June	160	29.0	29.3	25.0–30.5	143	27.6	27.6	12.1–33.9	192	17.3	16	9–90
July	9	29.4	29.8	29.3–30.5	9	27.6	27.6	25.4–28.6	9	27.3	21	16–70
August	433	28.1	28.6	27.6–32.2	433	28.8	29.4	11.8–34.2	433	194	235	11–470

[1] This method gives weight to distribution of larvae rather than distribution of stations.

they are largely covered by integument. The supraoccipital crest was resorbed by about 10.0–10.5 mm in Gulf larvae but still present on a 11.5-mm specimen from the U. S. Atlantic coast (Hildebrand and Cable, 1938).

The identity of Ryder's (1887) yolk-sac Atlantic spadefish larvae is uncertain (Johnson, 1978). Ryder's 3.5-mm and 4.0-mm larvae lack a supraoccipital crest and preopercular spines, both of which Hildebrand and Cable (1938) and we found by 2.5 mm in Atlantic spadefish larvae. Ryder's 4.0-mm larva also has an oil globule in the yolk sac and the gut does not have the single, tightly coiled loop we found in preflexion Atlantic spadefish. Neither Hildebrand and Cable (1938) nor we found an oil globule in Atlantic spadefish larvae of 2.0 mm or

2.5 mm, respectively. Differences between Ryder's and our study do not support identification of Ryder's larvae <4.0 mm as Atlantic spadefish even if we allow for specimen shrinkage (also noted by Johnson, 1978) and for slower development times due to cooler waters of Chesapeake Bay during the summer when Atlantic spadefish spawn.

Johnson (1984) characterized the sequence of fin completion in larval Atlantic spadefish as pattern A: dorsal and anal soft rays – spinous dorsal – pelvics – pectorals. We cleared and stained seven larvae and found the sequence of fin completion more closely resembles Johnson's (1984) pattern F with all elements of the pelvic fin present before dorsal and anal soft rays. This difference in fin completion pattern, however, may be due to differences in how we and Johnson interpreted spine formation and fin completion. We counted rays when first segmented and spines when present; Johnson may have counted pterygiophores. Pattern F is found in *Hapalogenys*, Monodactylidae, and Pempheridídae (Johnson, 1984).

Larvae of Atlantic spadefish are characterized by early development of specialized spinous scales or "prescales" (at about 5.5 mm, this study) that eventually transform into adult ctenoid scales. Spinous larval scales are present to about 15.0 mm (Johnson, 1984). Ctenoid scales are well developed by 18.0 mm (Hildebrand and Cable, 1938).

Developmental morphology and head spination of Atlantic spadefish is generally similar to that of Pacific spadefish (Martinez-Pecero et al., 1990). Both species are deep-bodied (usually 55–60% SL) and preanal length is about 60% SL. Pigmentation and standard length at which fins develop also are similar; a full complement of rays is present in all fins by 8.0–9.0 mm in both species (Hildebrand and Cable, 1938; Martinez-Pecero et al., 1990; this study). However, consolidation of pigment into lateral bands, resorption of the supraoccipital crest, and the beginning of transition to the juvenile stage occur earlier in Pacific spadefish than in Atlantic spadefish. Larvae of ephippids from the Indo-Pacific region differ from *Chaetodipterus* from the western Atlantic and Pacific Oceans in extent of head spination (Leis and Trnski, 1989; Martinez-Pecero et al., 1990; this study). Larvae of *Platax* from the Indo-Pacific have a median supraoccipital crest with a serrate leading edge (Leis and Trnski, 1989) but do not have the circumorbital series of spinous ridges, nor spines on the jugal, tabular, pterotic, or supracleithral bones found in *Chaetodipterus* (Martinez-Pecero et al., 1990; this study). Head spination in *Ephippus* larvae from the Indo-Pacific is similar to that of *Chaetodipterus* and these two genera are probably more closely related than either is to *Platax*. Other species-specific head spination found in *Chaetodipterus* larvae from the western Atlantic and Pacific Oceans, and in *Ephippus orbis*, *Platax batavianus*, and three *Platax* species from the Indo-Pacific region include a posttemporal spine which may be reduced to a ridge in some species, a supraorbital ridge that varies in size among species, and one or two subopercular spines (Leis and Trnski, 1989; Martinez-Pecero et al., 1990; this study).

Early larvae of Atlantic spadefish could be confused with priacanthids, lobotids, some carangids and stromateoids, the wreckfish—*Polyprion americanus*, and *Menticirrhus* spp. because of similarities in head spination or in body pigmentation. Priacanthids have an elongate, serrate, median supraoccipital crest that extends posteriorly over the mid- and hindbrain; serrations along the lower jaw and frontal bone; and the angle preopercular spine is elongate and serrate as is the pelvic spine. Tripletail, *Lobotes surinamensis*, have a vaulted, serrate supraoccipital crest in early larvae, the pelvics are inserted behind the pectoral fins, and have fewer anal fin elements than Atlantic spadefish (Atlantic spadefish: A. III, 17–18, tripletail: A. III, 11–12). In carangids, the two anteriormost anal spines are separated from the third by a distinct gap and most species have a low, median supraoccipital crest that has serrations along the dorsal edge; other carangids lack a supraoccipital crest entirely. Some carangids also have a precocious dorsal fin with anterior spines or rays elongate, or with serrations along the angle preopercular spine. Some stromateoids (e.g. *Ariommus* spp., *Nomeus gronovii*) resemble Atlantic spadefish in early body pigmentation, body shape, and by having precocious pelvics, but stromateoids lack a median supraoccipital crest, a large preopercular angle spine, and all but *Hyperoglyphe* have >30 myomeres. *Polyprion americanus* larvae have a small, peak-like median supraoccipital crest, but with serrations along the leading edge, and lack a serrate pterotic ridge and spines on the tabular bone (Johnson, 1984). Wreckfish also have 27 myomeres, fewer dorsal (22–24) and anal fin (11–13) elements, and the mouth is larger than in Atlantic spadefish. Larval Atlantic spadefish differ from early larvae of *Menticirrhus* spp. by lack of both preopercular spines and the median supraoccipital crest in the latter.

We recently examined specimens reported by Dawson (1971) as larval black driftfish, *Hyperoglyphe bythites*. These specimens had a supraoccipital crest, pterotic ridge, spine on the interopercle, other head spination, and a pigmentation pattern identical to Atlantic spadefish. Vertebral,

dorsal, and anal fin counts overlap between black driftfish and Atlantic spadefish, but teeth are found in a single band on the dentary in black driftfish (Ginsburg, 1954) and in two bands in Atlantic spadefish (Hildebrand and Cable, 1938; this study). Dawson's 5.7–7.9 mm specimens had teeth in two bands along the dentary. Because it is unlikely that black driftfish larvae have the same suite of characters as Atlantic spadefish, Dawson's specimens should be assigned to Atlantic spadefish.

Atlantic spadefish spawn from May through September based on seasonal abundance of Atlantic spadefish larvae in the northern Gulf; peak spawning occurs between June and August (Ditty et al., 1988; this study). Density estimates were highest during June in this study (Table 3), during July in a previous study of coastal waters off central Louisiana (Ditty, 1986), and during July and August off Mississippi Sound (Stuck and Perry, 1982). Neuston net collections were greatest during August (Table 3). Gonad maturity data off South Carolina support peak spawning of Atlantic spadefish during summer (Hayse, 1990).

Spatial distribution data indicate that Atlantic spadefish larvae are apparently rare in the eastern Gulf. Only one larva was collected east of Mobile Bay (Alabama) during this study, and one larva by Houde et al.[3] in a survey of Gulf waters off Florida. In addition, distribution of both larvae and station depths where larvae were collected indicates that Atlantic spadefish occur primarily in coastal waters (Ditty and Truesdale, 1984; this study), except near the Mississippi River delta where waters may offer additional habitat suitable to larvae because of lower salinities. The relatively high number of positive stations (26%) near the delta during August 1988 sampling of frontal zones suggests that frontal zones may concentrate larvae. Frontal zone waters may also provide a richer environment for feeding and growth of larvae because of higher phytoplankton and zooplankton biomass (Govoni et al., 1989; Grimes and Finucane, 1991). However, Powell et al. (1990) were unable to demonstrate consistently that larvae have a nutritional advantage when associated with the Mississippi River plume. A possible association of Atlantic spadefish larvae with riverine frontal areas requires further study.

In conclusion, understanding the biology, life history, and relations of Atlantic spadefish requires a knowledge of the morphology, distribution, and ecology of their larvae. Larval characters (e.g. degree of head spination) may also provide insight into the interrelationships among the Ephippidae and their relationship to other families. The potential use of larval characters in defining these relationships, however, cannot be clearly understood until larval development within the family is more fully documented (Watson and Walker, 1992).

[3] Houde, E. D., J. C. Leak, C. E. Dowd, S. A. Berkeley, and W. J. Richards. 1979. Ichthyoplankton abundance and diversity in the eastern Gulf of Mexico. Univ. Miami Report BLM Contract No. AA550-CT7-28, Miami, FL 33149, 546 p.

Acknowledgments

This study was supported by the Marine Fisheries Initiative (MARFIN) Program (contract numbers: NA90AA-H-MF111 and NA90AA-H-MF727). The authors would like to thank the Southeast Area Monitoring and Assessment Program (SEAMAP) and Gulf States Marine Fisheries Commission for providing specimens and environmental data; Churchill Grimes (NMFS, Panama City Lab, Florida) for access to neuston net collections off the Mississippi River delta during August 1988; and John Lamkin (NMFS, Pascagoula, MS) for providing specimens of the reported black driftfish for examination. We also thank Laura Younger for providing scanning electromicrographs of the head spines of Atlantic spadefish larvae. Finally, we thank the reviewers for their comments in substantially improving the manuscript. Jack Javech (NMFS, Miami, FL) illustrated the larvae.

Literature cited

Berry, F. H., and W. J. Richards.
1973. Characters useful to the study of larval fishes. Mid. Atl. Coast. Fish. Cent. Tech. Pap. 1:48–65.

Dawson, C. E.
1971. Notes on juvenile black driftfish, *Hyperoglyphe bythites*, from the northern Gulf of Mexico. Copeia 1971(4):732–735.

Ditty, J. G.
1986. Ichthyoplankton in neritic waters of the northern Gulf of Mexico off Louisiana: composition, relative abundance, and seasonality. Fish. Bull. 84(4):935–946.

Ditty, J. G., and F. M. Truesdale.
1984. Ichthyoplankton surveys of nearshore Gulf waters off Louisiana: January–February and July 1976. Assoc. Southeastern Biol. Bull. 31(2):55–56.

Ditty, J. G., G. G. Zieske, and R. F. Shaw.
1988. Seasonality and depth distribution of larval fishes in the northern Gulf of Mexico above 26°00'N latitude. Fish. Bull. 86(4):811–823.

Ginsburg, I.
1954. Four new fishes and one little known species from the east coast of the United States, includ-

ing the Gulf of Mexico. J. Wash. Acad. Sci. 44:256–264.

Govoni, J. J., D. E. Hoss, and D. R. Colby.
1989. The spatial distribution of larval fishes about the Mississippi River plume. Limnol. Oceanogr. 34(1):178–187.

Gregory, W. K.
1933. Fish skulls: a study of the evolution of natural mechanisms. Trans. Am. Philos. Soc. 23:75–481.

Grimes, C. B., and J. H. Finucane.
1991. Spatial distribution and abundance of larval and juvenile fish, chlorophyll and macrozooplankton around the Mississippi River discharge plume, and the role of the plume in fish recruitment. Mar. Ecol. Prog. Ser. 75:109–119.

Hayse, J. W.
1990. Feeding habits, age, growth, and reproduction of Atlantic spadefish *Chaetodipterus faber* (Pisces: Ephippidae) in South Carolina. Fish. Bull. 88(1):67–83.

Hildebrand, S. F., and L. E. Cable.
1938. Further notes on the development and life history of some teleosts at Beaufort, N. C. Bull. U.S. Bur. Fish. 48(24):505–642.

Hubbs, C. L., and K. F. Lagler.
1958. The fishes of the Great Lakes region. Univ. Mich. Press, Ann Arbor, 213 p.

Johnson, G. D.
1978. Development of fishes of the mid-Atlantic Bight, an atlas of egg, larval, and juvenile stages. Vol. IV: Carangidae through Ephippidae. U.S. Fish. Wildl. Serv.. Biol. Serv. Prog. FWS/OBS-78/12, 314 p.
1984. Percoidei: development and relationships. *In* H. G. Moser, W. J. Richards, D. M. Cohen, M. P. Fahay, A. W. Kendall Jr., and S. L. Richardson (eds.), Ontogeny and systematics of fishes, p. 464–498. Am. Soc. Ichthy. Herp., Spec. Publ. No. 1.

Leis, J. M., and T. Trnski.
1989. The larvae of Indo-Pacific shorefishes. Univ. Hawaii Press, Honolulu, 371 p.

Martinez-Pecero, R., E. Matus-Nivon, R. Ramirez-Sevilla, D. E. Hernandez-Ceballos, and M. Contreras-Olguin.
1990. Huevo, larva y juvenil del peluquero *Chaetodipterus zonatus* (Girard) (Pisces: Ephippididae). Rev. Biol. Trop. 38(1):71–78. (In Spanish.)

Nelson, J. S.
1984. Fishes of the world, 2nd ed. John Wiley & Sons, NY, 523 p.

Powell, A. B., A. J. Chester, J. J. Govoni, and S. M. Warlen.
1990. Nutritional condition of spot larvae associated with the Mississippi River plume. Trans. Am. Fish. Soc. 119:957–965.

Richardson, S. L., and W. A. Laroche.
1979. Development and occurrence of larvae and juveniles of the rockfishes *Sebastes crameri, Sebastes pinniger*, and *Sebastes helvomaculatus* (family Scorpaenidae) off Oregon. Fish. Bull. 77(1):1–46.

Ryder, J. A.
1887. On the development of osseous fishes, including marine and freshwater forms. Rep. U.S. Fish. Comm., Part 13, 1885 (1887):489–604.

Sanders, N., Jr., T. Van Devender, and P. A. Thompson.
1990. SEAMAP environmental and biological atlas of the Gulf of Mexico, 1986. Gulf States Marine Fish. Comm., Ocean Springs, MS, No. 20, 328 p.

SAS Institute, Inc.
1985. SAS User's Guide: statistics, 1985 ed. SAS Institute, Cary, NC, 584 p.

Schmied, R. L., and E. E. Burgess.
1987. Marine recreational fisheries in the southeastern United States: an overview. Mar. Fish. Rev. 49(2):1–7.

Smith, P. E., and S. L. Richardson.
1977. Standard techniques for pelagic fish egg and larva surveys. FAO Fish. Tech. Paper No. 175, 100 p.

Stuck, K. C., and H. M. Perry.
1982. Ichthyoplankton community structure in Mississippi coastal waters. *In* Fishery monitoring and assessment completion report, 1 January 1977 to 31 December 1981, p. VI-I-1 thru VI-I-53. Gulf Coast Res. Lab. (Ocean Springs, MS), Proj. No. 2-296-R.

Stuntz, W. E., C. E. Bryan, K. Savastano, R. S. Waller, and P. A. Thompson.
1985. SEAMAP environmental and biological atlas of the Gulf of Mexico, 1982. Gulf States Marine Fish. Comm., Ocean Springs, MS, No. 12, 145 p.

Thompson, P. A., and N. Bane.
1986a. SEAMAP environmental and biological atlas of the Gulf of Mexico, 1983. Gulf States Marine Fish. Comm., Ocean Springs, MS, No. 13, 179 p.
1986b. SEAMAP environmental and biological atlas of the Gulf of Mexico, 1984. Gulf States Marine Fish. Comm., Ocean Springs, MS, No. 15, 171 p.

Thompson, P. A., T. Van Devender, and N. J. Sanders Jr.
1988. SEAMAP environmental and biological atlas of the Gulf of Mexico, 1985. Gulf States Marine Fish. Comm., Ocean Springs, MS, No. 17, 338 p.

Watson, W., and H. J. Walker Jr.
1992. Larval development of sargo *(Anisotremus davidsonii)* and salema *(Xenistius californiensis)* (Pisces: Haemulidae) from the Southern California Bight. Bull. Mar. Sci. 51(3):360–406.

Appendix Table

Summary of total number of bongo net/neuston net stations examined for Atlantic spadefish larvae (*Chaetodipterus faber*) in the Gulf of Mexico. Acronyms are as follows: SEAMAP - Southeast Area Monitoring and Assessment Program; NMFS - National Marine Fisheries Service, Panama City, Florida. NS means no samples.

	Mar	Apr	May	Jun	Jul	Aug	Sep	Oct	Nov	Dec
SEAMAP										
1982	77[1]/0[2]	69/68	71/73	102/100	26/24	NS	NS	3/8	29/3	NS
1983	15/13	27/27	84/84	55/45	44/42	NS	NS	39/26	NS	24/23
1984	23/0	44/0	46/0	55/54	20/26	155/162	NS	24/0	6/0	36/36
1985	29/0	NS	NS	85/0	39/0	69/0	20/0	4/0	2/0	24/0
1986	NS	24/0	90/0	57/0	10/0	NS	145/0	43/0	73/0	24/0
Total	144/13	164/95	291/157	354/199	139/92	224/162	165/0	113/34	110/3	108/59
NMFS[2]										
1988	55	71	36							

[1] 60-cm bongo net, 0.333-mm mesh, oblique-tow from depth.
[2] 1 × 2 m neuston net, 0.947-mm mesh, 10 min. surface-tow, unmetered.

Larval development, distribution, and abundance of common dolphin, *Coryphaena hippurus*, and pompano dolphin, *C. equiselis* (family: Coryphaenidae), in the northern Gulf of Mexico*

James G. Ditty
Richard F. Shaw
Coastal Fisheries Institute, Center for Coastal, Energy, and Environmental Resources
Louisiana State University, Baton Rouge, LA 70803

Churchill B. Grimes
Southeast Fisheries Science Center, National Marine Fisheries Service, NOAA
Panama City Laboratory, 3500 Delwood Beach Road
Panama City, FL 32408

Joseph S. Cope
Coastal Fisheries Institute, Center for Coastal , Energy, and Environmental Resources
Louisiana State University, Baton Rouge, LA 70803

Abstract.— Dolphinfishes are highly prized commercial and recreational species of worldwide distribution in tropical and subtropical seas, but the development and distribution of their larvae are poorly understood. Common dolphin eggs hatch in about 38 hours at 25°C based on a predictive relationship among egg diameter, water temperature, and development time. Morphometrics are generally greater in pompano dolphin than in common dolphin. Pompano dolphin are deeper–bodied and have a larger eye by 9 mm, and a larger mouth and longer pre-anal length by about 13 mm. Differences in pigment along the caudal peduncle and its finfold separate common dolphin from pompano dolphin <4.0–4.5 mm SL; common dolphin lack pigment in these areas. Number of spines along the outer shelf of the preopercle also separate species although preopercle spines are often difficult to count on larvae not cleared and stained; common dolphin have four spines along the outer preopercular shelf and pompano dolphin have five. Pigmented pelvic fins and bands of pigment laterally on both the body and median fins of common dolphin are diagnostic for separating species >8 mm SL; pompano dolphin lack these characters. Both common dolphin and pompano dolphin larvae usually are found at ≥24°C, ≥33 ppt, and beyond the 50 m isobath. Preflexion larvae (<7.0–7.5 mm SL) were primarily collected in oceanic waters. Both species may spawn year–round, at least in the southern part of the survey area. Larval common dolphin are significantly more abundant than pompano dolphin.

The dolphinfishes, *Coryphaena hippurus* (common dolphin) and *C. equiselis* (pompano dolphin), are distributed worldwide in tropical and subtropical seas (Briggs, 1960). Highly prized as food, these fishes are important recreational and commercial species, but relatively little is known about their early life stages. Gibbs and Collette (1959) reviewed spawning and adult seasonal distribution for the western North Atlantic Ocean, and Palko et al. (1982) compiled dolphinfish biological data. Aoki and Ueyanagi (1989) discussed larval and early juvenile distribution for the eastern Pacific, and similar information is available for the western Pacific and Indian oceans (Shcherbachev, 1973). Preliminary distribution maps are available for the Gulf of Mexico (Gulf), but associated environmental data are not included (Richards et al., 1984; Kelley et al., 1986). Embryonic development is described for common dolphin (Mito, 1960; Hassler and Rainville, 1975; Hagood and Rothwell[1]) and osteological development for both species (Potthoff, 1980), but descriptive larval morphology is primarily limited to sizes >13 mm SL (Gibbs and Collette, 1959; Shcherbachev, 1973). Okiyama (1988) and Aoki and Ueyanagi (1989) provide information on developmental morphology of Pacific specimens <13 mm SL, but their illustrations are

[1] Hagood, R. W., and G. N. Rothwell. 1979. Sea Grant interim project report—1979. Aquaculture in tropical ocean—*Coryphaena* sp. Oceanic Inst., Makapuu Point, Waimanalo, HI 96795.

Manuscript accepted: 20 October 1993
Fishery Bulletin 92:275–291 (1994).

*Contribution No. LSU-CFI-92-5 of Louisiana State University Coastal Fisheries Institute.

insufficient to examine important details, and Okiyama's study is a general overview of exisitng information. The utility of early life stages of *Coryphaena* in examining previous phylogenetic hypotheses and evolutionary interrelationships of echeneoids (i.e. Coryphaenidae-Rachycentridae-Echeneididae) is discussed by Johnson (1984). Our objectives are 1) to describe and compare early larval development of common dolphin and pompano dolphin using the dynamic approach to larval description (Berry and Richards, 1973) and 2) to describe the spatial and temporal distribution and abundance of early life stages of dolphinfishes in the northern Gulf.

Materials and methods

Seasonal occurrence, distribution, and abundance of dolphinfish larvae were determined primarily from 814 neuston net collections taken during Southeast Area Monitoring and Assessment Program (SEAMAP) ichthyoplankton surveys of the Gulf between 1982 and 1984 (1982–276 stations, 1983–260, 1984–278). These years represent the first time interval for which a complete set of data was currently available. SEAMAP collections were made with an unmetered 1×2 m net (0.947-mm mesh) towed at the surface for 10 minutes at each station. The SEAMAP effort also involved the collection and processing of about 1,819 bongo net stations between 1982 and 1986 (1982–384 stations, 1983–288, 1984–409, 1985–272, and 1986–466) (SEAMAP 1983–1987)[2]. Bongo nets (60-cm net, 0.333-mm mesh) were towed obliquely to the surface from within 5 m of the bottom or from a maximum depth of 200 m. Sampling during April and May was primarily beyond the continental shelf, and that during March and from June to November was primarily over the shelf at stations <180 m depth. No samples were taken during January and February. Tows were made during both day and night depending on when the ship occupied the station. Latitude 24°30'N was the southern boundary of our survey area in the eastern Gulf and latitude 26°00'N the southern boundary of the central and western Gulf (Appendix Fig. 1). These coordinates approximate the U.S. Exclusive Economic Zone (EEZ)/Fishery Conservation Zone (FCZ). Additional information on temporal and spatial coverage of SEAMAP plankton surveys are found in Stuntz et al. (1985), Thompson and Bane (1986, a and b), Thompson et al. (1988), and Sanders et al. (1990).

Ichthyoplankton collections were also examined from riverine/oceanic frontal zones off the Mississippi River delta. These collections were from surface-towed 1×2 m neuston nets (0.947-mm mesh, 10–min. tows, sample n=311) and were obtained from the National Marine Fisheries Service (NMFS), Panama City, Florida (i.e. May 1988 [55 neuston samples]; August 1988 [71]; September 1986 [46], 1987 [68], and 1989 [35]; and December 1988 [36]).

A detailed examination of dolphinfish larvae was made to describe developmental morphology. We examined 25 common dolphin and 19 pompano dolphin larvae between 3.5 and 15.0 mm SL for differences in pigmentation, developmental morphology, and head spination, but only cursorily discuss fin development because of a thorough review of these structures by Potthoff (1980). Body measurements were made to the nearest 0.1 mm with a dissecting scope and ocular micrometer following Hubbs and Lagler (1958) and Richardson and Laroche (1979). We follow Leis and Trnski's (1989) criteria for defining length of preopercular spines, body depth, head length, and eye diameter. We consider notochord length in preflexion and flexion larvae synonymous with standard length (SL) in postflexion larvae and report all lengths as SL unless otherwise noted. Specimens were field-fixed in 10% formalin and later transferred to 70% ethyl alcohol. We used a compound scope to examine origin and location of epithelial spicules and the maxillary spine. Juveniles are those >25 mm, when specimens usually have developed a full complement of rays in all fins and scales (Johnson, 1984). Representative specimens were illustrated with a camera lucida (Figs. 1 and 2). Only three pompano dolphin <4 mm were collected and these were in too poor a condition to illustrate.

Estimates of larval catch (number of larvae/neuston tow) were calculated for each station. Mean catch estimates by month and season were calculated by dividing the sum of larvae (by species) by the total number of stations sampled within each category (month, season, etc.) and multiplying the result by 10 (number of larvae/10 neuston tows). Mean catch more closely reflects the abundance of larvae throughout the area by including total sampling effort in calculations. Catch was combined by month and by season across years. Seasons were defined as follows: spring=March to May; summer=June to August; and fall=September to November (Appendix Fig. 2).

Nonparametric tests were used to evaluate diel, seasonal, and overall differences in catch of common

[2] SEAMAP. 1983–1987. (plankton). ASCII characters. Data for 1982–1986. Fisheries-independent survey data/National Marine Fisheries Service, Southeast Fisheries Center: Gulf States Marine Fisheries Commission, Ocean Springs, MS (producer).

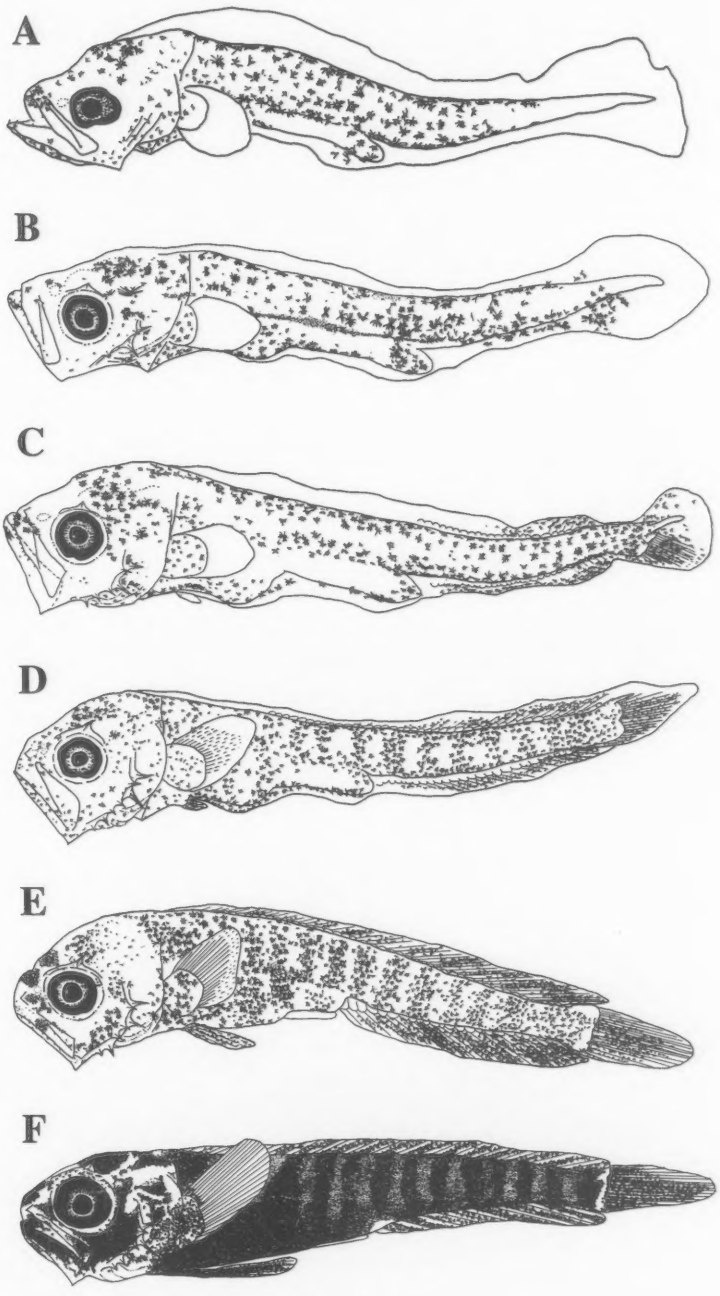

Figure 1

Larval development of common dolphin (*Coryphaena hippurus*) from the northern Gulf of Mexico. (**A**) 3.5 mm, (**B**) 5.0 mm, (**C**) 7.1 mm, (**D**) 9.5 mm, (**E**) 11.0 mm, (**F**) 14.0 mm. All measurements are in standard length (SL).

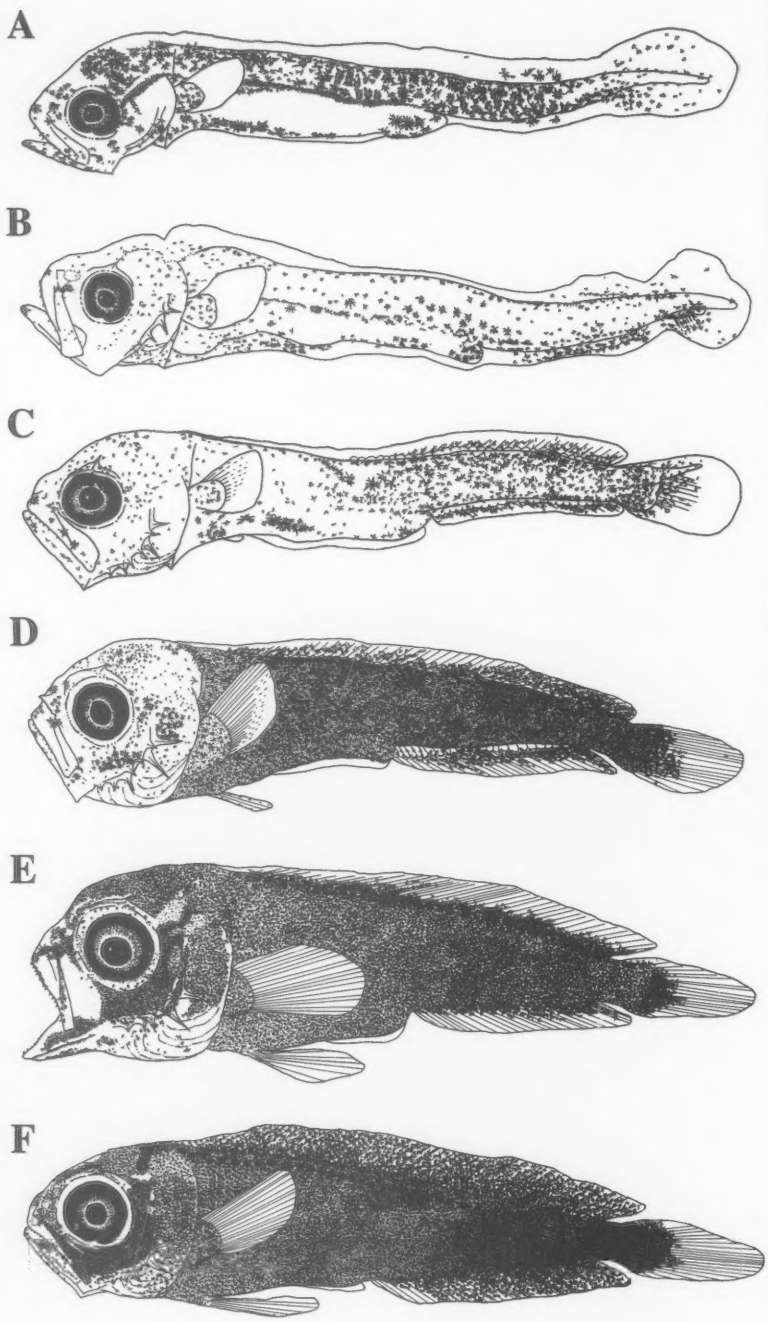

Figure 2

Larval development of pompano dolphin (*Coryphaena equiselis*) from the northern Gulf of Mexico. (**A**) 4.7 mm, (**B**) 5.5 mm, (**C**) 7.5 mm, (**D**) 9.7 mm, (**E**) 11.5 mm, (**F**) 15.0 mm. All measurements are in standard length (SL).

dolphin and pompano dolphin. Only those stations where either of the two species were present were included in analyses. A Kruskal-Wallis test was used to detect differences among groups (α=0.05) and a Tukey-type test to determine if mean differences were significant (Zar, 1984; SAS Institute, 1985). Dolphinfish >25 mm were excluded from analyses.

Temperature and salinity data were taken from the sea surface only. Hydrographic data were multiplied by number of larvae caught (by species) at each station to obtain an overall median and mean. This method gives weight to distribution of larvae rather than distribution of stations. We used a percent cumulative frequency of ≥75% for determining the relationship between distribution of dolphinfish larvae and surface water temperature, salinity, and station depth. Percent frequency indicates the range of hydrographic conditions most often associated with occurrences of larvae. Proc Univariate was used to calculate median, mean, and percent cumulative frequency statistics (SAS Institute, 1985). We divided the continental shelf into approximately equal geographic areas (i.e. into sq. km.) based on depth and designated the inner shelf as <50 m deep, outer shelf waters as those from 50 to 180 m deep, and oceanic waters as those beyond the continental shelf (i.e. >180 m).

Results

Morphology

A continuous median finfold extended posteriorly along the body of early larvae of both species from the posterior midbrain to the cleithral symphysis. Remnants of the finfold were visible ventrally along the hindgut (i.e. preanal finfold) at least through 15 mm. Minute epithelial spicules covered the body of each species by 4 mm and were best observed on the head and larval finfold. Spicules were more easily observed as larvae grew. Yolk-sac larvae <3.5 mm of common dolphin and pompano dolphin had unpigmented eyes. Preflexion larvae (<7.0–7.5 mm) of both species were elongate, with body depth usually ≤20% SL. The body became relatively deeper during flexion (about 7.5–9.0 mm) and pompano dolphin were deeper-bodied than were common dolphin by early postflexion (Table 1). The head was moderately long (i.e. between 20 and 33% SL) in both species and the snout was short and blunt. The eyes were round and larger in pompano dolphin than in common dolphin by early postflexion (Table 1). The mouth was large and oblique; upper jaw length usually ranged from 42 to 45% of head length in postflexion dolphinfish of both species. Pompano dolphin have a larger mouth than do common dolphin by 13 mm (Table 1). The foregut was partially convoluted and had a half-twist in preflexion larvae of both species and a single loop in larger larvae; the hindgut was straight. By 13 mm, however, preanal length was generally greater in pompano dolphin than in common dolphin (Table 1). Preanal length usually ranged from 60 to 65% SL during preflexion, but decreased thereafter to 55–60% SL in both species. The pelvic fins were moderately long (about 15–18% SL; Table 1) and extend to the tips of the pectorals by 12 mm. Myomeres were obscured by heavy

Table 1

Morphometrics of larval common dolphin (*Coryphaena hippurus*) and pompano dolphin (*C. equiselis*) from the northern Gulf of Mexico. Measurements are expressed as % standard length (SL).

SL (mm)	*N*	Preanal length	Head length	Snout length	Orbit diameter	Upper jaw length	Body depth cleithrum	Prepelvic distance	Pelvic length
C. hippurus									
3.5–4.9	5	57.0–65.0	23.0–25.0	4.0–6.0	9.0–10.0	11.0–12.5	16.5–18.5	—	—
5.0–6.9	4	61.0–65.0	24.0–27.0	5.0–6.0	8.0–9.5	9.0–13.0	17.0–22.0	31.0–34.0	bud
7.0–8.9	4	60.0–63.0	23.0–27.0	5.0–6.0	7.0–9.0	9.5–12.0	16.0–20.0	27.0–32.5	bud–3.0
9.0–10.9	3	56.0–59.0	25.0–28.0	5.5–6.0	9.5–11.0	12.0–13.0	19.0–21.0	27.0–30.0	4.5–11.0
11.0–12.9	5	54.0–57.0	24.0–27.0	5.0–6.0	10.0–11.0	11.0–13.0	20.0–23.0	27.0–28.0	11.0–15.0
13.0–14.9	4	54.0–56.5	25.0–28.0	4.0–5.0	11.0–11.5	12.0–12.5	21.0–22.5	26.0–30.0	17.0–18.5
C. equiselis									
3.7–4.9	3	60.0–65.0	23.0–27.5	5.0–6.0	9.5–10.0	11.5–13.0	19.0–21.0	—	—
5.0–6.1	4	60.0–62.0	23.0–24.0	5.0–6.0	8.5–10.0	10.0–13.0	16.0–20.0	—	—
7.5–8.9	2	46.0–47.0	19.0–22.0	4.0–4.5	8.0–9.5	10.0–12.0	16.0–22.0	22.0–24.0	bud–6.0
9.0–10.9	3	56.0–60.0	27.0–30.0	4.5–5.0	12.0–12.0	12.0–15.0	25.0–29.0	30.0–35.0	8.5–14.0
11.0–12.9	4	55.0–60.0	25.0–30.0	4.0–5.0	12.0–14.0	12.0–14.0	27.0–29.0	31.0–35.0	13.0–15.0
13.0–15.0	3	55.0–60.0	27.0–30.0	4.0–5.0	13.0–13.0	13.0–15.0	25.5–28.0	28.0–34.0	16.0–18.5

pigmentation and were difficult to count on dolphinfish larvae; however, a 5.5-mm pompano dolphin had 33 myomeres and a partially cleared 11-mm common dolphin had 30 vertebrae. Only two pompano dolphin between 6.1 and 9.7 mm were collected (7.5 and 8.5 mm) and morphometrics for these larvae were considerably smaller than for the other specimens (Table 1).

Pigmentation

Dolphinfish were heavily pigmented at all sizes, except the caudal peduncle and its finfold in early preflexion larvae of common dolphin which was unpigmented (Fig. 1). In common dolphin <4 mm, the length of the unpigmented portion of the caudal peduncle was 15–20% SL. By 4.5–5.0 mm, however, pigment was present along the caudal peduncle and on the caudal finfold (Fig. 1). Early preflexion pompano dolphin <4 mm had a row of melanophores along the caudal peduncle (both dorsally and ventrally) and pigment was scattered throughout the caudal finfold (Fig. 2). On the head, pigment was scattered externally over the premaxilla, snout, and fore-, mid-, and hind-brain of early larvae of each species. Pigment also was present along the dentary, lower jaw, isthmus, branchiostegal rays, and on the roof of the mouth. On the visceral mass, melanophores were scattered over the foregut and anus of early preflexion larvae of both species but the hindgut was sparsely pigmented laterally (Figs. 1 and 2). Gut pigmentation increased with length. Vertical bands of pigment first formed along the dorsal and anal fins of common dolphin at about 8 mm. These bands of pigment subsequently extended across the body; 12 to 13 poorly formed bands were visible by 10 mm. Vertical bands became more distinct as larvae grew (Fig. 1). Bands of pigment do not form in pompano dolphin, but this species does have a row of enlarged melanophores along the body dorso- and ventro-laterally (adjacent to the dorsal and anal fin bases) by 7.5 mm, which was not present in common dolphin (Figs. 1 and 2).

Pectoral buds were present on early larvae of each species. Pigment was scattered over the pectoral axilla and was heavier on pompano dolphin than on common dolphin of similar length. The proximal portion of the upper pectoral rays of common dolphin was pigmented by 14–15 mm; no pigment was present on the pectoral rays of pompano dolphin. Dorsal- and anal-fin bases were thickening by 5 mm in pompano dolphin and by 6 mm in common dolphin; the anal-fin base developed slightly before that of the dorsal base. Both fin bases and their ray anlagen developed in a posterior to anterior direction. Pelvic-fin buds of common dolphin were present by 6.5 mm and pigmented by 7.5 mm. No pompano dolphin between 6.1 and 7.5 mm were examined, but the pelvic buds were present by 7.5 mm. The pelvic rays of pompano dolphin remained unpigmented at all sizes. Pigment occurred on the developing caudal rays of each species by early flexion. By 10 mm, all but the distal tips of the caudal rays were pigmented in common dolphin; only about the proximal third of each caudal ray was pigmented in pompano dolphin. Differences in caudal-fin pigmentation were more pronounced as larvae grew (Figs. 1 and 2).

Head and body spination

Dolphinfish larvae developed two series of preopercle spines, one series along the posterior margin of the inner shelf and the other along the outer shelf. Number and location of spines along the outer shelf of the preopercle separate larval common dolphin from pompano dolphin. Two spines were present along the margin of both the inner and outer preopercular shelves of 4-mm common dolphin, the largest spines occurring on either side of the angle of the preopercle (Figs. 1 and 2). A third spine was added along both the inner and outer shelf by 7 mm; a fourth spine was added along the outer preopercle by 10.0–10.5 mm. A total of three spines occurred along the inner and four spines along the outer shelf of the preopercle of larval common dolphin (Fig. 1). Arrangement of preopercle spines in larval pompano dolphin <4 mm was similar to that in common dolphin except three rather than two spines were visible along the outer preopercular shelf. A third spine was added along the inner shelf by 7 mm and a fourth and fifth spine along the outer shelf by 9 mm. A total of three spines occurred along the inner and five spines along the outer preopercular shelf of larval pompano dolphin (Fig. 2). Number and placement of preopercle spines were consistent through at least 15 mm in both species. All preopercle spines were simple (Figs. 1 and 2).

Dolphinfish have several spines and ridges on the head. The pterotic area was swollen in both species by 5 mm and a laterally directed spine was present along the supraorbital ridge of each frontal bone of 6-mm pompano dolphin and 7-mm common dolphin (Figs. 1 and 2). The supraorbital ridge of each species usually had a single spine, but some pompano dolphin had two or three spines along the ridge. The swollen pterotics and supraorbital spine were best observed when specimens were viewed dorsally; both features were well developed by 7.5–8.0 mm. The frontal bone was notably thicker above the eye of pompano dolphin, but the supraorbital ridge was less well developed in pompano dolphin than in common dolphin by 9.5 mm. The supraorbital spine(s)

of pompano dolphin were regressing by 11–12 mm. A small spine was present anteriorly along the maxilla of each species by 5 mm (Figs. 1 and 2). The maxillary spine (difficult to locate because of its position and size) pointed dorso-laterally and was slightly better developed in pompano dolphin than in common dolphin of similar size. A posttemporal spine was present in both species by 9 mm and was most easily observed when specimens were viewed dorsally. The anterior portion of the lacrimal bone was prominent in dolphinfish larvae; the lacrimal was more pronounced in pompano than in common dolphin by late flexion (Figs. 1D and 2D).

Minute teeth were present anteriorly on the upper and lower jaws of each species by 3.8 mm. Number and size of teeth increased with SL. A pair of canine-like teeth were present in 10-mm pompano dolphin and 11-mm common dolphin.

Spatial and temporal distribution

Larval dolphinfish were collected during all months sampled, but small larvae of both species were found primarily during warm months. Preflexion larvae of common dolphin occurred mainly from April through November. One common dolphin larva (7.0 mm) was also collected during December (21, 1983), at a station due south of Caminada Pass, Louisiana (23.5°C, station depth: 531 m). Larval pompano dolphin were collected from March through October; larvae <10 mm were collected through late September. Only one pompano dolphin larva (5 mm) was collected during March (13, 1982; water temperature: 18°C), at a bongo-net station 29 m deep off Caminada Pass, Louisiana. Two pompano dolphin larvae (18.3 and 22.5 mm) were collected during October (14 and 17, 1983), but they were probably spawned during late September.

Larvae of common dolphin and pompano dolphin were collected primarily at water temperatures ≥24°C (90% of larvae) and salinities ≥33 ppt (≥75%) (Table 2, Fig. 3). The pompano dolphin collected during March was the only larva of either species taken at <21°C. Based on water temperatures when common dolphin larvae usually occurred (≥24°C) and using Pauly and Pullin's (1988) relationship between egg diameter and water temperature to predict development time in other marine fishes, we estimate a common dolphin egg of 1.4 mean-mm diameter would hatch in about 38 hours at 25°C and 26 hours at 30°C (Table 3). Few common dolphin larvae and no pompano dolphin were collected at <25 ppt (Table 2; Fig. 3).

Larval dolphinfish of both species were widely distributed in neritic and oceanic waters of the Gulf and most were collected near the surface. Over 90% of common dolphin and about 80% of pompano dolphin occurred over the outer continental shelf and in oceanic waters; preflexion larvae were usually taken in oceanic waters (stations >180 m deep) (Appendix Fig. 3). Overall, larval common dolphin were significantly more abundant than pompano dolphin (Kruskal-Wallis, $P \leq 0.0001$, df= 362; Table 4). Larval common dolphin were also collected at more stations than were pompano dolphin (15.0% versus 5.1% of all stations sampled, respectively; Table 4). Only 3.1% of oblique bongo-net samples (1982–86, n=1819) took common dolphin larvae (no. larvae=83, length=6.5 mm, range=3.2–21.8 mm) and <0.01% captured pompano dolphin (no. larvae=10, $\bar{x}$ length=4.6 mm, range=4.0–8.7 mm).

Differences in catch of common dolphin and pompano dolphin, respectively, were not significant among seasons or between day and night. About 25% of spring and 18% of fall neuston stations collected larval common dolphin, but <9% of those stations sampled during summer (Table 4). Larval pompano dolphin were collected at 7% of spring neuston stations, 2% of summer stations, and 8% of fall stations (Table 4). Only two neuston tows collected >13 larvae of either species; these two tows ac-

Table 2

Summary of hydrographic data for common dolphin (*Coryphaena hippurus*) and pompano dolphin (*C. equiselis*) larvae collected in the northern Gulf of Mexico. Data are from the sea surface only; median values are obtained from the distribution of larvae versus the hydrographic parameter. Bongo and neuston net data are combined. '*N*' is number of larvae used in obtaining median values. Discrepancies in '*N*' result from missing values in the hydrographic data.

	Salinity (ppt)			Water temperature (°C)			Station depth (m)		
	N	Median	Range	*N*	Median	Range	*N*	Median	Range
C. hippurus	537	34.0	18.7–37.8	590	28.0	21.4–32.0	599	195	11–3475
C. equiselis	80	35.1	25.0–37.8	94	27.6	18.0–30.4	94	195	11–3325

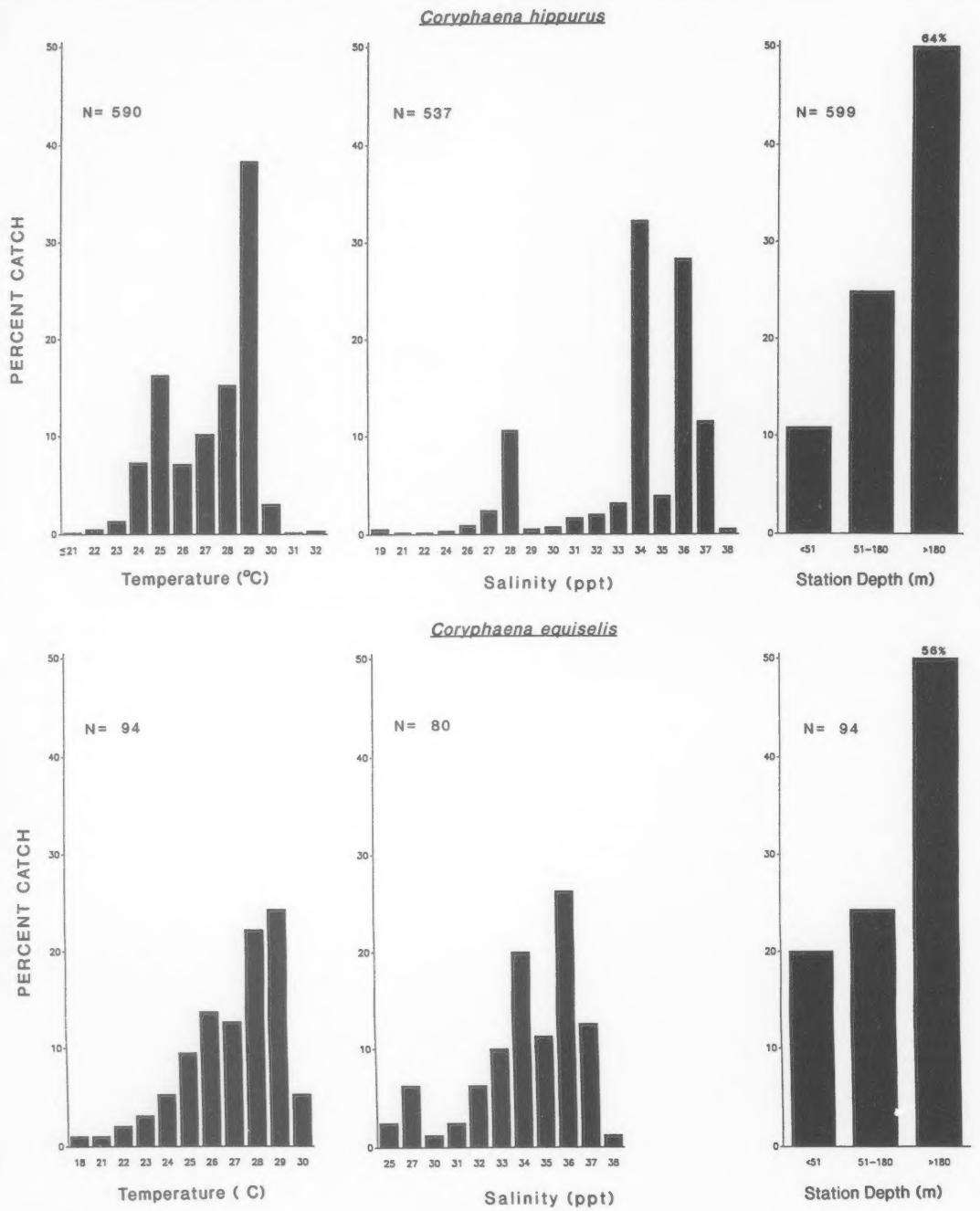

Figure 3

Summary of hydrographic data for larval common dolphin (*Coryphaena hippurus*) and pompano dolphin (*C. equiselis*) in the northern Gulf of Mexico. Data are from both bongo and neuston net tows. Hydrographic values are rounded to the nearest whole number. *N* = number of larvae. Discrepancies in '*N*' among parameters are the result of missing hydrographic data.

Table 3

Egg development time and hatching length (total length:TL) of common dolphin (*Coryphaena hippurus*).

Author	Egg diameter	°C	Hatching		Study location
			Time (hr)	TL (mm)	
Mito, 1960	1.28–1.62	21–29	48–60	3.95	Japan
Hassler and Rainville, 1975	1.3[1]	27[1]	—	3.0[2]	Atlantic
Hagood and Rothwell (see Footnote 1)	— 1.35[3]	26 26[3]	40 38[3]	— —	Hawaii Hawaii
Soichi, 1978	1.4–1.65	24–25	60	3.8–4.9[2]	Japan
Uchiyama et al., 1986	—	24–25	48–50	4.0–4.6	Hawaii
Lamadrid-Rose and Boehlert, 1988	1.52–1.66	26	54	4.3–5.4[4]	Hawaii
This study	1.4[5]	20 25 30	58[5] 38[5] 26[5]	— — —	Gulf of Mexico

[1] Mean.
[2] One-day-old larva.
[3] *C. equiselis.*
[4] Standard length.
[5] Mean egg diameter and predicted hatching times.

Table 4

Mean catch (no.larvae/10 neuston tows) of common dolphin (*Coryphaena hippurus*) and pompano dolphin (*C. equiselis*) larvae in the northern Gulf of Mexico by month. Collections for 1982–1984 are throughout the Gulf and those from 1986 to 1989 are primarily around the Mississippi River delta. Mean catch is calculated over all stations sampled by month; months are combined across years. Grand mean catch per 10 tows is calculated by dividing total number of larvae collected by all stations sampled. Numbers in parenthesis are positive catch stations over total stations sampled.

Taxa	N[1]	March	April	May	June	July	August	September	October	November	Grand Total
C. hippurus	517	0.0 (0/13)	3.4 (22/100)	7.6 (58/221)	2.9 (29/208)	0.5 (3/92)	0.5 (13/248)	13.4 (29/163)	3.9 (4/33)	16.7 (2/3)	4.8 (160/1081)
C. equiselis	85	0.8 (1/13)	1.2 (10/100)	0.9 (15/221)	1.0 (8/208)	0.2 (2/92)	<0.1 (1/248)	1.8 (16/163)	0.6 (2/33)	0.0 (0/3)	0.8 (54/1081)

[1] Number of larvae.

counted for about 40% of all common dolphin larvae taken. Both collections occurred off the Mississippi River delta, one during September 1986 (n=161, 195 m station depth) and the other during May 1988 (n=52, 63 m station depth).

Discussion

Early preflexion larvae (<4.0–4.5 mm) of pompano dolphin are separated from those of common dolphin by having melanophores along the caudal peduncle and scattered throughout the caudal finfold (Figs. 1 and 2). Number and placement of spines along the outer shelf of the preopercle also separate species (Table 5). Separation of dolphinfishes is particularly difficult between 4.5 and 8.0 mm because preopercle spines are often difficult to count on larvae not cleared and stained. At >8 mm, common dolphin are more easily separated from pompano dolphin by having pigment on the developing pelvic fins and bands of pigment laterally on the body and median fins (Figs. 1 and 2; Table 5). Differences in caudal-fin pigmentation also separate species by early

Table 5

Characters helpful in separating larvae of common dolphin (*Coryphaena hippurus*) from pompano dolphin (*C. equiselis*).

Species	Pigment			Outer preopercle spines	Meristics	
	Caudal peduncle	Pelvic fins	Vertical bands		Number of vertebrae	Dorsal fin rays
C. hippurus	Absent	Present[2]	Present[2, 3]	4	30–31	58–66
C. equiselis	Present[1]	Absent	Absent	5	33–44	52–59

[1] At <4.0–4.5 mm SL.
[2] At about 8.0 mm SL.
[3] Laterally on body and median fins.

postflexion (Figs. 1 and 2). In general, our findings agree with those of Aoki and Ueyanagi (1989). Lack of pelvic-fin pigment in pompano dolphin is diagnostic for separating the two species when common dolphin lose lateral banding through preservation or specimen deterioration. Although the 8.5-mm common dolphin larva illustrated in Johnson (1984) lacks pelvic pigment, this specimen has bands of pigment laterally on both the body and median fins.

Number of myomeres and dorsal-fin rays separate juvenile and adult common dolphin from pompano dolphin (30 or 31 vertebrae and 58–66 [$\bar{x}$=61] dorsal rays in common dolphin; 33 or 34 vertebrae and 52–59 [$\bar{x}$=55] dorsal rays in pompano dolphin; Collette et al., 1969; Potthoff, 1980). Great care must be taken when counting the most anterior dorsal-fin elements (Gibbs and Collette, 1959), however, because anterior dorsal rays are short and develop late (Potthoff, 1980). Myomeres are difficult to count without clearing and staining larvae because dolphinfish are heavily pigmented.

Early larval development of common dolphin and pompano dolphin from the Gulf is similar to that in the western Pacific Ocean (Aoki and Ueyanagi, 1989). Developmental milestones (e.g. initial formation of dorsal- and anal-fin bases, yolk-sac absorption, and lateral body banding) occur at similar sizes in common dolphin from both the Gulf and western Pacific Ocean. We found yolk-sac absorption in common dolphin complete by about 3.7 mm, as did Aoki and Ueyanagi (1989). Off Japan, however, common dolphin do not complete yolk-sac absorption until about 6 mm TL (Okiyama, 1988). Aoki and Ueyanagi (1989) did not discuss either maxillary or posttemporal spines or the epithelial spicules noted during this study.

Morphometrics are generally greater in pompano dolphin than in common dolphin from the gulf by early postflexion (Table 1). Differences in mean morphometric ratios (expressed as % SL) between species from the Pacific Ocean are significant (Student's *t*-test, α=0.05) for larvae 5–10 mm; relative growth of all body parts measured (except preanal length) were greater in pompano dolphin than in common dolphin (Aoki and Ueyanagi, 1989).

Distribution of dolphinfish larvae (Table 2, Fig. 3), juveniles, and adults is apparently limited by the 20°C isotherm (Gibbs and Collette, 1959). We found larval dolphinfish of both species primarily at temperatures ≥24°C and salinities ≥33 ppt, as did Fahay (1975), Powles (1981), and Aoki and Ueyanagi (1989). On the basis of water temperatures between 25 and 30°C (those when common dolphin larvae primarily occur), we estimate a common dolphin egg would hatch between 26 and 38 hours. Incubation time at 25°C predicted for common dolphin eggs from the Gulf was similar to that of Hagood and Rothwell[1] at 26°C, but less than incubation times predicted by other studies (Table 3).

Location of dolphinfish spawning is poorly documented. We believe that spawning occurs in oceanic waters based on the collection of preflexion larvae of both species at stations primarily beyond the continental shelf (Appendix Fig. 3). In addition, >80% of larvae of each species (Fig. 3) and 85% of stations where larvae occurred were over or beyond the outer continental shelf (Appendix Fig. 2). These findings support information from along the Atlantic coast of the southeastern U. S. that dolphinfish larvae are most abundant near or beyond the 180 m depth contour (Powles, 1981). In the Gulf, larvae of both common and pompano dolphin were collected over a similar median (Table 2), mean, and range of station depths (mean: 815 m for common dolphin and 782 m for pompano dolphin based on our weighted method of calculating these statistics). This similarity between species in distribution of larvae is reinforced by the average depth of stations where larvae were captured. Average station depth of capture was 1198 m for common dolphin (n=216 stations) and 1042 m for pompano dolphin (n=64 stations).

Other studies suggest that common dolphin in the tropical Atlantic (Gibbs and Collette, 1959) and Pacific (Aoki and Ueyanagi, 1989) spawn closer to shore than do pompano dolphin. In the Pacific, mid-oceanic occurrences of common dolphin larvae are limited to waters near islands (Aoki and Ueyanagi, 1989).

Overall, larval common dolphin are significantly more abundant than pompano dolphin in the northern Gulf (Table 4; Appendix Fig. 2) and along the southeastern United States (Fahay, 1975; Powles, 1981). Larvae of both common dolphin and pompano dolphin were particularly abundant around the Mississippi River delta. Higher larval dolphinfish abundances near the delta may reflect the generally higher abundance of fish larvae in the delta area (Ditty, 1986; Govoni et al., 1989; Grimes and Finucane, 1991) as compared to the open Gulf (Richards et al., 1989), or may reflect greater intensity of neuston sampling near the delta rather than the actual distribution of spawning adults. In the Pacific and Indian Oceans, larval pompano dolphin are more abundant than common dolphin (Shcherbachev, 1973; Aoki and Ueyanagi, 1989).

Dolphinfish may spawn year-round in the Gulf, at least in the southern part of the study area where seasonal water temperatures remain above about 24°C. Estimated spawning dates based on collection of preflexion common dolphin support spawning in the northern Gulf from at least April to December (Fig. 4). Peak spawning of common dolphin occurs during spring and early fall based on higher catches of larvae during these seasons, although differences among seasons are not significant. Along the Atlantic coast, eggs have been collected during July and August in the Gulf Stream (Hassler and Rainville, 1975) and larvae and early juveniles year-round along the southeastern United States (Fahay, 1975; Powles and Stender, 1976) and tropical Atlantic (Gibbs and Collette, 1959). Ripe female common dolphin occur in the Gulf Stream off Cape Hatteras (North Carolina) from at least May through July (Schuck, 1951; Rose, 1966), and in the Florida Current from November to July (March spawning peak, Beardsley, 1967). Pompano dolphin spawn in the Gulf from spring through at least early fall (Fig. 4; Gibbs and Collette, 1959). If larval pompano dolphin growth rates are similar to those for common dolphin (about 1 mm/day, Hassler and Rainville, 1975; Uchiyama et al., 1986), the two mid-October collected pompano dolphin larvae (18.3 and 22.5 mm) were spawned during late September. Pompano dolphin spawn year-round in tropical mid-Atlantic and South Atlantic Bight waters based on collection of larvae and juvenile length-frequency data (Potthoff, 1971; Fahay, 1975).

We found no significant diel differences in catch of larvae for either species as did Fahay (1975). Eldridge et al. (1977), however, found both common dolphin and pompano dolphin significantly more abundant at night, and that catch of larval common dolphin increased with concentration of *Sargassum*. Larval common dolphin <10 mm are more common in subsurface (i.e. depths of 20–30 m) than in surface tows during both day and night (Aoki and Ueyanagi, 1989). Larval pompano dolphin <10 mm are more frequently collected in subsurface tows during the day only; larvae >10 mm are more common near the surface during the night (Aoki and Ueyanagi, 1989).

New information on the larval morphology of pompano dolphin from this study corroborates Johnson's (1984) hypothesis of a relationship between Coryphaenidae and Rachycentridae rather than that previously hypothesized between Rachycentridae and Echeneididae. Larvae of dolphinfishes and cobia share similar patterns of head spination: laterally swollen pterotics; a single, simple spine on the supraorbital ridge of each frontal bone (except in *C. equiselis* which may have multiple spines along the ridge); a small posttemporal spine; and both dolphinfish and cobia have 3 or 4 spines along the inner shelf and 4 or 5 spines along the outer shelf of the preopercle with the largest spines on either side of the preopercular angle (Johnson, 1984; Ditty and Shaw, 1992; this study). Dolphinfishes have a small maxillary spine that cobia lack (Ditty and Shaw, 1992; this study), but no spine on the supracleithrum found in cobia (Dawson, 1971; Ditty and Shaw, 1992; this study). *Echeneis* lack head spines. Larval dolphinfishes and cobia also lack large hooked teeth anteriorly on the dentary found in *Echeneis* (Johnson, 1984; Leis and Trnski, 1989). Dolphinfishes differ from cobia by lacking dorsal and anal spines and by having more vertebrae (30–34 in dolphinfishes versus 25 in cobia). Dolphinfishes also have 50+ soft dorsal rays, whereas cobia have 27–33 (Ditty and Shaw, 1992).

Acknowledgments

This study was supported by the Marine Fisheries Initiative (MARFIN) Program (contract numbers: NA90AA-H-MF111 and NA90AA-H-MF727). The authors thank the Southeast Area Monitoring and Assessment Program (SEAMAP) and Gulf States Marine Fisheries Commission for providing specimens and environmental data. Bruce Mundy (NMFS, Honolulu Laboratory, Hawaii) provided a

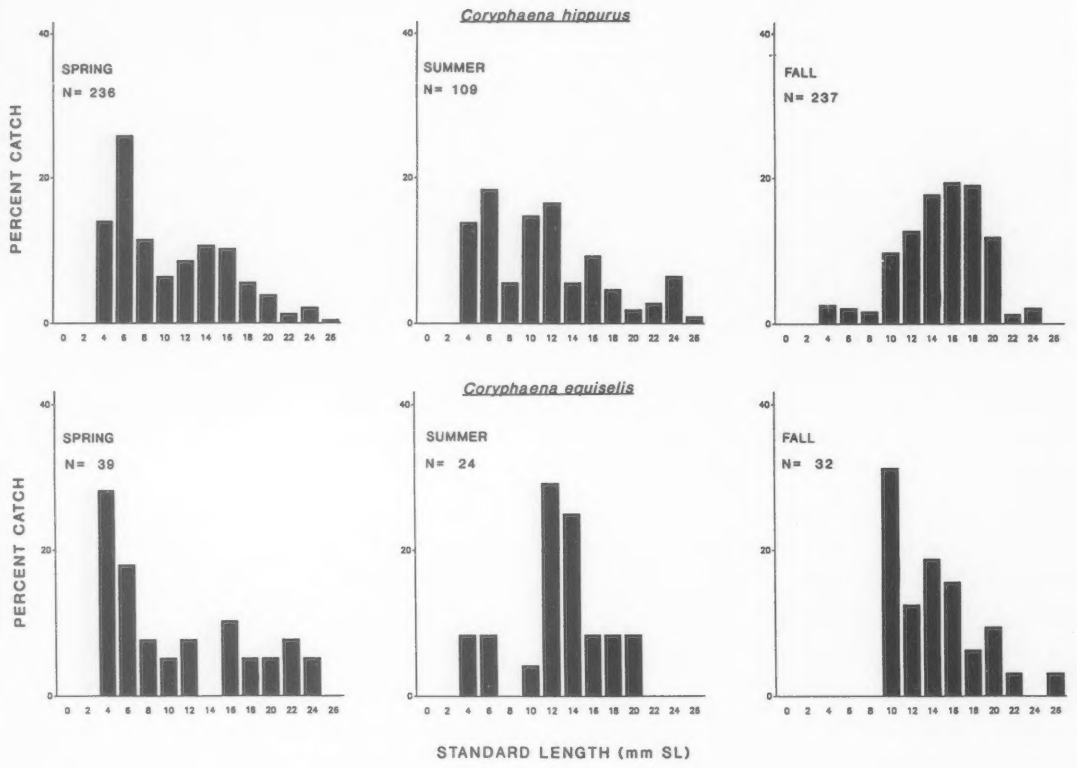

Figure 4

Length-frequency distribution of larval common dolphin (*Coryphaena hippurus*) and pompano dolphin (*C. equiselis*) in the northern Gulf of Mexico by season. Catches are from both bongo and neuston net tows; seasons are combined across years. Spring: March–May, Summer: June–August, Fall: September–November. Length categories are combined by 2-mm intervals; ≥0.5–mm increments are rounded to the nearest whole number. *N* = number of larvae.

copy of the English translation of Aoki and Ueyanagi (1989). We also thank Cathy Grouchy for illustrating the larvae.

Literature cited

Aoki, M., and S. Ueyanagi.
1989. Larval morphology and distribution of the dolphin-fishes, *Coryphaena hippurus* and *C. equiselis* (Coryphaenidae). Tokai Univ. Proc., Oceanogr. Sec., No. 28, p. 157–174. [In Japanese.]

Beardsley, G. L.
1967. Age, growth, and reproduction of the dolphin, *Coryphaena hippurus*, in the straits of Florida. Copeia 1967:441–451.

Berry, F. H., and W. J. Richards.
1973. Characters useful to the study of larval fishes. Mid. Atl. Coast. Fish. Cent. Tech. Pap. 1:48–65.

Briggs, J. C.
1960. Fishes of worldwide (circumtropical) distribution. Copeia 1960(3):171–180.

Collette, B. B., R. H. Gibbs, and G. E. Clipper.
1969. Vertebral numbers and identification of the two species of dolphin (*Coryphaena*). Copeia 1969(3):630–631.

Dawson, C. E.
1971. Occurrence and description of prejuvenile and early juvenile Gulf of Mexico cobia, *Rachycentron canadum*. Copeia (1):65–71.

Ditty, J. G.
1986. Ichthyoplankton in neritic waters of the northern Gulf of Mexico off Louisiana: composition, relative abundance, and seasonality. Fish. Bull. 84: 935–946.

Ditty, J. G., and R. F. Shaw.
1992. Larval development, distribution, and ecology of cobia, *Rachycentron canadum* (Family:

Rachycentridae), in the northern Gulf of Mexico. Fish. Bull. 90:668–677.

Eldridge, P. J., F. H. Berry, and M. C. Miller III.
1977. Test results of the Boothbay neuston net related to net length, diurnal period, and other variables. S. Car. Mar. Resour. Cent. Tech. Rep. No. 18, 22 p.

Fahay, M. P.
1975. An annotated list of larval and juvenile fishes captured with surface-towed meter net in the South Atlantic Bight during four RV *Dolphin* cruises between May 1967 and February 1968. NOAA Tech. Rep., NMFS SSRF-685, 39 p.

Gibbs, R. H., Jr., and B. B. Collette.
1959. On the identification, distribution, and biology of the dolphins, *Coryphaena hippurus* and *C. equiselis*. Bull. Mar. Sci. 9(2):117–152.

Govoni, J. J., D. E. Hoss, and D. R. Colby.
1989. The spatial distribution of larval fishes about the Mississippi River plume. Limnol. Oceanogr. 34(1):178–187.

Grimes, C. B., and J. H. Finucane.
1991. Spatial distribution and abundance of larval and juvenile fish, chlorophyll and macrozooplankton around the Mississippi River discharge plume, and the role of the plume in fish recruitment. Mar. Ecol. Prog. Ser. 75:109–119.

Hassler, W. W., and R. P. Rainville.
1975. Techniques for hatching and rearing dolphin, *Coryphaena hippurus*, through larval and juvenile stages. Univ. N. Carolina Sea Grant Prog., UNC-SG-75–31, 17 p.

Hubbs, C. L., and K. F. Lagler.
1958. The fishes of the Great Lakes region. Univ. Mich. Press, Ann Arbor, 213 p.

Johnson, G. D.
1984. Percoidei: development and relationships, p. 464–498. *In* H. G. Moser, W. J. Richards, D. M. Cohen, M. P. Fahay, A. W. Kendall Jr., and S. L. Richardson (eds.), Ontogeny and systematics of fishes, p. 464–498. Am. Soc. Ichthy. Herp., Spec. Publ. No. 1.

Kelley, S., T. Potthoff, W. J. Richards, L. Ejsymont, and J. V. Gartner.
1986. SEAMAP 1983—Ichthyoplankton. Larval distribution and abundance of Engraulidae, Carangidae, Clupeidae, Lutjanidae, Serranidae, Sciaenidae, Coryphaenidae, Istiophoridae, Xiphiidae, and Scombridae in the Gulf of Mexico. NOAA Tech. Mem., NMFS-SEFC-167, no pagination.

Lamadrid-Rose, Y., and G. W. Boehlert.
1988. Effects of cold shock on egg, larval, and juvenile stages of tropical fishes: potential impacts of ocean thermal energy conversion. Mar. Environ. Res. 25:175–193.

Leis, J. M., and T. Trnski.
1989. The larvae of Indo-Pacific shorefishes. Univ. Hawaii Press, Honolulu, 371 p.

Mito, S.
1960. Egg development and hatched larvae of the common dolphin-fish *Coryphaena hippurus* Linne. Bull. Jap. Soc. Sci. Fish. 26:223–226.

Okiyama, M.
1988. An atlas of the early stage fishes in Japan. Tokai Univ. Press, Tokyo, p. 481–483.

Palko, B. J., G. L. Beardsley, and W. J. Richards.
1982. Synopsis of the biological data on dolphinfishes, *Coryphaena hippurus* Linnaeus and *Coryphaena equiselis* Linnaeus. NOAA Tech. Rep., NMFS Circ. 443, 28 p.

Pauly, D., and R. S. V. Pullin.
1988. Hatching time in spherical, pelagic, marine fish eggs in response to temperature and egg size. Environ. Biol. Fish. 22(4):261–271.

Potthoff, T.
1971. Observations on two species of dolphin (*Coryphaena*) from the tropical mid-Atlantic. Fish. Bull. 69:877–879.

1980. Development and structure of fins and fin supports in dolphin fishes *Coryphaena hippurus* and *Coryphaena equiselis* (Coryphaenidae). Fish. Bull. 78:277–312.

Powles, H.
1981. Distribution and movements of neustonic young of estuarine dependent (*Mugil* spp., *Pomatomus saltatrix*) and estuarine independent (*Coryphaena* spp.) fishes off the southeastern United States. Rapp. P.-v. Reun. Cons. int. Explor. Mer 178:207–209.

Powles, H., and B. W. Stender.
1976. Observations on composition, seasonality and distribution of ichthyoplankton from MARMAP cruises in the South Atlantic Bight in 1973. South Car. Mar. Res. Cent. Tech. Rep. Ser. No. 11, 47 p.

Richardson, S. L., and W. A. Laroche.
1979. Development and occurrence of larvae and juveniles of the rockfishes *Sebastes crameri*, *Sebastes pinniger*, and *Sebastes helvomaculatus* (Family Scorpaenidae) off Oregon. Fish. Bull. 77:1–46.

Richards, W. J., T. Potthoff, S. Kelley, M. F. McGowan, L. Ejsymont, J. H. Power, and R. M. Olvera L.
1984. SEAMAP 1982—Ichthyoplankton. Larval distribution and abundance of Engraulidae, Carangidae, Clupeidae, Lutjanidae, Serranidae, Coryphaenidae, Istiophoridae, Xiphiidae, and Scombridae in the Gulf of Mexico. NOAA Tech. Mem., NMFS-SEFC-144, no pagination.

Richards, W. J., T. Leming, M. F. McGowan, J. T. Lamkin, and S. Kelley-Fraga.
1989. Distribution of fish larvae in relation to hydrographic features of the Loop Current boundary in the Gulf of Mexico. Rapp. P. v. Reun. Cons. int. Explor. Mer 191:161–176.

Rose, C. D.
1966. The biology and catch distribution of the dolphin *Coryphaena hippurus* (Linnaeus) in North Carolina waters. Ph.D. diss., N. Carolina State Univ., Raleigh, 153 p.

Sanders, N., Jr., T. Van Devender, and P. A. Thompson.
1990. SEAMAP environmental and biological atlas of the Gulf of Mexico, 1986. Gulf States Marine Fish. Comm., Ocean Springs, MS, No. 20, 328 p.

SAS Institute, Inc.
1985. SAS User's Guide: Statistics, 1985 ed. SAS Institute, Cary, NC, 584 p.

Schuck, H. A.
1951. Notes on the dolphin (*Coryphaena hippurus*) in North Carolina waters. Copeia 1951(1): 35–39.

Shcherbachev, Y. N.
1973. The biology and distribution of the dolphins (Pisces, Coryphaenidae). J. Ichthyol. 13:182–191.

Soichi, M.
1978. Spawning behavior of the dolphin, *Coryphaena hippurus*, in the aquarium and its eggs and larvae. Jap. J. Ichthyol. 24:290–294. [In Jap., Engl. summ.]

Stuntz, W. E., C. E. Bryan, K. Savastano, R. S. Waller, and P. A. Thompson.
1985. SEAMAP environmental and biological atlas of the Gulf of Mexico, 1982. Gulf States Marine Fish. Comm., Ocean Springs, MS, No. 12, 145 p.

Thompson, P. A., and N. Bane.
1986a. SEAMAP environmental and biological atlas of the Gulf of Mexico, 1983. Gulf States Marine Fish. Comm., Ocean Springs, MS, No. 13, 179 p.
1986b. SEAMAP environmental and biological atlas of the Gulf of Mexico, 1984. Gulf States Marine Fish. Comm., Ocean Springs, MS, No. 15, 171 p.

Thompson, P. A., T. Van Devender, and N. J. Sanders Jr.
1988. SEAMAP environmental and biological atlas of the Gulf of Mexico, 1985. Gulf States Marine Fish. Comm., Ocean Springs, MS, No. 17, 338 p.

Uchiyama, J. H., R. K. Burch, and S. A. Kraul Jr.
1986. Growth of dolphins, *Coryphaena hippurus* and *C. equiselis*, in Hawaiian waters as determined by daily increment on otoliths. Fish. Bull. 84:186–191.

Zar, J. H.
1984. Biostatistical analysis. Second ed., Prentice-Hall, Inc., NJ, 718 p.

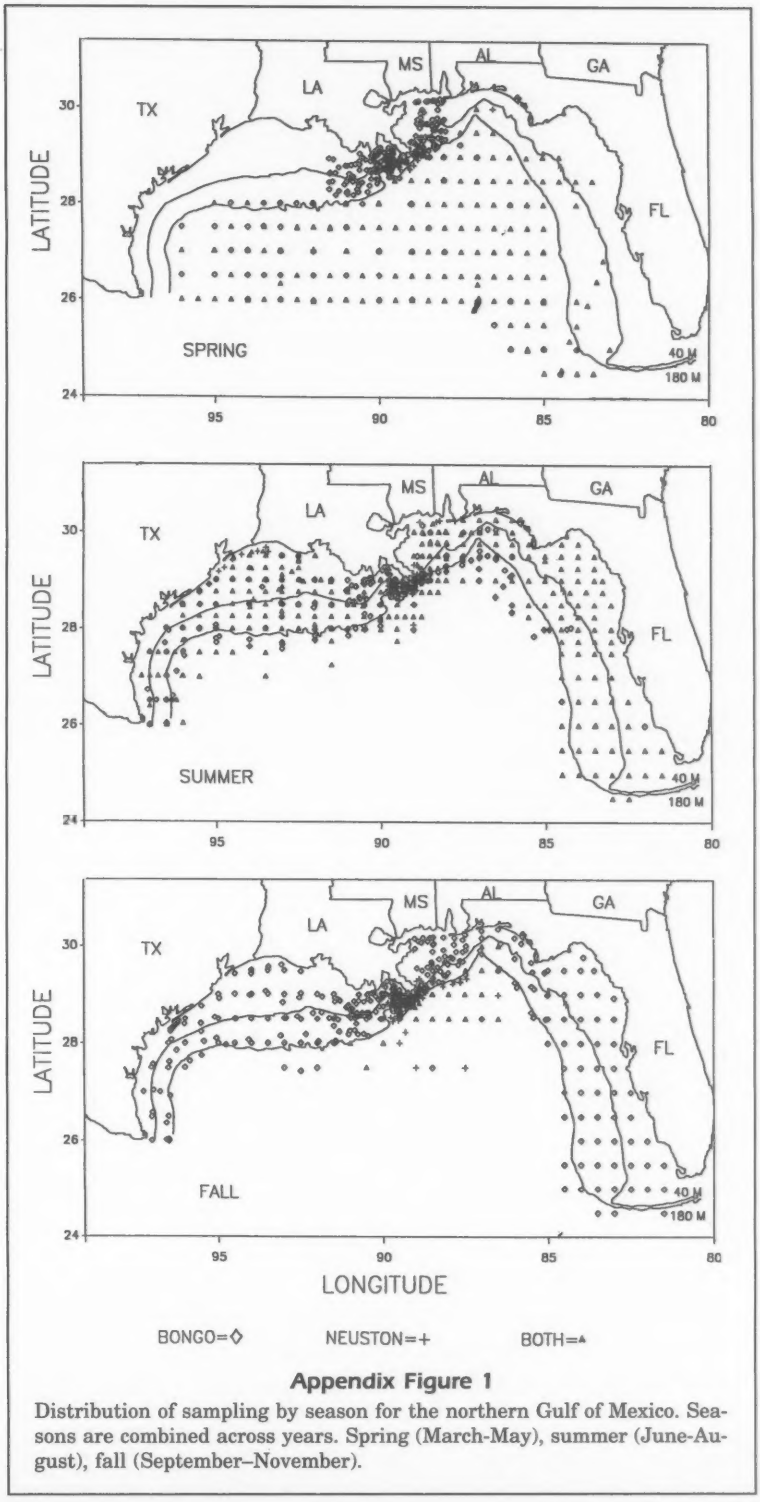

Appendix Figure 1

Distribution of sampling by season for the northern Gulf of Mexico. Seasons are combined across years. Spring (March-May), summer (June-August), fall (September–November).

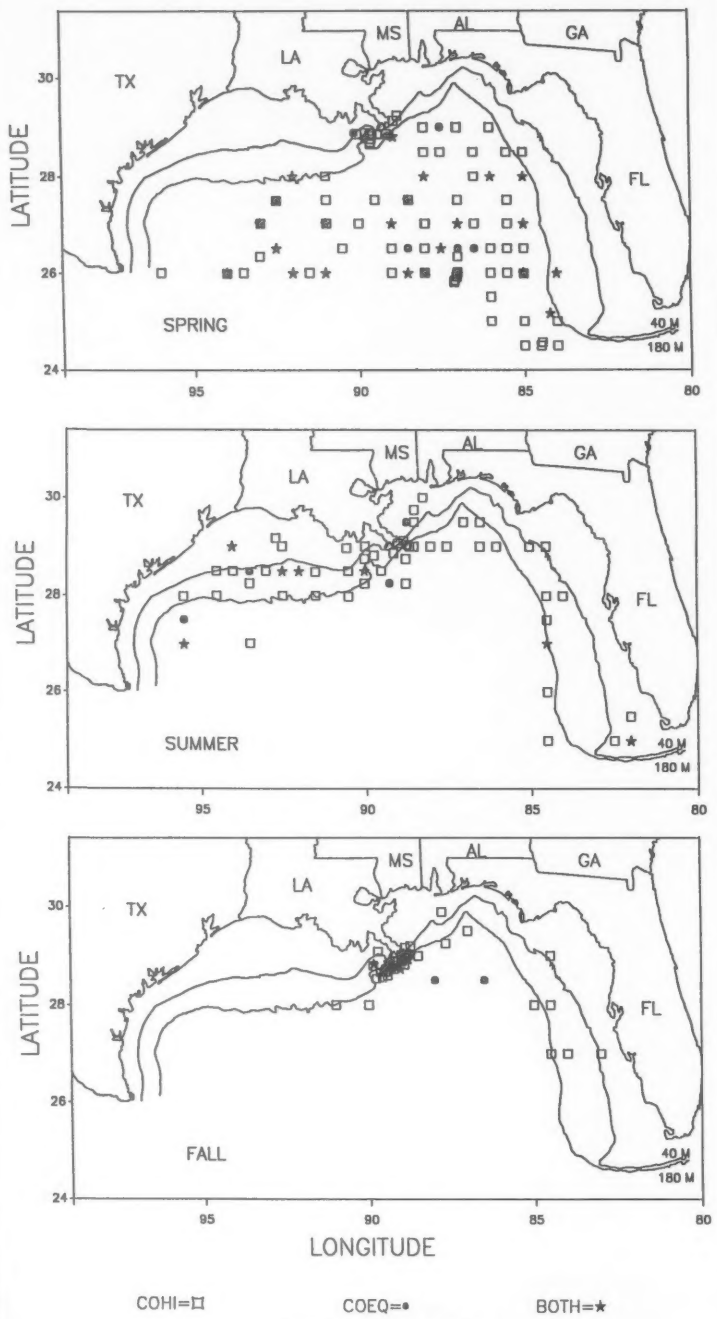

Appendix Figure 2

Distribution of common dolphin (*Coryphaena hippurus*) and pompano dolphin (*C. equiselis*) larvae in the northern Gulf of Mexico by season. Seasons are combined across years. Catches are from both bongo and neuston net tows. Spring (March–May), summer (June–August), fall (September–November).

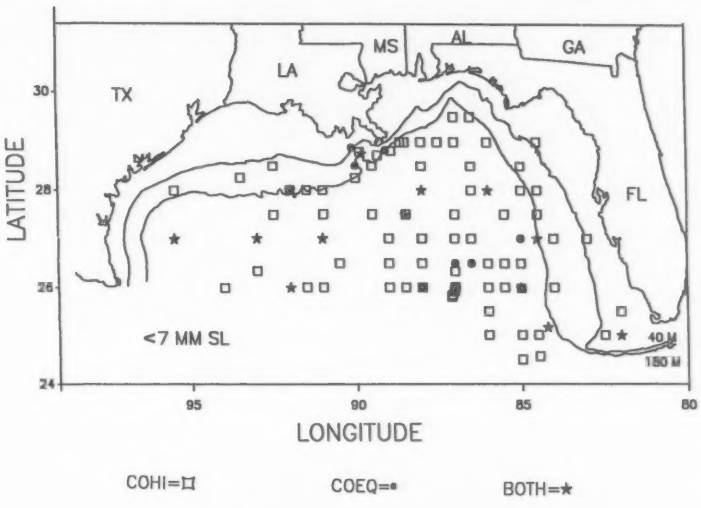

Appendix Figure 3

Distribution of early larval (<7.0 mm) common dolphin (*Coryphaena hippurus* [COHI]) and pompano dolphin (*C. equiselis* [COEQ]) in the northern Gulf of Mexico. Both bongo and neuston net tows are used in determining early larval distribution. Data are combined across seasons and years.

Using Pb-210/Ra-226 disequilibria for sablefish, *Anoplopoma fimbria*, age validation

Craig R. Kastelle
Daniel K. Kimura
Alaska Fisheries Science Center, National Marine Fisheries Service, NOAA
7600 Sand Point Way NE, Seattle, WA 98115-0070

Ahmad E. Nevissi
Donald R. Gunderson
School of Fisheries, WH-10, University of Washington
Seattle, WA 98195

Abstract.—Age determination of sablefish (*Anoplopoma fimbria*) is typically done by counting growth zones on the burnt cross-section of the otolith. The break-and-burn method of age determination is difficult to apply to sablefish. Therefore, we applied a relatively new method of fish age validation, using the disequilibrium of Pb-210/Ra-226 in the otoliths. This method of validation complements previous methods which used oxytetracycline (OTC) marking to validate incremental growth in sablefish otoliths. The Pb-210/Ra-226 disequilibria generally confirmed the ageing criteria used to interpret the otolith's burnt cross-section.

Sablefish (*Anoplopoma fimbria*) is an important commercial species distributed continuously along the North Pacific Rim from California to northern Japan. On central California's continental shelf, the spawning of sablefish takes place from October to February at depths of over 823 m (Hunter et al., 1989). Both eggs and larvae have been collected at depths of over 400 m in April off British Columbia. After hatching, postlarval sablefish move into the surface waters where onshore or offshore transport may take place (Mason et al., 1983). Postlarvae have been found offshore, but as juveniles they are usually seen inshore (Bracken, 1983; Mason et al., 1983). The juveniles are believed to reside inshore for several years and then move to deeper offshore waters as they near maturity and join the spawning population (Bracken, 1983; Mason et al., 1983). Mature sablefish are typically caught at 700 m (Mason et al., 1983). Funk and Bracken[1] note that the growth of young fish is fast compared to very slow growth of mature fish. An abrupt slowing of growth coincides with the onset of sexual maturity. Mean fork length increases with depth and the length at 50% maturity for females is 60 cm (Hunter et al., 1989).

At the Alaska Fisheries Science Center (AFSC) sablefish ages are determined by counting growth zones (assumed annular) seen on the distal surface of the otolith, or more frequently in the burnt dorsal-ventral cross-section (break-and-burn method, Beamish et al., 1983). Even though ageing criteria have been established for sablefish by using the break-and-burn method (Beamish and Chilton, 1982; Beamish et al., 1983), variability between individual sablefish in the morphology of their otoliths and the appearance of growth zones makes this method difficult to apply. Between-reader variability in sablefish ages are far greater than for any other species routinely aged at the AFSC (Kimura and Lyons, 1991).

Sablefish age validation has been examined by using oxytetracycline (OTC) studies, mark and recapture of known age fish, tagging studies, length-frequency analysis of young fish, and daily growth zone counts in juvenile sablefish otoliths (Beamish

[1] Funk, F., and B. E. Bracken. 1983. Growth of sablefish in southeastern Alaska. AK Dept. Fish and Game Info. Leaflet No. 223, 40 p.

Manuscript accepted 27 October 1993
Fishery Bulletin 92:292-301 (1994)

and Chilton, 1982; Beamish et al., 1983). The age range considered by Beamish and Chilton (1982) was from 0 to 43 years, but their study had few individuals from the upper end of the age range. The OTC method can validate only incremental growth zones after injection, leaving interpretation of earlier growth in any one fish questionable. Ideally, the age range of OTC-injected fish spans all ages. Younger OTC-injected fish can then be used to infer that incremental growth zones seen prior to an OTC injection on older fish are annuli. With these limitations, the procedures used by Beamish and Chilton (1982) and Beamish et al. (1983) confirmed that ages counted on the burnt cross-section were accurate.

Our goal was to use radiometric dating techniques to validate the break-and-burn ageing criteria used at the AFSC for sablefish aged to approximately 35 years. This validation used the measured ratio of Pb-210/Ra-226 in the otoliths to provide estimates of total age, thereby complementing previous OTC validation work which only confirmed incremental growth.

In the first application of radiometric ageing to fishes, Bennett et al. (1982) used the ratio of Pb-210/Ra-226 to validate ages up to 80 years for splitnose rockfish (*Sebastes diploproa*). More recently, these radioisotopes were used by Campana et al. (1990) and Fenton et al. (1990, 1991) in age validation and longevity studies in a variety of fish species. Additional radioisotope pairs such as Th-228/Ra-228 have also been used to age fish (Smith et al., 1991).

The isotopes Ra-226 and Pb-210 are part of the naturally occurring decay chain of U-238:

$$\begin{array}{l} U\text{-}238 \xrightarrow[4.5\times10^{9}\,yr]{} Ra\text{-}226 \xrightarrow[1600\,yr]{} Rn\text{-}222 \xrightarrow[3.8\,d]{} Pb\text{-}210 \\ Pb\text{-}210 \xrightarrow[22.3\,yr]{} Po\text{-}210 \xrightarrow[138\,d]{} Pb\text{-}206 \end{array} \qquad (1)$$

where the dashed lines indicate short-lived intermediary nuclides that are not shown.

Both Ra-226 and Pb-210 are found naturally in seawater. Ra-226 is a calcium (Ca) analogue which accompanies Ca through the food chain and is deposited in fish tissue, particularly calcified structures, along with Ca (Swanson, 1985; Porntepkasemsan and Nevissi, 1990). The otoliths of teleosts consist of an acellular organic protein matrix mineralized with aragonite, a form of calcium carbonate in which the radioisotopes are deposited (Mugiya, 1977; Campana and Neilson, 1985). Pb-210 is also accumulated by the biota through the food chain (Shannon et al., 1970; Heyraund and Cherry, 1979). In fish, Pb-210 is preferentially deposited in the bone or liver[2] (Swanson, 1985). Its initial activity in the otolith must be measured (later as R^*) for the application of radiometric ageing.

When Ra-226 is deposited in otoliths, like Ca it remains immobile, and a disequilibrium is created between Ra-226 and all of its progeny. With time, the activity of shorter-lived daughter products like Pb-210 will increase. In the pair of radioisotopes used here, Ra-226 and Pb-210, the difference between their half-lives is great (Eq. 1). Therefore, after about 100 years in a closed system the activity of both Ra-226 and Pb-210 will become equal, establishing a so called "state of secular equilibrium" (Faure, 1986). A chronometer is started when Ra-226 is first deposited in the otolith, and the activity ratio Pb-210/Ra-226 is a function of the time elapsed since deposition.

Radiometric dating applied to fish otoliths relies on three basic assumptions (Faure, 1986; Smith et al., 1991):

1 The otoliths are closed with respect to the loss or gain of any radioisotopes in the decay chain.
2 The initial activity ratio of Pb-210/Ra-226 in the otoliths should be much smaller than one, ideally close to zero, and known or measured.
3 The specific activity [disintegrations per minute per gram (dpm/g)] of the radioisotopes in the material incorporated into the otoliths must be constant.

These assumptions will be considered in detail later in the "Discussion" section. But first, it is important to consider Assumption 3 because it explains why we did not use whole otoliths. Assumption 3 is the most problematic of the three assumptions when applied to whole otoliths because it also requires assuming a mass-growth rate for the otoliths (Smith et al., 1991). Campana et al. (1990) used otolith cores in their application of radiometric dating to fish. When using otolith cores and individual measurements of Ra-226 for each sample being radiometrically aged, Assumption 3 becomes unnecessary. However, if measurements of Ra-226 are averaged over the different samples being radiometrically aged, Assumption 3 requires that the different core samples have the same activity levels. Our study followed the procedures of Campana et al. (1990) and used otoliths cores. But unlike Campana et al. (1990), we used individual Ra-226 measurements for each sample being aged so that Assumption 3 was unnecessary.

[2] Noshkin, V. E., K. M. Wong, R. J. Eagle, T. A. Jokela, and J. A. Brunk. 1988. Radionuclide concentrations in fish and invertebrates from Bikini Atoll. Lawrence Livermore National Laboratory, Livermore, Ca., UCRL-53846, 53 p.

Materials and methods

Otolith collection

Sablefish were collected along the Eastern Pacific Continental Shelf during two research cruises by the AFSC. The first collection was made from the research vessel *Alaska* on 8 August 1986 and contained 61 fish captured at 135 m in Morro Bay, California. The second collection was made from the vessel *American Viking* between 23 September and 31 October 1986 and contained 423 fish captured at depths of 246–1426 m off the California coast between 32°23'N and 42°23'N. Both sagittal otoliths were removed at sea. The sacculus membranes were removed and otoliths were stored in 50% ethanol.

Ages were estimated by the first author (Reader 1) from one otolith per fish applying the break-and-burn method, and the other otolith was used in the radiometric study. The criteria used to count annuli for this study were similar to those typically used by experienced age readers at the AFSC and Tiburon Laboratories of the National Marine Fisheries Service (NMFS), and were the same used by Beamish and Chilton (1982) and Beamish et al. (1983). By using these criteria, an age range of up to ±5 years for older fish was often possible. The oldest age consistent with these criteria was often assigned as the most probable age. When a fish was aged as 1 year old the otolith surface was usually adequate and no break-and-burn was done. The otoliths were subsequently pooled into four age categories (1 year, 9–11 year, 14–23 year, and 24–34 year), on the basis of Reader-1 ages.

For comparison, a subsample of otoliths initially aged ≥14 years (n=186) was read by a second experienced sablefish age reader at the AFSC (Reader 2). Additionally, all fish initially aged ≥14 years (n=266) were read by an experienced sablefish age reader at the Pacific Biological Station (PBS), Canadian Department of Fisheries and Oceans (Reader 3).

In the radiometric dating procedures, we used that part of the otolith which was deposited during the first year of life (i.e. the first year core). For age category 1, whole otoliths representing the first 15 to 18 months of growth were used. These otoliths were those classified as age 1 by Reader 1 and were intact and unburnt. For other age categories, the first year cores were isolated by grinding away excess otolith material. The grinding was done with a Buehler metallurgical polishing machine equipped with Buehler wet and dry #600 or #900 paper. Otolith material representing the first year was readily identifiable in older fish from the distal surface of the ground otolith, and from the broken-and-burnt section, viewed with a dissecting microscope (25×) as a guide. Removal of material was done slowly, with frequent viewing of the otolith during the grinding process (Kastelle, 1991). The position of the first annulus on the otolith has been confirmed by several authors in age validation studies of young sablefish (Beamish and Chilton, 1982; Beamish et al., 1983; McFarlane and Beamish, 1983). Average measurements of the core dimensions were not used as an aid in the grinding process. Instead, grinding was completed when the contours of the first year were approximated. Small inaccuracies in the grinding were inconsequential because samples were pooled into four categories based on age ranges.

All otolith cores were cleaned with an ultrasonic cleaner in distilled and deionized water for a minimum of 30 seconds. Any soft tissue remaining on the otolith after collection was visibly broken down by the ultrasonic cleaner. The goal of the cleaning was to remove any contamination from soft tissue or grinding paper. After cleaning, the otoliths were stored again in a fresh 50% ethanol solution prior to analysis for radioisotopes.

Approximately one gram of material was necessary for radioisotope activity to be measurable above background levels, which meant that 83 to 141 otoliths were used for each age category. To increase the weight of category 1 (1 year olds), an additional unburnt half of the aged otolith from some specimens was included with the intact otoliths (83 specimens total: 83 whole otoliths plus 65 half otoliths from some of the same fish).

Activity measurements

The methods employed in the chemical separation and counting techniques for Ra-226 and Pb-210 were similar to those used by Bennett et al. (1982) and are detailed in Kastelle (1991).

In general, the activity of Pb-210 in the otoliths was determined by counting the alpha decays of Po-210 (the granddaughter-proxy of Pb-210 with which it is in secular equilibrium, Eq. 1) by using a yield tracer of Po-209. Reagent blanks, with and without yield tracers, were processed with each age category as follows: category 1, one blank without yield tracer; categories 2 and 3 processed simultaneously, one blank with a yield tracer and one without; category 4, one blank with a yield tracer and one without. The counting time for each sample or reagent blank was approximately three weeks.

The activity of Ra-226 was determined by counting alpha decays of Rn-222 (the daughter-proxy of Ra-226 with which it grows into secular equilibrium,

Eq. 1) in a Lucas cell (Lucas, 1957). The samples were stored in a Rn-222 de-emanation flask for a minimum of three weeks prior to counting. During storage, Rn-222 reached secular equilibrium with Ra-226. Reagent blanks were processed with each sample. Lucas cell (Rn-222) counting times were 4,000 minutes for each sample or reagent blank. Lucas cell and electronic backgrounds (counting time 1,000 minutes) were measured multiple times before and after any sample or reagent blank. The counting efficiency (i.e. the percentage of decays that was detected) of the de-emanation technique, Lucas cells, and associated electronics was determined to be 53.75% with the use of a Ra-226 standard solution supplied by the U.S. Environmental Protection Agency. Activities of Ra-226 and associated errors were calculated by using the methods of Sarmiento et al. (1976). Details concerning incorporation of blank and background measurements into the activity calculation for Po-210 and Ra-226 are given in Kastelle (1991). All sources of error were propagated through the calculations to estimate errors (standard deviation or SD) for the Ra-226 and Pb-210 measurements.

Data analysis

ANOVA with contrasts was used to test whether break-and-burn otolith ages from the different age readers were significantly different within each age category. Statistical analyses of activity measurements from samples, backgrounds, and reagent blanks were conducted by using Z, t, and a likelihood ratio χ^2 test as described below. To test if the Ra-226 (or Pb-210) activity from each age category was statistically different, the likelihood ratio test was employed. Assuming X_i is distributed as $N(\mu_i,\sigma_i^2)$, where the σ_i^2 are known, the likelihood ratio χ^2 test for $H_o:\mu_1=\ldots=\mu_n$, is

$$\hat{\chi}^2=\sum(X_i-\hat{\mu})^2/\sigma_i^2$$

which is distributed as χ^2_{n-1}. Here X_i is the measured Ra-226 (or Pb-210) activity for age category i,

$$\hat{\mu}=\sum(X_i/\sigma_i^2)/\sum(1/\sigma_i^2),$$

and σ_i^2 is the variance for age category i. If σ_i^2's are underestimated, then the $\hat{\chi}^2$ would be inflated. Z tests were carried out between the reagent blanks plus background, and background alone, for Po-209 and Po-210 measurements; a t-test was performed between the mean Rn-222 reagent blank plus background and the background alone.

Two sets of estimated Pb-210/Ra-226 ratios were calculated: one by using the mean Ra-226 activity from the four categories and the second by using the Ra-226 activity measured for each category. The delta method was used to determine the variance of the ratios (Seber, 1982).

The measured ratio of Pb-210/Ra-226 in the otoliths can be used to predict a radiometric age from the curve:

$$\frac{A_2}{A_1}=1-e^{-\lambda_2 t}+R^*e^{-\lambda_2 t}, \quad (2)$$

where A_1 is the activity for Ra-226, A_2 and λ_2 are the activity and decay constant respectively (λ=ln (2)/half-life, for Pb-210, t is time (i.e. age), and R^* is the initial ratio of Pb-210/Ra-226 (Fig. 1, see also Kastelle [1991]). The initial ratio was estimated by solving Equation 2 for R^* and applying the activity ratio from age category 1 (R^*=-0.034). The negative value for R^* is due to measurement error. Therefore, we assume R^* = 0 in Figure 1. The actual fish ages were predicted from the radiometric ages by subtracting the time between collection and analysis (4.5 yr) from the radiometric ages in Figure 1. Alternatively, it is possible to calculate the radiometric ages by correcting the Pb-210 activity estimates to the time of otolith collection. These adjusted radiometric ages were then compared with ages read from the burnt otolith cross-section by the three readers. For each of the readers, a linear regression line was fit through the origin and compared with the 45° line of agreement by using a t-test.

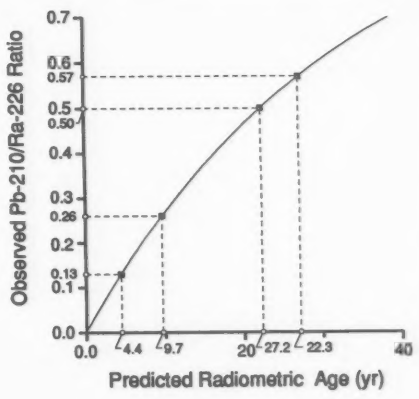

Figure 1

Predicted radiometric age of samples from observed activity ratios and curve of expected activity ratio (Eq. 2). Predicted radiometric age includes the 4.5 years between collection and analysis.

Results

ANOVA with contrasts showed the average age generated by the three age readers within each age category were all pair-wise significantly different ($P<0.001$). Reader 3 estimated the youngest ages, followed by Reader 1, and Reader 2 produced the highest ages (Table 1). Age categories were based on ages from Reader 1; therefore, the age ranges in each category for Readers 2 and 3 were greater.

The reagent blanks plus background for Po-210 and Po-209 did not contain significant activity above the background alone ($P>0.05$). The background activity for Po-209 and Po-210 ranged up to 6.413×10^{-4} $\pm1.472\times10^{-4}$ cpm (counts per minute) and 5.600×10^{-4} $\pm9.75\times10^{-5}$, respectively (Table 2). Therefore, the unadjusted sample data (including background counts) were reduced by the appropriate background only; no adjustment was made for the reagent blank. Specific activity of Pb-210 at the time of separation from Ra-226 ranged from 0.037 ±0.007 dpm/g in category 1 to 0.265 ±0.041 dpm/g in category 4 (Table 3). The Pb-210 activity levels were significantly different among the four age categories ($P<0.001$).

The average background count ($n=66$) for the Rn-222 system was 8.500×10^{-3} $\pm5.27\times10^{-4}$ cpm. The mean reagent blank plus background for Rn-222 was not significantly greater than the background alone ($P=0.077$). Mean Ra-226 activity ($n=4$) was 0.414 ±0.050 dpm/g (Table 3). Ra-226 values from the four age categories were significantly different ($P<0.001$). Therefore, the Ra-226 measurements were specific to each age category.

The adjusted radiometric ages (from category specific Ra-226 measurements) for age categories 1 to 4 respectively were –0.09, 5.21, 17.83, and 22.66 years. Although the adjusted radiometric ages were consistently younger than the burnt cross-section ages from Reader 1, there was general agreement between the two methods (Fig. 2). A t-test between the slope of a line fit through the origin vs. the 45° line did not show a significant difference for any of the age readers ($P>0.05$).

Discussion

Principal findings

The principal result of this study is that the radiometric ages generally confirmed the burnt otolith ageing criteria that are used to age sablefish by U.S. and Canadian age readers. A factor which facilitated this confirmation is that sablefish otoliths apparently accumulate higher levels of radioisotopes than do other fish species that have been previously studied. We found the specific activities of Pb-210 and Ra-226 in sablefish otoliths (Table 3) to be a full order of magnitude greater than values reported in other species (Bennett et al., 1982; Campana et al., 1990; Fenton et al., 1991). These large differences in activity levels may be explained by biological and environmental considerations. Radium-226 is incor-

Table 1

For each age category of sablefish, *Anoplopoma fimbria*, comparison of average estimated age, number of samples read, age range by each age reader, and radiometric age are shown. The time between collection and analysis (4.5 yr) was subtracted from the radiometric age at the time of analysis to make the ages comparable.

Age category	First Reader: average age (yr), n read, range (yr)	Second Reader: average age (yr), n read, range (yr)	Canada (PBS): average age (yr), n read, range (yr)	Radiometric age: average age (yr), n pooled, range (yr)[1]
1	1, n=83, (1)	—	—	–0.09, n=83 (–0.89, 0.74)
2	9.79, n=130, (9, 11)	—	—	5.21, n=130 (3.40, 7.12)
3	18.91, n=141, (14, 23)	22.07, n=101, (14, 42)	15.58, n=139, (8, 27)	17.83, n=141 (13.05, 23.44)
4	28.55, n=127, (24, 34)	31.01, n=85, (17, 49)	23.75, n=127 (11, 48)	22.66, n=127 (16.50, 30.30)

[1] Based on measured Pb-210/Ra-226 ratio and error with individual Ra-226 measurements and Eq. 2.

Table 2

Comparison of background (Bk) and blank (BL) activity reported in the literature for tracer spikes, Po-210 in equilibrium with Pb-210, and Ra-226. NR = not reported

		Tracer spike (Po-209 or Po-208)	Po-210	Ra-226
This study	Bk (cpm)	$1.867 \times 10^{-4} \pm 5.63 \times 10^{-5}$ to $6.413 \times 10^{-4} \pm 1.472 \times 10^{-4}$	$2.353 \times 10^{-4} \pm 6.53 \times 10^{-5}$ to $5.600 \times 10^{-4} \pm 9.75 \times 10^{-5}$	$8.500 \times 10^{-3} \pm 5.27 \times 10^{-4}$
	Bl (dpm)	Not significant	Not significant	Not significant
Bennett et al. (1982)	Bk (cpm)	NR	6.94×10^{-4}	1.4×10^{-2} to 2.8×10^{-2}
	Bl (dpm)	NR	Not measurable above Bk	3.9×10^{-2}
Campana et al. (1990)	Bk (cpm)	NR	6.94×10^{-4}	NR
	Bl (dpm)	NR	5×10^{-4}	NR
Fenton et al. (1990)	Bk (cpm)	NR[1]	NR[1]	
	Bl (dpm)	NR	$1.03 \times 10^{-2} \pm 2.7 \times 10^{-3}$	$1.25 \times 10^{-2} \pm 4.3 \times 10^{-3}$
Fenton et al. (1991)	Bk (cpm)	6.94×10^{-4}	6.94×10^{-4}	1.4×10^{-3} to 3.5×10^{-3}
	Bl (dpm)	NR	$1.03 \times 10^{-2} \pm 2.7 \times 10^{-3}$	$2.55 \times 10^{-2} \pm 2.3 \times 10^{-3}$

[1] Not reported specifically for this radioisotope, but this author suggested a lower value here than reported by Bennett et al. (1982).

Table 3

For each age category of sablefish, *Anoplopoma fimbria*, number of specimens, average estimated age and estimated age range (from Reader 1), specific activity (dpm/gram) of Ra-226 and Pb-210, and the ratios Pb-210/Ra-226 and the ratios Pb-210/mean Ra-226, at the time of analysis 4.5 years after collection are shown. Errors are ±1 SD and are rounded up in the last significant digit for presentation.

Age category	Number pooled	Average age (yr)	Age range (yr)	Ra-226 (dpm/g)	Pb-210 (dpm/g)	Pb-210 Ra-226[1]	Pb-210 Ra-226[2]
1	83	1	1	0.288 ± 0.012	0.037 ± 0.007	0.128 ± 0.023	0.089 ± 0.019
2	130	9.79	9–11	0.517 ± 0.021	0.135 ± 0.022	0.260 ± 0.043	0.325 ± 0.065
3	141	18.91	14–23	0.386 ± 0.017	0.193 ± 0.030	0.500 ± 0.080	0.467 ± 0.092
4	127	28.55	24–34	0.465 ± 0.019	0.265 ± 0.041	0.570 ± 0.091	0.640 ± 0.126

[1] Activity ratios calculated with Ra-226 measured from each group.
[2] Activity ratios calculated with mean Ra-226: 0.414 ± 0.050.

porated into the biota or food chain through a variety of sources, such as water during the osmoregulation process, from food (Porntepkasemsan and Nevissi, 1990) such as phytoplankton (Shannon and Cherry, 1971) and zooplankton (Evans et al., 1938), and from contact with sediments (Swanson, 1985). The geographic area the species inhabits, its vertical distribution in the water column, and the efficiency of transfer of Ra-226 through its food chain could play a role in the uptake of Ra-226 (Cochran,

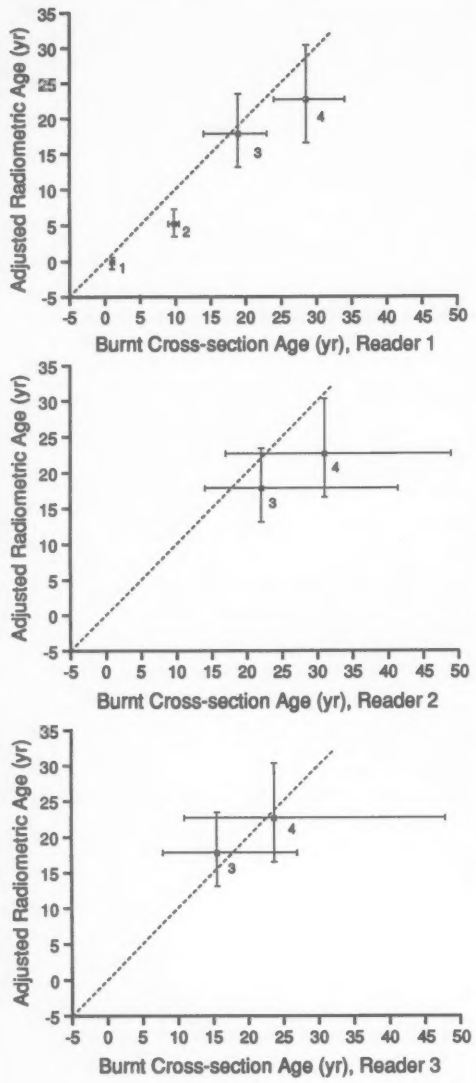
Adjusted Radiometric Age (yr)
Burnt Cross-section Age (yr), Reader 1
Adjusted Radiometric Age (yr)
Burnt Cross-section Age (yr), Reader 2
Adjusted Radiometric Age (yr)
Burnt Cross-section Age (yr), Reader 3

Figure 2

Comparison of burnt otolith cross-section ages (from Readers 1, 2, and 3) with adjusted radiometric ages (4.5 years were subtracted for the time between capture and analysis). Range in adjusted radiometric ages is 1 standard deviation, and the range in burnt otolith cross-section ages are the maximum and minimum in each age category (see Table 1). Ranges of burnt cross-section ages for Readers 2 and 3 are wider than for Reader 1 because age categories were defined by Reader 1 ages.

1982; Swanson, 1985; Fenton et al., 1990). Additionally, feeding rate, metabolic rate, and calcium deposition rate could all affect the specific activities found in otoliths. Sablefish are one of the fastest-growing epipelagic juvenile fishes (Shenker and Olla, 1986; Kendall and Matarese, 1987). Therefore, the higher Ra-226 and Pb-210 activity levels seen in sablefish otolith cores could be related to rapid uptake of Ra-226.

Assumptions for radiometric dating

We discussed three assumptions which must be satisfied for the radioisotope ageing of sablefish to be valid. Assumption 1, that otolith cores are closed with respect to loss or gain of any radioisotopes in the decay chain, has not been tested. Considering the decay chain containing Ra-226 (Eq. 1), Rn-222 is a source of concern. For Ra-226 to decay to Pb-210, it must first become Rn-222 (half-life=3.82 days) which is a noble gas. It is conceivable that Rn-222 could migrate in the otolith. A loss of Rn-222 would lead to underestimation of the true age. However, the calcium carbonate crystalline structure of the otolith probably prevents radioisotopes from migrating.[3]

Welden (1984) measured Pb-210 activity in the calcified cartilage of vertebral centrum from sharks, applying a procedure similar to the dating of sediments. The calcified cartilage allowed the Pb-210 to migrate in the vertebra so the assumption of a closed system did not hold true. Previous research by Goreau and Goreau (1960), Moore et al. (1973), Dodge and Thomson (1974), and Veeh and Burnett (1982) confirmed that calcium carbonate in coral acted as a chemically closed system. In Rn-222 diffusion experiments, Moore et al. (1973) could not detect migrations in coral.

For our study, Assumption 2 required that in the core of otoliths, initial ratios of the two radioisotopes be measured or known, and ideally be near zero. More Ra-226 than Pb-210 may be encountered by fish since Ra-226 is not in equilibrium with Pb-210 in seawater (Bacon et al., 1976). The environmental residence time of Ra-226 in seawater has been reported to be as high as 950 years (Szabo, 1967) and as low as 0.7 to 5.5 years (Shannon and Cherry, 1971). The environmental residence time of Pb-210 in surface waters has been reported to be as high

[3] At the "CSIRO, International workshop on otolith chemistry" 2–6 March 1992, in Hobart, Tasmania, Australia the possibility of Rn-222 migration was discussed with some enthusiasm. G. Fenton suggested that the otolith is relatively impermeable, and that Rn-222 migration is not a major problem.

as 3.5 years (Shannon et al., 1970) and as low as 1.4 years (Bacon et al., 1976). Pb-210 is incorporated into particulate matter whereby it is removed from the water column and deposited into sediments. To correct for Pb-210 incorporation, we measured the initial ratio, R^*, with young fish (1 yr olds). By analyzing very young splitnose rockfish, Bennett et al. (1982) found that the initial ratio of Pb-210/Ra-226 was between 0.1 and 0.2. Similar values for the initial ratio were also found in redfish (*Sebastes mentella*) (Campana et al., 1990), orange roughy (*Hoplostethus atlanticus*) (Fenton et al., 1991), and blue grenadier (*Macruronus novaezelandiae*) (Fenton et al., 1990). These results are comparable with the $R^*=0$ we used. The initial ratio cannot be estimated from older age categories because their true ages are uncertain. Therefore, $R^*=0$ for older age categories was assumed.

Assumption 3 states that the specific activity of Ra-226 incorporated into the otolith core be constant over the time span that the otoliths are receiving the radioisotopes. Assumption 3 is not required if only the otolith core is used and individual Ra-226 measurements are made for each age category. In sablefish the core of 1–year-old fish was appropriate because it is large, and there is a strong possibility that fish migration prior to maturity might cause a change in Ra-226 uptake. The likelihood ratio χ^2 test suggested that Ra-226 measurements differed among age categories. Therefore, ratios calculated by using individual Ra-226 measurements were preferred over those calculated with the Ra-226 mean. Campana et al. (1990), using cores composed of the first 5 years of growth, and a mean of 5 whole otolith samples (13 g per sample), found no significant difference in Ra-226 activity between the cores and whole otoliths. This suggested a constant rate of Ra-226 uptake. The differences we found between the Ra-226 activity measured in the four age categories were considerable (Table 3). Because the factors controlling Ra-226 uptake are complex and not well understood, the observed differences may well be real.

The use of whole otoliths requires modeling the mass growth rate of the otolith over the life of the fish and making assumptions concerning the uptake of Ra-226 and Pb-210 each year. Bennett et al. (1982) modeled the otolith's mass growth rate and assumed that the uptake of Ra-226 over the life span of the fish was proportional to otolith size (i.e. they assumed a constant rate of uptake). In whole otoliths from blue grenadier, the rate of uptake of Ra-226 changed over the life of the fish (Fenton et al., 1990). Therefore, the assumption of a constant rate of uptake of Ra-226 was violated. In whole otoliths from orange roughy, the Ra-226 specific activity increased with age (Fenton et al., 1991). Therefore, Fenton et al. (1991) used two Ra-226 averages: one for young age categories and a second for old age categories.

The conservative approach is to use the otolith core and individual category Ra-226 measurements making Assumption 3 unnecessary. Also, by using cores the closed system considered under Assumptions 1 and 2 is reduced. The behavior of otolith material deposited later in a fish's life need not be considered. The different approaches (otolith core, whole otolith, larger multi-gram samples, or any averaging of different age ranges) have trade-offs which should be evaluated in light of a species' biology.

Sources of error in ageing methodologies

Differences between the three sets of burnt cross-section ages are explainable. First, storage of broken-and-burnt otoliths in ethanol between readings may cause a fading of growth patterns. Second, variations in application of the otolith interpretation criteria of Beamish and Chilton (1982) and Beamish et al. (1983) could also lead to differences.

Even with the high specific activity (compared with other species) found in sablefish otoliths, the generally low activity levels of Po-210 and Ra-226 found in otoliths makes it important to carefully evaluate reagent blanks and background activities. Therefore, activity levels for reagent blank and background measurements reported in four previous studies (Bennett et al., 1982; Campana et al., 1990; and Fenton et al., 1990, 1991) were compared with those found here (Table 2). Considering the magnitude of errors, the Po-210 background we found was similar to other reported values (Table 2). The literature showed a much greater range of activities measured in the reagent blanks. Like Bennett et al. (1982), we found a nonsignificant activity level in the Po-210 reagent blank. The Po-210 reagent blank of 0.0103 ±0.0027 dpm reported by Fenton et al. (1990, 1991) seems high compared with the other findings. Also, we were the only study to report a nonsignificant Ra-226 reagent blank activity. Except for the Ra-226 reagent blank result, our background and reagent blank measurements for both Ra-226 and Pb-210 are in the same range as those reported in previous applications of radiometric ageing to fish.

The Ra-226 (or equivalent Rn-222) activity levels were low and difficult to measure. The signal to background ratio can be increased by using a greater sample weight. Fenton et al. (1991) argued that measuring Ra-226 by using barium co-precipitation with alpha spectroscopy (Sill, 1987) could also produce a better signal to background ratio. How-

ever, our measurements of Ra-226 background were similar to those of Fenton et al. (1991).

The low activity of Ra-226 and Pb-210 in the otoliths also requires that care be taken to avoid contamination. The otoliths were stored in 50% ethanol at sea. The grade of the ethanol was not ultra-pure which could introduce contaminating radioisotopes. Ethanol may also leach out some of the radioisotopes during storage. Some previous fish age-validation studies using Pb-210/Ra-226 (Fenton et al., 1990) stored the otoliths dry with desiccated adhering tissues. The dry tissue proved very difficult to remove and introduced Po-210 contamination. We relied on ultrasonic cleaning to break up any soft hydrated tissue after which the otoliths were rinsed thoroughly. This appeared to remove any organic material on the surface of the otolith. Contamination by Po-210 in the adherent tissues would increase the estimated radiometric age. In our study, the results from age category 1 indicate that this was not the case. Also, the grinding paper used could also introduce contamination.

Conclusions

The goal of this study was to validate the break-and-burn otolith ageing criteria used for sablefish at the AFSC. Although usually lower, the radiometric ages were within two standard deviations of the break-and-burn ages (Table 1; Fig. 2). If a range of possible ages occurred in the break-and-burn method, the older age was usually chosen. Since radiometric ages were consistently lower than burnt cross-section ages (from Reader 1), this method was probably not the best way to interpret the broken-and-burnt otolith. Possible migration of Rn-222 from the otolith, as discussed earlier, could also explain the difference.

Nevertheless, the break-and-burn method of age determination for sablefish has been validated by this study for fish up to 34 years old. This is the maximum age regularly seen in commercial or research catches. We have shown that the break-and-burn ageing criteria applied to sablefish otoliths produces, on average, ages similar to radiometric ages.

Acknowledgments

We thank age readers from the Pacific Biological Station, Canadian Department of Fisheries and Oceans, and the Alaska Fisheries Science Center, NMFS, for providing sablefish ages. We thank the Scientific Editor and three anonymous reviewers for comments which led to significant improvements in the paper.

Literature cited

Bacon, M. P., D. W. Spencer, and P. G. Brewer.
1976. $^{210}Pb/^{226}Ra$ and $^{210}Po/^{210}Pb$ disequilibria in seawater and suspended particulate matter. Earth Planet. Sci. Lett. 32:277–296.

Beamish, R. J., and D. E. Chilton.
1982. Preliminary evaluation of a method to determine the age of sablefish (*Anoplopoma fimbria*). Can. J. Fish. Aquat. Sci. 39:277–287.

Beamish, R. J., G. A. McFarlane, and D. E. Chilton.
1983. Use of oxytetracycline and other methods to validate a method of age determination for sablefish. *In* Proceedings of the second Lowell Wakefield fisheries symposium, Anchorage, AK, p. 95–116. Alaska Sea Grant Report 83-8.

Bennett, J. T., G. W. Boehlert, and K. K. Turekian.
1982. Confirmation of longevity in (*Sebastes diploproa*) (Pisces: Scorpaenidae) from $^{210}Pb/^{226}Ra$ measurements in otoliths. Mar. Bio. 71:209–215.

Bracken, B. E.
1983. Sablefish migration in the Gulf of Alaska based on tag recoveries. *In* Proceedings of the second Lowell Wakefield fisheries symposium, Anchorage, AK, p. 185–190. Alaska Sea Grant Report 83–8.

Campana, S. E., and J. D. Neilson.
1985. Microstructure of fish otoliths. Can. J. Fish. Aquat. Sci. 42:1014–1032.

Campana, S. E., K. C. T. Zwanenburg, and J. N. Smith.
1990. $^{210}Pb/^{226}Ra$ determination of longevity in redfish. Can. J. Fish. Aquat. Sci. 47:163–165.

Cochran, J. K.
1982. The oceanic chemistry of the U- and Th-series nuclides. *In* M. Ivanovich and R. S. Harmon (eds.), Uranium series disequilibrium: applications to environmental problems, p. 384–430. Oxford Univ. Press, NY.

Dodge, R. E., and J. Thomson.
1974. The natural radiochemical and growth records in contemporary hermatypic corals from the Atlantic and Caribbean. Earth Planet. Sci. Lett. 23:313–322.

Evans, R. D., A. F. Kip, and E. G. Moberg.
1938. The radium and radon content of Pacific Ocean water, life, and sediments. Am. J. Sci. 36:241–259.

Faure, G.
1986. Principles of isotope geology. John Wiley and Sons, New York, NY, 589 p.

Fenton, G. E., D. A. Ritz, and S. A. Short.
1990. $^{210}Pb/^{226}Ra$ disequilibria in otoliths of blue grenadier, *Macruronus novaezelandiae*: problems associated with radiometric ageing. Aust. J. Mar. Freshwater Res. 41:467–473.

Fenton, G. E., S. A. Short., and D. A. Ritz.
1991. Age determination of orange roughy, *Hoplostethus atlanticus* (Pisces: Trachichthyidae)

using ^{210}Pb:^{226}Ra disequilibria. Mar. Bio. 109:197–202.

Goreau, T. F., and N. I. Goreau.
1960. The physiology of skeleton formation in corals. IV: On isotopic equilibrium exchanges of calcium between corallum and environment in living and dead reef-building corals. Biol. Bull. Mar. Biol. Lab., Woods Hole 119:416–427.

Heyraund, M., and R. D. Cherry.
1979. Polonium-210 and lead-210 in marine food chains. Mar. Biol. 52:227–236.

Hunter, J. R., B. J. Macewicz, and C. A. Kimbrell.
1989. Fecundity and other aspects of the reproduction of sablefish (*Anoplopoma fimbria*) in central California waters. CalCOFI Rep. 30:61–72.

Kastelle, C. R.
1991. Radioisotope age validation and an estimate of natural mortality from the gonad to somatic weight index for sablefish (*Anoplopoma fimbria*). M.S. thesis, Univ. Washington, School of Fisheries, 87 p.

Kendall, A. W., and A. C. Matarese.
1987. Biology of eggs, larvae, and epipelagic juveniles of sablefish (*Anoplopoma fimbria*) in relation to their potential use in management. Mar. Fish. Rev. 49(1):1–13.

Kimura, D. K., and J. J. Lyons.
1991. Between-reader bias and variability in the age-determination process. Fish. Bull. 89:53–60.

Lucas, H. F.
1957. Improved low-level alpha scintillation counter for radon. Rev. Sci. Instruments 28(9): 680–683.

McFarlane, G. A., and R. J. Beamish.
1983. Preliminary observations on the juvenile biology of sablefish (*Anoplopoma fimbria*) in waters off the west coast of Canada. *In* Proceedings of the second Lowell Wakefield fisheries symposium, Anchorage, AK, p. 119–135. Alaska Sea Grant Report 83–8.

Mason, J. C., R. J. Beamish, and G. A. McFarlane.
1983. Sexual maturity, fecundity, spawning, and early life history of sablefish (*Anoplopoma fimbria*) off the Pacific coast of Canada. Can. J. Fish. Aquat. Sci. 40:2126–2134.

Moore, W. S., S. Krishnaswami, and S. G. Bhat.
1973. Radiometric determinations of coral growth rates. Bull. Mar. Sci. 23(2):157–176.

Mugiya, Y.
1977. Effect of acetazolamide on the otolith growth of goldfish. Bull. Jpn. Soc. Sci. Fish. 43(9):1053–1058.

Porntepkasemsan, B., and A. E. Nevissi.
1990. Mechanism of radium-226 transfer from sediments and water to marine fishes. Geochem. J. 24:223–228.

Sarmiento, J. L., D. E. Hammond, and W. S. Broecker.
1976. The calculation of the statistical counting error for ^{222}Rn scintillation counting. Earth Planet. Sci. Lett. 32: 351–356.

Seber, G. A. F.
1982. The estimation of animal abundance and related parameters. Macmillan, New York, NY, 654 p.

Shannon, L. V., and R. D. Cherry.
1971. Radium-226 in marine phytoplankton. Earth Planet. Sci. Lett. 11:339–343.

Shannon, L. V., R. D. Cherry, and M. J. Orren.
1970. Polonium-210 and lead-210 in the marine environment. Geochim. Cosmochim. Acta 34:701–711.

Shenker, J. M., and B. L. Olla.
1986. Laboratory feeding and growth of juvenile sablefish, *Anoplopoma fimbria*. Can. J. Fish. Aquat. Sci. 43:930–937.

Sill, C. W.
1987. Determination of Radium-226 in ores, nuclear wastes and environmental samples by high-resolution alpha spectrometry. Nucl. Chem. Waste Management 7:239–256.

Smith, J. M., R. Nelson, and S. E. Campana.
1991. The use of Pb-210/Ra-226 and Th-228/Ra-228 dis-equilibria in the ageing of otoliths of marine fish. *In* P. J. Kershaw and D. S. Woodhead (eds.), Radionuclides in the study of marine processes, p 350–359. Elsevier Applied Science, England.

Swanson, S. M.
1985. Food-chain transfer of U-series radionuclides in a northern Saskatchewan aquatic system. Health Phys. 49(5):747–770.

Szabo, B. J.
1967. Radium content in plankton and sea water in the Bahamas. Geochim. Cosmochim. Acta 31:1321–1331.

Veeh, H. H., and W. C. Burnett.
1982. Carbonate and phosphate sediments. *In* M.Ivanovich and R. S. Harmon (eds.), Uranium series disequilibrium: applications to environmental problems, p. 459–480. Oxford Univ. Press, NY.

Welden, B. A.
1984. Radiometric verification of age determination in elasmobranch fishes. M.S. thesis, Calif. State Univ., Hayward, Moss Landing Marine Labs, 108 p.

Distribution and abundance of two juvenile tropical *Photololigo* species (Cephalopoda: Loliginidae) in the central Great Barrier Reef Lagoon

Natalie A. Moltschaniwskyj
Department of Marine Biology, James Cook University of North Queensland
Townsville, Queensland 4811, Australia.

Peter J. Doherty
Australian Institute of Marine Science, PMB 3
Townsville, Queensland 4810, Australia.

Abstract.—This study quantified the temporal and spatial abundance of juveniles of two *Photololigo* species on the continental shelf off Townsville, Australia with the use of light-traps. The two *Photololigo* species (A and B) showed very distinct and separate spatial distribution patterns. *Photololigo* sp. A was found close to the coast and was the smaller and more abundant of the two species. This species was most abundant in surface waters, although larger individuals were generally caught deeper. There was no evidence of vertical movements during the night. The presence of small and large juvenile *Photololigo* sp. A during summer and winter months suggests spawning and recruitment occur throughout the year. In contrast, *Photololigo* sp. B was caught predominantly offshore. All sizes of *Photololigo* sp. B were caught both near the benthos and at the surface in the mid-lagoon, but farther offshore juveniles were deeper and larger. The presence of small juvenile squid of both species throughout the summer suggests that these species spawn for an extended period during the summer. This study demonstrates that light-traps are an effective way of sampling small cephalopods.

Manuscript accepted 8 November 1993
Fishery Bulletin 92: 302–312 (1994)

The current poor state of knowledge about processes important in squid population dynamics is mainly due to limited information about the juvenile phase (Voss, 1983; Boyle, 1990). Life-history characteristics have largely been derived from information about the adult phase. Our limited information about young squid is demonstrated in attempting to define the life-history phases (Young and Harman, 1988). Jackson and Choat (1992) suggest, given the comparatively short life time of tropical squid (<250 days), that a proportionally long period of the life cycle is spent as small individuals. In the case of *Loligo chinensis*, with a summer life time of 120 days, individuals less than 60 days old (<50-mm mantle length) have not been studied. Hence, for almost half the life history of most squid there is not even the most basic information. Temporal and spatial abundance patterns of juvenile squid will provide a basis for understanding the processes of mortality, growth, and recruitment. However, such information has traditionally been difficult to obtain because of problems in capturing and identifying a sufficient size range of juvenile cephalopods (Vecchione, 1987).

To examine the ecology of juvenile squid it is necessary to use techniques that catch a size range of individuals, hatchlings to juveniles, in good condition. Pelagic squid produce either benthic or pelagic eggs and have a planktonic juvenile phase (Boletzky, 1977). Juvenile squid are alert, mobile organisms that easily avoid capture by towed nets (Vecchione, 1987). The use of a combination of different towed nets to sample an area enables the collection of a wider size range of juvenile squid (Rodhouse et al., 1992). However, it is difficult to obtain replicates needed to provide density estimates from towed nets. In this study we have employed an alternative technique based on light-attraction that is effective in sampling pelagic juvenile fishes. Automated light-traps (Doherty, 1987) can overcome the problems of net avoidance and enable sampling at discrete depths in the water column. The ability to sample concurrently within an area ensures that estimates of variability in abundance are not confounded by time. This technique also collects live material in good condition, which can facilitate taxonomic identification. However, sampling an unknown volume of

water by individual traps requires cautious interpretation of abundance estimates (Choat et al., 1993).

There are four species of loliginid squid currently recognized in the Townsville region: *Sepioteuthis lessoniana, Loliolus noctiluca, Photololigo* sp. B, and *Photololigo* sp. A.[1] There are currently no morphological descriptions of the two *Photololigo* species, but they can be readily identified by using allozyme electrophoretic techniques (Yeatman and Benzie, in press). Previously both of these species have been referred to as *Photololigo* (*Loligo*) *chinensis* (Jackson and Choat, 1992; Yeatman and Benzie, in press), but neither correspond to *P. chinensis* from Thailand.[2] Electrophoretic analysis of a subset of juveniles collected during three months of the program found that all *Photololigo* sp. A were found less than 33 km offshore and 90% of the *Photololigo* sp. B were found 33 km or more offshore.[2] Because these species are morphologically identical as juveniles, we assumed that all individuals found at stations less than 33 km offshore were *Photololigo* sp. A and that *Photololigo* collected more than 33 km offshore were *Photololigo* sp. B. *Photololigo* sp. A (previously known as *Loligo chinensis*) has been the topic of recent growth studies using statolith aging techniques (Jackson and Choat, 1992). This species is a small short-lived neritic squid. Individuals are approximately 60 days old when they appear in the adult population and they can grow to 180 mm in 120 days. Little is known about the early life-history and juvenile distribution patterns of either *Photololigo* species. The objectives of this study were to describe the spatial and temporal distribution patterns of juvenile *Photololigo* species across the continental shelf in the Townsville region of the Great Barrier Reef.

Materials and methods

Sampling design

Two major habitat types are found on the continental shelf, off Townsville, Australia. The inshore habitat is a 56 km wide soft bottom coastal lagoon ranging in depth from 15 m to 40 m. The offshore habitat is a complex reef matrix of similar extent, dissected by channels ranging from 40 m to 75 m deep at the shelf break. To assess the cross-shelf distribution of juvenile squid, four automated light-traps (Doherty, 1987) were deployed at fifteen sampling stations spanning the continental shelf and the western Coral Sea (Fig. 1). Abundance along this transect was assessed over four months, October to January, during two austral summers, 1990/91 and 1991/92. At each station, the abundance of juvenile squid was determined at two depths by deploying two pairs of light-traps. In each pair, one light-trap was suspended immediately below the surface while the other light-trap was set deeper. In 1990/91, all deep light-traps were suspended 20 m below the surface. In 1991/92, the deep light-traps were suspended within 5 m of the bottom to a maximum of 100 m in the Coral Sea.

In all deployments, the two pairs of light-traps were released approximately 300 m apart and allowed to drift for one hour. Allowing the traps to drift in the water minimized potential problems with differential water movement among stations. The use of drifting light-traps has been shown to be a more effective way of catching pelagic organisms than anchored light-traps in open water (Thorrold, 1992). After one hour, the four light-traps were retrieved and the entire catch was fixed and preserved in 100% ethanol. Each evening the first light-trap was deployed after 1930 hours (Eastern Standard Time) and the last light-trap retrieved before 0430 hours. Travel time between each station allowed only five cross-shelf stations to be sampled per night. Thus, each night's activity concentrated on one of the two continental shelf habitats or the Coral Sea. Each monthly cruise consisted of nine nights during which time each of the 15 stations was sampled three times. However, sea conditions were not always favorable. Sampling effort at each station is shown in Table 1.

It was not logistically possible to sample all stations in each habitat simultaneously. Therefore, time of night is confounded with station position. Haphazard selection of the first station sampled each night ensured that no station was consistently sampled at the same time on all nights. Cruises were scheduled to include the new moon because this is the lunar phase when light attraction has proved most effective for fishes and various invertebrates (Milicich, 1992). Temperature and salinity profiles of the water column were collected at each station by using a Seabird Conductivity Temperature Device during the 1991/92 summer.

Concurrent with the summer cross-shelf sampling, light-traps were anchored within 100 m of the southeasterly side (weather-side) of four reefs; Keeper, Helix, Faraday, and Myrmidon, to sample near-reef water (Fig. 1). The use of drifting light-traps near the reefs was not possible. During the summer of 1990/91, four light-traps were anchored at each reef; three immediately below the surface

[1] C. C. Lu, Museum of Victoria, Australia, pers. commun. 1990.
[2] J. Yeatman, James Cook Univ., Australia, unpubl. data 1993.

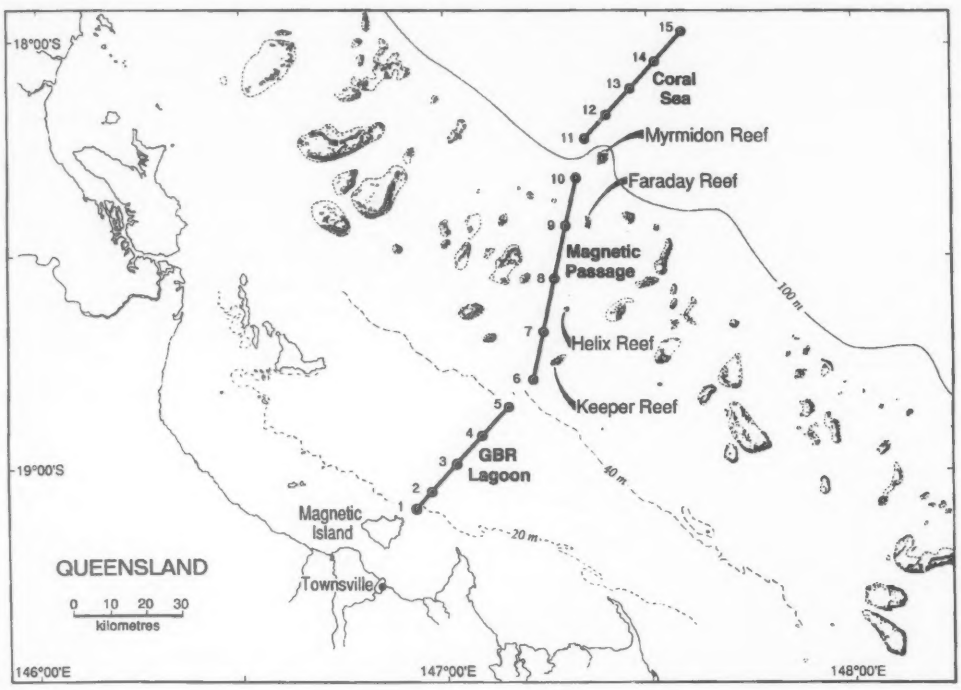

Figure 1

Map of the cross-shelf transect off Townsville, Australia, showing the position of each station along the transect. Station 1 = 19 km from Townsville, 2 = 24 km, 3 = 33 km, 4 = 43 km, 5 = 52 km, 6 = 61 km, 7 = 75 km, 8 = 92 km, 9 = 100 km, 10 = 115 km, 11 = 136 km, 12 = 145 km, 13 = 152 km, 14 = 163 km, and 15 = 172 km.

and one at 20 m below the surface. In 1991/92, an extra light-trap was added at 20 m. The anchored light-traps had an automatic timer, enabling the lights to be switched on and off automatically at predetermined periods during the night. Each light-trap on the reef fished for a total of three hours per night; lights came on for one hour at 2200 hours, 2400, and 0300 hours. Light-traps at all reefs were emptied the following day.

Squid were identified in the laboratory and the dorsal mantle length recorded for each individual. Individuals were measured within 14 days of preservation in 100% ethanol. A comparison of measurements of individuals (ranging in size from 5.3 mm to 29.5 mm) before and 14 days after preservation found that shrinkage was on average 0.5 mm.

Abundance patterns of the two *Photololigo* species during the two summers of sampling were examined by using 'planned comparisons,' where specific pregenerated hypotheses were examined (Day and Quinn, 1989). For each species we were interested in differences in abundance between years, locations, and depths.

To examine seasonality of juvenile *Photololigo* sp. A, the inshore station (19 km) was sampled during the austral winter months of May, June, July, and August 1991. Three sites at this station were sampled with four shallow and four deep (13-m) light-traps. Sites were sampled during the period of the new moon, on five nights in May and three nights in June, July, and August. Densities in summer and winter months were compared by using an unbalanced one-way analysis of variance (ANOVA), with month as the factor analyzed. Values in each light-trap for nights and sites within a month were treated as replicates.

To determine whether vertical migration might influence horizontal distribution patterns we examined the size structure of *Photololigo* sp. A at two depths during the night. On at least one occasion

Table 1

Total sampling effort for *Photololigo* spp. in each month in light-trap hours (and number of nights sampled) at each station during the two summers of sampling.

Year and month	Distance (km) from Townsville															Total no. sampled
	19	24	33	43	52	61	75	92	100	115	136	145	152	163	172	
1990																
Oct	8(2)	15(4)	16(4)	12(3)	16(4)	15(4)	4(1)	4(1)	4(1)	4(1)	12(3)	10(3)	10(3)	10(3)	10(3)	150(40)
Nov	12(3)	12(3)	12(3)	0(0)	16(3)	12(3)	12(3)	12(3)	12(3)	12(3)	8(2)	8(2)	8(2)	4(1)	4(1)	144(35)
Dec	8(2)	8(2)	4(1)	4(1)	4(1)	4(1)	4(1)	3(1)	4(1)	4(1)	4(1)	4(1)	4(1)	4(1)	4(1)	67(17)
1991																
Jan	12(3)	12(3)	12(2)	12(2)	12(2)	8(2)	8(2)	8(2)	8(2)	8(2)	8(2)	8(2)	4(2)	8(2)	8(2)	136(32)
Oct	12(3)	12(3)	12(3)	12(3)	12(3)	12(3)	8(2)	8(2)	8(2)	8(2)	4(1)	4(1)	4(1)	4(1)	4(1)	124(31)
Nov	12(3)	12(3)	11(3)	12(3)	12(3)	12(3)	12(3)	12(3)	12(3)	12(3)	4(1)	4(1)	4(1)	4(1)	4(1)	139(35)
Dec	12(3)	10(3)	11(3)	12(3)	12(3)	12(3)	8(2)	8(2)	8(2)	8(2)	4(1)	4(1)	4(1)	4(1)	4(1)	121(31)
1992																
Jan	12(3)	12(3)	12(3)	11(3)	12(3)	12(3)	8(2)	8(2)	8(2)	8(2)	4(1)	4(1)	4(1)	4(1)	4(1)	123(31)
Total	88(22)	93(24)	90(22)	75(18)	96(22)	87(22)	64(16)	63(16)	64(16)	64(16)	48(12)	46(12)	42(12)	42(11)	42(11)	1004(254)

in each month of the 1991/92 sampling period the 19- and 24-km stations were sampled both early and late in the night. The samples were separated into early (captured before 2400 hrs) and late (captured after 2400 hrs). By combining data from stations, across nights and months, it was possible to compare the size distributions between depths and time of night. A multiway-frequency analysis was used to determine the effect of time of night and depth on the size-frequency distribution.

Results

Distribution patterns

Juvenile *Photololigo* individuals were predominantly caught within 52 km of the mainland (Fig. 2). The few individuals found farther offshore were in the Magnetic Passage (five individuals) and on the reefs (six individuals). *Photololigo* species were not found in the Coral Sea. *Photololigo* sp. A was numerically the most abundant of the two species during both summers (Fig. 2); 856 individuals were caught in 181 hours of light-trapping (4.73 individuals caught per hour), compared with 379 *Photololigo* sp. B caught in 348 hours of light-trapping (1.09 individuals per hour). Catch per hour of light-trapping was greatest for *Photololigo* sp. A, especially at the 24-km station. The catch per unit of effort for *Photololigo* sp. B was greater at the 33-km station (Table 2). Overall, *Photololigo* sp. A juveniles were present in higher numbers at the 24-km station in the surface waters (Table 3). This pattern was consistent in both years, but higher numbers were caught in 1991/92 (Table 3), largely because of very high catches in December 1991 (Fig. 2). In comparison, highest numbers of *Photololigo* sp. B were consistently found at the 33-km station and abundance levels tended to decrease farther offshore (Fig. 2). Overall, *Photololigo* sp. B demonstrated no difference in abundance levels between the two years (Table 4). In contrast to *Photololigo* sp. A, juvenile *Photololigo* sp. B was more abundant deeper in the water column (Table 4). Farther offshore, *Photololigo* sp. B juveniles were present in very low numbers and were caught only in the deep light-traps (Fig. 2).

Photololigo sp. A ranged in size from 2.6 to 47.9 mm. The size-frequency distributions at the two depths were not significantly different between the 19-km and 24-km stations (χ^2=12.28; df=9; P=0.1979) (Fig. 3). There was no systematic change in the size-frequency distribution of *Photololigo* sp. A during either summer (Fig. 4). A modal shift in the size-frequency distribution in January 1992 suggested that fewer small individuals were available to be caught. However, catches were very low in this month.

Photololigo sp. B ranged in size from 3.6 to 61.6 mm (Fig. 3). From the size-frequency distributions it was clear that larger juveniles were found farther offshore and deeper in the water column (Fig. 3). No

modal shift in the size-frequency distribution during the summers was apparent (Fig. 4). However, catches were low in most months.

The multiway-frequency analysis established that the size-frequency distribution of juvenile *Photololigo* sp. A at both depths changed as a function of time of night (Table 5). Small juveniles dominated in the surface waters, but larger individuals were generally found closer to the benthos (Fig. 5). During the night, the relative abundance of small individuals decreased at both depths. Close to the benthos an increase in large individuals was evident. There was no discernible pattern of vertical migration; however, combining data across months to increase the number of juveniles in the analysis removed the possibility of detecting vertical migration in any one month.

The number of *Photololigo* sp. A juveniles captured during the winter months was similar to most of the summer monthly catches (Fig. 6); although winter catches never reached levels such as those seen in December 1991 (Table 6). The large number of small juveniles captured over the winter (Fig. 6) indicates that *Photololigo* sp. A spawns and hatches in both seasons. A similar size range was captured at each sampling during the summer months (Fig. 7).

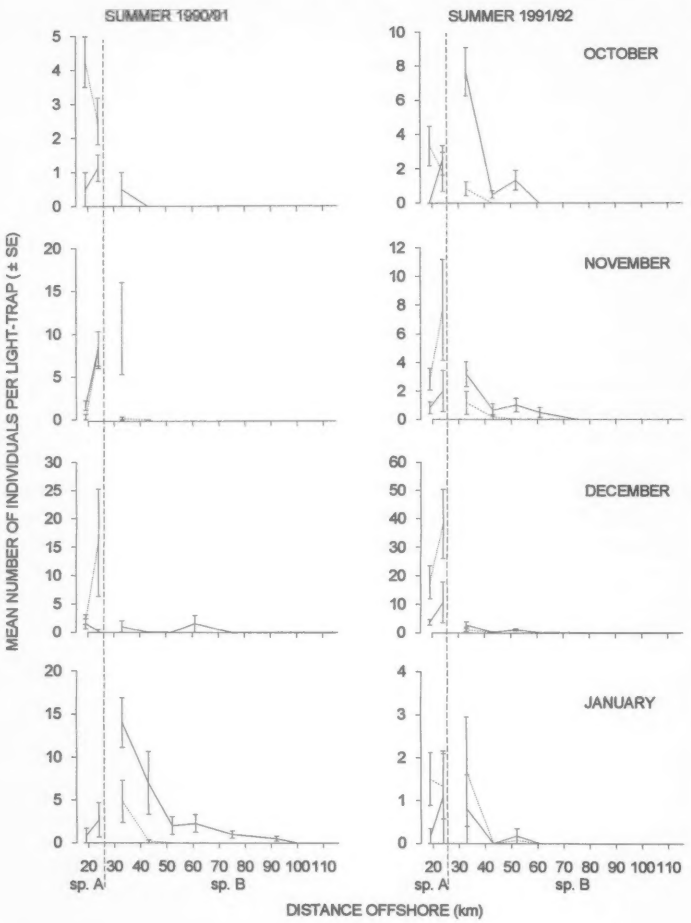

Figure 2

Catches of juvenile *Photololigo* sp. A (found at 19 and 24 km) and *Photololigo* sp. B (found at 33 km and greater) from Townsville, Australia. Most values are averages (± standard error) of six one-hour sets over three nights. See Table 1 for replicates at each station. (Solid lines, deep light-traps; dashed lines, shallow light-traps). Note the variable scale of the Y-axes.

Physical parameters

Both temperature and salinity decreased nonlinearly across the lagoon; discontinuities in both variables occurred midway across the Lagoon (Fig. 8). Temperature or salinity discontinuities were detected on at least six out of nine nights between the 33-km station and one or both of the neighbouring stations. This suggested that in the lagoon the water mass was heterogenous and may have influenced the distribution patterns of juvenile squid.

Salinity-temperature profiles of the water column at each station indicated thermoclines were present on some nights (Table 7). A thermocline was defined as a temperature change greater than 0.5°C between surface and bottom water; differences as great as 3°C were detected during January. However, these thermoclines were a temporally and spatially unstable feature of the water column, possibly due to variable wind conditions and the shallow body of water being sampled.

Discussion

Light-traps have provided a technique by which spatio-temporal distribution patterns of two *Pho-*

tololigo species can be described. Identification of *Photololigo* species using allozyme electrophoresis suggests that the two species are separated geographically across the Great Barrier Reef Lagoon (Yeatman and Benzie, in press). This separation occurs in a region of the coastal lagoon where temperature-salinity data indicate heterogeneity. High numbers of juvenile *Photololigo* sp. A at stations close to the mainland suggests that spawning grounds for this species may be close to the coast, a feature typical for loliginid squid (Mangold, 1987). Furthermore, the presence of small and large individuals during summer and winter months indicates that spawning, hatching, and recruitment are not seasonal events. This characteristic may be more common for tropical species that tend to have shorter lifespans than temperate species (Jackson and Choat, 1992). Large numbers of small juveniles collected during the winter may be a function of slower growth during the winter (Jackson and Choat, 1992). Little is known about *Photololigo* sp. B adults; however, the presence of juveniles in this region suggests that an adult population does occur in the Townsville region and that spawning occurs throughout the summer. The identification of juvenile *Photololigo* was confirmed on a subsample of specimens captured during the summer. Conclusions drawn from this study are based upon the assumption that the offshore distribution pattern of the two species was consistent in all other months of sampling.

Table 2

Catch per hour of light-trapping for each *Photololigo* species across the Great Barrier Reef Lagoon for eight months of summer sampling. *Photololigo* sp. A at stations 19 km and 24 km and *Photololigo* sp. B farther offshore.

	Species A		Species B				
Month	19km	24km	33km	43km	52km	61km	Total
1990							
Oct	2.38	1.81	0.25	0	0	0	0.62
Nov	0.75	8.25	5.42	—	0	0	2.88
Dec	1.88	8.00	0.50	0	0	0.75	2.63
1991							
Jan	0.42	1.33	9.42	3.58	1.00	1.13	2.91
Oct	1.67	2.17	4.25	0.25	0.67	0	1.50
Nov	1.83	4.83	2.17	0.42	0.50	0.25	1.67
Dec	10.67	24.42	1.92	0.17	0.50	0	6.28
1992							
Jan	0.83	1.75	1.67	0.17	0.08	0	0.75
Total	2.59	6.31	3.30	0.72	0.36	0.17	2.33

Table 3

Planned comparisons of juvenile *Photololigo* sp. A densities between depths, years, and sites.

Contrast	df	Contrast sums of squares	Mean squares	*F*-value	*P>F*
Depths	1	9.8165	9.8165	12.20	0.0006
Years	1	3.7565	3.7565	4.67	0.0320
Sites	1	8.6892	8.6892	10.80	0.0012
Residual	177	142.3838	0.8044		

Table 4

Planned comparisons of juvenile *Photololigo* sp. B densities between depths and years.

Contrast	df	Contrast sums of squares	Mean squares	*F*-value	*P>F*
Depths	1	17.0607	17.0607	37.85	0.0001
Years	1	0.0438	0.0438	0.10	0.7554
Residual	335	148.7448	0.4507		

Juvenile squid are not easily sampled with towed nets (Vecchione, 1979; Vecchione and Gaston, 1985; Holme, 1974). They have highly developed sensory and locomotor systems (Boletzky, 1974) and it is likely that these animals are often undersampled because of net avoidance. Choat et al. (1993) have shown that plankton nets select for small larval fish, but larger fish are captured from the same water column by using light attraction. Thorrold (1992), as well as this study, showed that light-traps are a useful technique for capturing juvenile squid. However, like most sampling techniques, the light-traps have biases. One problem is that light-traps sample an unknown volume of water. Nonetheless, they have

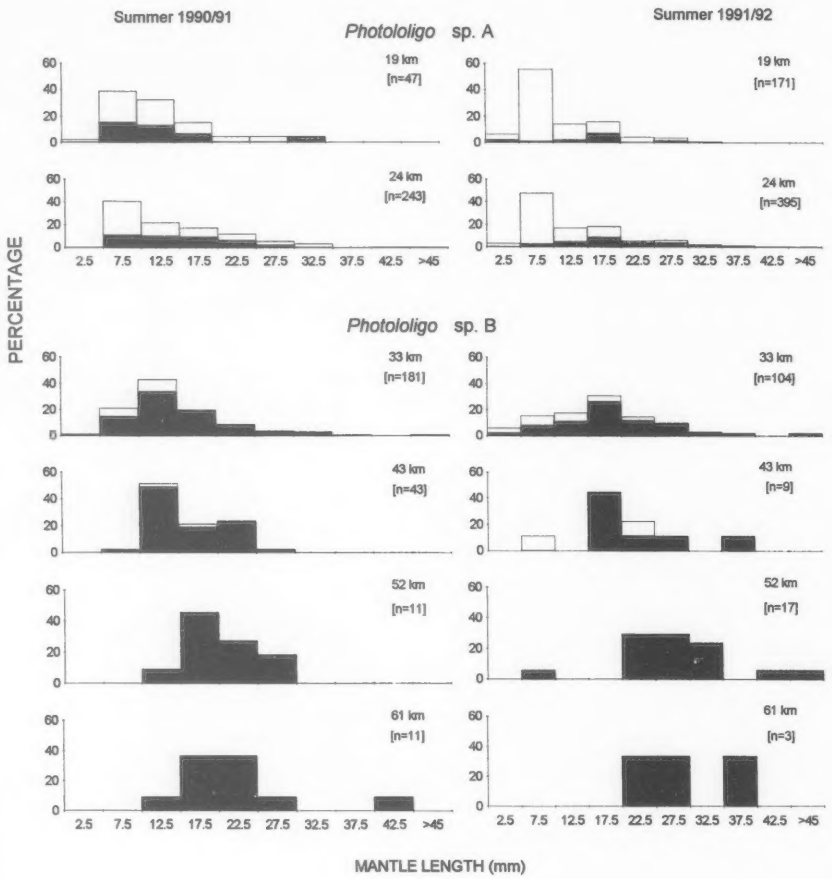

Figure 3

Size-frequency distribution of *Photololigo* sp. A and *Photololigo* sp. B caught at each station (pooled across months) in deep (shaded) and shallow (unshaded) light-traps. Total number of juveniles indicated in brackets.

Table 5

Results of the multiway frequency analysis to examine changes in the size distribution of *Photololigo* sp. A between time of night and depth.

Source	df	χ^2	*P*
Depth	1	92.8	0.00
Time	1	25.57	0.00
Depth × Time	1	0.19	0.66

been validated as useful devices for monitoring relative abundance patterns in larval supply of pelagic juvenile fish at fixed locations (Milicich et al., 1992).

Great care needs to be exercised when interpreting catch rates from different locations because changes in water transparency can bias light-trap efficiency. Similarly, it is not possible to quantitatively compare catches from drifting and anchored light-traps (Thorrold, 1992). This is because the former act as lagrangian drifters and sample photopositive organisms from within a constant light pool. In contrast, the moored light-traps experience a variable water flow that may greatly increase the volume of water swept in an hour of sampling. Despite more intensive sampling on the reefs, catches of *Photololigo* were low and we conclude that spawning does not occur near the reefs and that juvenile *Photololigo* individuals are concentrated in the lagoon. In the

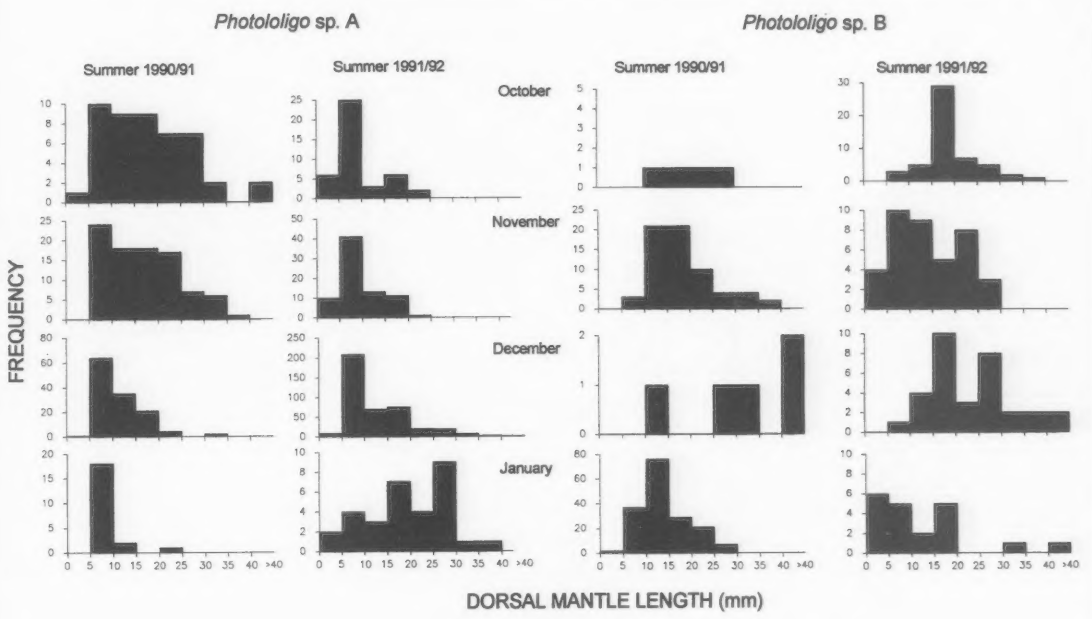

Figure 4

The size-frequency distribution of juvenile *Photololigo* sp. A and *Photololigo* sp. B during eight months of summer sampling. Size classes are mid-points of each class. Data are pooled across depths and stations.

present study, a gradient of turbidity across the shelf makes it possible that inshore catches would underestimate abundance if corrected for diminishing light-pools. However, if the error was significant, it would only exaggerate, not diminish, our observation that juvenile squid were more abundant within the coastal lagoon.

Table 6

Analysis of variance examining differences between densities of *Photololigo* sp. A at the 19 km station between summer months of 1990/91 and 1991/92 and winter months of 1991.

Source	df	Contrast sums of squares	Mean squares	*F*-value	*P>F*
Month	11	1118.200	101.654	9.55	0.0001
Residual	214	2277.910	10.644		

High catches of juvenile squid in the coastal lagoon were at locations where discontinuities were often observed in surface temperature and salinity. Hydrodynamic modelling of this region suggests that the coastal lagoon is often subject to velocity shear (King and Wolanski, 1992). Water in the lagoon typically flows southward under the influence of the poleward East Australian Current, which pushes water onto the outer shelf and through the reef matrix, especially through channels like the Magnetic Passage. Under typical south-easterly wind conditions the shallow body of water trapped against the coast moves in the opposite direction, northwards. The result is a velocity shear between the two water masses and a zone of low residual displacement. Modelling studies suggest that the cross-shelf location of this feature, referred to as a separation front (King and Wolanski, 1992), will shift seawards as the wind strength increases and vice versa. This mobility of the frontal region is consistent with the daily and monthly variability of salinity and temperature at the surface indicated by our physical monitoring during the second summer.

This low-shear zone is identified as a significant place for aggregation of planktonic organisms. Cross-shelf studies have shown highest abundances of larval reef fishes in a similar location near the

center of the Great Barrier Reef Lagoon (Thorrold, in press). These catches included individuals taken from reefs farther offshore, as well as piscivorous larvae of various scombrids from inshore (Thorrold, 1993). It is not clear whether aggregation of these stages is passive, due to hydrodynamics, or the result of attraction to the coastal boundary area by enhanced secondary productivity in this frontal zone (Thorrold and McKinnon, 1992). This discontinuity may be a mechanism separating the two *Photololigo* species geographically. The separation of juvenile cephalopod species in the Gulf Stream east of New England is thought to be closely related to mesoscale hydrological features (Vecchione and Roper, 1986). The importance of hydrological features in aggregating juvenile squid has been identified in a number of species (Rodhouse and Clarke, 1985; Brunetti and Ivanovic, 1992; Rodhouse et al., 1992). This suggests that these areas are ecologically important for juvenile squid.

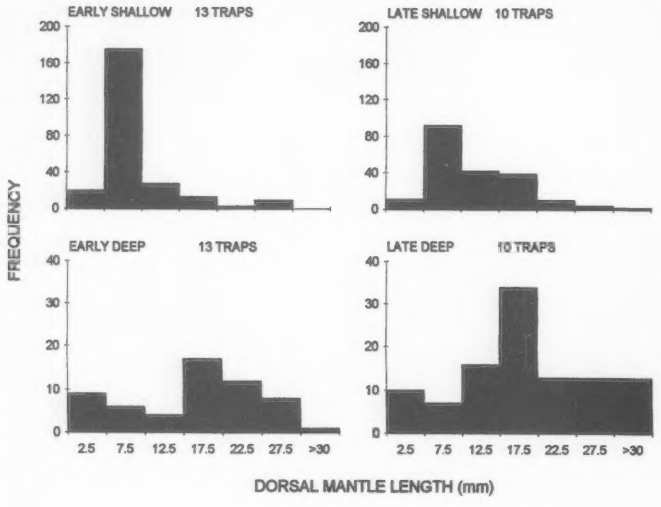
EARLY SHALLOW 13 TRAPS
LATE SHALLOW 10 TRAPS
EARLY DEEP 13 TRAPS
LATE DEEP 10 TRAPS
FREQUENCY
DORSAL MANTLE LENGTH (mm)
2.5 7.5 12.5 17.5 22.5 27.5 >30

Figure 5

Size-frequency distributions of juvenile *Photololigo* sp. A from the two inshore stations at two sampling depths (pooled across the summer months 1991/92), captured early (before 2400 hr) and late (after 2400 hr) in the night.

The second way in which shelf-scale hydrodynamics affects the stability of the water column is the intrusion of upwelled waters from the shelf-break driven onto the shelf by variations in the speed and position of the East Australian Current. These cold intrusions can be tracked into the Great Barrier Reef Lagoon (King and Wolanski, 1992) and the strong thermal stratification observed in January 1992 was consistent with an intrusion at this time. A cold bottom layer at 33 km was evident on one night in November, but the inner stations were not stratified. The presence of juvenile *Photololigo* at most stations in all months, despite a range of physical conditions, suggests juvenile *Photololigo* can tolerate substantial environmental variation. This tolerance is consistent with a nonseasonal reproductive strategy, which is essential for a species that lives for only four months.

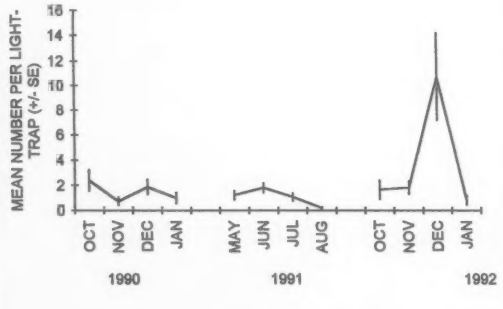

Figure 6

Catches of juvenile *Photololigo* sp. A at the 19-km station over twelve months: during summer 1990/91, winter 1991, and summer 1991/92. (Data pooled across depth and nights.)

During the night there was little evidence of a pronounced vertical migration such as the mass aggregations of juvenile *Loligo* spp. on the benthos (Vecchione and Gaston, 1985) or the general movement to the surface by juvenile *L. pealei* (Vecchione, 1981). The absence of vertical movement during the night suggests that the observed ontogenetic shift of *Photololigo* sp. B farther offshore and deeper is real and not a product of location confounded with time of night when sampling occurred. However, as was noticed in the catch-per-unit-of-effort values, both species are caught in relatively low numbers; hence, conclusions based on small differences that are not significantly different are limited. There was a problem with low numbers in all spatial and temporal trends described. However, this was a preliminary study with just two hours of sampling at each station per night. More intensive sampling in bound-

Table 7

Depth of the thermocline (m) at each station on each night of sampling during the three months of the 1991/92 summer.

Sampling period and situation	Depth of thermocline Day 1	Day 2	Day 3
October 1991			
19 km	14	11	Absent
24 km	13	14	Absent
33 km	10	13	Absent
43 km	10	Absent	Absent
52 km	25	Absent	Absent
61 km	31	Absent	—
November 1991			
19 km	Absent	Absent	Absent
24 km	Absent	Absent	Absent
33 km	Absent	Absent	20
43 km	Absent	Absent	22
52 km	Absent	Absent	25
61 km	Absent	Absent	29
January 1992			
19 km	7	7	9
24 km	9	9	9
33 km	11	13	12
43 km	15	15	18
52 km	28	24	27
61 km	31	47	—

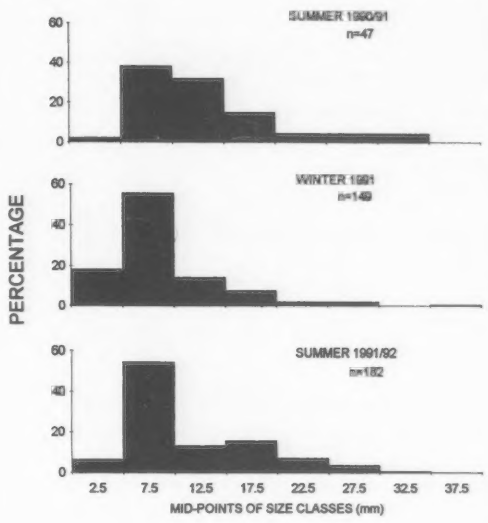

Figure 7

Size-frequency distributions of juvenile *Photololigo* sp. A at the 19-km station during the summer and winter months. (Numbers are pooled across months, depth, and nights.)

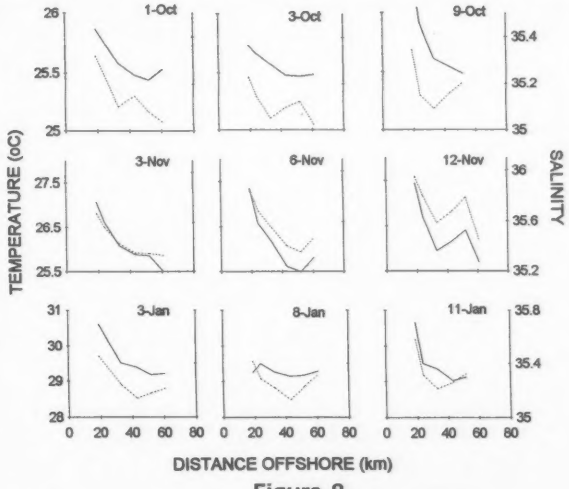

Figure 8

Surface temperature (dashed) and salinity (solid) profiles across the Great Barrier Reef Lagoon for each night of sampling in October and November 1991 and in January 1992. The Conductivity Temperature Device failed during the December cruise.

ary waters, both vertical and horizontal, is needed to understand how juvenile squid react to the physical environment. This study has shown that light-traps are useful devices for catching juvenile squid, providing a basis for a more intensive study of the early life-history of squid.

Acknowledgments

This project was funded by a FIRDC grant to P.J.D. and a Merit Research Grant to N.A.M. We thank the crew of the RV *Lady Basten* and volunteers who assisted with fieldwork. Identification of squid was assisted by C. C. Lu. We thank Julia Yeatman for access to electrophoretic data and discussions about species identification. This manuscript was greatly improved by the comments of J. H. Choat, A. Lewis, M. McCormick, the Coral Reef Discussion Group, and two anonymous reviewers. This research was conducted while N.A.M. was on a Commonwealth Scholarship.

Literature cited

Boletzky, S. v.
1974. The 'larvae' of Cephalopoda: a review. Thalassia Jugoslavica 10:45–76.
1977. Post-hatching behaviour and mode of life in cephalopods. Symp. Zool. Soc. Lond. 38:557–567.

Boyle, P. R.
1990. Cephalopod biology in the fisheries context. Fish. Res. 8:303–321.

Brunetti, N. E., and M. L. Ivanovic.
1992. Distribution and abundance of early life stages of squid (*Illex argentinus*) in the south-west Atlantic. ICES J. mar. Sci. 49:175–183.

Choat, J. H., P. J. Doherty, B. A. Kerrigan, and J. M. Leis.
1993. A comparison of towed nets, purse seine, and light-aggregation devices for sampling larvae and pelagic juveniles of coral reef fishes. Fish. Bull. 91:195–209

Day, R. W., and G. P. Quinn.
1989. Comparisons of treatments after an analysis of variance in ecology. Ecol. Monogr. 59:433–463

Doherty, P. J.
1987. Light-traps: selective but useful devices for quantifying the distributions and abundances of larval fishes. Bull. Mar. Sci. 41:423–431.

Holme, N. A.
1974. The biology of *Loligo forbesi* Steenstrup (Mollusca: Cephalopoda) in the Plymouth area. J. mar. biol. Assoc. U.K. 54:481–503.

Jackson, G. D., and J. H. Choat.
1992. Growth in tropical cephalopods: an analysis based on statolith microstructure. Can. J. Fish. Aquat. Sci. 49:218–228.

King, B., and E. Wolanski.
1992. Coastal dynamics along a rugged coastline. *In* D. Prandle (ed.), Dynamics and exchanges in estuaries and the coastal zone, p. 577–598. Coastal and Estuarine Studies 74, Springer-Verlag.

Mangold, K.
1987. Reproduction. *In* P. R. Boyle (ed.), Cephalopod life cycles. Vol 2: Comparative reviews, p. 157–200. Academic Press, NY.

Milicich, M. J.
1992. Light-traps: a novel technique for monitoring larval supply and replenishment of coral reef fish populations. Unpubl. Ph.D. thesis, Griffith University, 127 p.

Milicich, M. J., M. G. Meekan, and P. J. Doherty.
1992. Larval supply: a good predictor of recruitment of three species of reef fish (Pomacentridae). Mar. Ecol. Prog. Ser. 86:153–166.

Rodhouse, P. G., and M. R. Clarke.
1985. Growth and distribution of young *Mesonychoteuthis hamiltoni* Robson (Mollusca: Cephalopoda): an Antarctic squid. Vie Milieu 35:223–230.

Rodhouse, P. G., C. Symon, and E. M. C. Hatfield.
1992. Early life cycle of cephalopods in relation to the major oceanographic features of the southwest Atlantic Ocean. Mar. Ecol. Prog. Ser. 89:183–195.

Thorrold, S. R.
1992. Evaluating the performance of light traps for sampling small fish and squid in open waters of the central Great Barrier Reef lagoon. Mar. Ecol. Prog. Ser. 89:277–285.
1993. Post-larval and juvenile scombrids captured in light traps: preliminary results from the central Great Barrier Reef lagoon. Bull. Mar. Sci. 52:631–641.
In press. Coupling of pre-settlement reef fish distribution and hydrography in the central Great Barrier Reef lagoon. Proc. Seventh International Coral Reef Symposium, 1992.

Thorrold, S. R., and A. D. McKinnon.
1992. Biological significance of the coastal boundary layer off Townsville, North Queensland. *In* D. A. Hancock (ed.), Larval biology. Australian Society for Fish Biology Workshop, Hobart 1991. Bureau of Rural Resources Proceedings 15:104–109.

Vecchione, M.
1979. Larval development of *Illex* Steenstrup, 1880, in the northwestern Atlantic, with comments on *Illex* larval distribution. Proc. Biol. Soc. Wash. 91:1060–1075.
1981. Aspects of the early life history of *Loligo pealei* (Cephalopoda; Myopsida). J. Shellfish Res. 1:171–180.
1987. Juvenile ecology. *In* P. R. Boyle (ed.), Cephalopod life cycles. Vol 2: Comparative reviews, p. 61–84. Academic Press, NY.

Vecchione, M., and G. R. Gaston.
1985. In-situ observations on the small-scale distribution of juvenile squids (Cephalopoda: Loliginidae) on the northwest Florida shelf. Vie Milieu 35:231–235.

Vecchione, M., and C. F. E. Roper.
1986. Occurrence of larval *Illex illecebrosus* and other young cephalopods in the slope water/Gulf Stream interface. Proc. Biol. Soc. Wash. 99:703–708.

Voss, G. L.
1983. A review of cephalopod fisheries biology. Mem. Natl. Mus. Victoria 44:229–241.

Yeatman, J., and J. A. H. Benzie.
In press. Genetic structure and distribution of *Photololigo* in Australia. Mar. Biol.

Young, R. E., and R. F. Harman.
1988. "Larva," "paralarva," and "subadult" in cephalopod terminology. Malacologia 29:201–207.

Observations on the distribution and activities of rockfish, *Sebastes* spp., in Saanich Inlet, British Columbia, from the *Pisces IV* submersible

Debra J. Murie*
Daryl C. Parkyn
Bruce G. Clapp*
Geoffrey G. Krause**
Department of Biology, University of Victoria
Victoria, B.C., Canada V8W 2Y2

Abstract.— The distribution and activities of rockfish, *Sebastes* spp., inhabiting depths between 21 and 150 m in the coastal fjord of Saanich Inlet, British Columbia, were assessed by using the *Pisces IV* submersible. Quillback rockfish, *S. maliger*, was the numerically dominant rockfish, attaining a median density of 5.7 fish·100m^{-2} between 21 m and 100 m of depth. Copper rockfish, *S. caurinus*, tiger rockfish, *S. nigrocinctus*, yellowtail rockfish, *S. flavidus*, yelloweye rockfish, *S. ruberrimus*, and green-striped rockfish, *S. elongatus*, were all observed in consistently low densities (<1 fish·100m^{-2}). The greatest densities of rockfish occurred over complex habitat of broken rock and boulders. The majority (>50%) of rockfish were observed either perched on open substrate, hovering, or swimming. All rockfish species were observed near quillback rockfish (>75% occurrence); and quillback, copper, and yellowtail rockfishes were also found in association with conspecifics.

Prior to the advent of submersibles, in situ observations of deep-water demersal fish assemblages were constrained by time-depth limitations of SCUBA, which restrict observations of fish assemblages primarily to depths above 40 m (130 ft) (e.g. Moulton, 1977; Larson, 1980; Hallacher and Roberts, 1985; Richards, 1987; Murie, 1991). Distributional studies of fishes inhabiting waters deeper than 30–40 m have therefore relied on hook-and-line surveys, box trapping, or net trawling, all of which have known biases and limitations (Westrheim, 1970; Uzmann et al., 1977; Krieger, 1993). The recent availability of small submersibles for research purposes has allowed direct visual assessment of the depth distribution, density, and habitat of a variety of deep-water fish species (Uzmann et al., 1977; Carlson and Straty, 1981; Richards, 1986; Dennis and Bright 1988; Pearcy et al., 1989; Stein et al., 1992; Krieger, 1993).

Rockfish (*Sebastes* spp.) are important to nearshore recreational and commercial fisheries along the northeastern Pacific coast (Patten, 1973; Richards, 1987). Many inshore rockfish species are believed to be ecologically and morphologically similar, and are primarily benthic, sedentary fishes (Patten, 1973; Moulton, 1977; Mathews and Barker, 1983; Richards, 1986, 1987; Murie, 1991). Distributions of nearshore rockfish may depend on a variety of factors, including depth, habitat, and the presence of con- and hetero-specifics. Various species are known to segregate bathymetrically (Larson, 1980; Hallacher and Roberts, 1985; Richards, 1986, 1987; Pearcy et al., 1989), reducing or eliminating the potential for competitive interactions between otherwise ecologically similar species (Larson, 1980). Using a submersible, it is possible to observe directly the species-specific depth distributions, as well as to estimate each species' numerical abundance or density with depth. Changes in density with depth within a rockfish species may ultimately be related to fish size because rockfish size is often posi-

*Present address: Department of Fisheries and Oceans, Pacific Biological Station, Marine Fish Division, Nanaimo, B.C., Canada V9R 5K6
**Present address: Explorations Unlimited, #1-1012 Richardson St., Victoria, B.C., Canada V8W 3C5.

Manuscript accepted 18 October 1993
Fishery Bulletin 92: 313–323 (1994)

tively correlated with depth (Westrheim, 1970; Boehlert, 1980; Wilkins, 1980; Richards, 1986).

Nearshore rockfish are usually found in close association with the substrate or vertical relief (e.g. kelp beds) and their density may be dependent on the type of habitat available (e.g. boulder fields, shelter holes, etc.) (Patten, 1973; Moulton, 1977; Richards, 1986, 1987; Pearcy et al., 1989; Stein et al., 1992). Depth and density distributions of nearshore rockfish in British Columbia have been assessed primarily by hook-and-line surveys (e.g. Richards et al., 1988) and observations from submersibles are lacking. To date, only one study has assessed the distribution of nearshore rockfish in British Columbia using direct observations from a submersible (Richards and Cass, 1985; Richards, 1986). In their study, the depth and habitat distributions of rockfish were surveyed at depths of 21–140 m in coastal waters of the northeastern Strait of Georgia. In addition to observations on depth and type of habitat frequented by various rockfish species, however, submersibles also provide a unique opportunity to observe the behavioral activities of the fishes and their associations with conspecifics and heterospecifics. To date, there has been a lack of submersible studies that attempt to quantitatively assess the in situ activities of rockfish.

In the present study, we examined the distribution of rockfish observed from a submersible deployed in Saanich Inlet, a coastal fjord in the southern Strait of Georgia, British Columbia (Fig. 1). Fjords in British Columbia differ from open coastal areas, such as those surveyed by Richards (1986), in that they typically rely on estuarine-type circulation for mixing but have submerged sills which restrict mixing of waters below the sill depth (Thomson, 1981). For fjords of Vancouver Island, B.C., limited circulation results in low dissolved oxygen levels in relatively deep water (Pickard, 1963). In Saanich Inlet, restricted mixing at depth results in oxygen-deficient waters (<2.0 $mg \cdot L^{-1}$) below 100 m throughout most of the year and intermittent, seasonal (usually during January–August) anoxia with production of hydrogen sulfide (Herlinveaux, 1962; Liu, 1989), which is toxic to aerobic organisms (Martin et al., 1981). Various studies of invertebrates in Saanich Inlet have shown that the concentration of dissolved oxygen in the water limits their depth distribution (e.g. Burd, 1983; Mackie and Mills, 1983; Jamieson and Pikitch, 1988; Liu, 1989). Field studies have also demonstrated that the vertical or horizontal distribution of fishes is positively correlated with oxygen concentration (reviewed in Kramer, 1987). We therefore speculated that depth distributions for rockfish species in Saanich Inlet would be relatively shallow when compared to their reported maximum depths in open coastal areas.

The present study is the first to examine in situ species composition and density of rockfish in a coastal fjord in British Columbia. In addition, in situ behavioral activities and species associations of nearshore rockfish at depths greater than 30 m in coastal waters of British Columbia have been described for the first time.

Methods

The *Pisces IV* submersible (Department of Fisheries and Oceans, Canada) was used to survey rockfish populations in Saanich Inlet on 9–10 December 1986. A comprehensive description of the *Pisces IV* submersible was given by Mackie and Mills (1983). The inlet has a steep, rocky slope bottom interspersed with sand-shell valleys and is 7.2 km at its

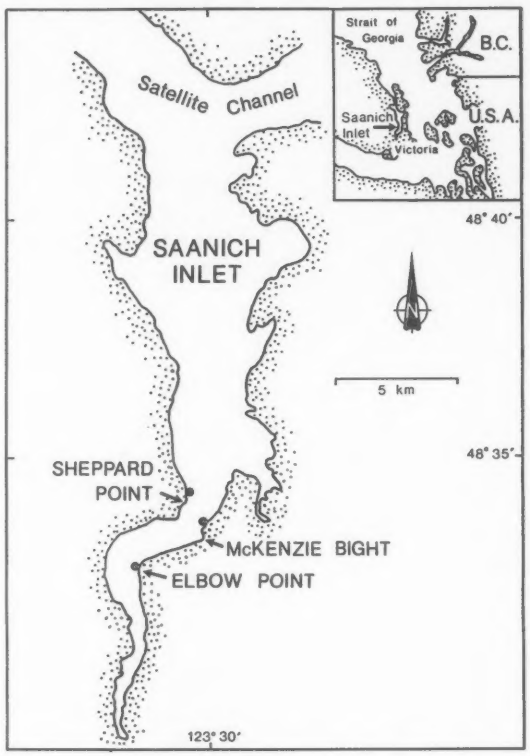

Figure 1

Location of transect sites (•) in Saanich Inlet, Vancouver Island, British Columbia. Inset: Location of Saanich Inlet in relation to the mainland of B.C.

widest. Specifics of the oceanographic characteristics of Saanich Inlet are detailed elsewhere (Herlinveaux, 1962; Anderson and Devol, 1973). Of relevance is that the basin of the inlet reaches a maximum depth of 234 m, but a submerged sill at 75 m at its mouth in Satellite Channel restricts the renewal of deep-water into the inlet. The resulting oxygen deficiency, anoxia, and production of hydrogen sulfide is offset in some years when well-oxygenated, dense bottom-water intrudes over the sill (Herlinveaux, 1962; Anderson and Devol, 1973). We therefore did a hydrocast at depths of 0–225 m to determine the depth of the oxycline in the inlet and whether hydrogen sulfide was present at the time of the surveys. The sampling station was located at lat. 48°37.80'N and long. 123°30.00'W (Liu, 1989).

Three sites within Saanich Inlet were surveyed: five transects were traversed at Elbow Point, eight in an area north of McKenzie Bight, and three in an area north of Sheppard Point (Fig. 1). These areas were known from preliminary SCUBA dive surveys to have rockfish present in >30 m water depth (Murie et al., pers. obs.). All surveys were conducted during daylight hours (09:30 hours to 16:00 hours) and were also restricted to a depth range between 20 and 150 m because the buoyancy of the *Pisces IV* is not finely controlled above 20 m, and bottom time restrictions precluded the transects starting at the basin floor (~200 m). Depth at which each transect started therefore varied among sites owing to slope and positioning of the submersible, with starting depths of 95–109 m at Elbow Point, 92–154 m at McKenzie Bight, and 67–74 m at Sheppard Point.

At the start of each transect, the *Pisces IV* submerged in open water and on reaching depth the external floodlights were lit and the submersible was manoeuvred horizontally, slowly, toward the cliff face. Once the bottom substrate (cliff) was located, the submersible began a slow vertical ascent (~5 $m \cdot min^{-1}$), keeping the viewing ports (port, pilot, and starboard) directed perpendicular to and approximately 3 m from the substrate. Underwater visibility at the time of the surveys was ~5–6 m with external illumination.

On ascent, an audio-record was made of the species, time, depth, estimated size (whenever possible), activity, and habitat for each rockfish observed. Each observer (port and starboard) recorded all rockfish encountered within a plane bisecting the pilot's viewport and extending outward at an angle of approximately 45°, corresponding to approximately 3 m of horizontal distance across the substrate (i.e. viewing width). To avoid counting the same fish twice, any rockfish swimming across the path of the submersible or positioned close to the pilot's viewing area was pointed out to the other observer. Size was visually estimated (±5 cm) by comparing the fish with an externally mounted graduated rod. Rockfish were designated as small (≤20 cm total length [TL]) and large (>20 cm TL); large referring to the size at which they enter recreational and commercial fisheries (Richards, 1986). Activity of each fish was scored according to whether the fish was perched in the open, positioned in a crevice, occupying a shelter hole, hovering off the substrate, or swimming. Habitat was categorized as vertical wall (may have cracks, small crevices, or ledges; score=1), complex (comprising broken rock and boulder fields; score=2), or sand-mud (score=3). Any change in the habitat or slope of the substrate (±10°) was recorded and the depth noted.

Rockfish density was estimated for each habitat type over 20–m depth intervals. The total number of fish recorded by both observers within each habitat type over a 20–m depth interval was divided by the total area of that habitat type viewed over the depth interval. The area viewed was calculated by multiplying the viewing width of both observers (i.e. 6 m) by the ratio of the change in depth to the sine of the slope.

Median densities of small and large fish were calculated for each habitat type and 20–m depth interval, with transects pooled for increased sample size. Density distributions for rockfish were skewed so densities were calculated as medians with 25% and 75% quartiles. Densities of quillback rockfish, *S. maliger,* among depth intervals and habitats were analyzed by using Kruskal-Wallis tests (SAS, 1985), as this species had an adequate median density (>1 $fish \cdot 100m^{-2}$). Statistical significance was indicated by $P \leq 0.05$. Analyses for the other rockfish species (median densities <1 $fish \cdot 100m^{-2}$) were limited to qualitative comparisons of their depth distributions and numerical abundances.

Activity of each species of rockfish was analyzed using percent occurrence, which was calculated by dividing the sum of all individuals observed in each activity by the total number of individuals of the species for which activities were recorded, and multiplying by 100%. Species associations were determined for individual fish of each species by scoring the presence of a conspecific or a heterospecific within 3 m. The sum of the number of individuals which were observed in the presence of a con- or hetero-specific was then expressed as a percentage of the total number of individuals of the species. Individual rockfish with no other rockfish within 3 m were considered to be 'alone' (solitary).

Results

Physical habitat

An area of approximately 10,521 m^2 was surveyed from the submersible, of which 38% was wall, 47% complex, and 15% sand-mud habitat. Area of coverage among habitat types differed with depth (Fig. 2). The area of complex and sand-mud habitat covered in the surveys decreased with depth whereas that of wall habitat increased. Sand-mud habitat was encountered only at depths of <60 m and the median area surveyed among transects was zero. Wall habitat was the only habitat type observed at depths greater than 120 m. The slope of the substrate was correlated with depth (Spearman rank correlation: r_s=0.37, P<0.001) and habitat (r_s =-0.71, P<0.001). This was evident in that wall habitat found primarily in deep water provided vertical or near-vertical relief (~70–90° slope), whereas complex and sand-mud habitats in shallower depths provided a graded substrate (~20–70° slope).

The area of each type of habitat surveyed differed among survey sites (Kruskal-Wallis: P=<0.001, 0.03, and <0.001 for wall, complex, and sand-mud habitat respectively). Elbow Point and McKenzie Bight had similar habitats whereas Sheppard Point had less wall and complex habitat and more sand-mud habitat than the Elbow Point and McKenzie Bight sites.

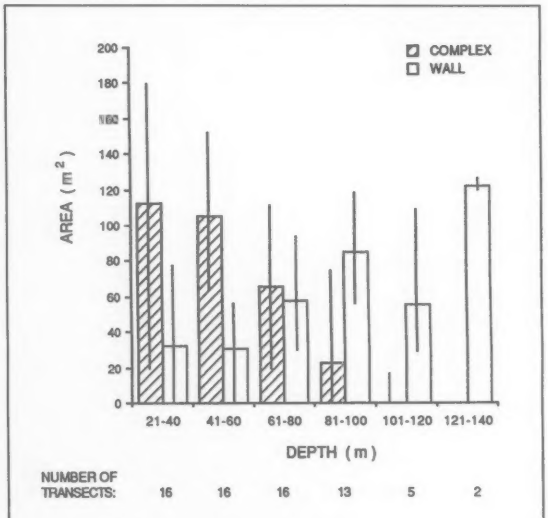

Figure 2

Overall median area of survey coverage for complex and wall habitat in relation to depth. Vertical bars represent the interquartile ranges ($Q_{0.25}$ to $Q_{0.75}$). Median area of sand-mud habitat surveyed was zero.

At the time of the surveys, Saanich Inlet was not anoxic although waters below 100 m were deficient in dissolved oxygen (Liu, 1989) (Table 1). Hydrogen sulfide was not present at any depths sampled in the inlet. Temperature and salinity were relatively stable below depths of 100 m.

Depth, size, and density distributions

Quillback rockfish represented 88% (681/770) of all rockfish sighted and were observed at a median depth of 54 m (Table 2). Density of quillback rockfish did not differ among depth intervals between 21–100 m (P=0.35) (Fig. 3A). Only three quillback rockfish were seen at depths >100 m. In total, the median size of 460 quillback rockfish was 23 cm (Table 2). Quillback rockfish size was positively correlated with depth (r^2=0.23, P<0.001, n=460) and the density of small and large quillback rockfish varied among depth intervals (P=0.01 and P=0.02 respectively) (Fig. 3B). Density of small quillback rockfish was similar to that of large quillback rockfish in the 21–40 m depth interval (P=0.66), but it was less at depth intervals greater than 40 m (all P<0.05) (Fig. 3B). In contrast, the median density of large quillback rockfish at depth intervals between 41–100 m was greater than their density in the 21–40 m depth interval (Fig. 3B).

Tiger rockfish, *S. nigrocinctus*, copper rockfish, *S. caurinus*, yellowtail rockfish, *S. flavidus*, greenstriped rockfish, *S. elongatus*, and yelloweye rockfish, *S. ruberrimus*, all had median densities of zero in 21–150 m depths in Saanich Inlet (Table 2).

Table 1

Temperature, salinity, and dissolved oxygen measured throughout depths in Saanich Inlet on 12 December 1986. Hydrogen sulfide was not present at any of the depths sampled.

Depth (m)	Temperature (°C)	Salinity (‰)	Dissolved oxygen ($mg \cdot L^{-1}$)
0	6.24	26.68	7.01
10	8.70	30.18	5.83
30	8.94	30.31	4.50
50	9.40	30.56	3.80
75	9.19	30.96	2.80
100	9.19	31.25	1.39
125	9.23	—	0.41
150	9.28	31.44	0.50
175	9.27	—	0.87
200	9.29	31.47	1.70
225	9.29	—	1.75

Table 2

Numerical abundance, median density, median depth, and median estimated size of *Sebastes* species observed at depths of 21–150 m in Saanich Inlet from the *Pisces IV* submersible.

		Density (fish·100m^{-2})		Depth (m)		Size (cm)	
Species	Number	Median	Range	Median	Range	Median	Range
S. maliger	681	5	(0–31)	54	(21–115)	23	(5–41)
S. nigrocinctus	28	0	(0– 2)	55	(33– 97)	28	(20–46)
S. caurinus	24	0	(0– 4)	44	(21– 65)	25	(5–36)
S. flavidus	23	0	(0– 7)	49	(41– 65)	35	(20–40)
S. elongatus	8	0	(0– 1)	65	(52–114)	18	(15–23)
S. ruberrimus	5	0	(0– 4)	89	(76–103)	28	(18–46)
Unidentified sp.	1			42		—	

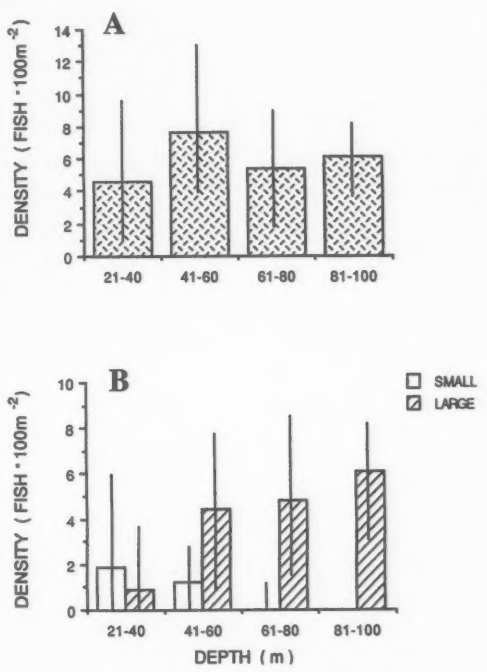

Figure 3

(**A**) Overall median densities of all quillback rockfish, *Sebastes maliger*, over depth; and (**B**) median densities of small and large quillback rockfish over depth. Vertical bars represent the interquartile ranges ($Q_{0.25}$ to $Q_{0.75}$). Median density of quillback rockfish in depths >100 m was zero.

Tiger rockfish accounted for 4%, and copper rockfish 3%, of the rockfish encountered; both were most abundant in 41–60 m (0.6 fish·100m^{-2}). Yellowtail rockfish also represented 3% of all rockfish observed with their density reaching a maximum of 6.3–6.6 fish·100m^{-2} in the 41–80 m depth intervals. Greenstriped rockfish (n=8), yelloweye rockfish (n =5), and one unidentified rockfish each represented less than 1% of all observed rockfish. Greenstriped and yelloweye rockfish both occurred in relatively deeper waters (Table 2).

The size of tiger rockfish was not correlated with depth (P=0.27, n=15) and only relatively large fish were seen from the submersible (Table 2). Copper rockfish size was positively correlated with depth (r^2=0.36, P=0.02, n=15), and no small copper rockfish were seen at depths greater than 40 m. Yellowtail rockfish seen were all relatively large fish (Table 2) and their size was not correlated with depth (P=0.46, n=21). All greenstriped rockfish observed were small (Table 2). Two juvenile yelloweye rockfish (18–20 cm TL) were observed at depths greater than 95 m and three subadult and adult yelloweye rockfish (36–46 cm TL) occurred between 80 and 90 m.

Habitat distribution

Density of quillback rockfish differed among survey sites (P=0.001). Densities observed at the Elbow Point and McKenzie Bight sites were similar (P=0.236), with a pooled median density of 5.7 fish·100m^{-2}. In contrast, the median density of quillback rockfish at Sheppard Point was zero.

Overall, quillback rockfish density was highest in areas of complex habitat (5.8 fish·100m^{-2}), followed

by wall habitat (3.5 fish·100m^{-2}) (Fig. 4). Only four quillback rockfish were observed over sand-mud habitat. Quillback rockfish densities, whether in complex or wall habitat, did not differ among depth intervals ≤100 m (P=0.52 and P=0.64 respectively) (Fig. 4).

Tiger, copper, yellowtail, and yelloweye rockfish were observed only over complex or wall habitats, whereas greenstriped rockfish occurred mostly over sand-mud habitat (Table 3). Tiger rockfish tended to occur in both complex and wall habitats, whereas copper, yellowtail, and yelloweye rockfish were seen mostly in complex habitat.

Activities

Quillback, copper, and greenstriped rockfish did not appear to be attracted to or obviously repelled by the presence of the submersible and its lights. At times, rockfish actively finned to maintain station after the submersible had produced currents. Any observed movements away from or towards the submersible were always relatively slow and, at times, hovering quillback rockfish would move slightly away from the path of the submersible, stop, and then resume hovering. Tiger and yelloweye rockfish appeared to have a delayed response to the submersible, in that it was possible to observe them prior to their actually moving into a shelter hole or crevice. In contrast, some spotted ratfish, *Hydrolagus colliei*, and a sixgill shark, *Hexanchus griseus*, were obviously attracted to the *Pisces*. These fish swam back-and-forth around the front of the submersible, repeatedly approaching the viewing ports near the external lights.

Activities were determined for a total of 662 quillback rockfish and the majority were observed hovering or perched on substrate in the open (Fig. 5), regardless of depth interval (all P>0.10). Copper rockfish were also observed primarily hovering and perched in the open, but were seen swimming more frequently than quillback rockfish. Both species were observed infrequently in crevices and rarely in shelter holes. Tiger rockfish were also observed most frequently perched in the open or occupying crevices. Yellowtail rockfish were all observed either hovering or swimming close to the substrate. All eight greenstriped rockfish were observed perched on the substrate. Of the five yelloweye rockfish observed, one was in a shelter hole, three were in crevices, and one was hovering.

Table 3

Numerical abundance of rockfish (*Sebastes* spp.) observed in densities of ≤1 fish·100m^{-2} over complex, wall, and sand-mud habitat in Saanich Inlet.

Species	Complex	Wall	Sand-Mud
S. nigrocinctus	13	15	0
S. caurinus	20	4	0
S. flavidus	21	2	0
S. elongatus	0	1	7
S. ruberrimus	4	1	0

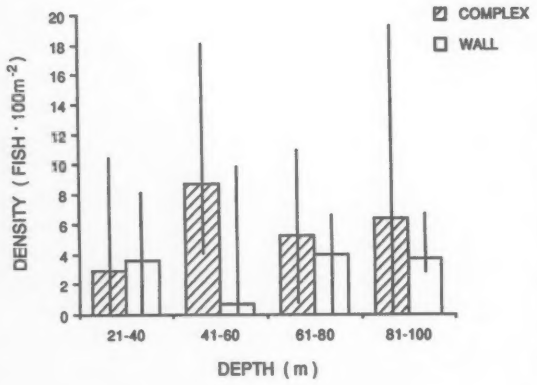

Figure 4

Median densities of quillback rockfish, *Sebastes maliger*, in complex and wall habitats among depths. Vertical bars represent interquartile ranges ($Q_{0.25}$ to $Q_{0.75}$). Median densities of quillback rockfish over sand-mud habitat were zero.

Species associations

The majority of quillback rockfish (94% occurrence) were observed within 3 m of at least one other quillback rockfish (Fig. 6). Quillback rockfish were almost never observed alone (2%) and were observed in the presence of other species relatively infrequently (~20% occurrence or less). Quillback rockfish formed loose conspecific aggregations that were distinctly different from the conspecific schools of yellowtail rockfish observed from the *Pisces*. When schooling, yellowtail rockfish formed tight groups of fish that orientated and moved together in the same direction, whereas in the aggregations of quillback rockfish, individual fish were orientated in various directions and engaged in various activities. Small groups of quillback rockfish (2–5 fish) observed from the submersible were interspersed between larger aggregations of more than 15 fish. Copper rockfish occurred within 3 m of quillback rockfish 92% of the time (Fig. 6), but also tended to occur near other copper rockfish

(64% occurrence) and tiger rockfish (32%). Copper rockfish, while usually near quillback rockfish, were also observed in conspecific aggregations and they were seldom seen alone (4%). Tiger rockfish were almost always observed near quillback rockfish (96% occurrence) and, to a much lesser extent, near other tiger rockfish (21%) (Fig. 6). The majority of yellowtail rockfish were observed in proximity to quillback rockfish (96%) and other yellowtail rockfish (91%). All five of the yelloweye rockfish seen were near quillback rockfish. Six greenstriped rockfish were observed near quillback rockfish whereas two were alone.

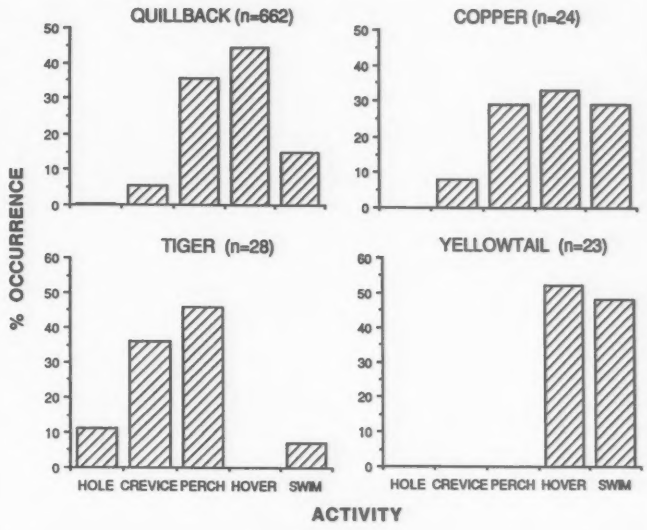

Figure 5

Percent occurrence of behavioral activities for quillback rockfish, *Sebastes maliger*; copper rockfish, *S. caurinus*; tiger rockfish, *S. nigrocinctus*; and yellowtail rockfish, *S. flavidus*, observed in Saanich Inlet from the *Pisces* submersible.

Discussion

Quillback rockfish are the numerically dominant rockfish species at depths of 21–100 m in nearshore areas of southern British Columbia, based on submersible observations in a fjord (this study) and in relatively open coastal areas (Richards, 1986). Based on both of these submersible studies, the main depth distribution of quillback rockfish is between 41 and 60 m, and their density at this depth is more than eight times greater than that of any other rockfish species observed at 41–60 m (Fig. 3A; Richards, 1986). As in Saanich Inlet, greenstriped and yelloweye rockfish were also observed in relatively low densities in the northeastern Strait of Georgia (means of ≤2 fish·100m^{-2} in various habitat types) (Richards, 1986), as well as tiger and copper rockfish (Richards and Cass, 1985). Yellowtail rockfish were not seen during submersible dives in the northeastern Strait of Georgia (Richards and Cass, 1985). In Saanich Inlet, complex habitat dominated by broken rock and boulder fields appears to be a common feature for the occurrence of the majority of these rockfish species. Based on *Pisces* surveys in the northeastern Strait of Georgia, Richards (1986) also observed that quillback and yelloweye rockfish were most abundant in complex habitat. Similarly, densities of copper and quillback rockfish were highest in complex habitat or in areas of highly irregular relief in Saanich Inlet in <40 m depth (Murie, 1991) and in the northern Strait of Georgia in <18 m depth (Richards, 1987). In SCUBA surveys, Matthews (1990) found the greatest densities of large copper and large quillback rockfish on high-relief rocky reefs in Puget Sound, Washington. Additionally, submersible observations in the vicinity of Heceta Bank, Oregon (Pearcy et al., 1989), suggested that tiger, yelloweye, and yellowtail rockfish were most frequently encountered over rock and rubble habitat. The densities of these near-bottom species may be greatest in this type of habitat because of increased protection from predators or increased density of prey due to the increase in microhabitat and vertical structure.

Stein et al. (1992) observed fish from a submersible at Heceta Bank and determined that the occurrence of fish species was related to specific substrates. Given the propensity of quillback rockfish to aggregate over complex habitat, differences in their density among sites surveyed in our study was not surprising. Sheppard Point, which had more sand-mud areas and a shallower slope, was noticeably different from Elbow Point and McKenzie Bight. It was also the only site where greenstriped rockfish were observed, which is consistent with the apparent habitat distribution of this species (Richards, 1986; Pearcy et al., 1989; Stein et al., 1992).

The overlap in the depth ranges, as well as the similarity in the median depths and the occurrence of fish over complex and wall habitats, suggested that quillback, copper, tiger, and yellowtail rockfish do not segregate in Saanich Inlet within the range

of bathymetry or habitat surveyed from the submersible. Yellowtail rockfish may be segregated spatially from tiger rockfish and, to some degree, copper and quillback rockfish, because the activities of yellowtail rockfish consistently placed them in the water column near the substrate but never in direct contact with the bottom. The appearance of quillback and copper rockfish near to one another (Fig. 6) was consistent with observations from SCUBA dive surveys at Saanich Inlet in 20–40 m. Sympatric aggregations of quillback and copper rockfish over complex habitat in Saanich Inlet can be dense (~25–50 fish·100m^{-2}) (Murie, 1991).

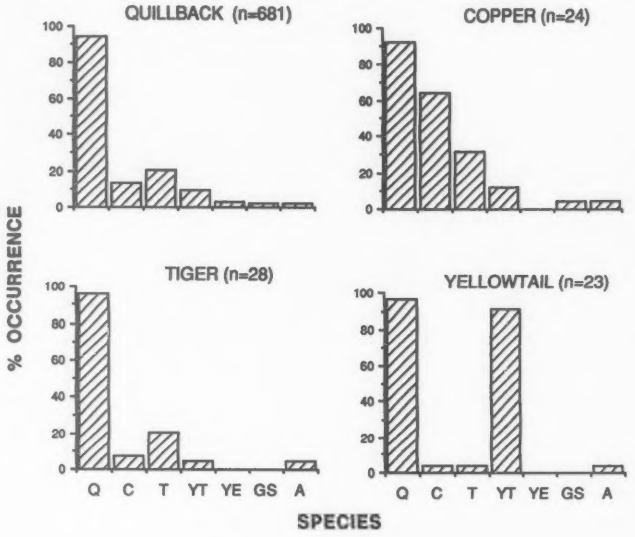

Figure 6

Percent occurrence of conspecific and heterospecific rockfish in association with quillback rockfish, *Sebastes maliger*; copper rockfish, *S. caurinus*; tiger rockfish, *S. nigrocinctus*; and yellowtail rockfish, *S. flavidus*; Species key: Quillback rockfish (Q), copper rockfish (C), tiger rockfish (T), yellowtail rockfish (YT), yelloweye rockfish (YE), greenstriped rockfish (GS), and alone (A).

Published information on in situ behavioral activity, species associations, and density of tiger rockfish is scarce, no doubt in part due to the consistently low densities in which this species is encountered. Tiger rockfish have been observed in low densities, and primarily as only a single fish encountered at any one time, in waters <30 m deep in Puget Sound (Moulton, 1977), in 21–140 m in the northeastern Strait of Georgia (Richards and Cass, 1985), in 64–305 m depths off Oregon (Pearcy et al., 1989), and in <30 m in Saanich Inlet (Murie, 1991). As 21% (6/28) of *S. nigrocinctus* were observed within 3 m of another tiger rockfish in our study (Fig. 6), this species may not be as 'solitary' as indicated by the previous studies. Density of tiger rockfish may be limited by the availability and defense of suitably large shelter holes, which the fish retreat into upon approach by a SCUBA diver (Murie, pers. obs.).

The depth distribution of rockfish in Saanich Inlet, and hence any size or species associations, may be influenced by a number of factors, including a) the physical regime of the inlet; b) the paucity of observations for relatively uncommon species; and c) the actual depth range and total number of transects surveyed with the submersible. The year-round oxygen deficiency in waters >100 m in Saanich Inlet, and the intermittent anoxia that occurs in waters of 125–234 m depth during January to August (Liu, 1989), may act to compress or shift the depth distribution of rockfish compared to open coastal waters where relatively deep water is not limiting in dissolved oxygen. In Saanich Inlet, squat lobsters, *Munida quadrispina,* migrate vertically en masse to avoid decreasing oxygen levels (Burd, 1983) although catastrophic mortality of spot prawns, *Pandalus platyceros,* in 85–90 m depth has been attributed to a sudden intrusion of displaced anoxic bottom-water into midwater depths (Jamieson and Pikitch, 1988). For mobile organisms (such as rockfish) decreasing oxygen levels may elicit a behavioral response involving a vertical or horizontal habitat shift (Kramer, 1987). Of three transects in Saanich Inlet that started at 150 m, no rockfish were observed at depths >115 m, and only three quillback rockfish were seen at depths >100 m (note: one of these transects was not used in the overall analysis owing to loss of the audio-track at <80 m). With the exception of copper rockfish, Hart (1973) reports maximum depths of >250 m for the other rockfish species. In addition, quillback, tiger, greenstriped, and yellowtail rockfish have been observed from submersibles at depths >120 m (Richards and Cass, 1985; Pearcy et al., 1989).

The scarcity of observations on relatively low density species of rockfish, especially in combination with time limitations of the submersible, could also affect our interpretation of rockfish depth distribution. In Saanich Inlet, few rockfish other than quill-

back rockfish were observed during the submersible dives. The depth range and density of the relatively uncommon species of rockfish may have been improved if we had been able to do more transects and, in the instance of maximum depths, by doing deeper transects. Bias in using submersible transects was exemplified by the downward bias (i.e. deeper) in the observed minimum depth ranges for tiger, yellowtail, and yelloweye rockfish in Saanich Inlet (Table 2). These rockfish species have been observed during SCUBA dives in Saanich Inlet in water as shallow as 15–25 m (Murie, pers. obs.). The density estimate and depth range for copper rockfish was probably also biased because of the reduced ability to maintain fine control of the *Pisces* buoyancy as it approaches shallower depths (~20 m). We know that copper rockfish in Saanich Inlet occur from near-surface waters (~2 m) and their distribution extends visibly below 40 m depth (Murie, 1991). The density of copper rockfish on rocky reefs in 20–30 m of water, however, can approach 50 fish·100m^{-2} (Murie, 1991), far in excess of any density observed for copper rockfish from the submersible (Table 2). In general, however, copper rockfish do occur in shallower water than quillback rockfish (Moulton, 1977; Richards, 1987; Murie, 1991), as was observed from the submersible transects in Saanich Inlet.

Another potentially important bias in the use of the *Pisces IV* to observe densities and activities of rockfish is whether the fish are attracted or noticeably repelled by the size, noise, and lights of the submersible. Similar to our study, Carlson and Straty (1981) noted that most of the rockfish were neither repelled nor attracted to the submersible while they observed them in southeastern Alaska. In addition, Richards (1986) observed that none of the common fish species seen in the northeastern Strait of Georgia seemed disturbed by the *Pisces IV* submersible. A notable exception in Carlson and Straty's (1981) study was large (7–10 kg) yelloweye rockfish that were obviously attracted to the submersible and actually followed it, similar to the ratfish and sixgill shark in our study. Pearcy et al. (1989) also noted that large schools of yellowtail rockfish were attracted to their submersible and followed it over substantial periods of time and depth; there was no visible evidence, however, of schools of yellowtail rockfish following the *Pisces* in our study.

The occurrence of perching and hovering activities observed for the majority of rockfish in Saanich Inlet from the *Pisces* was consistent with behavioral activities of quillback and copper rockfish observed with SCUBA in Saanich Inlet (Murie, 1991). Observations from the submersible were limited in this respect because it was impossible to look into all crevices or into shelter holes under rocks for the presence of fish. Tiger and yelloweye rockfish could be seen in shelter holes and crevices but their size could not always be estimated. Although the *Pisces* approaches shelter holes from below (during its ascent), fish in deep shelter holes and crevices may not be detected. The presence of fish in crevices and shelter holes was therefore probably underestimated. Nevertheless, at present, submersibles and remotely-operated vehicles (ROVs) provide the best means of observing the activities of rockfish occupying complex habitat in deep water.

Although it is evident from submersible observations that estimates of abundance and activities of rockfish involve a variety of biases, these direct visual assessments can provide quantitative information on the densities and depth distributions of rockfish species in habitats that cannot be surveyed adequately using bottom trawls. In addition, submersibles allow direct observation of the behavioral activities and associations of individual fish in relation to specific habitat types. This type of information has not been attainable using conventional survey techniques of fisheries.

Acknowledgments

We are especially grateful to T. Fitch and the pilots and crew of the *Pisces IV* (Institute of Ocean Sciences, Department of Fisheries and Oceans, Sidney, B.C.) who provided the opportunity and expertise to work efficiently with the submersible. We thank Q. Liu for analyzing the hydrocast samples, and J. Gilbert and C. Steinhoff for rockfish observations. Constructive comments by F. Matthews, L. Richards, J. McInerney, N. Wilimovsky, P. Gregory, V. Tunnicliffe, D. Mitchell, C. Tolman, and two anonymous reviewers improved the manuscript. Financial support was provided by a Postgraduate Scholarship from the Natural Sciences and Engineering Research Council of Canada (DJM) and by the Biology Department, University of Victoria.

Literature cited

Anderson, J. J., and A. H. Devol.
1973. Deep water renewal in Saanich Inlet, an intermittently anoxic basin. Estuarine and Coastal Mar. Sci. 1:1–10.

Boehlert, G. W.
1980. Size composition, age composition, and growth of canary rockfish, *Sebastes pinniger*, and splitnose rockfish, *S. diploproa*, from the 1977 rockfish survey. Mar. Fish. Rev. 42: 57–63.

Burd, B. J.
1983. The distribution, respiration and gills of a low oxygen tolerant crab, *Munida quadrispina* (Benedict, 1902) (Galatheidae, Decapoda) in an intermittently anoxic fjord. M.Sc. thesis, Biology Dept. Univ. Victoria, Victoria, B.C., 151 p.

Carlson, H. R., and R. R. Straty.
1981. Habitat and nursery grounds of Pacific rockfish, *Sebastes* spp., in rocky coastal areas of southeastern Alaska. Mar. Fish. Rev. 43:13–19.

Dennis, G. D., and T. J. Bright.
1988. Reef fish assemblages on hard banks in the northwestern Gulf of Mexico. Bull. Mar. Sci. 43:280–307.

Hallacher, L. E., and D. A. Roberts.
1985. Differential utilization of space and food by the inshore rockfishes (Scorpaenidae: *Sebastes*) of Carmel Bay, California. Env. Biol. Fish. 12:91–110.

Hart, J.
1973. Pacific fishes of Canada. Fish. Res. Board Can. Bull. 180:407–443.

Herlinveaux, R.
1962. Oceanography of Saanich Inlet in Vancouver Island, British Columbia. J. Fish. Res. Board Can. 19:1–37.

Jamieson, G. S., and E. K. Pikitch.
1988. Vertical distribution and mass mortality of prawns, *Pandalus platyceros*, in Saanich Inlet, British Columbia. Fish. Bull. 86:601–608.

Kramer, D. L.
1987. Dissolved oxygen and fish behavior. Env. Biol. Fish. 18:81–92.

Krieger, K.
1993. Distribution and abundance of rockfish determined from a submersible and by bottom trawling. Fish. Bull. 91:87–96.

Larson, R. J.
1980. Competition, habitat selection, and the bathymetric segregation of two rockfish (*Sebastes*) species. Ecol. Monogr. 50: 221–239.

Liu, Q.
1989. Ecophysiological studies of *Orchomenopsis affinis* (Holmes) (Lysianassidae, Amphipoda) in an intermittently anoxic fjord. M.Sc. thesis, Biology Dept., Univ. Victoria, Victoria, B.C., 122 p.

Mackie, G. O., and C. E. Mills.
1983. Use of the *Pisces IV* submersible for zooplankton studies in coastal waters of British Columbia. Can. J. Fish. Aquat. Sci. 40:763–776.

Martin, D. W., P. A. Mayes, and V. W. Rodwell.
1981. Harper's review of biochemistry, 18th ed. Lange Medical Pub., Los Altos, CA, 126 p.

Mathews, S. B., and M. W. Barker.
1983. Movements of rockfish (*Sebastes*) tagged in northern Puget Sound. Fish. Bull. 82: 916–922.

Matthews, K. R.
1990. A comparative study of habitat use by young-of-the-year, subadult, and adult rockfishes on four habitat types in central Puget Sound. Fish Bull. 88:223–239.

Moulton, L.
1977. An ecological analysis of fishes inhabiting the rocky nearshore regions of northern Puget Sound, Washington. Ph.D. diss., Univ. Washington, Seattle, WA, 181 p.

Murie, D. J.
1991. Comparative ecology and interspecific competition between the sympatric congeners *Sebastes caurinus* (copper rockfish) and *S. maliger* (quillback rockfish). Ph.D. diss., Univ. Victoria, Victoria, B.C., 287 p.

Patten, B. G.
1973. Biological information on copper rockfish in Puget Sound, Washington. Trans. Am. Fish. Soc. 102:412–416.

Pearcy, W. G., D. L. Stein, M. A. Hixon, E. K. Pikitch, W. H. Barss, and R. M. Starr.
1989. Submersible observations of deep-reef fishes of Heceta Bank, Oregon. Fish. Bull. 87:955–965.

Pickard, G. L.
1963. Oceanographic characteristics of inlets of Vancouver Island, British Columbia. J. Fish. Res. Board Can. 20:1109–1144.

Richards, L. J.
1986. Depth and habitat distributions of three species of rockfish (*Sebastes*) in British Columbia: observations from the submersible *Pisces IV*. Env. Biol. Fish. 17:13–21.
1987. Copper rockfish (*Sebastes caurinus*) and quillback rockfish (*Sebastes maliger*) habitat in the Strait of Georgia, British Columbia. Can. J. Zool. 65:3188–3191.

Richards, L. J., and A. J. Cass.
1985. Transect counts of rockfish in the Strait of Georgia from the submersible *Pisces IV*, October and November 1984. Can. Fish. Aquat. Sci. Data Rep. No. 511, 99 p.

Richards, L. J., C. M. Hand, and J. R. Candy.
1988. 1988 research catch and effort data on nearshore reef-fishes in British Columbia statistical areas 12 and 13. Can. Fish. Aquat. Sci. Man. Rep. No. 2000, 89 p.

SAS (SAS Institute Inc.).
1985. SAS User's guide: statistics, vers. 5. Cary, NC, 956 p.

Stein, D. L., B. N. Tissot, M. A. Hixon, and W. Barss.
1992. Fish-habitat associations on a deep reef at the edge of the Oregon continental shelf. Fish. Bull. 90:540–551.

Thomson, R. E.
1981. Oceanography of the British Columbia coast. Can. Spec. Publ. Fish. Aquat. Sci. 56, 291 p.

Uzmann, J. R., R. A. Cooper, R. B. Theroux, and R. L. Wigley.
1977. Synoptic comparison of three sampling techniques for estimating abundance and distribution of selected megafauna: submersible vs. camera sled vs. otter trawl. Mar. Fish. Rev. 39:11–19.

Westrheim, S.J.
1970. Survey of rockfishes, especially Pacific ocean perch, in the northeastern Pacific Ocean, 1963–66. J. Fish. Res. Board Can. 27:1781–1809.

Wilkins, M.E.
1980. Size composition, age composition, and growth of chilipepper, *Sebastes goodei,* and bocaccio, *S. paucispinis,* from the 1977 rockfish survey. Mar. Fish. Rev. 42:48-53.

Reexamination of geographic variation in cranial morphology of the pantropical spotted dolphin, *Stenella attenuata*, in the eastern Pacific

William F. Perrin
Southwest Fisheries Science Center, National Marine Fisheries Service, NOAA
P.O. Box 271, La Jolla, CA 92038

Gary D. Schnell
Daniel J. Hough
Oklahoma Biological Survey and Department of Zoology, University of Oklahoma
Norman, OK 73019

James W. Gilpatrick Jr.
Jerry V. Kashiwada
Southwest Fisheries Science Center, National Marine Fisheries Service, NOAA
P.O. Box 271, La Jolla, CA 92038

Abstract.—The spotted dolphin (*Stenella attenuata*) is found throughout much of the eastern tropical Pacific Ocean. A previous study evaluated morphological variation in skull morphology, but now specimens are available for a greater portion of the range. Also, corrections have been made in data and an assessment has been made evaluating repeatability of character measurements. We reassessed geographic variation in 30 cranial features (26 morphometric measures and 4 tooth counts) based on 611 museum specimens. All characters except two tooth counts showed statistically significant geographic variation, while 21 of the 30 characters exhibited significant sexual dimorphism. Males were larger in most characters; females were larger in some length measurements involving the rostrum and ramus. As in previous analyses, inshore *S. attenuata* were found to be very distinctive, so subsequent analyses focused on offshore spotted dolphins from 29 5° latitude-longitude blocks. Mantel tests and matrix correlations for 19 of the 30 features demonstrated significant "regional patterning," whereas 22 of the characters were shown to have "local patterning." Principal-components, canonical-variates, and cluster (UPGMA and function-point) analyses also were employed to assess geographic variation. In the eastern portion of the range, the subdivision between northern and southern offshore *S. attenuata* found in the previous investigation was confirmed. In general, blocks to the west (including one encompassing part of the Hawaiian Islands) were more like the southern blocks than those of the northeast. Morphological patterns were similar to those found in a number of environmental variables, particularly water depth, solar insolation (January), sea surface temperature (January and July), surface salinity, and thermocline depth (winter and summer). Present management units are inconsistent with the pattern of cranial variation; spotted dolphins from west of lat. 120°W probably should not be pooled with those to the east, as they show closer affinity with the Southern Offshore unit. In addition, the boundary between the Northern and Southern units should probably be moved north to about lat. 5°N.

Manuscript accepted 12 October 1993
Fishery Bulletin 92:324-346 (1994)

Spinner and spotted dolphins (*Stenella longirostris* and *S. attenuata*) have broadly overlapping ranges in the eastern tropical Pacific Ocean (Perrin et al., 1983). Information concerning geographic variation of these species is of both intrinsic scientific and practical interest. Dolphins in the region are killed as a result of purse-seining for yellowfin tuna (*Thunnus albacares*; Allen, 1985). The tuna often are found in association with these two dolphin species (or with *Delphinus delphis*), and fishermen set nets on the dolphin schools to capture tuna found below the dolphins. Estimates indicate that from 1985 to 1990 roughly 53,000 to 129,000 dolphins were killed annually as a result of fishing operations (Hall and Boyer 1987, 1988, 1989, 1990, 1991, 1992). Most recently the annual kill has dropped to approximately 15,000 to 27,000 (Hall and Lennert[1,2]). Government regulations in the United States set limitations on U.S. vessels with respect to the extent of dolphin mortality that will be permitted. Dolphins are managed by defining a series of management stocks. Data, such as those on skull morphology, can provide insight into the underlying population subdivision and may be of considerable value in defining geographic boundaries of biologically relevant management stocks (Dizon et al., 1992).

Douglas et al. (1992) have provided a detailed assessment of geographic variation in cranial morphology of spinner dolphins. For spotted dolphins, the most recent geographic-variation analyses using skull characteristics were by Douglas et al. (1984) and Schnell et

[1] Hall, M. A., and C. Lennert. 1992. Estimates of incidental mortality of dolphins in the purse-seine fishery for tunas in the eastern Pacific Ocean in 1991. Int. Whal. Commn. meeting doc. SC/44/SM6, 5 p.

[2] Hall, M. A., and C. Lennert. 1993 Incidental mortality of dolphins in the eastern Pacific Ocean tuna fishery in 1992. Int. Whal. Commn. meeting doc. SC/45/SM1, 5 p.

al. (1986). Numerous additional specimens have become available, particularly from the western portion of the range and Hawaii. The repeatability of 36 skull measures used in previous studies (Douglas et al., 1984; Schnell et al., 1986) was appraised, as was done previously by Douglas et al. (1992) for spinner dolphins. Also, some immature specimens had inadvertently been incorporated into the previous spotted dolphin analyses. For these reasons, we have undertaken a reassessment of geographic variation and sexual dimorphism of spotted dolphins from the eastern tropical Pacific. This study provides an opportunity to re-evaluate variation patterns previously described and to compare directly patterns of variation found in spotted and spinner dolphins.

Materials and methods

Overall, data-gathering and assessment procedures outlined by Douglas et al. (1992) were used. We measured 611 adult museum specimens (maturity evaluated on the basis of premaxilla fusion with maxilla at distal end of rostrum; Dailey and Perrin, 1973) of spotted dolphins (Fig. 1). These included 534 of 613 specimens used in earlier studies (Douglas et al., 1984; Schnell et al., 1986; 79 specimens previously used had been incorrectly aged or had inadequate locality data) along with 77 new specimens.

As was done with spinner dolphins (Douglas et al., 1992), the first specimen set was measured by M. E. Douglas and the new specimens by W. F. Perrin. In addition, Perrin remeasured 81 specimens of spinner and spotted dolphins measured by Douglas to determine whether measurements were repeatable. Initially, 36 characters were evaluated (illustrations and character definitions given in Schnell et al., 1985). Comparisons of measurements taken on the same specimens by the two investigators indicated that 6 of the original 36 measurements (i.e. width of left premaxillary [at midline of nares], width of right premaxillary [at midline of nares], separation of pterygoids, length of left tympanic cavity, length of right tympanic cavity, and width at pterygobasioocipital sutures) should be deleted, because we were not able consistently to repeat these measurements. For some other measurements, there were differences between investigators, but the differences were consistent (e.g. one obtained measurements that were smaller than those reported by the other). Therefore, we calculated regression equations for each of the remaining characters based on the 81 jointly measured specimens. These regression equations were used to convert the measurements from the rest of the initial specimens to appropriate values for inclusion with the measurements taken by Perrin. Through these procedures, we developed a data set of 30 characters (see Table 1) for the 611 specimens.

Specimens were not used if, because of damaged parts, we could not obtain most of the 30 measurements. Missing values (0.50% of total) for included specimens were estimated by linear regression[3] onto the character that explained the greatest proportion of the variance for the variable being considered.

Animals were assigned to 5° latitude-longitude blocks and each geographic block assigned a numerical code (see Fig. 1). These codes were modified slightly from those employed by Schnell et al. (1986) to accommodate new specimens from more westerly blocks. We had specimens available from 41 blocks, 8 of which were represented by only a single specimen and 4 of which were inshore blocks (i.e. contained only specimens of the inshore form; Douglas et al., 1984). The 29 blocks that were not inshore blocks and had more than one specimen were used as the basis for most geographic variation analyses. While several of the 29 blocks have relatively small samples, geographic-patterning tests (described below) suggested that, in general, sample values are representative of what is expected for these blocks based on their geographic positions.

Schnell et al. (1985) showed *S. attenuata* to be sexually dimorphic for 23 of 36 characters. Because some specimens used in that analysis were removed and new specimens added (see above), we conducted a two-way analysis of variance (ANOVA) for block and sex, based on specimens in the 11 blocks with at least four of each sex (Fig. 1). Correction terms were obtained to adjust measurements of the larger sex downward and the smaller sex upward, thus producing sex-adjusted or "zwitter" measurements (method described in more detail by Schnell et al., 1985). As a result, we were able to combine specimens for both sexes in an overall analysis of geographic variation.

To assess whether combining specimens from different cruise sets within blocks confounded geographic patterns based on blocks, we performed a nested ANOVA for cruise sets within the 12 blocks for which two specimens were obtained from at least two cruise sets. Blocks employed in this analysis (with numbers of cruise sets in parentheses) were the following: 0215 (4), 0216 (3), 0312 (2), 0506 (2), 0507 (2), 0512 (9), 0513 (10), 0515 (2), 0612(6), 0613 (7), 0615 (3), and 0712 (2).

[3] "Missing Data Estimator" program by Dennis M. Power, Santa Barbara Mus. Nat. Hist., pers. commun. 1975.

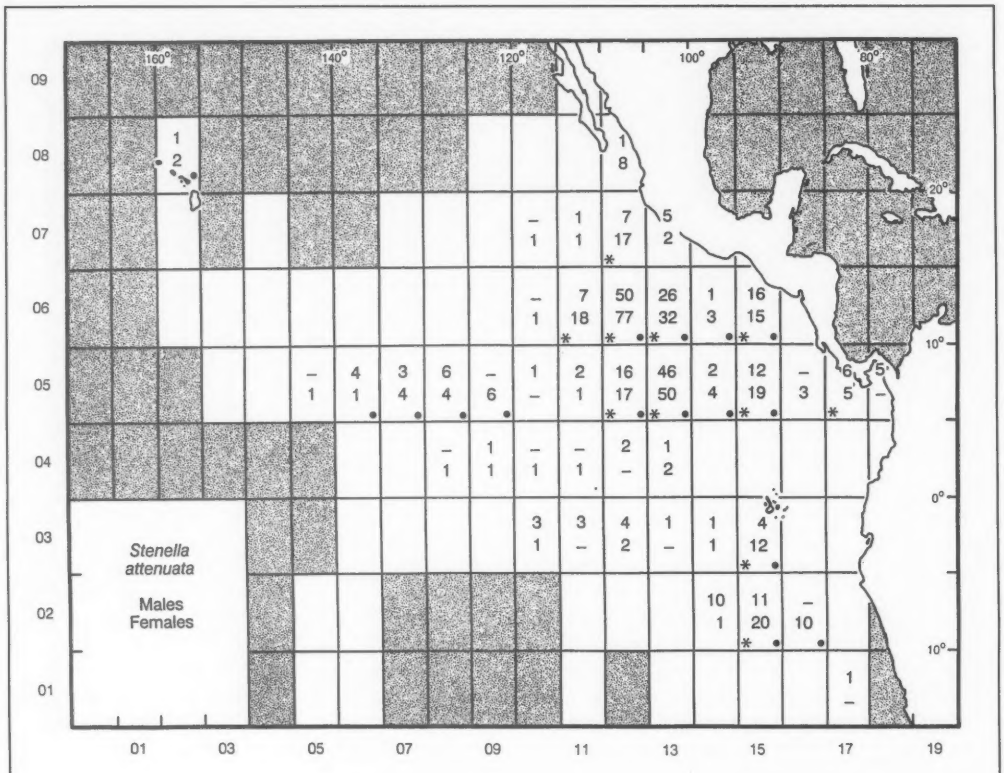

Figure 1

Known range of *Stenella attenuata* in eastern tropical Pacific Ocean (based on Perrin et al., 1983), with numbers of males (above) and females (below) available for each 5° latitude-longitude block (total of 611 specimens). Each block is identified by numerical code (numbers on left and bottom margins are combined; e.g. block 0802 encompasses the northern Hawaiian Islands). Asterisks indicate the 11 blocks included in analysis of sexual dimorphism. Initial analyses indicated that specimens in four blocks (0516, 0517, 0518, 0812) represented a well differentiated inshore form (see Douglas et al., 1984); thus, these were not used in subsequent evaluations. The remaining 29 blocks with two or more specimens were used as the basis for analyses of geographic variation; for some evaluations, the eight blocks with single specimens were projected onto axes based on the other 29 blocks. For the 16 blocks marked with a dot in lower-right corner, sufficient numbers of *S. attenuata* and *S. longirostris* (i.e. at least two of each species) were available for interspecific comparison of geographic trends.

Correlation, ordination, and clustering

After conversion to zwitters, characters were standardized (means=0, standard deviations=1). Product-moment correlations were computed among characters, and associations among characters were summarized by clustering characters (unweighted pair-group method with arithmetic averages; UPGMA). This technique is a type of hierarchical cluster analysis that also was used to summarize average distance coefficients (Sneath and Sokal, 1973) calculated for all pairs of blocks based on standardized data. Cophenetic correlation coefficients indicate the extent to which distances in resulting dendrograms accurately represented original interblock morphologic distances.

Standardized data also were summarized by using a nonhierarchical *K*-group method (function-point cluster analysis; described in Katz and Rohlf [1973] and Rohlf et al. [1979]). Through use of this technique, blocks are assigned to subgroups at a specified level. A *w*-parameter value used in function-point clustering was varied. An hierarchical, but not necessarily nonoverlapping, system of clusters was

Table 1

Geographic variation and sexual dimorphism in *Stenella attenuata* evaluated for 30 characters.

Character[1]	*F*–value[2]		Mean[3]		Correction factor[4]	Percentage difference[5]
	Block	Sex	Male	Female		
1 Condylobasal L.	10.59***	1.94	397.0	398.2	–0.74	–0.30
2 L. Rostrum (from Base)	6.94***	13.49***	236.7	239.5	–1.55	–1.20
3 L. Rostrum (from Pterygoid)	6.88***	6.84**	278.5	281.0	–1.31	–0.87
4 W. Rostrum (at Base)	14.20***	25.13***	83.3	81.8	0.73	1.85
5 W. Rostrum (at 1/4 L.)	12.25***	51.82***	57.1	55.2	0.90	3.32
6 W. Rostrum (at 1/2 L.)	13.82***	47.61***	42.4	40.9	0.78	3.78
7 W. Premax. (at 1/2 L.)	8.51***	72.88***	23.6	22.4	0.60	5.25
8 W. Rostrum (at 3/4 L.)	8.65***	73.90***	29.9	28.0	0.96	6.66
9 Preorbital W.	16.92***	45.92***	149.5	146.6	1.43	1.97
10 Postorbital W.	22.46***	42.23***	167.8	165.1	1.31	1.63
11 Skull W. (at Zygomatic P.)	21.98***	51.05***	167.4	164.5	1.46	1.79
12 Skull W. (at Parietals)	5.73***	54.11***	129.6	136.4	1.58	2.34
13 Ht. Braincase	10.61***	53.87***	95.9	93.7	1.04	2.36
14 L. Braincase	15.67***	39.94***	113.1	111.2	0.95	1.71
15 Max. W. Premax.	8.89***	4.45*	66.2	65.7	0.27	0.85
16 W. External Nares	7.38***	0.03	42.5	42.5	0.01	0.02
17 L. Temporal Fossa	22.41***	16.79***	70.1	68.4	0.82	2.53
18 W. Temporal Fossa	20.60***	28.50***	55.2	53.2	0.93	3.72
19 Orbital L.	2.97**	0.06	47.4	47.4	0.02	0.10
20 L. Antorbital P.	8.33***	4.30*	36.9	36.4	0.24	1.43
21 W. Internal Nares	9.58***	12.80***	47.4	46.6	0.36	1.58
22 L. Up. Toothrow	6.20***	10.56**	204.3	206.7	–1.29	–1.16
23 No. Teeth (Up. Lf.)	0.96	1.54	41.4	41.2	0.10	0.47
24 No. Teeth (Up. Rt.)	0.98	0.65	41.3	41.1	0.07	0.33
25 No. Teeth (Low. Lf.)	2.89*	0.02	41.0	40.9	–0.01	–0.02
26 No. Teeth (Low. Rt.)	2.82**	1.02	40.8	41.0	–0.08	–0.36
27 L. Low. Toothrow	5.38***	11.63***	198.6	201.2	–1.40	–1.28
28 Ht. Ramus	16.13***	0.12	57.3	57.1	0.38	0.24
29 Tooth W.	12.14***	19.65***	3.4	3.3	0.06	3.55
30 L. Ramus	9.02***	8.86**	335.5	338.3	–1.48	–0.82

[1] Abbreviations: Ht. = height; L. = length; Lf. = left; Low. = lower; Max. = maximum; No. = number; P. = process; Premax. = premaxillary; Rt. = right; Up. = upper; W. = width.
[2] *F*-values from main effects two-way analysis of variance (5° block vs. sex) involving 11 blocks (*$P < 0.05$; **$P < 0.01$; ***$P < 0.001$). Total of 170 individuals. Degrees of freedom 10 for among-block variation and 1 for between sexes.
[3] Unweighted mean for 11 blocks.
[4] Added to all individual female measurements and subtracted from all individual male measurements to correct for sexual differences.
[5] Difference between sexes (males minus females) multiplied by 100; the resulting value was divided by average of male and female means.

obtained by repeating the analysis at different clustering levels. Results are displayed in modified skyline diagrams (Wirth et al., 1966).

Using standardized data, we constructed scatter diagrams by projecting blocks onto the first two principal components (Sneath and Sokal, 1973) extracted from a matrix of correlations among the 30 characters. Canonical-variates analysis also was employed to obtain the subset of variables that shows the greatest interblock separation relative to intrablock variation (Program P7M of BMDP statistical software; Dixon, 1990). Plots of the first two canonical variables show the maximum separation of blocks in two-dimensional space.

Mantel test for geographic patterning

A Mantel (1967) test was used to assess interlocality variation in each character and determine whether measures are geographically patterned or, alterna-

tively, vary spatially at random. The observed association between sets of character differences and geographic distances was tested relative to its permutational variance, and the resulting statistic compared against a Student's t-distribution with infinite degrees of freedom. We performed analyses using GEOVAR, a computer-program library for geographic variation analysis (written by David M. Mallis and provided by Robert R. Sokal, State University of New York at Stony Brook).

Character differences were compared first with actual geographic distances (in nautical miles) between centers of blocks and then with reciprocals of distances. In evaluations of reciprocals, where distances are scaled in a nonlinear manner, longer distances are considered effectively to be equal, and the portion of the scale involving smaller distances is expanded. Thus, use of reciprocals of distances increases the power of analyses to reveal geographic patterns that are "local" in nature (i.e. involving closely placed blocks), whereas tests involving nautical-mile distances evaluate "regional" trends. Positive associations of character differences and nautical-mile distances are indicated by positive t-values, while negative t-values denote such associations when using distance reciprocals. Douglas et al. (1992) provided a simplified example to demonstrate use of the Mantel procedure.

We also computed matrix correlations (Sneath and Sokal, 1973) between character differences and the associated geographic distances or reciprocals of distances between localities. The statistical significance of these coefficients cannot be tested in the conventional way, because all pairs of localities were used and these are not statistically independent. However, the resulting values can be used as descriptive statistics indicating the degree of association of difference values.

Morphological-environmental covariation

We calculated product-moment correlations of block means for morphological characters with environmental variables. Data were available for 13 environmental variables for the eastern tropical Pacific Ocean (Table 2; data sources summarized in Douglas et al., 1992). The list of environmental variables used is somewhat different than that employed by Schnell et al. (1986), because data for some of the variables were not available for all blocks in the broader geographic range being considered in the current study. We also used UPGMA to summarize associations among these environmental variables for 51 blocks; since these two dolphin species have broadly overlapping distributions in the eastern tropical Pacific, the blocks used are representative of areas inhabited by *S. attenuata*.

In order to obtain summary variables reflecting overall environmental trends, we conducted a principal-components analysis of the 13 environmental variables for 51 blocks with specimens of *S. longirostris* (Douglas et al., 1992) or *S. attenuata* or both. Individual blocks were projected onto the resulting environmental principal components based

Table 2

Environmental measurements compiled for each 5° latitude-longitude block.[1]

1 Sea Current (N., Winter)—Average northern component (in knots) of surface water current in winter.

2 Sea Current (W., Winter)—Average western component (in knots) of surface water current in winter.

3 Water Depth—Average sea depth (in m).

4 Solar Insolation (Jan.)—Average incoming solar radiation for January (in gm·cal/cm^2).

5 Solar Insolation (Annual)—Average annual incoming solar radiation in gm·cal/cm^2).

6 Sea Surface Temp. (Jan.)—Average January sea surface temperature (in°C).

7 Sea Surface Temp. (July)—Average July sea surface temperature (in°C).

8 Sea Surface Temp. (Ann. Var.)—Average annual sea surface temperature variation (in°C).

9 Oxygen Min. Layer (Depth)—Annual mean depth (in m) of absolute oxygen minimum surface with respect to the vertical.

10 Surface Salinity—Average salinity (‰) of surface sea water.

11 Thermocline Depth (Winter)—Mean depths (in m) to top of thermocline for January, February, and March.

12 Thermocline Depth (Summer)—Mean depths (in m) to top of thermocline for July, August, and September.

13 Surface Dissolved Oxygen—Annual mean dissolved oxygen (mL/L) of surface sea water.

[1] Data sources listed in Douglas et al. (1992: table 2). Abbreviations: Ann. Var. = annual variation; Jan. = January; Min. = minimum; N. = north; Temp. = temperature; W. = west.

on standardized data. These environmental components served as composite environmental variables for comparisons with morphological variables.

Matrix correlations and Mantel tests were used to test for local and regional patterning of environmental variables. Also, differences between each pair of blocks for a given morphological variable were compared with those for an environmental variable.

Interspecific comparisons

The predominant trends in the data sets for each of *S. attenuata* and *S. longirostris* were summarized with principal components and canonical variables. Information is available for 16 blocks from which both offshore *S. attenuata* and *S. longirostris* were sampled (Fig. 1). These blocks are representative of the total geographic range investigated in our studies. In order to compare general patterns of variation in the two species, we calculated product-moment correlations, Mantel tests, and matrix correlations for individual morphological characters, principal-component projections, and canonical-variable projections of these 16 blocks.

In our analyses, average distances based on morphological characters were computed between each pair of localities. To evaluate the extent of similarity in geographic patterns, the original distance matrices for each species were modified such that only distances among the 16 localities common to both species were included. These matrices were then compared by using the Mantel test and computing the matrix correlation.

Results

Sexual dimorphism

Table 1 includes mean measurements for males and females based on 11 blocks. For two-way ANOVAs assessing geographic block and sex (df=21, n=461), all but 5 of the 30 were very highly significant (P<0.001). The probability was 0.02 for number of teeth (lower right) and 0.007 for orbital length. Two characters showed no significant variation (upper tooth counts) and one character (number of teeth [lower left]) was close to significant (P<0.06). Statistically significant interactions (P<0.05) between block and sex were found for five of the characters: condylobasal length; width of rostrum (at 1/4 length); width of rostrum (at 1/2 length); width of rostrum (at 3/4 length); and width of internal nares. Interaction denotes that the degree of sexual dimorphism differs among blocks for these characters.

Sexual dimorphism was significant for 22 of the 30 characters (Table 1). Females had longer rostrums, which is reflected in a number of characters (i.e. 2, 3, 22, 27, 30). In general, males had wider skulls and tended to be larger for nonrostral portions of the skull. Percentage differences between sexes are presented in Table 1. The average absolute difference (i.e. sign ignored) between the sexes for the 30 characters was 1.78%. For 8 characters where females were larger, the average difference was 0.75%, whereas for 22 characters where males were larger the average difference was 2.16%. The greatest differences were found for width of premaxillary (at 1/2 length) and width of rostrum (at 3/4 length)—5.25% and 6.66%, respectively.

Table 3 shows the results for the nested ANOVA for cruise sets within blocks. Twenty-three of the 30 characters showed highly significant or very highly significant block effects, whereas only three characters (those involving the temporal fossa and length of braincase) reflected highly significant or very highly significant effects for cruise set. Even in those three cases, block effects were more pronounced. Therefore, we conclude that combining cruise sets into blocks did not have an important confounding influence on geographic patterns found among blocks.

Correlation, ordination, and clustering

Most character pairs had positive correlations. An exception was tooth counts and temporal fossa measurements, which tended to have negative correlations with skull width measurements. The dendrogram in Figure 2 summarizes absolute correlations (i.e. sign of correlation ignored) among characters based on 29 blocks to provide an assessment of character covariation. The width of external nares was the character with the least association with other measures. Tooth characters join and are separated from the remaining morphometric characters. Braincase measures and skull width (at parietals) cluster in another relatively distinct group. The remaining characters are arranged in two groups. The cluster at the top of Figure 2 includes most length measurements and height of ramus. Width measurements along with length of antorbital process, orbital length, and length of temporal fossa are included in the adjoining major cluster (Fig. 2).

Table 4 includes character loadings on the first two principal components based on data for 29 blocks. Component I explains 45.0% of the total variance for the 30 characters, whereas component II summarizes an additional 16.8% (cumulative total of 61.8%). Projections of blocks onto the two components are depicted in Figure 3, and a map (Fig. 4) is included that renders geographic block projections onto the first component. Component I repre-

Table 3

Results of nested ANOVA (*F*-values) for different cruise sets within 12 latitude-longitude blocks of offshore *Stenella attenuata*.

	F–value	
Character[1]	Cruise set	Block
1 Condylobasal L.	1.28	3.03***
2 L. Rostrum (from Base)	1.34	3.25***
3 L. Rostrum (from Pterygoid)	1.65*	4.36***
4 W. Rostrum (at Base)	1.25	8.86***
5 W. Rostrum (at 1/4 L.)	1.60*	7.51***
6 W. Rostrum (at 1/2 L.)	1.12	8.34***
7 W. Premax. (at 1/2 L.)	1.29	5.25***
8 W. Rostrum (at 3/4 L.)	1.01	5.39***
9 Preorbital W.	1.25	10.87***
10 Postorbital W.	1.22	11.31***
11 Skull W. (at Zygomatic P.)	1.27	10.81***
12 Skull W. (at Parietals)	0.97	1.11
13 Ht. Braincase	1.55*	1.55
14 L. Braincase	1.83**	3.59***
15 Max. W. Premax.	1.22	4.01***
16 W. External Nares	0.95	3.00***
17 L. Temporal Fossa	2.13***	7.54***
18 W. Temporal Fossa	1.87**	9.48***
19 Orbital L.	1.29	1.24
20 L. Antorbital P.	0.82	5.00***
21 W. Internal Nares	1.09	3.47***
22 L. Up. Toothrow	1.33	2.67**
23 No. Teeth (Up. Lf.)	1.23	1.22
24 No. Teeth (Up. Rt.)	1.19	0.78
25 No. Teeth (Low. Lf.)	1.47*	2.57**
26 No. Teeth (Low. Rt.)	1.45*	2.57**
27 L. Low. Toothrow	1.63*	2.45**
28 Ht. Ramus	1.09	1.77
29 Tooth W.	1.31	1.45
30 L. Ramus	1.25	2.37**

* $P < 0.05$; ** $P < 0.01$, *** $P < 0.001$.
[1] Abbreviations identified in Footnote 1 of Table 1.

Table 4

Principal component loadings for offshore *Stenella attenuata* involving character means for 29 latitude-longitude blocks.

	Component[2]	
Character[1]	I	II
1 Condylobasal L.	**0.812**	–0.505
2 L. Rostrum (from Base)	0.786	–0.483
3 L. Rostrum (from Pterygoid)	0.795	–0.446
4 W. Rostrum (at Base)	**0.867**	0.206
5 W. Rostrum (at 1/4 L.)	**0.923**	0.157
6 W. Rostrum (at 1/2 L.)	**0.855**	0.308
7 W. Premax. (at 1/2 L.)	**0.863**	0.161
8 W. Rostrum (at 3/4 L.)	**0.868**	0.211
9 Preorbital W.	**0.930**	0.235
10 Postorbital W.	**0.940**	0.181
11 Skull W. (at Zygomatic P.)	**0.938**	0.173
12 Skull W. (at Parietals)	0.740	0.270
13 Ht. Braincase	–0.002	0.225
14 L. Braincase	0.508	–0.325
15 Max. W. Premax.	0.366	–0.059
16 W. External Nares	0.286	–0.311
17 L. Temporal Fossa	–0.544	–0.576
18 W. Temporal Fossa	–0.375	–0.541
19 Orbital L.	0.655	–0.018
20 L. Antorbital P.	**0.805**	0.203
21 W. Internal Nares	0.604	0.000
22 L. Up. Toothrow	0.705	–0.588
23 No. Teeth (Up. Lf.)	–0.137	**–0.668**
24 No. Teeth (Up. Rt.)	–0.112	**–0.726**
25 No. Teeth (Low. Lf.)	–0.301	**–0.673**
26 No. Teeth (Low. Rt.)	–0.341	**–0.635**
27 L. Low. Toothrow	0.680	**–0.632**
28 Ht. Ramus	0.608	0.355
29 Tooth W.	–0.129	0.118
30 L. Ramus	**0.803**	–0.528

[1] Abbreviations identified in Footnote 1 of Table 1.
[2] Relatively high loadings highlighted in bold as follows: (component I) > |0.8|; (II) >|0.6|.

sents general size, with relatively high character loadings (Table 4) for most characters, the exceptions being tooth characters and the two measurements of the temporal fossa. The specimens from blocks in the northeastern portion of the range tend to be small (Figs. 3 and 4), whereas those to the south and southwest typically are larger. The largest specimens were found in block 0802, which encompasses a portion of the Hawaiian Islands. Component II reflects tooth counts and measurements associated with toothrow length (Table 4). Blocks with relatively high values for these characters are found near the top of Figure 3, whereas those with low values tend to be near the bottom.

Blocks with single specimens were not used in the delineation of the principal components but have been projected onto components calculated by using the 29 blocks (Fig. 3). In general, the single-specimen blocks fall close to where one would predict based on their geographic position; some exceptions are expected based simply on expected chance variation.

Interblock morphological differences are summarized in the phenogram in Figure 5. Two blocks (0312 and 0802) are loosely joined in the most disparate cluster. Remaining blocks are divided into two clusters. The one represented at the top of Figure 3 includes the blocks from the south, southwest, and west, whereas the other includes blocks from the northeastern portion of the range.

Clusters based on the function-point procedure are summarized in the modified skyline diagram in Figure 6A. The most distinctive block is 0802 (en-

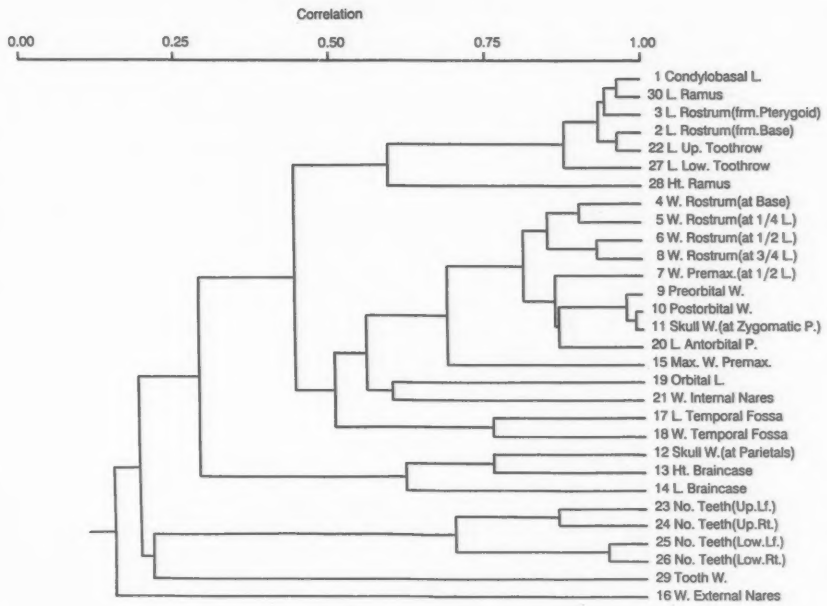

Figure 2

Correlations among characters based on character means for 29 latitude-longitude blocks. Clustering performed using UPGMA on absolute correlations among characters (i.e. negative signs removed). Cophenetic correlation coefficient is 0.87.

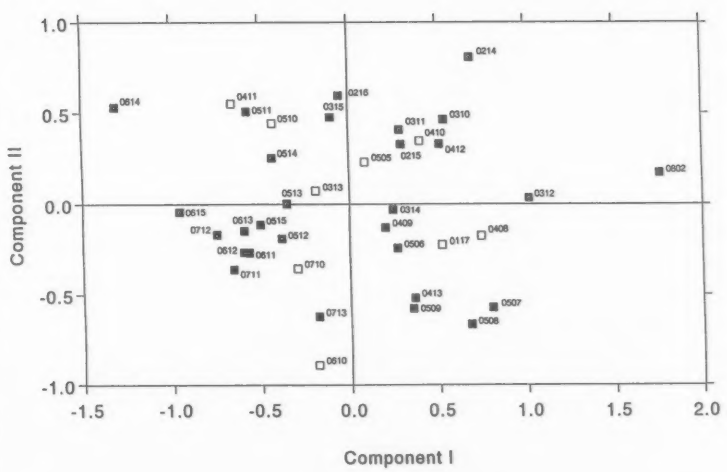

Figure 3

Projections of blocks onto first two principal components based on 30 characters. Solid symbols indicate 29 latitude-longitude blocks on which analysis was conducted. Open symbols represent blocks with only single specimens projected onto axes generated from 29 blocks with two or more specimens.

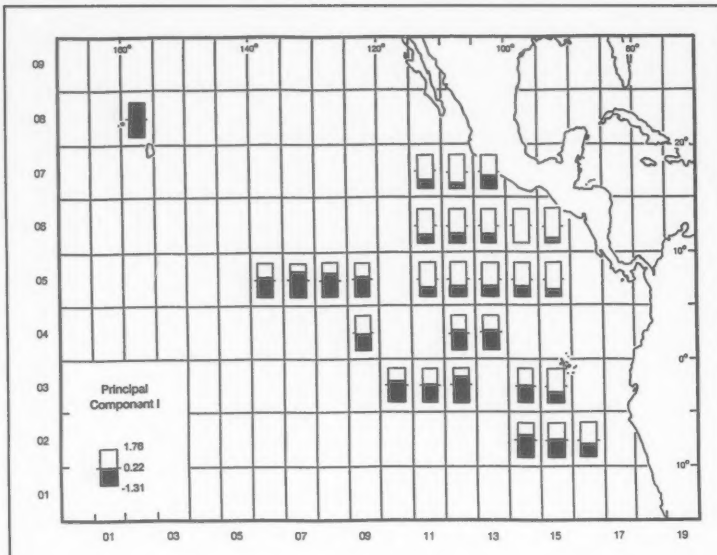

Figure 4

Geographic variation in principal component I. Bar represents range (low to high block values), and midpoint is marked. Darkened part of bar indicates value for particular latitude-longitude block.

compassing part of Hawaiian Islands) at the right of the diagram. A number of single blocks (0312, 0314, 0311) are separated from the others at w-values of 3.10 and 2.87. Most of the blocks from the northeastern portion of the range were included in a single cluster at lower w-values, although some individual blocks were separated by themselves (e.g. 0614, 0711).

In Figure 6B, a skyline diagram is included that is based on five characters: length of rostrum (from pterygoid); preorbital width; length of braincase; length of temporal fossa; and width of temporal fossa. These variables were identified by using canonical-variates analysis (reported below) as those that in combination provided the greatest discrimination among blocks. The use of function-point clustering on these selected characters provided clusters that persisted through several clustering levels. At the w-value of 1.38, four clusters were formed. The Hawaiian Island block (0802) is in a group by itself (on left side of Fig. 6B). The blocks to the south, southwest, and west are in a second assemblage (i.e. 0214 through 0506), while the northeastern blocks form the other major cluster (i.e. 0513 through 0713). Block 0711 is separated into its own group. At w-values less than 1.38, the second cluster is subdivided and the southern blocks are included with some from the southwest.

Canonical-variates analysis selected five characters (Table 5). Blocks are projected onto the first two canonical variables resulting from this analysis (Fig. 7), whereas Figure 8B shows geographically the distribution of geographic variation projections onto canonical variable 1. The eigenvalue for canonical variable 1 is 1.00, while that for variable 2 is 0.19. The two together summarize 82.4% of the variance in the five characters. In the scatter diagram (Fig. 7), blocks with only single specimens are projected onto the canonical variables generated by using the other 29 blocks. As indicated in Table 5, the most important character in the canonical-variates analysis was postorbital width. (Fig. 8A). It has relatively small values in the northeastern portion of the range, and considerably larger values in other areas to the south, southwest, and west. The largest postorbital width measurements are found in specimens taken near the Hawaiian Islands (0802). The geographic configuration of this character is very similar to the general pattern exhibited by the first canonical variable (Fig. 8B). Canonical variable 1 and principal component I (Fig. 4) have similar geographic patterns. Canonical variable 2 does not reflect any particular geographic pattern. It basically contrasts three blocks (0711, 0802, and 0311) with the others, as indicated by these three being separated in the upper portion of Figure 7 from other blocks.

Mantel test for geographic patterning

Results of Mantel tests and matrix correlations comparing interblock character differences with geographic distances (in nautical miles) and with the reciprocals of geographic distances are presented in Table 6. Regional patterning, as indicated by a significant association with geographic distance, was found for 18 (60.0%) of the 30 characters. In these characters, the localities the farthest apart tended to exhibit the greatest morphological difference. Local patterning, which is judged based on a significant negative association between geographic distance-reciprocals and morphological differences, was found in 22 (73.3%) of the characters. Not unexpectedly, virtually all characters (i.e. all but one) exhib-

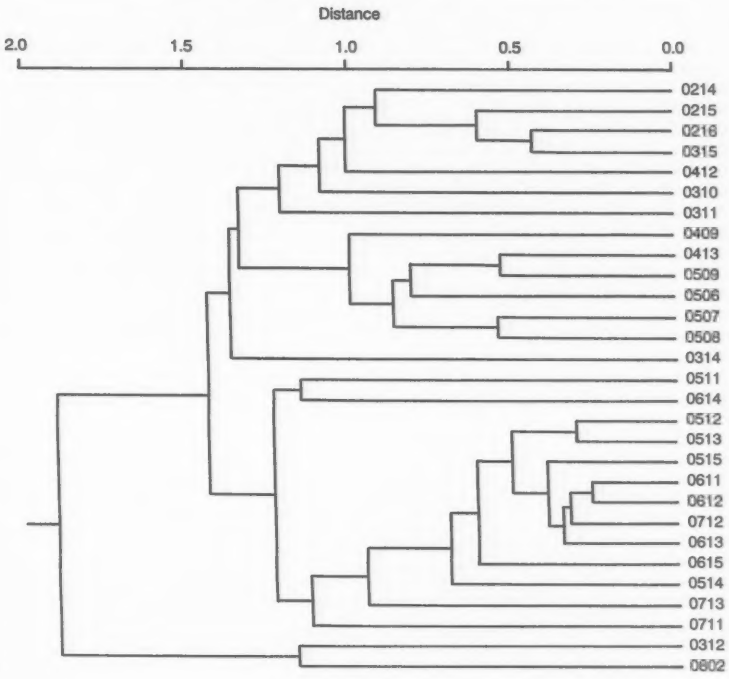

Figure 5

Distance phenogram summarizing UPGMA clustering of 29 latitude-longitude blocks based on 30 characters. Cophenetic correlation is 0.76.

Table 5

Canonical variates analysis of all specimens of *Stenella attenuata* from 29 latitude-longitude blocks.

Character[1]	*F*–value to enter	Order of entry	Coefficients[2] 1		2	
3 L. Rostrum (from Pterygoid)	2.88	4	0.0062	(0.0665)	–0.0731	(–0.7900)
9 Preorbital W.	9.19	1	0.1932	(0.8774)	0.0031	(0.3650)
14 L. Braincase	2.53	5	–0.0266	(–0.0851)	0.2243	(0.7179)
17 L. Temporal Fossa	2.84	3	–0.1113	(–0.4674)	0.0895	(0.3759)
18 W. Temporal Fossa	7.22	2	–0.1167	(–0.4305)	–0.0812	(–0.2996)
Constant			–13.5670		–18.3837	

[1] Abbreviations identified in Footnote 1 of Table 1.
[2] Unstandardized coefficients (with standardized values in parentheses) for canonical variates.

iting a significant regional pattern also showed local patterning.

Our tests showed strong regional and local patterning for principal component I and canonical variable 1, whereas principal component II has significant local patterning (Table 6). Mantel tests and correlations confirm a point made earlier—that canonical variable 2 does not exhibit a systematic geographic pattern.

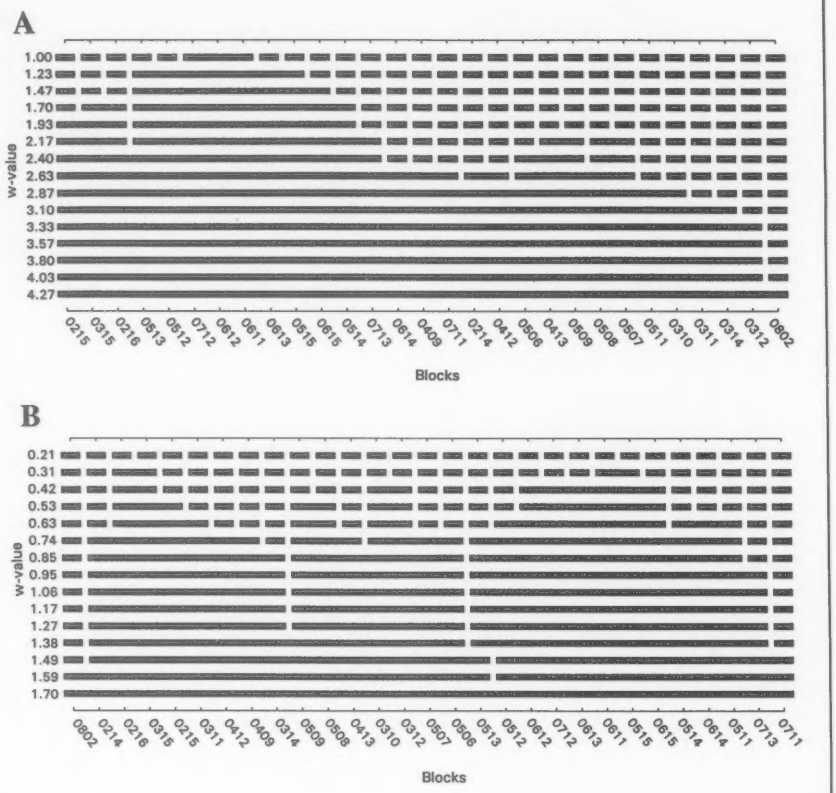

Figure 6

Modified skyline diagrams for 29 latitude-longitude blocks, indicating groups formed using function-point clustering procedures and based on: (**A**) all 30 characters; (**B**) five characters that, in combination, best discriminate among blocks (preorbital width, width of temporal fossa, length of temporal fossa, length of rostrum [from pterygoid], length of braincase). For given *w*-value (i.e. row), blocks connected in common line are in same cluster.

Morphological-environmental covariation

Douglas et al. (1992: fig. 9) included a dendrogram summarizing absolute correlations among 13 environmental variables (listed in Table 2) for blocks having either *S. attenuata* or *S. longirostris* or both. These variables were partitioned into five clusters. Sea current (N., winter) is separated by itself, whereas sea current (W., winter) and oxygen minimum layer (depth) form a second cluster, which groups with an assemblage of five variables involving surface measures of temperature, oxygen, and salinity (variables 6, 7, 8, 10, and 13). The fourth cluster has the two solar insolation variables (4 and 5), while the fifth includes three measures indicating water and thermocline depths (variables 3, 11, and 12).

A principal-components analysis was conducted to obtain variables that would summarize general environmental trends; three components were presented from Douglas et al. (1992: table 6). Highest loadings for environmental variables on principal component I included those for sea surface temperatures (variables 6, 7, and 8), particularly July temperatures. The correlation with sea surface temperature (annual variable) is negative. The second component reflected thermocline depth (variable 11 and 12), as well as water depth and surface salinity. The

third had relatively high loadings with the two characters involving solar insolation (variables 4 and 5). A more detailed description of character associations with the principal components is available in Douglas et al. (1992).

Projection values for environmental principal component I are summarized in Figure 9A for the 29 blocks with larger samples of *S. attenuata*. It reflects the fact that sea surface temperatures are considerably higher in northern than southern blocks, and that the northern blocks exhibit relatively little annual variation in surface temperatures. Block projections on environmental principal component II are portrayed in Figure 9B, which summarizes the increases in thermocline depth, water depth, and surface salinity as one proceeds west and south.

Correlations of morphologic variables, principal components, and canonical variables with environmental variables and environmental principal components are summarized in Table 7. The sea current measures (variables 1 and 2) have virtually no statistical association with morphological characters, while water depth (variable 3) has positive correlations with lengths and widths of the rostrum, as well as principal component I and canonical variable 1 (Table 7).

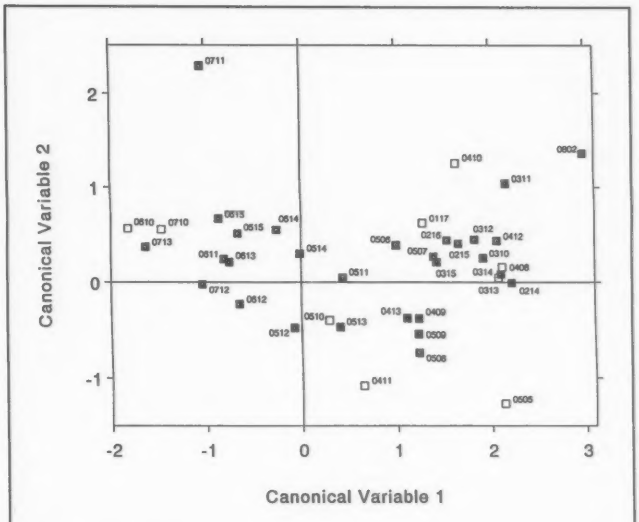

Figure 7

Projections of latitude-longitude blocks onto first two canonical variables based on 30 characters. Solid symbols indicate 25 blocks on which analysis was conducted. Open symbols represent blocks with only single specimens, which were projected onto axes generated from 29 blocks with two or more specimens.

Solar insolation (Jan.), the fourth variable, has larger values in the south; values become smaller to the north. It has significant positive correlations with nine morphologic variables, and negative associations with six others. The negative associations with the two temporal fossa measures are particularly strong (width of temporal fossa summarized in Fig. 10A). This environmental variable has relatively high correlations with canonical variable 1 and principal component II (Table 7).

Not unexpectedly, the fifth variable, solar insolation (annual) exhibits high values at the equator. Readings are lower for blocks closer to either pole. It has few significant statistical associations with morphologic characters, although the negative correlations with length of braincase and width of temporal fossa (Fig. 10A) are relatively high (Table 7).

The sixth and seventh environmental measures (surface temperatures in January and July) have negative associations with a number of width measurements, as well as with a few length variables (Table 7). They have very strong positive correlations with temporal fossa measures. Figure 10 summarizes the values for sea surface temperature (July), as well as for the closely associated width of temporal fossa (r=0.799; the highest correlation of an environmental and a morphological variable). Sea surface temperature (annual variable), the eighth environmental variable, has significant correlations with relatively few morphologic characters (Table 7), although its pattern has affinities with those summarized by principal component II and canonical variable 1. Environmental variable 9, oxygen minimum layer (depth), shows very few statistically significant correlations with morphological measurements (Table 7).

Surface salinity, variable 10, exhibits strong covariation with numerous measurements, particularly those involving the anterior portion of the skull (Table 7). It also has high correlations with principal component I (Fig. 4) and canonical variable 1 (Fig. 8B). Salinity, which was depicted in Douglas et al. (1992: fig. 13B) for *S. longirostris* blocks, shows east-west changes from lower to higher values at a given latitude, as well as a north-to-south trend of increasing values (below 15°N).

The eleventh variable, thermocline depth (winter), is summarized in Figure 11B. It has positive correlations with 12 morphological measures and a negative correlation with 1 character. The correlation of this environmental variable with skull width (at parietals), shown in Figure 11A, is 0.610. Variable

12, thermocline depth (summer), has strong positive correlations with a large number of variables, particularly those reflecting measurements in the anterior portion of the skull. Given its covariation with water depth, it is not surprising that thermocline depth (winter) has significant correlations with principal component I and canonical variable 1. Surface dissolved oxygen (variable 13) has only a few weak statistical associations with morphological characters.

Environmental principal component I (Fig. 9A) has a pattern similar to those for sea surface temperatures in January and July (variables 6 and 7). The highest correlation (0.733) of this component is with width of temporal fossa (Fig. 10A). The second environmental component (Fig. 9B) is strongly associated with numerous characters (Table 7), reflecting the general trends from the northeast to the west, southwest, and south. The third component, which is negatively associated with canonical variable 2 (Table 7), has only one strong association with a morphological variable, that being with tooth width (r=–0.680; Table 7). The third environmental component exhibits decreasing values as one moves away from the equator. Tooth width shows an opposite pattern, which is particularly emphasized with the relatively thick teeth in specimens from the Hawaiian Islands (block 0802).

In Table 8, Mantel t-values and matrix correlations are provided for associations of environmental variables (including environmental principal components) with the five morphologic characters selected for inclusion during the canonical-variates analysis. With this approach, covariation patterns are assessed on the basis of difference values between all block pairs. Preorbital width shows a strong association with water depth, the two measures of solar insolation, the sea surface temperatures in January and July, oxygen minimum layer (depth), and surface salinity (Table 8). It also exhibits a pattern that is statistically associated with all three environmental components. The two measures of the temporal fossa show concordance with patterns for solar insolation (January, as well as annual), all sea surface temperature measures, oxygen minimum layer (depth), surface salinity, and the first environmental principal component. The length of temporal fossa also has a weak statistical

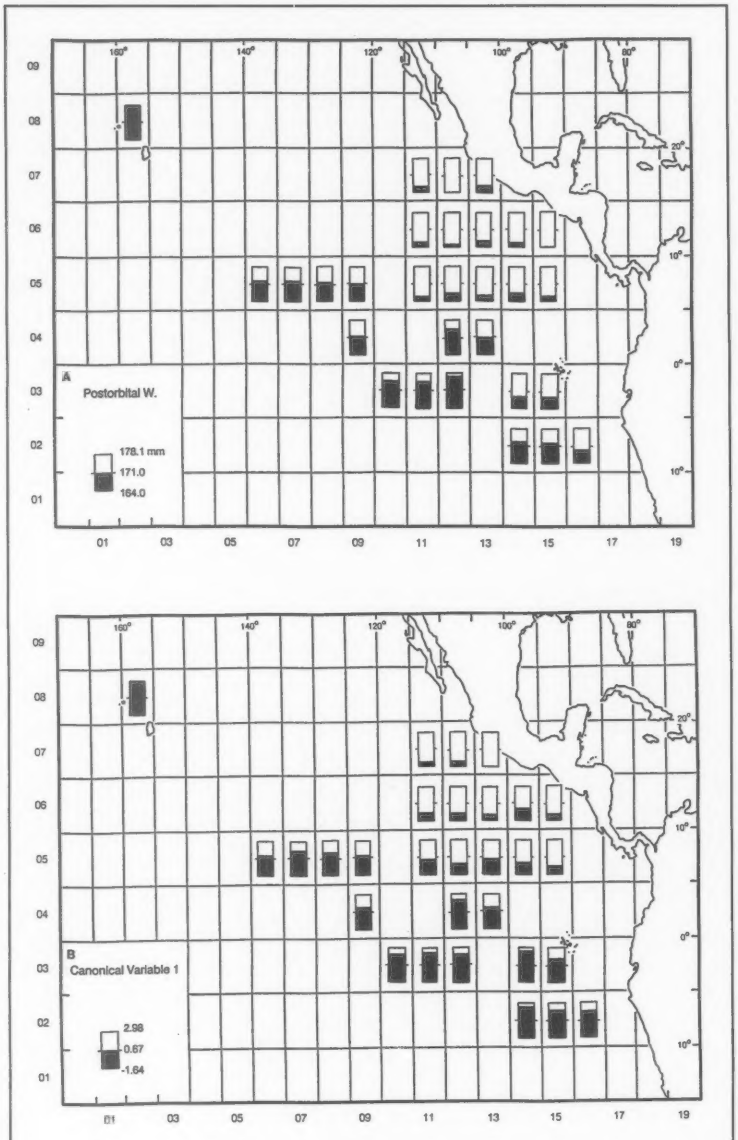

Figure 8

Geographic variation in (**A**) postorbital width and (**B**) canonical variable 1. Darkened part of bar indicates value for particular latitude-longitude block.

association with environmental component III. Table 8 indicates that the pattern for length of rostrum (from pterygoid) is associated statistically with those for water depth and thermocline depth (summer). This morphologic character also is shown to have geographic patterning statistically similar to that exhibited by environmental components II and III. For length of braincase, the Mantel tests were significant (but weak) only for sea current (N., winter) and solar insolation (Jan.). The strongest association of length of braincase is with environmental component III; its pattern also is linked statistically to the second environmental component.

Table 6

Association of interlocality character differences with geographic distances (in nautical miles) and the reciprocals of these distances. Results from Mantel tests (t) and matrix correlations (r) for offshore *Stenella attenuata*.

	Distance		Reciprocal of distance	
Character[1]	t	r	t	r
1 Condylobasal L.	4.19***	0.460	−4.19***	−0.303
2 L. Rostrum (from Base)	4.34***	0.449	−4.45***	−0.310
3 L. Rostrum (from Pterygoid)	3.59***	0.352	−4.10***	−0.276
4 W. Rostrum (at Base)	4.53***	0.493	−5.07***	−0.365
5 W. Rostrum (at 1/4 L.)	4.11***	0.446	−4.84***	−0.348
6 W. Rostrum (at 1/2 L.)	3.76***	0.413	−4.73***	−0.343
7 W. Premax. (at 1/2 L.)	1.28	0.134	−2.88**	−0.203
8 W. Rostrum (at 3/4 L.)	3.14**	0.347	−4.11***	−0.300
9 Preorbital W.	5.00***	0.464	−6.83***	−0.445
10 Postorbital W.	4.61***	0.397	−6.66***	−0.416
11 Skull W. (at Zygomatic P.)	4.22***	0.380	−6.21***	−0.398
12 Skull W. (at Parietals)	4.81***	0.583	−4.34*	−0.336
13 Ht. Braincase	1.81	0.227	−1.81	−0.143
14 L. Braincase	2.60**	0.339	−1.85	−0.151
15 Max. W. Premax.	1.64	0.159	−3.53***	−0.236
16 W. External Nares	0.78	0.066	−1.38	−0.085
17 L. Temporal Fossa	1.49	0.152	−3.13**	−0.216
18 W. Temporal Fossa	0.90	0.097	−2.86**	−0.206
19 Orbital L.	−0.25	−0.031	−0.35	−0.027
20 L. Antorbital P.	0.89	0.078	−3.65***	−0.229
21 W. Internal Nares	0.44	0.046	−1.09	−0.077
22 L. Up. Toothrow	4.08***	0.422	−3.93***	−0.274
23 No. Teeth (Up. Lf.)	1.57	0.173	−1.68	−0.123
24 No. Teeth (Up. Rt.)	3.03**	0.296	−3.68***	−0.247
25 No. Teeth (Low. Lf.)	1.75	0.188	−1.89	−0.135
26 No. Teeth (Low. Rt.)	2.44*	0.283	−2.39*	−0.180
27 L. Low. Toothrow	2.99**	0.364	−3.20**	−0.249
28 Ht. Ramus	1.74	0.181	−1.69	−0.116
29 Tooth W.	3.36***	0.398	−3.82***	−0.292
30 L. Ramus	3.02**	0.361	−2.88**	−0.221
Component I	4.54***	0.474	−5.51***	−0.386
Component II	1.42	0.122	−2.75**	−0.172
Canonical Variable 1	3.76***	0.289	−6.69***	−0.393
Canonical Variable 2	1.11	0.143	−1.47	−0.119

* $P<0.05$; **$P<0.01$, ***$P < 0.001$.
[1] Abbreviations identified in Footnote 1 of Table 1.

Interspecific comparisons

The study by Douglas et al. (1992) reported comparable statistical analyses on skulls of *S. longirostris*, a dolphin species that overlaps broadly with *S. attenuata* in the eastern tropical Pacific. The projections onto the first two principal components for *S. attenuata* were evaluated against projections on the two components obtained for *S. longirostis* (for summary information on these components, see Fig. 3 and Table 4 for offshore *S. attenuata*, and fig. 3 and table 3 of Douglas et al. [1992] for *S. longirostris*). A strong correspondence exists between the first principal components for the two species, as indicated by product-moment correlations, Mantel t-tests, and matrix correlations comparing the component projections. The second principal components for the two studies are not similar (Table 9); they summarize different general trends in variation.

A similar interspecific comparison was made of projections of the 16 blocks onto canonical variables (Table 9). The first canonical variable for *S. attenuata* and that for *S. longirostris* are virtually identical, reflecting highly concordant geographic patterns for the two species (Table 9). While block projections on the first canonical variables for the two species were very similar, the actual characters incorporated into the canonical variables are not the same (see our Table 5 and table 4 of Douglas et al. 1992). Of the five characters entered for each species, only length of rostrum (from pterygoid) was present in both character sets. However, the first and most important character entered into the analyses—preorbital width for *S. attenuata* and postorbital width for *S. longirostris* are highly correlated (see close association of these two characters in *S. attenuata* indicated in Fig. 2); because these two characters exhibit very similar variation pat-

terns, a canonical-variates analysis typically would not select both for inclusion, since they provide basically the same information for separating blocks.

The second canonical variables for the two studies also were compared (Table 9). They showed no statistical association.

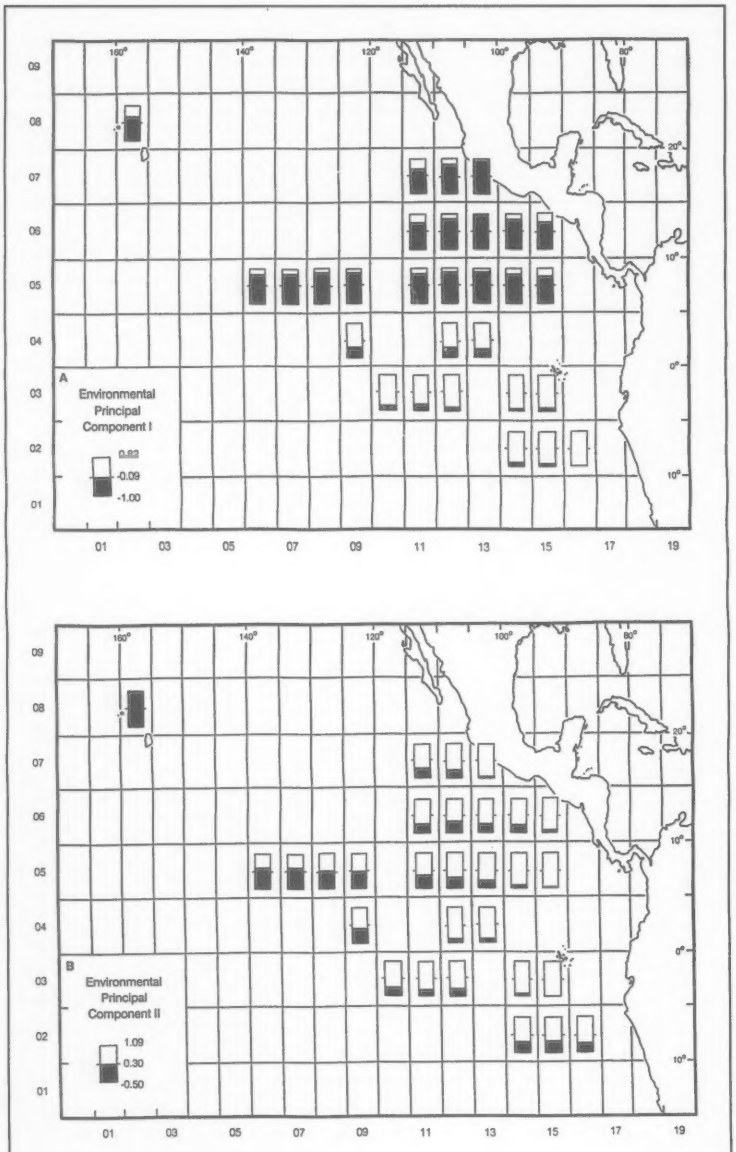

Figure 9

Geographic variation in environmental variables as summarized in (**A**) principal component I and (**B**) principal component II. Darkened part of bar indicates value for particular latitude-longitude block.

Table 10 includes results of Mantel tests, matrix correlations, and product-moment correlations of interspecific comparisons for individual morphological characters. Thirteen of the 30 *t*-values for Mantel tests of interlocality differences for the same character in the two species were significant, while 15 of 30 product-moment correlations indicated statistical associations. Nine of 11 characters with positive correlations were width measures. Furthermore, a tenth (length of antorbital process) is essentially a width character as well (for illustration of measurement, see Schnell et al. 1985). The two characters involving upper tooth counts, as well as length of temporal fossa, exhibited significant negative correlations. For *S. attenuata*, upper tooth counts tend to be higher for the western blocks (but not for the Hawaiian Island block), whereas in *S. longirostris*, higher upper tooth counts are found in the Hawaiian and eastern blocks. The length of temporal fossa is greater in northern localities of *S. attenuata* (Fig. 10A), whereas the shorter fossae are found in northeastern blocks for *S. longirostris* (see Douglas et al. 1992: fig. 11).

Discussion

Sexual dimorphism

Schnell et al. (1985) conducted the most recent analysis of sexual dimorphism of *S. attenuata* in cranial morphology. They found statistically significant dimorphism for 23 of 36 characters. Our analyses used many of the same specimens, with some added and some deleted, and 30 of the same characters. For the 30 characters we analyzed, Schnell et al. (1985) found the same 22 to have statistical differences between sexes (one statistically significant character analyzed earlier was not used in our analysis). Results from the two studies on sexual dimorphism are essentially the same. Thus, for *S. attenuata*, our current findings simply update information in Schnell et

Table 7

Product-moment correlations of block means for morphological variables and components versus environmental variables and components based on 29 latitude-longitude blocks of offshore *Stenella attenuata*.[1]

	Environmental variable[3]													Environmental component		
Character[2]	1	2	3	4	5	6	7	8	9	10	11	12	13	I	II	III
1 Condylobasal L.			++							+	++	+++			+++	
2 L. Rostrum (from Base)			++								++	+++			+++	
3 L. Rostrum (from Pterygoid)			++							+	+	+++			++	
4 W. Rostrum (at Base)			++			--	-			+++	++	+++			+++	
5 W. Rostrum (at 1/4 L.)			++			---	--			+++	+	++		--	++	
6 W. Rostrum (at 1/2 L.)			+	+		---	---	+		+++		+		--	+	
7 W. Premax. (at 1/2 L.)			+	+		--	--			++		+		--		
8 W. Rostrum (at 3/4 L.)			++	+		--	--			+++		+		-	+	
9 Preorbital W.			+++	+		---	---			+++	+	++		--	++	
10 Postorbital W.			+++	+		---	---			+++		++		--	++	
11 Skull W. (at Zygomatic P.)			++			---	---	+	-	+++		++		---	+	
12 Skull W. (at Parietals)				-	-						+++				++	
13 Ht. Braincase											++					
14 L. Braincase				--	---						++					---
15 Max. W. Premax.				+		--	--			++		++		-		
16 W. External Nares	-															
17 L. Temporal Fossa				---	-	+++	+++	--		---		-	---	+++		
18 W. Temporal Fossa				---	---	+++	+++	---		---				+++		-
19 Orbital L.						-	-		-	++				--		
20 L. Antorbital P.				++		---	---	+	--	+++		+		---		
21 W. Internal Nares						---	--	+	-	++				-		
22 L. Up. Toothrow		-	+					-			++	+++			+++	
23 No. Teeth (Up. Lf.)	++												-			
24 No. Teeth (Up. Rt.)													-			+
25 No. Teeth (Low. Lf.)			-			++				-				+		
26 No. Teeth (Low. Rt.)						+				-	-		-		-	
27 L. Low. Toothrow			+								+	++			++	
28 Ht. Ramus																
29 Tooth W.			-	-	--											---
30 L. Ramus			+								++	+++			++	
Component I			++			---	--			+++	+	+++		-	++	
Component II				++		--	--	+++		+			++	--		
Canonical Variable 1			+++	+++	+	---	---	++		+++		++		---	+	
Canonical Variable 2					-											---

[1] Blanks indicate nonsignificant correlations. Individual symbols refer to significant positive or negative correlations ($P<0.05$; greater than 0.367), double symbols indicate highly significant correlations ($P<0.01$; greater than 0.470), and triple symbols represent very highly significant correlations ($P<0.001$; greater than 0.580).

[2] Abbreviations identified in Footnote 1 of Table 1.

[3] Environmental variables: (1) Sea Current (N., winter); (2) Sea Current (W., winter); (3) water depth; (4) solar insolation (Jan.); (5) solar insolation (annual); (6) sea surface temp. (Jan.); (7) sea surface temp. (July); (8) sea surface temp. (ann. var.); (9) oxygen min. layer (depth); (10) surface salinity; (11) thermocline depth (winter); (12) thermocline depth (summer); and (13) surface dissolved oxygen.

al. (1985) to reflect a modified sample size and a reduced character set.

Douglas et al. (1992) analyzed sexual dimorphism in skull measures for *S. longirostris* from the eastern tropical Pacific. They found 15 of the 30 characters to be statistically different between sexes. Since *S. longirostris* samples are somewhat smaller, one might expect fewer significant differences in this species simply due to sample size. Nevertheless, inspection of the results indicates support for the conclusion reached by Douglas et al. (1986: 542–543) "that the degree of sexual dimorphism in spotted dolphins is greater than in spinner dolphins." They also pointed out that "the trends are basically the same for both species, suggesting that common behavioral and/or ecological factors are influencing sexual dimorphism in these dolphins."

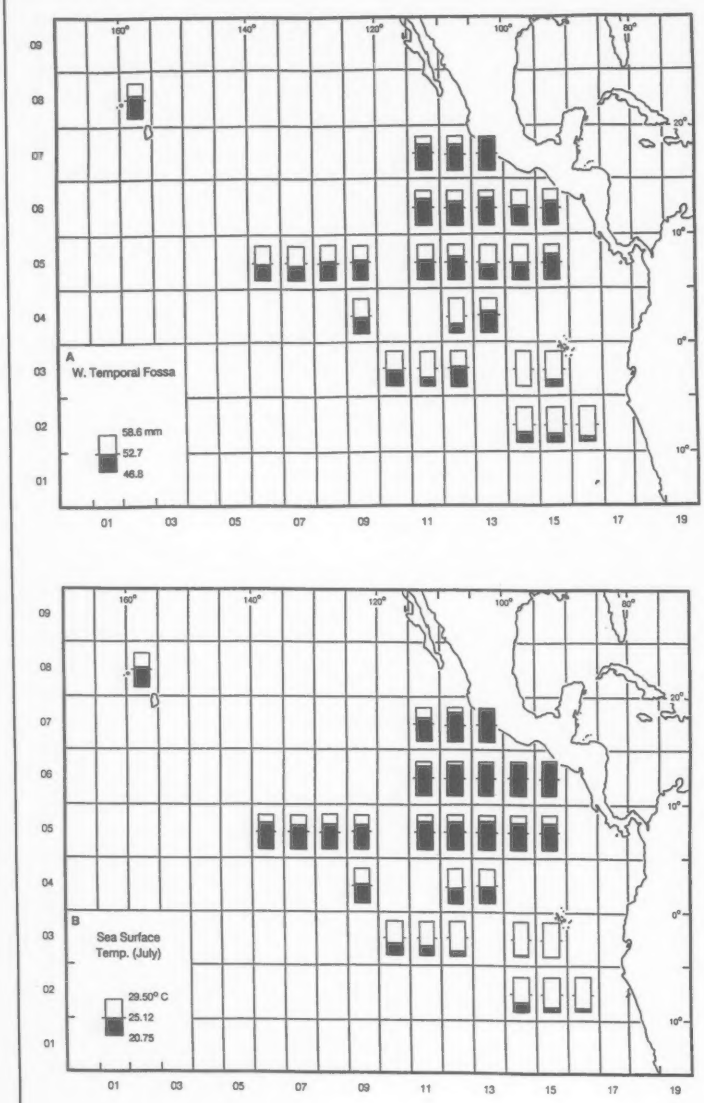

Figure 10

Geographic variation in (**A**) width of temporal fossa and (**B**) sea surface temperature (July). Darkened part of bar indicates value for particular latitude-longitude block.

Geographic variation

From an initial group of specimens, Perrin et al. (1979a) described differences between dolphin skulls available from southern areas and those from more northerly locations. Schnell et al. (1986), based on larger sample sizes, indicated that available information "strongly implies a significant degree of isolation between northern and southern forms." They did not have specimens from west of 125°W and called for additional material from west of 120°W to help clarify the relationship between southern *S. attenuata* and other populations, particularly in light of the notation by Perrin et al. (1979a) of similarities of specimens from the southern group with those from Hawaii. In the eastern portion of the range, the subdivision between northern and southern offshore *S. attenuata* found previously by Perrin et al. (1979a) and Schnell et al. (1986) was confirmed by our analyses with a geographically expanded specimen base. In general, blocks to the west (including those from the waters adjacent to Hawaii) are more like the southern blocks than blocks of the northeast. We found a general concentric pattern of geographic variation (see Fig. 8B), much like that established by Douglas et al. (1992) for the broadly overlapping *S. longirostris*. This also was suggested by Perrin et al. (1985).

Reilly (1990) provided some insight as to possible reasons why samples of *S. attenuata* and *S. longirostris* from the south, southwest,

and west would show close morphologic affinities. He analyzed large-scale dolphin distribution patterns and environmental patterns based on research-vessel surveys conducted in the eastern tropical Pacific from June through November, comparing his results with those of Au and Perryman (1985). Reilly's (1990) distributional comparisons between seasons indicated that along 10°N *S. attenuata* and *S. longirostris* occur in relatively high density west of 120°N during the summer. Furthermore, they were not in high densities along 4°N between 90 and 120°W, and along 6°N between 88 and 110°W—regions with relatively high concentrations of these two species in the winter (Au and Perryman, 1985). Reilly (1990) indicated that "One hypothesis suggested by these complementary changes is an intraregional, seasonal movement." Data from mark-recapture efforts (Perrin et al., 1979b; Hedgepeth[4]) are consistent with respect to the hypothesized direction of such migrations, although the distances are greater than those suggested by the very limited data from these studies. Reilly (1990) also noted that the suggested movement patterns are at least partially explainable based on seasonal atmospheric and oceanographic changes in the region.

Morphological-environmental covariation

In the earlier study of *S. attenuata*, Schnell et al. (1986) assessed environmental-morphological covariation for a similar, although not identical, set of environmental parameters. Since their investigation was restricted largely to eastern blocks, different findings with respect to covariation are possible. Schnell et al. (1986) noted that the strongest morphological-environmental associations involved solar insolation (Jan.). Sea surface temperatures also covaried with a number of morphological characteristics, as did oxygen minimum layer (depth).

The environmental principal components indicated that a number of environmental measures have a north-south component (see Fig. 9A), while others (particularly thermocline depth and water

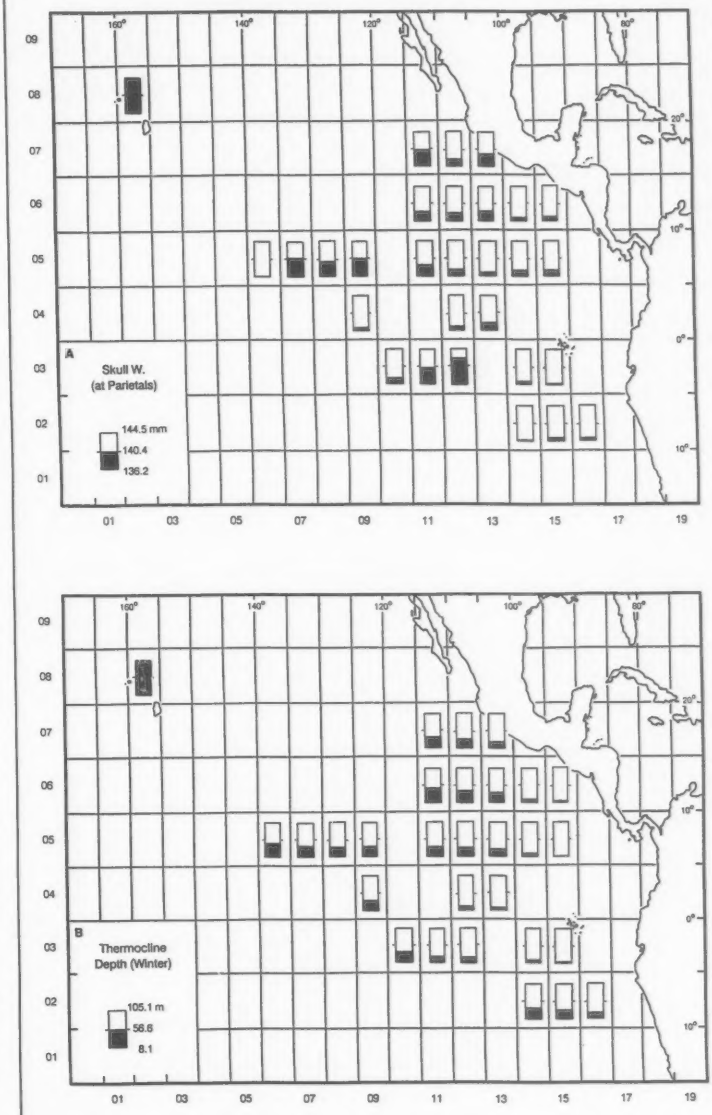

Figure 11

Geographic variation in (**A**) skull width (at parietals) and (**B**) thermocline depth (winter). Darkened part of bar indicates value for particular latitude-longitude block.

[4] Hedgepeth, J. B. 1985. Database for dolphin tagging operations in the eastern tropical Pacific, 1969–1978, with discussion of 1978 tagging results. Southwest Fisheries Center Admin. Rep. No. LJ-85-03, 40 p.

Table 8

Results of Mantel tests (t) and matrix correlations (r) for offshore *Stenella attenuata*. Comparison of interlocality differences for 13 environmental variables and 3 environmental components against those for five morphological variables selected in canonical-variates analysis.

Environmental variable	Preorbital width		Width of temporal fossa		Length of temporal fossa		Length of rostrum (from pterygoid)		Length of braincase	
	t	r	t	r	t	r	t	r	t	r
1 Sea Current (N.,winter)	−1.34	−0.114	2.43*	0.318	−0.20	−0.026	0.67	0.085	2.41*	0.322
2 Sea Current (W.,winter)	0.02	0.001	−1.95	−0.139	−1.68	−0.119	1.94	0.136	0.82	0.059
3 Water Depth	4.12***	0.259	−0.45	−0.033	−1.08	−0.080	3.24**	0.236	1.17	0.088
4 Solar Insolation (Jan.)	7.38***	0.466	6.39***	0.479	6.47***	0.481	−0.56	−0.041	−2.29*	−0.173
5 Solar Insolation (ann.)	7.58***	0.502	2.85**	0.238	2.91**	0.241	0.68	0.056	−0.84	−0.071
6 Sea Surface Temp. (Jan.)	5.53***	0.371	5.71***	0.493	4.70***	0.401	−1.15	−0.097	−1.43	−0.125
7 Sea Surface Temp. (July)	5.59***	0.369	6.97***	0.579	4.08***	0.335	−0.94	−0.076	−1.30	−0.109
8 Sea Surface Temp. (ann. var.)	1.69	0.114	6.23***	0.547	2.87**	0.249	−0.74	−0.064	−0.82	−0.073
9 Oxygen Minimum Layer (depth)	4.18***	0.236	3.60***	0.191	3.75***	0.200	−0.56	−0.030	−0.79	−0.042
10 Surface Salinity	9.52***	0.594	5.31***	0.386	4.66***	0.337	0.32	0.023	−1.20	−0.088
11 Thermocline Depth (winter)	0.40	0.026	0.90	0.070	1.88	0.144	0.20	0.016	−0.39	−0.031
12 Thermocline Depth (summer)	1.21	0.085	−0.07	−0.007	0.84	0.079	2.60**	0.240	0.00	0.000
13 Surface Dissolved Oxygen	−1.85	−0.147	0.76	0.089	1.83	0.211	−0.40	−0.045	−0.01	−0.001
Environmental Component I	3.71***	0.238	6.75***	0.476	4.57***	0.309	−1.69	−0.111	−1.31	−0.104
Environmental Component II	3.77***	0.364	−0.26	−0.030	0.39	0.041	3.45***	0.352	2.63**	0.359
Environmental Component III	4.64***	0.449	0.52	0.059	2.36*	0.252	2.22*	0.227	4.54***	0.623

*$P<0.05$; **$P<0.01$; ***$P<0.001$.

depth) show trends from the east to the west, southwest, and south. Not unexpectedly, a mosaic of variation patterns is present in the suite of morphologic characters we assessed. Some, like width of temporal fossa (Fig. 10A), align closely with environmental variables—such as sea surface temperature (July) (Fig. 10B)—subsumed under environmental component I (Fig. 9A). Others, like skull width (at parietals) (Fig. 11A), display patterns similar to those of thermocline depth (winter) (Fig. 11B) and other environmental measures summarized by environmental component II (Fig. 10B). However, the overall, general morphological trend is reflected best by projections onto the first canonical variable based on morphologic data (Fig. 4), which has a relatively strong negative correlation with environmental component I and a weaker positive one with environmental component II.

By adding the more westerly blocks to the analysis, environmental-morphological covariation patterns that emerged, in some cases, were different from those reported by Schnell et al. (1986). For example, the previous statistically significant correlations they found for several morphologic characters with sea current (N., winter) and sea surface temperature (annual variation) were not repeated

in our expanded study. Likewise, strong associations with measures of solar insolation were substantially reduced for all but a few characters (i.e. length of braincase, length of temporal fossa, and width of temporal fossa; Table 7). Some characters, such as sea current (W., winter) and oxygen minimum layer (depth), did not have variation patterns in either study that corresponded to those for morphologic variables. Water depth, however, has significant correlations with more characters now that western blocks have been added. At least three environmental measures—sea surface temperature (Jan.), sea surface temperature (July) (Fig. 10B), and surface salinity—had relatively strong covariation patterns that stayed relatively constant through the two studies.

Availability in the future of better information on environmental variation and, possibly, on other relevant parameters reflecting environmental heterogeneity will allow researchers to analyze dolphin-environmental covariation in a more meaningful way. For example, better environmental data and more comprehensive information on dolphin feeding ecology could provide a basis for testable predictions concerning why certain morphological characters covary with specific environmental variables. Our admittedly descriptive analyses demonstrate some striking cases of dolphin-environmental covariation and, thus, provide initial guidance in terms of possible causal relationships that may be examined with greater sophistication by future investigators.

Interspecific covariation

In this paper we have presented statistical data for trends in geographic covariation of *S. longirostris* and *S. attenuata* skulls from 16 blocks for which samples of both species were available (brief comments on covariation were included by Douglas et al. 1992). Geographic patterns in 13 of the 30 morphological characters showed statistical correspondence based on Mantel tests, whereas

Table 9

Comparisons of principal component and canonical variable projections for offshore *Stenella attenuata* and *S. longirostris* based on corresponding data for 16 latitude-longitude blocks.

	Principal component		Canonical variable	
Statistic	I	II	1	2
Product-moment correlation	0.745***	0.289	0.896***	–0.328
Mantel *t*-value	3.46**	0.32	6.65***	1.62
Matrix correlation	0.528	0.039	0.741	0.204

*$P<0.05$; **$P<0.01$; ***$P<0.001$. *P*-values for Mantel tests based on number of times permutational Z-values less than or equal to observed *Z*-values (one-tailed test).

Table 10

Results of Mantel tests, matrix correlations, and product-moment correlations for 16 overlapping latitude-longitude blocks of offshore *Stenella attenuata* and *S. longirostris*. Comparison of interlocality differences for 30 morphological variables.

Character[1]	Mantel *t*-value	Matrix correlation	Product-moment correlation
1 Condylobasal L.	1.21	0.184	0.256
2 L. Rostrum (from Base)	1.28	0.178	0.159
3 L. Rostrum (from Pterygoid)	0.55	0.074	0.150
4 W. Rostrum (at Base)	4.65***	0.626	0.837***
5 W. Rostrum (at 1/4 L.)	4.14***	0.337	0.693**
6 W. Rostrum (at 1/2 L.)	4.57***	0.495	0.775***
7 W. Premax. (at 1/2 L.)	–0.49	–0.066	0.351
8 W. Rostrum (at 3/4 L.)	1.01	0.120	0.540*
9 Preorbital W.	5.70***	0.737	0.865***
10 Postorbital W.	6.24***	0.693	0.861***
11 Skull W. (at Zygomatic P.)	6.37***	0.732	0.883***
12 Skull W. (at Parietals)	2.71**	0.446	0.616*
13 Ht. Braincase	0.60	0.093	0.294
14 L. Braincase	2.91*	0.494	0.613*
15 Max. W. Premax.	2.88**	0.318	0.675**
16 W. External Nares	–0.64	–0.073	0.224
17 L. Temporal Fossa	0.79	0.088	–0.499*
18 W. Temporal Fossa	0.62	0.077	–0.443
19 Orbital L.	0.92	0.148	0.383
20 L. Antorbital P.	4.10**	0.396	0.658**
21 W. Internal Nares	1.61	0.205	0.613*
22 L. Up. Toothrow	1.19	0.165	0.069
23 No. Teeth (Up. Lf.)	2.98**	0.501	–0.753***
24 No. Teeth (Up. Rt.)	2.99**	0.517	–0.691**
25 No. Teeth (Low. Lf.)	0.03	0.004	–0.223
26 No. Teeth (Low. Rt.)	0.66	0.104	–0.428
27 L. Low. Toothrow	0.59	0.090	0.015
28 Ht. Ramus	2.34*	0.298	0.408
29 Tooth W.	0.20	0.038	–0.260
30 L. Ramus	0.70	0.111	0.174

* $P<0.05$; **$P<0.01$; ***$P<0.001$. *P*-values for Mantel tests based on number of times permutational *Z*-values less than or equal to observed *Z*-values (one-tailed test).
[1] Abbreviations identified in Footnote 1 of Table 1.

product-moment correlations were significant for 15 characters. Some of these associations were very strong (i.e. correlations as high as 0.883; see Table 10). Given that we are comparing two species, entities that have independent gene pools, the most likely explanation for common positive trends in morphologic covariation is that the two species are being subjected to similar forces of natural selection.

However, we found several striking examples where covariation was negative. A significant negative association was found for length of temporal fossa, while the negative correlation for width of temporal fossa was nearly significant statistically. The number of upper teeth (characters 23 and 24) also show significant negative correlations (Table 10). Muscles associated with the feeding apparatus are positioned in the temporal fossa; obviously, tooth numbers could be related to prey types taken. One suspects that the presence of antithetical trends in these particular skull characteristics is a result of competitive interactions involving these two interacting species. This may be an example of ecological character displacement related to differences in feeding and food types taken (Perrin, 1984). Certainly, the two species are found in close association over much of the eastern tropical Pacific (Au and Perryman, 1985; Reilly, 1990); 49% of *S. attenuata* schools included some *S. longirostris*, while 73% of the schools of the less common *S. longirostris* included *S. attenuata* (Reilly, 1990).

The information available to date indicates that spinner and spotted dolphins may have different feeding habits or preferences in areas of co-occurrence in the eastern tropical Pacific. Based on analysis of stomach contents of spinner and spotted dolphins captured together in purse-seine hauls in the tuna fishery, Perrin et al. (1973) concluded tentatively that while some prey species are taken by both, spinner dolphins in the mixed-species associations specialize in small mesopelagic fishes (mainly myctophids and gonostomatids) and squids, whereas the spotted dolphins consume larger and more epipelagic species such as flying fishes, small scombroids (e.g. *Auxis* sp.), and larger squids. In addition, state of digestion of the stomach contents indicted that the spinner and spotted dolphins had fed at different times of the day. Stomachs of a spotted dolphin from Hawaii, where the two species do not school together, and from two spotted dolphins from the far western portion of the range in the eastern Pacific, where the mixed species associations are less common than in the core area of the tuna fishery off Mexico and Central America (Au and Perryman, 1985; fig. 11), contained a large proportion of small mesopelagic species like those eaten by the spinner dolphin in the mixed species associations farther to the east. This geographic variation in feeding habits may reflect resource partitioning where the two species associate closely, which in turn may be manifested in morphological character displacement.

Genetic subdivision, management units, and implications of cranial variation

The results suggest that gene flow is not uniform throughout the range of *S. attenuata* in the eastern Pacific; the morphological heterogeneity probably reflects genetic subdivision, a conclusion also reached as a result of the earlier study by Schnell et al. (1986). A similar inference was drawn by Douglas et al. (1992) based on morphologic studies of *S. longirostris*. For *S. attenuata*, we found that 93.3% of the 30 morphologic characters had statistically significant geographic variation, with 60.0% exhibited regional patterning and 73.3% local patterning. This geographic partitioning of morphologic variance was demonstrable even with pooling of specimens taken over a number of months and years, a process that would tend to shroud such relationships.

The boundaries of management units presently employed (Perrin et al., 1985) are not fully consistent with the general pattern of morphologic variation described here. It appears that animals west of about 120°W longitude have greater affinity with those in the Southern Offshore management unit than they do with *S. attenuata* from the eastern portion of the present Northern Offshore unit, the unit in which they are presently included. Further, the present boundary between the Northern and Southern Offshore units, at 1°S latitude, is probably too far south; a boundary at about 5°N would be more consistent with the general pattern of cranial variation.

The proposed Northern Offshore unit bounded by 5°N and 120°W would be nearly congruent with the "conservation zone" suggested for *S. longirostris* (Perrin et al., 1991). This is to be expected based on the correlated trends of covariation with environmental variables; the two species, as they exist in this region, apparently are parts of an endemic fauna uniquely adapted to the far eastern tropical Pacific and, as such, are "evolutionarily significant units" (Dizon et al., 1992).

The cranial results are only one line of evidence useful for delineation of management units; others, such as patterns in movements, external morphology or life-history parameters, also should be taken into consideration. For example, other data may indicate that *S. attenuata* west of 120°W differ sig-

nificantly in some regard from those south of 5°N and should be managed separately (yielding three management units instead of the present two). Certainly, the specimens from the Hawaiian Islands are generally larger than those from the south, southwest, and west with which they have their closest morphologic affinity.

Note added in proof Based in part on the results and recommendations in this paper, the management unit boundaries for the offshore spotted dolphin in the eastern Pacific have been changed. The boundary of a new "Northeastern stock" runs south along the 120°W meridian to 5°N and then east to the mainland. Offshore spotted dolphins outside this zone to the west and south are now part of a "Western/Southern stock." February, 1994.

Acknowledgments

Support for aspects of this research was received by the University of Oklahoma through Contract 79-ABC-00167 from the U.S. Department of Commerce, National Oceanographic and Atmospheric Administration, and Purchase Orders 84-ABA-02177 and 40JGNF0532 from the National Marine Fisheries Service, Southwest Fisheries Science Center, La Jolla, CA. We thank individuals (listed in Douglas et al., 1992) who provided access to museum specimens. M. E. Douglas measured the initial set of specimens used in this study. Pamela A. Pogorelc assisted with preparation of some of the figures. Paul Fiedler, Steven Reilly, Michael Scott, and an anonymous reviewer provided useful suggestions on earlier drafts of this paper.

Literature cited

Allen, R. A.
1985. Dolphins and the purse-seine fishery for yellowfin tuna. *In* J. R. Beddington, R. J. H. Beverton and D. M. Lavigne (eds.), Marine mammals and fisheries, p. 236–252. Allen and Unwin, London, 354 p.

Au, D. W. K., and W. L. Perryman.
1985. Dolphin habitats in the eastern tropical Pacific. Fish. Bull. 83:623–643.

Dailey, M. D., and W. F. Perrin.
1973. Helminth parasites of porpoises of the genus *Stenella* in the eastern tropical Pacific, with descriptions of two new species: *Mastigonema stenellae* gen. et sp. n. (Nematoda:Spiruroidea) and *Zalophotrema pacificum* sp. n. (Trematoda: Digenea). Fish. Bull. 71:455–471.

Dixon, W. D. (chief ed.).
1990. BMDP statistical software. Vol. 1. Univ. California Press, Berkeley, CA.

Dizon, A. E., C. Lockyer, W. F. Perrin, D. P. DeMaster and J. Sisson.
1992. Rethinking the stock concept: a phylogenetic approach. Conserv. Biol. 6:24–36.

Douglas, M. E., G. D. Schnell, D. J. Hough, and W. F. Perrin.
1992. Geographic variation in cranial morphology of spinner dolphins (*Stenella longirostris*) in the eastern tropical Pacific Ocean. Fish. Bull. 90:54–76.

Douglas, M. E., G. D. Schnell, and D. J. Hough.
1984. Differentiation between inshore and offshore spotted dolphins in the eastern tropical Pacific Ocean. J. Mammal. 65:375–387.
1986. Variation in spinner dolphins (*Stenella longirostris*) from the eastern tropical Pacific Ocean: sexual dimorphism in cranial morphology. J. Mammal. 67:537–544.

Hall, M. A., and S. D. Boyer.
1987. Incidental mortality of dolphins in the eastern tropical Pacific tuna fishery in 1985. Rep. Int. Whal. Commn. 37:361–362.
1988. Incidental mortality of dolphins in the eastern tropical Pacific tuna fishery in 1986. Rep. Int. Whal. Commn. 38:439–441.
1989. Estimates of incidental mortality of dolphins in the eastern Pacific fishery for tropical tunas in 1987. Rep. Int. Whal. Commn. 39:321–322.
1990. Incidental mortality of dolphins in the tuna purse-seine fishery in the eastern Pacific Ocean during 1988. Rep. Int. Whal. Commn. 40:461–462.
1991. Incidental mortality of dolphins in the tuna purse-seine fishery in the eastern Pacific Ocean during 1989. Rep. Int. Whal. Commn. 41:507–509.
1992. Estimates of incidental mortality of dolphins in the purse-seine fishery for tunas in the eastern Pacific Ocean in 1990. Rep. Int. Whal. Commn. 42:529–531.

Katz, J. O., and F. J. Rohlf.
1973. Function-point cluster analysis. Syst. Zool. 22:295–301.

Mantel, N.
1967. The detection of disease clustering and a generalized regression approach. Cancer Res. 27:209–220.

Perrin, W. F.
1984. Patterns of geographical variation in small cetaceans. Acta Zool. Fennica 172:137–140.

Perrin, W. F., R. R. Warner, C. H. Fiscus, and D. B. Holts.
1973. Stomach contents of porpoise, *Stenella* spp., and yellowfin tuna, *Thunnus albacares*, in mixed-species aggregations. Fish. Bull. 71:1077–1092.

Perrin, W. F., P. A. Sloan, and J. R. Henderson.
1979a. Taxonomic status of the 'southwestern stocks' of spinner dolphin, *Stenella longirostris*, and spotted dolphin, *S. attenuata*. Rep. Int. Whal. Commn. 29:175–184.

Perrin, W. F., W. E. Evans, and D. B. Holts.
1979b. Movements of pelagic dolphins (*Stenella* spp.) in the eastern tropical Pacific as indicated by results of tagging, with summary of tagging operations, 1969–1976. U.S. Dep. Commerce, NOAA Tech. Rep. NMFS SSRF-737, 14 p.

Perrin, W. F., M. D. Scott, G. J. Walker, F. M. Ralston, and D. W. K. Au.
1983. Distribution of four dolphins (*Stenella* spp. and *Delphinus delphis*) in the Eastern Tropical Pacific, with an annotated catalog of data sources. U.S. Dep. Commerce, NOAA Tech. Memo. NMFS, 65 p.

Perrin, W. F., M. D. Scott, G. J. Walker, and V. L. Cass.
1985. Review of geographical stocks of tropical dolphins (*Stenella* spp. and *Delphinus delphis*) in the eastern Pacific. U.S. Dep. Commerce, NOAA Tech. Rep. NMFS 28, 28 p.

Perrin, W. F., P. A. Akin, and J. V. Kashiwada.
1991. Geographic variation in external morphology of the spinner dolphin, *Stenella longirostris*, in the eastern Pacific and implications for conservation. Fish. Bull. 89:411–428.

Reilly, S. B.
1990. Seasonal changes in distribution and habitat differences among dolphins in the eastern tropical Pacific. Mar. Ecol. Prog. Ser. 66:1–11.

Rohlf, F. J., J. Kishpaugh, and D. Kirk.
1979. NT-SYS. Numerical taxonomy system of multivariate statistical programs. State Univ. New York, Stony Brook, New York.

Schnell, G. D., M. E. Douglas, and D. J. Hough.
1985. Sexual dimorphism in spotted dolphins (*Stenella attenuata*) in the eastern tropical Pacific Ocean. Mar. Mamm. Sci. 1:1–14.

1986. Geographic patterns of variation in offshore spotted dolphins (*Stenella attenuata*) of the eastern tropical Pacific Ocean. Mar. Mamm. Sci. 2:186–213.

Sneath, P. H. A., and R. R. Sokal.
1973. Numerical taxonomy. W. H. Freeman and Co., San Francisco.

Wirth, M., G. F. Estabrook, and D. F. Rogers.
1966. A graph theory model for systematic biology with an example for the Oncidiinae (Orchidaceae). Syst. Zool. 15:59–69.

Modeling oyster populations. IV: Rates of mortality, population crashes, and management*

Eric N. Powell
Department of Oceanography, Texas A&M University
College Station, TX 77843

John M. Klinck
Eileen E. Hofmann
Center for Coastal Physical Oceanogrphy, Crittenton Hall
Old Dominican University, Norfolk, VA 23529

Sammy M. Ray
Department of Marine Biology, Texas A&M University
College Station, TX 77843

Abstract.—A time-dependent energy-flow model was used to examine how mortality affects oyster populations over the latitudinal gradient from Galveston Bay, Texas, to Chesapeake Bay, Virginia. Simulations using different mortality rates showed that mortality is required for market-site oysters to be a component of the population's size-frequency distribution; otherwise a population of stunted individuals results. As mortality extends into the juvenile sizes, the population's size frequency shifts toward the larger sizes. In many cases adults increase despite a decrease in overall population abundance. Simulations, in which the timing of mortality varied, showed that oyster populations are more susceptible to population declines when mortality is restricted to the summer months. Much higher rates of winter mortality can be sustained. Comparison of simulations of Galveston Bay and Chesapeake Bay showed that oyster populations are more susceptible to intense population declines at higher latitudes. The association of population declines with disease agents causing summer mortality and the increased frequency of long-term declines at high latitudes result from the basic physiology of the oyster and its population dynamics cycle. Accordingly, management decisions on size limits, seasons and densities triggering early closure must differ across the latitudinal gradient and in populations experiencing different degrees of summer and winter mortality relative to their recruitment rate. More flexible size limits might be an important management tool. When fishing is the primary cause of mortality, populations should be managed more conservatively in the summer. The latitudinal gradient in resistance to mortality requires more conservative management at higher latitudes and different management philosophies from those used in the Gulf of Mexico.

Manuscript accepted 12 October 1993
Fishery Bulletin 92:347–373 (1994)

One of the unfortunate characteristics of oyster *Crassostrea virginica* populations is their susceptibility to periods of heavy mortality, which can extend from a few months to a few years in duration. Oyster population abundances drop precipitously during these times and may remain low for extended periods (Schlesselman, 1955; Engle, 1956; Laird, 1961; Engle and Rosenfield, 1962). Why populations decline over several years or crash over shorter periods of time can usually be explained by killing floods (Andrews et al., 1959; Soniat and Brody, 1988; Soniat et al., 1989) or disease epizootics (Needler and Logie, 1947; Andrews and Hewatt, 1957; Mackin and Hopkins, 1962) although predators and overfishing have occasionally received some credit (Moore and Pope, 1910; Menzel et al., 1957; Quast et al., 1988).

A review of the literature shows that declines and crashes in oyster populations have some interesting characteristics (Mackin and Wray, 1950; Mackin et al., 1950; Menzel, 1950, a and b; Menzel and Hopkins, 1953; Owen, 1953; Gunter, 1955; Mackin and Sparks, 1962; Hofstetter et al., 1965; Copeland and Hoese, 1966; Hofstetter, 1966; Gilmore et al., 1975; and previously cited references):

1 With the exception of killing floods, the times of the year with the most intense mortality are usually restricted to the summer and early fall and to areas of higher salinity. Warm temperatures and high salinities promote the growth of the disease-producing organisms *Perkinsus marinus* and *Haplosporidium nelsoni* (Ray and Chandler, 1955; Andrews and Hewatt, 1957) and predation by such pests as the oyster drill, *Thais haemastoma* (Garton and Stickle, 1980; Stickle, 1985).
2 Population crashes or significant declines have been documented throughout the oyster's latitudinal range. However, except for permanent changes in salinity,

* Parts I-III have been published in the *Journal of Shellfish Research* (Part I in 11:387-398; Part III in 11:399-416; Part II is in press).

owing to levee building for instance (Mackin and Hopkins, 1962), population recovery rates appear to be more rapid at lower latitudes (compare Owen, 1953; Hofstetter, 1983; Stanley and Sellers, 1986; Mackenzie, 1989).

3 Major population crashes resulting in long-term loss or decline of the *C. virginica* fishery have occurred almost exclusively along the northeast coast of North America. Moreover, significant population declines occurred earlier in the century at higher latitudes (viz. Canada, 1910s, Mid-Atlantic area, 1950s; Delaware and Chesapeake Bays, 1980s) (Stanley and Sellers, 1986; Mountford and Reynolds, 1988; Mackenzie, 1989; and others referenced previously), although more than one significant population has declined in some areas.

These trends in oyster population dynamics gleaned from the literature are not well documented. Much literature is anecdotal and significant exceptions do exist. Nevertheless, taken as a whole, these trends suggest two hypotheses: 1) a latitudinal gradient in susceptibility to population crashes exists in oyster populations; and 2) as temperature varies both latitudinally and seasonally, temperature, through its effect on oyster physiology (e.g. Koehn and Bayne, 1989), may determine the susceptibility of oyster populations to potentially destabilizing episodes of mortality.

In this study, we tested these hypotheses using a population dynamics model. The results of the modeling exercise were then used to examine some basic decisions required for fishery management; viz. the timing and length of the fishing seasons and the size limits set for the fishery to obtain a maximum sustainable yield (e.g. Glude, 1966; Hofstetter and Ray, 1988; Young and Martin, 1989).

The model

Perspective and basic characteristics

The oyster population model shown in Figure 1 is designed to investigate the dynamics of the post-settlement phase of the American eastern oyster's, *Crassostrea virginica*, life from newly settled juvenile through adulthood. The model consists of a system of ten coupled ordinary differential equations, with each equation representing a size class of oyster; however, the ten size classes are not evenly divided across the length or biomass spectrum (Table 1). Size class 1 includes newly settled juveniles (Dupuy et al., 1977). Size class 10 corresponds to oysters that are larger than those normally found in natural populations. The boundaries between size classes 4 and 5, 5 and 6, and 6 and 7 represent size limits that have been used or considered for market-size oysters: 2.5 in; 3.0 in and 3.5 in, respectively. We define adults, individuals capable of spawning, as individuals weighing more than 0.65 g ash-free dry weight, about 50 mm in length (Hayes and Menzel, 1981). Therefore, size classes 1 to 3 are juveniles.

Table 1

Biomass and length dimensions of the oyster *Crassostrea virginica* size classes used in the model. Biomass is converted to size using the relationship given in White et al. (1988).

Model Size class	Biomass (g ash-free dry wt)	Length (mm)
1	1.3×10^{-7} – 0.028	0.3 – 25.0
2	0.028 – 0.10	25.0 – 35.0
3	0.10 – 0.39	35.0 – 50.0
4	0.39 – 0.98	50.0 – 63.5
5	0.98 – 1.94	63.5 – 76.0
6	1.95 – 3.53	76.0 – 88.9
7	3.53 – 5.52	88.9 – 100.0
8	5.52 – 7.95	100.0 – 110.0
9	7.95 – 12.93	110.0 – 125.0
10	12.93 – 25.91	125.0 – 150.0

All calculations were done in terms of energy in $cal \cdot m^{-2}$. When necessary, oyster energy is converted to oyster biomass by using a caloric conversion of 6100 $cal \cdot g$ dry wt^{-1} for oysters (Cummins and Wuycheck, 1971) and biomass to an approximate length by using White et al.'s (1988) biomass-length conversion. To calculate any gain, loss, or transfer of energy (or biomass) between size classes, an additional conversion was made to express the gain, loss or transfer in terms of a specific rate (day^{-1}) which was then multiplied by the caloric quantity in a size class. Transfers between size classes were scaled by the ratio of the average weight of the current size class (in g dry wt or cal) to that of the size class from which energy was gained or to which energy was lost. This ensured that the total number of individuals in the model was conserved, in the absence of recruitment and mortality. Because, the size classes in the model are not equivalent in dimension, each specific rate for each transfer between size classes was scaled by the ratio between the two size classes:

$$\text{for transfers up:} \quad W_j/(W_{j+1}-W_j)$$

$$\text{for transfers down:} \quad W_j/(W_j-W_{j-1}),$$

where W is the median biomass (in g dry wt) in size class j. For simplicity, we will not include any of these conversions and scaling factors in the equations given subsequently.

Governing equation

The change in oyster standing stock with time in each size class (O_j) is the result of changes in net production (NP_j), taken to be the sum of the production of somatic (P_{gj}) and reproductive (P_{rj}) tissue, and the addition of individuals from the previous size class or loss to the next largest size class by growth. Following White et al. (1988), net productivity is assumed to be the difference between assimilation (A_j) and respiration (R_j),

$$NP_j = P_{gj} + P_{rj} = A_j - R_j. \quad (1)$$

Accordingly,

$$\frac{dO_j}{dt} = P_{gj} + P_{rj} + (\text{gain from } j-1) - (\text{loss to } j+1) \quad (2)$$

for j = 1,10 recognizing P_{rj} = 0 for j = 1,3.

Resorption of either gonadal or somatic tissue results in loss of biomass. When NP_j<0, oysters lose biomass and transfer into the next lower size class. This is an important difference between our size class model and a size class model based on linear dimensions; shell size does not change, however biomass does during periods of negative scope for growth. This is the basis for the use of condition index as a measure of health in oysters (e.g. Newell, 1985; Wright and Hetzel, 1985). To allow for this, equation 2 must be modified as

$$\frac{dO_j}{dt} = P_{gj} + P_{rj} + (\text{gain from } j-1) - (\text{loss to } j+1) + (\text{gain from } j+1) - (\text{loss to } j-1) \quad (3)$$

for j = 1,10. The last two terms on the right side of Equation 3 represent the individuals losing biomass and, thus, translating down to the next lower size class.

The relationships used to parameterize the processes in Equation 3 are described in the following sections. More details and a discussion of the assumptions and supporting data for the model were presented by Klinck et al. (1992), Powell et al. (1992) and Hofmann et al. (1992). Accordingly, the basic oyster size class model is outlined only briefly. However, calculations of spawning size and recruitment, mortality, and the effect of oyster density on feeding are specific to this study and are described in more detail.

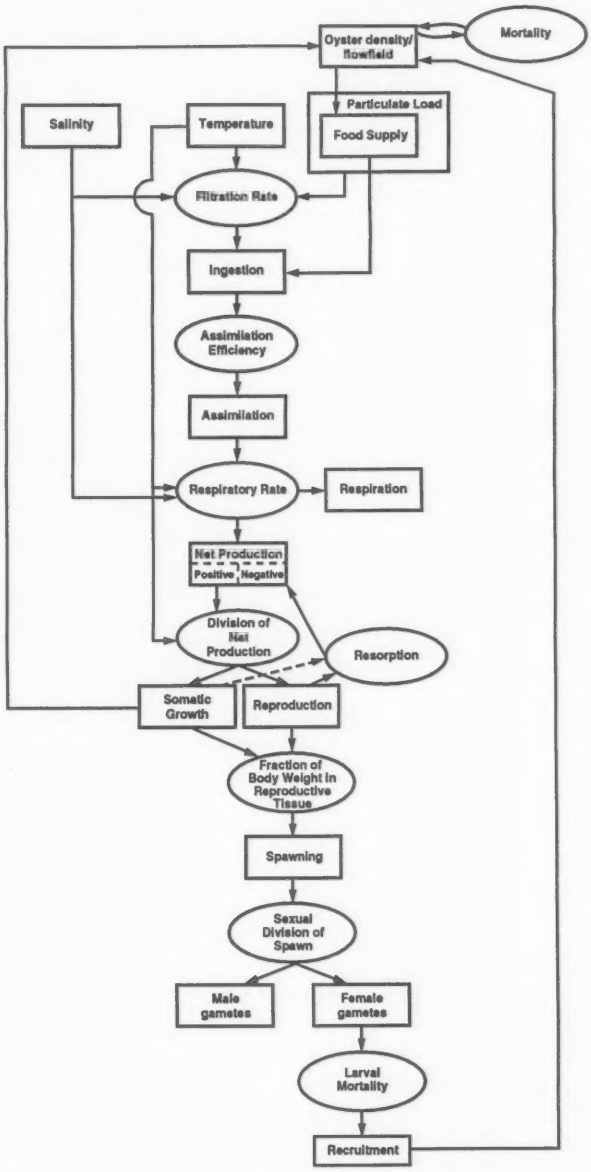

Figure 1
Schematic diagram of the energy flow model.

Feeding and assimilation

Ingestion rate depends upon the filtration rate and the ambient food concentration. We adapted Doering and Oviatt's (1986) equa-

tion for filtration rate to oysters (Powell et al., 1992) to obtain filtration rate as a function of biomass and temperature (T):

$$FR_j = \frac{K_j^{0.96} T^{0.95}}{2.95}, \quad (4)$$

and

$$K_j = W_j^{0.317} 10^{0.669}, \quad (5)$$

where filtration rate (FR_j) is in mL filtered ind^{-1} min^{-1} and W_j is the ash-free dry weight in g for each size class. Equation 4 contains the temperature-dependency described by Loosanoff (1958).

Filtration rate was further modified by salinity as described by Loosanoff (1958). Filtration rate decreases as salinity drops below 7.5‰ and ceases at 3.5‰. In mathematical terms:

$$\begin{array}{ll} \text{at } S \geq 7.5‰ & FR_{sj} = FR_j \\ \text{at } 3.5 < S < 7.5‰ & FR_{sj} = FR_j (S - 3.5)/4.0 \\ \text{at } S \leq 3.5‰ & FR_{sj} = 0. \end{array} \quad (6)$$

where S is ambient salinity and FR_j is the filtration rate obtained from Equation 4.

The reduction in feeding efficiency at high particulate loads was included as a reduction in filtration rate according to Loosanoff and Tommers (1948)

$$\tau = (4.17 \times 10^{-4})(10^{0.0418x}), \quad (7)$$

where τ is the total particulate content (inorganic + organic) in g·L^{-1} and x is the percent reduction in filtration rate.

Solving Equation 7 for the percent reduction in filtration rate gives a modified expression for filtration rate of the form:

$$FR_{tj} = FR_{sj}\left[1 - 0.01\left(\frac{\log_{10}\tau + 3.38}{0.0418}\right)\right]. \quad (8)$$

Equation 8, if applied to total particulate content (inorganic + organic), limits ingestion rate to approximately the maximum value found by Epifanio and Ewart (1977). Therefore, an additional term to lower ingestion efficiency at high food concentrations was not used.

The effect of oyster density on food availability was parameterized from measurements given in Lund (1957) as

$$f = \frac{k}{[k/f_o - 1]e^{-rd} + 1}, \quad (9)$$

where f is the fractional reduction in food, d is oyster density expressed as L filtered hr^{-1}·m^{-2}, and f_0=0.001, an arbitrarily low number conforming to the expectation that food supply is not affected by low oyster density. For the high flow (59 L hr^{-1}) conditions given in Lund (1957), k = 0.31 and r = 1.36×10^{-6}. For low flow (12 L hr^{-1}) conditions, k = 0.57 and r = 9.746×10^{-7}. Food availability at a given oyster density is estimated as (1–f) times the ambient food concentration. Filtration rate times the ambient available food concentration then gives oyster ingestion. Assimilation is obtained from ingestion using an assimilation efficiency of 0.75 (Powell et al., 1992).

Respiration

Oyster respiration as a function of temperature and oyster weight was obtained from Dame (1972) as

$$R_j = (69.7 + 12.6T) W_j^{b-1}, \quad (10)$$

where R_j is in µL 0_2 consumed hr^{-1}·g dry wt^{-1} and b = 0.75.

Salinity effects on oyster respiration were parameterized from data given in Shumway and Koehn (1982) by obtaining a ratio (R_r) of respiration at 10‰ to respiration at 20‰, $R_r = \frac{R_{10‰}}{R_{20‰}}$, and regressing this ratio against temperature. This yielded two equations:

$$\begin{array}{ll} \text{at } T < 20°C & R_r = 0.007T + 2.099; \\ \text{at } T \geq 20°C & R_r = 0.0915T + 1.324; \end{array} \quad (11)$$

which were then used to obtain respiration rate as follows:

$$\begin{array}{ll} S \geq 15‰ & R_{Tj} = R_j; \\ 10‰ < S < 15‰ & R_{Tj} = R_j\left(1 + [(15 - S)(R_r - 1)/5]\right); \\ S \leq 10‰ & R_{Tj} = R_j R_r. \end{array} \quad (12)$$

Shumway and Koehn (1982) identified effects of salinity on respiration at 20‰; however, we used a 15‰ cutoff to conform to Chanley's (1958) observations on oyster growth.

Reproduction

For adult oysters (j=4,10), net production was apportioned into growth and reproduction by using a temperature-dependent reproduction efficiency of the form

$$R_{effj} = 0.054T - 0.729 \quad (13)$$

for January to June and

$$R_{effj} = 0.047T - 0.809 \quad (14)$$

for July to December. Equations 13 and 14 were derived empirically from the field observations of Soniat and Ray (1985) and may not hold north of Delaware Bay (Hofmann et al., in press).

The portion of net productivity going into reproduction is given by

$$P_{rj} = R_{effj} NP_j, \text{ for } j = 4,10. \quad (15)$$

Somatic growth is the remaining fraction. In cases where $NP_j < 0$, we assume preferential resorption of gonadal tissue to cover the debt. For juveniles and adults with no gonadal tissue, resorption of somatic tissue occurs. We assume that reduced reproduction at low salinity (Engle, 1947; Butler, 1949) results from decreased filtration rate and increased respiratory rate and so include no specific relationship for this effect.

Spawning of the oyster population occurs when the total cumulative reproductive biomass of the population exceeds 20% of the total oyster biomass (Choi et al., 1993). This value is lower than the estimates of Galtsoff (1964) and Deslous-Paoli and Heral (1988), but comes from direct measurements of egg content. Once spawning occurs, the total reproductive biomass is apportioned into male and female biomass according to Kennedy (1982)

$$f_{ratio} = 0.021L_b - 0.62. \quad (16)$$

where f_{ratio} is the ratio of females to males and L_b is shell length in mm obtained from biomass (White et al., 1988). Oysters can change their sex, and Kennedy (1982) suggested that the ratio of males to females is affected by oyster density, salinity, and stress. While perhaps important in some situations, no data exist to parameterize these relationships adequately. They are not included in the model.

The female portion of reproductive biomass (R_f) is converted into eggs spawned by

$$\text{Number of eggs spawned} = R_f \ 1/6133 \ 1/W_{egg} \quad (17)$$

where 6133 is the egg's caloric content (cal g dry wt^{-1}) (Klinck et al., 1992) and W_{egg} is egg weight obtained from

$$W_{egg} = 2.14 \times 10^{-14} V_{egg}, \quad 18$$

where oyster egg volume (V_{egg}) is from Gallager and Mann (1986). The factor 2.14×10^{-14} represents conversions for density, dry wt to wet wt, and μm^3 to cm^3. The egg weight, 13 ng dry wt, calculated from Equation 18 is close to experimentally determined egg weights (Lee and Heffernan, 1991; Choi et al., 1993).

Larval recruitment and mortality

Larval growth rate, which determines the time spent in the plankton, is controlled by ambient food concentration, temperature, salinity, and turbidity. Therefore, larval life span can range from twenty to sixty days (Dekshenieks et al., in press). For the purposes of this modeling study, larval life span was assumed to be twenty days, which may be an underestimate for some environmental conditions, but is in general agreement with observations (Prytherch, 1929; Dupuy et al., 1977; Bahr and Lanier, 1981). We allow an additional 10 days for the larvae to grow to the mean biomass represented by size class one in the post-settlement model. Thus, thirty days after spawning, larvae appear in the simulated post-settlement oyster population as new recruits to the first size class (j=1).

While in the plankton, oyster larvae undergo considerable mortality from a variety of sources. Larval mortality is included in the model by using a simple linear relationship of the form

$$\text{Number of larvae recruited spawn}^{-1} = s(\text{Number of eggs spawned}) \quad (20)$$

where s determines the rate at which individuals are lost per spawn (in spawn^{-1}). No attempt is made to differentiate among sources of oyster larval mortality.

Post-settlement population mortality

Post-settlement oyster populations undergo natural mortality from diseases and predators and man-induced mortality through fishing. Both natural and man-induced mortality vary with season and size of individual. Adult mortality was modeled by using a linear mortality relationship of the form

$$\text{Number dying time}^{-1} = k_d \ (\text{Number living}), \text{ for } j = k,l \quad (21)$$

where k_d determines the daily mortality rate (in day^{-1}) and k and l are the inclusive size classes being affected by mortality. As with larval mortality, this approach does not differentiate among the many sources of oyster mortality. However, the ef-

fect of these mortality sources is implicit in the value chosen for k_d and the size class range used (k,l).

Environmental forcing

Monthly-averaged time series of temperature measured in Galveston Bay (Soniat and Ray, 1985) and Chesapeake Bay (Galtsoff et al., 1947) were used as input to the model (Fig. 2). Each time series is two years in length and each shows temperature trends expected for mid-latitude temperate bays: cool in fall and spring and warm in summer. For a 6-year simulation, the 2-year time series shown in Figure 2 was repeated three times. Salinity values were held constant throughout the year at 24‰ to simplify the discrimination between salinity and temperature effects.

Monthly-averaged values of food concentration were also input into the model (Fig. 2). However, unlike the temperature time series, idealized time series, constructed to illustrate particular types of food availability, were used. This approach was used so that the occurrence and magnitude of features such as the spring and fall phytoplankton blooms could be manipulated (Fig. 2, A and C) or eliminated (Fig. 2B). However, the general characteristics of the idealized food time series are representative of measured values (Soniat et al., 1984; Berg and Newell, 1986). The basic idealized food time series consisted of low winter levels (0.5 $mg \cdot L^{-1}$), higher summer levels (0.75 $mg \cdot L^{-1}$) and still higher values for two months in the spring and fall to simulate spring and fall bloom levels (1.25 $mg \cdot L^{-1}$). A summary of the environmental conditions used for each simulation is given in Table 2.

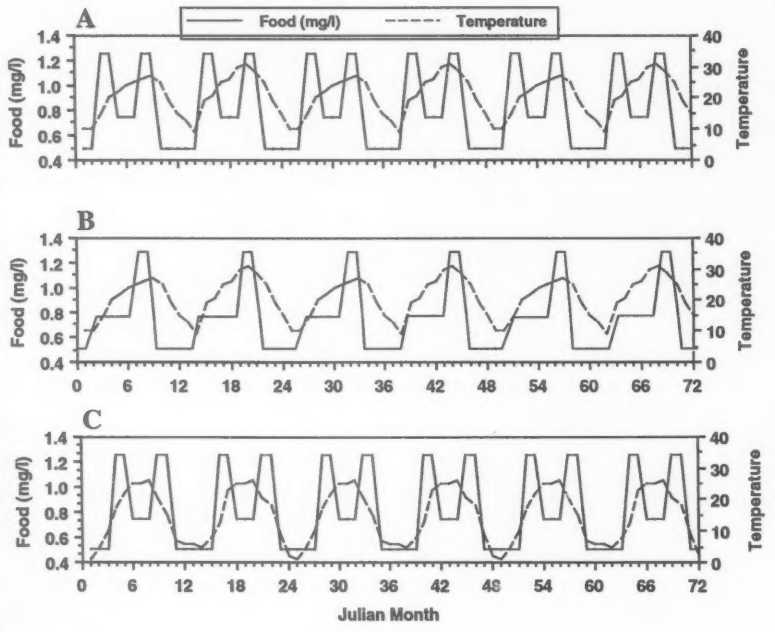

Figure 2

Monthly-averaged time series of temperature and food concentration used as environmental forcing for the oyster population model. (**A**) Temperatures from Galveston Bay (Soniat and Ray, 1985) and plankton biomass for years having blooms in March–April and August–September. (**B**) Temperatures from Galveston Bay and plankton biomass for years having one bloom in August-September. (**C**) Temperatures from Chesapeake Bay with plankton biomass for years having blooms in April-May and September-October. See Table 2 for a description of the food time series used.

Table 2

Summary of environmental and biological conditions used for the oyster *Crassostrea virginica* population simulations. The figure (F) or table (T) displaying the results of each simulation is indicated. All simulations were run using a constant salinity of 24‰, no turbidity, and low flow conditions characteristic of sheltered reefs. An appropriate seasonal time series for temperature was used for Galveston Bay (GB) or Chesapeake Bay (CB) as required (Fig. 2). Three initial densities were used. The numbers per size class for the 10 size classes at these densities are:

low (L):	0	0	0	0	0	0	10	0	0	0
medium (M):	0.1	1.5	5.1	9.2	13.3	5.6	1.4	0.1	0	0
high (H):	490	2240	3637	3217	2502	289	6	0	0	0

A series of standardized food time series was used as depicted in Figure 2. These consisted of 5 winter months at 0.5 $mg \cdot L^{-1}$, 3 or 5 summer months at 0.75 $mg \cdot L^{-1}$ and 2 or 4 bloom months in the spring and/or fall of 1.25 $mg \cdot L^{-1}$. Blooms were of 2-month duration. When two blooms occurred, the two 2-month blooms were separated by 3 summer months. When one 2-month bloom occurred, the bloom was preceded or succeeded by 5 summer months. Table designations are: A/S, August–September bloom; M/A-A/S, March–April and August–September blooms; A/M-S/O, April–May and September–October blooms. Mortality was expressed as a yearly rate: a rate of 99% for instance would have removed 99% of the biomass in one year if no recruitment or growth occurred. For yearly (Y) mortality, this rate was applied for the entire year. For summer (S) mortality, this yearly rate was applied only to the months of April through September. For winter (W) mortality, the yearly rate was applied only to the months of October through March. Recruitment was the fraction of eggs spawned that successfully recruited to the population. In each case, the lowest size class suffering mortality is given (e.g. 5). In every case, all larger size classes also suffered mortality at the same yearly rate: all smaller size classes were unaffected. All simulations began on Julian day 1 (January 1) and were run for 6 years.

Case	Table or figure	Bay	Food time series	Fraction of spawn recruited	Yearly mortality rate	Season of mortality	Size class suffering mortality	Beginning density (day 1)
1	F-3	GB	M/A-A/S	10^{-7}	NA	NA	NA	L
2	F-4,T-2	GB	M/A-A/S	10^{-7}	50%	Y	≥5	H
3	T-2	GB	M/A-A/S	10^{-7}	75%	Y	≥5	H
4	T-2,3,4	GB	M/A-A/S	10^{-7}	90%	Y	≥5	H
5	T-2	GB	M/A-A/S	10^{-7}	99%	Y	≥5	H
6	F-5,T-2,3,4	GB	M/A-A/S	10^{-7}	99.9%	Y	≥5	H
7	T-3	GB	M/A-A/S	10^{-7}	90%	Y	≥3	H
8	F-6	GB	M/A-A/S	10^{-7}	99%	Y	≥3	H
9	F-7,T-3	GB	M/A-A/S	10^{-7}	99.9%	Y	≥3	H
10	F-8	GB	M/A-A/S	10^{-7}	99%	Y	≥1	H
11	F-10e,T-3,4	GB	A/S	10^{-7}	90%	Y	≥5	H
12	F-10f,T-3,4	GB	A/S	10^{-7}	99.9%	Y	≥5	H
13	T-3,4	GB	A/S	10^{-7}	90%	Y	≥3	H
14	F-9,T-3	GB	A/S	10^{-7}	99.9%	Y	≥3	H
15	T-4	GB	A/S	10^{-8}	90%	Y	≥3	H
16	F-10g	GB	A/S	10^{-8}	75%	Y	≥3	H
17	F-10h	GB	A/S	10^{-8}	50%	Y	≥3	H
18	F-10a	GB	A/S	10^{-8}	75%	Y	≥5	H
19	F-10b,T-4	GB	A/S	10^{-8}	90%	Y	≥5	H
20	F-10c	GB	A/S	10^{-8}	99%	Y	≥5	H
21	F-10d,T-4	GB	A/S	10^{-8}	99.9%	Y	≥5	H
22	T-4	GB	M/A-A/S	10^{-8}	99.9%	Y	≥5	H
23	T-4	GB	M/A-A/S	10^{-8}	90%	Y	≥5	H
24	F-11,13,T-5	GB	M/A-A/S	10^{-8}	99.9%	W	≥5	H
25	T-5,6	GB	M/A-A/S	10^{-8}	99%	W	≥5	H
26	T-5	GB	M/A-A/S	10^{-8}	90%	W	≥5	H
27	T-5	GB	M/A-A/S	10^{-8}	90%	S	≥5	H
28	T-5,6	GB	M/A-A/S	10^{-8}	99%	S	≥5	H
29	F-12,13,T-5	GB	M/A-A/S	10^{-8}	99.9%	S	≥5	H
30	T-5,6	GB	M/A-A/S	10^{-8}	90%	S	≥3	H
31	F-14,T-5	GB	M/A-A/S	10^{-8}	99%	S	≥3	H

Table 2 (Continued)

Case	Table or figure	Bay	Food time series	Fraction of spawn recruited	Yearly mortality rate	Season of mortality	Size class suffering mortality	Beginning density (day 1)
32	F-14,T-5	GB	M/A-A/S	10^{-8}	99%	W	≥3	H
33	T-5,6	GB	M/A-A/S	10^{-8}	90%	W	≥3	H
34	F-17,18	GB	M/A-A/S	10^{-8}	99%	S	≥5	M
35	F-17,18	GB	M/A-A/S	10^{-8}	99%	W	≥5	M
36	F-17,18	GB	M/A-A/S	10^{-8}	99%	S	≥6	M
37	F-17,18	GB	M/A-A/S	10^{-8}	99%	W	≥6	M
38	F-17,18	GB	M/A-A/S	10^{-8}	99%	S	≥7	M
39	F-17,18	GB	M/A-A/S	10^{-8}	99%	W	≥7	M
40	T-5	GB	A/M-S/O	10^{-8}	99.9%	W	≥5	H
41	F-15,16,T-5	GB	A/M-S/O	10^{-8}	99.9%	S	≥5	H
42	T-5	GB	A/M-S/O	10^{-8}	90%	W	≥3	H
43	T-5,6	GB	A/M-S/O	10^{-8}	90%	S	≥3	H
44	F-19,20	CB	A/M-S/O	10^{-8}	99%	S	≥5	H
45	T-6	CB	A/M-S/O	10^{-8}	90%	S	≥3	H
46	T-6	CB	M/A-A/S	10^{-8}	90%	S	≥3	H
47	T-6	CB	M/A-A/S	10^{-8}	99%	S	≥5	H
48	F-21,T-6	CB	M/A-A/S	10^{-8}	99%	W	≥5	H
49	T-6	CB	M/A-A/S	10^{-8}	90%	W	≥3	H
50	T-6	CB	A/M-S/O	10^{-8}	90%	W	≥3	H
51	F-20	CB	A/M-S/O	10^{-8}	99%	W	≥5	H

Model solution

The model described by Equation 3 was solved numerically by using an implicit (Crank-Nicolson) tridiagonal solution technique. The time step for model integration was one day. Simulations were run for six years which is sufficient time for the model solutions to adjust so that trends in population levels could be identified in the simulations.

Results

Model initialization

The system of equations given by Equation 3 requires that an initial oyster population size-frequency distribution be specified. The simulations described in the following sections are designed to investigate seasonal and latitudinal mortality effects on oyster population size frequency and stability. Therefore, it proved useful to begin the simulations with a size-frequency distribution representative of a crowded population; that is, one suffering little mortality. In this way, changes in the simulated oyster populations will be the result of mortality only. Also, using the same initial population distribution allows for comparison between simulations throughout the entire 6-year simulated time period.

The initial oyster size-frequency distribution was obtained from a simulation that was started with 10 individuals·m^{-2} in size-class 7 on 1 January. The food time series for this simulation contained two phytoplankton blooms of two months duration (March/April, August/September) with intervening summer months and winter months as detailed in Figure 2. Dense bivalve populations can deplete the surrounding water column of food (Fréchette et al., 1991). We used Lund's (1957) low flow conditions to simulate the effect of oyster density on food supply. Such conditions might be typical of an enclosed or sheltered reef (Powell et al., 1987). No mortality was allowed in any size class.

The time development of the simulated population (Fig. 3A) shows that the mean size of the population slowly declines from size class 7 to size class 3, as population density increases about 3 orders of magnitude. These trends are characteristic of a crowded population: high population density and reduced adult size. Reproduction continues throughout the simulation (Fig. 3, A and C) with a strong fall spawning pulse (Fig. 3B) occurring in response to the fall phytoplankton bloom (Hofmann et al., 1992). Therefore, food limitation is not sufficient to cap population growth; however, the rate of population increase has dramatically declined over the 6-year simulation. It is the population size-frequency distribution at the end of the 6-year simulation (Fig. 3D) that is used to initialize the mortality simulations described in the following sections.

Effect of continuous mortality

The first set of simulations considered the oyster population that would be produced in Galveston Bay, Texas, when continuous mortality (mortality throughout the year) is imposed on size classes 5 and larger. Oyster size class 5 approximates the 2.5 in size limit often desired by the oyster fishery as opposed to the standard size limit of 3 now enforced in most areas. Over this series of simulations, the rate of yearly mortality was varied from 50% to 99.9%, the two extremes being depicted in Figures 4 and 5. For an oyster population with no recruitment, these rates would result in a reduction of the population by 0.5 and 0.999, respectively, in one year. In our simulations, where recruitment and mortality constantly change population abundance, a 50% mortality rate does not necessarily result in the loss of one-half of the individuals in the population in one year.

Over this series of simulations (Table 3, Figs. 4 and 5), as mortality rate increases from 50% to 99.9%, density declines by about 80% and the size-frequency distribution shifts slightly to lower size classes. Population reproductive effort declines as the number of adults declines, but individual reproductive effort increases. At the lower mortality rate, spawning is primarily confined to a single strong pulse in the fall. At the higher mortality rate, spawning effort is distributed between a spring and fall spawning peak; the fall peak is stronger and extends over a longer time (Fig. 4A vs. Fig. 5A).

Moreover, spawning is higher in every other year (Figs. 4C and 5C). In the temperature time series for Galveston Bay (Fig.

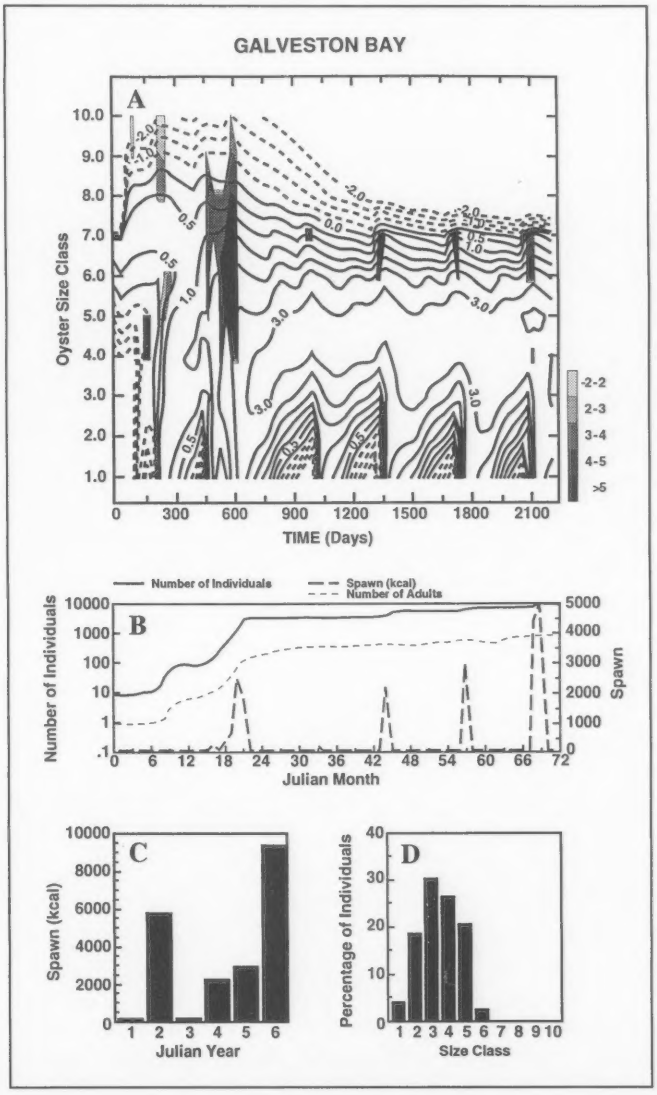

Figure 3

Simulated time development and population distribution of a Galveston Bay *Crassostrea virginica* population with no mortality, allowing the population to approach the carrying capacity of the environment. (**A**) The number of individuals per size class and reproductive effort per size class. Values are plotted opposite the size class designation, not halfway between; hence all individuals in size class 7 are opposite the grid mark labeled 7 on day 1 of this simulation. Isolines, for number of individuals, are the logarithms of the number of oysters ($\log_{10}$N). Hence, the zero contour corresponds to one individual. Population concentrations less than this are indicated by dashed lines; population concentrations greater than this by solid lines. Shading for the amount of reproductive effort (spawn) represents the logarithm of cal ($\log_{10}$cal) with the darkest shades corresponding to highest values. Contour interval is 0.5 for the number of individuals and 1.0 for reproductive effort. (**B**) Monthly-averaged values of the number of individuals, the number of adults (j=4, 10), and the monthly reproductive effort in kcal for the 6-year simulation. Values can be converted into joules by multiplying by 4.16 $j \cdot cal^{-1}$; into biomass by using 6100 cal·g dry wt^{-1}; and into the equivalent number of fully developed eggs by 13 ng·egg^{-1} $\times 6.133 \times 10^{-6}$ cal·ng^{-1}. (**C**) The yearly reproductive effort (number of kcal spawned). (**D**) The final size class distribution in the population at day 2,160. Additional data and explanation in Table 2, case 1.

2A), one winter is colder and one summer warmer than the other. As a result, the first year in each pair is characterized by lower reproductive effort as decreased temperatures reduce filtration and ingestion rate and switch net production towards somatic growth. Warmer temperatures the second year result in a larger reproductive effort.

Within these simulated oyster populations, a complex interaction exists between population density, size frequency, and mortality rate. Increasing mortality removes individuals, thereby increasing the available food supply for the remaining individuals. Increased food supply results in increased spawning effort, which then increases population density. This in turn then gives reduced spawning effort. This feedback results in potential population equilibria of different densities and size frequencies for each level of mortality (Table 3). Even at 99.9% yearly mortality, however, the population sustains itself at a fairly dense level. Of more significance, each population approaches an equilibrium or nearly so, such that recruitment balances mortality over this range of mortality rates. Year-to-year shifts in population size over the 6-year simulation show neither continually strong declines nor increases in population density for any of the mortality rates.

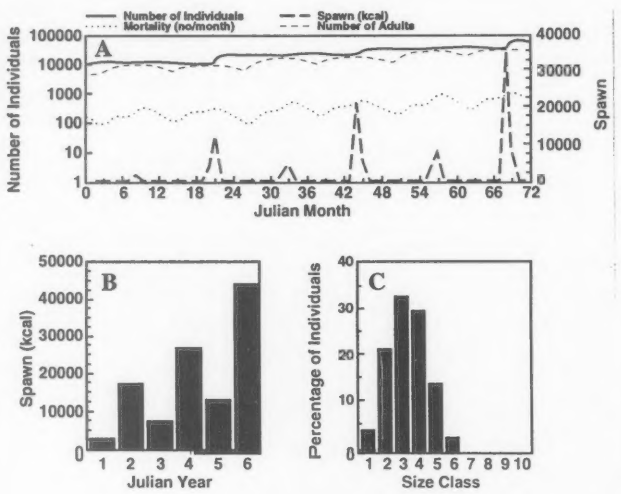

Figure 4

Simulated time development and population distribution of a Galveston Bay *Crassostrea virginica* population exposed to a continuous mortality rate of 50% per year on size classes 5 and larger. (**A**) Monthly averaged values of the number of individuals, the number of adults (j=4, 10), and the monthly reproductive effort in kcal for the 6-year simulation. (**B**) The yearly reproductive effort (number of kcal spawned). (**C**) The final size class distribution in the population at day 2,160. Further explanation in Figure 3 and Table 2, case 2.

In Figures 6–8, we compare the time-development of oyster populations exposed to similar overall mortality levels, but in which mortality extends into lower size classes than in Figures 4 and 5. In these simulations, mortality was imposed either on all adult sizes and the larger juveniles (Figs. 6 and 7) or on all size classes (Fig. 8). Figures 7 and 5 differ only in the size classes exposed to mortality (5 and larger vs. 3 and larger) as do Figures 6 and 8 (3 and larger vs. 1 and larger). As high (90–99.9%) yearly mortality rates are imposed on smaller oyster size classes (Figs. 6–8), the population becomes more susceptible to significant population declines. For example, a 99.9% yearly mortality rate had little effect when mortality was restricted to size classes 5 and larger (Fig. 5), but results in a population crash if size classes 3 and larger are similarly exposed (Fig. 7). Many more individuals die before reproducing in the latter case than in the former. A mortality rate of 99.9% is required for a population crash at size classes 3 and larger (Fig. 7), but only 99% at size class 1 and larger (Fig. 8). As mortality extends into the smaller size classes, the mortality rate that the population can sustain decreases. We note that, although these mortality rates seem high, they are well within the typical range for juvenile survivorship in bivalve communities (e.g. Powell et al., 1984; Cummins et al., 1986).

Table 3

A comparison of final density in simulated *Crassostrea virginica* populations after 6 years and total reproductive effort in year 6 at various rates of yearly mortality. Additional details in Table 2.

Case	Mortality rate (%)	Ending density (day 2160) (ind·m^{-2})	Total reproductive effort in year 6 (kcal·m^{-2})
2	50	50,748	43,158
3	75	16,966	15,093
4	90	33,112	46,426
5	99	12,295	14,211
6	99.9	16,565	19,896

Furthermore, as mortality extends into lower size classes, the size-frequency distribution shifts to larger sizes (Figs. 6C, 7C, 8C). The effect is significant because only in cases where mortality is high do oysters grow large enough to reach marketable size for the oyster fishery (size class 6 and larger). Removal of smaller individuals increases the available food supply for the survivors, thereby allowing some to attain market-size.

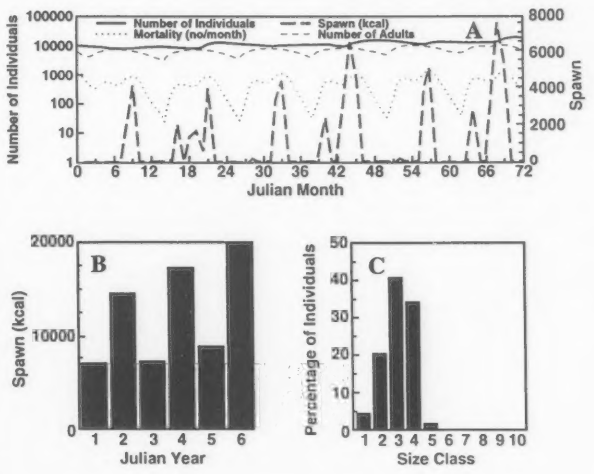

Figure 5

Simulated time development and population distribution of a Galveston Bay *Crassostrea virginica* population exposed to a continuous mortality rate of 99.9% per year on size classes 5 and larger. (**A**) Monthly-averaged values of the number of individuals, the number of adults (j=4, 10), and the monthly reproductive effort in kcal for the 6-year simulation. (**B**) The yearly reproductive effort (number of kcal spawned). (**C**) The final size class distribution in the population at day 2,160. Further explanation in Figure 2 and Table 2, case 6.

Effect of food supply

Interactions between food supply and mortality rate are potentially important in determining population density and size-frequency distribution. In years in which a spring bloom is reduced or fails to occur (Fig. 2B), the available food spectrum is shifted in time and total food supply for the year is reduced. In Figure 9, we examine the effect of the failure of the spring bloom. Figure 9 can be compared directly with Figure 7, the two differing only in food supply. A failed spring bloom shifts the food spectrum as well as decreasing the total food available over the year.

Hofmann et al. (1992) showed that the food supply time series used for Figure 9 results in a strong fall spawning pulse. With an imposed yearly mortality of 99.9% in size classes 3 and larger and no spring bloom, the simulated oyster populations (Fig. 9) are not substantially different from those shown in Figures 6–8. However the simulated oyster population shown in Figure 9 is characterized by a stronger fall spawning pulse, as expected, whereas the previous simulations generally had spawning more evenly distributed over the spawning season. The population still reaches a stable distribution and the size-frequency distribution includes individuals in the larger size classes (Fig. 9C). Thus, continuous yearly mortality overrides the effects of variations in the timing of food supply.

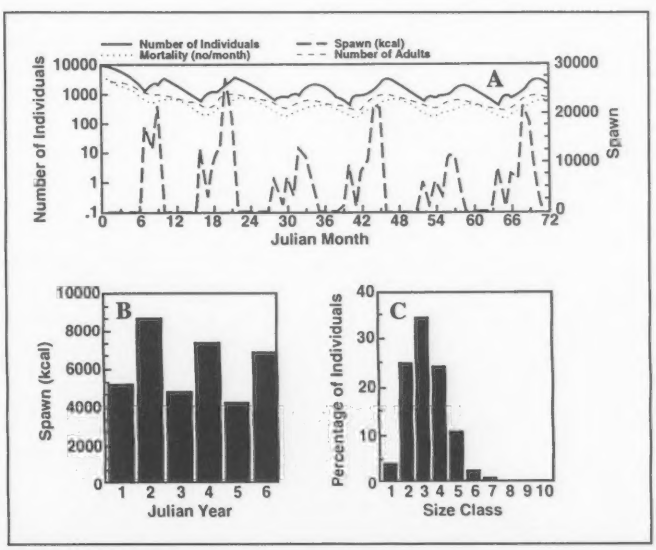

Figure 6

Simulated time development and population distribution of a Galveston Bay *Crassostrea virginica* population exposed to a continuous mortality rate of 99% per year restricted to size classes 3 and larger. (**A**) Monthly-averaged values of the number of individuals, the number of adults (j=4, 10), and the monthly reproductive effort in kcal for the 6-year simulation. (**B**) The yearly reproductive effort (number of kcal spawned). (**C**) The final size class distribution in the population at day 2,160. Further information in Figure 3 and Table 2, case 8.

However, in this and other simulations, the population density is consistently higher after six years with the lower, more restricted food supply associated with the missing spring bloom (e.g. Fig. 7 vs. 9; Table 4). The effect occurs regardless of the size-class distribution of mortality or the mortality rate. The initial surmise that more food should result in higher densities is not confirmed. Reproductive effort is higher at the higher food supply only in the first year (Fig. 7 vs. 9) and declines more rapidly thereafter as population density declines. Initially this would appear to be counterintuitive; more food should result in higher population densities and greater reproductive effort. However, increased food in the spring increases growth rate so that more oysters grow more rapidly into size classes suffering mortality. As a result, the number of adults and population reproductive potential declines. This results in a lower population density. The model simulations indicate that oyster population abundance is the result of a complicated interplay between the timing of food supply, reproductive effort, and mortality.

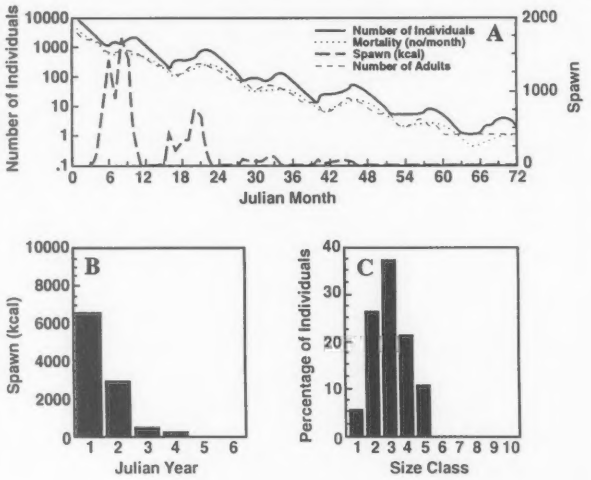

Figure 7

Simulated time development and population distribution of a Galveston Bay *Crassostrea virginica* population exposed to a continuous mortality rate of 99.9% restricted to size classes 3 and larger. (**A**) Monthly-averaged values of the number of individuals, the number of adults (j=4, 10), and the monthly reproductive effort in kcal for the 6-year simulation. (**B**) The yearly reproductive effort (number of kcal spawned). (**C**) The final size class distribution in the population at day 2,160. Further information in Figure 3 and Table 2, case 9.

Lowered recruitment success

An additional source of mortality for oyster populations is through decreased survivorship of the planktonic larvae (Table 5, Fig. 10). Lower larval survivorship results in decreased recruitment success and lower population densities, as expected. However, loss of the spring bloom enhances oyster population density as before (Table 5). Nevertheless, a reduction in recruitment success, when combined with mortality on the post-settlement population, results in populations that are less resistant to population crashes. For example, a tenfold reduction in recruitment success in a population exposed to a 75% mortality rate in size classes 3 and larger produces the effect observed for a mortality rate of 99.9% with an order of magnitude higher recruitment success.

One additional important concept arises from this series of simulations. Simulations that included high recruitment success and various mortality rates produced final size-frequency distributions similar to those shown in Fig. 10, E and F. Few individuals are found in size classes 5 and larger. The legal size for the oyster fishery is typically size classes 6 and larger. No fishery could exist under these conditions. High population density produces stunted individuals. A reduction in recruitment success over a range of mortality rates (Fig. 10, A–D) gives size-frequency distributions shifted towards the larger size classes. In fact, more market-sized animals exist in these populations than in the ones shown in Figure 10, E and F. Shifting mortality to lower size classes results in even more market-size individuals (Fig. 10, G–H). A successful fishery requires some degree of mortality, including juvenile mortality.

Effect of seasonal mortality

The commercial oyster fishery is typically confined to a winter season. In some cases, a restricted summer season is also allowed. Agents of natural mortality, like *Perkinsus marinus* and *Thais haemastoma*, typically extract a greater toll during the summer. The effect of mortality restricted to the summer and to the winter is illustrated in Figures 11 and 12, respectively, and in Table 6. For this series of simulations, we define winter as the months of October through March and summer as the months of April through September. Thus each simulated oyster population has the same number

of days (180) with and without mortality. Regardless of the mortality rate, when mortality is restricted to size classes 5 and larger, populations suffer a greater reduction in density when mortality is restricted to the summer (compare Fig. 11B and 12B; Table 6). Summer mortality depresses reproductive effort and depressed reproductive effort, continued over time, results in lower population density.

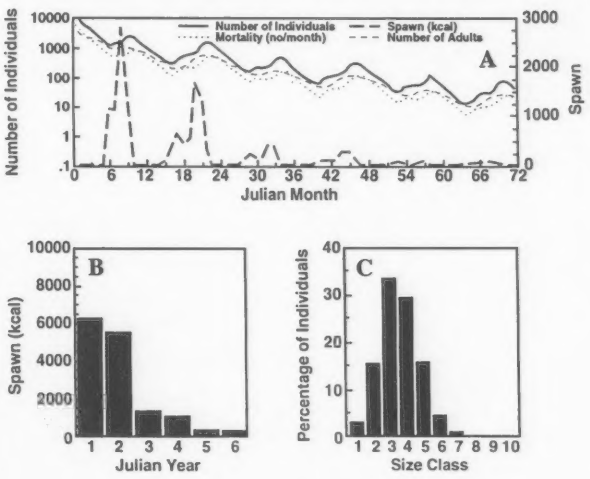

Figure 8

Simulated time development and population distribution of a Galveston Bay *Crassostrea virginica* population exposed to a continuous mortality rate of 99% imposed on all size classes. (**A**) Monthly averaged values of the number of individuals, the number of adults (j=4, 10), and the monthly reproductive effort in kcal for the 6-year simulation. (**B**) The yearly reproductive effort (number of kcal spawned). (**C**) The final size class distribution in the population at day 2,160. Further information in Figure 3 and Table 2, case 10.

Examining the population size-frequency distribution over the year for simulated oyster populations suffering winter (Fig. 13, A and B) and summer (Fig. 13, C and D) mortality suggests an explanation for the more detrimental effect of summer mortality on population density. Figure 13 shows snapshots of the population's size-frequency distribution at various times during the year. When mortality is imposed only during the winter, the population size-frequency distribution shifts to larger size classes in the summer in response to increased growth rate produced by warmer temperatures. Therefore, during the fall spawning season the population is dominated by the larger size classes that account for much of the reproductive effort. Winter mortality then shifts the population size-frequency distribution back to smaller individuals (Fig. 13B) and the cycle begins again. Hence, winter mortality allows the population to replace, during the next summer and fall, the individuals that are lost.

In contrast, restricting mortality to summer months produces a population size-frequency distribution that varies little over a year (Fig. 13, C and D). The variation that does occur is a shift towards smaller individuals in the summer. For example, more individuals are found in size classes 6 and 7 in September in populations that experi-

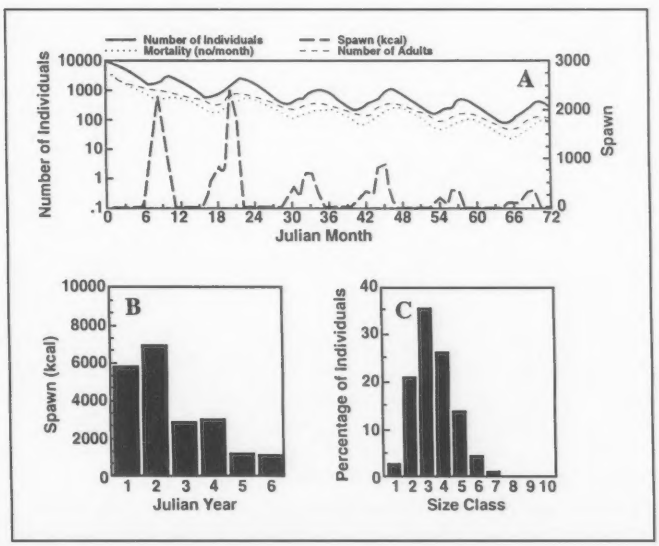

Figure 9

Simulated time development and population distribution of a Galveston Bay *Crassostrea virginica* population exposed to a continuous mortality rate of 99.9% restricted to size classes 3 and larger and in which the food time series contained only the fall bloom. The case is comparable to Figure 7 in which two blooms occurred. (**A**) Monthly averaged values of the number of individuals, the number of adults (j=4, 10), and the monthly reproductive effort in kcal for the 6-year simulation. (**B**) The yearly reproductive effort (number of kcal spawned). (**C**) The final size class distribution in the population at day 2,160. Further information in Figure 3 and Table 2, case 14.

ence winter (Fig. 13B) rather than summer (Fig. 13D) mortality. The shift to smaller individuals in populations with summer mortality results in lowered reproductive effort. Hence, lost individuals are not replaced in the fall and winter and the population declines.

As mortality extends into the juvenile size classes, the difference in winter and summer mortality should decrease and the seasonal shift in size-frequency as a function of mortality should disappear because a greater fraction of the total mortality occurs in individuals contributing relatively little to the population's spawning potential. This is confirmed by the model (Fig. 14, Table 6). Interestingly, although the seasonal variations in size-frequency distributions are muted, changes in size-frequency distribution over the year are still greater for populations that experience winter mortality. These populations show a slight shift to smaller size classes in the winter.

To examine the effect of varying food supply, we placed the spring and fall blooms one month later in the year (April/May and August/September) and then compared the time development of oyster populations suffering winter or summer mortality with those previously described when the blooms occurred one month earlier (Tables 6 and 7). For populations experiencing winter mortality, delaying the spring and fall blooms by one month (Fig. 2C) does not significantly change the simulated populations from those obtained for the earlier blooms, even when mortality extends to the juvenile size classes (3 and larger). However, for summer mortality, delaying the blooms by one month dramatically improves the population's ability to sustain itself (Fig. 12 vs. Fig. 15; Table 5). Moving the spring and fall blooms one month later in the year produces 1) a strong spring spawning pulse as well as the fall pulse and 2) a shift in the population size-frequency distribution toward the larger size classes, although yearly changes in the size-frequency distribution are still characteristic of summer mortality (Fig. 16 vs. 13). As a result, spawning effort increases under the delayed-bloom condition as fall spawning extends beyond the summer season of mortality. Accordingly, variation in the timing of food supply, under certain circumstances, can be important in the success of an oyster population, particularly in cases where adult mortality is restricted to the summer months.

Table 4

A comparison of final density in simulated *Crassostrea virginica* populations after six years and total reproductive effort in year 6 with and without a spring phytoplankton bloom. Additional details in Table 2.

Case	Spring bloom?	Ending density (day 2,160) ($ind \cdot m^{-2}$)	Total reproductive effort in year 6 ($kcal \cdot m^{-2}$)
9	Yes	2	12
14	No	248	1,003
7	Yes	2,602	7,787
13	No	2,788	7,398
6	Yes	16,565	19,896
12	No	32,513	36,569
4	Yes	33,112	46,426
11	No	42,758	39,217

Table 5

A comparison of final density in simulated *Crassostrea virginica* populations after 6 years and total reproductive effort in year 6 at various rates of recruitment, with and without a spring phytoplankton bloom. Additional details in Table 2.

Case	Mortality rate	Recruitment	Ending density (day 2,160) ($ind \cdot m^{-2}$)	Total reproductive effort in year 6 ($kcal \cdot m^{-2}$)
		No spring bloom		
13	90%	10^{-7}	2,788	7,398
15		10^{-8}	2	26
11	90%	10^{-7}	42,758	39,217
19		10^{-8}	1,067	12,480
12	99.9%	10^{-7}	32,513	36,569
21		10^{-8}	11	236
		Spring bloom		
6	99.9%	10^{-7}	16,565	19,896
22		10^{-8}	1	40
4	90%	10^{-7}	33,112	46,426
23		10^{-8}	328	4,935

Size limits for the fishery

Three size limits have been used or considered as the legal limit for market-size oysters: 2.5 in, 3.0 in,

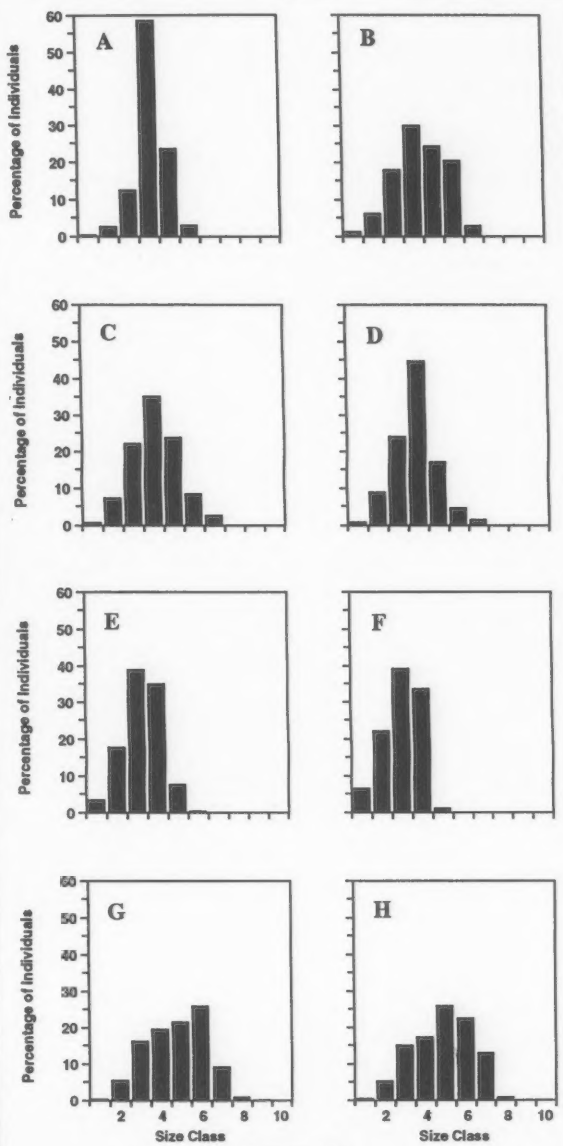

Figure 10

A comparison of the final size-frequency distributions (day 2,160) in simulated *Crassostrea virginica* populations exposed to a Galveston Bay temperature time series following 6 years of recruitment, growth, and mortality under varying degrees of recruitment and mortality. In each case, size classes 5 and larger were exposed to continuous mortality at a yearly rate of (**H**) 50%, (**A** and **G**) 75%, (**B**) 90%, (**C** and **E**) 99%, (**D** and **F**) 99.9%. Recruitment was tenfold higher (or larval mortality tenfold less severe) in E and F. Mortality rates extend down into size classes 3 and 4 in G and H. Further information in Figure 3 and Table 2, cases 11, 12, 16–21.

and 3.5 in. These correspond to size classes 5, 6, and 7 in the model. The simulations used to test the effect of these size limits were initialized with a population size-frequency distribution having a component in the larger size classes (Fig. 12). With a yearly mortality rate of 99%, oyster populations increase when mortality is restricted to size class 7 and larger (3.5 in) but decline rapidly if mortality includes size classes 5 and 6 (2.5 in) (Fig. 17). Hence, a change in the legal size limit may have a substantial effect on the fishery and on the oyster population as a whole. Of course, the specific results would vary according to the biomass-to-length conversion used.

As the fishing season typically is confined to the winter, we examined the effect of changing size limits when mortality was restricted to the winter or to the summer months (Fig. 17). Overall, the same pattern persisted in both seasons. Populations declined more under the smaller size limits. However, several significant differences are also observed:

1 Populations in which mortality was restricted to the summer had a stronger spring spawning pulse; most spawning occurred in the midsummer and early fall in populations suffering only winter mortality.
2 Reproductive effort and population density was consistently higher in populations suffering winter mortality (Fig. 18, C, D, and E), density by a factor of 2 to 4, reproduction by a factor of 2 to 8; increased reproductive effort occurred both because the number of adults increased and because those adults spawned more with the result that reproduction was more than proportionately higher.
3 The size-frequency distribution was shifted toward the smaller size classes in populations having winter mortality (Fig. 18, A and B) but had little impact on the size-frequency distribution with summer mortality.

Overall, the number of market-size oysters available at the end of the simulation was higher at the larger size limits (Fig. 18F). As a result, a greater potential yield was available to the fishery at the larger size limits. One reason for the higher yield available to the fishery at the larger size limit (≥3.5 in) is the shift in size-frequency distribution toward larger size classes with adult mortality. A second reason is the protection of a larger portion of the reproductive population. However, if unchecked, the continually growing population in the last set of simulations, where

Table 6

A comparison of final density in simulated *Crassostrea virginica* populations after six years and total reproductive effort in year 6 with mortality restricted to the winter or the summer season and with the spring and fall phytoplankton blooms early in the year or one month later. Additional details in Table 2.

Case	Season	Ending density (day 2,160) ($ind \cdot m^{-2}$)		Total reproductive effort in year 6 ($kcal \cdot m^{-2}$)	
	Mortality: ≥5	Bloom: Early	Late	Bloom: Early	Late
24, 40	Winter	287	220	5,168	4,344
29, 41	Summer	36	500	606	6,904
25	Winter	467		7,365	
28	Summer	253		3,586	
26	Winter	1,400		4,529	
27	Summer	1,333		13,107	
	Mortality: ≥3				
33, 42	Winter	403	595	5,890	8,664
30, 43	Summer	623	692	7,766	8,829
32	Winter	5		111	
31	Summer	5		91	

Table 7

A comparison of final density in simulated *Crassostrea virginica* populations after six years and total reproductive effort in year 6 with mortality restricted to the winter or the summer season and with the spring and fall phytoplankton blooms early in the year or one month later, in Chesapeake Bay and Galveston Bay. Additional details in Table 2.

Case	Bay	Ending density (day 2,160) ($ind \cdot m^{-2}$)		Total reproductive effort in year 6 ($kcal \cdot m^{-2}$)	
	Mortality: ≥5	Bloom: Early	Late	Bloom: Early	Late
	Winter				
48	Chesapeake	394		3,924	
25	Galveston	467		7,365	
	Summer				
47	Chesapeake	102		644	
28	Galveston	253		3,586	
	Mortality: ≥3				
	Summer				
46, 45	Chesapeake	72	85	328	542
30, 43	Galveston	623	692	7,766	8,829
	Winter				
49, 50	Chesapeake	122	84	832	606
33, 42	Galveston	403	595	5,890	8,664

mortality was restricted to size class 7 and larger (≥3.5 in), would eventually negate both effects as population density increased.

Effect of latitude on population stability

In Figure 19 and Table 7, we compare the time-development of oyster populations under the temperature conditions of Chesapeake Bay with those under the temperature conditions of Galveston Bay (Fig. 15). In comparison with the Galveston Bay populations, those in Chesapeake Bay are characterized by densities 2 to 5 times lower, reproductive efforts as much as a factor of 10 lower, size-frequency distributions considerably shifted toward the large size classes (Figs. 20 and 21), and discrete spo-

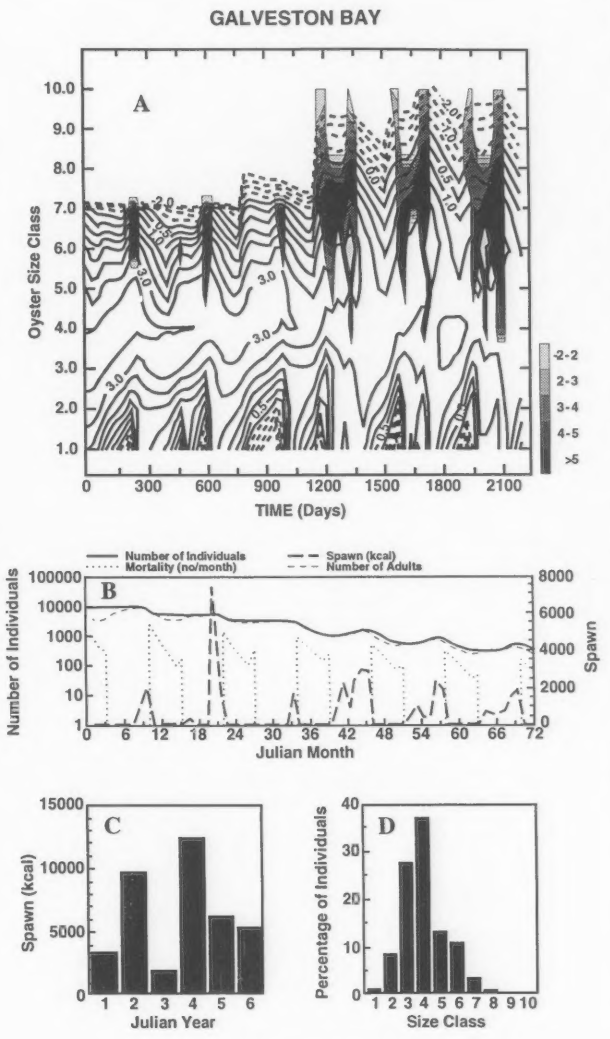

Figure 11

Simulated time development and population distribution of a Galveston Bay *Crassostrea virginica* population exposed to a continuous mortality rate of 99.9% restricted to size classes 5 and larger and in which mortality occurred only during the winter. Compare Figure 12. (**A**) The number of individuals per size class and reproductive effort per size class. Isolines, for number of individuals, are the logarithms of the number of oysters ($\log_{10}$N). Shading for the amount of reproductive effort (spawn) represents the logarithm of cal ($\log_{10}$cal). (**B**) Monthly averaged values of the number of individuals, the number of adults (j=4, 10), and the monthly reproductive effort in kcal for the 6-year simulation. (**C**) The yearly reproductive effort (number of kcal spawned). (**D**) The final size class distribution in the population at day 2,160. Further information in Figure 3 and Table 2, case 24.

radic spawning pulses typically strongest in midsummer. Like Galveston Bay populations, a shift in the timing of the spring and fall blooms has little effect on the seasonal changes in size-frequency distribution (Fig. 21) but considerable effect on the resulting population density in some cases. Populations experiencing winter mortality are more affected by variations in the timing of the food supply than populations experiencing summer mortality. Unlike Galveston Bay populations, populations experiencing summer mortality have lower population densities than populations experiencing winter mortality only when the blooms occur in March/April and August/September. Delaying the blooms by one month results in little variation between populations experiencing summer and winter mortality. The most significant factor producing differences between the Galveston Bay and Chesapeake Bay populations is the cooler temperatures that characterize Chesapeake Bay. This results in reduced reproductive effort with more net production going to support somatic tissue growth (Table 7).

Discussion

The importance of mortality

Unlike an oyster population, an oyster fishery cannot persist without large adult individuals. One of the consistent messages of this modeling exercise is the requirement of mortality for the population to produce larger, market-size individuals. Either adult or juvenile mortality will suffice, as both juveniles and adults compete for food (Powell et al., 1987). Low rates of mortality result in crowding, food limitation, and a stunted population. As mortality extends into the juvenile size classes, and finally into the larval stages (modeled as a reduction in recruitment, reduced reproductive effort, or produced by the colder temperatures of Chesapeake Bay) the population on the average becomes skewed more and more towards the larger adult size classes. Frequently, this proportional shift was sufficient to result in an increase in adult density despite an overall lower population density. An even higher rate of mortality reversed this trend; the popula-

tion size-frequency shifted again towards smaller size classes as adult individuals were rapidly removed from the population. Clearly, for a successful fishery, a delicate balance exists between sufficient mortality to permit the fishery to exist and too much mortality which will reduce the harvestable yield.

Food supply is a complicating factor. Increased food supply will not always result in increased population density or increased harvestable yield. The timing of the food supply interacts in subtle ways with the timing and intensity of mortality, sometimes producing higher densities and sometimes lower ones. The simulations show that the effect of variations in food supply is complex; no simple rules apply and a number of feedback mechanisms exist. In one case, for example, lower population density resulted from increased food supply because increased growth permitted more oysters to enter the size classes that were exposed to mortality, thereby resulting in a population that declined. In another case, a one-month change in the timing of the spring and fall blooms changed population density by a factor of 2 at the same mortality rate. In other cases, little impact occurred in the population despite, for example, the complete failure of the spring bloom.

Population stability and population crashes

The stability of oyster populations is sensitive to several factors, including the timing and intensity of mortality, latitude, and food supply. (We use the term stable in the sense of Underwood [1989] for populations able to recover quickly from perturbation. The terms elasticity and resiliency might also be used.) Increased mortality reduced population density in every comparison. Oftentimes, a relatively stable equilibrium occurred as recruitment balanced mortality over the long term. In all cases, however, mortality rates sufficient to destabilize this equilibrium could be found and a population decline resulted. When mortality extended over a wider range of size classes or affected larval survivorship, population destabilization occurred more easily. In the former case, more oysters

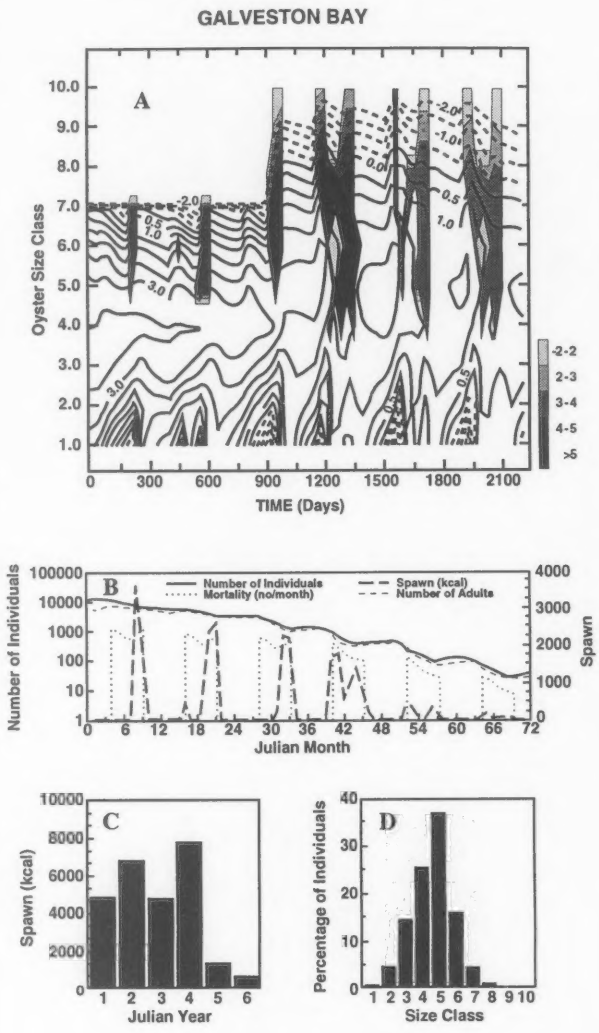

Figure 12

Simulated time development and population distribution of a Galveston Bay *Crassostrea virginica* population exposed to a continuous mortality rate of 99.9% restricted to size classes 5 and larger and in which mortality occurred only during the summer. Compare Figure 11. (**A**) The number of individuals per size class and reproductive effort per size class. Isolines, for number of individuals, are the logarithms of the number of oysters ($\log_{10}$N). Shading for the amount of reproductive effort (spawn) represents the logarithm of cal ($\log_{10}$cal). (**B**) Monthly averaged values of the number of individuals, the number of adults (j=4, 10), and the monthly reproductive effort in kcal for the 6-year simulation. (**C**) The yearly reproductive effort (number of kcal spawned). (**D**) The final size class distribution in the population at day 2,160. Further information in Figure 2 and Table 2, case 29.

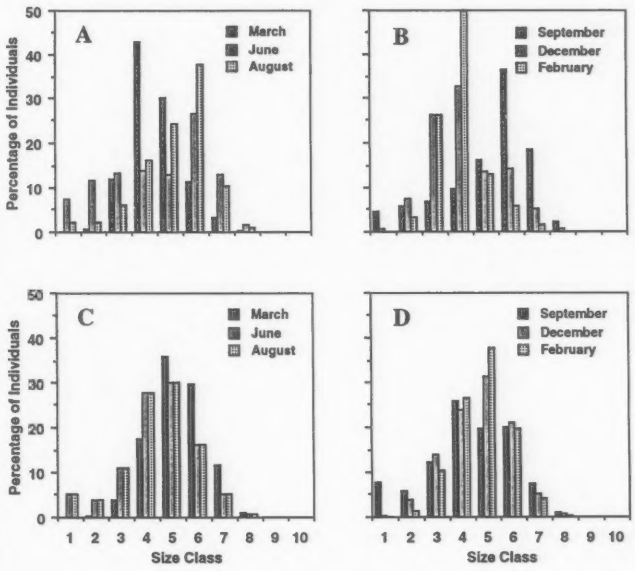

Figure 13

A comparison of the changes in size-frequency distribution through the year in the two *Crassostrea virginica* populations depicted in Figures 11 and 12. (**A** and **B**) a population suffering winter mortality; (**C** and **D**) a population suffering summer mortality. Mortality in both cases was restricted to size classes 5 and larger.

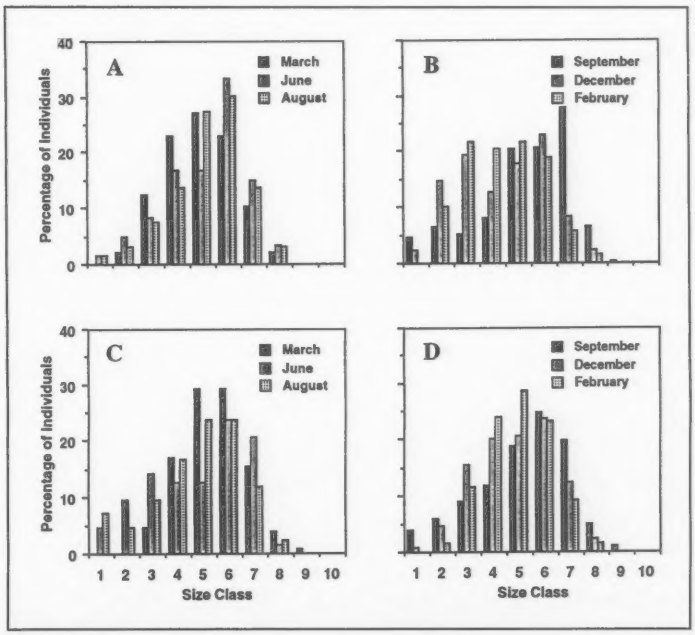

were exposed to mortality. In the latter case, lowered recruitment no longer balanced the higher rates of mortality.

In cases where mortality was imposed for time periods of less than one year, mortality restricted to the six summer months (April–September) nearly always resulted in decreased population density compared to mortality restricted to the winter months. Rarely did the two yield similar results. Never did summer mortality have a lesser impact. The effect was noted at different latitudes, in populations having mortality restricted to a variety of differing size classes, and in populations varying in larval survivorship. However, adult mortality was required. Extending mortality into the juvenile size classes minimized the effect.

Nearly all reports of population crashes in oyster populations result from adult summer mortality, recruitment failure, or floods. Most predators and parasites are most effective in the summer. The series of simulations presented here suggests that the explanation for the importance of adult summer mortality does not necessarily reside in the fact that the most significant agents of adult mortality (except the fishery) operate most effectively in the summer. Although this may well be true, the oyster itself would appear to be more susceptible to mortality in the summer. That is, a greater chance of population crashes in the summer may be physiologically preordained. One potentially important mechanism causing this increased susceptibility is the temperature control on the partitioning of somatic tissue and reproductive tissue in the winter, spring, and summer. Fewer individuals are present in the adult size

Figure 14

A comparison of the changes in size-frequency distribution through the year in simulated *Crassostrea virginica* populations having size classes 3 and larger exposed to mortality. Compare to Figure 13 where mortality was restricted to size classes 5 and larger. (**A** and **B**) mortality restricted to the winter; (**C** and **D**) mortality restricted to the summer. More information in Figure 3 and Table 2, cases 31 and 32.

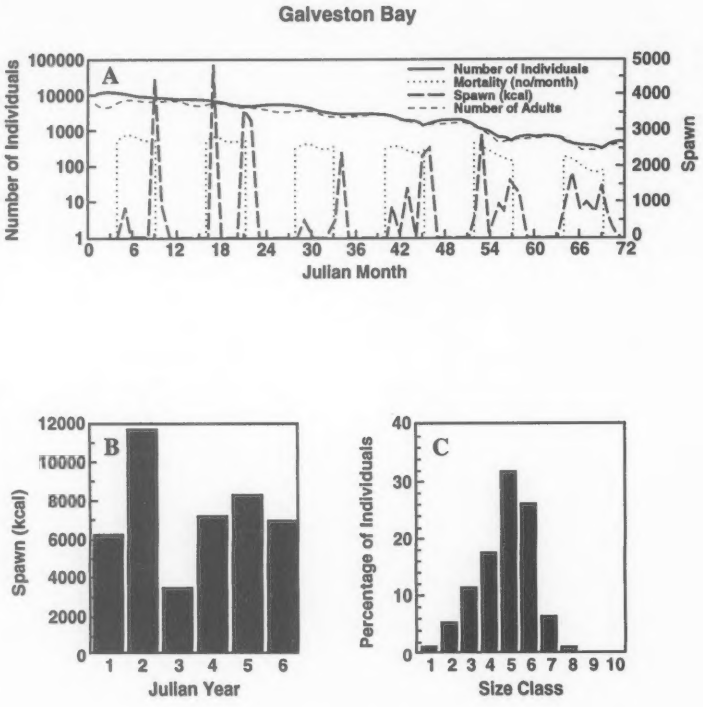

Figure 15

Simulated time development and population distribution of a Galveston Bay *Crassostrea virginica* population exposed to summer mortality at a yearly rate of 99.9% restricted to size classes 5 and larger and in which the food time series contained blooms in April/May and September/October. Figure 12 contains comparable results in which the food time series contained two blooms one month earlier. For additional information, see Figure 3 and Table 2, case 41.

classes in the winter, hence losses are minimized. Juveniles grow rapidly to adulthood in the spring and spawn in the summer. As a result, reproductive effort is higher and population stability is enhanced when mortality is restricted to the winter.

One of the interesting observations from the simulations is the consistent difference in the seasonal shifts in size-frequency distribution exhibited by populations suffering adult summer or winter mortality. Populations impacted most significantly by summer mortality had relatively stable size-frequency distributions over the year. Winter mortality produced strong seasonal shifts in the size-frequency distribution. The results suggest that seasonal shifts in size-frequency distributions might provide a useful measure of the relative importance of summer and winter mortality and of adult mortality in oyster populations. For example, the seasonal cycle in market-sized individuals on some Galveston Bay reefs (e.g. Figure 2.1 in Quast et al., 1988) is similar to the seasonal shifts observed in simulated populations in which mortality was restricted to the winter months, suggesting that the fishery might be an important source of mortality in these populations.

Latitudinal gradient in stability

Although not conclusive, the literature reviewed earlier suggests a latitudinal gradient may exist in oyster population stability. Populations at higher latitudes may be more susceptible to population crashes. The Galveston Bay and Chesapeake Bay simulations support this possibility. Simulated popu-

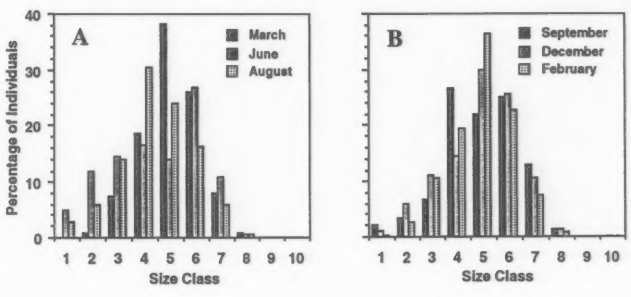

Figure 16

The seasonal changes in size-frequency distribution of the *Crassostrea virginica* population depicted in Figure 15. Figure 13 gives comparable results for the comparable simulation depicted in Figure 12.

lations in Chesapeake Bay were more susceptible to population crashes than those in Galveston Bay. Simulated populations in Galveston Bay consistently had higher population densities after 6 years. Reproductive effort was higher because more of the year occurred within the temperature range conducive to spawning. Higher reproductive effort balanced a larger rate of mortality; hence mortality rates had to be substantially higher in Galveston Bay to effect a population crash. Although not simulated, recovery rates should have been faster as well. Like the distinction between winter and summer mortality, this latitudinal gradient in population stability would appear to result from the basic physiology of the oyster. The fundamental physiological mechanisms associated with reproduction and the division of net production into somatic and reproductive growth would appear to be responsible.

Implications for fisheries management

The methods for managing the *C. virginica* fishery are generally limited to three somewhat interconnected decisions: 1) what size limit should be set; 2) what season should be allowed; and 3) what population density should trigger season closure? The setting of size limits may depend on biological and economic issues. Only biological issues will be considered here. Two aspects of oyster physiology are most important in determining size limits.

First, under conditions of crowding and at lower latitudes, oysters fail to grow to large size. The former is due to food-limiting conditions. The latter is due to warmer temperatures resulting in the shunting of net production into reproductive growth (Hofmann et al., in press). A considerable body of data supports food limitation in oyster populations, from aspects of spatial distribution (Powell et al., 1987), to reduced growth in crowded locations (Osman et al., 1989), and the observation of increased growth coincident with high mortality (Crosby et al., 1991). A latitudinal gradient in size bespeaks of the importance of temperature in determining the degree to which net production is allocated to somatic growth (Hofmann et al., in press). Both phenomena are reproduced by the model. Clearly, in either case, the setting of size limits as currently done has the effect of artificially reducing yield. If economic considerations warrant it, lower size limits should be set in these populations. In crowded conditions, adult mortality might even increase adult size and yield.

Second, raising size limits increases population density and, under certain conditions, the resulting increase in reproductive effort can eventually result in an increased number of market-size oysters at the larger size limit. Such conditions are met in populations of relatively low density where oysters of legal size are already abundant. Of importance is the recognition that this condition occurs only in populations suffering a relatively high degree of mortality relative to the recruitment rate. Many other agents of mortality, besides the fishery, are important in oyster populations and these agents generally do not respect legal size limits. The model suggests that raising size limits will only be effective if the fishery is the predominant cause of mortality in the population or if other agents of mortality are generally restricted to these same size classes. If all adults are affected, then raising size limits will be ineffective.

Besides the setting of size limits, management policy normally includes a restriction of the fishing season. Fishing seasons on public grounds are generally restricted to the winter months. In some cases, certain areas are set aside for a summer season as well. Natural mortality rates are high in oyster populations, generally greater that 70% per year (Mackin, 1959). Oyster populations in the Gulf of Mexico withstand this degree of mortality without long-term population declines. In this sense, the populations are stable (other species are stable at much higher mortality rates, e.g. Zonneveld [1991]). Rates of recruitment are sufficient to balance mortality over the long term. Nevertheless, population declines do occur (Sindermann, 1968; and others referenced previously) and these have, on occasion,

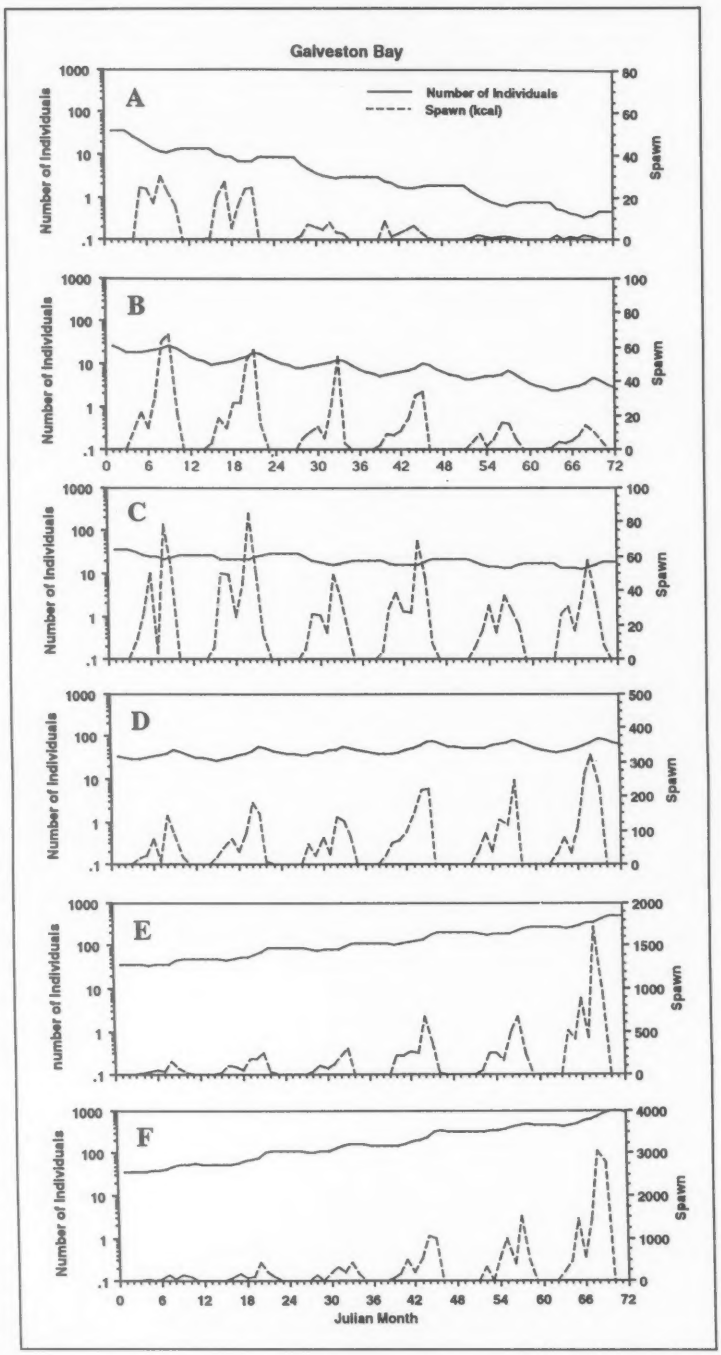

Figure 17

Comparison of the time development of simulated *Crassostrea virginica* populations exposed to mortality in three differing size classes: (**A** and **B**), sizes 5 and larger; (**C** and **D**) sizes 6 and larger; (**E** and **F**) sizes 7 and larger. Cases A, C, and E show the time development under conditions where mortality was restricted to the summer. Cases B, D, and F show the time development under conditions where mortality was restricted to the winter. Further information in Figure 3 and Table 2, cases 34–39.

been blamed on overfishing. Although no adequate data are available, one suspects that the fishery may be a principle source of mortality in the winter, but not in the summer when the various other agents of mortality, such as diseases and predators, are active.

Oyster populations are more resistant to winter mortality than to summer mortality. The increased likelihood of an intense population decline during the summer observed throughout the oyster's latitudinal range is a product of the basic physiology of the oyster. Simulated oyster populations were most resistant to population declines when mortality was restricted to the winter months under nearly all conditions of recruitment, size-class specific mortality and food supply; they were never less resistant. The simulations suggest that oyster populations can withstand substantially higher rates of mortality in the winter than in the summer and, under conditions where fishing is the primary cause of mortality, populations should be managed more conservatively during the summer season.

A latitudinal gradient in stability exists in oyster populations. Population declines without short-term recovery are more likely at higher latitudes. The simulations suggest that populations should be more and more sensitive to natural agents of mortality and to management decisions at ever increasing latitudes. In effect, populations in the Gulf of Mexico, by their physiology, can withstand the vagaries of nature and the mistakes of man much easier than populations on the Mid-Atlantic and northeast coasts of the United States. The evidence suggests the need for more conservative oyster management at higher latitudes. In effect, the Gulf of Mexico populations and the northeastern

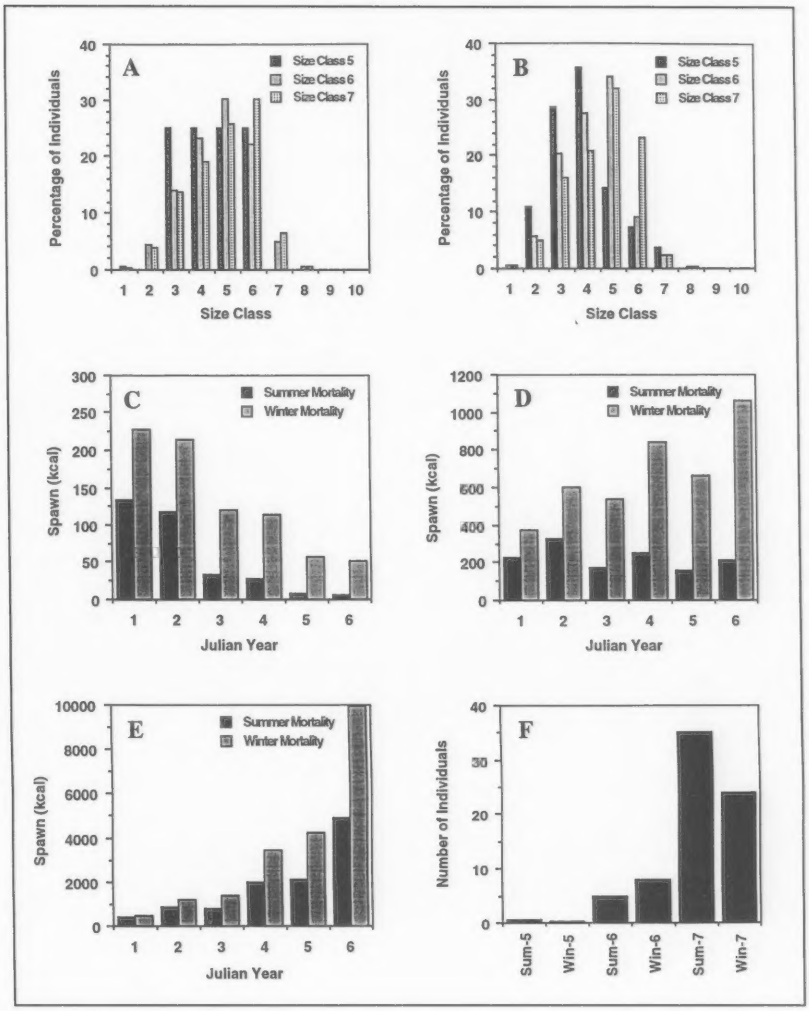

Figure 18

A comparison of the final size-frequency distributions (day 2,160) (**A** and **B**), the yearly reproductive efforts (**C, D,** and **E**) and the number of market-size individuals in the *Crassostrea virginica* population after 6 years (**F**) for the simulations depicted in Figure 17. (A) mortality restricted to the summer (Fig. 17, A, C, and E). (B) mortality restricted to the winter (Fig. 17, B, D, and F). (C) Yearly reproductive effort for populations exposed to mortality in sizes 5 and larger (Fig. 17, A and B). (D) Yearly reproductive effort for populations exposed to mortality in sizes 6 and larger (Fig. 17, C and D). (E) Yearly reproductive effort for populations exposed to mortality in sizes 7 and larger (Fig. 17, E and F). (F) The number of market-size individuals in the population after 6 years, restricting the calculation of market-size individuals to the same classes suffering mortality, 5 and larger (sum-5, Fig. 17A; win-5, Fig. 17B), 6 and larger (sum-6, Fig. 17C; win-6, Fig. 17D) and 7 and larger (sum-7, Fig. 17E; win-7, Fig. 17F).

populations exist under different physiological constraints and these constraints demand different management philosophies and decisions.

Acknowledgments

We thank Elizabeth Wilson-Ormond and Stephanie Boyles for help in data acquisition. This research was supported by an institutional grant NA89-AA-D-SG139 to TAMU by the National Sea Grant College Program, National Oceanic and Atmospheric Administration (NOAA), U.S. Department of Commerce, grant DACW64-91-C-0040 from the Army Corps of Engineers, Galveston District Office, and computer funds from the College of Geosciences and Maritime Studies Research Development Fund. Additional computer resources and facilities were provided through the Center for Coastal Physical Oceanography at Old Dominion University. We appreciate this support.

Literature cited

Andrews, J. D., D. Haven, and D. B. Quayle.
1959. Fresh-water kill of oysters (*Crassostrea virginica*) in James River, Virginia, 1958. Proc. Natl. Shellfish. Assoc. 49:29–49.

Andrews, J. D., and W. G. Hewatt.
1957. Oyster mortality studies in Virginia. II: The fungus disease caused by *Dermocystidium marinum* in oysters in Chesapeake Bay. Ecol. Monogr. 27:1–26.

Bahr, L. M., and W. P. Lanier.
1981. The ecology of intertidal oyster reefs of the South Atlantic coast: a community profile. U.S. Fish Wildl. Serv., Biol. Serv. Program, FWS/OBS-81/15, 105 p.

Berg, J. A., and R. I. E. Newell.
1986. Temporal and spatial variations in the composition of seston available to the suspension feeder *Crassostrea virginica*. Estuarine Coastal Shelf Sci. 23:375–386.

Butler, P. A.
1949. Gametogenesis in the oyster under conditions of depressed salinity. Biol. Bull. (Woods Hole) 96:263–269.

Chanley, P. E.
1958. Survival of some juvenile bivalves in water of low salinity. Proc. Natl. Shellfish. Assoc. 48:52–65.

Choi, K- S., D. H. Lewis, E. N. Powell, and S. M. Ray.
1993. Quantitative measurement of reproductive output in the American oyster, *Crassostrea virginica* (Gmelin), using an enzyme-linked immunosorbent assay (ELISA). Aquaculture Fish. Manag. 24:299–322.

Copeland, B.J., and H.D. Hoese.
1966. Growth and mortality of the American oyster, *Crassostrea virginica*, in high salinity shallow bays in central Texas. Publ. Inst. Mar. Sci. Univ. Tex. 11:149–158.

Crosby, M. P., C. F. Roberts, and P. D. Kenny.
1991. Effects of immersion time and tidal position on in situ growth rates of naturally settled eastern oysters, *Crassostrea virginica* (Gmelin, 1791). J. Shellfish Res. 10:95–103.

Cummins, K. W., and J. C. Wuycheck.
1971. Caloric equivalents for investigations in ecological energetics. Int. Ver. Theor. Angew. Limnol. Verh. 18:1–158.

Cummins, H., E. N. Powell, R. J. Stanton Jr., and G. Staff.
1986. The size-frequency distribution in palaeoecology: the effects of taphonomic processes during formation of death assemblages in Texas bays. Palaeontology (Lond.). 29:495–518.

Dame, R. F.
1972. The ecological energies of growth, respiration and assimilation in the intertidal American oyster *Crassostrea virginica*. Mar. Biol. (Berl.) 17:243–250.

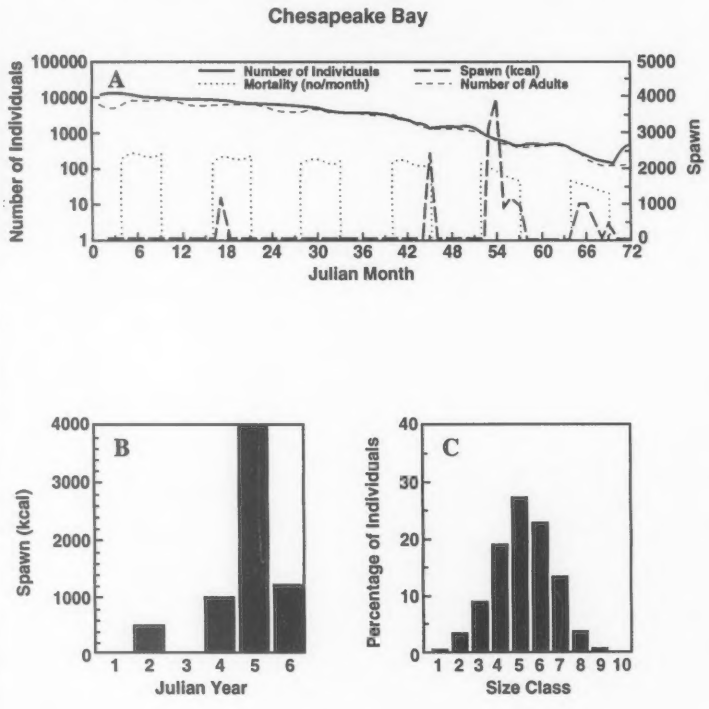

Figure 19
The time development of a simulated *Crassostrea virginica* population exposed to a seasonal temperature regime for Chesapeake Bay and summer mortality. Additional information in Figure 3 and Table 2, case 44.

Dekshenieks, M. M., E. E. Hofmann, and E. N. Powell.
In press. Environmental effects on the growth and development of *Crassostrea virginica* (Gmelin) larvae: a modeling study. J. Shellfish Res.

Deslous-Paoli, J- M., and M. Heral.
1988. Biochemical composition and energy value of *Crassostrea gigas* (Thunberg) cultured in the Bay of Marennes-Oleron. Aquat. Living Resour. 1:239–249.

Doering, P. H., and C. A. Oviatt.
1986. Application of filtration rate models to field populations of bivalves: an assessment using experimental mesocosms. Mar. Ecol. Prog. Ser. 31:265–275.

Dupuy, J. L., N. T. Windson, and C. E. Sutton.
1977. Manual for design and operation of an oyster seed hatchery. Virginia Institute of Marine Science, Gloucester Point, VA, 104 p.

Engle, J. B.
1947. Commercial aspects of the upper Chesapeake Bay oyster bars in light of the recent oyster mortalities. Proc. Natl. Shellfish. Assoc. for 1946, p. 42–46.

1956. Ten years of study on oyster setting in a seed area in upper Chesapeake Bay. Proc. Natl. Shellfish. Assoc. 46:88–99.

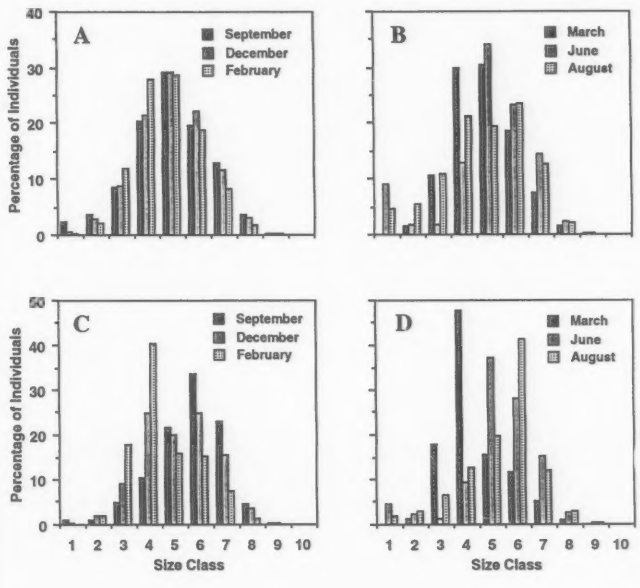

Figure 20

The seasonal shift in size-frequency distribution for two *Crassostrea virginica* populations in Chesapeake Bay. (**A** and **B**) exposed to summer mortality; (**C** and **D**) exposed to winter mortality. (A and B) coincide with the simulation depicted in Figure 19. (C and D) coincide with Table 2, case 51.

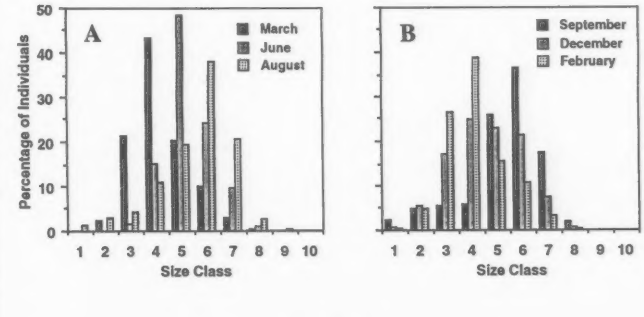

Figure 21

The seasonal shift in size-frequency distribution of a *Crassostrea virginica* population in Chesapeake Bay exposed to an (**A**) early spring (March/April) and (**B**) early fall (August/September) bloom. The complementary case of two later blooms is depicted in Figure 20, C and D. More information can be found in Table 2, case 48.

Engle, J. B., and A. Rosenfield.
1962. Progress in oyster mortality studies. Proc. Gulf Carib. Fish. Inst. 15:116–124.

Epifanio, C. E., and J. Ewart.
1977. Maximum ration of four algal diets for the oyster *Crassostrea virginica* Gmelin. Aquaculture 11: 13–29.

Fréchette, M., D. A. Booth, B. Myrand, and H. Bérard.
1991. Variability and transport of organic seston near a mussel aquaculture site. ICES Mar. Sci. Symp. 192:24–32.

Gallager, S. M., and R. Mann.
1986. Growth and survival of *Mercenaria mercenaria* (L.) and *Crassostrea virginica* (Gmelin) relative to broodstock conditioning and lipid content of eggs. Aquaculture 56:105–121.

Galtsoff, P. S.
1964. The American oyster *Crassostrea virginica* Gmelin. U.S. Fish Wildl. Serv. Fish. Bull. 64:1–480.

Galtsoff, P. S., W. A. Chipman Jr., J. B. Engle, and H. N. Calderwood.
1947. Ecological and physiological studies of the effect of sulphate pulp mill wastes on oysters in the York River, Virginia. U.S. Fish Wildl. Serv. Fish. Bull. 51:58–186.

Garton, D., and W. B. Stickle.
1980. Effects of salinity and temperature on the predation rate of *Thais haemastoma* on *Crassostrea virginica* spat. Biol. Bull. (Woods Hole) 158:49–57.

Gilmore, G. H., S. M. Ray, and D. V. Aldrich.
1975. Growth and mortality of two groups of oysters (*Crassostrea virginica* Gmelin), maintained in cooling water at an estuarine electric power generating station. Texas A&M Univ. Proj. Rep. TAMU-SG-75–207, 67 p.

Glude, J. B.
1966. Criteria of success and failure in the management of shellfisheries. Trans. Am. Fish. Soc. 95:260–263.

Gunter, G.
1955. Mortality of oysters and abundance of certain associates as related to salinity. Ecology 36:601–605.

Hayes, P. F., and R. W. Menzel.
1981. The reproductive cycle of early setting *Crassostrea virginica* (Gmelin) in the northern Gulf of Mexico, and its implications for population recruitment. Biol. Bull. (Woods Hole) 160:80–88.

Hofmann, E. E., E. N. Powell, J. M. Klinck, and E. A. Wilson.
1992. Modeling oyster populations. III: Critical feeding periods, growth and reproduction. J. Shellfish Res. 11:399–416.

Hofmann, E. E., J. M. Klinck, E. N. Powell, S. Boyles, and M. Ellis.
In press. Modeling oyster populations. II: Adult size and reproductive effort. J. Shellfish Res.

Hofstetter, R. P.
1966. Oyster mortality studies along the Texas coast during 1966. Texas Parks Wildl. Dept. Coastal Fish. Proj. Rep., p. 55–68.
1983. Oyster population trends in Galveston Bay 1973–1978. Tex. Parks Wildl. Dept. Management Data Ser. no. 51, 33 p.

Hofstetter, R. P., and S. M. Ray.
1988. Managing public oyster reefs: Texas experience. J. Shellfish Res. 7:213.

Hofstetter, R. P., T. L. Heffernan, and B. D. King III.
1965. Oyster (*Crassostrea virginica*) mortality studies along the Texas coast. Tex. Parks Wildl. Dep. Coastal Fish. Proj. Rep., p. 119–131.

Kennedy, V. S.
1982. Sex ratios in oysters, emphasizing *Crassostrea virginica* from Chesapeake Bay, Maryland. Veliger 25:329–338.

Klinck, J. M., E. N. Powell, E. E. Hofmann, E. A. Wilson, and S. M. Ray.
1992. Modeling oyster populations: the effect of density and food supply on production. Proc. Adv. Mar. Technol. Conf. 5:85–195.

Koehn, R. K., and B. L. Bayne.
1989. Towards a physiological and genetical understanding of the energetics of the stress response. Biol. J. Linn. Soc. 37:157–171.

Laird, M.
1961. Microecological factors in oyster epizootics. Can. J. Zool. 39:449–485.

Lee, R. F., and P. B. Heffernan.
1991. Lipids and proteins in eggs of eastern oysters (*Crassostrea virginica* Gmelin, 1791) and northern quahogs (*Mercenaria mercenaria* Linnaeus, 1758). J. Shellfish Res. 10:203–206.

Loosanoff, V. L.
1958. Some aspects of behavior of oysters of different temperatures. Biol. Bull. (Woods Hole) 114:57–70.

Loosanoff, V. L., and F. D. Tommers.
1948. Effect of suspended silt and other substances on rate of feeding of oysters. Science (Wash. D.C.) 107:69–70.

Lund, E. J.
1957. A quantitative study of clearance of a turbid medium and feeding by the oyster. Publ. Inst. Mar. Sci. Univ. Tex. 4:296–312.

MacKenzie, C. L., Jr.
1989. A guide for enhancing estuarine molluscan shellfisheries. Mar. Fish. Rev. 51(3):1–47.

Mackin, J. G.
1959. A method of estimation of mortality rates in oysters. Proc. Natl. Shellfish.Assoc. 50:41–51.

Mackin, J. G., and S. H. Hopkins.
1962. Studies on oyster mortality in relation to natural environments and to oil fields in Louisiana. Publ. Inst. Mar. Sci. Univ. Tex. 7:1–131.

Mackin, J. G., and A. K. Sparks.
1962. A study of the effect on oysters of crude oil loss from a wild well. Publ. Inst. Mar. Sci. Univ. Tex. 7:230–261.

Mackin, J. G., and D. A. Wray.
1950. Report on the second study of mortality of oysters in Barataria Bay, Louisiana, and adjacent areas. Texas A&M Research Foundation Proj. Rep., Proj. 9, 39 p.

Mackin, J. G., B. Welch, and C. Kent.
1950. A study of mortality of oysters of the Buras area of Louisiana. Texas A&M Research Foundation Proj. Rep., Proj. 9, 41 p.

Menzel, R. W.
1950a. Report on oyster studies in Caillou Island oil field, Terrebonne Parish Louisiana. Texas A&M Research Foundation Proj. Rep., Proj. 9, 60 p.
1950b. Report of oyster studies in Lake Felicity and Bayou Bas Bleu, Terrebonne Parish, Louisiana. Texas A&M Research Foundation Proj. Rep., Proj. 9, 46 p.

Menzel, R. W., and S. H. Hopkins.
1953. Report on oyster experiments at Bay Sainte Elaine oil field. Texas A&M Research Foundation Proj. Rep., Proj. 9, 170 p.

Menzel, R. W., N. C. Hulings, and R. R. Hathaway.
1957. Causes of depletion of oysters in St. Vincent Bar, Apalachicola Bay, Florida. Proc. Natl. Shellfish. Assoc. 48:66–71.

Moore, H. F., and T. E. B. Pope.
1910. Oyster culture experiments and investigations in Louisiana. U.S. Dep. Commerce Labor Bur. Fish. Document No. 731, 52 p.

Mountford, K., and R. C. Reynolds.
1988. Potential biological effects of modeled water quality improvements resulting from two pollutant reduction scenarios. *In* Understanding the estuary: advances in Chesapeake Bay research. Proceedings of a conference 29–31 March 1988. Chesapeake Research Consortium Publ. 129, Baltimore, MD, p. 593–606.

Needler, A. W. H., and R. R. Logie.
1947. Serious mortalities in Prince Edward Island oysters caused by a contagious disease. Trans. R. Soc. Canada Ser. III Sect. V 41:73–89.

Newell, R. I. E.
1985. Physiological effects of the MSX parasite *Haplosporidium nelsoni* (Haskin, Stauber & Mackin) on the American oyster *Crassostrea virginica*. J. Shellfish Res. 5:91–95.

Osman, R. W., R. B. Whitlatch, and R. N. Zajac.
1989. Effects of resident species on recruitment into a community: larval settlement versus post-

settlement mortality in the oyster *Crassotrea virginica*. Mar. Ecol. Prog. Ser. 54:61–73.

Owen, H. M.
1953. Growth and mortality of oysters in Louisiana. Bull. Mar. Sci. Gulf Caribb. 3:44–54.

Powell, E. N., H. Cummins, R. J. Stanton Jr., and G. Staff.
1984. Estimation of the size of molluscan larval settlement using the death assemblage. Estuarine Coastal Shelf Sci. 18:367–384.

Powell, E.N., M.E. White, E.A. Wilson, and S.M. Ray.
1987. Small-scale spatial distribution of oysters (*Crassostrea virginica*) on oyster reefs. Bull. Mar. Sci. 41:835–855.

Powell, E. N., E. E. Hofmann, J. M. Klinck, and S. M. Ray.
1992. Modeling oyster populations.I: A commentary on filtration rate. Is faster always better? J. Shellfish Res. 11:387–398.

Prytherch, H. F.
1929. Investigation of the physical conditions controlling spawning of oysters and the occurrence, distribution, and setting of oyster larvae in Milford Harbor, Connecticut. Bull. Bur. Fish. 44:429–503.

Quast, W. D., M. A. Johns, D. E. Pitts Jr., G. C. Matlock, and J. E. Clark.
1988. Texas oyster fishery management plan source document. Texas Parks Wildl. Dept Coastal Fish. Branch, Austin, TX, 178 p.

Ray, S. M., and A. C. Chandler.
1955. *Dermocystidium marinum*, a parasite of oysters. Exp. Parasitol. 4:172–200.

Schlesselman, G. W.
1955. The Gulf coast oyster industry in the U.S. Geogr. Rev. 45:531–541.

Shumway, S. E., and R. K. Koehn.
1982. Oxygen consumption in the American oyster *Crassostrea virginica*. Mar. Ecol. Prog. Ser. 9:59–68.

Sindermann, C. J.
1968. Oyster mortalities, with particular reference to Chesapeake Bay and the Atlantic coast of North America. U.S. Fish Wildl. Serv. Bur. Comm. Fish. Spec. Sci. Rep. Fisheries No. 569, 10 p.

Soniat, T. M., and S. M. Ray.
1985. Relationships between possible available food and the composition, condition and reproductive state of oysters from Galveston Bay, Texas. Contrib. Mar. Sci. 28:109–121.

Soniat, T. M., and M. S. Brody.
1988. Field validation of a habitat suitability index model for the American oyster. Estuaries 11:87–95.

Soniat, T. M., S. M. Ray, and L. M. Jeffrey.
1984. Components of the seston and possible available food for oysters in Galveston Bay, Texas. Contrib. Mar. Sci. 27:127–141.

Soniat, T. M., L. E. Smith, and M. S. Brody.
1989. Mortality and condition of the American oyster in Galveston Bay, Texas. Contrib. Mar. Sci. 31:77–94.

Stanley, J. G., and M. A. Sellers.
1986. Species profile: life histories and environmental requirements of coastal fishes and invertebrates (Gulf of Mexico)—American oyster. U.S. Fish Wildl. Serv. Biol. Rep. 82 (11.64), U.S. Army Corps of Engineers, TR EL-82–4, 25 p.

Stickle, W. B.
1985. Effects of environmental factor gradients on scope for growth in several species of carnivorous marine invertebrates. *In* J. S. Gray and M. E. Christiansen (eds.), Marine biology of polar regions and effects of stress on marine organisms. John Wiley & Sons Ltd., New York, p.601–616.

Underwood, A. J.
1989. The analysis of stress in natural populations. Biol. J. Linn. Soc. 37:51–78.

White, M. E., E. N. Powell, and S. M. Ray.
1988. Effects of parasitism by the pyramidellid gastropod *Boonea impressa* on the net productivity of oysters (*Crassostrea virginica*). Estuarine Coastal Shelf Sci. 26:359–377.

Wright, D. A., and E. W. Hetzel.
1985. Use of RNA:DNA ratios as an indicator of nutritional stress in the American oyster *Crassostrea virginica*. Mar. Ecol. Prog. Ser. 25:199–206.

Young, P. C., and R. B. Martin.
1989. The scallop fisheries of Australia and their management. Crit. Rev. Aquat. Sci. 1:615–638.

Zonneveld, C.
1991. Estimating death rates from transect counts. Ecol. Entomol. 16:115–121.

A suite of extensions to a nonequilibrium surplus-production model*

Michael H. Prager

Miami Laboratory, Southeast Fisheries Science Center
National Marine Fisheries Service, NOAA
75 Virginia Beach Drive, Miami, Florida 33149

Cooperative Unit for Fisheries Education and Research
Rosenstiel School of Marine and Atmospheric Science
University of Miami, 4600 Rickenbacker Causeway, Miami, Florida 33149

Abstract.—Surplus-production models, because of their simplicity and relatively undemanding data needs, are attractive tools for many stock assessments. This paper reviews the logistic production model, starting with the basic differential equation and continuing with a description of the model development without the equilibrium assumption. It then describes several extensions, including "tuning" the model to a biomass index; partitioning fishing mortality by gear, time, or area; and making projections. Computation of confidence intervals on quantities of interest (e.g. maximum sustainable yield (MSY), effort at MSY, level of stock biomass relative to the optimum level) can be done through bootstrapping, and the bootstrap can also be used to construct nonparametric tests of hypotheses about changes in catchability. To fit the model, an algorithm that uses a forward solution of the population equations can be implemented on a small computer. An example of the utility of surplus-production models (illustrating several of these extensions) is given. The example is loosely based on swordfish (*Xiphias gladius*) in the North Atlantic Ocean, but is not intended to describe the actual status of that stock.

Despite the prevalence of age-structured population models, surplus-production models—which generally do not incorporate age structure—remain useful for analysis of fish population dynamics. These models are of particular value when the catch cannot be aged, or cannot be aged precisely, and therefore age-structured models cannot be applied. Surplus-production models are also useful as a complement to age-structured models, providing another view of the data and the fisheries. An especially appealing aspect of production models is their simplicity; from a scientific point of view, this makes exploration of their properties easier; from a management point of view, it makes their results easier to present and understand (Barber, 1988).

In this paper, I show that another benefit of these models' simplicity is that model extensions are easily made. Examples of such extensions include modeling several simultaneous or sequential fisheries on the same stock, "tuning" the model to a biomass index (as is often done in age-structured models; e.g. the CAGEAN model of Deriso et al., 1985; the CAL model of Parrack, 1986; the ADAPT model of Gavaris, 1988), modeling changes in catchability or population characteristics (e.g. carrying capacity), and estimating missing values of fishing effort. Many of these extensions have not been presented before.

The comprehensiveness of a production model can be further increased by introducing another extension: computation of nonparametric estimates of variability in the results. These can be obtained by bootstrapping, and can be used both to describe the results more completely and to learn more about the model's behavior under a variety of circumstances.

After reviewing the formulation of the simplest surplus-production model (the logistic model), a number of extensions to the model are described. An example, loosely based on swordfish, *Xiphias gladius,* in the North Atlantic Ocean, is presented to illustrate typical results from the model and the use of many of the extensions. The example, which is not intended to be an assessment of that stock, should not be used to make inferences about stock status.

Manuscript accepted 18 October 1993
Fishery Bulletin 92:374–389 (1994)

* Contribution MIA-92/93-58 of the Miami Laboratory, Southeast Fisheries Science Center, National Marine Fisheries Service.

Model formulation and fitting

Basic differential equations

Surplus-production models characterize a population as an undifferentiated biomass. The number of individuals present or harvested plays no part in these models, nor is age or size structure considered. A quantity termed "surplus production" is used to characterize population dynamics at different levels of population size (measured in biomass). Surplus production is the algebraic sum of three major forces: recruitment, growth, and natural mortality. The adjective "surplus" refers to the surplus of recruitment and growth over natural mortality; i.e. the net production. In this article, surplus production will often be termed simply "production," and the models termed "production models."

In the simplest production model, the logistic or Graham-Schaefer (Graham, 1935; Schaefer, 1954, 1957) model, a first–order differential equation describes the rate of change of stock biomass B_t due to production. In the absence of fishing, the population's rate of increase or decrease is assumed to be a function of the current population size only:

$$\frac{dB_t}{dt} = rB_t - \frac{r}{K}B_t^2, \qquad (1)$$

where B_t is the population biomass at time t and r and K are parameters. The right side of Equation 1 is simply the start of the Taylor expansion of an arbitrary function $\Phi(B)$ passing through the origin (Lotka, 1924).

Equation 1 is written in the parameterization of population ecology, in which K represents the maximum population size, or carrying capacity, and r represents the stock's intrinsic rate of increase (in proportion per unit time). In this paper, both are assumed constant. Other parameterizations could be used, and indeed a slightly different parameterization is used for simplicity in the next section.

Adding fishing mortality F_t to the model, it becomes

$$\frac{dB_t}{dt} = (r - F_t)B_t - \frac{r}{K}B_t^2. \qquad (2)$$

This model, like many fisheries models, is much simpler than the real world. In particular, it excludes such factors as environmental variation, interspecific effects, or the possible presence of more than one stable regime.

Time trajectories of biomass and yield

Integration of Equation 2 with respect to time allows modeling the biomass and yield through time. Before integration, simplify notation by defining $\alpha_t = r - F_t$ and $\beta = r/K$ to express Equation 2 more simply as

$$\frac{dB_t}{dt} = \alpha_t B_t - \beta B_t^2. \qquad (3)$$

Equation 3 can be conveniently solved for biomass under the assumption that F_t is constant and that therefore α_t is constant. This is a weak assumption, for if F_t varies, time can be divided into short periods of constant or nearly constant F and a solution found for each period. Fitting would then require knowing the catch and effort for each short period.

For the period beginning at $t = h$ and ending at time $t = h + \delta$, during which the instantaneous fishing mortality rate is F_h, the solution to Equation 3 is

$$B_{h+\delta} = \frac{\alpha_h B_h e^{\alpha_h \delta}}{\alpha_h + \beta B_h (e^{\alpha_h \delta} - 1)} \quad \text{when } \alpha_h \neq 0, \text{ or} \qquad (4a)$$

$$B_{h+\delta} = \frac{B_h}{1 + \beta \delta B_h} \quad \text{when } \alpha_h = 0. \qquad (4b)$$

Equation 4a is the familiar logistic equation. However, if $\alpha_h = 0$ (i.e. if $F_h = r$), Equation 4a is undefined and Equation 4b is used in its place.

Modeling the yield during the same period involves another integration with respect to time:

$$Y_h = \int_{t=h}^{h+\delta} F_h B_t \, dt, \qquad (5)$$

where B_t, the biomass at instant t, is defined by Equations 4a and 4b; F_h is the (constant) instantaneous rate of fishing mortality during the time period; and Y_h is the yield taken during the period. Performing the integration in Equation 5,

$$Y_h = \frac{F_h}{\beta} \ln\left[1 - \frac{\beta B_h (1 - e^{\alpha_h \delta})}{\alpha_h}\right] \quad \text{when } \alpha_h \neq 0, \text{ or} \qquad (6a)$$

$$Y_h = \frac{F_h}{\beta} \ln(1 + \delta \beta B_h) \quad \text{when } \alpha_h = 0. \qquad (6b)$$

Equation 6a was apparently first given by Pella (1967) (and a similar form developed by Schnute [1977]); Equations 4b and 6b seem not to have been presented in fishery biology before now.

It follows from the definition of F that the estimated average biomass during the period is simply Y_h / F_h. The surplus production P_h during the time period can be determined by mass balance:

$$P_h = B_{h+\delta} - B_h + Y_h. \qquad (7)$$

When yield is equal to surplus production, the population is in equilibrium.

Parameter estimation

Parameter estimation for this model can be accomplished by a number of methods. The method presented here is a slight modification of one originated by Pella (1967), later used by Pella and Tomlinson (1969), and recently termed the "time-series method" by Hilborn and Walters (1992). Although it is not necessary to use equal time periods, the treatment in the balance of this paper assumes, for simplicity, that there are T equal time periods, indexed by $\tau = \{1, 2, ..., T\}$, and that a period is one year in duration. The following symbols are used:

B_τ population biomass at the start of year τ
Y_τ yield in biomass during year τ
P_τ surplus production during year τ,
f_τ fishing effort rate during year τ,
F_τ fishing mortality rate during year τ,
α_τ function of F_τ; $\alpha_\tau = r - F_\tau$.

Estimates of the first five of these quantities are represented by $\hat{B}_\tau, \hat{Y}_\tau, \hat{P}_\tau, \hat{f}_\tau$, and $\hat{F}_\tau$.

An important additional assumption is that, for all τ, $F_\tau = qf_\tau$; in other words, that fishing mortality rate is proportional to fishing effort rate and that the catchability coefficient q is constant. (The assumption of constant q is slightly relaxed later.)

The data required for fitting are, for each time period τ, data on effort f_τ and the yield Y_τ, where $\tau = \{1, 2, ..., T\}$ and $T > 4$. The parameters to be estimated are r and K in Equation 1, q, and B_1, the biomass at the beginning of the first year. The simplest procedure accumulates residuals in yield. To perform the estimation, the following algorithm is used:

A1 Obtain starting guesses for the four parameters.
A2 Beginning with the current estimate of B_1, project the population through time according to Equations 4a and 4b. For each year of the projection, compute estimated yield from Equations 6a and 6b.
A3 Compute the objective function to be minimized. Assuming a multiplicative error structure in yield, this is

$$\sum_{\tau=1}^{T}\left[\log(Y_\tau) - \log(\hat{Y}_\tau)\right]^2.$$

A4 Monitor the objective function for convergence. If achieved, end. Otherwise, revise the parameter estimates (using a standard minimization scheme) and continue at step A2.

The simplex or "polytope" algorithm (Nelder and Mead, 1965; Press et al., 1986) works well as the minimization scheme in this application. Although not as rapid computationally as some other methods, the simplex algorithm is quite robust to starting values and is easily manipulated (by restarts) to avoid local minima (see Press et al., 1986, p. 292). Rivard and Bledsoe (1978) used the Marquardt (1963) algorithm successfully for estimation in a similar model.

The estimation method just described uses the recorded effort in each year to estimate yield. Alternatively, one could use the recorded yield in each year to estimate the fishing mortality rate (or equivalently, the fishing effort rate). The solutions of Equations 6a and 6b for fishing mortality rate are

$$F_\tau = \frac{\beta Y_\tau}{\ln\left[\frac{\beta B_t (e^{\alpha_\tau - 1})}{\alpha_\tau} + 1\right]} \quad \text{when } \alpha_\tau \neq 0, \text{ or} \tag{8a}$$

$$F_\tau = \frac{\beta Y_\tau}{\ln[1 + \beta B_\tau]} \quad \text{when } \alpha_\tau = 0. \tag{8b}$$

To use this approach, one must revise the second and third steps of the algorithm to become—

A2′ Beginning with the current estimate of B_1, compute the estimated fishing effort for each year by solving Equation 8a or 8b and dividing by $\hat{q}$. Project the population to year-end with Equation 4.
A3′ Compute the objective function to be minimized. Assuming a multiplicative error structure in effort, this is

$$\sum_{\tau=1}^{T}\left[\log(f_\tau) - \log(\hat{f}_\tau)\right]^2.$$

This is equivalent to minimizing the sums of squared residuals in the logarithm of catch per unit of effort, i.e. to minimizing

$$\sum_{\tau=1}^{T}\left[\log(C_\tau / f_\tau) - \log(C_\tau / \hat{f}_\tau)\right]^2.$$

A significant practical advantage of the second approach is that it simplifies the analysis of data with some missing data on effort. During parameter estimation, effort is estimated for all years; for years of missing effort, the contribution to the objective function is simply defined to be zero. In contrast, the computations for the first approach are not possible without data on effort for each year.

Estimating effort from yield introduces two small practical difficulties. The first difficulty is that Equation 8a is not an explicit solution for effort (because α_τ includes f_τ), so it must be solved iteratively. This is accomplished by putting a starting guess $\tilde{F}_\tau$ into the right–hand side of the equation, solving, and substituting the result repeatedly until convergence is achieved. A logical starting guess is $\tilde{F}_\tau = Y_\tau / \hat{B}_\tau$.

The second difficulty involves a fundamental difference between predicting yield and predicting effort. For a given starting biomass and effort, one can always compute the corresponding yield. For a given starting biomass, however, there are some yields that can never be obtained, no matter how high the effort. Under these circumstances, the catch equation (6a or 6b) has no solution. Unless a tactic is devised for such cases, it becomes impossible to compute the objective function when they occur, and thus impossible to conduct its minimization. A tactic suggested by R. Methot[1] as useful in his stock-synthesis model (Methot, 1989, 1990) is to place a constraint on the maximum allowable value of F_τ (and consequently of f_τ). When an estimate of F_τ reaches this constraint, it is not allowed to increase further, and the quantity $[\log(Y_\tau) - \log(\hat{Y}_\tau)]^2$ is added to the objective function along with the usual squared residual in effort. This allows computation of a reasonable value of the objective function for such regions of the solution space that may be encountered during optimization. In my experience, however, final estimates have always come from a solution in which yield is always matched exactly.

In fitting a linear regression, observation error in the predictor variables causes problems with the parameter estimates, including inconsistency and, in the bivariate linear case, bias towards zero (Thiel, 1971; Kennedy,1979). The problems induced into nonlinear models are less well understood, but are believed to be similar. Schnute (1989) has illustrated how the choice of dependent variable in a fisheries model can affect the results substantially. In fisheries contexts, yield is usually observed more precisely than fishing effort; for that reason, it seems preferable on statistical grounds to use the second approach, estimating effort from yield, rather than estimating yield from effort.

Whichever approach is chosen, the estimation process results in direct estimates of B_1, r, K, and q, which define unique estimates of the stock biomass levels B_2, B_3, ..., B_T and the stock's production during each period of time. The corresponding estimate of maximum sustainable yield (MSY) under the logistic model is $\widehat{\text{MSY}} = \hat{K}\hat{r}/4$. According to the theory of production modeling, MSY can be attained as a sustainable yield only at one specific stock size; for the logistic model this is $B_{\text{MSY}} = K/2$, estimated by $\hat{B}_{\text{MSY}} = \hat{K}/2$. The instantaneous fishing mortality that generates MSY at B_{MSY} is $F_{\text{MSY}} = r/2$; the corresponding rate of fishing effort is $f_{\text{MSY}} = r/2q$, with estimates given by substituting $\hat{r}$ and $\hat{q}$ for the unknown true values in these two expressions.

[1] Methot, R. Alaska Fisheries Science Center, 7600 Sand Point Way NE, Seattle, WA 98115. Personal commun., 1993.

The logarithmic objective function assumes multiplicative errors with constant variance. The solution obtained is the maximum-likelihood solution if the transformed residuals are independent, of constant variance, and normally distributed (see Seber and Wild, 1989). However, maximum-likelihood methods, while generally desirable, are not necessarily robust to outliers, nor do they necessarily have desirable small-sample properties. Use of a robust-regression method (such as least absolute values regression) would be an interesting research topic.

Another management benchmark

An analogue of the management benchmark $F_{0.1}$ can be computed for this model (or for any production model). The derivative of equilibrium yield with respect to fishing mortality rate for this model is

$$\frac{dY_e}{dF} = K\left(1 - \frac{2F}{r}\right). \tag{9}$$

At $F = 0$, this derivative is equal to K. We define as $F_{0.1}$ for this model as the value of F at which Equation 9 equals $0.1K$. Substitution into Equation 9 gives the following results: $F_{0.1} = 0.45r$, and $Y_{0.1} = 0.2475rK$ (where $Y_{0.1}$ is the equilibrium yield corresponding to $F_{0.1}$). An equivalent statement is that $F_{0.1}$ is 90% of F_{MSY}, and $Y_{0.1}$ is 99% of MSY. Punt (1990) used the concept of $F_{0.1}$ for a production model but did not explicitly state these relationships.

Penalty for large estimates of B_1

Logistic production theory implies that B_1 should always be less than K, but the objective functions used here are relatively insensitive to the estimate of B_1. In practice, I have found that the estimate of B_1 obtained from some data sets tends to be much larger than the estimate of K. Such results could be eliminated by introducing a fixed constraint into the solution, but I have used another method successfully: adding a penalty term to the objective function when $\hat{B}_1 > \hat{K}$. Including this term, the complete logarithmic objective function (assuming residuals in effort) becomes

$$L = \sum_{\tau=1}^{T}\left[\log(f_\tau) - \log(\hat{f}_\tau)\right]^2 + \phi\left[\log(\hat{B}_1) - \log(\hat{K})\right]^2, \tag{10}$$

where $\phi \equiv 1$ if $\hat{B}_1 > \hat{K}$, and $\phi \equiv 0$, otherwise. While constraining the value of B_1 seems logical in accordance with the underlying population theory, such constraints can change the estimates of other parameters, compared to an unconstrained solution. The amount of change can be examined by estimating with and without the penalty term or fixed constraint.

Extensions to the model

A great strength of the model presented here is the ease with which it can be extended and modified. Such extensions can include, for example, modeling fisheries divided by space, time, or gear type; analyzing data series including some years of no effort, as would occur during a closure; analyzing data series with years of missing or highly uncertain effort data; incorporating changes in catchability within the data series, perhaps after periods of closure or following regulatory changes; and tuning the model to fishery-independent estimates or indices of population biomass.

Missing data

Gaps in the effort and yield time series do not present a problem to these dynamic production model analyses. Years with no effort (and therefore no catch) can easily be treated by defining the residual to be zero. Although such years do not influence parameter estimation directly, the time lag during the years of closure carries information that is incorporated in fitting the model, and an estimate of population biomass for each missing year is made according to the logistic growth model. In contrast, years of closure contribute no information to production models that assume equilibrium conditions.

A slightly more difficult problem is the correct treatment of years in which effort is known to have existed, but for which the data are missing or highly uncertain. In such a case, the framework presented here can be used to estimate, simultaneously with the other parameters, effort levels for a limited number of such years within the series. As in any estimation scheme, the total number of estimated parameters should be kept reasonably small in comparison to the number of years of nonzero data. If residuals are constructed in effort (rather than yield) the estimation of missing effort becomes trivial, as a predicted effort is computed for each year during parameter estimation.

More than one data series

Another simple extension of the basic estimation framework is analysis of stocks fished by two or more different gear types, either in the same years or serially. For convenience, I refer to these as different fisheries on the same stock. To define the situation more precisely, there are J different fisheries, indexed by $j = \{1, 2, ..., J\}$. The effort applied by fishery j in period τ is $f_{j\tau}$, the catchability coefficient of that fishery is q_j, and the yield in period τ is $Y_{j\tau}$. All q_j are assumed time–invariant. The total instantaneous fishing mortality in period τ is

$$F_\tau = \sum_{j=1}^{J} q_j f_{j\tau}. \tag{11}$$

Biomass and yield projections can be computed by Equations 4a, 4b, 6a, and 6b as before. The estimated yield from fishery j in period τ is

$$\hat{Y}_{j\tau} = \frac{\hat{q}_j \hat{f}_{j\tau}}{\hat{F}_\tau} \hat{Y}_\tau, \tag{12}$$

where $\hat{Y}_\tau$ is the total yield in period τ. During parameter estimation, a residual is obtained for each fishery having nonzero effort in period τ. The contribution to the objective function for each period is thus composed of a sum of terms, one for each fishery with nonzero effort. In addition, the individual fisheries may carry different statistical weights to reflect varying levels of confidence in the data from each fishery. Inverse-variance weighting can be approximated by iteratively examining the mean-squared error (MSE) from each series, weighting, and re-estimating the parameters.

Model tuning

If an external series of population biomass estimates is available, it can be incorporated into the analysis in a procedure analogous to tuning an age-structured analysis. The external estimates are compared to the population estimates derived within the production model and the residuals incorporated in computation of the objective function. Rivard and Bledsoe (1978) suggested this possibility, but did not pursue the idea, and it has also been described by Hilborn and Walters (1992). The external biomass series need not be continuous, but may contain missing values; the series' contribution to the objective function is set to zero for years with missing values. An external *index* of biomass can be used similarly, with the cost of estimating one more parameter (the catchability associated with the index).

The model formulation involved in tuning the model is similar to that used when fitting more than one fishery. As in that situation, each year's contribution to the objective function consists of a sum of terms. Here, the sum includes a term from each fishery and a term for each biomass–estimate or index series. For a maximum–likelihood solution, the components should carry statistical weights inversely proportional to their variances.

Varying catchability

In many situations, catchability is thought to change relatively suddenly, perhaps because more efficient

gear for finding or catching the fish is introduced. In such cases, the formulation represented by Equations 11 and 12 can be used to estimate different catchability coefficients for segments of a single time series. In formulating such a model, the time segments would be treated as separate fisheries, each having nonzero catch and effort data only during its respective time period. Each additional time segment would add one additional parameter to the model.

A common concern is determining whether the improvement in fit obtained from a more complex model is statistically significant. A production model with added catchability parameters can be tested against the simpler model (with one estimated q) with a standard F-ratio test. (Here F refers to the F distribution of statistics, not to fishing mortality rate.) The test statistic F^* is

$$F^* = \frac{(\mathrm{SSE_s} - \mathrm{SSE_c})/v_1}{\mathrm{SSE_c}/v_2}, \qquad (13)$$

where $\mathrm{SSE_s}$ and $\mathrm{SSE_c}$ are the error sums of squares of the simple and complex models, respectively; v_1 is the difference in number of estimated parameters between the two models; and v_2 is the number of data points less the total number of estimated parameters. The significance probability of F^* can be obtained from tables of the F-distribution with v_1 and v_2 degrees of freedom. As pointed out by a referee, this is equivalent to to a likelihood-ratio test assuming log-normal error structure, which is implicit in using the SSE from log-transformed data. Because of the possibility of specification error, any such significance test must be considered approximate.

A nonparametric test of the null hypothesis $q_1 = q_2$ can also be conducted by examining a bias-corrected confidence interval on the ratio of the two catchability coefficients. (Construction of bias-corrected confidence intervals is described later.) As an example, assume that the alternative hypothesis is $q_1 \neq q_2$. The null hypothesis would be rejected at $P<0.05$ if a 95% confidence interval on the ratio q_1 / q_2 did not include the value 1.0. Like the F-test, this test is approximate because of the possibility of specification error.

In other cases, catchability is thought to vary in more subtle ways than the step function just suggested (Paloheimo and Dickie, 1964; Gulland, 1975; MacCall, 1976; Peterman and Steer, 1981; Winters and Wheeler, 1985), and one could incorporate any number of catchability models into the estimation framework. It would be straightforward to model a linear trend (increase or decrease) in catchability with time. This could be parameterized by estimating the first and last years' values of q and generating intermediate years' values by linear interpolation, so that only one additional parameter would be estimated. One could also add some form of density–dependent catchability model with a minimal cost in terms of number of parameters estimated; the foundation of such an approach was presented by Fox (1975). However, it might prove difficult to distinguish varying catchability from trends in biomass itself. If so, the use of external estimates or indices of biomass, as explained above, might be especially valuable.

Bootstrap estimates of bias and variability

The bootstrap (Efron, 1982; Stine, 1990) is a sample reuse technique often used to estimate sampling variances, confidence intervals, bias, and similar properties of statistics, including parameter estimates. Major advantages of the bootstrap, compared to alternative methods (such as those based on the information matrix), are its flexibility and relative freedom from distributional assumptions. A minor drawback is that it demands a great deal of computer time.

Bootstrapping is often performed by resampling the original observations. However, in fitting nonequilibrium production models, the order of the catch-effort pairs is as significant as the data themselves. For time-series models (in the broad sense), Efron and Tibshirani (1986) describe a method, used here, that preserves the original time structure of the data. For each bootstrap trial (of which there may be 250 to several thousand), a set of synthetic observations is constructed by combining the ordered predictions from the original fit with residuals chosen at random (with replacement) from the set of residuals from the original fit. The model is then refit to this set of synthetic observations.

The bootstrap can be used to estimate bias in parameter estimates. The median estimation bias B'_θ in a parameter θ is estimated by

$$\hat{B}'_\theta = \hat{\theta}_m - \hat{\theta}, \qquad (13a)$$

where $\hat{\theta}$ is the conventional estimator of θ, and $\hat{\theta}_m$ is the median value of θ obtained from the bootstrap trials (Efron,1982; Efron and Gong, 1983). A bias–corrected estimator $\hat{\theta}_{BC}$ of a parameter θ can therefore be given by

$$\hat{\theta}_{BC} = \hat{\theta} - \hat{B}'_\theta. \qquad (13b)$$

It appears that the median bias correction, rather than a mean correction, has been adopted in the bootstrapping literature because a mean correction (which would be expected to produce an "unbiased" estimate in the usual sense) can have extremely high variance (Hinkley, 1978). The resulting problems are

avoided by use of a median correction, which is quite resistent to outliers. However, the use of a median correction implies that the estimated bias correction will be nonzero for an estimator that is unbiased (in the usual sense) but arises from a distribution in which the median does not equal the mean. That is, the use of a median bias correction transforms the estimator into a median estimator.

Several methods have been developed for computing bias–corrected confidence intervals from the bootstrap (Efron, 1982; Efron, 1987; Noreen, 1989). The most widely used at present appears to be the BC method of Efron (1982). To compute a BC interval, let $N(z)$ be the cumulative distribution function (CDF) of the standard normal distribution and let N^{-1} be the inverse–normal CDF. Let $\hat{C}$ be the empirical bootstrap CDF of the parameter θ; i.e. $\hat{C}(g)$ is the proportion of realizations of $\hat{\theta}$ in the bootstrap distribution that falls below any arbitrary value g. Define the constant

$$z_0 \equiv N^{-1}\left[\hat{C}(\hat{\theta})\right], \tag{14}$$

where $\hat{\theta}$ is the conventional estimator. Then, the $(1 - 2a)$ BC central confidence interval on $\hat{\theta}$ is defined as

$$\theta \in \left\{\hat{C}^{-1}\left[N\left(2z_0 + N^{-1}(a)\right)\right], \hat{C}^{-1}\left[N\left(2z_0 - N^{-1}(a)\right)\right]\right\}. \tag{15}$$

This method assumes that a transformation exists under which the distribution of θ becomes normal and homoscedastic. However, the form of the transformation need not be known (Efron and Gong, 1983). Kizner (1991) constructed bootstrap confidence intervals on production-model results, but he did not state whether bias corrections were used.

This discussion of bootstrapping has referred to estimated "parameters" for simplicity, but the method can be used to estimate bias corrections and bias–corrected confidence intervals for any estimated quantity. Such quantities might include estimates of MSY, f_{MSY}, the population biomass in the final (or any other) year, $f_{0.1}$, projections of biomass levels (discussed next), and so forth.

Projections

Because a production model implicitly includes a recruitment function, it can be used to make projections based on hypothetical catch or effort quotas. As noted above, the historical population biomass trajectory is estimated during parameter estimation. The modeled population can then be projected forward in time by using the same population equations (4, 6, 8), and a proposed set of yields or effort rates. If the bootstrap is used following parameter estimation, the results of each bootstrap trial can be projected forward. From the results, it is possible to compute bias–corrected point estimates and confidence intervals on the projection results.

Example: North Atlantic swordfish

Many aspects of the production model discussed above are illustrated in this example, which is loosely based on swordfish, *Xiphias gladius,* in the North Atlantic Ocean. The example comprises two analyses, the difference between them being the use of an abundance index for tuning the second analysis. Both the base analysis and the tuned analysis used the same yield and fishing-effort data (Table 1; Fig. 1); the tuned analysis also used a hypothetical index of abundance constructed for this purpose (Table 1; Fig. 1). In both analyses, errors were assumed to occur in fishing effort and to follow a lognormal distribution; in other words, the "second estimation approach" described previously was used. Each analysis included a projection of five years beyond the actual data; during those five years, it was assumed that a yield of 12,000 metric tons would be taken annually. Each analysis included a bootstrap with 1,000 trials.

This example is not intended as, and should not be considered to be, a formal assessment of the swordfish fishery. Such an assessment would normally include additional information and analysis, including age-structured population models and numerous sensitivity analyses. Also, the abundance index used here was developed solely to serve an example, and is not believed to be an accurate reflection of abundance over time.

The North Atlantic swordfish fishery enjoyed a high catch rate in 1962 and 1963, but it declined in the late 1960s (Fig. 1). The U.S. and Canadian portions of the fishery were sharply reduced in the early 1970s because of FDA regulations prohibiting interstate transportation or importation of fish with mercury concentrations exceeding the allowable level of 0.5 ppm (Hoey et al., 1989). In 1978, the FDA increased the allowable mercury content to 1 ppm, and since then, the catch has increased, but the CPUE has slowly declined (Fig. 1B). For the years 1971–73, early years of the FDA regulations, data are available on catch but not on fishing effort.

Results from the two analyses were similar, but they illustrate how tuning can influence the results of a production model. In each analysis, the model fits the effort data reasonably well (Fig. 2); however, because the hypothetical abundance index does not match the observed CPUE well (Fig. 1B), the fit in the last years of the tuned model was a compromise

between matching the observed effort (Fig. 2B) and matching the index (Fig. 2C). The tuned analysis gave lower estimates of MSY, f_{MSY}, and a less optimistic impression of the current level of the stock, as represented by the ratio B_{1992}/B_{MSY} (Table 2). It also estimated that the recent fishing mortality rate, as represented by the ratio F_{1991}/F_{MSY}, was somewhat higher.

Estimated median biases from each analysis were small. In the base analysis, no management benchmark was estimated to have a bias exceeding 1.5% of the corresponding uncorrected estimate (Table 2). Estimated median biases for the tuned analysis were only slightly higher; with only the estimated bias in f_{MSY} slightly exceeding 2%. Estimates of median bias in individual model parameters (such as r and K) were slightly higher yet, but only for B_1 was bias estimated as higher than about 2.5%.

Table 1

Data used in two production model analyses loosely based on swordfish, *Xiphias gladius*, in the North Atlantic Ocean. Yield and standardized fishing-effort-rate data are from Hoey et al. (1993) with minor revisions. Hypothetical abundance index data are the mean of ages 3 through 5+ in numbers from Scott et al. (1992). The index was constructed solely for illustrative purposes, and is designated "hypothetical" because it probably is not a good indicator of total-stock biomass.

Year	Yield (t)	Fishing effort rate (10^6 hooks/yr)	Hypothetical abundance index
1962	5,342	6.45	—
1963	10,189	8.54	—
1964	11,258	24.45	—
1965	8,652	25.30	—
1966	9,338	31.39	—
1967	9,084	28.90	—
1968	9,137	40.11	—
1969	9,138	43.23	—
1970	9,425	38.47	—
1971	5,198	—	—
1972	4,727	—	—
1973	6,001	—	—
1974	6,301	19.22	—
1975	8,776	22.97	—
1076	6,587	21.17	—
1977	6,352	18.14	—
1978	11,797	20.40	—
1979	11,859	40.13	—
1980	13,527	35.44	—
1981	11,126	34.85	1.000
1982	12,832	40.73	0.816
1983	14,423	55.10	0.488
1984	12,516	49.44	0.483
1985	14,255	59.55	0.526
1986	18,278	80.75	0.411
1987	19,959	98.91	0.377
1988	19,137	97.08	0.368
1989	17,008	90.46	0.359
1990	15,594	85.86	0.352
1991	13,212	69.86	—

Approximate 80% nonparametric confidence intervals computed by Equations 14 and 15 were derived from the bootstrap. These were computed for the individual model parameters, management benchmarks, indicators of stock position, and for each year's relative stock size estimate (Table 2; Fig. 3). A unitless nonparametric measure of the precision of estimates was constructed by dividing the bias–corrected 50% confidence interval (interquartile range; not shown here) by the corresponding median bias–corrected estimate. The resulting statistic, the relative interquartile range (RIR) is a nonparametric analog of the coefficient of variation. The RIR was of similar magnitude for both models, and was smallest in MSY and f_{MSY}, the benchmarks that do not depend on q. Estimates of the quantities that depend on q, and that thus involve absolute scaling, exhibited relative IQ ranges of about 50% (Table 2).

Estimates of relative biomass (B_τ scaled to B_{MSY}) and fishing mortality rate (F_τ scaled to F_{MSY}) were also similar from the two models (Fig. 3). They show a declining biomass through 1991, with an increase expected thereafter (at the projected harvest rate of 12,000 t/yr, which is less than the MSY estimates). As expected, the precision of estimates during the projection period was less than during the period for which data were available.

In summary, this example demonstrates that much more than MSY can be estimated from a production model. Biomass trajectories can be computed easily, as can estimated confidence intervals derived through the bootstrap. If an independent index of abundance is available, the model can be tuned to that index. Another useful feature is that projections can be used to estimate the probable effects of quotas or other management measures.

Discussion

The modeling framework described here is based on the logistic population model. The history of this model was summarized by Kingsland (1982), who pointed out that the model originated in the work of Verhulst (1845) and Robertson (1923), was popularized by Pearl and Reed (1920), and was also studied by Lotka (1924). The model was introduced to fishery science by Graham (1935) and Schaefer (1954,

1957). In modeling fish populations, one could just as easily use the exponential yield model of Fox (1970) or a model of more flexible shape, such as that of Pella and Tomlinson (1969) or its alternative formulation by Fletcher (1982). (Fletcher's formulation lacks the estimated exponent that has been found to complicate estimation [Ricker 1975, p. 326].) Unfortunately, those formulations can not supply an analytical formulation similar to Equations 6 and 8, which means that numerical integration would have to be used, as in the GENPROD computer program of Pella and Tomlinson (1969). Another alternative would be to use a discrete-time model, rather than the continuous-time model presented here. Such models are simpler mathematically, but usually entail assumptions that the growth, recruitment, and catching seasons are brief. The logistic model was used here because it is a simple case, not because using other models would be impractical or inferior.

For what types of stocks are the models presented here appropriate? Research is lacking to answer this question definitively, but general comments are possible. One group of fishes for which production models seem to work well is the tropical tunas. These species are characterized by relatively fast growth, relatively constant recruitment, and reduced annual seasonality in the life processes. Density dependence in growth has been demonstrated in a related species, *Scomber japonicus* (Prager and MacCall, 1988); such plasticity in growth would allow the compensation inherent in a production model to be expressed in a way beyond recruitment variability. For modeling fish stocks with more seasonality in growth, reproduction, and harvest, a discrete-time production model might prove superior to the continuous-time model presented here.

In many fish stocks, recruitment is extremely variable. Ordinary production models may not work well when applied to stocks with large recruitment fluctuations that are unrelated to population size, especially when the catch–effort series is short. If recruitment fluctuations can be linked to external factors (such as variation in rainfall or sea–surface temperature), a production model incorporating these factors might work well (Freon, 1986). It would be simple to modify the logistic model to incorporate an environmental factor, perhaps as an influence on r on an annual basis.

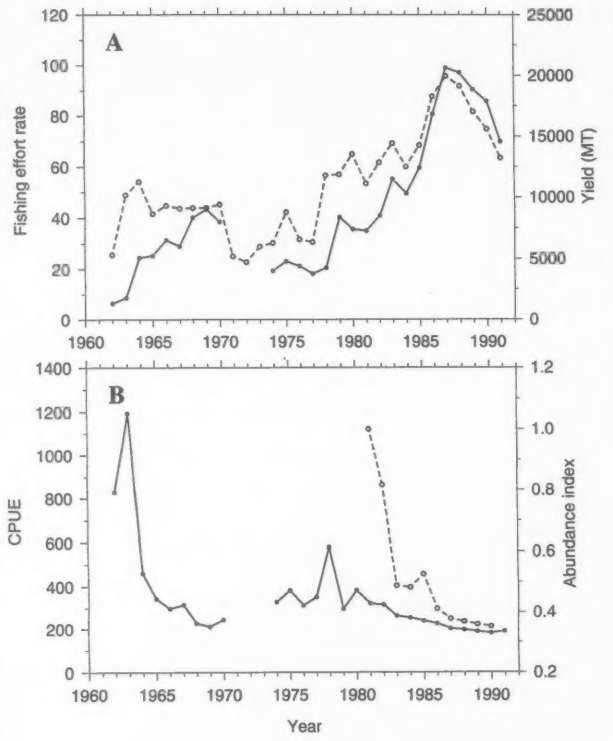

Figure 1

Data used to fit production model examples loosely based on swordfish, *Xiphias gladius* , in the North Atlantic Ocean. (**A**) Standardized effort rate (•) and total yield (○). (**B**) CPUE trajectory (•) computed from data in (A), and index of abundance (○) used to tune the second example. The index, which was used for illustrative purposes only, is not a good measure of total-stock abundance.

Other extensions

Many other extensions to the production model have been published. An incomplete list includes these: Fox (1975, 1977) presented a logistic production model with mixing of two stocks; Deriso (1980) and Hilborn (1990) demonstrated different methods of fitting production models to age-structured populations (but see also Ludwig and Walters, 1985); Freon (1986) introduced environmental variables into a production model that used the equilibrium assumption; Laloë (1989) and Die et al. (1990) incorporated fished area into production models; Polovina (1989) demonstrated a system of production models in which some parameters are common among models; and Hoenig and Warren (1990) demonstrated Bayesian

and empirical Bayes methods for fitting production models. Most of the extensions described by these investigators could be combined with techniques presented here (e.g. tuning, bootstrapping), as required for a particular analysis.

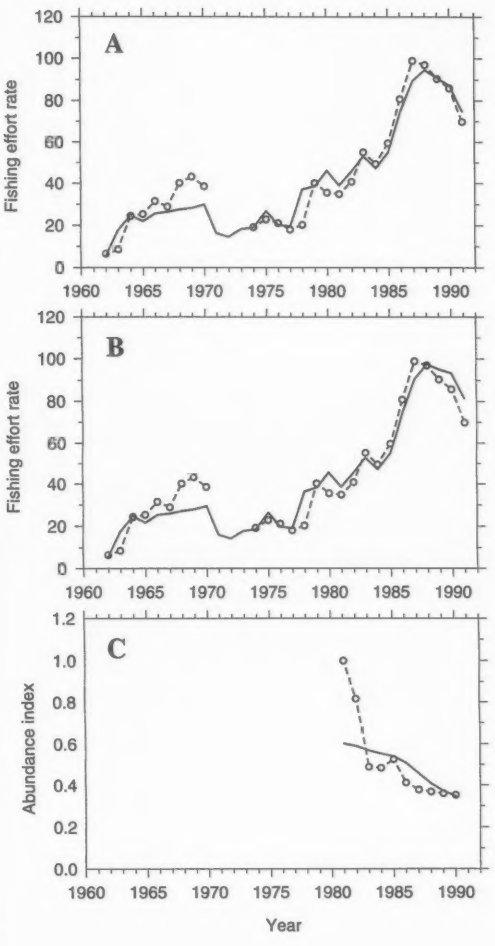

Figure 2

Goodness-of-fit of two production model analyses loosely based on swordfish, *Xiphias gladius*, in the North Atlantic Ocean. These analyses are illustrative and are not intended as an assessment of swordfish. Model 2 differs from Model 1 in being tuned to a hypothetical index of abundance. (**A**) Observed (o) and estimated (——) fishing effort rate from Model 1. (**B**) Observed (o) and estimated (——) effort rate from Model 2. (**C**) Observed (o) and estimated abundance-index from Model 2.

Autocorrelation

Because catch and effort data are usually autocorrelated, the residuals from fitting—whether computed in yield or effort—may also be autocorrelated. A matter of statistical concern is whether a method of fitting that takes the autocorrelation into account (such as one based on time-series analysis sensu Box and Jenkins [1976]) might be more appropriate. Some results relevant to this question were obtained by Ludwig et al. (1988) in a study that used two different objective functions to fit production models to simulated data. The first was a total-least-squares objective function, which did not take autocorrelation into account; the second, an approximate-likelihood objective function, which did. Ludwig et al. (1988) found that the two methods produced very similar estimates; the authors concluded that the added complexity of the approximate-likelihood method was probably not warranted. In addition, the approximate-likelihood method frequently failed to converge from poor starting values. This does not mean that autocorrelation should be ignored in all fisheries modeling; however, it was not a major concern in the study cited.

Process error

The model presented here assumes that the production of biomass is a deterministic function of the current biomass; stochasticity occurs only in the observation of catch or effort or in the relation of fishing effort to fishing mortality rate (if effort is being estimated from catch). In reality, production is undoubtedly stochastic to some degree. In recognition of this, fisheries models that explicitly incorporate process error have been developed (e.g. Ludwig et al., 1988; Sullivan, 1992). Because process errors are propagated forward in time, it would seem that time-series fisheries models (e.g. production models), should include corrections for process errors, so that the system can be modeled as correctly as possible.

Despite the undeniable logic of including process error in fisheries models, there are also negative aspects, and the practical merit of including process error in fisheries applications remains a topic for research. The theory of models including process error was largely developed in process control (Kalman, 1960), a field in which large data sets are common. Including both observation error and process error in a model generally entails either estimating a large number of nuisance parameters (the process errors), making strong assumptions about the form or value of the process error component, or both. In some cases, the need to estimate additional parameters can make it difficult or impossible to estimate parameters of interest, such as MSY, without additional

Table 2

Results of two bootstrapped production model analyses loosely based on swordfish, *Xiphias gladius,* in the North Atlantic Ocean. The base model used only yield and standardized effort data. The tuned model also used a hypothetical index of abundance (Table 1). Each conventional parameter estimate is designated $\hat{\theta}$, the corresponding bias-corrected estimate is designated $\hat{\theta}_{BC}$. Nonparametric bias-corrected 80% confidence intervals are derived from the bootstrap; as with most fishery analyses, these are conditional on correct model structure and probably underestimate true uncertainty (see text). The relative interquartile (IQ) range, a unitless measure of precision, is the 50% confidence interval divided by the median bias-corrected estimate. All results are rounded to three significant digits.

	Base model					Tuned model				
Quantity estimated	$\hat{\theta}$	$\hat{\theta}_{BC}$	80% lower CL	80% upper CL	Relative IQ range	$\hat{\theta}$	$\hat{\theta}_{BC}$	80% lower CL	80% upper CL	Relative IQ range
Management benchmarks										
MSY	13,800	13,700	11,800	15,100	11.8%	13,400	13,400	11,700	14,900	11.7%
F_{MSY}	0.257	0.259	0.161	0.393	45.3%	0.264	0.269	0.169	0.432	50.9%
f_{MSY}	72.6	71.1	61.7	82.2	14.5%	68.7	68.3	0.590	0.781	14.1%
B_{MSY}	53,800	53,100	37,400	79,700	40.7%	50,900	50,000	33,600	71,900	39.6%
B_{1992}/B_{MSY}	0.932	0.929	0.755	1.17	21.8%	0.829	0.820	0.650	1.01	23.6%
F_{1991}/F_{MSY}	1.03	1.03	0.750	1.32	28.3%	1.18	1.18	0.892	1.53	29.3%
Directly estimated parameters										
r	0.514	0.517	0.323	0.785	45.3%	0.528	0.537	0.337	0.865	50.9%
K	108,000	106,000	74,800	159,000	40.7%	102,000	100,000	67,200	144,000	39.6%
q	0.00354	0.00363	0.00236	0.00541	43.3%	0.00384	0.00393	0.00260	0.00612	45.7%

information or assumptions. (For an example, see Conser et al., 1992, and Prager, 1993). This would not be a serious objection if estimates made by models without process error were known to be severely flawed, but to my knowledge the fisheries literature includes no comprehensive comparisons of equivalent models with and without process error.

The work by Ludwig et al. (1988) does shed some light on this question, as their simulations and models included both types of error. The authors found that when observation error was ignored (its variance assumed to be zero) during parameter estimation, the resulting estimates were biased and resulted in an average loss in harvest value of at least 20%. In contrast, when the relative variance of the process error component was assumed to be half of its correct value, a substantially smaller loss in harvest value resulted. Unfortunately, Ludwig et al. (1988) did not present results for estimation under the assumption that process error was zero. Further research into estimation methods for systems with both process error and observation error would allow fishery scientists and managers to better balance complexity and accuracy in population models.

Precision of estimates

Production models tend to estimate some quantities much more precisely than others. Hilborn and Walters (1992) discuss this phenomenon at some length; the comments here reflect my own experiences. For most stocks, the main biological reference points (MSY, f_{MSY}) are estimated relatively precisely. However, absolute levels of stock biomass B_τ and fishing mortality rate F_τ are usually estimated much less precisely. This occurs because very few data sets contain sufficient information to estimate q well. (The example illustrates this point well—Table 2.) By dividing biomass and fishing–mortality estimates by estimates of the corresponding biological reference points, the effects of imprecision in estimating q can be removed. The relative levels thus obtained are useful measures in their own right: the relative level of biomass $\hat{B}_\tau / \hat{B}_{MSY}$ describes whether a population is above or below the level at which MSY can be obtained, and the relative level of fishing mortality rate $\hat{F}_\tau / \hat{F}_{MSY}$ suggests whether an increase or decrease in fishing effort might provide a higher sustainable yield.

When two or more catchability coefficients are estimated, ratios of catchability coefficients are typically estimated more precisely than the individual values of q. Thus it is possible to compare two different gears without being able to estimate very precisely the catchability of either one. If a parameterization involving K and r is used in fitting, the estimates of these quantities are usually quite impre-

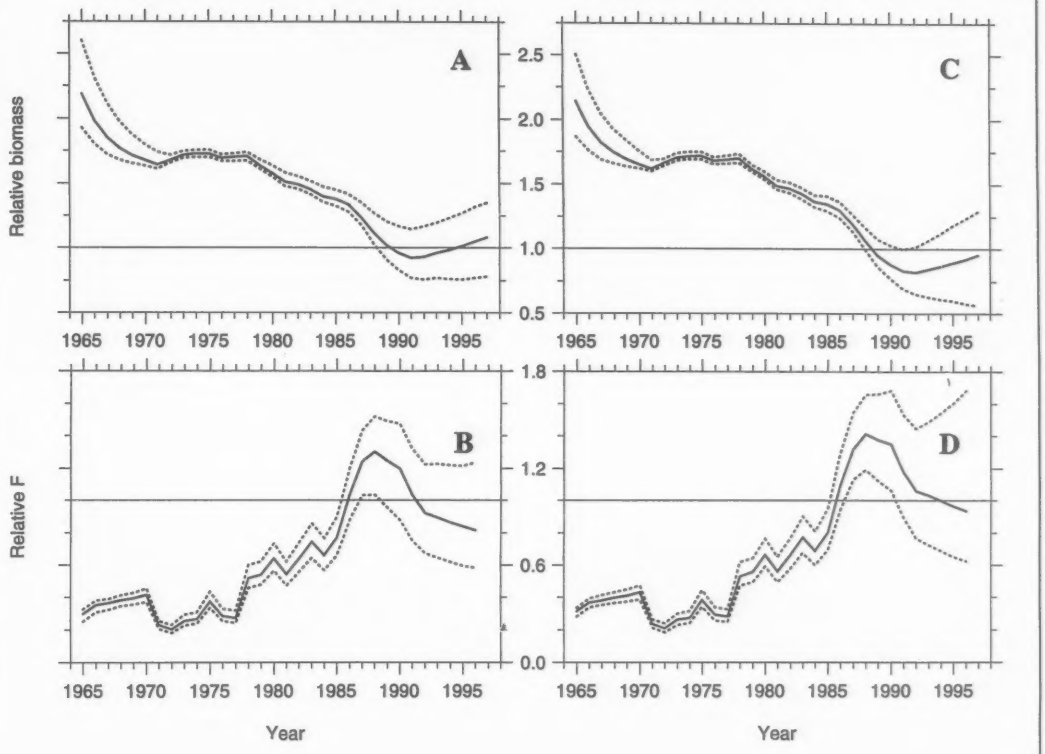

Figure 3

Estimated trajectories of relative biomass and relative fishing mortality rate from two production model analyses (including proposed yields from 1992 through 1996) loosely based on swordfish, *Xiphias gladius*, in the North Atlantic Ocean. These analyses are illustrative and are not intended as an assessment of swordfish. "Relative biomass" is the stock biomass divided by B_{MSY}, the biomass at which maximum sustainable yield (MSY) can be obtained; "relative fishing mortality rate" is the fishing mortality rate (F) divided by the rate (F_{MSY}) that yields MSY when the stock is at B_{MSY}. Production models estimate these relative quantities more precisely than the corresponding absolute quantities. Trajectories (——) are shown with approximate 80% confidence intervals (---) from the bootstrap. Model 2 differs from Model 1 in being tuned to a hypothetical index of abundance. Panels (**A**) and (**B**), estimates from Model 1; (**C**) and (**D**), estimates from Model 2.

cise, but because they are correlated, the corresponding estimates of MSY and optimum effort can nonetheless be quite precise.

The estimate of B_1, the starting biomass in the first year, is usually quite imprecise even when normalized to B_{MSY}. It is also my impression that it can be biased for some data sets, although this does not significantly affect relative biomass estimates beyond the first few years. I would therefore not recommend using a production model to draw any inferences about the population biomass during the first few (perhaps 2 to 4) years, unless auxiliary information is available. Such information might comprise a biomass index (for tuning) or knowledge to support using an assumption of the type $B_1 = sK$, where s is a proportionality constant known a priori. Punt, 1990, provides an example. This indeterminacy in production modeling is similar to the inability of sequential population (age-structured) analyses to say much about population dynamics in the most recent years unless auxiliary information is used. In practice, it does not seem to degrade the estimates of MSY and optimum effort when a reasonably long time series is used.

Validity of bias corrections and confidence intervals

Bootstrap confidence intervals are approximations, and bias-correction methods can at times worsen the

approximation. DiCiccio and Tibshirani (1987) demonstrate an example in which "the BC and BC_a methods seem to pull the percentile interval in the wrong direction and hence the coverage gets worse." (The BC_a method, due to Efron [1987], incorporates a second-order correction to the BC method.) In that example, bias correction for the point estimate would also have made it worse. The example presented by DiCiccio and Tibshirani (1987) (estimating the variance of a correlation coefficient, true value 0.9, from a data set of 15 observations) seems rather extreme, but it does serve to emphasize that model results, including estimated bias corrections, must not be accepted blindly.

Confidence intervals estimated by bootstrap methods entail fewer assumptions than those made by parametric methods, but most likely are still optimistic. In a study of an econometrics equation (including a lagged term) that was fit by generalized least squares with an estimated covariance matrix, Freedman and Peters (1984) found the bootstrap estimates of standard error far superior to those made with asymptotic assumptions. The bootstrap estimates were 20% to 30% too low, but estimates from asymptotic formulas were too low by factors of almost three. One reason for underestimation by the bootstrap was that, due to the effect of fitting, the residuals used for resampling were smaller than the true values of the disturbance term (Freedman and Peters, 1984). A suggested correction is given by Stine, 1990, p. 338.

There are other reasons why estimated confidence intervals for fisheries models are likely to be optimistic. The time frame encompassed by the data used to fit fisheries models is usually short and does not encompass the full range of environmental variation that can add unexplained variation to observed data. As the time series becomes longer, the random effects of environmental variation tend to become more extreme, making earlier confidence intervals appear overly optimistic (Steele and Henderson, 1984). Another cause of optimistic confidence intervals is the use of preliminary models (e.g. ANOVA) to construct abundance indices; such models tend to filter the indices and thus reduce apparent variance. There may also be systematic errors in the data (from, e.g. gradual changes in q or gradual or sudden changes in the proportion of the catch reported); these can bias the results, but the confidence intervals include only the effects of variability, not bias from model misspecification. Schenker (1985) stated that "bootstrap confidence intervals should be used with caution in complex problems." It is probably appropriate to consider estimated confidence intervals from fisheries population models to be, in general, minimum estimates.

Is there life after death?

The concept of maximum sustainable yield was given its epitaph about 15 years ago in a critical review by Larkin (1977). Notwithstanding the title of his paper, Larkin's main target was not the concept of MSY itself, but what he called the "religion" of applying MSY dogmatically to every stock. Undoubtedly, one must recognize that MSY is not an immutable quantity, and that model results should not be used dogmatically. However, compensation in population dynamics does give rise to some form of maximum sustainable yield. Whether MSY is estimable from the data available for a given stock, and whether it is a useful concept given the stock's dynamics, are reasonable questions that, even if answered in the negative, do not invalidate the concept of MSY.

In a response to Larkin's (1977) paper, Barber (1988) pointed out that MSY, far from being dead, was still in widespread use. Barber cited the utility of MSY as a formal management objective; its simplicity and ability to be understood by the fishing industry, administrators, and managers; and the grounding of the MSY concept in basic ecological theory. He concluded by repeating Holt's (1981) suggestion that MSY be considered part of a multi–faceted management scheme.

Shortly following Larkin's (1977) paper, Sissenwine (1978) discussed several shortcomings of MSY as the basis for optimum yield (OY), the "legally mandated immediate objective of marine fisheries management in the coastal waters of the United States beyond the territorial sea of the individual states." In this section, I address those items not discussed earlier. Sissenwine pointed out that it is difficult to estimate q, and that q may vary with population size. This difficulty might be overcome, to some degree, by the methods described earlier for estimating changes in q. More importantly, this problem is not unique to production models. The common use of CPUE series to tune age-structured models also requires strong assumptions about q. Indeed, because an age-structured model generally provides little information about a cohort before it has been substantially fished, its estimate of population biomass in a year close to the present may be more influenced by random variations in q than would a similar estimate from a production model.

Sissenwine (1978) made a number of criticisms of production models fit by equilibrium assumption. The methods described here do not use the equilibrium assumption and are not subject to those problems. Once the assumption is dropped, one is much less likely to get a good, but spurious, fit, when modeling a population whose dynamics are not approximated

by the model. This is an excellent reason (but not the only one) to avoid the equilibrium assumption.

A final important point raised by Sissenwine (1978) is that, because the world is stochastic, one is truly more interested in maximum average yield (MAY) than MSY. Several studies (Doubleday, 1976; May et al., 1978; Sissenwine, 1978) have shown that in general MAY < MSY; thus harvesting MSY indefinitely would lead to stock collapse. This result does not make production models less useful, but does emphasize the necessity to use their results in the context of other knowledge about the stock and as part of an evolving view of stock dynamics. Fishery assessment and management are dynamic processes that must adapt to changing conditions and new knowledge. It is inconceivable that we will ever know enough about any wild stock to establish a management regime that could be effective into the indefinite future. The failure of MSY to be such a regime is no failure at all.

Notes added in proof

1 I have recently been made aware of several production-model applications that were circulated in the Collected Papers of the International Commission on Southeast Atlantic Fisheries (ICSEAF). Pertinent documents include those by Butterworth et al., 1986; Andrew et al., 1989; and Punt, 1989.

2 Anyone attempting to implement the methods described here should be aware that Equation 6, when solved for F, can be double-valued.

Acknowledgments

I thank A. Anganuzzi, J. Bence, R. Deriso, A. Fonteneau, K. Hiramatsu, W. Lenarz, A. MacCall, R. Methot, C. Porch, J. Powers, A. Punt, W. Richards, G. Scott, P. Tomlinson, J. Zweifel, and two anonymous referees for comments on the manuscript or assistance with the techniques described. In addition, suggestions from J. Hoenig and V. Restrepo were particularly helpful in improving many parts of the work. Portions of this work result from research sponsored by NOAA Office of Sea Grant, U.S. Department of Commerce, under federal Grant No. NA90AA–D–SG045 to the Virginia Graduate Marine Science Consortium and the Virginia Sea Grant College Program.

Literature cited

Barber, W. E.
1988. Maximum sustainable yield lives on. N. Am. J. Fish. Manage. 8:153–157.

Box, G. E. P., and G. M. Jenkins.
1976. Time series analysis: forecasting and control, revised ed. Holden-Day, San Francisco.

Conser, R., J. M. Porter, and J. J. Hoey.
1992. Casting the Shepherd stock-production model in a statistical framework suitable for swordfish stock assessment and management advice. Int. Comm. Cons. Atl. Tunas (Madrid), Coll. Vol. Sci. Pap. 39:593–599.

Deriso, R. B.
1980. Harvesting strategies and parameter estimation for an age-structured model. Can. J. Fish. Aquat. Sci. 37:268–282.

Deriso, R. B., T. J. Quinn II, and P. R. Neal.
1985. Catch-age analysis with auxiliary information. Can. J. Fish. Aquat. Sci. 42:815–824.

DiCiccio, T., and R. Tibshirani.
1987. Bootstrap confidence intervals and bootstrap approximations. J. Am. Stat. Assn. 82:163–170.

Die, D. J., V. R. Restrepo, and W. W. Fox Jr.
1990. Equilibrium production models that incorporate fished area. Trans. Am. Fish. Soc. 119:445–454.

Doubleday, W. C.
1976. Environmental fluctuations and fisheries management. Int. Comm. Northw. Atl. Fish., Sel. Pap. 1:141–150.

Efron, B.
1982. The jackknife, the bootstrap, and other resampling plans. Society for Industrial and Applied Mathematics, Philadelphia, 92 p.
1987. Better bootstrap confidence intervals. J. Am. Stat. Assn. 82:171–200.

Efron, B., and G. Gong.
1983. A leisurely look at the bootstrap, the jackknife, and cross-validation. Am. Statistician 37:36–48.

Efron, B., and R. Tibshirani.
1986. Bootstrap methods for standard errors, confidence intervals, and other measures of statistical accuracy. Stat. Sci. 1:54–75.

Fletcher, R. I.
1982. A class of nonlinear productivity equations from fishery science and a new formulation. Math. Biosci. 61:279–293.

Fox, W. W., Jr.
1970. An exponential yield model for optimizing exploited fish populations. Trans. Am. Fish. Soc. 99:80–88.
1975. An overview of production modeling. Int. Comm. Cons. Atl. Tunas (Madrid), Coll. Vol. Sci. Pap. 3:142–156.
1977. Some effects of stock mixing on management decisions. Int. Comm. Whal. Rep. 27:277–279.

Freedman, D. A., and S. C. Peters.
1984. Bootstrapping a regression equation: some empirical results. J. Am. Stat. Assn. 79:97–106.

Freon, P.
1986. Introduction of environmental variables into global production models. Proc. Int. Symp. Long Term Changes Mar. Fish Pop., Vigo (Spain), p. 481–528.

Gavaris, S.
1988. An adaptive framework for the estimation of population size. Can. Atl. Fish. Sci. Adv. Comm., Res. Doc. 88/29.

Graham, M.
1935. Modern theory of exploiting a fishery, and application to North Sea trawling. J. Cons. Int. Explor. Mer 10:264–274.

Gulland, J. A.
1975. The stability of fish stocks. J. Cons. Int. Explor. Mer 37:199–204.

Hilborn, R.
1990. Estimating the parameters of full age-structured models from catch and abundance data. *In* L.-L. Low (ed.), Proceedings of the symposium on application of stock assessment techniques to gadids. Int. N. Pac. Fish. Comm. Bull. 50:207–213.

Hilborn, R., and C. J. Walters.
1992. Quantitative fisheries stock assessment: choice, dynamics, and uncertainty. Chapman and Hall, NY, 570 p.

Hinkley, D. V.
1978. Improving the jackknife with special reference to correlation estimation. Biometrika 65:13–21.

Hoenig, J. M., and W. G. Warren.
1990. Bayesian and related approaches to fitting stock production models. ICES CM-1990/D:13, 21 p.

Hoey, J. J., R. J. Conser, and A. R. Bertolino.
1989. The western north Atlantic swordfish. *In* W. J. Chandler (ed.), Audubon wildlife report 1989/1990, p. 456–477. Academic Press, San Diego.

Hoey, J. J., J. Mejuto, J. Porter, and Y. Uozumi.
1993. A standardized biomass index of abundance for North Atlantic swordfish. Int. Comm. Cons. Atl. Tunas (Madrid), Coll. Vol. Sci. Pap. 40:344–352.

Holt, S. J.
1981. Maximum sustainable yield and its application to whaling. *In* J. Gordon Clark (ed.), Mammals in the seas, vol. 3, p.22–55. FAO Fish. Ser. 5.

Kalman, R. E.
1960. A new approach to linear filtering and prediction problems. J. Basic Eng. 82:34–45.

Kennedy, P.
1979. A guide to econometrics. MIT Press, Cambridge, MA, 175 p.

Kingsland, S.
1982. The refractory model: the logistic curve and the history of population ecology. Q. Rev. Biol. 57:29–52.

Kizner, Z. I.
1991. Bootstrap estimation of the confidence intervals of stock and TAC assessments with the use of dynamic surplus production models. NAFO Sci. Coun. Studies 16: 149–152.

Laloë, F.
1989. Un modèle global avec quantité de biomasse inaccessible dépendand de la surface de pêche. Application aux données de la pêche d'albacore (*Thunnus albacares*) de l'Atlantique Est. Aquat. Liv. Res. 2:231–239.

Larkin, P. A.
1977. An epitaph for the concept of maximum sustained yield. Trans. Am. Fish. Soc. 106:1–11.

Lotka, A. J.
1924. Elements of physical biology. Reprinted 1956 as "Elements of mathematical biology" by Dover Press, NY, 465 p.

Ludwig, D., and C. J. Walters.
1985. Are age-structured models appropriate for catch-effort data? Can. J. Fish. Aquat. Sci. 42:1066–1072.

Ludwig, D., C. J. Walters, and J. Cooke.
1988. Comparison of two models and two estimation methods for catch and effort data. Nat. Res. Modeling 2:457–498.

MacCall, A. D.
1976. Density dependence of catchability coefficient in the California Pacific sardine, *Sardinops sagax caerulea*, purse seine fishery. Calif. Coop. Ocean. Fish. Invest. Rep. 18:136–148

Marquardt, D. W.
1963. An algorithm for least squares estimation of nonlinear parameters. J. Soc. Ind. Appl. Math. 2:431–441.

May, R. M., J. R. Beddington, J. W. Horwood, and J. G. Shepherd.
1978. Exploiting natural populations in an uncertain world. Math. Biosci. 42:219–252

Methot, R. M.
1989. Synthetic estimates of historical abundance and mortality for northern anchovy. Am. Fish. Soc. Symp. 6:66–82.
1990. Synthesis model: an adaptable framework for analysis of diverse stock assessment data. *In* L.-L. Low (ed.), Proceedings of the symposium on application of stock assessment techniques to gadids, p. 259–277. ICNAF Bull. 50.

Nelder, J. A., and R. Mead.
1965. A simplex method for function minimization. Comp. J. 7:308–313.

Noreen, E. W.
1989. Computer–intensive methods for testing hypotheses: an introduction. John Wiley & Sons, NY, 229 p.

Paloheimo, J. E., and L. M. Dickie.
1964. Abundance and fishing success. Rapp. P.–v. Réun. Cons. int. Explor. Mer 155:152–163.

Parrack, M. L.
1986. A method of analyzing catches and abundance indices from a fishery. Int. Comm. Cons. Atl. Tunas (Madrid), Coll. Vol. Sci. Pap. 24:209–221.

Pearl, R., and L. J. Reed.
1920. On the rate of growth of the population of the United States since 1790 and its mathematical representation. Proc. Nat. Acad. Sci. U.S.A. 6:275–288.

Pella, J. J.
1967. A study of methods to estimate the Schaefer model parameters with special reference to the yellowfin tuna fishery in the eastern tropical Pacific ocean. Ph.D. diss., Univ. of Washington, Seattle, 156 p.

Pella, J. J. and P. K. Tomlinson.
1969. A generalized stock production model. Bull. Inter-Am. Trop. Tuna Comm. 13:419–496.

Peterman, R. M., and G. Steer.
1981. Relation between sport-fishing catchability coefficients and salmon abundance. Trans. Am. Fish. Soc. 110:585–593.

Polovina, J. J.
1989. A system of simultaneous dynamic production and forecast models for multispecies or multiarea applications. Can. J. Fish. Aquat. Sci. 46:961–963.

Prager, M. H.
1993. A nonequilibrium production model of swordfish: data reanalysis and possible further directions. Int. Comm. Cons. Atl. Tunas (Madrid), Coll. Vol. Sci. Pap. 40:433–437.

Prager, M. H., and A. D. MacCall.
1988. Revised estimates of historical spawning biomass of the Pacific mackerel, *Scomber japonicus*. Calif. Coop. Ocean. Fish. Invest. Rep. 29:81–90.

Press, W. H., B. P. Flannery, S. A. Teukolsky, and W. T. Vetterling.
1986. Numerical recipes: the art of scientific computing. Cambridge Univ. Press, Cambridge, 818 p.

Punt, A. E.
1990. Is $B_1 = K$ an appropriate assumption when applying an observation error production-model estimator to catch-effort data? S. Afr. J. Mar. Sci. 9:249–259.

Ricker, W. E.
1975. Computation and interpretation of biological statistics of fish populations. Bull. Fish. Res. Board Can. 191, 382 p.

Rivard, D., and L. J. Bledsoe.
1978. Parameter estimation for the Pella-Tomlinson stock production model under nonequilibrium conditions. Fish. Bull. 76:523–534.

Robertson, T. B.
1923. The chemical basis of growth and senescence. J. B. Lippincott, Philadelphia.

Schaefer, M. B.
1954. Some aspects of the dynamics of populations important to the management of the commercial marine fisheries. Bull. Inter-Am. Trop. Tuna Comm. 1(2):27–56.
1957. A study of the dynamics of the fishery for yellowfin tuna in the eastern tropical Pacific Ocean. Bull. Inter-Am. Trop. Tuna Comm. 2:247–268.

Schenker, N.
1985. Qualms about bootstrap confidence intervals. J. Am. Stat. Assn. 80:360–361.

Schnute, J.
1977. Improved estimates from the Schaefer production model: theoretical considerations. J. Fish. Res. Board Can. 34:583–603.
1989. The influence of statistical error on stock assessment: illustrations from Schaefer's model. *In* R. J. Beamish and G. A. McFarlane (eds.), Effects of ocean variability on recruitment and an evaluation of parameters used in stock assessment models, p. 101–109. Can. Spec. Publ. Fish. Aquat. Sci. 108.

Scott, G. P., V. R. Restrepo, and A. Bertolino.
1992. Standardized catch rates for swordfish (*Xiphias gladius*) from the U.S. longline fleet through 1990. Int. Comm. Cons. Atl. Tunas (Madrid), Coll. Vol. Sci. Pap. 39:554–571.

Seber, G. A. F., and C. J. Wild.
1989. Nonlinear regression. John Wiley & Sons, NY, 768 p.

Sissenwine, M. P.
1978. Is MSY an adequate foundation for optimum yield? Fisheries 3(6):22–42.

Steele, J. H., and E. W. Henderson.
1984. Modeling long–term fluctuations in fish stocks. Science 224:985–987.

Stine, R.
1990. An introduction to bootstrap methods: examples and ideas. *In* J. Fox and J. S. Long (eds.), Modern methods of data analysis, p. 325–373. Sage Publs., Newbury Park, CA, 446 p.

Sullivan, P. J.
1992. A Kalman filter approach to catch-at-length analysis. Biometrics 48:237–257.

Thiel, H.
1971. Principles of econometrics. John Wiley & Sons, NY, 736 p.

Verhulst, P.-F.
1845. Recherches mathématiques sur la loi d'accroissement de la population. Mem. Acad. Roy. Belg. 18:1–38.

Winters, G. H., and J. P. Wheeler.
1985. Interaction between stock area, stock abundance, and catchability coefficient. Can. J. Fish. Aquat. Sci. 42:989–998.

Experimental outplanting of juvenile queen conch, *Strombus gigas*: comparison of wild and hatchery-reared stocks

Allan W. Stoner
Megan Davis
Caribbean Marine Research Center, 805 E. 46th Place
Vero Beach, FL 32963

Abstract.—Stock enhancement with hatchery-reared juvenile queen conch, *Strombus gigas* L., has been suggested as a means to rehabilitate overfished populations in Florida and the Caribbean region. A 15-month field experiment was conducted in the Bahamas to compare the survival, growth, morphology, and behavior of hatchery-reared and wild juvenile conch (85–120 mm shell length). Two experimental sites were established. Site C1 contained a resident conch population whereas few conch occurred naturally at site C2. Survival was higher for wild conch than for hatchery-reared conch. After 7 months, 28% of the original wild conch were recovered compared with only 9% of the hatchery-reared conch. Thin shells, short spines, and low burial frequency in hatchery-reared conch may have caused them to be more vulnerable to predators. In a tethering experiment, about twice as many hatchery conch were killed as wild conch, but the difference was not significant inside enclosures. Survivorship was higher at the site with resident juveniles, probably because of density-dependent protection from predation. After a period of high mortality in free-ranging conch during the first two months, tag recovery curves for both stock types reached a plateau. Also, near the end of the study, shell characteristics of wild and hatchery conch were identical as was survivorship. Analysis of movement patterns indicated that both stock types moved toward the natural population center. Although survivorship was higher at the site with resident conch, growth rates for both stock types were often lower at this site. Algal foods may have been more abundant at the site without conch because of lower grazing pressure. Athough highest mean daily growth occurred at 1.0 conch·m^{-2}, growth rates of conch enclosed at 0.5, 1.0, and 2.5 individuals·m^{-2} were not significantly different in most cases. Growth rates were higher for wild conch than for hatchery conch. In summer, free-ranging and tethered wild conch grew twice as fast as hatchery-reared conch. Success in rehabilitating depleted queen conch populations will require the release of high quality, hatchery-reared juveniles in large numbers in appropriate habitats.

Manuscript accepted 4 October 1993
Fishery Bulletin 92:390–411 (1994)

Widespread depletion of natural fishery stocks, particularly in inshore coastal and estuarine habitats, has resulted in increasing interest in enhancement and restoration of wild populations through releases of hatchery-reared individuals. Among the molluscs, relatively sedentary bivalves such as oysters, *Crassostrea* spp. (Burrell et al., 1981; Goodwin[1]), clams, *Mercenaria mercenaria* (Flagg and Malouf, 1983), mussels, *Mytilus edulis* (Dare and Edwards, 1976), and giant clams, *Tridacna* spp. (Heslinga et al., 1984; Heslinga and Watson, 1985) have been restocked most successfully. Experimental reseeding of scallops, *Argopecten* and *Patinopecten* spp. (Saito, 1984; Aoyama, 1989; Tettelbach and Wenczel, 1991) and abalone, *Haliotis* spp. (Kojima, 1981; Saito, 1984; Uki, 1984; Searcy and Salas, 1985; Tegner and Butler,1985; Tong et al., 1987; Ebert, 1989; Emmett and Jamieson, 1989) also show promise.

Queen conch, *Strombus gigas*, is one of the most important fishery species in the Caribbean region (Brownell and Stevely, 1981; Berg and Olsen, 1989), with an estimated annual value of 30 million U.S. dollars (Appeldoorn and Rodriquez, 1993). Heavy fishing for queen conch in shallow water habitats has resulted in a decline of this species throughout most of its biogeographic range (Appeldoorn et al.,1987; Appeldoorn and Rodriguez, 1993), and the U.S. fishery has been closed completely since 1986 (Berg and Olsen, 1989). Mariculture has been suggested as a way to rehabilitate queen conch populations (Berg, 1976; Siddall, 1984a; Davis et al., 1987), and research efforts during the past two decades have made it possible to culture large numbers of juvenile conch for stock enhancement (Brownell, 1977; Ballantine and Appeldoorn, 1983; Hensen, 1983; Laughlin and Weil, 1983; Cruz, 1986; Davis et al., 1987; Heyman et al., 1989; Creswell,1993; Davis, 1993). Unfortunately, field outplants of hatchery-reared stock have met with little success because of very high mortality (Appeldoorn and Ballantine, 1983; Laughlin and Weil, 1983; Appeldoorn, 1985; Marshall et al., 1993; Dalton, 1993). Also, little is known about the relative viability of wild and hatchery-reared conch.

This study uses a large-scale outplant experiment, together with enclosure and tether experiments, to compare the survival, growth, morphology, and behavior of hatchery-reared and wild juvenile conch released into a well-studied nursery

[1] Goodwin, W.F. 1981 Use of seed oysters to supplement oyster production in southern North Carolina. Report, North Carolina Division of Marine Fisheries, NCDMF - Project - 2/314-R, 109 p.

site (Stoner and Sandt, 1991, 1992). This research provides further insight into the potential for using cultured conch in a stock enhancement program, and elucidates possible limitations.

Methods and materials

Site description

During the 15–month period from March 1990 to May 1991, all field outplant, enclosure, and tether experiments were carried out at two different sites designated C1 and C2 (Fig. 1). The study sites, each a 100–m square area delineated by buoys, were located 0.8 km west of Children's Bay Cay and 5.0 km southeast of the Caribbean Marine Research Center field station on Lee Stocking Island, in the southern Exuma Cays, Bahamas (lat. 23°44.5'N, long. 76°04.4'W) (Fig. 2). A shallow sand bank is to the southwest. The two sites are in a homogeneous seagrass meadow of *Thalassia testudinum* with moderate shoot density (500–700 shoots·m^{-2}) in 3.2 m depth. Tidal currents run northwest (flood) and southeast (ebb) at velocities to 50 cm·sec^{-1} with a tidal range of approximately 1.0 m. Clear water from the Exuma Sound flows over the sites on flood tides, resulting in high underwater visibility that facilitated field experiments and recovery of tagged conch.

Site C1 was established within a well-studied queen conch nursery area that has carried as many as 500,000 individuals in densities between 0.5 and 2.0 conch·m^{-2} since at least 1984 (Wicklund et al., 1991; Stoner et al. 1993, unpubl. data). Site C1 has been the location of numerous investigations on conch mass migration (Stoner et al., 1988; Stoner 1989a), distribution (Stoner and Waite, 1990), and diet (Stoner and Waite, 1991).

Site C2 was approximately 0.3 km to the southeast of site C1 and had very few juvenile conch (< 0.05 conch·m^{-2}). In 1988, small-scale transplants in enclosures showed that young conch survived and grew at nearly identical rates at sites C1 and C2 despite the absence of wild conch at the latter (Stoner and Sandt, 1992). This suggested that certain unpopulated areas of the extensive seagrass meadows in the Exuma Cays could support outplanted conch stocks.

Density estimates were obtained by counting the conch (tagged and untagged) in as many as 20 haphazardly placed circles of 4-m radius at each site at five different times during the experiment. The purpose of these estimates was to assess the natural population of conch prior to the transplant, to exam-

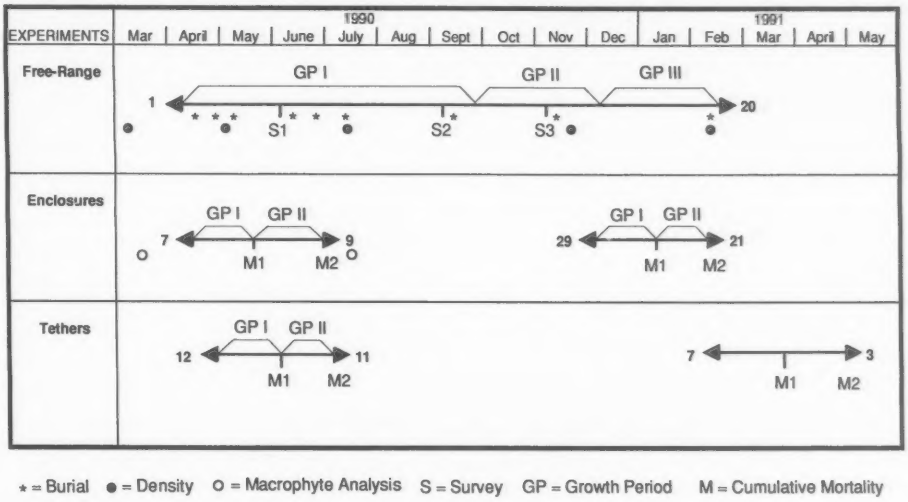

Figure 1

Calendar of free-ranging, enclosure, and tether experiments; showing duration of experiments, data collection points, and time periods for growth and mortality of queen conch, *Strombus gigas*. The total study period extended from March 1990 to May 1991. See text for descriptions of the measurements and experiments.

ine the density of conch at the end of the experiment, and to observe movements by the population. On each date up to 100 conch were measured for shell length (apex to siphonal canal).

Seawater temperature for the study site was recorded with a Ryan Temp Mentor placed on the bottom between sites C1 and C2. Temperature was recorded (+ 0.2°C) every 30 minutes, and seven-day mean temperatures were calculated for plotting (Fig. 3).

Experimental animals

Approximately 6,000 wild and 6,000 hatchery-reared conch were used in the experiments described below. Wild conch were collected from the Children's Bay Cay nursery site (C1); all were between 85 and 120 mm shell length (SL). Hatchery-reared conch were purchased from Tradewind Industries, Ltd. (Caicos Conch Farm) in Providenciales, Turks, and Caicos Islands. These conch originated from 12 egg masses collected near Providenciales in the summer of 1988. The larvae were fed with Caicos *Isochrysis* and postlarvae with flocculated *Chaetoceras gracilis* and blended *Enteromorpha* sp. (Davis et al., 1992). Between December 1988 and March 1989, 50-mm juveniles were transplanted to a protected nursery habitat near the hatchery (Davis and Dalton, 1991).

Between 26 and 29 March 1990, 6,000 hatchery-reared conch comparable in size to the 1+ year class conch native to Children's Bay Cay nursery (85–120 mm SL)(Table 1) were collected from the grow-out area and held in two 8 × 8 m holding pens. On the morning of 30 March the conch were loaded into 32 large burlap sacks wrapped in plastic bags and transported via cargo plane to Lee Stocking Island. The conch were kept cool and moist during the 7-hour period out of the water. Upon arrival, conch were immediately taken to either site C1 or C2. The plastic was removed and the burlap bags were placed on the bottom of the respective sites. On 31 March they were released into two temporary pens (10 m^2) already constructed at each of the study sites. All hatchery-reared conch were tagged and measured over the next 10 days. Wild conch were tagged and placed in temporary pens during a 10-day period prior to the arrival of the hatchery-reared conch.

All conch were marked with orange spaghetti tags (Floy Manufacturing Co.) tied around the spire, and total shell length was measured to the nearest millimeter (±1 mm) with calipers. Tags were both letter coded and numbered so that conch type and release site could be identified immediately in the field.

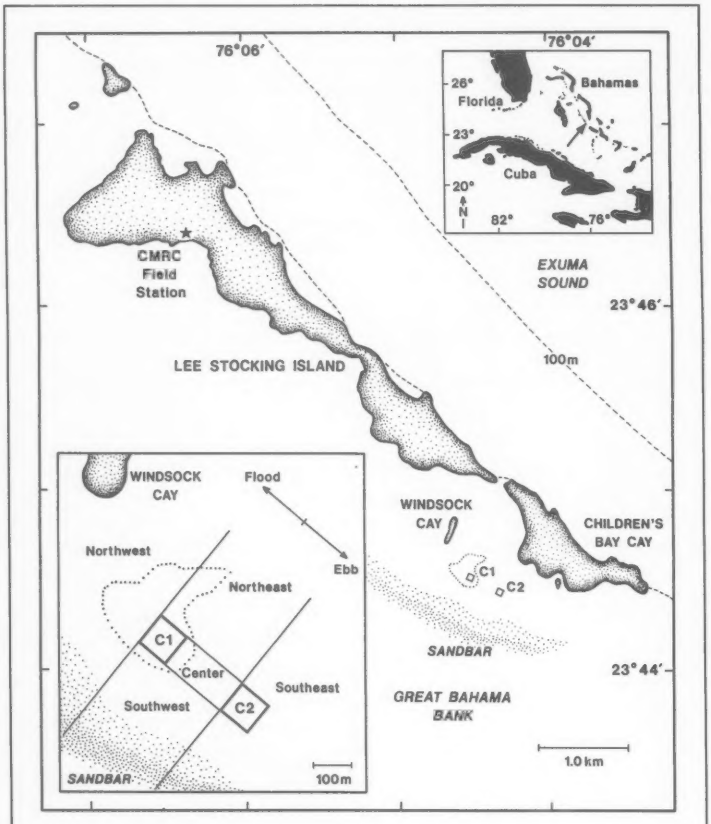

Figure 2

Map of Lee Stocking Island and Children's Bay Cay in the southern Exuma Cays, Bahamas. Study sites C1 and C2 are shown as squares, the dotted line around C1 represents the approximate boundaries of the natural queen conch, *Strombus gigas*, population in July 1990. The lower insert shows the geographic zones surveyed during each tag recovery.

Free-ranging experiment

Hatchery-reared and wild tagged conch were haphazardly released throughout each of the two 100 m × 100 m experimental sites (C1 and C2) to examine survivorship, growth, morphology, and behavior of free-ranging juveniles between 1 April 1990 and 20 February 1991. The size ranges for hatchery and

wild conch released at site C1 were 80–117 mm SL (mean=102, SD=8, n=2,552) and 85–117 mm SL (mean=100, SD=7, n=2,543), respectively. For site C2, the size ranges for hatchery and wild conch were 80–117 mm SL (mean=101, SD=8, n=2,540) and 83–117 mm SL (mean=101, SD=6, n =2,490), respectively.

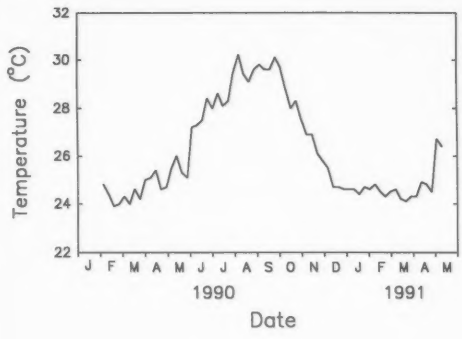

Figure 3

Bottom-water temperature recorded between sites C1 and C2, during the study period. Seven-day averages for recordings made every 30 minutes are plotted.

Table 1

Density of juvenile queen conch (*Strombus gigas*) in two field sites (C1 and C2) prior to the release of tagged conch (2 Mar. 1990), during the release experiment, and at the end of the experiment (21 Feb. 1991). Density was measured by counting conch, including tagged conch, in up to 20 randomly-selected 4-m diameter circles (50 m^2) at each site. Mean shell length for up to 100 individuals was measured for conch found in each survey. Values are mean ± SD (n).

Date	Number of plots	Density (mm)	Shell length (no./m^2)
Site C1			
2 Mar 90	20	0.26 + 0.12	105 + 14 (100)
2 May 90	20	1.27 + 1.01	n/a
16 Jul 90	20	0.66 + 0.31	111 + 12 (100)
27 Nov 90	5	0.22 + 0.12	113 + 16 (55)
21 Feb 91	6	0.19 + 0.19	129 + 13 (56)
Site C2			
2 Mar 90	20	0.01 + 0.01	99 + 14 (9)
2 May 90	20	0.03 + 0.03	n/a
16 Jul 90	20	0.62 + 0.74	119 + 10 (100)

Tag recovery Tag recapture surveys were conducted in June, September, and November 1990, to provide a relative index of survivorship over time and space. Searches encompassed the transplant sites, the zone between the sites, and adjacent seagrass and sand habitats. The search area was sectioned arbitrarily (see insert, Fig. 2), and several divers using snorkel or SCUBA gear drifted repeatedly side by side over the area using the flood tidal current for transport. Conch location was recorded by section, and searches continued until no additional conch were found. After each survey, all recaptured conch were returned to their original transplant sites (C1 or C2). Because very few hatchery-reared conch remained alive in February 1991, collections were made for shell growth and morphology, but the complete survey was not conducted.

Tag recovery does not measure absolute survivorship because of potential emigration from the study site and possible inefficiency in finding tagged animals; however, the search effort was intensive, and clear water (usually >10 m horizontal visibility) facilitated the efficiency of the searches. In two blind tests 87 and 92% of 200 uniquely tagged conch were recovered by using standard search procedure (unpubl. data). The surveys were conducted over periods from 7 to 20 days depending upon the number of divers available. Because of known limitations, tag recovery data were used as a relative indicator of survivorship in the two stock types and two study sites.

Growth Seasonal growth rates (mm·day^{-1}) were determined for three periods: summer (April to September 1990), fall (September to November 1990), and winter (November 1990 to February 1991) by comparing shell lengths of individual, tagged conch at the beginning and end of the survey periods.

Shell morphology At the beginning (1 April 1990) and end of the experiment (20 February 1991), representative samples of at least 30 hatchery-reared and 30 wild conch (collected alive) were measured for shell length and width, and shell and tissue weight. Maximum shell width was the distance between the last complete spine formed near the shell aperture and the spine on the opposite side of the shell. Total weight of the shell and soft tissue (live weight) was recorded to the nearest 0.01 g. After freezing and subsequent thawing, the soft tissue of the animal was extracted, lightly blotted, and weighed. Weights of the clean, air-dried shells were also recorded.

Behavior Nine times during the study, observations on burial behavior were made for the first 30 hatch-

ery-reared and 30 wild conch (tagged individuals) at each outplant site. Burial frequency was quantified as the percentage of conch that had at least part of the shell buried in the sediment, detritus, or algae. Counts for the two sites were pooled for each of the conch types. General observations on locomotory activity were also recorded.

Data from the tag recovery surveys provided information on the movements of free-ranging conch. During each tag recovery the type (wild or hatchery-reared), initial site of transplant (C1 or C2), and number of tagged conch found in different regions around the initial release sites (Fig. 2) were recorded. The total number of conch found in each survey was used to calculate the percentage of hatchery or wild conch from site C1 or C2 in each area surveyed.

Enclosure experiments

Experiment I Enclosure experiments were designed to determine the significance of density-dependent growth and survival of hatchery-reared and wild conch in identical habitats. The first 3-month experiment was conducted from 7 April to 9 July 1990. At each site (C1 and C2) 12 circular pens (30 cm high, 20 m^2) without covers were constructed of vinyl coated wire mesh (2.5 × 5.0 cm). Prior to the experiment (23 February–12 March) three haphazardly placed 25 × 25 cm quadrants per cage were sampled for *Thalassia testudium* components to ensure habitat similarity among the pens, both within and between stations. In each quadrant, seagrass shoot density was estimated, and all above-ground parts were collected into 3–mm mesh nylon bags. Living blades and detritus were separated in the laboratory, dried at 80°C and weighed. Detritus measurements were made again at the end of the experiment (9–13 July 1990) to test for potential depletion of this important food source.

At each site tagged hatchery and wild conch were placed in pens at three different densities, in two random blocks. Stocking densities, spanning the high range of natural densitites in the wild, were 0.5, 1.0, and 2.5 conch·m^{-2} (10, 20, 49 conch·pen^{-1}). The size ranges for hatchery-reared and wild conch were 90–109 mm SL (mean=100, SD=3) and 92–115 mm SL (mean=102, SD=3), respectively. Before stocking the pens with experimental conch, all visible epibenthic predators such as tulip snails, *Fasciolaria tulipa*, apple murex, *Murex pomum*, and the giant hermit crab, *Petrochirus diogenes*, and sea urchins *Tripneustes esculentus* were removed. Every two weeks throughout the experiment, dead conch were replaced to ensure constant density; replacements were not used in growth and survivorship measurements.

Cumulative mortality was calculated by subtracting the number of live conch remaining from the initial loading number. Mortality was examined statistically at the midpoint (day 37) and at the end (day 93) of the experiment. Shell length was measured at the start, near the middle (day 37), and at the end (day 93) of the experiment, and growth rates were calculated for the two periods.

Experiment II A second 3-month enclosure experiment was conducted at sites C1 and C2 to compare survival and growth of hatchery-reared and wild conch in the winter (29 November 1990–21 February 1991). Enclosures built for experiment I were reused in this experiment after having been clear of conch since July 1990. Four enclosures at each site were stocked with 10 hatchery-reared and 10 wild conch (1.0 conch·m^{-2}) gathered from the surrounding free-ranging populations. This density was chosen because highest mean growth rates frequently occurred at this density in enclosure experiment I. The initial size of the hatchery-reared conch ranged from 104–130 mm SL (mean=118, SD=5) and the wild conch ranged from 109–134 mm SL (mean=122, SD=5).

Dead conch were replaced with similar sized free-ranging conch every two weeks. As in the first experiment cumulative mortality and growth rates were determined only for the original stock, not the replacements. Mortality was calculated five times throughout the experiment, and analyzed statistically at the midpoint (day 35) and end (day 84) of the experiment. Growth rates were calculated for two growth periods, 29 November 1990 to 3 January 1991 and 3 January to 21 February 1991.

Tether experiments

Experiment I The first three-month tethering experiment was conducted during the summer (12 April to 11 July 1990) at sites C1 and C2 to examine survivorship, tag effects, and growth rates. The size ranges for hatchery-reared and wild conch were 82–116 mm SL (mean=100, SD=9) and 89–115 mm SL (mean=101, SD=6), respectively. Each conch was secured to a 0.5-m long stainless steel welding rod by a 1 m length of 20-lb test monofilament line that was attached to the shell spire with a clear nylon cable tie. The tether rods were marked with uniquely numbered tags and pushed 40 cm into the substratum approximately 2 m apart. Conch were tethered in four rows of 20 individuals. Each row contained 10 hatchery-reared conch and 10 wild conch in an alternating pattern. For each type of conch, the shell of every second individual was tagged to determine potential tagging effects on conch mortality in the free-ranging experiment.

Cumulative mortality was examined by using the same procedure as enclosure experiment I. Mortality was calculated three times throughout the experiment, and analyzed statistically at the midpoint (day 45) and end (day 90) of the experiment. Growth rates were calculated for two growth periods: 12 April to 27 May and 27 May to 11 July 1990.

Experiment II The second 3-month tethering experiment was conducted during the winter (7 February–3 May 1991) at site C1. Too few of the original hatchery-reared conch remained alive to set up the experiment at the second site. Hatchery-reared conch ranged from 100 to138 mm SL (mean=116, SD=8), and wild conch were 111–133 mm SL (mean=124, SD=5). Tethers were set up as in experiment I with four replicated rows of 20 individuals (10 hatchery-reared and 10 wild conch), except the conch themselves were not tagged. The conch were checked for mortality three times during the experiment and analyzed statistically at days 42 and 84.

Because cable ties were secured behind long apical spines, escape from tether apparatus would be possible only in the event of failure in the cable tie, monofilament line, or connections. Failure appears to be unlikely because nearly all kills observed in this study were found as empty shells attached to the tether apparatus or as crushed shells within 1 m of the original location.

Data Analysis

Analysis of variance (ANOVA), following the guidelines of Day and Quinn (1989), was used extensively in the interpretation of growth and mortality data. The statistical procedures started with full model ANOVA that included all independent effects. When interactions were significant, one- or two-way ANOVAs were performed to examine the effects of site and stock type, the variables most critical in this study. For brevity, non-significant interaction terms in multiple-way ANOVAs are not addressed in the text but are reported in tables. Mortality data were normally examined at the mid-point of individual experiments and at the end.

Cochran's test was used to test for homogeneity of variances. Log and arcsine transformations of data were used in some cases to remove heteroscedasticity; these are noted in the text. Where repeated measurements were made within one experimental enclosure (i.e. growth rates determined for conch in one pen), mean growth rates in the enclosures were used as replicates rather than individual measurements to eliminate pseudoreplication (Hurlburt, 1984). Analysis of covariance (ANCOVA) was used to test for differences in morphological characteristics (shell weight, shell diameter, and tissue weight) between hatchery-reared and wild conch. Shell length was the covariate.

After release, tagged, free-ranging conch dispersed from the initial 1-ha study sites. Chi-square analysis was used to compare dispersion of the two stock types, where the distribution of tagged wild conch was used for the expected frequency in different survey zones.

Results

Conditions at the outplant sites

During the 15–month study period, bottom-water temperature ranged from 24°C in February 1990 to 30°C in late September 1991, then declined rapidly and remained between 24 and 25°C until early May, when temperature rose to 27°C (Fig. 3).

Density estimates made 1 month prior to the beginning of the free-ranging experiment (2 March 1990) showed that the density of conch at site C1 was 16 times higher than at site C2 (Table 1). Between March and May, conch density at site C1 increased to over 1.2 conch·m^{-2}, owing to immigration of the natural population. Transplanted conch from the free-ranging experiment made up 7–15% of the conch in the density estimates; however, on 2 May 1990, transplanted conch accounted for 88% of estimated density. In July, there were nearly equal densities of conch at sites C1 and C2, but in November 1990 and February 1991, densities were close to the original values first observed in March 1990. This may be due to directional changes in movement of conch (towards the northeast) during the winter, which took them away from the transplant sites C1 and C2 (see Behavior).

As expected, shell length measurements taken during the density surveys show an increase in length over time for wild conch tagged at C1 (from mean=105 ± 14 SD in March 1990 to mean=129 ± 13 SD in February 1991)(Table 1). This represents an overall growth rate of 0.07 mm·day^{-1}, similar to that measured in free-ranging tagged conch. No growth rate was calculated for C2, because density surveys yielded low numbers; however, the mean sizes appear to be comparable to those measured at site C1 (Table 1).

Handling and tag effects

Transporting hatchery-reared conch appeared to have little adverse effect on their subsequent survivorship in the field. Conch were left out of water for 7 hours, and all remained alive during the 7 days after transport while they were tagged and placed in enclosures for Experiment I.

Table 2

Mortality of tagged and untagged queen conch (*Strombus gigas*) on tethers at the two experimental sites. Ten tagged and ten untagged conch were tethered in each of four replicate blocks at each site. Values are mean percent mortality ± SD (number of dead conch).

	Mortality	
Site	Tagged	Untagged
C1	52.5 ± 12.6 (21)	45.0 ± 12.9 (18)
C2	40.0 ± 21.6 (16)	52.5 ± 9.6 (21)

In the first tethering experiment percent mortalities (arcsine-transformed) did not differ among any of the tag and site treatments (Table 2) (ANOVA, $F_{3,12}$=0.722, P =0.558 for C1; $F_{3,12}$=0.679, P =0.581 for C2).

Free-ranging experiment

Tag recovery Tag recapture rates for free-ranging juvenile conch were related to both stock type and location (Table 3, Fig. 4). Exhaustive searches in and beyond the study area recovered all visible live conch, and there is no reason to believe that hatchery conch were seen and collected by the divers less often than wild conch. In fact, wild conch had burial rates higher than hatchery conch (see Behavior); therefore, the reverse bias is more likely.

In November 1990, approximately 7.5 months after initial release, 206 of hatchery-reared conch were recovered from site C1 and 248 from C2, an overall recapture of 9% of the original release (Fig. 4). Recoveries of wild conch from sites C1 and C2 numbered 542 and 820 conch, respectively, an overall recapture rate of 28%. The highest proportion of loss occurred during the first two months (April and May 1990). After May, recovery curves for both hatchery and wild conch leveled off at both sites. Tag recapture was consistently higher for wild conch released at site C2 (34% at experiment end) than for those released at C1 (22%), despite the presence of large num-

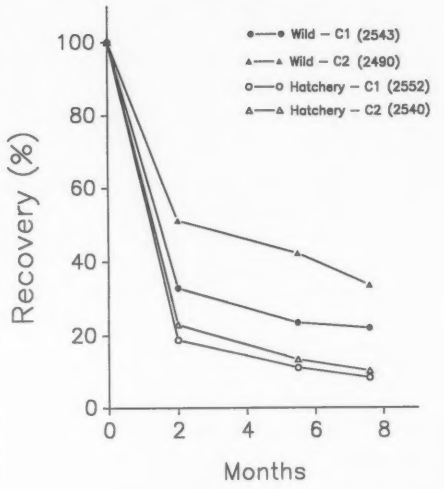

Figure 4

Recovery rates for free-ranging hatchery-reared and wild queen conch, *Strombus gigas*, transplanted to sites C1 and C2 in April 1990. Values are percentages of the original conch (April releases) found in June, September, and November surveys. In parentheses are the original numbers of tagged conch.

Table 3

Tag recovery summaries for hatchery-reared and wild queen conch (*Strombus gigas*) released in two study sites near Children's Bay Cay, Bahamas, in 1990. Adjustments to the original numbers of conch released in April account for tagged conch taken from the free-ranging study to be used in enclosure and tether experiments; these were subtracted from the original number.

	Site			
	C1		C2	
Stock type	Hatchery	Wild	Hatchery	Wild
April to June (64 days)				
Original Number Released in April	2552	2543	2540	2490
Recovered Live	480	837	586	1270
% Recovered Live	18.8	32.9	23.1	51.0
June to September (100 days)				
Adjusted Number Released	2517	2467	2472	2451
Recovered Live	277	582	328	1035
% Recovered Live	11.0	23.6	13.3	42.2
September to November (66 days)				
Adjusted Number Released	2502	2452	2457	2436
Recovered Live	206	542	248	820
% Recovered Live	8.2	22.1	10.1	33.7

bers of untagged, wild conch at the C1 area. Hatchery stocks were recovered in about equal proportions at the two sites.

Growth Free-ranging wild conch had higher growth rates (log-transformed) than hatchery-reared conch during all three seasons examined (Table 4). During summer, the difference was approximately two times (Fig. 5), but the rates began to converge in the fall. Growth rates were highest during summer and fall, and lowest during winter, following patterns of water temperature (Fig. 3). Conch grew significantly faster at site C2 than at C1 during both summer and winter; site differences were not significant in the fall (Table 4, Fig. 5).

Morphology At the beginning of the free-ranging experiment, shells of hatchery-reared conch were significantly lighter than those of wild conch from the Children's Bay Cay nursery site (slopes were homogeneous, F=0.833, P=0.365; ANCOVA: F=92.62, P< 0.001) (Fig. 6A). Lower shell weight in hatchery-reared conch is a function of either thinner shells or differences in shell form compared to wild conch. Regressions of shell width with shell length (Fig. 6B) showed that the spines were, in fact, longer in wild conch than in hatchery-reared stock (slopes were homogeneous, F=1.76, P= 0.190; ANCOVA: F=73.99, P< 0.001). Regressions of tissue wet weight with shell length show no significant difference in tissue weight between wild and hatchery-reared conch (Fig. 6C), (slopes were homogeneous, F=1.76, P=0.190; ANCOVA: F=3.24, P=0.077).

Measurements made on shells of hatchery-reared and wild conch at the end of the experiment in February 1991 show that lines for shell weight and width had converged (Fig. 7, A and B). Shell weights of hatchery-reared conch were still lighter than those of wild conch (slopes were homogeneous, F=0.189, P=0.665; ANCOVA: F=7.44, P=0.008) (Fig. 7A), but the lines were closer than in April 1990 (Fig. 6A). Stock type did not affect the relationship between shell length and shell width in February (Fig. 7B) (slopes were homogeneous, F=2.01, P=0.160; ANCOVA: F=0.957, P=0.331). Hatchery-reared conch

Table 4

Results of two-way ANOVAs for growth rates in free-ranging queen conch (*Strombus gigas*). "Site" refers to the two experimental sites C1 and C2. "Stock type" refers to hatchery-reared versus wild conch.

Source	df	MS	F	P
Period I (April to September 1990—64 days)				
Site × stock type	1	<0.001	1.205	0.273
Site	1	0.003	22.157	0.001
Stock type	1	0.045	322.407	<0.001
Error	396	<0.001		
Period II (September to November 1990—100 days)				
Site × stock type	1	<0.001	1.332	0.249
Site	1	<0.001	0.418	0.518
Stock type	1	0.004	16.967	<0.001
Error	396	<0.001		
Period III (November 1990 to February 1991—66 days)				
Site × stock type	1	<0.001	0.714	0.400
Site	1	0.001	7.541	0.007
Stock type	1	0.001	8.697	0.004
Error	115	<0.001		

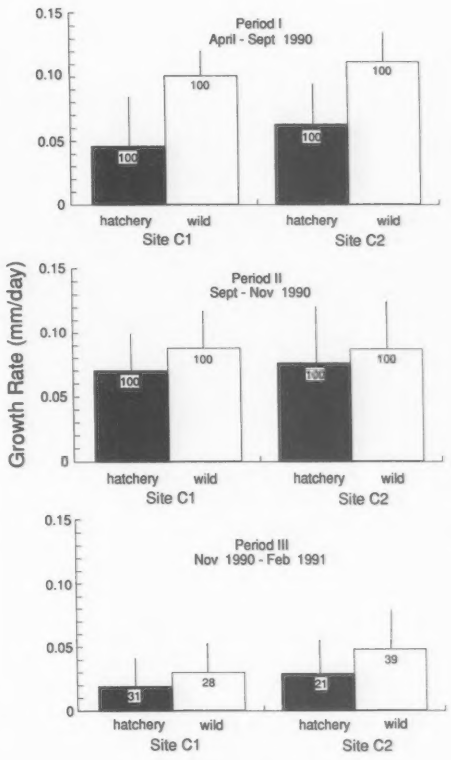

Figure 5

Comparison of growth rates of free-ranging hatchery-reared and wild queen conch, *Strombus gigas*, at sites C1 and C2. Growth periods I–III represent summer, fall, and winter, respectively. Values are mean ± SD, with the number of conch measured shown inside the vertical bars.

had heavier tissue wet weight than wild conch (slopes were homogeneous, F=0.163, P=0.688; ANCOVA: F=7.12, P= 0.010) (Fig. 7C). This can be explained by examining the ratio between tissue and shell weight. At the beginning of the experiment these ratios for hatchery and wild conch were 0.34 ± 0.04 and 0.22 ± 0.03 (mean ± SD), respectively. This indicates that hatchery conch had lighter shells and heavier soft tissue than wild conch. At the end of the experiment ratios for hatchery and wild conch were 0.30 ± 0.04 and 0.25 ± 0.04 (mean ± SD), respectively. The lower ratio for hatchery conch indicates that both the tissue and shell weight were increasing.

Hatchery-reared conch that survived 11 months in the field either developed morphological characteristics of wild conch, or the survivors had such characteristics at release. Because there was little overlap in regressions of shell width versus shell length at the beginning of the experiment, change in shape is the most plausible explanation for characteristics measured in hatchery-reared conch at the end of the experiment. Presence of short spines on pretran-

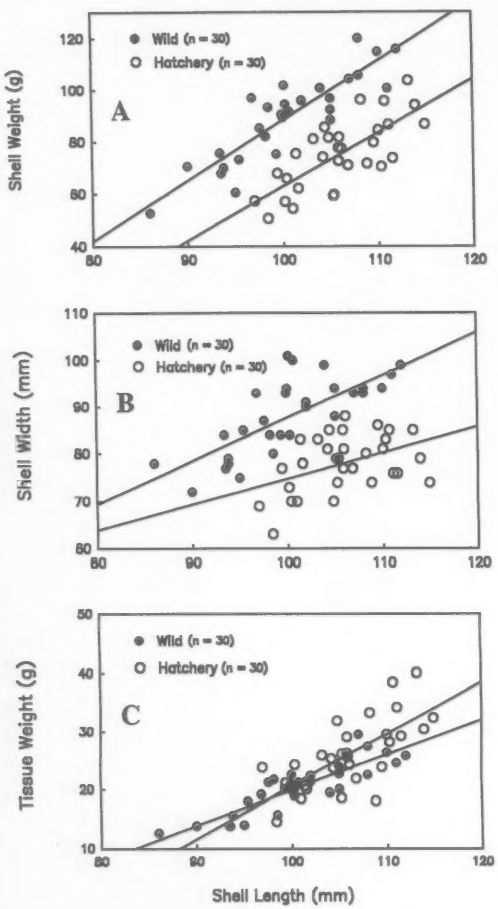

Figure 6

Shell weights (**A**), shell widths (**B**), and tissue weights (**C**) of hatchery-reared and wild queen conch, *Strombus gigas*, shown as a function of shell length. Measurements were taken for conch of each stock type collected at the beginning of the free-ranging experiment (1 April 1990).

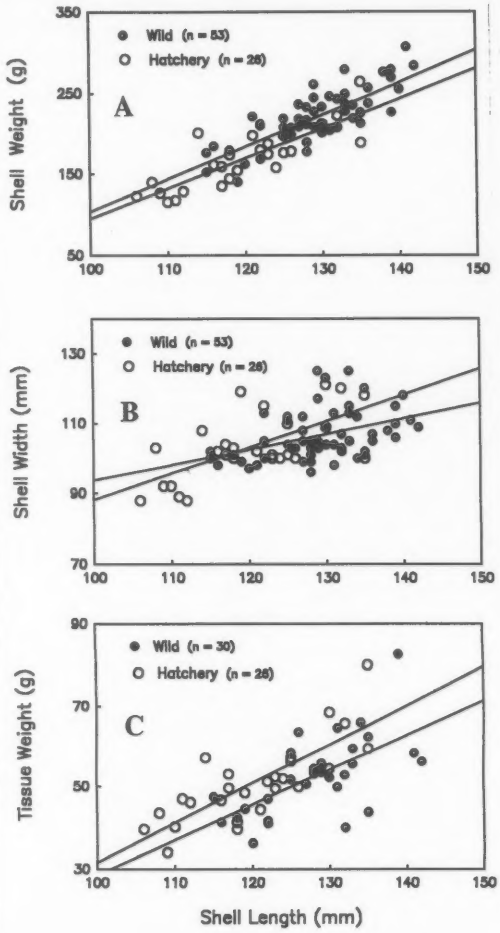

Figure 7

Shell weights (**A**), shell widths (**B**), and tissue weights (**C**) of hatchery-reared and wild queen conch, *Strombus gigas*, shown as a function of shell length. Measurements were taken for conch of each stock type collected at the termination of the free-ranging experiment (21 Feb. 1991).

splant portions of the shells followed by long spines on the outer (newer) portions of the last shell whorl support the hypothesis of changing shell shape. Although it is normal for spine length to increase proportionally with shell length in queen conch, the posttransplant increase in hatchery-reared stock was extreme and obviously disproportionate in most shells.

Behavior On all nine dates when burial was examined for free-ranging animals, a higher percentage of wild conch were buried than of hatchery-reared individuals (Fig. 8). Pairwise ANOVA of burial frequency on arcsine-transformed data from dates as blocks showed that the difference in burial rates between stock types was significant ($F_{1,15}$=8.51, P=0.011). Hatchery and wild conch showed nearly parallel patterns of burial frequency over time. However, plots of burial frequency should not be interpreted as seasonal trends, because juvenile conch appear to demonstrate tidal periodicity in locomotory activity (pers. observ.). Although the patterns were not quantified, it was frequently noted during field observations that hatchery conch were more active than wild conch. While hatchery-reared individuals were almost always moving, wild conch were frequently found nestled motionless beneath algae or detritus.

Given the relatively small area of the two outplant sites (1 ha each) tagged conch often dispersed relatively far from their original release sites (Fig. 9, A and B). For example, in June 1990 only 15% of the recovered hatchery-reared conch released at site C1 were found in that zone and 35% were found northwest of C1. Tagged conch tended to move to the northeast and northwest between April and June 1990. By June, hatchery-reared and wild conch initially released at site C1 were widely dispersed and differentially distributed (χ^2=18.01, df=4, P=0.05). Hatchery-reared conch released at C2 tended to disperse more widely than wild conch (i.e., from the southwest sandbar to the north zones); the difference was significant (χ^2=255.6, df=6, P=0.05). Wild conch moved toward the center zone between site C1 and C2 (Fig. 9B). Between June and September 1990 a large percentage of conch released at site C1 were found between C1 and C2 (Fig. 9A), while conch from site C2 continued to be found north of the release area (Fig. 9B). In both cases the difference in dispersion between hatchery and wild was significantly different (C1: χ^2=-6.4, df=5, P=0.05; C2: χ^2=17.6, df=5, P=0.05). By November 1990, hatchery and wild conch released at site C1 (χ^2=9.1, df=5, P=0.05) and C2 (χ^2=12.6, df=6, P=0.05) had similar distributions. Conch released at site C2 consistently moved toward the adjacent natural juvenile population centered at C1 (see Fig. 2).

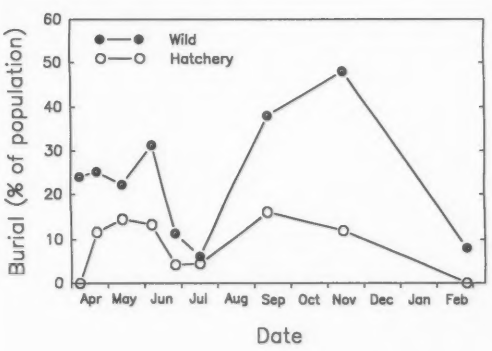

Figure 8

Percentage of queen conch, *Strombus gigas*, buried during each observation for hatchery-reared and wild conch. Values are based upon observations on 30 haphazardly chosen conch of each stock type on each date.

Enclosure experiments

Experiment I

Mortality In the first enclosure experiment (7 April to 9 July 1990), mortality data for the midpoint and end of the experiment (Fig. 10) were examined with two separate three-way ANOVAs, by using numbers of dead conch (Table 5). Except when highest mortality occured at site C2 at the end of the experiment, mortality did not differ between sites or among the three stocking densities. Differences in mortality between stock types were never significant in the enclosures (Table 5).

Growth Trends of growth (log-transformed) in the first enclosure experiment (Fig. 11) were similar to those observed in free-ranging conch during the summer (Fig. 5) (i.e. rates were higher at C2 than at C1, and wild conch grew faster than hatchery conch). In growth period I (7 April–14 May 1990), wild and hatchery conch grew faster at site C2 than at C1, and wild conch grew faster than hatchery conch at both sites (Table 6). There was also a significant density effect (Table 6); highest growth occurred in conch held at 1.0 individuals·m^{-1} (Fig. 11).

In growth period II (14 May–9 July 1990), there were numerous two-way interactions in the ANOVA (Table 6), particularly at site C1. In one-way ANOVAs, there was no density effect for hatchery ($F_{2,3}$ = 5.74, P=0.094) or for wild ($F_{2,3}$ =7.139, P=0.072) conch at site C1; however, hatchery and wild conch

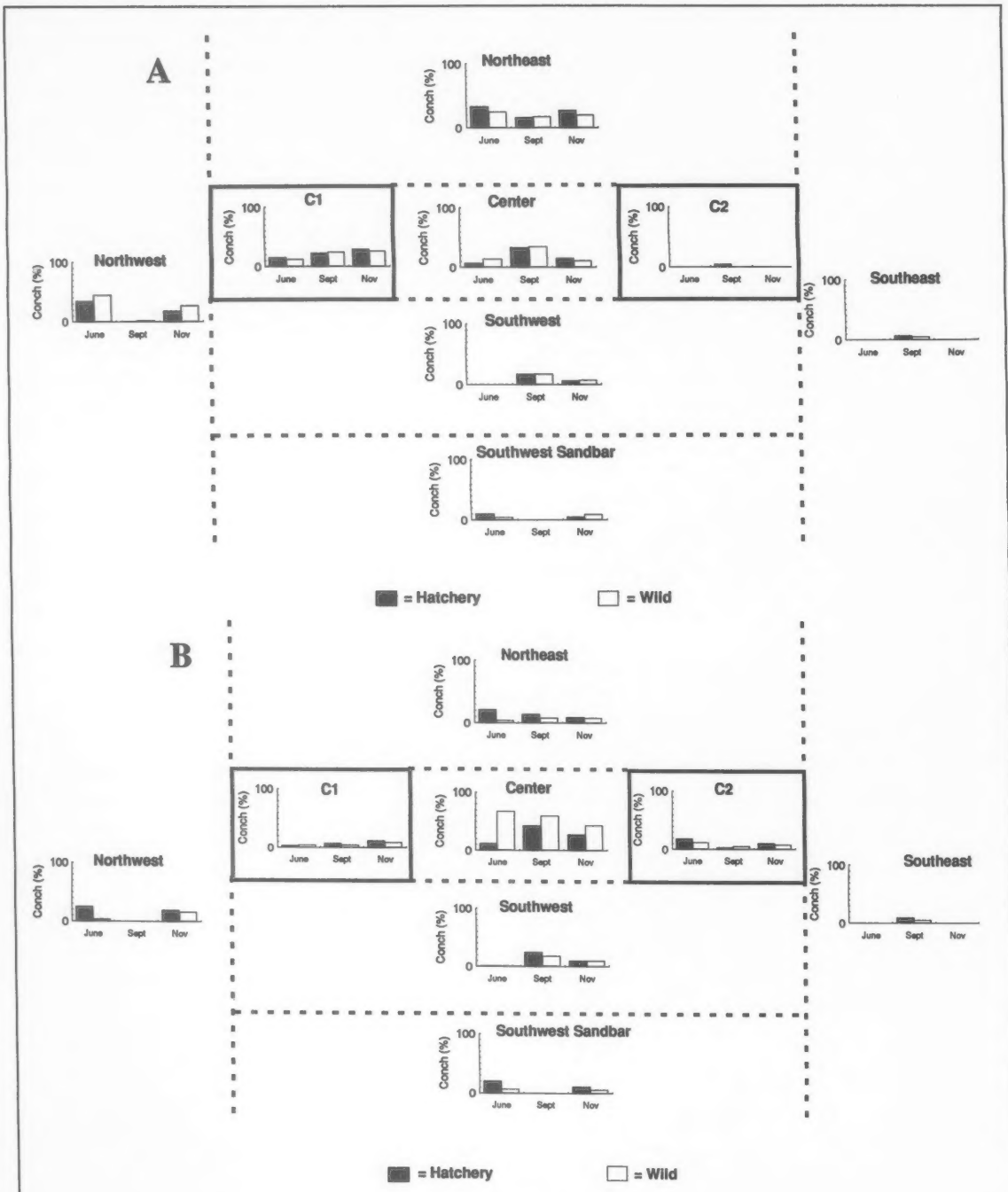

Figure 9

Recoveries of tagged queen conch, *Strombus gigas*, in the eight zones (not to scale) searched during the June, September, and November surveys. Values shown are the percentages of total capture for each stock type found in each zone, (**A**) conch released at site C1, and (**B**) conch released at site C2. See Figure 2 for true distances between the zones.

Table 5

Results of three-way ANOVAs for mortality of queen conch (*Strombus gigas*) in enclosure experiment I. "Site" refers to the two experimental sites C1 and C2. "Stock type" refers to hatchery-reared versus wild conch. "Density" is the density of conch tested in enclosures.

Source	df	MS	*F*	*P*
Period I (7 April to 14 May 1990—37 days)				
Site × type × density	2	0.015	1.266	0.317
Site × stock type	1	0.015	1.259	0.284
Site × density	2	0.003	0.258	0.777
Stock type × density	2	0.003	0.281	0.760
Site	1	0.028	2.400	0.147
Stock type	1	0.004	0.353	0.564
Density	2	0.001	0.108	0.898
Error	12	0.012		
Period II (14 May to 9 July 1990—56 days)				
Site × type × density	2	0.018	1.465	0.270
Site × stock type	1	0.010	0.839	0.378
Site × density	2	0.001	0.109	0.897
Stock type × density	2	0.018	1.447	0.273
Site	1	0.095	7.710	0.017
Stock type	1	0.008	0.691	0.422
Density	2	<0.001	0.028	0.973
Error	12	0.012		

differed in growth rate ($F_{1,10}$=10.75, P=0.008). At site C2 there were no differences in growth rate either between hatchery and wild conch or among the stocking densities (Table 6).

Prior to the beginning of the enclosure experiment, pen locations were chosen for similarity in macrophyte characteristics (Table 7). Seagrass shoot density ($F_{23,48}$=0.55, P=0.938) and macrophyte biomass ($F_{23,48}$=1.37, P=0.177) did not differ among the 24 cages. Although ANOVA showed that detritus differed ($F_{23,48}$=2.00, P=0.022) among the cages, Tukey's multiple comparison test did not detect the differences (P>0.05). At the end of the experiment dry weight of seagrass detritus did not differ among the cages (Table 7)($F_{23,24}$=0.900, P=0.598), and there were no differences in individual cages between the beginning and end of the experiment ($F_{1,142}$=0.090, P=0.764). There is no evidence, therefore, that detritus was depleted even at the high density of 2.5 conch·m^{-2}. When comparing shoot density between the beginning and end of the experiment, there was no difference ($F_{1,142}$=2.95, P=0.088), but biomass of living seagrass did differ between the dates ($F_{1,142}$=37.01, P<0.001), probably related to blade growth in the spring season.

Experiment II

Mortality At the termination (day 85) of enclosure experiment II (29 November 1990–21 February 1991) mortality was obviously higher at site C2 than at C1 for both hatchery and wild conch (Fig. 12), similar to the results of enclosure experiment I (Fig. 10). Midway through the experiment there was no significant mortality difference between site C1 and C2; however, the difference was significant by the end of the experiment (Table 8); mortality was higher at site C2. Similar to enclosure experiment I, there were no differences in mortality between hatchery and wild conch (Table 8).

Growth Growth rates were low in enclosure experiment II (0.01–0.06 mm·d^{-1}) (Fig. 13), paralleling the trend observed in free-ranging conch (Fig. 4) and associated with low winter temperatures (Fig. 3). There were significant site × stock type interactions for period I ($F_{1,12}$=5.949, P=0.031) and period II ($F_{1,12}$=5.004, P=0.045) because of differences in growth rate between hatchery and wild conch at site C1 (period I: $F_{1,6}$=6.48, P=0.044; period II: $F_{1,6}$=9.747, P=0.021); but not at site C2 (period I: $F_{1,6}$=0.008, P=0.932; period II: $F_{1,6}$=0.207, P=0.665). At site C1 wild conch grew approximately twice as fast as hatchery conch.

Tether experiments

Experiment I

Mortality The first tether experiment, conducted from 11 April to 11 July 1990, confirmed that the difference in tag recovery rate between hatchery-reared and wild conch was related to predation (Fig. 14). Hatchery conch were killed at a frequency approximately twice that of wild conch for day 45 and day 88 (Table 9, Fig. 14). Site effects were not significant at either midpoint or end of the experiment (Table 9, Fig. 14).

Growth Growth rates in both hatchery and wild conch on tethers were higher at site C2 than at site C1 by the end of the study period (11 July 1990) (Fig. 15). This difference also occurred in free-ranging conch (Fig. 5) and enclosure experiment I (Fig. 11). During period I (April and May 1990) there was a significant site × type interaction (Table 10) because wild conch grew faster at site C2 than C1 ($F_{1,64}$=49.28, P<0.001), and hatchery conch grew at

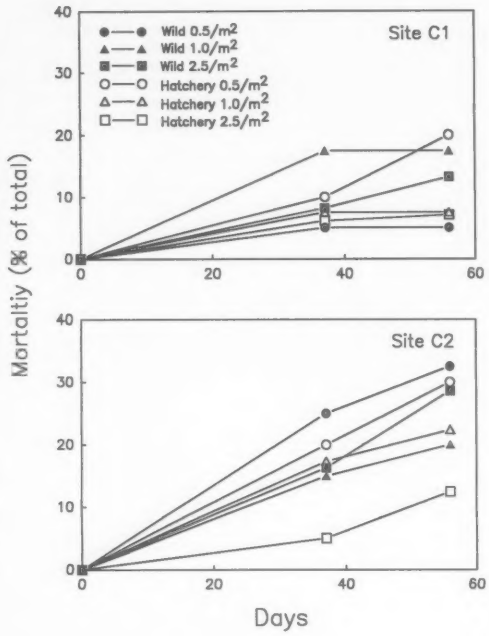

Figure 10

Cumulative mortality curves for enclosure experiment I. Hatchery-reared and wild queen conch, *Strombus gigas*, were held at three different densities at sites C1 and C2. Initial numbers of conch in the enclosures were 10, 20 and 49, yielding densities of 0.5, 1.0, and 2.5 conch·m^{-2}, respectively.

the same rate at both sites ($F_{1,43}$=0.105, P= 0.747). Wild conch grew significantly faster than hatchery conch at site C1 ($F_{1,55}$=14.54, P<0.001) and C2 ($F_{1,52}$=69.06, P<0.001) (Fig. 15). In growth period II (June and July 1990) wild conch grew faster than hatchery conch at both sites (Table 10, Fig. 15).

Experiment II A second tether experiment conducted at site C1 from 7 February to 3 May 1991, using wild conch and the few remaining hatchery-reared conch from the free-ranging experiment, resulted in mortality curves (Fig. 16) different from the first tether experiment (Fig. 14). Mortality rates did not differ between stock types at either 42 ($F_{1,6}$=0.871, P=0.387) or 84 days ($F_{1,6}$<0.001, P=1.000). Mortalities were identical (65%) at the 84–day termination of the experiment (Fig. 16).

Comparison of experiments

Mortality rates in hatchery-reared conch were higher than or equal to those of wild conch in all experiments and at both study sites (Table 11). Equivalent mortality rates were found in enclosures and in tether experiment II run at the end of the study period. Growth rates were higher in wild conch than in hatchery-reared conch except during the second 5-week period of enclosure experiment I at site C2 and in enclosure experiment II at site C2, when growth rates were equivalent.

Site differences in mortality rates were relatively consistent across experiments and stock types (Table 11). Mortality was always lower for both wild and hatchery-reared conch at site C1 than at C2, except

Table 6

Results of multi-way ANOVAs for growth rates of queen conch (*Strombus gigas*) in enclosure experiment I. Sources are the same as described in Table 5.

Source	df	MS	*F*	*P*
3-way ANOVA for Period I (7 April to 14 May 1990—37 days)				
Site × type × density	2	<0.001	0.481	0.630
Site × stock type	1	<0.001	0.893	0.363
Site × density	2	<0.001	2.456	0.128
Stock type × density	2	<0.001	2.284	0.144
Site	1	0.001	28.210	<0.001
Stock type	1	<0.001	16.511	0.002
Density	2	<0.001	4.649	0.032
Error	12	<0.001		
3-way ANOVA for Period II (14 May to 9 July 1990—56 days)				
Site × type × density	2	<0.001	3.546	0.062
Site × stock type	1	0.001	8.722	0.012
Site × density	2	<0.001	1.281	0.313
Stock type × density	2	<0.001	4.261	0.040
Site	1	<0.001	0.778	0.395
Stock type	1	0.0022	3.171	<0.001
Density	2	<0.001	4.787	0.030
Error	12	<0.001		
2-way ANOVA for Period II (Site C1)				
Stock type × density	2	0.001	9.513	0.014
Stock type	1	0.002	36.836	0.001
Density	2	<0.001	4.619	0.061
Error	6	<0.001		
2-way ANOVA for Period II (Site C2)				
Stock type × density	2	<0.001	0.015	0.985
Stock type	1	<0.001	1.465	0.272
Density	2	<0.001	1.935	0.225
Error	6	<0.001		

for equivalent mortality rates measured in tether experiment I. Most experiments showed that growth rates were lower at site C1 than at C2 with certain exceptions (Table 11). A significantly higher growth rate was found at C1 in wild conch during the second enclosure experiment, and equivalent growth rates were found in hatchery-reared conch in the same experiment. Growth rate did not differ between sites during fall in free-ranging conch.

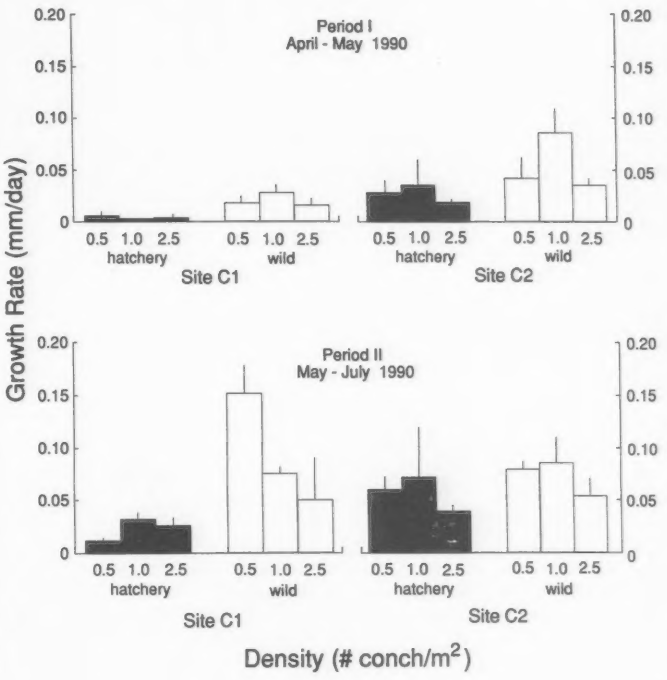

Figure 11

Growth rate comparisons for enclosure experiment I. Hatchery-reared and wild queen conch, *Strombus gigas*, were held at three different densities at sites C1 and C2. Values are mean ± SD for average growth rates in two replicate enclosures.

Discussion

Importance of seed stock quality

Stock enhancement and rehabilitation depend upon the ability of fisheries managers to place viable seed animals in optimal habitats at appropriate times (Stoner, in press). Hatcheries in the Turks and Caicos Islands, Belize, Mexico, and Florida are now producing juvenile queen conch with the expectation that hatchery-reared conch will be seeded into local waters for restoration of depleted resources. Releases of hatchery-reared conch in several small-scale pilot programs have been relatively unsuccessful in terms of conch survival (Appeldoorn and Ballantine, 1983; Appeldoorn, 1984; Iversen et al., 1986; Coulston et al., 1987; Rathier, 1987; Davis et al., 1992), but it is unknown whether low survivorship was related to characteristics of the habitat or the outplanted conch. The only published field comparison of wild and hatchery-reared queen conch (Marshall et al.[2]) showed that hatchery-reared conch may be more vulnerable to predation than are wild conch. Additionally, Jory and Iversen (1988) found that hatchery-reared conch may have shells with lower breaking strengths than those of wild conch. The present study shows that potential differences in physiology, behavior, morphology, and survival must all be considered.

Differences in growth rate between wild and hatchery-reared conch at Children's Bay Cay study sites are surprising given that the hatchery conch had been in a field grow-out enclosure with natural substrata and food for 6 months. Several explanations

[2] Marshall, L. S., Jr., C. Cox, and R. N. Lipcius. 1992. Survival of wild and hatchery-reared juvenile queen conch in natural habitats. Unpubl. manuscr.

Table 7

Seagrass components in 24 cages at the beginning and end of enclosure experiment I. *Thalassia* biomass included all above-ground live blades. *Thalassia* detritus included senescent and decomposing seagrass blades retained in a 3 mm mesh bag. Values are mean (± SD).

Seagrass components	March 1990	July 1990
Thalassia shoot density (shoots·m^{-2})	674.1 (±92.2)	649.3 (±79.8)
Thalassia biomass (g dry wt·m^{-2})	77.2 (±18.5)	107.2 (±37.5)
Thalassia detritus (g dry wt·m^{-2})	317.9 (±131.7)	324.32 (±25.4)

Table 8

Results from two-way ANOVAs for mortality of queen conch (*Strombus gigas*) in enclosure experiment II. Sources are the same as described in Table 4.

Source	df	MS	*F*	*P*
Period I (29 November 1990 to 3 January 1991—35 days)				
Site × stock type	1	0.563	0.239	0.634
Site	1	5.063	2.150	0.168
Stock type	1	0.563	0.239	0.634
Error	12	2.354		
Period II (3 January to 21 February 1991—50 days)				
Site × stock type	1	0.250	0.143	0.712
Site	1	110.250	63.000	<0.001
Stock type	1	0.250	0.143	0.712
Error	12	1.750		

Table 9

Results of two-way ANOVAs for mortality of queen conch (*Strombus gigas*) in tether experiment I. Sources are the same as described in Table 4.

Source	df	MS	*F*	*P*
Period I (12 April to 27 May 1990—45 days)				
Site × stock type	1	1.563	0.926	0.355
Site	1	0.063	0.037	0.851
Stock type	1	14.063	8.333	0.014
Error	12	1.688		
Period II (27 May to 11 July 1990—45 days)				
Site × stock type	1	<0.001	<0.001	1.000
Site	1	0.250	0.098	0.759
Stock type	1	12.250	4.820	0.049
Error	12	2.542		

Table 10

Results of two-way ANOVAs for growth rates of queen conch (*Strombus gigas*) in tether experiment I. Sources are the same as described in Table 4.

Source	df	MS	*F*	*P*
Period I (12 April to 27 May 1990—45 days)				
Site × stock type	1	0.004	28.152	<0.001
Site	1	0.005	31.072	<0.001
Stock type	1	0.014	85.104	<0.001
Error	107	<0.001		
Period II (27 May to 11 July 1990—45 days)				
Site × stock type	1	<0.001	0.535	0.467
Site	1	0.016	50.410	<0.001
Stock type	1	0.002	7.629	0.007
Error	72	<0.001		

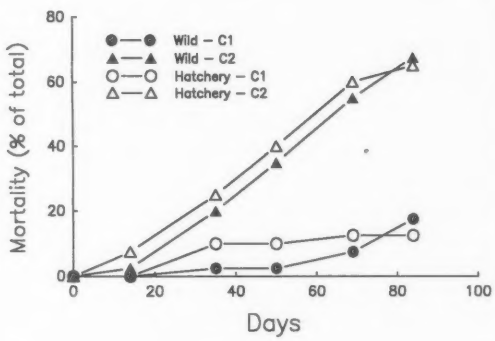

Figure 12

Cumulative mortality curves for enclosure experiment II. Hatchery-reared and wild queen conch, *Strombus gigas*, were compared at sites C1 and C2. Forty conch of each stock type were held at each site.

may be speculated: 1) hatchery and wild conch were different in their metabolic functions, such as partitioning of energy into somatic and shell growth, 2) slow growth in hatchery-reared conch was a sublethal effect of transport, or 3) poor growth was related to behavioral characteristics of hatchery-reared conch, such as a reduced ability to recognize foods in the new habitat or unusually high motility. Laboratory experiments by Siddall (1984b) showed that 10-mm juvenile queen conch held at high density had high locomotory activity and associated low growth rates. Seemingly constant motion and lack of burial in our hatchery-reared animals suggest that their metabolic demands may have been high. However, high growth rates in the hatchery conch later in our investigation showed that the problem was not a permanent characteristic of the stock type, and others have shown that hatchery-reared conch can have normal growth rates in the field (Appeldoorn and Ballantine, 1983; Davis et al., 1992). Nevertheless, as suggested earlier (Stoner and Sandt, 1991, 1992), growth appears to be a very sensitive indicator of a seed animal's physiological performance in a new habitat.

A more serious difference occurred in mortality rates. From the first field experiments with hatchery-reared queen conch juveniles (Appeldoorn and Ballantine, 1983) it has been clear that small conch are highly susceptible to predation. Recommendations for release size range from 4 cm shell length

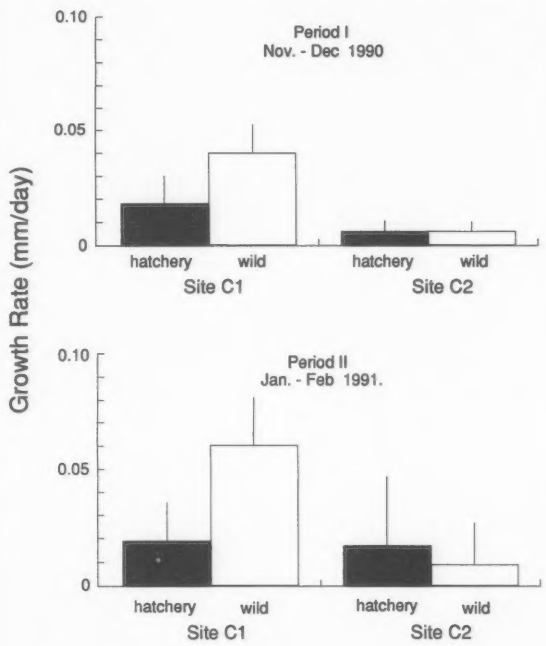

Figure 13

Growth rate comparisons for enclosure experiment II. Hatchery-reared and wild queen conch, *Strombus gigas*, were held at 1.0 conch·m^{-2} at sites C1 and C2. Values are mean ± SD for average growth rates in four replicate enclosures.

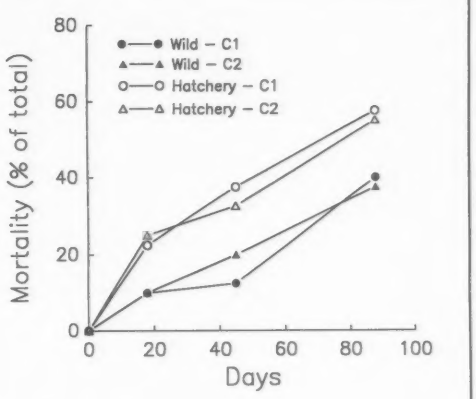

Figure 14

Cumulative mortality curves for tether experiment I. Hatchery-reared and wild queen conch, *Strombus gigas*, were compared at sites C1 and C2. Forty conch of each stock type were tethered at each site.

(Berg, 1976) to 10 cm or larger (Jory and Iversen, 1983). Even with the use of 8–12 cm shell length test animals in this investigation, hatchery-reared conch on tethers were killed at a rate nearly twice the rate of wild conch early in the study. Morphological and behavioral differences are probably the most important factors influencing mortality. Thin shells and short apical spines observed in the hatchery-reared conch would present a smaller, more vulnerable prey to predators. Palmer's (1979) experiments have shown that spination is an important shell characteristic for minimizing predation in intertidal gastropods.

Shell weight and spination are malleable traits in queen conch. Alcolado (1976) observed that shell form in the species was related to water depth and habitat type, with thin shells and short-spines being associated with rapid growth in shallow water. Environmental mediation of shell form was tested experimentally by Martin-Mora (1992) near Lee Stocking Island. She found that transplanted wild conch took on the morphology of local conch within several months, and that high shell weight and long spines were associated with slow growth rate. Given the importance of shell quality in molluscan biology, attention has been given to relationships between shell properties and diets, substrata, temperature, salinity, and other physical factors (Wilbur, 1964; Carter, 1980). It is likely, therefore, that culture techniques can be developed to provide seed conch which are less vulnerable to predation.

Survivorship of hatchery-reared conch may also have been influenced by their low burial frequency. Wild conch tend to shelter under detritus or algae, and remain partially buried and unmoving for long periods of time. This probably provides a certain degree of protection from larger visual predators. Low burial frequency in hatchery-reared conch may be related to the fact that the field grow-out area in the Caicos Islands, where they spent several months before being transplanted to the Exuma Cays, was primarily a hard-bottom environment. Behavioral differences between hatchery-reared and wild stocks are rarely documented; however, Schiel and Welden (1987) found that hatchery-reared red abalone, *Haliotis rufescens*, did not move to concealed locations as did wild abalone, resulting in higher predatory mortality.

There are at least three limitations of the present investigation. One is not knowing whether convergence in the morphology and survivorship of wild and hatchery-reared conch was related to

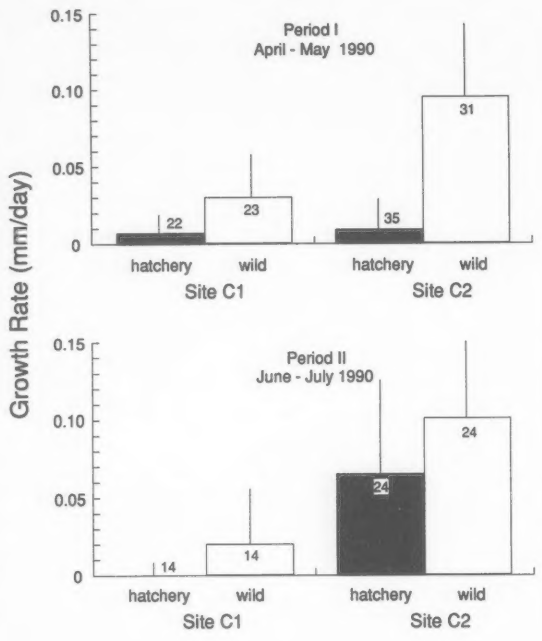

Figure 15

Growth rates of hatchery-reared and wild queen conch, *Strombus gigas*, held on tethers at sites C1 and C2 during experiment I. Values are mean ± SD, with the number of conch measured shown inside the vertical bars.

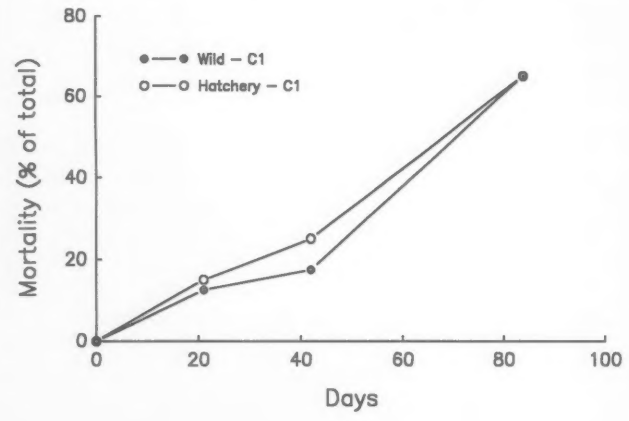

Figure 16

Cumulative mortality curves for hatchery-reared and wild queen conch, *Strombus gigas*, held on tethers at site C1 during experiment II. Forty conch of each stock type were tethered at each site.

adaptation by individuals over the course of the investigation, or is explained simply by differential survivorship (i.e. the most fit hatchery-reared conch survived to the end of the experiments). As discussed earlier, a strong case for adaptation can be made because of the obvious changes in shell morphology over time within individual conch. Second, hatchery-reared conch used in this study were from one season's production in a single hatchery. We know that different hatcheries and different cultures from individual hatcheries can produce conch with different characteristics. For example, Jory and Iversen (1988) found different shell strengths among cultures of queen conch. Because juvenile conch are reared from egg masses collected from the wild, and because both shell morphology and behavior appear to be relatively plastic characteristics in queen conch, we believe that differences shown between hatchery-reared animals and native stocks can be alleviated through modifications in diets, hatchery substrata, and other culture techniques. Field viability must be considered continuously throughout the hatchery-rearing process. Third, morphological effects on survival may vary with site because of differences in predator assemblages. For example, at a site where molluscs (such as tulip snails, *Fasciolaria tulipa*) are the most important predators, size and escape behavior may be more important than spine length and shell thickness. More site comparisons and better knowledge of predator-prey relationships are needed.

Importance of stock enhancement sites

Site selection for stock enhancement with queen conch is a complex issue and the subject of several earlier papers (Stoner and Sandt, 1991, 1992; Stoner et al., 1993; Stoner, in press). It is clear from experiments reported here that even carefully chosen locations, such as our non-conch study site C2, may not support juvenile conch over the long term. Conch at this site demonstrated consistently higher growth than conch at the traditional nursery site (C1), but mortality was also higher in both tethered and free-ranging conch.

Site differences in mortality could be associated with patterns of predator abundance or diversity, or both. Although predators may accumulate where prey density is high, the most likely explanation for lower predation rate at site C1

Table 11

Summary of results from free-ranging, enclosure, and tether experiments on mortality and growth of hatchery-reared and wild queen conch (*Strombus gigas*) at two field sites (C1 & C2). W = wild conch. H = hatchery-reared conch. PI, PII, and PIII refer to different growth periods within the experiment. Signs indicate statistically significant differences (see text).

	Stock type		Differences	
Experiment	Site C1	Site C2	Mortality	Site differences
Free-ranging	W < H	W < H	C1 < C2	
Enclosure expt. I	W = H	W = H	C1 < C2	
Enclosure expt. II	W = H	W = H	C1 < C2	
Tether expt. I	W < H	W < H	C1 = C2	
Tether expt. II	W = H	—	—	
Growth free-ranging				
summer (PI)	W > H	W > H	W > H	W > H
fall (PII)	W > H	W > H	C1 < C2	C1 = C2
winter (PIII)	C1 < C2			
Enclosure expt. I	W > H	W > H (PI)	W = H (PII)	C1 < C2
Enclosure expt. II	W > H	W = H	W: C1 > C2	H: C1 = C2
Tether expt. I	W > H	W > H	C1 < C2	

than C2 is that juvenile conch realize density-dependent protection from predation. *Strombus* species often live in aggregations (Catterall and Poiner, 1983; Stoner et al., 1993), and recent experiments have shown that juvenile queen conch actually increase their survivorship by living in densities sufficiently high to compromise growth rate in certain cases (Stoner and Ray, 1993; Ray and Stoner, 1994). This aggregation or "herding" behavior probably reduces predation by providing a "probability refuge" (Bertram, 1978; Pulliam and Caraco, 1984); that is, the effects of predators are diluted by the presence of large numbers of alternative prey. Gregariousness provides an explanation for repeated movements of tagged conch from release site C2 toward C1, which was centered in a known juvenile aggregation. Stoner and Ray (1993) observed a similar response in queen conch translocated at another site near Lee Stocking Island. High growth rates were found outside an aggregation, but mortality was high, and movements were always toward the center of the aggregation. Regardless of the exact mechanisms involved, it is clear that both density and absolute numbers of conch released may be critical factors in an equation for success in stock enhancement. Typical nursery aggregations in the Exuma Cays range in size from less than 100,000 to several million juvenile conch (Wicklund et al.,1991; Stoner, unpubl. data). We speculate that releases at individual sites will need to be made with tens of thousands of conch; however, new research should be designed to determine the optimal number that can be released in an area, and how releases at several sites instead of just one or two might improve the probability of stock enhancement.

In this study there was no significant effect of density on growth rate over the ranges tested (0.5 and 2.5 conch·m^{-2}); however, inverse density-dependent growth was observed in another study at the same site (C1) with conch densities ranging from 1.0 to 4.0 conch·m^{-2} (Stoner, 1989b). It is not surprising therefore, that juvenile aggregations in the Exuma Cays are normally found with less than 2.0 conch·m^{-2} (Stoner et al., 1993). Such values are probably site specific. For example, at least one long-term nursery site near Lee Stocking Island rarely has more than 0.2 conch·m^{-2} (Stoner, unpubl. data). Stocking density will need to be evaluated carefully.

Different kinds of testing

General patterns of growth and mortality between the two stock types and the two outplant sites were relatively consistent among three kinds of experiments (free-ranging conch, enclosures, and tethers) (Table 11); however, the actual values measured were undoubtedly influenced by different manipulations. For example, recovery of free-ranging conch during the first two months of the experiment ranged from only 19 to 52%, whereas during the same period 70–95% survival was observed in enclosures. The coverless enclosures apparently excluded some important predators (such as the tulip snail, *Fasciolaria tulipa*),

and not all free-ranging survivors were recovered. High mortality of conch on tethers at site C2 was probably a result of the low density of conch surrounding the tethers, lack of protection provided by enclosures, and reduced ability to avoid predators. Where the density of ambient conch was high (site C1), mortality rates in enclosures and on tethers were nearly identical, suggesting the significance of alternative prey, already discussed.

Comparisons of growth rates among experimental treatments in this study are difficult to make because of different times and durations of the growth periods. For example, high growth rates in free-ranging conch calculated for April to September 1990 reflect the high temperature season. Best comparisons are provided by enclosure and tether experiments run concurrently between April and June 1990, and by growth rates for free-ranging and enclosed conch measured between December 1990 and February 1991. In both cases the conch had relatively similar growth rates within stock type and site, suggesting that caging and tethering did not affect the nutritional state of experimental animals.

Given potential artifacts of enclosures and tethers on survivorship, measurements made on free-ranging conch will be preferred for certain questions, particularly those related to behavioral patterns and natural mortality (as opposed to relative mortality measured with tethers). On the other hand, it is impossible to recover all free-ranging conch and tag recovery can not be translated directly into survivorship. Mark-recapture data can be used to estimate population changes, with certain inherent limitations (Skalski and Robson, 1992); this may be a good approach for those primarily concerned with survivorship in large outplants. Those more interested in the role of habitat, stocking densities, and mechanisms of mortality will probably wish to maintain more control over the experimental animals. Covered enclosures, such as those used by Ray and Stoner (in press), offer the best means for testing growth potential in different habitats; meanwhile tethers give good information on relative rates of mortality for comparison of different sites, conch sizes or types.

Conclusions

One of the most striking implications of Appeldoorn's (1988) estimates of natural mortality in queen conch, is that juvenile mortality is very high. For example, survivorship in the first two years of life (to approx. 130 mm SL) may be as low as 35%. Our results on recovery of free-ranging wild conch over a 7–month period corroborate Appeldoorn's calculations. One may conclude from such survivorship curves that it will take a very large number of seed conch to enhance a local stock size. The problem would be exacerbated by poor seed stock quality, releases in suboptimal habitats, or release procedures which place the conch at unusual disadvantage (e.g. poor handling and acclimation, season of release, stocking density, and seed stock size).

Success in enhancing molluscan populations with hatchery-reared stocks has been variable. For example, Tegner and Butler (1985) recovered only 1% of their outplanted red abalone, *Haliotis rufescens*, one year after release. With the same species, Ebert (1989) reported high growth coupled with modest survivorship and some individuals reached sexual maturity with ripe gonads. In Japan, considerable success has been documented with the ezo abalone, *Haliotis discus lannai* (Saito, 1984). Hatchery-reared bay scallops, *Argopecten irradians,* released into the field at 20 mm were all lost within a month in one year; however, in another year the scallops lived to reproduce (Tettelbach and Wenczel, 1991). Despite failures, success is usually achieved as a result of adequate research. Stock rehabilitation via aquaculture may be the only viable means of restoring populations depleted to near-extinction levels, as is the case for queen conch in some regions of the Caribbean (Appeldoorn et al., 1987; Berg and Olsen, 1989).

Several steps will be required for restoration of queen conch stocks in the field:

1 The quality of hatchery-reared stock must be high and consistent. Morphology, physiology, and behavior must be considered, and stock quality should be field tested before major releases. Models of the effects of hatchery stock releases on a fishery (e.g. Madenijian et al., 1991; Polovina, 1991) will be useful only if hatchery-reared and wild stocks are identical in growth and mortality.
2 Sites for releases should be chosen with respect to information on historically significant nursery grounds, and preliminary tests for habitat suitability must be run with juvenile conch of the sizes to be seeded.
3 Release techniques must be developed to optimize conch survivorship. Factors which require further research are animal size, stocking density, minimum numbers to be released, release timing (season and time of day), and animal handling and acclimation. High numbers of individuals will need to be released given natural mortality rates and success might be improved by making releases at several sites.
4 Released conch and natural stocks will need to be managed in a comprehensive, multidisciplinary

plan for the nursery habitat, considering water quality, sediments, macrophytes, and predator species, as well as the conch populations themselves.

Hatchery techniques are well developed for queen conch, but the production of high numbers of juveniles does not insure the success of stock rehabilitation programs. Success will require much basic research on the life history and ecology of the species, particularly with respect to nutrition, growth, and predator-prey interactions. A close interaction between hatchery managers, fisheries biologists, and ecologists will be key to success.

Acknowledgments

This research was supported by a grant from the National Undersea Research Program, NOAA, U.S. Department of Commerce. We thank K. Schwarte and J.-P. Thonney for conducting most of the field work, along with D. Mansfield, E. Martin, S. Oberlink and V. Sandt. Dozens of yachtsmen assisted in the initial tagging and measurement of conch. L. Marshall provided helpful suggestions related to tethering experiments. A. Dalton and W. Hartman of the Caicos Conch Farm were especially helpful in providing the hatchery-reared conch and information on their culture. R. Glazer, J. Lin, M. Ray, S. Tettelbach, and anonymous reviewers made valuable suggestions for improving the manscript.

Literature cited

Alcolado, P. M.
1976. Crecimiento, variaciones morfologicas de la concha y algunas datos biologicos del cobo *Strombus gigas* L. (Mollusca, Mesogastropoda). Acad. Cien. Cuba, Instit. Oceanol. No. 34, 36 p.

Aoyama, S.
1989. The Mutsu Bay scallop fisheries: scallop culture, stock enhancement, and resource management. *In* J. F. Caddy (ed.), Marine invertebrate fisheries: their assessment and management. Wiley & Sons, New York, p. 525–539.

Appeldoorn, R. S.
1984. The effect of size on mortality of small juvenile conchs (*Strombus gigas* Linné and *S. costatus* Gmelin). J. Shellfish Res. 4:37–43.
1985. Growth, mortality, and dispersion of juvenile, laboratory-reared conchs, *Strombus gigas* and *S. costatus*, released at an offshore site. Bull. Mar. Sci. 37:785–793.
1988. Ontogenetic changes in natural mortality rate of queen conch, *Strombus gigas* (Mollusca: Mesogastropoda). Bull. Mar. Sci. 42:159–165.

Appeldoorn, R. S., and D. L. Ballantine.
1983. Field release of cultured queen conchs in Puerto Rico: implications for stock restoration. Proc. Gulf Caribb. Fish. Inst. 35:89–98.

Appeldoorn, R. S., G. D. Dennis, and O. Monterrosa-Lopez.
1987. Review of shared demersal resources of Puerto Rico and the lesser Antilles region. *In* R. Mahon (ed.), Report and proceedings of the expert consultation on shared fishery resources of the Lesser Antilles region. FAO Fishery Report 383:36–106.

Appeldoorn, R. S., and B. Rodriguez Q. (eds.)
1993. Queen conch biology, fisheries and mariculture. Fundacion Cientifica Los Roques, Caracas, Venezuela.

Ballantine, D. L., and R. S. Appeldoorn.
1983. Queen conch culture and future prospects in Puerto Rico. Proc. Gulf Caribb. Fish. Inst. 35:57–63.

Berg, C. J., Jr.
1976. Growth of the queen conch *Strombus gigas*, with a discussion of the practicality of its mariculture. Mar. Biol. 4:191–199.

Berg, C. J., Jr., and D. A. Olsen.
1989. Conservation and management of queen conch (*Strombus gigas*) fisheries in the Caribbean. *In* J. F. Caddy (ed.), Marine invertebrate fisheries: their assessment and management. Wiley & Sons, New York, p. 421–442.

Bertram, B. C.
1978. Living in groups: predators and prey. *In* J. R. Krebs and N. B. Davies (eds.), Behavioural ecology: an evolutionary approach. Blackwell Scientific Publ., Oxford, p. 64–96.

Brownell, W. N.
1977. Reproduction, laboratory culture, and growth of *Strombus gigas*, *S. costatus*, and *S. pugilis* in Los Roques, Venezuela. Bull. Mar. Sci. 27:668–680.

Brownell, W. N., and J. M. Stevely.
1981. The biology, fisheries, and management of the queen conch, *Strombus gigas*. Mar. Fish. Rev. 43:1–12.

Burrell, V. J., Jr., J. J. Manzi, and W. Z. Carson.
1981. Growth and mortality of two types of seed oysters from the Wando River, South Carolina. J. Shellfish Res. 1:1–7.

Carter, J. G.
1980. Environmental and biological controls of bivalve shell mineralogy and microstructure. *In* D. C. Rhoads and R. A. Lutz (eds), Skeletal growth of aquatic organisms, biological records of environmental changes. Plenum Press, New York, p. 69–113.

Catterall, C. P., and I. R. Poiner.
1983. Age- and sex-dependent patterns of aggregation in the tropical gastropod *Strombus luhuanus*. Mar. Biol. 77:171–182.

Coulston, M. L., R. W. Berey, A. C. Dempsey, and P. Odum.
1987. Assessment of the queen conch (*Strombus gigas*) population and predation studies of hatch-

ery-reared juveniles in Salt River Canyon, St. Croix, US Virgin Islands. Proc. Gulf Caribb. Fish. Inst. 38:294–306.

Creswell, L.R.
1993. An historical overview of queen conch mariculture. *In* R. S.Appeldoorn and B. Rodriquez Q. (eds.), Queen conch biology, fisheries and mariculture. Fundacion Cientifica Los Roques, Caracas, Venezuela.

Cruz, R.S.
1986. Avances en la experimentacion de produccion massiva de caracol en Quintana Roo, Mexico. Proc. Gulf Caribb. Fish. Inst. 37:12–20.

Dalton, A.
1993. Mariculture of queen conch (*Strombus gigas* L.): development of nursery and grow-out techniques. *In* R. S. Appeldoorn and B. Rodriquez Q. (eds.), Queen conch biology, fisheries and mariculture. Fundacion Cientifica Los Roques, Caracas, Venezuela.

Dare, P. J., and D. B. Edwards.
1976. Experiments on the survival, growth, and yield of relaid mussels (*Mytilus edulis*) in the Menai Straits, North Wales. J. Cons., Cons. Intern. Explor. Mer 37:16–28.

Davis, M.
1993. Mariculture techniques for queen conch (*Strombus gigas* Linné): egg mass to juvenile stage. *In* R. S. Appeldoorn and B. Rodriquez Q. (eds.), Queen conch biology, fisheries and mariculture. Fundacion Cientifica Los Roques, Caracas, Venezuela.

Davis, M., and A. Dalton.
1991. New large-scale culturing techniques for *Strombus gigas* post larvae in the Turks and Caicos Islands. Proc. Gulf Caribb. Fish. Inst. 40:257–66.

Davis, M., A. Dalton, and P. Higgs.
1992. Recent developments in conch mariculture in the Turks and Caicos Islands. Proc. Gulf Caribb. Fish. Inst. 42:397–402.

Davis, M., C. Hesse, and G. Hodgkins.
1987. Commercial hatchery procedures for queen conch, *Strombus gigas*, seed for the research and grow-out market. Proc. Gulf Caribb. Fish. Inst. 38:326–335.

Day, R. W., and G. P. Quinn.
1989. Comparisons of treatments after an analysis of variance in ecology. Ecol. Monogr. 59:433–463.

Ebert, T. B.
1989. Growth of hatchery reared red abalone at Fitzgerald Marine Reserve: one year post-release. Calif. Fish. Game 75:178–179.

Emmett, B., and G. S. Jamieson.
1989. An experimental transplant of northern abalone, *Haliotis kamtschatkana*, in Barkley Sound, British Columbia. Fish. Bull. 87:95–104.

Flagg, P. J., and R. E. Malouf.
1983. Experimental planting of juveniles of the hard clam *Mercenaria mercenaria* (Linné) in the waters of Long Island, New York. J. Shellfish Res. 3:19–27.

Hensen, R. R.
1983. Queen conch management and culture in the Netherlands Antilles. Proc. Gulf Carib. Fish. Inst. 35:53–56.

Heslinga, G. A., F. E. Perron, and O. Orak.
1984. Mass culture of giant clams (F. Tridacnidae) in Palau. Aquaculture 39:197–215.

Heslinga, G. A., and T. C. Watson.
1985. Recent advances in giant clam mariculture. Proc. 5th Intern. Coral Reef Symp. 5:531–538.

Heyman, W. D., R. A. Dobberteen, L. A. Urry, and A. M. Heyman.
1989. Pilot hatchery for the queen conch, *Strombus gigas*, shows potential for inexpensive and appropriate technology for larval aquaculture in the Bahamas. Aquaculture 77:277–285.

Hurlbert, S. H.
1984. Pseudoreplication and the design of ecological field experiments. Ecol. Monogr. 54:187–211.

Iversen, E. S., D. E. Jory, and S. P. Bannerot.
1986. Predation on queen conchs, *Strombus gigas*, in the Bahamas. Bull. Mar. Sci. 39:61–75.

Jory, D. E., and E. S. Iversen.
1983. Conch predators: not a roadblock to mariculture. Proc. Gulf Carib. Fish. Inst. 35:108–111.
1988. Shell strength of queen conch, *Strombus gigas* L.: aquaculture implications. Aqua. Fish. Manag. 19:45–51.

Kojima, H.
1981. Mortality of young Japanese black abalone, *Haliotis discus discus*, after transplantation. Bull. Jpn. Soc. Sci. Fish. 47:151–159.

Laughlin, R. A., and E. Weil M.
1983. Queen conch mariculture and restoration in the Archipelago de Los Roques. Proc. Gulf Carib. Fish. Inst. 35:64–72.

Madenijian, C.P., B.M. Johnson, and S.R. Carpenter
1991. Stocking strategies for fingerling walleyes: an individual-based model approach. Ecol. Appl. 1:280–288.

Martin-Mora E.
1992. Developmental plasticity in the shell of the queen conch *Strombus gigas*. M.S. thesis, Florida State Univ., Tallahassee, 52 p.

Palmer, A. R.
1979. Fish predation and the evolution of gastropod shell sculpture: experimental and geographic evidence. Evolution 33:697–713.

Polovina, J. L.
1991. Evaluation of hatchery releases of juveniles to enhance rockfish stocks with application to Pacific ocean perch *Sebastes alutus*. Fish. Bull. 89:129–136.

Pulliam, H. R., and T. Caraco.
1984. Living in groups: is there an optimal group size? *In* J. R. Krebs and N. B. Davies (eds.), Behavioral ecology: an evolutionary approach, 2nd ed. Sinauer Assoc., Sunderland, Mass., p. 122–147.

Rathier, I.
1987. Etat d'avancement des recherches sur l'elevage du lambi (*Strombus gigas*) en Martinique. Proc. Gulf Carib. Fish. Inst. 38:336–344.

Ray, M., and A. W. Stoner.
In press. Experimental analysis of growth and survivorship in a marine gastropod aggregation: balancing growth with safety in numbers. Mar. Ecol. Prog. Ser.

Saito, K.
1984. Ocean ranching of abalones and scallops in northern Japan. Aquaculture 39:361–373.

Schiel, D. R., and B. C. Welden.
1987. Responses to predators of cultured and wild red abalone, *Haliotis rufescens*, in laboratory experiments. Aquaculture 60:173–188.

Searcy, R., and A. Salas.
1985. Studies on the ecology and re-seeding of abalone in Baja California. Trans. CIBCASIO 10:106–122.

Siddall, S. E.
1984a. Synopsis of recent research on the queen conch *Strombus gigas* Linné. J. Shellfish Res. 4:1–3.
1984b. Density-dependent levels of activity of juveniles of the queen conch *Strombus gigas* Linné. J. Shellfish Res. 4:67–74.

Skalski, J. R., and D. S. Robson.
1992. Techniques for wildlife investigations: design and analysis of capture data. Academic Press, San Diego, Calif., 237 p.

Stoner, A. W.
1989a. Winter mass migration of juvenile queen conch, *Strombus gigas*, and their influence on the benthic environment. Mar. Ecol. Prog. Ser. 56:99–104.
1989b. Density-dependent growth and the grazing effects of juvenile queen conch (*Strombus gigas* L.) in a tropical seagrass meadow. J. Exp. Mar. Bio. Ecol. 130:119–127.
In press. Significance of habitat and stock pre-testing for enhancement of natural fisheries: experimental analyses with queen conch. J. World Aquacult. Soc.

Stoner, A. W., M. D. Hanisak, N. P. Smith, and R. A. Armstrong.
1993. Large-scale distribution of queen conch nursery habitats: implications for stock enhancement. *In* R. S. Appeldoorn and B. Rodriquez Q. (eds.), Queen conch biology, fisheries and mariculture. Fundacion Cientifica Los Roques, Caracas, Venezuela.

Stoner, A. W., R. N. Lipcius, L. S. Marshall Jr., and A. T. Bardales.
1988. Synchronous emergence and mass migration in juvenile queen conch. Mar. Ecol. Prog. Ser. 49:51–55.

Stoner, A. W., and M. Ray.
1991. Experimental analysis of habitat quality for juvenile queen conch in seagrass meadows. Fish. Bull. 89:693–700.
1992. Transplanting as a test procedure before large-scale outplanting of juvenile queen conch. Proc. Gulf Caribb. Fish. Inst. 41:447–458.
1993. Aggregation dynamics in juvenile queen conch, *Strombus gigas*: population structure, mortality, growth, and migration. Mar. Biol. 116:571–582.

Stoner, A. W., and J. M. Waite.
1990. Distribution and behavior of queen conch, *Strombus gigas*, relative to seagrass standing crop. Fish. Bull. 88:573–585.
1991. Trophic biology of *Strombus gigas* in nursery habitats: diets and food sources in seagrass meadows. J. Moll. Stud. 57:451–460.

Tegner, M. J., and R. A. Butler.
1985. The survival and mortality of seeded and native red abalones, *Haliotis rufescens*, on the Palos Verdes peninsula. Calif. Fish Game 71:150–163.

Tettelbach, S. T., and P. Wenczel.
1991. Reseeding efforts and the status of bay scallop populations in New York following the appearance of brown tide. J. Shellfish Res. 10:273.

Tong, L. J., G. A. Moss, and J. Illingworth.
1987. Enhancement of a natural population of the abalone, *Haliotis iris*, using cultured larvae. Aquaculture 62:67–72.

Uki, N.
1984. Abalone culture in Japan. Proc. 9th and 10th US-Japan meetings on Aquaculture. Dep. Commer., NOAA Tech. Report NMFS 16:83–88.

Wicklund, R. I., L. J. Hepp, and G. A. Wenz.
1991. Preliminary studies on the early life history of the queen conch, *Strombus gigas*, in the Exuma Cays, Bahamas. Proc. Gulf Caribb. Fish. Inst. 40:283–298.

Wilbur, K. M.
1964. Shell formation and regeneration. *In* K. M. Wilbur and C M. Yonge (eds), Physiology of mollusca, Vol. 1. Academic Press, New York, p. 243–282.

A snow crab, *Chionoecetes opilio* (Decapoda, Majidae), fishery collapse in Newfoundland

David M. Taylor
Paul G. O'Keefe
Charles Fitzpatrick
Science Branch, Department of Fisheries and Oceans
P. O. Box 5667, St. John's, Newfoundland A1C 5X1

Abstract.—A fishery for snow crab, *Chionoecetes opilio*, began in 1979 in a shallow water (<200 m) area off the Avalon Peninsula of southeastern Newfoundland and developed rapidly with landings peaking at 8609 metric tons (t) in 1981. Landings began to decline in 1982, and dropped to 74 t in 1985. This fishery collapse coincided with similar declines in catch per unit of effort (CPUE) and abundance of newly molted male snow crab. In Bonavista Bay, a deep water (>200 m) fishing area north of the Avalon Peninsula, CPUE declined less and the proportion of newly molted male snow crab remained relatively constant during the same period. Coincident with the decline of the Avalon Peninsula fishery was a pronounced drop in mean bottom temperature on the commercial fishing grounds, from –0.6° C to –1.4°C, a phenomenon not observed in Bonavista Bay. This decline in water temperature appears to have been the cause of the fishery collapse because temperatures became low enough to interrupt the molting cycle of snow crab off the Avalon Peninsula. If the potential impact of the lower water temperatures and subsequent long-term cessation of growth and recruitment within the snow crab population had been recognized, the available pool of commercial-sized crab could have been harvested more slowly over a period of years to lessen the disruption of the fishery.

Manuscript accepted 18 October 1993
Fishery Bulletin 92: 412–419.

The Newfoundland snow crab, *Chionoecetes opilio*, fishery began in 1968, and until 1978 was confined to deep water (>220 m) bays and areas within 30 km of the coast. In 1978, fishing effort in offshore areas east of the Avalon Peninsula (Fig. 1) increased markedly, resulting in peak landings in 1981 (Fig. 2) of 8609 t (Taylor and O'Keefe[1]).

The Canadian Atlantic Fisheries Scientific Advisory Committee (CAFSAC) recommended that annual exploitation rates for commercially harvested snow crab stocks not exceed 50–60% of annual productivity in order to prevent overexploitation (Anon.[2]). The Committee adopted this guideline because the fishery targets males only and most males have an opportunity to mate at least once before reaching the minimum legal size, thereby ensuring adequate recruitment into the fishery and the reproductive integrity of the populations. However, should there be a recruitment failure, the reproductive potential is maintained by sublegal sexually mature males in the population and females that can produce at least two clutches of viable eggs from one copulation using stored sperm (Paul, 1984).

The fishery occurs from April until November each year. Typically, catch per unit of effort (CPUE) declines throughout the fishing season until July and August when a high level of molting activity results in an increased abundance of newly molted recruits. As fishermen are discouraged by processors from landing these low-yield soft-shelled crabs, new-shelled animals of legal size (≥95 mm carapace width (CW)) generally enter the fishery in the following spring. Their recruitment is evident by high CPUE values at the beginning of the next fishing season (Taylor and O'Keefe[1]).

Between 1979 and 1982, exploitation rates off the Avalon Peninsula remained within recommended levels, but beginning in 1982 catch rates declined rapidly until 1984 when fishing became uneconomical (Taylor and O'Keefe[3]). Other areas in Newfoundland, such as Bonavista Bay (Fig. 1), have consistently had exploitation rates in excess of recommended levels and consequently have experienced reductions in catch rates. However, the

[1] Taylor, D. M., and P. G. O'Keefe. 1984a. Assessment of Newfoundland snow crab (*Chionoecetes opilio*) stocks, 1982. Can. Atl. Fish. Sci. Advis. Comm. CAFSAC Res. Doc. 84/13, Dartmouth, Nova Scotia, 35 p.

[2] Anonymous, 1981. Advice on some invertebrate and marine plant stocks. Can. Atl. Fish. Sci. Advis. Comm. CAFSAC Advisory Document 81/1, Dartmouth, Nova Scotia, 6 p.

[3] Taylor, D. M., and P. G. O'Keefe. 1986. Analysis of the snow crab, *Chionoecetes opilio*, fishery in Newfoundland for 1985. Can. Atl. Fish. Sci. Advis. Comm. CAFSAC Res. Doc. 86/57, Dartmouth, Nova Scotia, 24 p.

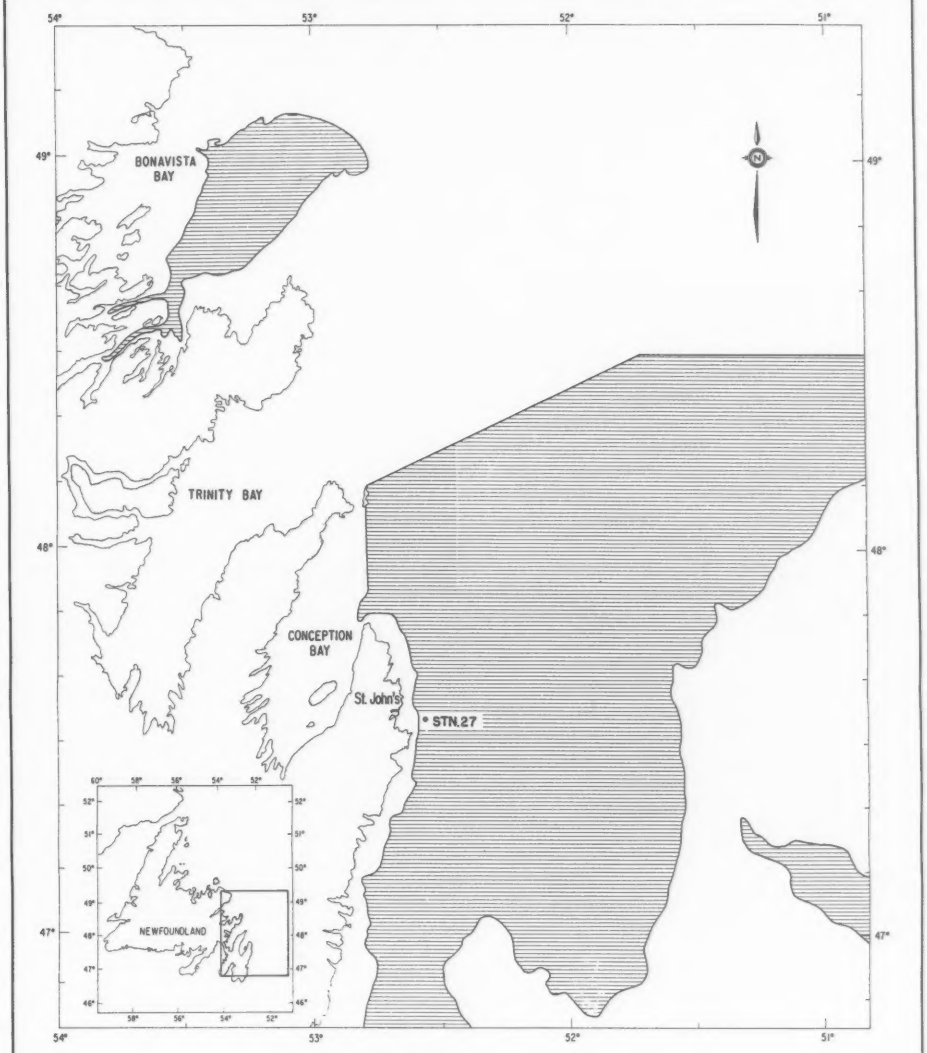

Figure 1

Offshore Avalon Peninsula and Bonavista Bay, Newfoundland, *Chionoecetes opilio* fishing grounds.

magnitude of the collapse in catch rates and landings off the Avalon Peninsula is unprecedented.

This paper examines biological data, fishermen's log returns, and temperature records from the Avalon Peninsula in comparison with similar data from Bonavista Bay in an attempt to describe possible reasons for this collapse.

Materials and methods

A total of 27 spring and fall cruises were conducted on the commercial fishing grounds off the Avalon Peninsula and in Bonavista Bay (Fig. 1) during 1979–88 to monitor population characteristics and catch rates. Fishing stations were selected randomly and strati-

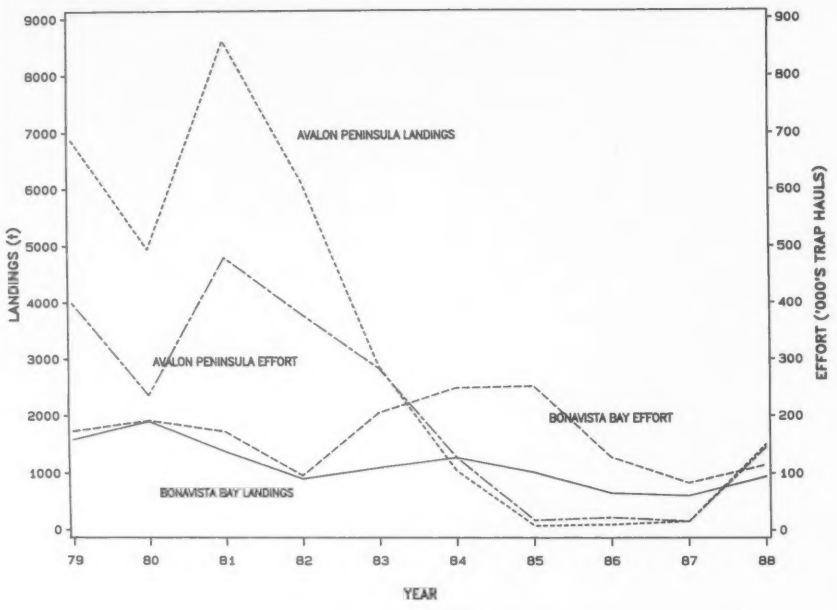

Figure 2

Summary of annual commercial landings and fishing effort for *Chionoecetes opilio* from offshore Avalon Peninsula and Bonavista Bay, Newfoundland.

fied by depth. Japanese-style conical traps baited with approximately two kg of northern shortfin squid, *Illex illecebrosus*, or with a mixture of squid and Atlantic mackerel, *Scomber scombrus*, and set in longline fleets of 12 were used to catch crabs. Although an attempt was made to duplicate the methodology employed by fishermen, space limitations onboard the research vessels restricted fleets of traps to 12 rather than the 50–70 used in commercial fishing. Weather permitting, traps were hauled after a 24–hour soak.

Crabs were removed from the traps, carapace width (CW) measured to the nearest 1 mm and shell condition determined. Three shell condition classes were used, based upon the following criteria described by Miller and O'Keefe (1981) and modified by Taylor et al. (1989):

Soft Shell (1) Carapace is brightly colored and free of epibiotic growth. Ventrally the crab is off-white to cream in color. Chelae bend, break, or crack with slight pressure. Bright iridescence present on dorsal margin of chelae. Animals within this category are considered as having molted not more than 90 days prior to capture.

New/Hard (2) Carapace is duller in color and a number of tube worms are present. Shell is hard and ventrally may be dark-cream colored and covered with discolored scratches. Chela does not bend or break when moderate thumb pressure is applied. Iridescence on chelae is reduced in intensity. This category generally applies to animals that have molted up to two years prior to capture.

Old/Hard (3) Carapace is dull brown in color and an assortment of calcareous tube worms and barnacles are present. The shell, although still hard, may have a slight "leathery" feel. Ventrally, the shell is brownish in color and many dark scratches evident. Iridescence on chelae is faint or absent. This category applies to animals that have not molted for at least two years.

Bottom temperatures from depths ≥170 m were obtained from an oceanographic station (Station 27) near the Avalon Peninsula fishing grounds (Fig. 1). There is no oceanographic station in Bonavista Bay, but bottom temperatures were obtained during eight research cruises by using expendable bathythermographs, or reversing thermometers.

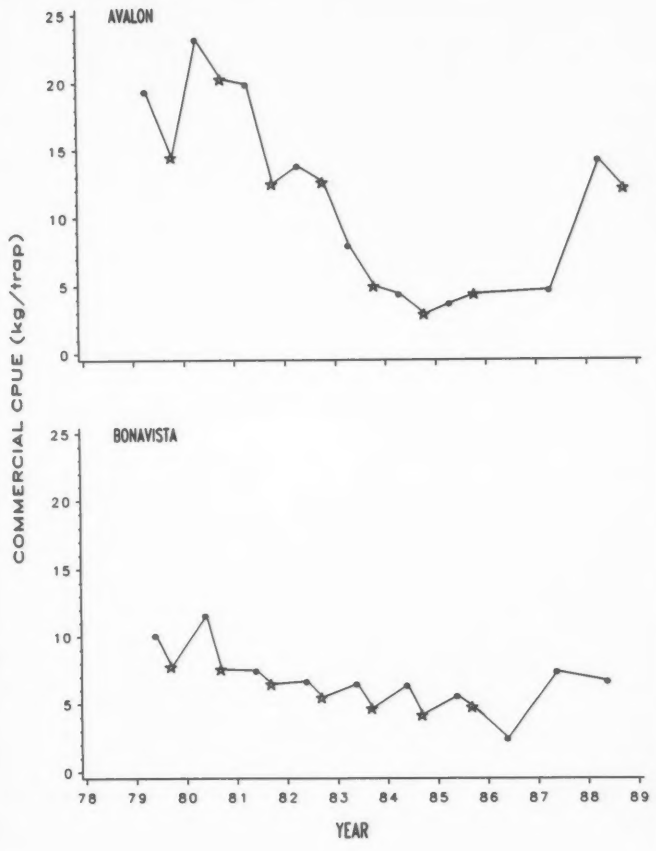

Figure 3

Commercial CPUE's for the Avalon Peninsula and Bonavista snow crab, *Chionoecetes opilio*, fisheries, 1979–88. Solid circles represent spring catch rates; stars represent fall catch rates.

CPUE's were derived for research fishing by multiplying the number of commercial crab caught per trap haul by a conversion factor of 0.45 kg/crab (Taylor, unpubl. data). Fishermen's logbook catch data were checked against processors' purchase slips. CPUE from logbook data was corrected for the percentage of sublegal crab in their catch as determined from sampling at processing plants conducted simultaneously with the research cruises. Total catch reported by log/purchase slips was then multiplied by the percentage of legal-sized animals and divided by the reported effort for the same time period to obtain a CPUE value comparable to that derived from a coincident research cruise.

Results

Logbook data

Landings and effort data from commercial logbooks are summarized in Figure 2. The drop in effort and landings for the Avalon Peninsula in 1980 is the result of a labor dispute and probably does not reflect abundance. Fishery CPUE in both the Avalon and Bonavista Bay areas was at its highest levels during the spring 1980 at 23.2 kg/trap haul and 11.6 kg/trap haul, respectively (Fig. 3). However, off the Avalon Peninsula, catch rates dropped to 19.9 kg/trap haul during the 1981 spring fishery as landings peaked at approximately 8500 t. CPUE declined to 13.8 kg/trap haul in 1982 despite logbook reports that new commercial fishing grounds were being exploited in the offshore areas (>100 km from land). This decline continued, reaching 3.7 kg/trap haul in the spring fishery of 1985 (Fig. 3), a drop of 84% from 1980 levels. This decline in CPUE was accompanied by a dramatic reduction in effort falling from 480,000 trap hauls in 1981 to 17,000 in 1985 (Fig. 2).

In comparison, the commercial spring fishery in Bonavista Bay, although overexploited (Taylor and O'Keefe[4]), has maintained a comparatively stable level of landings and CPUE since 1981 (905–1805 t and 4.1–to 8.2 kg/trap haul, respectively, despite an overall increase in effort from 1980 levels [Fig. 2]). Unlike the Avalon Peninsula fishery, spring catch rates in this area consistently reflect growth and recruitment into the commercial biomass as newly molted individuals recover to commercial acceptability over winter.

Research cruise CPUE and shell condition data

Logbook-derived commercial CPUEs and research cruise CPUE data with calculated confidence intervals are represented in Figures 3 and 4, respectively. Confidence intervals for most offshore Avalon research cruise CPUE data are fairly tight, with the exception of those data from a February 1986 cruise.

[4] Taylor, D. M., and P. G. O'Keefe. 1987. Analysis of the snow crab (*Chionoecetes opilio*) fishery in Newfoundland for 1986. Can. Atl. Fish. Sci. Advis. Comm. CAFSAC Res. Doc. 87/57, Dartmouth, Nova Scotia, 26 p.

These CPUE values were derived from only four fishing sets that were placed on the commercial fishing grounds opportunistically.

On the commercial fishing grounds off the Avalon Peninsula, CPUE's derived from research cruises were nearly identical to those of commercial enterprises at approximately 19.5 kg/trap haul in 1979 (spring). However, CPUEs diverged over the years primarily because commercial vessels had a greater fishing range than the research vessels. Nevertheless, the sharp drop in CPUE between 1982 and 1983 was reflected in both the commercial and research cruise data. In the commercial fishery, CPUE dropped from 13.8 kg/trap haul in the spring of 1982 to 8.0 kg/trap haul in the spring of 1983 (Fig. 3). This decline in crab abundance was mirrored in research cruise data, which indicate a decline from 9.3 kg/trap haul to 2.9 kg/trap haul over the same period (Fig. 4).

Research cruise data for this period in Bonavista Bay are not available. Logbook data, however, indicate that CPUE dropped by only 0.2 kg/trap haul (Fig. 4).

Data on shell conditions of legal-sized and prerecruit crabs from research cruises conducted off the Avalon Peninsula demonstrate that the drop in CPUE coincided with a decline in the proportion of new-shelled crabs from 52.4% to 18.6% (Fig. 5). In Bonavista Bay, the percentage of new-shelled animals dropped to 68.4% in the fall of 1983 from 97.7% in the spring of 1982. However, the proportion of new-shelled animals quickly rebounded to 97% in 1984 as opposed to 40.6% off the Avalon Peninsula during the same year.

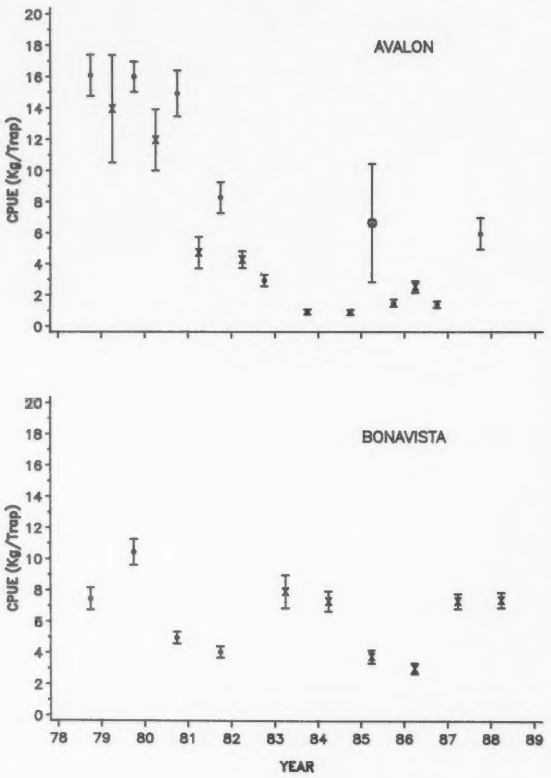

Figure 4

Research cruise CPUE's with calculated confidence intervals for the Avalon Peninsula and Bonavista Bay, 1979–88. Solid circles represent spring cruises and X's represent fall cruises. A circled 'X' is used to highlight data from the February 1986 cruise during which only 4 stations were fished in a nonrandom manner.

Temperature data

From the spring of 1978 through the first half of 1982, mean bottom temperature ranged from –0.3° C to –0.8°C off the Avalon Peninsula (Fig. 5). During the second half of 1982, the beginning of a trend towards colder bottom temperatures was evident. Bottom temperatures during this period dropped as low as –1.6° C and rarely rose above –1.0°C the entire period of mid 1982 to 1986. Two brief periods of warming occurred in both 1983 and 1984 but these periods were short-lived and weak. In 1986 a general warming trend began with an increase from the 1985 low of –1.6°C to around –1.1°C, a trend that has continued to the present.

The drop in temperature and the decrease in the proportion of new-shelled crabs appeared to coincide with bottom temperatures declining during April–May of 1982 whereas the percentage of new-shelled crabs dropped from 52.4% in April to 17.0% in September. Figure 5 illustrates that between 1982 and 1986 there were two brief periods (1983 and 1984) when mean bottom temperature at Station 27 increased slightly and coincidental increases in the proportion of new-shelled animals followed in 1984 and 1985. This delay between increase in water temperatures and appearance of new-shelled crabs is consistent with our current understanding of snow crab molting mechanisms (Moriyasu[5]).

The warming trend in July 1984 was short-lived (Fig. 5). During 1985 water temperatures dropped to the lowest level of all the years examined. Shell

[5] Moriyasu, M. Dept. Fisheries And Oceans, Gulf Fisheries Centre, Box 5030, Moncton, N.B. E1C 9B6. Personal commun. April, 1987.

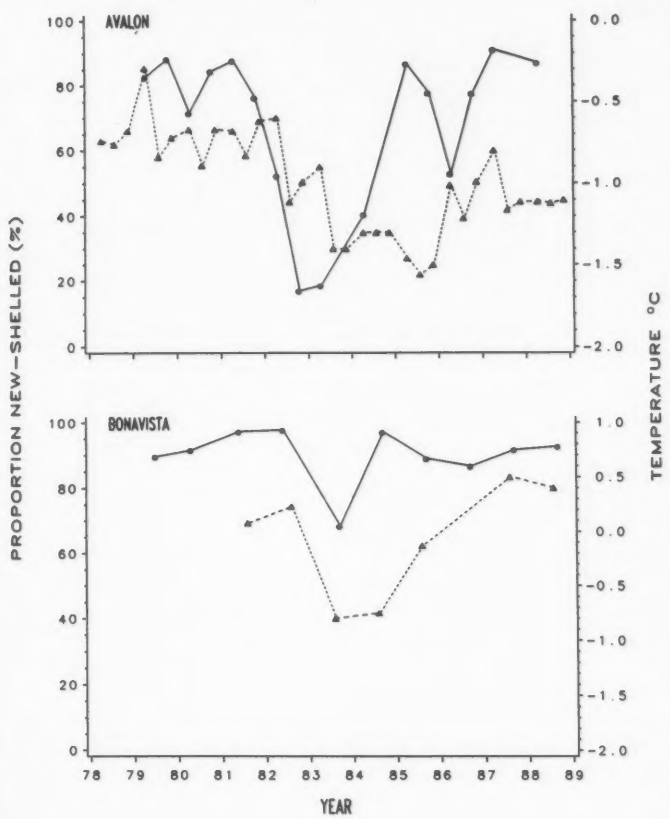

Figure 5

Changes in the percentages of new-shelled Avalon Peninsula and Bonavista Bay *Chionoecetes opilio* males ≥ 70 mm CW in relation to changes in bottom water temperatures on snow crab commercial fishing grounds, 1979–88. Solid circles connected by solid lines represent the proportion of new-shelled crabs and the triangles connected by a broken line represent bottom water temperature.

condition sampling in February 1986 indicated no molting activity during the summer and fall of 1985 (Fig. 5).

A further indication that the impact of these increases in new-shelled animals was minimal is illustrated by continuing low CPUE's (Figs. 3 and 4). Large proportions of new-shelled animals and higher CPUEs were not observed until the warming trend of 1986 was firmly established. While the decline in temperature between 1982 and 1983 is mirrored in data collected during Bonavista Bay research cruises (Fig. 5), the lowest temperatures encountered in Bonavista Bay are roughly equivalent to normal temperatures at Station 27 off Avalon Peninsula.

Although there was a significant decline in the proportion of new-shelled crab in 1983 after the water temperature declined (68.4% vs. 97.7%) in the spring of 1982 this value quickly rebounds in 1984 to 97.0% despite only a marginal warming of the water (Fig. 5).

Discussion

The tight confidence intervals for the Avalon Peninsula research cruise CPUE's (Fig. 4) for 1982–1987 (except February 1986) are indicative of just how severe, widespread, and enduring the resource depletion was in this area. Each research survey fished stations randomly selected and stratified by depth and covered virtually all the approximately 3600 sq. km. of commercial snow crab fishing grounds (Taylor et al.[6]). Had a sustained recovery been made by the crab population in any section of the commercial fishing grounds, it would have almost certainly been detected, either by our research cruises or by commercial crab fishermen.

Little is known about environmental factors that affect snow crab molting physiology. Low water temperatures may inhibit molting in crabs (Hiatt, 1948; Adelung, 1971; Leffler, 1972; Warner, 1977) and other decapods (Travis, 1954; Aiken, 1980; Ennis, 1983).

Foyle (1987) determined that snow crab from Cape Breton Island are able to maintain normal physiological functions at temperatures much higher than their normal temperature range. At high temperatures however and at temperatures below 1°C, reproductive growth and net energy consumption become slightly negative. Snow crab on the northeast coast of Newfoundland live at much lower water temperatures (<-0.75°C) than do those off the Cape Breton Island and a drop in temperature may result in such a "deficit" in their energy budget that molting physiology is impaired.

[6] Taylor, D. M., W. R. Squires, and P. G. O'Keefe. 1983. An alternate methodology for estimating snow crab (*Chionoecetes opilio*) populations in commercially fished areas. Can. Atl. Fish. Sci. Advis. Comm. CAFSAC Res. Doc. 83/1, Dartmouth, Nova Scotia, 10 p.

Aiken (1980) demonstrated that molting is inhibited in American lobsters, *Homarus americanus*, at 5° C if active premolt is not achieved before water temperature drops to that level. A similar physiological response to declining temperature may have contributed to the apparent reduction in molting in the snow crab population off the Avalon Peninsula after temperature dropped in 1982.

Molting in Newfoundland snow crab in this area generally occurs during May–August. The sharp decline in abundance of new-shelled crab in September indicated that many animals that would normally molt during this period apparently failed to do so, possibly as a result of extremely cold water temperatures.

Both Bonavista Bay and the offshore Avalon are affected by the Labrador Current. In 1982 the current became wider and deeper than in previous years causing a cooling effect throughout the water column (Akenhead[7]). Whereas this phenomenon affected the entire east coast of Newfoundland, it was most severe near the Avalon Peninsula primarily because of its comparative shallowness (174–200 m). Bonavista Bay is 220–486 m deep on the crab grounds and its depth may reduce the cooling effect of the Labrador Current (Akenhead[8]). This may explain why snow crab molting activity here was not as adversely affected as it was on the Avalon crab fishing grounds (Fig. 5).

The lack of recruitment into the fishery, between 1982 and 1986, meant that the snow crab resource off the Avalon Peninsula had been in effect "mined" rather than harvested as a renewable resource. The impact of the decline in snow crab abundance was dramatic. This marked decline in landings, from the Avalon Peninsula area, resulted in a substantial drop in employment and earnings from the snow crab fishery (Collins[9]).

Evidence of a link between temperature and molting is circumstantial. However, the drop in water temperature followed by a rapid decline in molting activity (Fig. 5), and subsequently CPUE (Fig. 4), makes a compelling argument that the yearly proportion of snow crab molting in an area is largely dependent on environmental conditions in the particular case where temperatures are very low and variable. The argument is supported by the observation that twice between 1984 and 1988 water temperatures rose and fell, affecting subsequent changes in the proportions of crabs molting off the Avalon Peninsula (Fig. 5). If molting of pre-recruit snow crabs and consequent recruitment into the fishery are affected by changes in water temperature, the impact of these changes should be included in resource management programs. The existing policy of allowing yearly exploitation rates of 50–60% should be re-examined. As the effects of these environmental changes may be long term, recommended exploitation rates could be reduced to prolong a fishery in which recruitment has been interrupted. Assessments of the fishery off the Avalon Peninsula (Taylor and O'Keefe[4]) indicate that exploitation rates were <65% between 1979 and 1981. However, owing to the failure of undersized males to molt into the fishery beginning in 1982, each successive year's standing stock was reduced until fishing was no longer economically viable. In contrast, although exploitation rates in Bonavista Bay consistently exceeded 75% (Taylor and O'Keefe[10], 1983[11], 1984b[12], and 1987[4]), molting within the population continued to provide sufficient recruitment for a viable fishery even though catch rates declined. With the exception of 1983 when the incidence of new-shelled animals (shell condition 1 and 2) in research cruise catches fell to 68% (Fig. 5), new-shelled animals composed in excess of 85% of the catch of legal-sized and immediate pre-recruits. This high level of molting appears to have prevented the precipitous decline in catches experienced in the offshore Avalon Peninsula area.

To prevent future declines of such proportions it may be advisable to monitor temperature, catch rates, and crab shell condition more closely on a seasonal basis. Efforts should also be made to determine thermal requirements for molting in snow crab. The implications for resource management strategy are simply that, regardless of exploitation levels, changes in temperature likely affect molting and hence recruitment to the standing stock to such an extent that assumptions regarding long-term sustainability of annual landings are not justified.

---

[7] Akenhead, S. A. 1986. The decline of summer subsurface temperatures on the Grand Bank, at 47°N, 1978–1985. NAFO SCR Doc. 86/25, 8 p.

[8] Akenhead, S. A. Institute of Ocean Sciences, Box 6000, Saanick Rd. Sydney, B.C. V8l 4B2. Personal commun., April 1987.

[9] Collins, J. F. Chief, Economic Analysis Division, Program Coordination & Economics Branch, Northwest Atlantic Fisheries Centre, P.O. Box 5667, St. John's, Newfoundland A1C 5X1. Personal commun. September 1993.

[10] Taylor, D. M., and P. G. O'Keefe. 1981. Assessment of snow crab (*Chionoecetes opilio*) stocks in Newfoundland, 1979. Can. Atl. Fish. Sci. Advis. Comm. CAFSAC Res. Doc. 81/57, Dartmouth, Nova Scotia, 34 p.

[11] Taylor, D. M., and P. G. O'Keefe. 1983. Assessment of snow crab (*Chionoecetes opilio*) stocks, in Newfoundland in 1980. Can. Atl. Fish. Sci. Advis. Comm. CAFSAC Res. Doc. 83/3, Dartmouth, Nova Scotia, 40 p.

[12] Taylor, D. M., and P. G. O'Keefe. 1984b. Assessment of Newfoundland snow crab (*Chionoecetes opilio*) stocks in Newfoundland for 1982. Can. Atl. Fish. Sci. Advis. Comm. CAFSAC Res. Doc. 84/3, Dartmouth, Nova Scotia, 30 p.

Acknowledgments

The authors are indebted to the crews of the C. S. S. *Shamook* and *Marinus* who provided able support during the research cruises. G. P. Ennis, J. Hoenig, R. Knoechel, D. G. Parsons, and P. Schwinghamer provided helpful comments on the manuscript. P. Collins, H. Mullett and G. King prepared the figures while M. Hynes and J. Lannon typed the manuscript.

Literature cited

Adelung, D.
1971. Studies on the molting physiology of decapod crustaceans as exemplified by the shore crab (*Carcinus maenas*). Sci. Mar. Res. at Heligloland 22:66–119. (English translation by Fish. Res. Board Can., Transl. Ser. No. 1877.)

Aiken, D. E.
1980. Molting and growth, Chapter 2. *In* J. S. Cobb and B. F. Phillips (eds.), The biology and management of lobsters, Vol. 1: Physiology and behavior. Academic Press, 463 p.

Ennis, G. P.
1983. Variation in annual growth in two Newfoundland lobster (*Homarus americanus*) populations in relation to temperature conditions. ICES C.M.1983/K:24, 11 p.

Foyle, T. P.
1987. Metabolism and energetics in a cold-water crustacean: the snow crab, *Chionoecetes opilio*. M.Sc. thesis, Dalhousie Univ., 83 p.

Hiatt, R. W.
1948. The biology of the lined shore crab, *Pachygrapsus crassipes* Randall. Pacific Sci. 2:135–218.

Leffler, C. W.
1972. Some effects of temperature on the growth and metabolic rate of juvenile blue crabs, *Callinecetes sapidus*, in the laboratory. Mar. Biol. 4:104–110.

Miller, R. J., and P. G. O'Keefe.
1981. Seasonal and depth distribution, size, and molt cycle of the spider crabs, *Chionoecetes opilio*, *Hyas araneus*, and *Hyas coarctatus* in a Newfoundland bay. Can. Tech. Rep. Fish. Aquat. Sci. 1003:iv + 18 p.

Paul, A. J.
1984. Mating frequency and viability of stored sperm in the tanner crab *Chionoecetes bairdi* (Decapoda, Majidae). J. Crust. Biol. 4(3):375–381.

Taylor, D. M., G. W. Marshall, and P. G. O'Keefe.
1989. Shell hardening in snow crabs *Chionoecetes opilio* tagged in soft-shelled condition. N. Am. J. Fish. Manage. 9:504–508.

Travis, D. F.
1954. The molting cycle of the spiny lobster, *Panulirus argus* Latreille. I: Molting and growth in laboratory-maintained individuals. Biol. Bull. 107:433–450.

Warner, G. F.
1977. The biology of crabs. Van Nostrand Reinhold Company, New York, 202 p.

Spawning time and recruitment dynamics of larval Atlantic menhaden, *Brevoortia tyrannus*, into a North Carolina estuary

Stanley M. Warlen

Beaufort Laboratory, Southeast Fisheries Science Center
National Marine Fisheries Service, NOAA
101 Pivers Island Road, Beaufort, North Carolina 28516–9722

Abstract.—Larval Atlantic menhaden, *Brevoortia tyrannus*, were collected weekly during their expected recruitment (November–April) to the estuary near Beaufort, North Carolina, over seven consecutive years beginning 1985–86. The larval density in nighttime quantitative samples was calculated and ages determined from otolith microstructure. Back-calculated birthdates and larval abundance data were used to estimate the relative contribution of weekly age cohorts to seasonal recruitment of larvae. Summaries of these data were measures of the spawning distributions. Larvae were recruited to the estuary from mid-November through April, with about 86% collected during February–April. In all years, age and size of larvae increased linearly throughout recruitment until the end of March and then declined. The mean age of recruited larvae over all years was 61 days and the mean standard length was 24.6 mm. Atlantic menhaden spawning season was protracted, lasting 4–6 months. In every spawning season, a dominant birthweek mode in either December or January contributed from 25–43% of the total recruits. More than 76% of all spawning occurred in the December– January period. Individual birthweek cohorts recruited to the estuary over periods from one week to several months. Cohorts that usually contributed the greatest number of individuals to estuarine recruitment usually recruited over longer periods. Atlantic menhaden have apparently selected a spawning season and location that ensures transport of larvae across the southeast United States continental shelf and arrival of most larvae during a time when conditions are conducive to optimal survival in the estuary.

Manuscript accepted 20 October 1993
Fishery Bulletin 92:420–433 (1994)

The Atlantic menhaden, *Brevoortia tyrannus*, is a commercially important clupeid that ranges on the east coast of the United States from the Gulf of Maine to the central coast of Florida. Tagging studies have shown that this species makes extensive seasonal migrations northward along the coast in spring and southward in fall and winter (Dryfoos et al., 1973; Nicholson, 1978). Most of the population is thought to overwinter in the area between Cape Hatteras, North Carolina, and northern Florida (Ahrenholz et al., 1987). Spatial and temporal trends in Atlantic menhaden spawning have been suggested by studies on the distribution of eggs and larvae (Reintjes, 1961; Kendall and Reintjes, 1975; Judy and Lewis, 1983) and studies on ovarian maturity and fecundity (Higham and Nicholson, 1964; Lewis et al., 1987). Those studies show that spawning occurs off New England from late spring to early summer and again in early fall, off the mid-Atlantic states in spring and fall and off the southeastern states from October to March. Maximum numbers of menhaden probably spawn in winter in offshore waters south of Cape Hatteras (Reintjes, 1969; Judy and Lewis, 1983) and waters off the North Carolina coast may be one of the major spawning grounds for Atlantic menhaden (Higham and Nicholson, 1964).

Plankton collections taken off North and South Carolina suggest that Atlantic menhaden may continuously spawn from late fall to early spring. Collections taken in the vicinity of Beaufort, North Carolina, from 1955 to 1961 (unpubl. data, National Marine Fisheries Service, Beaufort Laboratory, cited by Higham and Nicholson, 1964) showed larvae in samples beginning in November or early December and continuously thereafter until mid-April. Subsequent work supported these estimates of the timing of estuarine immigration of menhaden larvae. Lewis and Mann (1971) sampled larval menhaden semimonthly as the fish recruited to the estuary near Beaufort Inlet in the fall/winter 1966–67 and 1967–68 seasons, to estimate relative indexes of abundance. Densities of menhaden larvae recruited to estuaries were reported for North Carolina (Hettler and Chester, 1990; Warlen and Burke, 1990) and South Carolina (Allen and Barker, 1990).

Examination of otolith microstructure to count daily growth increments has made possible reasonably accurate estimates of the age and growth of the early life history stages of fishes. Age at estuarine recruitment can be tracked within and among seasons or years. Age at

recruitment is also a measure of the total time from offshore spawning to recruitment to the estuary. Valuable new information on the early life history of larvae can be obtained when estimates of recruitment densities are combined with estimates of seasonal age composition of the catches. Back-calculated birthdate distributions of larvae in each sample can be multiplied by the catch density to determine the relative contribution of birthweek cohorts to the number of immigrants.

The purposes of this seven-year study were to document the duration and relative abundance of larval Atlantic menhaden recruitment to the estuary near Beaufort, North Carolina; to measure size and estimate ages of recruited larvae; to back-calculate birthdate distributions of larvae; and to determine the contribution of birthweek cohorts to the number of immigrants for an estimation of temporal spawning within and among sampling years.

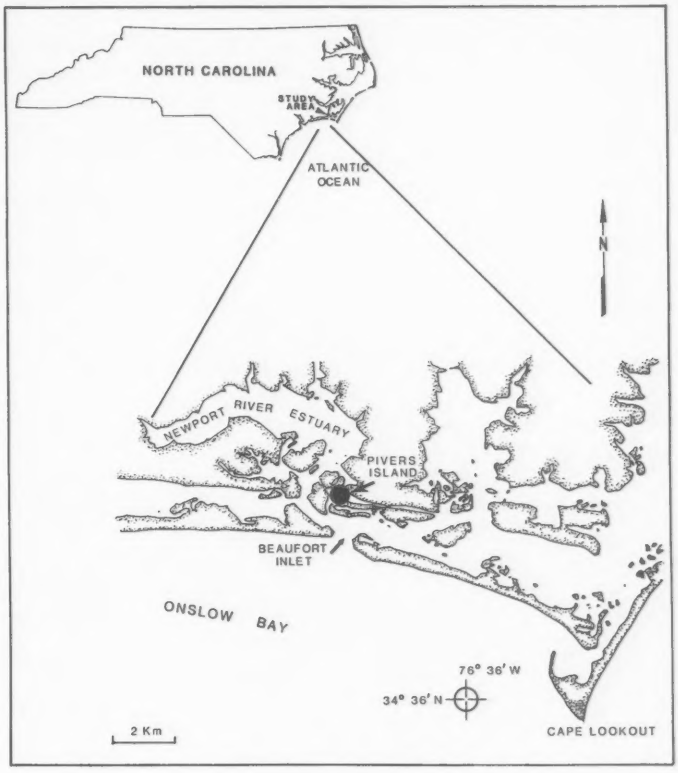

Figure 1

Location of the sampling site for larval Atlantic menhaden, *Brevoortia tyrannus*, in the lower Newport River estuary near Pivers Island, North Carolina.

Methods

Larval collection

Larval Atlantic menhaden were collected at a station adjacent to Pivers Island (Fig. 1) as they recruited to the Newport River estuary from the Atlantic Ocean. Sampling, designed to cover the expected recruitment period of mid-November to April (Lewis and Mann, 1971), ran for seven consecutive years beginning with the 1985–86 sampling year. Larvae were sampled from 13 November 1985 to 23 April 1986 with a 60-cm bongo frame with paired 505-μm mesh nets and flow meters pulled by a 6.7-m boat. Tows were made weekly during nighttime hours just after mid-flood tide, when the current was strongest, to reduce potential net avoidance by larvae. Data from the catch of both nets from two consecutive tows, one surface-bottom-surface (double oblique) in 3–5 m of water and one just under the surface (subsurface), were averaged to estimate larval density (number larvae/100 m^3 water fished) and to provide fish for ageing. The lack of a significant difference (paired comparison t-test, $P>0.05$) in catch density from subsurface and double oblique tows allowed the paired data to be combined. In the other six sampling years (19 November 1986–30 April 1987, 10 November 1987–4 May 1988, 16 November 1988–3 May 1989, 15 November 1989–2 May 1990, 14 November 1990–24 April 1991, and 13 November 1991–6 May 1992) larvae were collected, with a 1 × 2 m neuston net frame fitted with a 945-μm mesh net and flow meter fished just under the water surface from a bridge platform over the center of the channel adjacent to Pivers Island. This location was only meters from the site sampled with the bongo nets in 1985–86. As in 1985–86, all samples were collected weekly during nighttime hours at mid-flood tide. Three consecutive sets were made each night in 1986–87 and four each night in subsequent years. Because of the expected seasonal variation in menhaden abundance, sets were between 2 and 16 minutes long; most were 5–7 minutes long. Volume of

water fished by the net ranged from 41 to 805 m^3 but most sets filtered 150–350 m^3. Ichthyoplankton samples were preserved with 95% ethanol and diluted so that the final alcohol concentration was ≥70%. Samples not sorted within 24 hours were rinsed and represerved in 70% ethanol. As for bongo nets, these catches were standardized as the number of Atlantic menhaden/100 m^3 of water fished. The mean of the density data from all sets on a given night (bongo nets in 1985–86 and neuston nets in other years) was used as the estimate of density of Atlantic menhaden larvae recruited during the flood tide.

Simultaneous larval collections were made with bongo and neuston nets on 17 December 1986 (3 sets) and 18 March 1987 (4 sets) to test for differences in menhaden catch density between gear type. There were no significant differences in density of menhaden caught by gear type (ANOVA, $P>0.54$) or among sets (ANOVA, $P>0.24$). Hence, the catch data from bongo and neuston nets are comparable. The mean age or standard length (SL) also did not differ between the two types of nets.

Larval ageing

Larvae for ageing were subsampled from individual weekly night net sets in proportion to their contribution to the total nightly catch. In catches of up to 20 fish, all larvae were used. In catches of >20 fish, subsample sizes were proportional to catch but generally no more than 50 fish were aged per week. The ages of 3,864 larvae were determined.

The standard length of each larva to be aged was measured to the nearest 0.1 mm with an ocular micrometer. Sagittal otoliths were removed from their surrounding soft tissue, cleaned in distilled water, and placed on a glass microscope slide under a thin layer of Flo-Texx mounting medium. Otoliths were observed with transmitted light on a compound microscope fitted with a television camera. Growth increments were counted from images on a video monitor at microscope magnifications of 400× or 1,000×. One person made dual readings of otoliths from each fish. Readings were averaged if they differed by a count of four or less; if they differed by ≥5 increments, the fish was excluded from further analyses. Increment counts of about 2% of the aged fish differed by five or more. Estimated age was the number of increments counted plus an empirically derived value for the number of days (5) from spawning to first increment formation (Warlen, 1992). The otolith ageing technique for Atlantic menhaden larvae has been validated by Maillet and Checkley (1990), who established that larvae form one otolith growth increment per day. I assumed that the age at initial increment deposition did not vary and that the otolith increment deposition rate was constant within and between sampling seasons. A spawning date (birthdate) was assigned to each ageable larva by using the estimated age of the fish in days to back-calculate from the date of capture. Larvae spawned in a given calendar week were considered in the same calendar birthweek cohort.

Estuarine recruitment of birthweek cohorts

The percentage contribution of Atlantic menhaden larvae of all birthweek cohorts to the total recruitment was measured for each of the seven years from 1985–86 to 1991–92. For each weekly collection, the percentage of larvae spawned in each back- calculated birthweek was determined. Each percentage was then multiplied by the total larval density (number/100 m^3) for the week. Based on these results, density estimates were made for larvae from each birthweek cohort recruiting to the estuary on a given collection night.

Densities for each birthweek cohort were summed over all collections within a sampling year. The proportion that each birthweek cohort contributed was determined by dividing the individual birthweek sums by the total density of all birthweek cohorts for the recruitment year. These computations produced estimates of the relative contribution that each birthweek cohort made to the total recruitment of menhaden larvae into the estuary near Beaufort.

Results

Larval recruitment abundances

Larval Atlantic menhaden recruited to the estuary near Beaufort over a 5 to 5½ month period from mid-November to the end of April (Fig. 2). Larvae were generally recruited in highest densities during February–April and contained, on average, about 86% of the total estuarine recruitment during those months (Table 1). Recruitment was low in November and seldom extended into May. There was a distinct density mode in each of the seven years (Fig. 2). Except for 1988–89, modal density always occurred in March or April (Fig. 2, Table 2). Highest densities in a 3-week period (modal week plus adjoining weeks) in any year contributed 32–89% of the total density of Atlantic menhaden larvae for the year (Table 2).

During the recruitment period, most Atlantic menhaden larvae recruited to the estuary in pulses. Mean density varied from zero to about 570 larvae/100 m^3 and most samples contained <20 larvae/100 m^3 (Figs. 2 and 3). Catch densities varied among sets on any given night and the standard deviation in catch densities generally increased with the mean catch den-

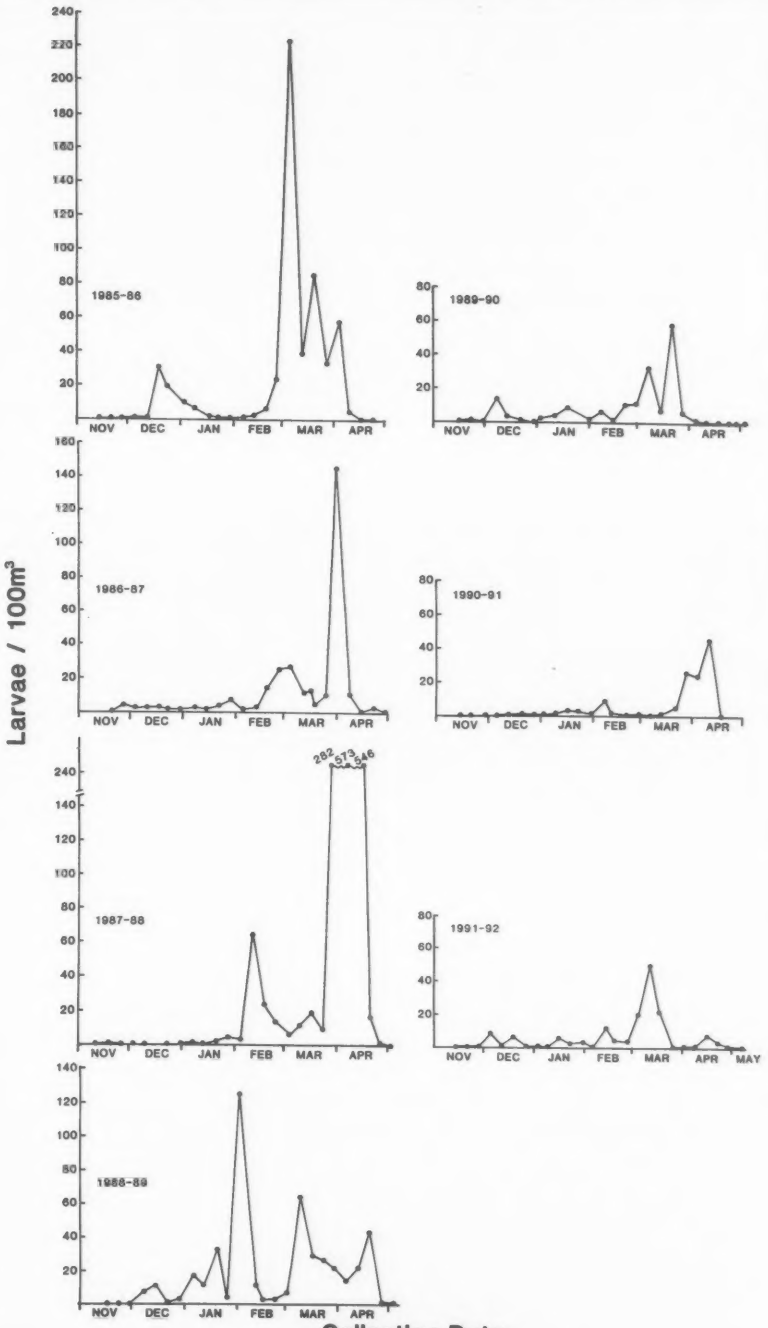

Figure 2

Weekly mean density (larvae/100 m^3) of Atlantic menhaden, *Brevoortia tyrannus*, larvae in collections at Pivers Island, North Carolina, in the lower Newport River estuary during seven consecutive estuarine recruitment years.

sity (Fig. 3). Relative abundance of larvae also varied among years (Fig. 2). The sum of weekly densities for individual sampling years differed by more than an order of magnitude (Table 2). Lowest relative abundances were observed for the last three sampling years.

I assumed that larval Atlantic menhaden caught each week were newly recruited to the estuary and that they were in transit past Pivers Island to upper portions of the estuary. These assumptions are supported by the presence of an abundance mode on 19 December 1985 (Fig. 2) and the presence of similar modes from bongo net sampling in the same estuary one-week later about 6 km up-estuary and two-weeks later about 11 km up-estuary (Warlen, unpubl. data). Also, the generally narrow 95% confidence limits in the age of larvae within each collection, along with no increase in the confidence limits through the recruitment year (Fig. 4), does not suggest an increase in the number of different birthweek cohorts in the lower estuary. In a number of cases, the week following a peak in density showed relatively low recruitment (Fig. 2), a pattern that did not suggest substantial carryover and accumulation of larvae from week to week. While a single sampling location may not reflect patterns of larval estuarine recruitment for all areas south of Cape Hatteras, it does provide a time-series description of relative larval recruitment abundances over several years inside a large inlet near the presumed major fall/winter spawning area.

Table 1

Percentage of the sum of the weekly mean densities (number/100 m^3) of larval Atlantic menhaden, *Brevoortia tyrannus*, recruited to the estuary near Pivers Island, North Carolina, November–May of each recruitment year.

Recruitment year	Month						
	Nov	Dec	Jan	Feb	Mar	Apr	May
1985–86	0.0	9.4	3.9	6.3	68.8	11.6	0.0
1986–87	1.6	4.1	5.5	15.1	18.5	55.2	0.0
1987–88	<0.1	<0.1	0.5	6.7	20.8	71.9	<0.1
1988–89	<0.1	5.0	14.4	30.9	32.2	17.4	<0.1
1989–90	1.2	10.7	12.8	16.9	57.0	1.4	0.0
1990–91	0.0	2.1	7.3	10.0	26.1	54.5	0.0
1991–92	0.5	10.4	8.5	13.5	57.5	9.5	0.1
Mean	0.5	6.0	7.6	14.2	40.1	31.6	<0.1

Table 2

Sum of weekly mean densities (number/100 m^3) by year, relative abundance (related to 1990–91), and peak recruitment density period (highest three consecutive sampling-date catches including the mode) of larval Atlantic menhaden, *Brevoortia tyrannus*, collected at Pivers Island, North Carolina, by recruitment year.

Recruitment year	Sum of weekly mean densities	Relative abundance	Peak recruitment density			
			Period of highest three consecutive catches			% of year
1985–86	554	4.3	Mar	5–Mar	19	59.9
1986–87	288	2.3	Mar	25–Apr	8	57.7
1987–88	1581	12.4	Mar	30–Apr	13	88.6
1988–89	459	3.6	Jan	19–Feb	1	32.2
1989–90	173	1.4	Mar	7–Mar	21	53.4
1990–91	128	1.0	Mar	27–Apr	10	75.2
1991–92	163	1.3	Mar	4–Mar	17	56.7

Age and size of larvae

In every sampling year the age of larvae increased linearly throughout estuarine recruitment until about the end of March after which the mean age declined (Fig. 4). Linear regressions of the mean estimated age over time, excluding the end-of-season down trending values, were significant (ANOVA, $P<0.001$) for each recruitment year. Young larvae were always collected early in each recruitment year (Fig. 4). Virtually all larvae collected in November were less than 40 days old. Larvae collected about late March were 2–4 times older than larvae collected early in the recruitment year. Except in a few cases, the within-sample age variation was small and the 95% confidence limits were within ±5 days of the mean age.

Larvae recruited to the estuary during peak recruitment were also the older larvae. Peak recruitment densities were in February–April (Fig. 2) and those larvae were older, generally age 60–90 days or older, as in 1987–88 when some were up to age 115 days (Fig. 4). The recruitment-year mean age of larvae varied between 55 and 74 days for the seven years. The mean age of larvae over all years was 61 days.

The standard length of larvae also increased significantly (ANOVA, $P<0.001$) within each recruitment year. The mean size of larvae increased to the end of March then decreased slightly to

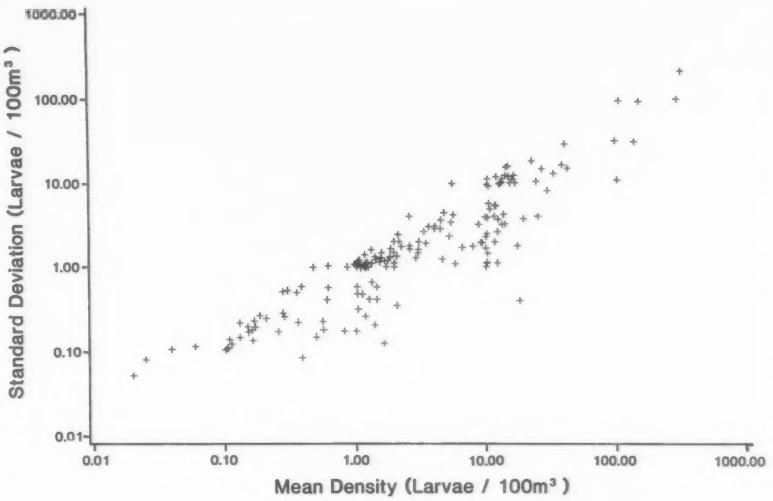

Figure 3

Plot of standard deviation versus mean density (larvae/100 m^3) for each collection night for larval Atlantic menhaden, *Brevoortia tyrannus*, sampled at Pivers Island, North Carolina, for seven consecutive recruitment years.

the end of the recruitment year (Fig. 5). Larvae recruited to the estuary were always >20 mm SL, except early in the recruitment year (November–December) when the mean size could be as low as 15 mm (Fig. 5). The overall recruitment year mean SL of larvae varied between 23.2 and 25.4 mm for the seven years and the mean SL over all years was 24.6 mm.

Spawning time

The menhaden spawning season in North Carolina was estimated from the birthdate distributions of larvae that survived to recruit to the estuary. The percentage distribution of spawning by week (Fig. 6) was based on the relative abundance of larvae collected at Pivers Island throughout the recruitment year. The spawning season was protracted, lasting four to six months (Fig. 6). Estimated spawning was variable among birthweeks. In every spawning season, there was a dominant birthweek mode that contributed from 25 to 43% of the total estuarine recruits. Except for 1987–88 (20 December 1987), these modes occurred very close to the new moon phase of the lunar cycle (10 January 1986, 31 December 1986, 9 December 1988, 28 December 1989, 15 January 1991, and 6 December 1991). Median spawning and modal spawning peaks were always in December or January as were the second and third quartile intervals of the distributions, except in 1989–90 when the second quartile interval extended into November (Fig. 6). Over all seven years, an average of more than 76% of all spawning occurred in December–January (Table 3). Earlier season spawning (October–November) contributed an average of 16% of the total, although November spawning alone could sometimes account for about 26% (Table 3). Little spawning occurred in February (. 7%) and in only two years did the March contribution exceed 1%.

The data suggest that within-season spawning frequency may be multimodal. There was an indication in 1985–86, 1986–87, 1989–90, 1990–91, and 1991–92 that a small, early mode may have occurred in October or November (Fig. 6). If there was an early mode in 1988– 89, it may have blended with the mode for later spawned fish. A small, late season mode (February or March) may also have been present and was most evident in the 1986–87, 1988–89, 1989–90, and 1991–92 spawning seasons.

Recruitment of birthweek cohorts

Individual birthweek cohorts were recruited to the estuary over periods from one week to several months (Fig. 7). Those birthweek cohorts that recruited over the shortest time periods were generally spawned either early (October) or late (February–March) in the season. Birthweek cohorts spawned from mid-November through January usually recruited over

Table 3

Percentage monthly spawning of Atlantic menhaden, *Brevoortia tyrannus*, estimated from the density-weighted, back-calculated birthdate distributions of larvae recruited to the estuary near Pivers Island, North Carolina, during November–April each recruitment year.

Recruitment year	Spawning month					
	Oct	Nov	Dec	Jan	Feb	Mar
1985–86	0.4	12.8	17.3	68.3	1.2	0.0
1986–87	4.2	7.3	64.4	21.1	2.9	0.1
1987–88	0.1	5.9	63.4	30.5	0.1	0.0
1988–89	0.6	26.5	49.2	9.1	12.9	1.7
1989–90	6.6	22.4	31.9	36.4	2.5	0.2
1990–91	0.0	8.4	11.6	54.2	25.8	0.0
1991–92	7.6	9.2	62.3	16.5	2.1	2.3
Mean	2.8	13.2	42.9	33.7	6.8	0.6

the longest time periods. However, 70% or more of any cohort were usually recruited in ≤3 consecutive weeks. In each recruitment year, those birthweek cohorts with the greatest numbers of individuals contributed most to the estuarine recruitment mode (Fig. 7). Also, within the larval catch of any given week, from one to 10 birthweek cohorts were represented (Fig. 7).

Discussion

Relatively large schools of larger-sized Atlantic menhaden, migrating from New England and mid-Atlantic states, along with local (North Carolina at least) Atlantic menhaden emigrating from estuaries, spawn off the southeast Atlantic states. The area from Cape Hatteras to about northern Florida is thought to be the major spawning location for this species (Higham and Nicholson, 1964; Reintjes, 1969; Nelson et al., 1977; Judy and Lewis, 1983; Lewis et al., 1987). Although the previous studies suggested that Atlantic menhaden spawn in the fall and winter off the southeast Atlantic states, none were able to estimate within season spawning intensity. The present study, which utilized samples collected throughout the recruitment year, estimated within season spawning intensity based on survivors entering an estuary. However, without any knowledge of egg production and the survival of cohorts between offshore spawning and estuarine recruitment, it was not possible to know how closely the estimates of the birthdate distributions represented the actual seasonal egg production.

In each year, the Atlantic menhaden spawning season was protracted. This long spawning season might indicate a "bet hedging" strategy (Lambert and Ware, 1984) where eggs are released continuously over the spawning season to ensure some reproduction during the most favorable periods for survival. Based on the birthdate distributions of larvae that recruit to the estuary, the most favorable period each year appears to be for those fish spawned in a relatively short period between early December and mid-to-late January. For all seven years, it was within this major spawning period that the week of peak spawning occurred. Larvae from this major spawning period are probably progeny of the large menhaden schools migrating southward from the New England and mid-Atlantic states. These schools, which contain many fish of spawning age (3+ years), are harvested from about late November to late January during the North Carolina fall purse seine fishery (Smith et al., 1987). Larvae spawned earlier (October–November), may originate from adults inhabiting North Carolina coastal waters and estuaries in the summer or from early fall adult immigrants to North Carolina waters (Wilkens and Lewis, 1971). Larvae spawned late (February–March) may have been spawned further south and immigrated to the estuary late in the season or were the offspring from northward migrating adults in early spring. This late spawned group contributed the younger, smaller larvae observed at the end of the recruitment year (Figs. 4 and 5).

Spawning locations, and routes and rates of transport probably account for the variation in age of larvae recruited to the estuary. While the precise locations of menhaden spawning are not known, the general area is thought to be on the mid- to outer-continental shelf off North Carolina (Checkley et al., 1988; Warlen, 1992). However, accounts of the occurrence of eggs are limited (Reintjes, 1969; Judy and Lewis, 1983) and no records of actual spawning events exist. Although some early season spawning may occur closer to shore, the largest contribution of recruited larvae to the estuary is later in the season, probably from the warm, plankton rich areas closer to the Gulf Stream. Water temperatures are generally ≥18°C (Govoni, 1993), even in winter. These warm temperatures are due, in part, to intrusions of warm surface water onto the middle continental shelf (Atkinson, 1985). Frequent upwelling events (Pietrafesa et al., 1985) stimulate primary productivity by providing nutrients (Atkinson, 1985; Yoder, 1985) for phytoplankton growth (Yoder et al., 1983)

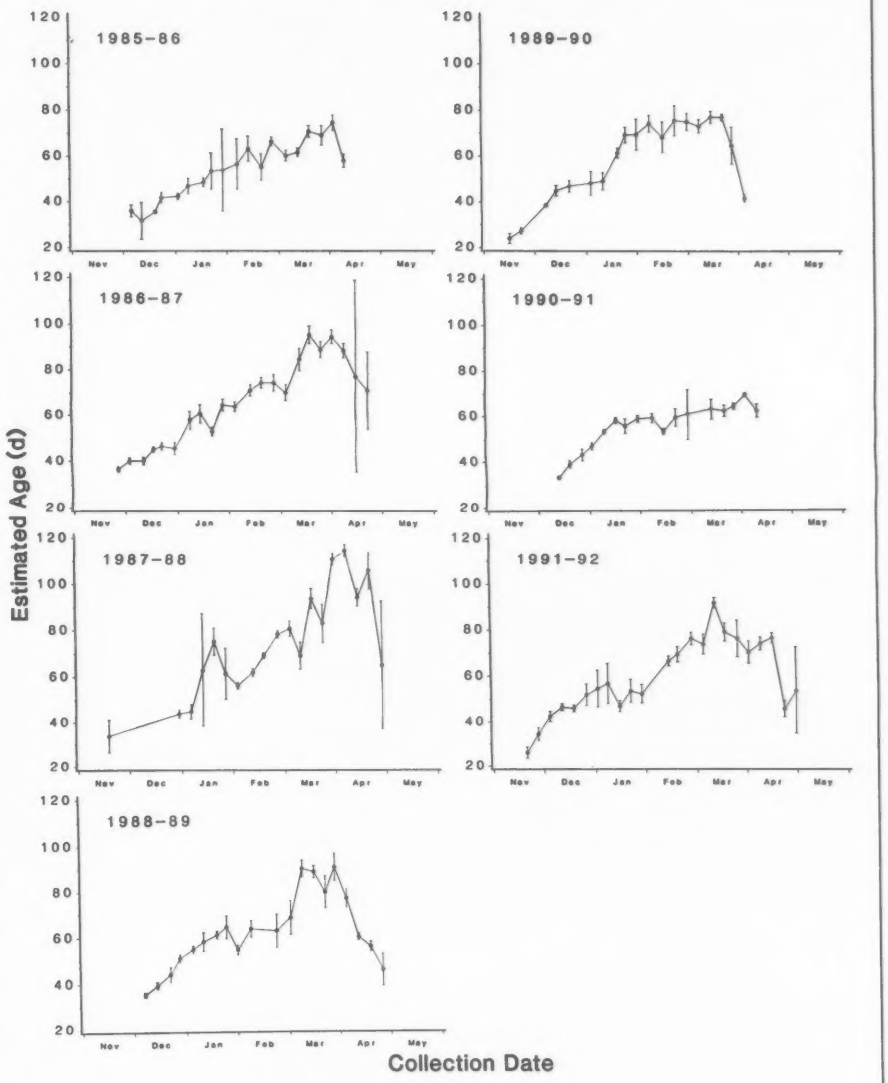

Figure 4

Mean of estimated ages (days) with 95% confidence limits of larval Atlantic menhaden, *Brevoortia tyrannus*, collected weekly over seven years during their estuarine recruitment at Pivers Island, North Carolina.

thus increasing secondary production (Paffenhöfer, 1985). This productive area is probably utilized by larval fishes spawned nearby.

Atlantic menhaden appear to spawn during periods (daily, seasonal) of lower light intensity. They probably spawn at night, and may have a diel pattern of ovulation and spawning that may be linked to the daily cycle of light and darkness as noted for many marine fishes (Bye, 1990). Reintjes (1969) examined Atlantic menhaden eggs at sea and concluded that estimated ages of groups of eggs of different stages suggested that "spawning occurred after mid-

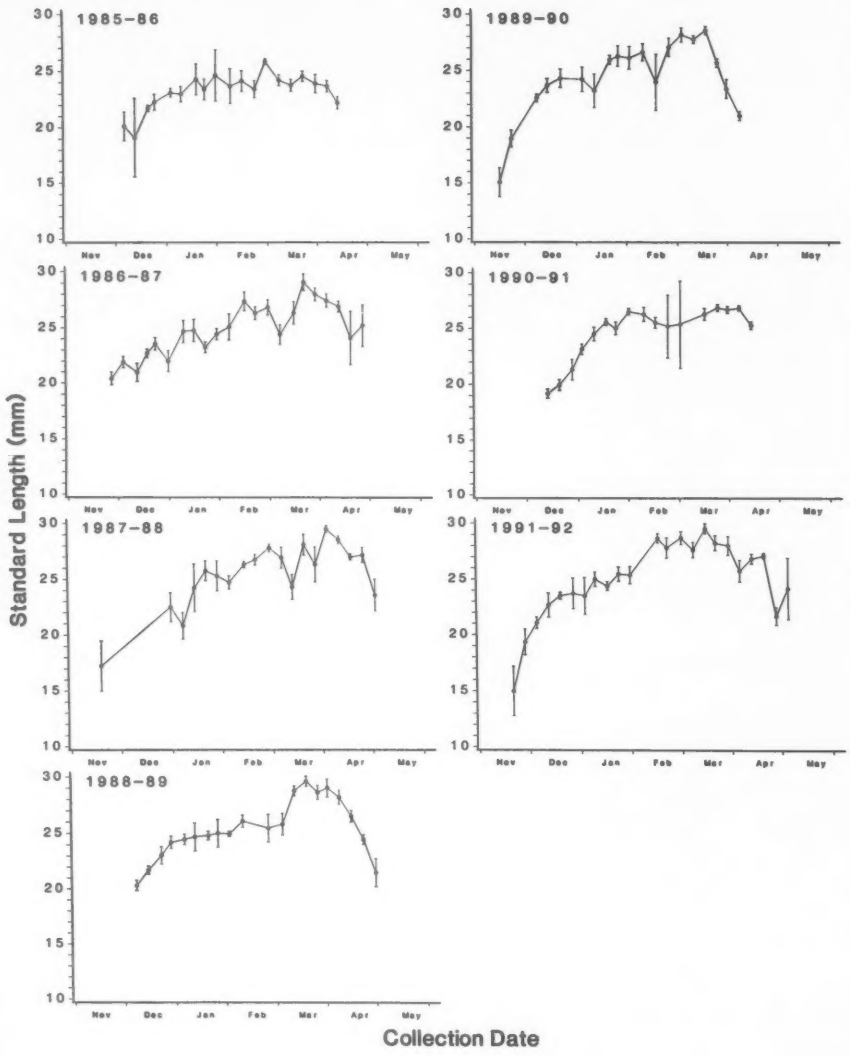

Figure 5

Mean standard length (mm) with 95% confidence limits of larval Atlantic menhaden, *Brevoortia tyrannus,* collected weekly over seven years during their estuarine recruitment at Pivers Island, North Carolina.

night but before dawn on three consecutive days." Ferraro (1981) also noted that Atlantic menhaden spawned at night and suggested that night spawning might be a means of reducing predation on spawners and eggs or of avoiding the deleterious effects of ultraviolet irradiation during early embryogenesis.

The relatively constant year-to-year spawning mode during December–January, observed in this study, occurs when the daily hours of darkness are maximal, 13 1/2–14 hours between sunset and sunrise, and when overcast days are more frequent. Peak spawning in each year (except 1987–88) also occurs very

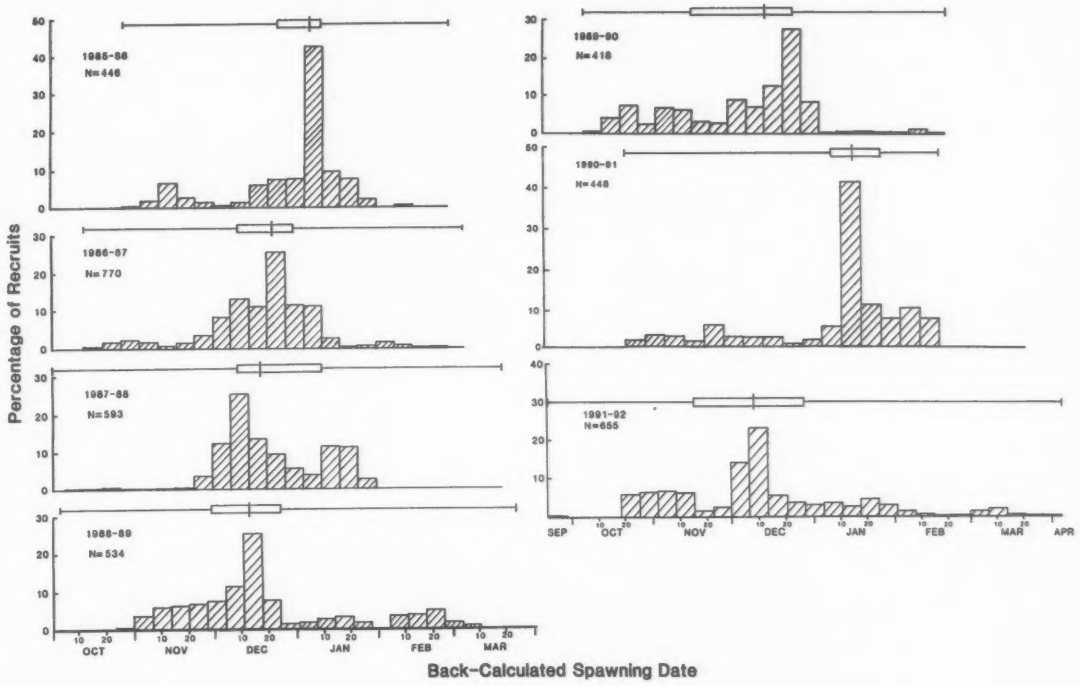

Figure 6

Birthdate frequency distributions calculated from the relative abundances of larval Atlantic menhaden, *Brevoortia tyrannus,* collected in the lower estuary at Pivers Island, North Carolina, in each of seven recruitment years. In each distribution, the vertical line is the median value and the box represents the 2nd and 3rd quartile intervals (central 50%). Lines beyond the boxes represent the range of data.

close to the new moon phase of the lunar cycle, which would also reduce available light during spawning.

Spawning of Atlantic menhaden off the southeastern Atlantic states is apparently timed to ensure transport of larvae across the continental shelf and arrival of most of the larvae (about 85% on average) during a time of optimal survival conditions in the estuary. Atlantic menhaden larvae that recruit to the estuary during the peak period (February–April) arrive when the water temperature is rising, prey abundance is high, and predator abundance and estuarine resident larval fishes and invertebrate (ctenophore) competitor abundances are low (Warlen and Burke, 1990). Some Atlantic menhaden larvae (about 15%) recruited to the estuary early in the season, November–December, before the period of coldest water temperatures in January (Warlen and Burke, 1990). These early recruited larvae may experience cold-related mortality if estuarine water temperatures drop to <4°C (Lewis, 1966; Wilkens and Lewis, 1971). However, larval Atlantic menhaden may tolerate lower temperatures than larvae of other species (e.g. spot, *Leiostomus xanthurus*) that recruit over the same period in the Beaufort area (Hoss et al., 1988). In milder winters, earlier recruited larvae may survive overwinter and, in the following spring and summer, may be larger than the more abundant Atlantic menhaden larval groups recruited several months later. Ahrenholz et al. (1989) observed a multi-modal distribution in lengths of juvenile menhaden collected in the summer in North Carolina which may reflect several seasonal abundance groups of immigrating larvae (early, middle, late) from a single spawning season.

Variation in egg production, mortality of eggs and larvae, and losses of larvae by advection to other areas of the coast probably account for the observed differences in relative recruitment abundances at the Pivers Island collection site. There was more than an order of magnitude difference between the relative abundances of the most abundant and the least abundant years. Lewis and Mann (1971) also ob-

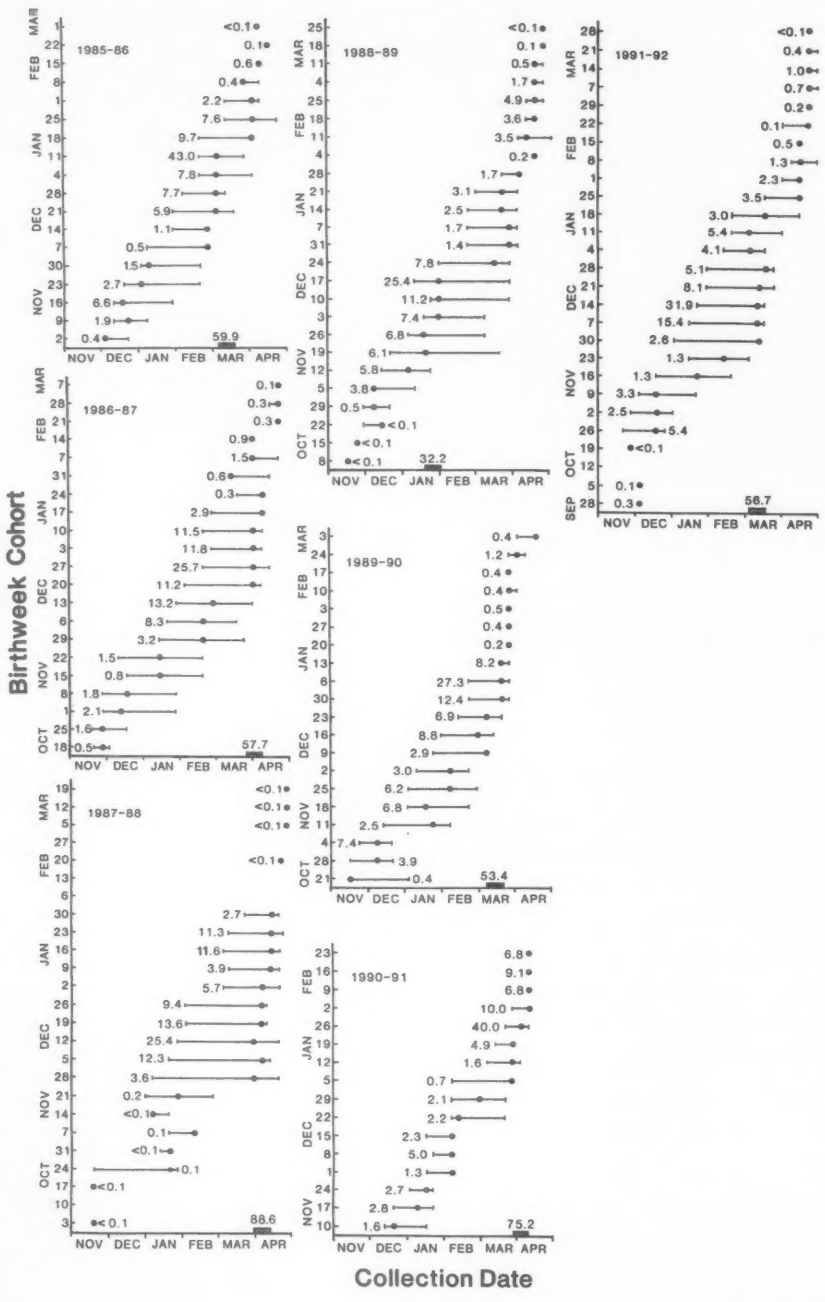

Figure 7

Percentage of total recruitment by birthweek cohort by year. The temporal range of collections of each birthweek cohort is denoted by a horizontal line and the mode by a closed circle. The peak recruitment density period (highest three consecutive sampling-date catches including the mode) and its percentage in each sampling season is indicated by the bar on the abscissa.

served a similar difference (13-fold) in relative abundances of Atlantic menhaden larvae at Pivers Island between 1966–67 and 1967–68. Their low year (1967–68) estimate was about one half that of the low year (1990–91) estimate in this study. Although relative abundances give estimates of larval recruitment among years, it is not known how representative the estimates are of coastwide year-class strength of the species. Virtual population analyses (VPA) indicate that recruitment to the commercial fishery to age-1 from the 1987–88 year class was about double that of the previous two years, 1985–86 and 1986–87 (Vaughan, 1993). In comparison, the estimate of larval recruitment for 1987–88 was about 3–5 times larger than the 1985–86 and 1986–87 estimates.

An increase in SL of Atlantic menhaden larvae recruited through each of seven seasons has also been observed in earlier studies. Higham and Nicholson (1964) noted that in plankton collections taken in the vicinity of Beaufort, North Carolina, Atlantic menhaden larvae were smallest in December and largest in April. Lewis and Mann (1971) found that the condition factor (weight/length^3) of larval Atlantic menhaden also increased throughout the season. Checkley et al. (1988) showed that the mean SL of Atlantic menhaden larvae about 10 km offshore increased over the period from January 15 to early March. The mean SL of Atlantic menhaden collected by Hettler and Chester (1990) increased from 16.0 mm in November to 27.6 mm in March then decreased to 24.0 mm in April. Similar trends in increasing size of larvae collected throughout the recruitment season have been observed for spot (Allen and Barker, 1990; Flores-Coto and Warlen, 1993), Atlantic croaker, *Micropogonias undulatus* (Allen and Barker, 1990; Warlen and Burke, 1990) and pinfish, *Lagodon rhomboides* (Warlen and Burke, 1990), all species that recruit to the estuary with Atlantic menhaden.

The total time required for transport of larvae from the area of hatching offshore to the estuary can be estimated from the ages of larvae caught at Pivers Island. The observed similarities in patterns of ages over each of the seven recruitment years suggest that similar transport mechanisms operate from year to year. Youngest larvae, which are only recruited at the beginning or end of each season, must be recruited most efficiently to the estuary, while at other times in the season transport becomes less efficient as larvae require longer to get to the estuary. Also, as the season progresses it is likely that spawning may occur further offshore (Warlen, 1992) as suitable spawning temperature water is found farther offshore and, consequently, larvae must be transported a greater distance to estuaries. The extended period of transport allows for mixing of birthweek cohorts offshore as evidenced by the greater mix of birthweek cohorts during the late season recruitment peaks. Mixing could also occur if there is "pooling" of larvae outside the inlet. Warlen (1992) suggested that larval Atlantic menhaden transported from offshore in North Carolina to the estuary was rapid in November–December. However, in the January–March period transport was only rapid to about the mid-shelf frontal zone, after which the overall transport rate was much slower. It is this latter spawned group that apparently makes up the largest fraction of estuarine immigrating larvae each recruitment season.

In summary, during an extended period (fall/winter/early spring) Atlantic menhaden spawn and their larvae are recruited to estuaries in the northern portion of the South Atlantic Bight. Although there is variation, consistent temporal patterns of spawning, recruitment density, and age and size trends are observed from year to year. Back-calculated modes in spawning suggest the importance of short periods within the total spawning season and peaks in estuarine recruitment suggest the importance of larval across-continental-shelf transport and near-shore concentrating mechanisms.

Acknowledgments

I gratefully acknowledge the work of Mary Boyd, William Rugen, and Elisabeth Laban who prepared and read otoliths. David Colby gave valuable assistance with statistical problems and data management. Peter Hanson helped with the use of a statistical graphics program and Elisabeth Laban worked on data summaries. Lynn Barker, Douglas Vaughan, and David Peters provided helpful, critical reviews of an earlier draft of the manuscript. This research could not have been completed without the able assistance of many persons who helped make the larval fish collections, especially on many cold winter's nights; I sincerely appreciate their help. Support for portions of this study was received from the South Atlantic Bight Recruitment Experiment (SABRE) program of the National Oceanic and Atmospheric Administration's Coastal Fisheries Ecosystem/Coastal Ocean Program.

Literature cited

Ahrenholz, D. W., W. R. Nelson, and S. P. Epperly.
1987. Population and fishery characteristics of Atlantic menhaden, *Brevoortia tyrannus*. Fish. Bull. 85:569–600.

Ahrenholz, D. W., J. F. Guthrie, and C. W. Krouse.
1989. Results of abundance surveys of juvenile Atlantic and gulf menhaden, *Brevoortia tyrannus* and

B. patronus. Dep. Commer., NOAA Tech. Rep. NMFS 84, 14 p.

Allen, D. M., and D. L. Barker.
1990. Interannual variations in larval fish recruitment to estuarine epibenthic habitats. Mar. Ecol. Prog. Ser. 63:113–125.

Atkinson, L. P.
1985. Hydrography and nutrients of the southeastern U.S. continental shelf. *In* L. P. Atkinson, D. W. Menzel, and K. A. Bush (eds.), Oceanography of the southeastern U.S. continental shelf, p. 77–92. Am. Geophys. Union, Wash. D.C.

Bye, V. J.
1990. Temperate marine teleosts. *In* A. D. Munro, A. P. Scott, and T. J. Lam (eds.), Reproductive seasonality in teleosts: environmental influences, p. 125–143. CRC Press, Boca Raton, FL.

Checkley, D. M., Jr., S. Raman, G. L. Maillet, and K. M. Mason.
1988. Winter storm effects on the spawning and larval drift of a pelagic fish. Nature (Lond.) 335: 346–348.

Dryfoos, R. L., R. P. Cheek, and R. L. Kroger.
1973. Preliminary analysis of Atlantic menhaden, *Brevoortia tyrannus*, migrations, population structure, survival and exploitation rates, and availability as indicated by tag returns. Fish. Bull. 71:719–734.

Ferraro, S. P.
1981. Eggs and larvae of Atlantic menhaden (*Brevoortia tyrannus*) in the Peconic Bays, New York in 1972–74. Rapp. P.-v. Réun. Cons. Int. Explor. Mer 178:181–182.

Flores-Coto, C., and S. M. Warlen.
1993 Spawning time, growth and recruitment of larval spot (*Leiostomus xanthurus*) into a North Carolina estuary. Fish. Bull. 91:8–22.

Govoni, J. J.
1993. Flux of larval fishes across frontal boundaries: examples from the Mississippi River plume front and the western Gulf Stream front in winter. Bull. Mar. Sci. 53:538–566.

Hettler, W. F., Jr., and A. J. Chester.
1990. Temporal distribution of ichthyoplankton near Beaufort Inlet, North Carolina. Mar. Ecol. Prog. Ser. 68:157–168.

Higham, J. R., and W. R. Nicholson.
1964. Sexual maturation and spawning of Atlantic menhaden. Fish. Bull. 63:255–271.

Hoss, D. E., L. Coston-Clements, D. S. Peters, and P. A. Tester.
1988. Metabolic responses of spot, *Leiostomus xanthurus*, and Atlantic croaker, *Micropogonias undulatus*, larvae to cold temperatures encountered following recruitment to estuaries. Fish. Bull. 86:483–488.

Judy, M. H., and R. M. Lewis.
1983. Distribution of eggs and larvae of Atlantic menhaden, *Brevoortia tyrannus*, along the Atlantic coast of the United States. Dep. Commer., NOAA Tech. Rep. NMFS SSRF-774, 23 p.

Kendall, A. W., Jr., and J. W. Reintjes.
1975. Geographic and hydrographic distribution of Atlantic menhaden eggs and larvae along the Middle Atlantic Coast from RV *Dolphin* cruises, 1965–66. Fish. Bull. 73:317–335.

Lambert, T. C., and D. M. Ware.
1984. Reproductive strategies of demersal and pelagic spawning fish. Can. J. Fish. Aquat. Sci. 41:1565–1569.

Lewis, R. M.
1966. Effects of salinity and temperature on survival of larval Atlantic menhaden, *Brevoortia tyrannus*. Trans. Am. Fish. Soc. 95:423–426.

Lewis, R. M., and W. C. Mann.
1971. Occurrence and abundance of larval Atlantic menhaden *Brevoortia tyrannus*, at two North Carolina inlets with notes on associated species. Trans. Am. Fish. Soc. 100:296–301.

Lewis, R. M., D. W. Ahrenholz, and S. P. Epperly.
1987. Fecundity of Atlantic menhaden, *Brevoortia tyrannus*. Estuaries 10:347–350.

Maillet, G. L., and D. M. Checkley Jr.
1990. Effects of starvation on the frequency of formation and width of growth increments in sagittae of laboratory-reared Atlantic menhaden *Brevoortia tyrannus* larvae. Fish. Bull. 88:155–165.

Nelson, W. R., M. C. Ingham, and W. E. Schaaf.
1977. Larval transport and year-class strength of Atlantic menhaden, *Brevoortia tyrannus*. Fish. Bull. 75:23–41.

Nicholson, W. R.
1978. Movements and population structure of Atlantic menhaden indicated by tag returns. Estuaries 1:141–150.

Paffenhöfer, G.-A.
1985. The abundance and distribution of zooplankton on the southeastern shelf of the United States. *In* L. P. Atkinson, D.W. Menzel, and K. A. Bush (eds.), Oceanography of the southeastern U.S. continental shelf, p. 104–117. Am. Geophys. Union, Wash. D.C.

Pietrafesa, L. J., G. S. Janowitz, and P. A. Wittman.
1985. Physical oceanographic processes in the Carolina Capes. *In* L. P. Atkinson, D. W. Menzel, and K. A. Bush (eds.), Oceanography of the southeastern U.S. continental shelf, p. 23–32. Am. Geophys. Union, Wash. D.C.

Reintjes, J. W.
1961. Menhaden eggs and larvae from MV *Theodore N. Gill* cruises, South Atlantic coast of the United States, 1953–54. U.S. Fish Wildl. Serv. SSRF-393, Dep. Interior, Bur. Comm. Fish., 7 p.
1969. Synopsis of biological data on the Atlantic menhaden, *Brevoortia tyrannus*. U.S. Fish Wildl. Serv. Circ. 320, Dep. Interior, Bur. Comm. Fish., 30 p.

Smith, J. W., W. R. Nicholson, D. S. Vaughan, D. L. Dudley, and E. A. Hall.
1987. Atlantic menhaden, *Brevoortia tyrannus*,

purse seine fishery, 1972–84, with a brief discussion of age and size composition of the landings. Dep. Commer., NOAA Tech. Rep. NMFS 59, 23 p.

Vaughan, D.S.

1993. A comparison of event tree risk analysis to Ricker spawner-recruit simulation: an example with Atlantic menhaden. *In* S. J. Smith, J. J. Hunt, and D. Rivard (eds.), Risk evaluation and biological reference points for fisheries management, p. 231–241. Can. Spec. Publ. Fish. Aquat. Sci., No. 120.

Warlen, S. M.

1992. Age, growth and size distribution of larval Atlantic menhaden off North Carolina. Trans. Am. Fish. Soc. 121:588– 598.

Warlen, S. M., and J. S. Burke.

1990. Immigration of larvae of fall/winter spawning marine fishes into a North Carolina estuary. Estuaries 13:453–461.

Wilkens, E. P. H., and R. M. Lewis.

1971. Abundance and distribution of young Atlantic menhaden, *Brevoortia tyrannus*, in the White Oak River estuary, North Carolina. Fish. Bull. 69:783–789.

Yoder, J. A.

1985. Environmental control of phytoplankton production on the southeastern U.S. continental shelf. *In* L. P. Atkinson, D. W. Menzel, and K. A. Bush (eds.), Oceanography of the southeastern U.S. continental shelf, p. 93–103. Am. Geophys. Union, Wash. D.C.

Yoder, J. A., L. P. Atkinson, S. S. Bishop, E. E. Hofmann, and T. N. Lee.

1983. Effect of upwelling on phytoplankton productivity on the outer southeastern U.S. continental shelf. Continental Shelf Res. 1:385–404.

Interannual variability of dolphin habitats in the eastern tropical Pacific. I: Research vessel surveys, 1986-1990

Stephen B. Reilly
Paul C. Fiedler
Southwest Fisheries Science Center, National Marine Fisheries Service, NOAA
P.O. Box 271, La Jolla, CA 92038

Abstract.—We used canonical correspondence analysis (CCA), an eigenvector ordination technique that includes direct gradient analysis, to investigate habitat use by spotted, *Stenella attenuata*, spinner, *S.longirostris*, striped, *S. coeruleoalba*, and common, *Delphinis delphis*, dolphins in the eastern tropical Pacific during 1986–90. Data were collected during annual research vessel cruises conducted in August–November of each year. Environmental variables included in the analyses were surface temperature, salinity, sigma-t, and chlorophyll, and thermocline depth and thickness. The dominant pattern in the species-environment relationship (1st canonical axis) separated common dolphins from spotted and spinner dolphins, based on their associations with cool upwelling habitat and warm tropical habitat, respectively. The second axis separated whitebelly spinners from eastern spinner dolphins. Both occurred in tropical water, but were separated primarily by thermocline topography. The species-environment correlations were 0.67 on the first axis, 0.42 on the second. Overall, the environmental data explained 15% of the variance in the species data. For individual school types this ranged from 36% for common dolphins to 6% for striped dolphins. Interannual variability in the species data was small but was judged significant by a Monte Carlo randomization test. Residual interannual variance was insignificant after removing variance associated with environmental variables.

Manuscript accepted 27 September 1993
Fishery Bulletin 92:434–450 (1994)

The eastern tropical Pacific (ETP) supports a diverse and abundant cetacean fauna of over 25 species (Leatherwood et al., 1982; Au and Perryman, 1985). It is a vast area, larger than the entire North Atlantic. Its waters are truly pelagic, except near a few islands and over a narrow continental shelf. Prior to the 1960s almost nothing was known of the distribution and ecology of the region's cetaceans beyond summaries of catch localities from nineteenth century fisheries for large whales (Townsend, 1935).

By the late 1960s, it became clear that large numbers of dolphins were being killed in the ETP in tuna purse seine operations (Perrin, 1969). The U.S. government initiated a program at that time to place scientific observers on purse seiners to monitor dolphin mortality (Smith, 1983). Beginning in 1974, research vessels were dispatched to the region to supplement the observer data (Holt et al., 1987). The combination of these efforts has produced unprecedented amounts of information on pelagic cetaceans. In this study we focused on the dolphin species affected by the tuna fishery: spotted dolphins, *Stenella attenuata*, two subspecies of spinner dolphins, *S. longirostris*, "whitebelly spinners" and "eastern spinners" (Perrin, 1990), striped dolphins, *S. coeruleoalba*, and common dolphins, *Delphinus delphis*.

Dolphin distribution patterns have been described from sighting and collection localities (e.g. Evans, 1975; Perrin, 1975; Perrin et al., 1983, 1985; Au and Perryman, 1985). Au and Perryman (1985) studied cetacean habitats of the eastern tropical Pacific from sightings and oceanographic data collected during the northern winter. They described two complementary patterns, both with apparent links to regional oceanography. One pattern, shown by common and striped dolphins, coincided with "upwelling-modified" conditions found along the equator and at the tropical terminations of eastern boundary currents off Baja California and the coasts of Ecuador and northern Peru (described in more detail below in Study Area). The second pattern, shown by spotted and spinner dolphins, coincided with largely tropical waters off Mexico, where warm, low-salinity surface waters occur over a strong, relatively shallow thermocline.

Reilly (1990) examined ETP dolphin distributions during the northern summer, and quantitatively tested Au and Perryman's habitat hypotheses. He found an apparent offshore shift in spotted, spinner, and striped (but not common) dolphins coincident with seasonal shoaling of a thermocline ridge along 10°N (Fig. 1). This seasonal shoaling is part of the dominant

pattern of seasonal change in the ETP, associated with the north-south movement of the Intertropical Convergence Zone between the trade winds (Fiedler, 1992). Statistical tests supported the habitat hypotheses of Au and Perryman (1985) for spotted, spinner, and common dolphins, but not for striped dolphins. During the summer, striped dolphins occupied habitat that was geographically complementary with habitats of both common and of spotted/spinner dolphins (Fig. 1). Striped dolphin habitat was indistinguishable statistically from either the upwelling-modified or tropical habitats with the variables used, indicating that other factors or processes act to separate these dolphins from the others.

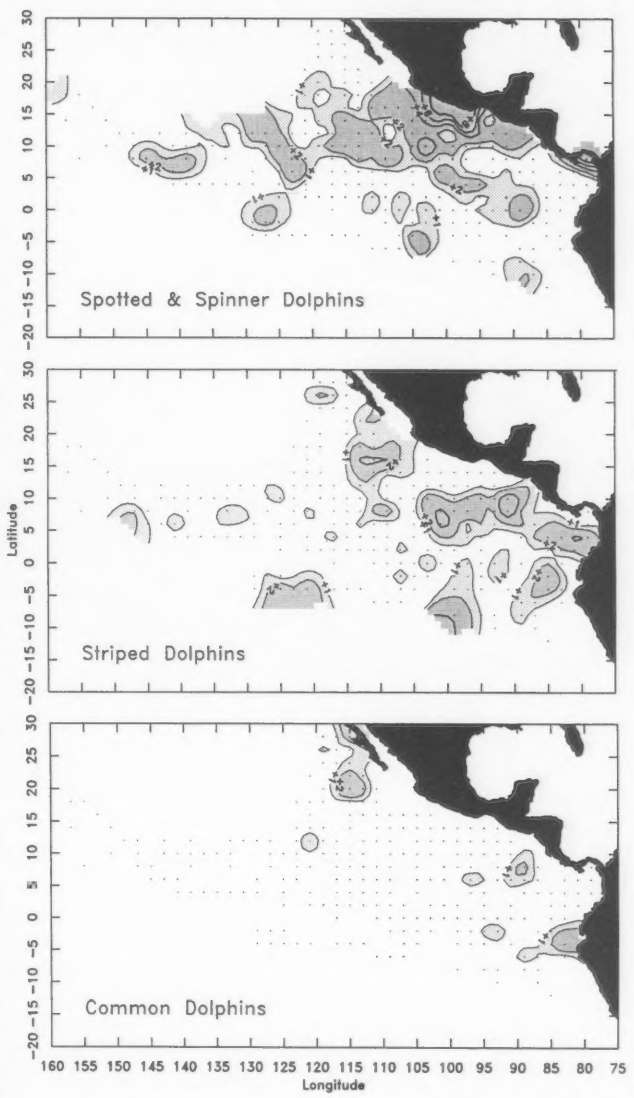

Figure 1

Dolphin distributions in the northern summer in the eastern tropical Pacific, from Reilly (1990). Contours are for encounter rates per 185 km searched. Dots represent centers of 2° squares in which there was at least 185 km search effort.

Interannual variation in the region's oceanography is dominated by the quasi-periodic El Niño-Southern Oscillation (ENSO; Enfield, 1989). Interannual variation exceeds seasonal variation in much of the ETP (Fiedler, 1992). ENSO variability affects all of the patterns and processes so far identified with cetacean habitats in the ETP. From this we hypothesized that dolphin distributions might change interannually in response to changes in the distribution of their habitats. If so, this could have important implications for the monitoring of trends in animal abundance now in progress from research vessel surveys (Gerrodette and Wade, 1991) and tuna vessel observer data (Anganuzzi and Buckland, 1989).

The primary objective of this study was to examine interannual variability in dolphin habitats, defined by multivariate techniques, for the years 1986–90. We also suggest methods for the use of habitat information in the monitoring of trends in cetacean abundance. That is, given a quantitative definition of habitat and a record of interannual changes in habitat distribution, can we help reduce variance or bias, or both, in the estimation of abundance or tests for trends?

Study area

The basic physical features of the upper ocean in the eastern tropical Pacific have been described by Wyrtki (1966, 1967), and Tsuchiya (1974). Fiedler (1992) updated this description and summarized seasonal and interannual variability. Major surface water masses and currents are depicted in Figure 2. Warm, low-salinity tropical surface water is found in the center of the ETP. Cooler, higher-salinity equatorial surface water is found south of about lat.

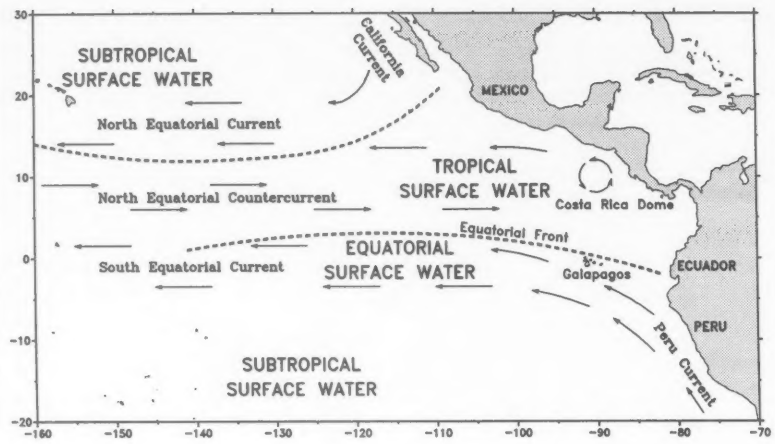

Figure 2

Schematic representation of the surface circulation and water masses of the eastern tropical Pacific.

3°N. Peru Current and California Current Waters are found along the coasts of Peru-Ecuador and Baja California, respectively. The Peru and California Currents feed into the westward South and North Equatorial Currents (SEC, NEC). The North Equatorial Countercurrent (NECC) flows eastward between the NEC and SEC into the center of the Tropical Surface Water mass. The NECC is strong during September–December and weak or absent during February–April.

A permanent shallow thermocline underlies most of the region, shoaling towards the coast (Wyrtki, 1966). Zonal thermocline ridges are found below surface divergences in the SEC along the equator and between the NEC and NECC along lat. 10°N (Fiedler, 1992). Upwelling driven by equatorward longshore winds off Peru and Baja California and by trade winds along the equator brings cold, nutrient-rich water from below the shallow thermocline (nutricline) into the surface layer. This nutrient input maintains optimal (saturating) concentrations of nitrogen at the surface and results in high levels of new production in equatorial and eastern boundary current systems (Chavez and Barber, 1987). Biological productivity is also enhanced by upwelling at the Costa Rica Dome (a quasi-permanent cyclonic eddy at the eastern end of the thermocline ridge along lat. 10°N; Wyrtki, 1964; King, 1986), and by intermittent, topographically induced offshore winds at several points along the coast of Central America (e.g. the Gulf of Tehuantepec, McCreary et al., 1989). Secondary and higher level productivity and standing stocks are generally high in areas of high primary productivity (Blackburn et al., 1970). Within this and other large oceanic regions, the abundance of animals from plankton to large nekton is patchy on a variety of spatial and temporal scales (Haury et al., 1978), with major consequences for the ecology of pelagic predators (e.g. Carr, 1987).

Data and methods

Field data collection

Dolphin sightings and oceanographic data were collected by two ships operating in different parts of the ETP from 28 July through 6 December each year from 1986 to 1990 (e.g. Holt et al., 1987). Track lines are shown in Figure 3. The surveys were conducted at 10 knots (18.5 km/hr) with three observers simultaneously on watch. One observer covered each side of the ship with a pair of 25× binoculars to search an arc from the bow to about 100° to the beam. The third observer covered the track line with hand-held binoculars and the naked eye. Sightings were approached when necessary to allow estimation of numbers within groups and species identification (Holt and Sexton, 1990).

While the ships were underway, surface temperature and salinity were recorded continuously by thermosalinograph (ODEC Model TSG-102, Inter-

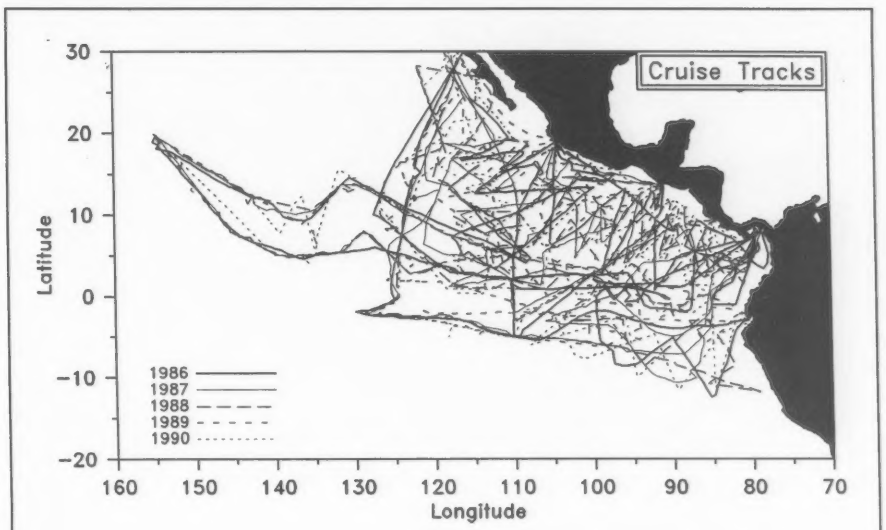

Figure 3

Cruise tracks of RV *David Starr Jordan* and *McArthur* during August–November, 1986–90.

Ocean Model 541, or Seabird SEACAT Model 21). Vertical structure was sampled in two ways. Expendable bathythermographs (XBTs) were deployed four to six times daily (every 55 to 110 km). Twice daily, just before dawn and just after dusk, the ships stopped to deploy conductivity-temperature-depth instruments (CTDs) to 1000 m. Sea water samples were collected with Niskin rosettes for chlorophyll and nutrient analysis. Surface chlorophyll was monitored continuously with a Turner Designs Fluorometer calibrated from discrete samples drawn at the surface at least six times per day (see Fiedler et al., 1990 for details).

The research vessels searched a total of 140,597 km (Fig. 3), and recorded a total of 2,014 sightings of dolphin schools of the seven types considered here, during five annual cruises, 1986 through 1990 (Table 1). The environmental data used include continuous temperature, salinity and fluorescence measurements along most of the trackline, 17,303 surface chlorophyll measurements, 4,726 XBT deployments and 1,596 CTD stations (Table 2).

Analytic methods

We estimated dolphin relative abundance as the number of schools sighted per unit distance searched, for each day, for seven pod-type categories (Table 1). These are the most frequently sighted types of dolphin schools in the region. They are also the types captured by the purse seine fishery. Only days with at least two hours of sighting effort (approximately 37 km) during periods of fair or better sighting conditions (Beaufort 5 or less) were used in the analyses. The distance searched in one day varied between 37 and 222 km. We analyzed daily sightings in relation to environmental conditions measured during that day. Our use of Beaufort 5 as the cut-off follows results from Holt (1987) who analyzed the effects of sea state on dolphin school sightability from ETP ship surveys.

Reilly (1990) found that dolphin habitats in the ETP could be defined statistically by a combination of thermocline depth, surface temperature, and salinity (where temperature and salinity were combined into sigma-t, an index of surface water density, by using a simple linear function described by Pickard and Emery, 1982). We used thermocline depth, surface temperature, salinity, and sigma-t, plus surface chlorophyll (log-transformed), and a measure of thermocline strength (the difference in depth between the 20° and 15° isotherms). Surface temperature, salinity, and chlorophyll were averaged from the day's continuous sampling during sighting effort. Thermocline depth (represented by the depth of the 20°C isotherm: Donguy and Meyers, 1987) and strength were estimated from XBT casts made during or within a few hours of sighting effort. We included sigma-t, in addition to both temperature and salinity, in the multivariate analyses as a form of

Table 1

Search effort and number of cetacean schools recorded by year, 1986–90, from the Monitoring of Porpoise Stocks expedition in the eastern tropical Pacific.

	Year					
	1986	1987	1988	1989	1990	Total
Km. searched	28,917	27,735	24,224	27,323	32,398	140,597
Number of Sightings of						
Spotted dolphins[1]	71	85	47	78	78	359
Common dolphins[2]	57	41	73	59	54	284
Spotted with Eastern Spinner[3]	44	40	33	51	33	201
Spotted with Whitebelly Spinner[3]	33	29	23	24	15	124
Eastern Spinner	27	18	6	19	13	83
Whitebelly Spinner	8	10	18	8	10	54
Striped dolphins[4]	158	180	206	213	152	909
Total sightings used in this analysis	398	403	406	452	355	2014
Other cetacean sightings	501	500	462	512	523	2498
Totals	899	903	868	964	878	4512

[1] *Stenella attenuata.*
[2] *Delphinus delphis.*
[3] *S. longirostris.*
[4] *S. coeruleoalba.*

"product variable," to see if it contributed additional information for determining dolphin habitats. In summary, the six oceanographic variables included were 1) surface temperature, TEMP; 2) surface salinity, SAL; 3) surface density, SIGMAT; 4) thermocline depth, Z20; 5) thermocline strength, ZD; and 6) chlorophyll, LOGC.

We examined the effects of interannual variability by including years (scaled 1–5) as categorical variables (details below). Additionally, we examined the contribution of fixed geographic effects by including latitude and longitude in some analyses. All environmental variables (oceanographic and geographic) were normalized prior to multivariate analyses to remove effects from differing scales of measurement.

Table 2

Oceanographic data from the Monitoring of Porpoise Stocks expedition, 1986–90, used in the canonical correspondence analyses. Table entries list numbers of observations for discrete measurements, or number of km covered during continuous measurements. XBT = expendable bathythermograph; CTD = conductivity-temperature-depth.

Data type	1986	1987	1988	1989	1990	Total
Surface temperature, salinity (km)	28,917	27,735	24,224	27,323	32,398	140,597
Surface chlorophyll measurements	3,763	1,927	3,613	3,552	4,448	7,303
XBT measurements (drops)	1,144	1,160	835	778	809	4,726
CTD measurements (stations)	244	280	352	352	368	1,596

Relationships between dolphin school distributions and environmental variation were analyzed by using canonical correspondence analysis (CCA; Ter Braak, 1986). We used the computer program CANOCO (Ter Braak, 1985). Correspondence analysis is an eigenvector ordination technique, similar to principal components analysis, that can be used to investigate community structure. These methods extract dominant, orthogonal axes of variation in abundance indices for multiple species at multiple sites. Typically, the ordination axes are then interpreted indirectly with the help of external knowledge and data on environmental gradients, either qualitatively or with regression methods (Gauch, 1982).

In contrast to principal components analysis and other linear methods, correspondence analysis (CA, also called reciprocal averaging) fits nonlinear Gaussian (unimodal) models to the species abundance data. Canonical correspondence analysis is an extension of CA in which the species ordination is done directly and iteratively in relation to environmental variables. CCA is an efficient ordination tech-

nique when species have bell-shaped response curves or surfaces with respect to environmental gradients (Ter Braak, 1986), which is consistent with general ecological knowledge (e.g.Whittaker et al., 1973). The models and algorithm used in the CANOCO implementation of canonical correspondence analysis are documented in Ter Braak (1986).

As part of the species-environment ordination, CCA estimates a series of site scores (here, site=day) that are linear combinations of the environmental variables that maximize the species-environment correlation. One set of site scores is estimated for each canonical ordination axis. The interpretation of environmental patterns represented by the axes is made from the correlation coefficients and the multiple regression or "canonical" coefficients of the original environmental variables with the canonical axes (Ter Braak, 1986).

The results of canonical correspondence can be best interpreted from an ordination "biplot," on which species and sites can be represented by points and environmental variables by arrows. The biplot displays the mean species scores or "optima" on two canonical axes, usually the first two, which explain the majority of the variance. The directions and relative lengths of the arrows for environmental variables represent their contributions to the ordination. More important environmental variables are therefore represented by longer arrows. In making biplots we used Hill's scaling (Ter Braak, 1986) in which site scores were computed as weighted averages of species scores (S=–1 in our implementation of CANOCO).

Community ordination was not our primary objective, but we used CCA for three reasons. It provides a quantitative definition of habitat for each species/stock in reduced dimensionality. The method estimates habitats using a nonlinear, unimodal model, avoiding the unrealistic assumption of a linear relationship between animal abundance and environmental gradients. CANOCO is also insensitive to a high frequency of zero observations (Ter Braak, 1985), typically found in animal survey data.

In assessing the contributions of environmental variables we took the liberal approach of retaining variables unless their contribution to the ordination was almost entirely encompassed by other, more influential variables. That is, a variable of marginal significance was not excluded if the apparent direction of its influence was different from the other environmental variables. Precision in estimating canonical coefficients was not compromised by retaining these marginal variables because we had 956 cases and a maximum of only 13 environmental variables (considering years as five dummy variables). We did not use stepwise procedures, which appear to offer an objective approach to variable selection, but are notoriously problematic for other reasons (e.g. Pimentel, 1979, p. 42–43).

We examined the importance of interannual variability in two related ways. First, as noted above, we included years as categorical explanatory variables, in addition to the oceanographic variables. The importance was then gauged by comparing ordination results to those with just the oceanographic variables. Second, we removed the variance associated with the environmental variables (by defining them as covariables), and then extracted axes associated with variance among years, to test for interannual differences in the species data not associated directly with interannual environmental variation.

The significance of an ordination axis was determined by testing the null hypothesis that its eigenvalue was not different from zero. The procedure used was a Monte Carlo randomization test (e.g. Hope, 1968) supplied with the program CANOCO. This procedure randomly associated sets of environmental variables from one case with sets of species data from another, then extracted canonical axes, and estimated their eigenvalues. The procedure was run 1,000 times to produce a reference set of eigenvalues representing random variability. The significance of the eigenvalues from the original data was determined by comparison to these distributions.

We extended the use of canonical correspondence analysis in two ways for our study of interannual variation in cetacean habitats. First, we mapped the spatial distributions of the site scores from the first two CCA axes, lightly smoothed and contoured. We then plotted the localities of cetacean sightings over these contours to allow visual appraisal of species-environment patterns. We did this as an alternative to plotting species and hundreds of sites together on a biplot, which we found to be uninformative. Second, we suggest two ways in which the results of the canonical correspondence analysis can be used in the monitoring of trends in cetacean abundance.

Results

Table 3 gives the weighted correlation matrix for the six oceanographic variables, the four species axes and four environmental axes from the CCA. The "species-environment" correlations are the values for equivalent axes, e.g. the correlation between the dominant species axis (no. 1) and the first environmental axis is 0.67. The correlation between the second axes is 0.42, and so on.

The ordination including the six oceanographic variables explained 14.7% of the variance in the dol-

Table 3

Correlation coefficients among environmental variables, canonical species axes and environmental axes estimated by a canonical correspondence analysis of cetacean abundances in the eastern tropical Pacific during 1986–90. Values marked with an * are significantly different from zero at a $P \leq 0.05$.

SPEC AX1	1.0000												
SPEC AX2	0.0085	1.0000											
SPEC AX3	0.0046	–0.0523	1.0000										
SPEC AX4	0.0283	0.0916	–0.0078	1.0000									
ENVI AX1	0.6692*	0.0000	0.0000	0.0000	1.0000								
ENVI AX2	0.0000	0.4152*	0.0000	0.0000	0.0000	1.0000							
ENVI AX3	0.0000	0.0000	0.1957	0.0000	0.0000	0.0000	1.0000						
ENVI AX4	0.0000	0.0000	0.0000	0.1196	0.0000	0.0000	0.0000	1.0000					
TEMP	–0.5885*	0.1445	–0.0143	0.0197	–0.8794*	0.3481*	–0.0730	0.1650	1.0000				
SAL	0.0599	–0.1110	0.0396	–0.0395	0.0895	–0.2674*	0.2022	–0.3304*	–0.4747*	1.0000			
LOGC	0.3246*	0.1354	–0.0803	–0.0721	0.4850*	0.3260*	–0.4106*	–0.6023*	–0.3697*	–0.0209	1.0000		
SIGMA T	0.4054*	–0.1646	0.0172	–0.0333	0.6058*	–0.3964*	0.0879	–0.2781	–0.8892*	0.8186*	0.2280	1.0000	
Z20	–0.4702*	–0.2630*	0.0239	0.0036	–0.7026*	–0.6336*	0.1224	0.0296	0.3921*	0.0811	–0.5103*	–0.2032	1.0000
ZD	0.2993*	0.0152	–0.0347	0.0788	0.4472*	0.0366	–0.1774	0.6588*	–0.3560*	0.0205	0.0476	0.2286	–0.2032
	SPECAX1	SPECAX2	SPECAX3	SPECAX4	ENVIAX1	ENVIAX2	ENVIAX3	ENVIAX4	TEMP	SAL	LOGC	SIGMA T	Z20

phin school abundance data as a whole, with a range from 33.5% for common dolphins to just 5.1% for whitebelly spinner dolphins (Table 4). The eigenvalues for the ordination axes indicate that only the first two are important (Table 4). Axes 3 and 4 together represent only 6% of the variation of the species—environment data. Ter Braak (1985) suggests that eigenvalues less than 0.02 be disregarded. The first axis accounts for 70% of the variance extracted, the second accounts for 24%, together they represent 94%. Further results and discussion therefore relate primarily to axes 1 and 2.

The relationships between most of the species categories of interest and the first two environmental axes were unimodal (Fig. 4), satisfying a primary assumption of CCA. One exception was common dolphins on axis 1, where there is evidence of bimodality.

The Monte Carlo randomization test resulted in rejection of the null hypothesis of no relationship between the species encounter rates and the environmental data (H_0 : λ=0). One thousand random permutations produced no ordinations with a trace (eigenvalue total) larger than the observed 0.443, giving a

Table 4

Ordination results from a canonical correspondence analysis of dolphin abundance and oceanographic conditions (surface temperature, salinity, sigma-t, chlorophyll, thermocline depth and thermocline strength) in the eastern tropical Pacific, August–November, 1986–90. "S-E total" is the sum of the species-environment eigenvalues, i.e. the species variation related to the environmental variables. "Overall total" is the total of all variation in the species encounter rate data. *P*-values are from a Monte Carlo randomization test with 1,000 repetitions.

	Canonical axes				S-E total	Overall total
	1	2	3	4		
Eigenvalues	0.309	0.107	0.020	0.005	0.443	3.002
P-values	<0.001				<0.001	
Species-environment correlations	0.669	0.415	0.196	0.120		
Cumulative percentage variance						
species-environment relation	69.8	93.9	98.4	99.5		
total species data	10.3	13.8	14.5	14.7		
spotted dolphin[1]	7.9	7.9	8.1	8.1		
common dolphin[2]	33.7	34.9	35.5	35.5		
spotted and eastern spinner[3] dolphins	13.1	22.2	22.3	22.5		
spotted and whitebelly spinner[3] dolphins	8.3	9.3	9.5	9.7		
eastern spinner dolphin	6.6	7.4	7.4	8.3		
whitebelly spinner dolphin	0.9	3.7	4.8	5.1		
striped dolphin[4]	1.7	2.8	5.9	5.9		

[1] *Stenella attenuata.*
[2] *Delphinus delphis.*
[3] *Stenella longirostris.*
[4] *S. coeruleoalba.*

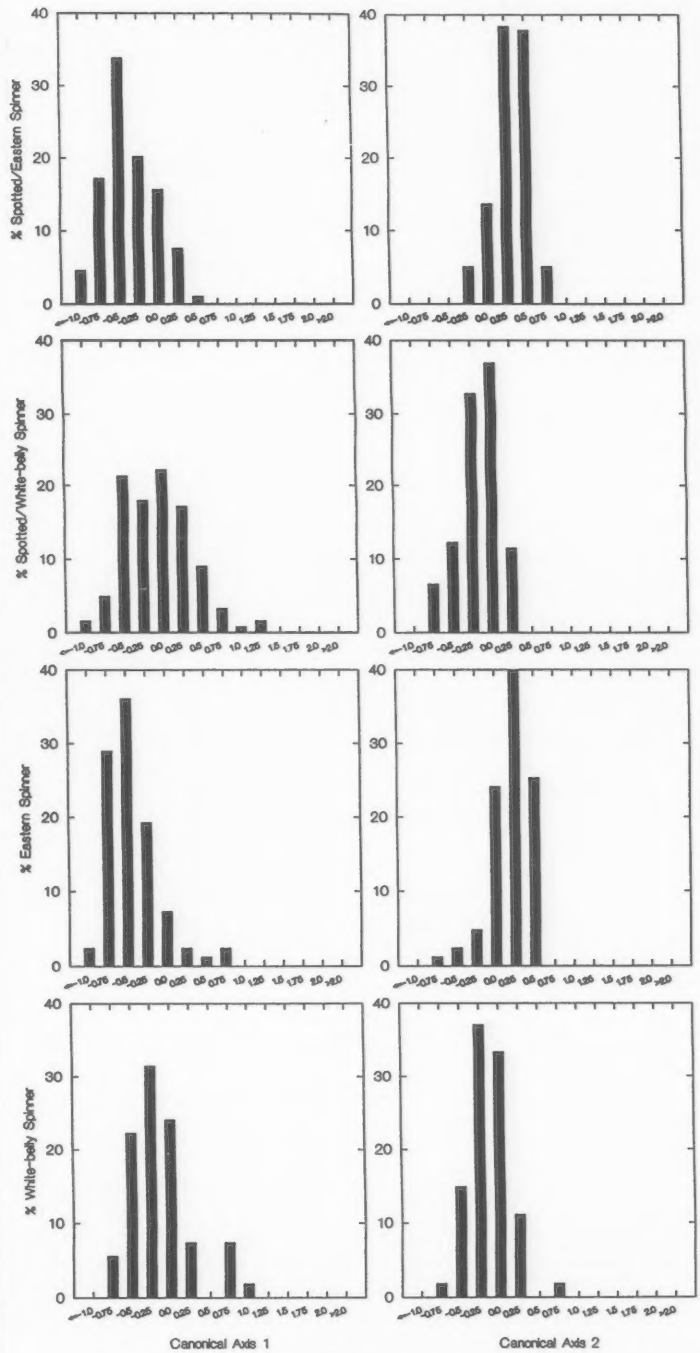

Figure 4

Frequency histograms, transformed to percentages, of the first two environmental axis scores in areas where cetaceans were sighted for seven species/stocks.

P-value < 0.001. The same was true for the first axis alone; no random permutation had an eigenvalue larger than the observed 0.309, again giving a *P*-value < 0.001. These results indicate that the probability of a Type-I error is less than 0.1%. (The CCA program, CANOCO, provided this test only for the trace and first axis, so no test was done for subsequent axes).

The species-environment biplot (Fig. 5A) displays the results for the six variable 'oceanographic' ordination. Fig. 5B shows the ordination with species tolerances, but without the visual distraction of the environmental vectors. The first axis separates common dolphins from all school types containing spotted and spinner dolphins. Positive scores on axis 1 are associated with cooler temperature (r=–0.88, Table 3), a thermocline that is shallower (i.e. smaller Z20, r=–0.70), yet weaker (larger difference in depth between 20° and 15°C isotherms, r =+0.45), denser surface water (higher sigma-t, r=+0.61) and high chlorophyll (r=+0.49). These are characteristics of "cool upwelling" habitat, as found in Equatorial and Peru/California Current surface waters. The distinct placement of common dolphins in the positive region of this axis indicates this is their preferred habitat. Negative scores on axis 1 are associated with warm temperature, a deeper and stronger thermocline, and lower chlorophyll, as found in less productive Tropical Surface Water. The placement of all spotted and spinner school types in the negative region indicates that these oceanographic conditions help define their preferred habitats.

Site or species scores on axis 2 are uncorrelated with scores on axis 1, by definition. Positive axis-2 scores are associated with a relatively shallow thermocline (r=–0.63, Table 3) and high chlorophyll (r=+0.40) as for axis 1, but also with warmer temperatures and lower salinity (lower sigma-t) rather than cool

temperature. These are characteristics of "coastal tropical" habitat found along the coast of Central America, where the surface layer is more stratified and upwelling is more intermittent and localized than in the cool upwelling habitat. Whitebelly spinners, alone and with spotted dolphins, had large negative axis-2 scores, while eastern spinners with spotted dolphins had positive scores. There was a strong separation on axis 2 between mixed schools of whitebelly spinners with spotted dolphins, and schools of eastern spinners with spotted dolphins. Schools of spotted dolphins alone had near-zero axis 2 scores. Striped dolphins loaded near the origin of both axes.

The spatial distributions of yearly axis 1 scores are mapped in Figure 6. Areas with positive scores are shaded to allow quick appraisal of changes between years (interpreted below). Also plotted in Figure 6 are sighting localities for spotted and common dolphins. Spotted dolphins occurred mostly in negative areas, common dolphins in positive areas, but with some overlap.

Spatial distributions of yearly axis 2 scores are mapped in Figure 7, with positive scores shaded. Whitebelly spinners occurred almost exclusively in waters with negative axis-2 scores (Figs. 5 and 7). Eastern spinners ranged throughout both positive and negative areas; a modest majority were found in positive areas. They were less closely associated with this axis than whitebelly spinners (Fig. 5) and seemed to be found in the eastern (more coastal) part of the warm tropical habitat defined by negative axis-1 scores.

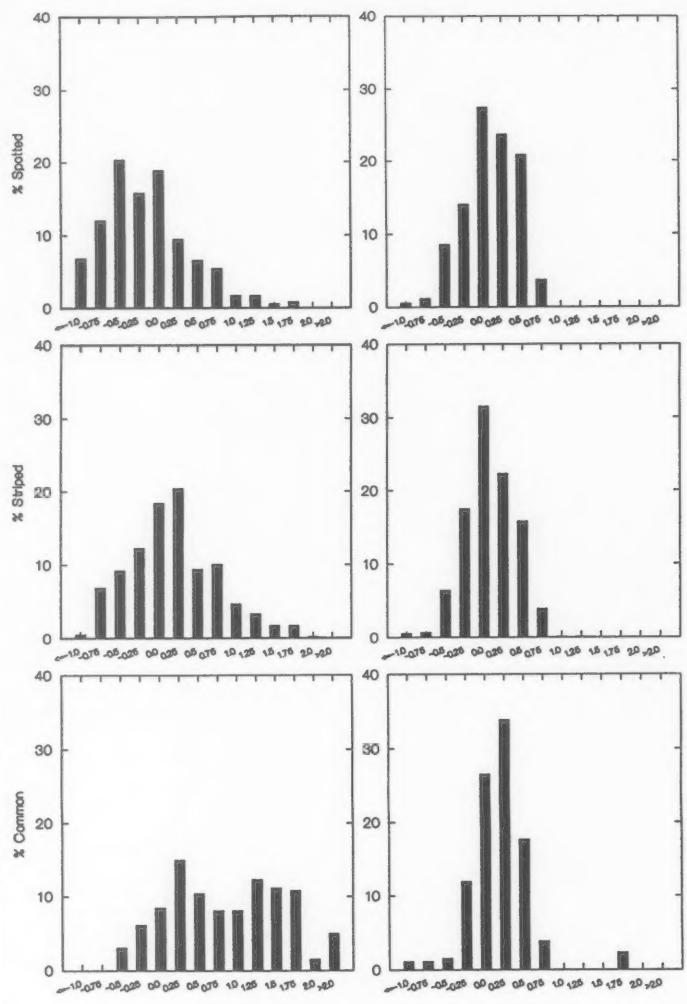

Figure 4 (Continued)

Interannual variability

We obtained only a slight increase in the percent of variance explained for the dolphin data (14.7% to 15.1%, Table 5) from addition of categorical variables representing the five sampled years, in addition to the six oceanographic variables. An ordination biplot from this analysis (Fig. 8) shows that the centroid for 1988 (year 3) loads farthest from the origin. Its location represents the cooler, more productive conditions associated with the 1988 La Niña.

An analysis including just years as categories, without oceanographic variables, explained only about 2% of the dolphin variance, but the dominant eigenvalue and trace were both significantly different from zero (Monte Carlo P-values=0.01 and 0.02, respectively). After extraction of the variance associated with the six oceanographic variables (by defining them as covariables) the ordination was not significant (Monte Carlo P=0.058, Table 5).

Fixed geographic effects

Inclusion of latitude and longitude in addition to the six oceanographic variables produced a notable increase in dolphin variance explained, from 14.7% to 20.5% (Table 5). The amount of additional influence indicated for fixed geographic effects varied substantially among school types. The largest increases were for whitebelly spinners, alone and with spotted dolphins. No improvement in explaining variance was made for schools of spotted dolphins alone.

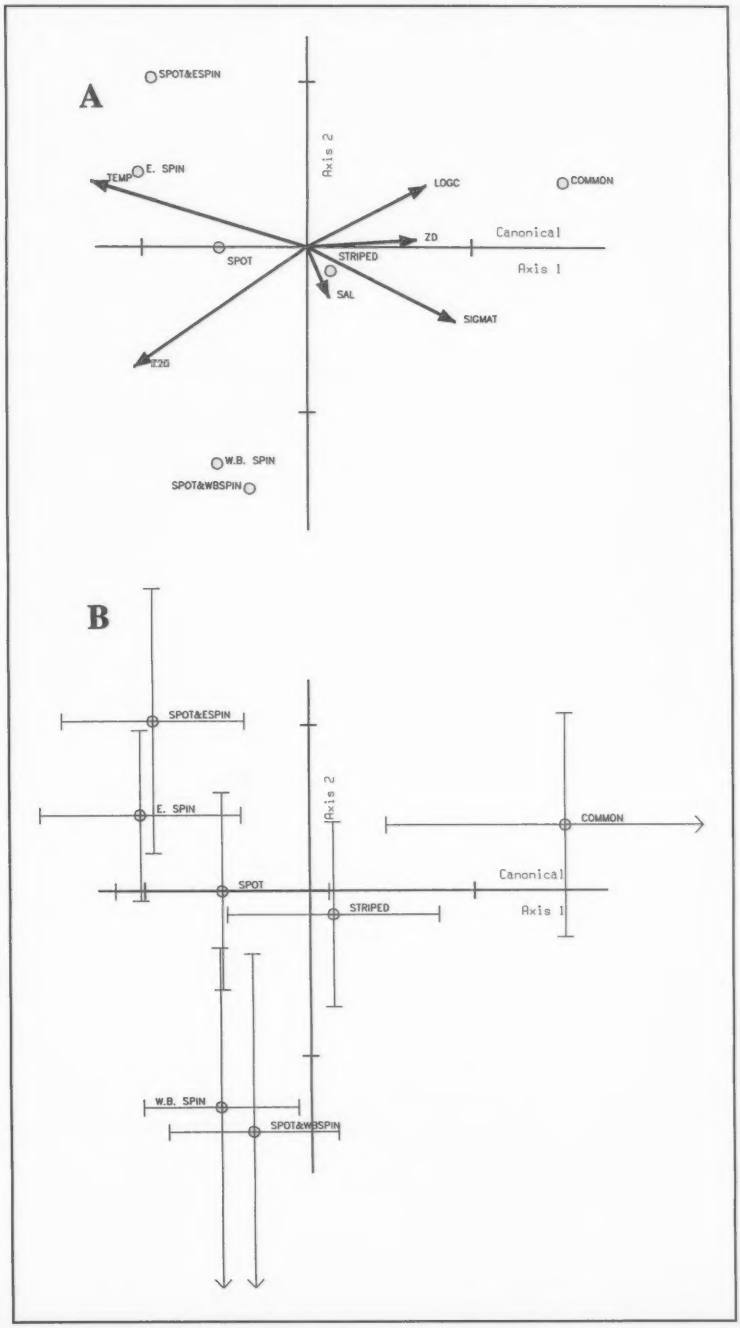

Group size effects

This study used encounter rates as an index of abundance. This index does not encompass effects of varying group size. There is some evidence for geographic patterns in group size for the dolphin school types studied (Gerrodette and Wade, 1991), so the analyses reported here were also run with the dependent variables modified as follows. Encounters with schools were weighted by the number of individuals estimated to be in the school. The weighted rate was then log-transformed. Canonical correspondence analyses run with these modified dependent variables produced essentially the same patterns as before, but with a small loss of explanatory power: the cumulative percent of the species variance explained was 14.2%, down from 14.7%.

Discussion

Species-environment patterns

The ordination results were generally consistent with past studies of

Figure 5

Ordination results from canonical correspondence analysis of cetacean species/stocks and environmental conditions in the eastern tropical Pacific. (**A**) Biplot of first two canonical axes and environmental variables. (**B**) Ordination showing 95% confidence limits for the species loadings. The environmental variables, represented by arrows in 5A, are surface temperature (TEMP), surface salinity (SAL), thermocline depth indexed by 20°C isotherm depth (Z20), thermocline strength, indexed by the difference in depth between the 20°C and 15°C isotherms (ZD), surface water density (SIGMAT), and surface chlorophyll, log-transformed (LOGC). These two axes represent 94% of the species-environment variance, 15% of the total encounter rate variance.

ETP cetacean ecology. The first axis contrasts the habitat use of common dolphins with spotted and spinner dolphins. The placement of common dolphins into cool upwelling habitat is consistent with results reported by Au and Perryman (1985) and Reilly (1990). The placement of spotted and spinner dolphins in contrasting habitat (negative axis-1 values; essentially warm tropical water) is also as reported earlier. Consistency with results of Reilly (1990) is not surprising, because that study shared data from 1986 and 1987 with this study, but is somewhat reassuring because different analytical techniques were used.

The second axis separated eastern spinners from whitebelly spinner dophins. This separation was even clearer between sightings of eastern spinners mixed with spotted dolphins and whitebelly spinners mixed with spotted dolphins. The ordination placement of whitebelly spinner dolphins in habitat with a deeper thermocline (negative axis 2) follows from their more offshore distribution and the general tendency for the thermocline to become deeper to the west in the ETP. Spotted dolphins alone occurred intermediate to these mixed schools. If this is a general pattern it suggests that the two mixed-school types of spotted and spinner dolphins are utilizing habitats as different as those used by separate species (e.g. common dolphins and spotted dolphins on axis 1). These results are consistent with the hypothesis that the morphological distinctness of the endemic eastern spinner dolphin subspecies reflects adaptation to local habitat conditions (Dizon et al., 1991), and the recent finding that spotted dolphins north of the equator and east of long. 120°W, i.e. those available to school with eastern spinner dolphins, comprise a distinct 'stock' (Dizon et al., in press).

The ordination of striped dolphins near the origin of both axes 1 and 2 indicates either that this is near their optimum habitat or that their distribution is unrelated to the environmental patterns represented in the canonical axes. The low "R^2" for striped dolphins (Table 4), and their widespread spatial distribution (Fig. 1; Reilly, 1990) support the latter interpretation.

The species-environment correlations observed were quite high: 0.67 for the first species and environment axes, 0.42 for the second axes. However, variation extracted by the canonical correspondence analysis accounted for just 15% of the total encounter rate variance. (This was increased to over 20% when fixed geographic effects were considered.) This modest explanatory power is in fact fairly good, given the unknown but surely large sampling variability inherent in daily encounter rates, and is consistent with levels of explanatory power in similar CCA analyses of abundance data (e.g. Ter Braak, 1986). Dolphins are very mobile and patchily distributed large predators, and are known to have complex social and behavioral interactions with their own and other species. These characteristics combine to produce highly variable abundance indices.

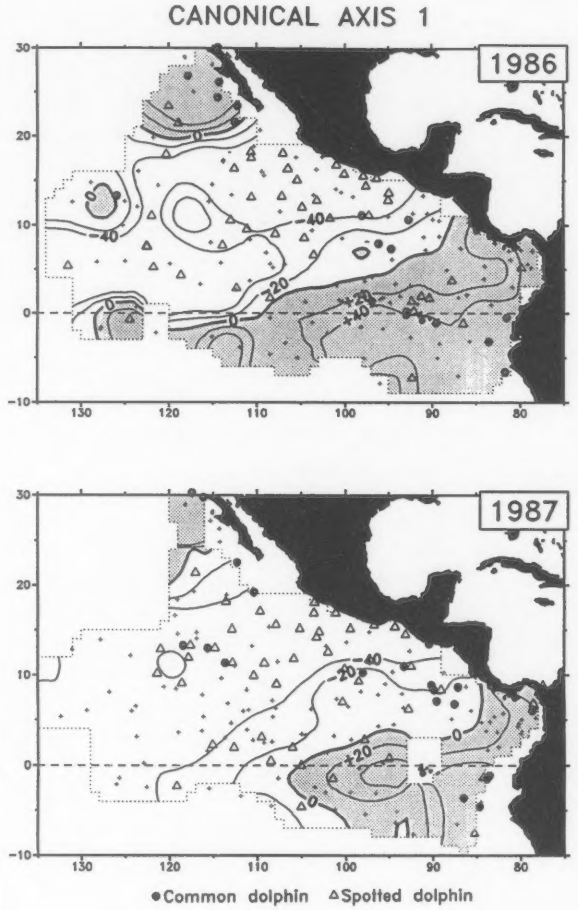

Figure 6

Maps of distribution of canonical axis 1 for 1986–90. Positive areas are shaded. Spotted dolphin, *Stenella coeruleoalba*, sighting localities are shown as open triangles, common dolphin, *Delphinus delphis*, localities as closed circles. A "+" represents a sighting day during which neither spotted nor common dolphins were seen.

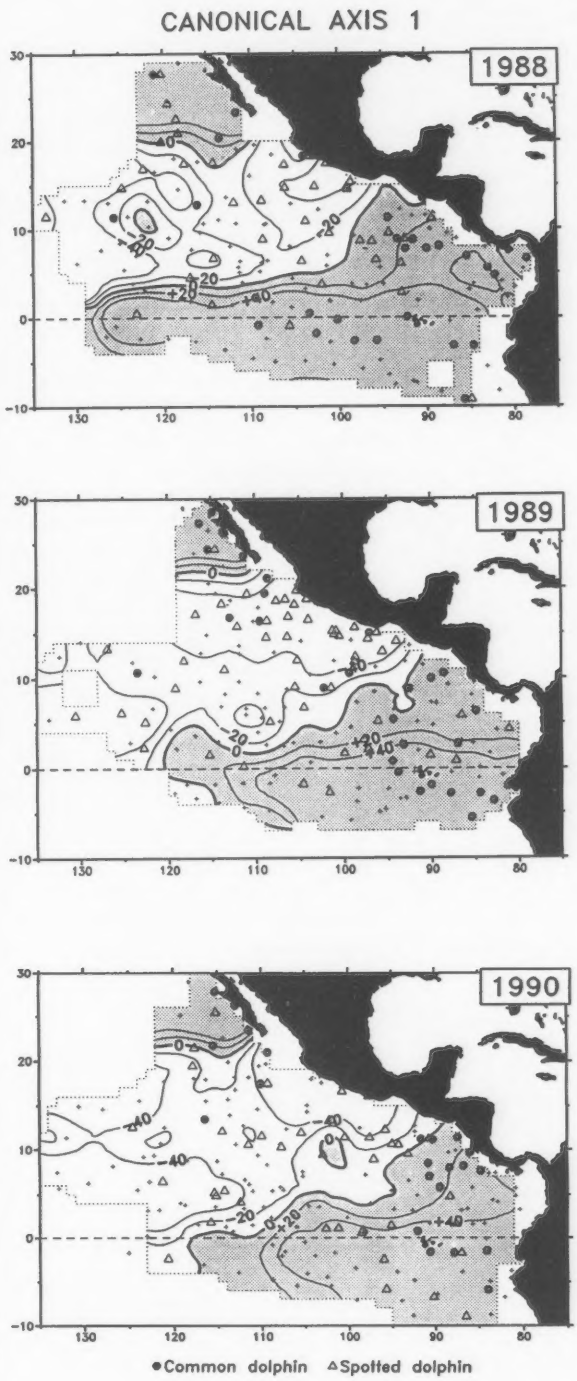

Figure 6 (Continued)

Explanatory power for common dolphins was surprisingly high: 36% with the six oceanographic variables, and 42% with fixed geography included. This result indicates that common dolphins have the tightest association with the environmental variables of the seven school types studied here. It also demonstrates the robustness of CCA, considering the bimodal distribution of common dolphins on axis 1 (Fig. 4).

The notable increase in performance for whitebelly spinner dolphins resulting from consideration of fixed geography raises interesting questions. Are they directly responding to some geophysical cue, such as magnetic anomalies (Kirschvink et al., 1986; Klinowska, 1985)? Or, does this result simply reflect orientation to oceanographic features or processes (e.g. prey distribution) not represented in our data?

Interannual variability

Interannual environmental variability is apparent in the geographic distributions of the canonical axis scores, and to a lesser extent in locations of dolphin sightings (Figs. 6 and 7). In 1986, cool upwelling habitat was found along the equator to long. 130°W, north of the equator to about lat. 10°N along the coast of Central America, and off the coast of Baja California. In 1987, cool upwelling habitat south of Baja California did not extend west of 110°W or north of 4°N, except in the Gulf of Panama. The study area was dominated by warm, low-productivity tropical water (negative axis-1 scores). This change was caused by a moderate El Niño event that began in late 1986 and lasted through 1987 (Kousky and Leetmaa, 1989). In 1988, cool upwelling water extended far north of the equator and south of Baja California, considerably reducing the area covered by tropical water. 1988 was a strong anti-El Niño or La Niña year (Leetmaa, 1990; Fiedler et al., 1992). In 1989 and 1990, conditions represented by axis-1 scores returned to a state similar to 1986. Interannual variation along axis 2 was not strongly related to ENSO variability. The area with positive axis-2 scores ("coastal tropical" habitat) was small in 1986 and 1987, increased in 1988 and again in 1989, and showed some diminishment in 1990.

Common dolphin distribution was previously observed to show no apparent seasonal changes (Reilly, 1990) but was observed here to change interannually more than the other school types studied, and these changes appear related to

ENSO variability. In 1987, with "cool upwelling" conditions contracted eastward and southward at the equator as part of that year's El Niño, in the southern ETP (south of about 2°S) common dolphins occurred only in the far east off South America. In 1988 during the strong La Niña these conditions were well established along the equator to the western extent of the study area, and common dolphins occurred in equatorial waters as far west as 110°W.

The maps in Figures 6 and 7 are imprecise representations of species-environment patterns derived by CCA for two reasons. First, the maps show only presence-absence, while we used an effort-corrected index of abundance (daily encounter rate) in the CCA. Second, the contouring requires some smoothing and interpolation between sites, while the CCA compared abundance indices only to environmental variables measured during the same day, along the same track lines where the cetaceans were sighted. These species are apparently separating more strongly on a smaller scale than we could effectively represent on the maps. A further consideration is that the scaling of axes for biplot presentation was done by using a method in which the canonical scores (as plotted on the maps here) are rescaled to produce biplot locations (Ter Braak, 1988). The resulting ordination gives an accurate relative placement of species centroids, but does not allow direct projection of centroids or tolerances onto canonical axis values as mapped in Figures 6 and 7.

The small but significant interannual variation in the species data was effectively accounted for by interannual variation in the environment. This was demonstrated by the low eigenvalue (λ=0.02, P=0.06) for interannual differences after extracting variance associated with the six oceanographic variables. This result does not necessarily apply to total population abundances, however, because in the above analyses we did not include school size estimates in our species data.

Group size effects

Inclusion of group-size data in the dolphin abundance index produced ordinations that were very similar to those using simple encounter rates, but with a slight decrease in explanatory power from the environmental data. We interpret this result to indicate that schools of all sizes occupy approximately the same habitats, and that school size variability within these habitats is not strongly related to the environmental variables analyzed here.

Applications to dolphin assessments

We suggest two approaches to use the results of this study in cetacean abundance and trend monitoring.

Table 5

Comparative ordinations from canonical correspondence analyses of seven types of dolphin school in the eastern tropical Pacific, with six different sets of environmental variables. Set 1 = surface temperature (SST), thermocline depth (Z20) and thermocline strength (ZD). Set 2 = SST, Z20, ZD, surface salinity (SAL), surface chlorophyll (LOGC) and surface density (SIGMA-T). Set 3 = Set 2 plus years (1–5) as categorical variables. Set 4 = Set 2 plus latitude and longitude. Set 5 = Set 2 plus both latitude & longitude and years. Set 6 = years (1–5) as categorical variables, after removing variance associated with all other environmental variables (Set 5).

	Environmental variable set					
	1	2	3	4	5	6
Eigenvalue sum	0.384	0.443	0.464	0.622	0.644	0.022
P-value	<0.001	<0.001	<0.001	<0.001	<0.001	0.058
Percent variance accounted for						
total species data	12.8	14.7	15.1	20.5	21.1	0.9
spotted dolphin[1]	7.8	8.1	8.8	8.8	9.6	0.8
common dolphin[2]	32.6	35.5	36.2	41.2	42.2	1.0
spottted and eastern spinner dolphins[3]	18.8	22.5	22.8	25.0	25.3	0.3
spotted and whitebelly spinner dolphins[3]	9.2	9.7	9.9	16.4	17.3	1.0
eastern spinner dolphin	7.5	8.3	9.5	10.4	11.2	0.9
whitebelly spinner dolphin	3.6	5.1	6.4	20.0	20.3	0.3
striped dolphin[4]	1.9	5.9	6.6	12.6	13.8	1.9

[1] *Stenella attenuata.*
[2] *Delphinus delphis.*
[3] *S. longirostris.*
[4] *S. coeruleoalba.*

Other, perhaps more sophisticated approaches are possible. We present these only as examples. The most straightforward approach, involving minimal assumptions, would be to post-stratify the data for each year separately, based on the spatial distribution of CCA axis scores and the weighted mean and standard deviation of those scores for the species of interest. This would be done to improve precision of abundance estimates. Populations that have similar means and standard deviations could use common strata. For example, separate strata could be defined by using axis 1 for common and spotted dolphins. Axis 2 could be used to provide strata for whitebelly spinner dolphins. Because we have probability distributions for the occurrence of these species along the canonical axes, we would not be limited to use just two strata but could use three or four. After the data were stratified based on the species annual habitat distributions, standard line transect methodology would be followed. This is generically similar to the post-stratification approach taken by Anganuzzi and Buckland (1989) to reduce bias in estimates of dolphin abundance from tuna vessel observer data.

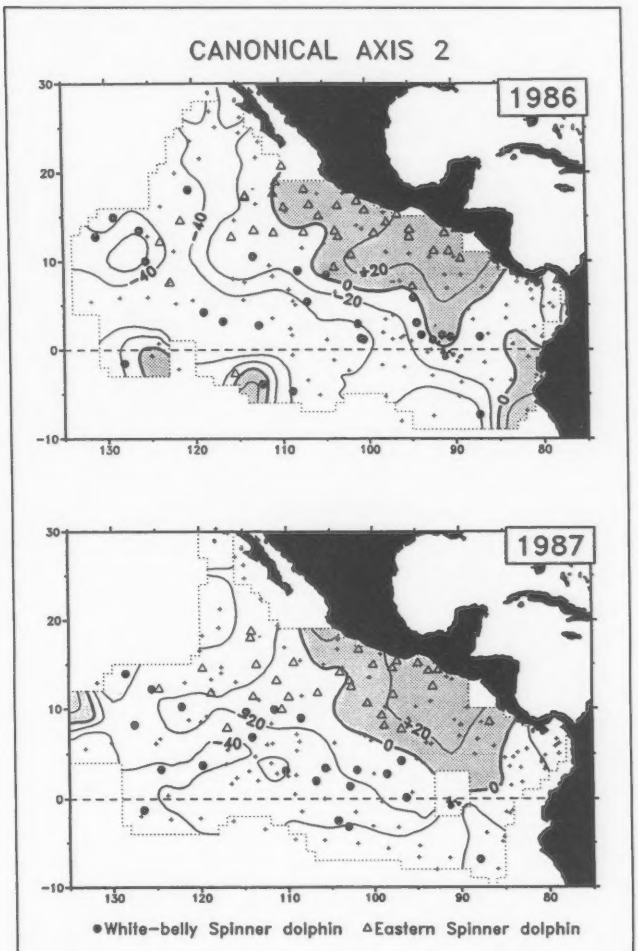

Figure 7

Maps of distribution of canonical axis 2 for 1986–90. Negative areas are shaded. Eastern spinner dolphin, *Stenella longirostris*, sighting localities are represented by closed circles, whitebelly spinner dolphin, *S. longirostris*, localities by open triangles.

A second possible approach, aimed at improving accuracy, would quantify the amount of habitat available within the study area each year, for each population. The simplest quantification scheme would define only two strata for each. The cut-point between strata could be the 95% limit of the population's distribution on the axis, or, less conservatively, the appropriate upper or lower quartile. More complex schemes using more than two strata could be developed, as with the post-stratification, based on additional information in the species probability distributions. The amount of any stratum available in a year could be quantified by, say, lightly smoothing and interpolating the CCA site scores (to provide values for all locations) and "sampling" the distribution with the actual cruise tracks for the year. If for example common dolphin habitat was to be defined as axis 1 > [some value], the amount of ocean sampled with axis 1 > [some value] in 1986 could be scaled as 1.0. The amount sampled in subsequent years could be scaled to the 1986 amount. The result would be a vector of values representing the amount of common dolphin habitat available within the ETP by year. This vector could then be applied to the encounter rate portion of the line transect abundance estimate for each year to account for changing availability of common dolphin habitat. If interannual differences were subsequently observed in the line transect abundance estimates, we could be more confident that they represent real changes in abundance, rather than just apparent changes due to spatial redistribution relative to sampling effort following habitat shifts.

In a separate study (Fiedler and Reilly, 1994) we applied the CCA ordination approach developed here to investigate interannual variability in abundance indices for ETP dolphins estimated from tuna vessel observer data. We calculated annual indices of habitat quality for each dolphin species targeted by the tuna fishery, for the years 1975–90, then compared these

habitat indices to Anganuzzi et al.'s (1991) abundance estimates. We used a subset of three environmental variables from those used here, to enable use of existing, large data bases on oceanography of the ETP, to allow computation of environmental axes for years prior to 1986. We found that, for some species, environmental variability does appear to influence abundance estimates made from tuna vessel observer data. We are now working on using environmental data to reduce error in dolphin abundance estimates derived from both research vessel and tuna vessel sightings data. Gerrodette et al.[1] applied the results of this study in a preliminary attempt to account for movements in and out of the study area when estimating total abundance of dolphins.

Acknowledgments

The efforts of many people were required to collect and process the data used in this analysis. Cetacean sightings were made and recorded by S. Beavers, S. Benson, C. Bisbee, P. Boveng, K. Brownell, S. Buckland, J. Caretta, J. Cotton, A. Dizon, G. Friedrichsen, S. Hill, A. Hohn, W. Irwin, A. Jackson, S. Kruse, C. LeDuc, R. LeDuc, M. Lynn, M. Newcommer, R. Pitman, J. Raffetto, K. Rittmaster, L. Robertson, R. Rowlett, S. Sinclair, D. Skordal, B. Smith, P. Stangl, V. Thayer and M. Webber. Oceanographic data were collected by J. Echols, J. Ellingson, J. Fleishman, L. Gearin, L. Lierheimer, B. McDonald, D. Niemer, V. Philbrick, B. Tershey, V. Thayer, G. Thomas and S. Strickland. C. Oliver, R. Holland, A. Jackson, R. Rasmussen and K. Blum contributed data editing and processing. Holland contributed computer programming for the analyses and produced the figures. We thank these people, plus the officers and crew of the NOAA research vessels *David Starr Jordan* and *McArthur* for their contributions. Helpful comments on various drafts were made by D. Au, J. Barlow, L. Ballance, D. DeMaster, W. Perrin, W. Perryman, P. Wade and two anonymous reviewers. Doug DeMaster provided enthusiastic support and encouragement during the course of this study.

[1] Gerrodette, T., P. C. Fiedler, and S. B. Reilly. 1991. Including habitat variability in line transect estimation of abundance and trends. NOAA-NMFS Admin. Rep. LJ-91-37.

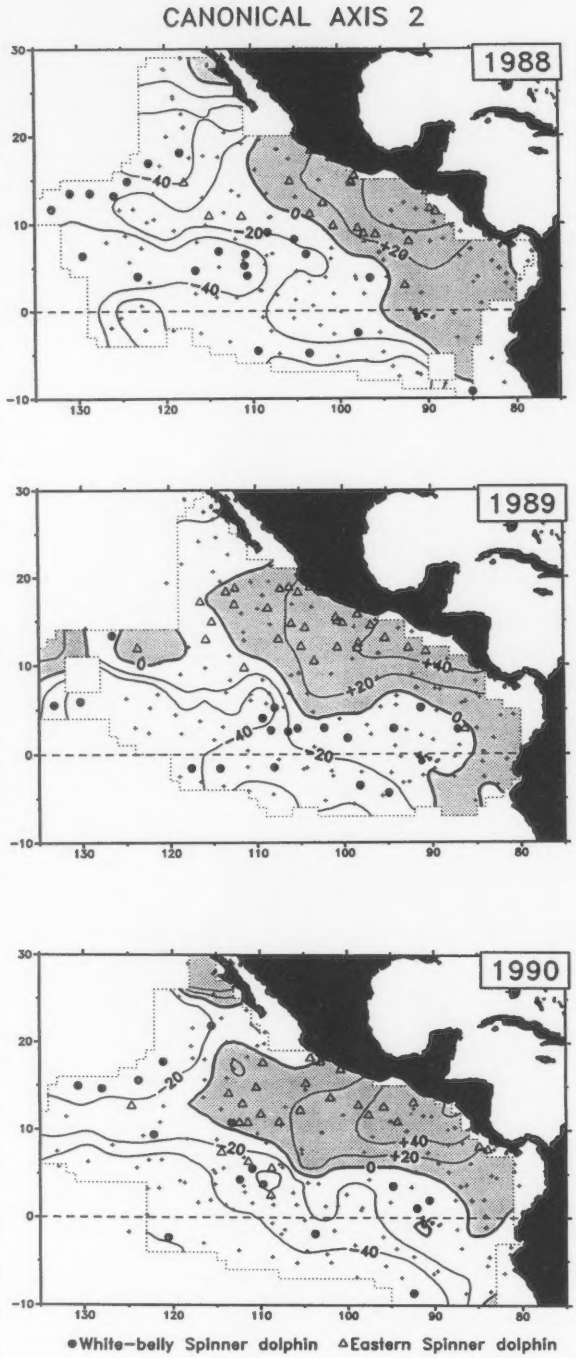

Figure 7 (Continued)

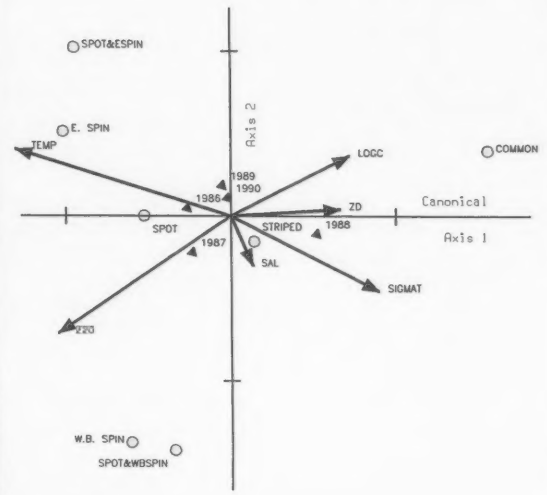

Figure 8

Ordination biplot from canonical correspondence analysis of seven dolphin school types in relation to six oceanographic variables (see Fig. 5 for definitions), with the five sampled years as categories. Mean values for each year are represented by triangles, YEAR 1 = 1986, YEAR 2 = 1987, etc.

Literature cited

Anganuzzi, A. A., and S. T. Buckland.
1989. Reducing bias in trends in dolphin abundance, estimated from tuna vessel data. Rep. Int. Whal. Comm. 39: 323–334.

Anganuzzi, A. A., S. T. Buckland, and K. L. Cattanach.
1991. Relative abundance of dolphins associated with tuna in the eastern tropical Pacific, estimated from tuna vessel sightings for 1988 and 1989. Rep. Int. Whal. Comm. 42:497–506.

Au, D.W. K., and W. L. Perryman.
1985. Dolphin habitats in the eastern tropical Pacific. Fish. Bull. 83:623–643.

Blackburn, M., R. M. Laurs, R. S. Owen, and B. Zeitschel.
1970. Seasonal and areal changes in standing stocks of phytoplankton, zooplankton and micronekton in the eastern tropical Pacific. Mar. Biol. 7:14–31.

Carr, A.
1987. New perspectives on the pelagic stage of sea turtle development. Conserv. Biol. 1(2):103–121.

Chavez, F. P., and R. T. Barber.
1987. An estimate of new production in the equatorial Pacific. Deep-Sea Res. 24:1229–1243.

Dizon, A. E., S. O. Southern, and W. F. Perrin.
1991. Molecular analysis of mtDNA types in exploited populations of spinner dolphins (*Stenella longirostris*). *In* R. Hoelzel (ed.), Genetic ecology of whales and dolphins. Rep. Int. Whal. Comm., Spec. Issue 13:183–202.

Dizon, A. E., W. F. Perrin, and P. A. Akin.
In press. Stocks of dolphins (*Stenella* spp. and *Delphinus delphis*) in the eastern tropical Pacific: a phylogeographic classification. NOAA Technical Rep. NMFS.

Donguy, J. R., and G. Meyers.
1987. Observed and modelled topography of the 20°C isotherm in the tropical Pacific. Oceanologica Acta 10:41–48.

Enfield, D. B.
1989. El Niño, past and present. Rev. Geophys. 27:159–187.

Evans, W. E.
1975. Distribution, differentiation of populations, and other aspects of the natural history of *Delphinus delphis* Linnaeus in the northeastern Pacific. Ph.D. thesis, Univ. Calif. Los Angeles.

Fiedler, P. C.
1992. Seasonal climatologies and variability of eastern tropical Pacific surface waters. NOAA Tech. Rep. NMFS 109, 65 p.

Fiedler, P. C., and S. B. Reilly.
1994. Interannual variability of dolphin habitats in the eastern tropical Pacific. II: Effects on abundances estimated from tuna vessel sightings, 1975–1990. Fish. Bull. 92:451–463.

Fiedler, P. C., L. J. Lierheimer, S. B. Reilly, S. N. Sexton, R. S. Holt, and D. P. DeMaster.
1990. Atlas of eastern tropical Pacific oceanographic variability and cetacean sightings, 1986–1989. NOAA Tech. Memo. NMFS-SWFSC-144.

Fiedler, P. C., F. P. Chavez, D. W. Behringer, and S. B. Reilly.
1992. Physical and biological effects of Los Niños in the eastern tropical Pacific. Deep-Sea Res. 39(2):199–219.

Gauch, H. G., Jr.
1982. Multivariate analysis in community ecology. Cambridge Univ. Press.

Gerrodette, T., and P. R. Wade.
1991. Monitoring trends in dolphin abundance in the eastern tropical Pacific: analyses of 1989 data. Rep. Int. Whal. Comm. 41:511–515.

Haury, L. R., J. A. McGowan, and P. H. Wiebe.
1978. Patterns and processes in the time-space scales of plankton distributions. *In* J. H. Steele (ed.), Spatial pattern in plankton communities. Plenum Press, New York.

Holt, R. S.
1987. Estimating density of dolphin schools in the eastern tropical Pacific Ocean by line transect methods. Fish. Bull. 85:419–434.

Holt, R .S., and S. N. Sexton.
1990. Monitoring trends in dolphin abundance in the eastern tropical Pacific using research vessels over a long sampling period: analyses of 1986 data, the first year. Fish. Bull. 88: 105–111.

Holt, R. S., T. Gerrodette, and J. B. Cologne.
1987. Research vessel survey design for monitoring dolphin abundance in the eastern tropical Pacific. Fish. Bull. 85:435–446.

Hope, A. C. A.
1968. A simplified Monte Carlo significance test procedure. R. Statist. Soc. J. Ser. B 30(3):582-598.

King, F. D.
1986. The dependence of primary production in the mixed layer of the eastern tropical Pacific on the vertical transport of nitrate. Deep-Sea Res. 33(6):733–754.

Kirschvink, J. L., A. E. Dizon, and J. A. Westphal.
1986. Evidence from strandings for geomagnetic sensitivity in cetaceans. J. Exp. Biol. 120:1–24.

Klinowska, M.
1985. Cetacean stranding sites relate to geomagnetic topography. Aquatic Mammals 1:27–32.

Kousky, V. E., and A. Leetmaa.
1989. The 1986–87 Pacific warm episode: evolution of oceanic and atmospheric anomaly fields. J. Clim. 2:254–267.

Leatherwood, S., R. R. Reeves, W. F. Perrin, and W. E. Evans.
1982. Whales, dolphins and porpoises of the eastern North Pacific and adjacent waters, a guide to their identification. NOAA Tech. Rep. NMFS Circ. 444.

Leetmaa, A.
1990. The interplay of El Niño and La Niña. Oceanus 32:30–34.

McCreary, J. P., H. S. Lee, and B. B. Enfield.
1989. The response of the coastal ocean to strong offshore winds: with application to circulations in the Gulfs of Tehuantepec and Papagayo. J. Mar. Res. 47:81–109.

Perrin, W. F.
1969. Using porpoise to catch tuna. Wld. Fish. 18(6):42–45.
1975. Distribution and differentiation of populations of dolphin of the genus *Stenella* in the eastern tropical Pacific. J. Fish. Res. Board. Can. 32:1059–1067.
1990. Subspecies of *Stenella longirostris* (Mammalia: Cetacea: Delphinidae). Proc. Biol. Soc. Wash. 103(2):453–463.

Perrin, W. F., M. D. Scott, G. J. Walker, F. M. Ralston, and D. W. K. Au.
1983. Distribution of four dolphins (*Stenella* spp. and *Delphinus delphis*) in the eastern tropical Pacific. NOAA Tech. Memo. NMFS-SWFC-38, 65 p.

Perrin, W. F., M. D. Scott, G. J. Walker, and V. Cass.
1985. Review of geographical stocks of tropical dolphins (*Stenella* spp. and *Delphinus delphis*) in the eastern tropical Pacific. NOAA Tech. Rep. NMFS 28, 28 p.

Pickard, G. L., and W. J. Emery.
1982. Descriptive physical oceanography, 4th (SI) enlarged ed. Pergamon Press, Oxford, 249 p.

Pimentel, R. A.
1979. Morphometrics. The multivariate analysis of biological data. Kendall/Hunt Publ. Co., Dubuque, Iowa, 276 p.

Reilly, S. B.
1990. Seasonal changes in distribution and habitat differences among dolphins in the eastern tropical Pacific. Mar. Ecol. Prog. Ser. 66(1–2):1–11.

Smith, T. D.
1983. Changes in size of three dolphin (*Stenella* spp.) populations in the eastern tropical Pacific. Fish. Bull. 81:1–13.

Ter Braak, C. J. F.
1985. Correspondence analysis of incidence and abundance data: properties in terms of a unimodal response model. Biometrics 41:859–873.
1986. Canonical correspondence analysis: a new eigenvector technique for multivariate direct gradient analysis. Ecology 67(5):1167–1179.
1988. CANOCO— a FORTRAN program for canonical community ordination by [partial] [detrended] [canonical] correspondence analysis, principal components analysis and redundancy analysis (version 2.1). Tech. Rep. LWA-88-02, Groep Landbouwwiskunde, Postbus 100,6700 AC Wageningen, The Netherlands.

Townsend, C. H.
1935. The distribution of certain whales as shown by logbook records of American whaleships. Zoologica Sci. Contrib. N.Y. Zool. Soc. 19(1):1–50.

Tsuchiya, M.
1974. Variation of surface geostrophic flow in the eastern intertropical Pacific Ocean. Fish. Bull. 72(4):1075–1086.

Whittaker, R. H., S. A. Levin, and R. B. Root.
1973. Niche, habitat and ecotope. Am. Nat. 107:321–338.

Wyrtki, K.
1964. Upwelling in the Costa Rica Dome. Fish. Bull. 63:355–372.
1966. Oceanography of the eastern equatorial Pacific Ocean. Oceanogr. Mar. Biol. Ann. Rev. 4:33–68.
1967. Circulation and water masses in the eastern equatorial Pacific Ocean. Int. J. Oceanol. Limnol. 1:117–147.

Young, T. L., and M. L.Van Woert.
1987. PLOT88 software library. Plotworks, Inc., La Jolla, CA.

Interannual variability of dolphin habitats in the eastern tropical Pacific. II: Effects on abundances estimated from tuna vessel sightings, 1975–1990

Paul C. Fiedler
Stephen B. Reilly
Southwest Fisheries Science Center, National Marine Fisheries Service, NOAA
P. O. Box 271, La Jolla, CA 92038

Abstract.—The results of a canonical correspondence analysis (CCA) of data from research vessel surveys of the eastern tropical Pacific were applied to time series of estimated dolphin abundances from tuna vessel sightings. The research vessel survey data consisted of daily dolphin school sightings and concurrent environmental variables for August–November of 1986 through 1990. Seasonal fields of habitat quality for 1975-90 were calculated from historical bathythermograph data by using the CCA ordination results. For spotted (*Stenella attenuata*) and eastern spinner (*S. longirostris orientalis*) dolphins, annual abundance estimates or interannual changes in those estimates are significantly correlated with habitat quality. This effect is at least partly due to expansion of high quality habitat beyond the geographic ranges assumed for the abundance estimate. We discuss ways that environmental data could be used to reduce error in dolphin abundance estimates.

Manuscript accepted 18 October 1993
Fishery Bulletin 92:451–463 (1994)

The eastern tropical Pacific Ocean (ETP) supports a diverse and abundant cetacean fauna. By the late 1960s, it had become clear that large numbers of dolphins were being killed in tuna purse seine operations (Perrin, 1969). The dolphin species affected by the tuna fishery, known as "target species," are spotted dolphin (*Stenella attenuata*), the "whitebelly" form and "eastern" subspecies of spinner dolphin (*S. longirostris* and *S. l. orientalis*, Perrin, 1990), common dolphin (*Delphinus delphis*), and striped dolphin (*S. coeruleoalba*). In 1973, the U.S. government initiated a formal program to place observers on purse seiners to monitor dolphin mortality (Smith, 1983). In 1975, the Inter-American Tropical Tuna Commission began putting observers on the international fleet. The tuna vessel observer data from these programs includes sightings of cetaceans, as well as mortality data and biological samples from incidental catches.

Time series of target species abundance have been estimated from tuna vessel observer data (Buckland et al., 1992). These are yearly estimates of stocks of spotted, spinner, and common dolphins within nominal stock boundaries known as the Status of Porpoise Stocks or SOPS boundaries.[1] Buckland et al. (1992) analyzed smoothed time series of these estimates and detected significant trends for some stocks.

Time series of dolphin abundance estimates are subject to considerable sampling error plus the effects of environmental variability on abundance and distribution. The effect of environmental factors on abundance estimates must be quantified before such a time series can be properly interpreted in terms of abundance changes or trends. This paper analyzes relationships between abundance estimates from tuna vessel observer data and environmental variability. Since little or no environmental data are collected on these ships, we base our analysis on species-environment relationships derived from research vessel data (Reilly and Fiedler, 1994).

National Marine Fisheries Service research vessels have surveyed the ETP several times since 1974 to collect data for abundance estimates and supplement the tuna vessel observer data (Holt et al., 1987). The most extensive research vessel observer data were collected

[1] Au, D. W. K., W. L. Perryman, and W. F. Perrin. 1979. Dolphin distribution and the relationship to environmental features in the eastern tropical Pacific. NOAA/SWFC Admin. Rep. No. LJ-79-43, 59 p.

for the Monitoring of Porpoise Stocks (MOPS) program during August-November in 1986 through 1990 (Wade and Gerrodette, 1992). The MOPS surveys were designed to cover the SOPS spotted, spinner, and common dolphin stock boundaries. Reilly and Fiedler (1994) showed that sighting rates of dolphin species or school types on the MOPS surveys were related to concurrently measured environmental variables. We used a robust and efficient multivariate technique, canonical correspondence analysis, to examine relations between spatial distributions of dolphin species and environmental variables.

Canonical correspondence analysis (CCA) was developed to relate community composition to known variation in the environment. It is a form of direct gradient analysis that directly estimates ordination axes as linear combinations of observed environmental variables (Ter Braak, 1986). The advantages of CCA for multivariate species-environment analyses and details of the method are discussed by Reilly and Fiedler (1994). CCA estimates unimodal (Gaussian) responses of species along the ordination axes. In general, the response is observed abundance or probability of occurrence. We assume that a species response (abundance observed at a site in time and space) reflects the suitability of environmental conditions at that site relative to the species' optimal habitat or niche. This suitability, or habitat quality, is defined by the response distribution along the axes. An observed response will also include error caused by behavioral responses to the environment that affect the detectability of schools.

In this paper, we analyze relations between abundance estimates and habitat quality. It must be stated at the outset that in a 15-year record of populations with growth rates of only ~0.02 yr^{-1} (Reilly and Barlow, 1986), we are able to detect short-term environmental effects on sampling but not long-term effects on population size. Nevertheless, we demonstrate that some of the interannual variability in estimated abundances of ETP dolphins can be explained by environmental factors.

Methods

We used archived bathythermograph data to quantify variability of surface temperature, thermocline depth, and thermocline thickness in the MOPS study area since 1975. These variables were shown to be important in explaining variations in encounter rates in the MOPS surveys (Reilly and Fiedler, 1994). Other important variables (salinity and chlorophyll concentration) have not been routinely observed with sufficient frequency to be used in this historical analysis. Seasonal fields (gridded values) of surface temperature, thermocline depth, and thermocline thickness for the period 1975–90 were derived from a bathythermograph data base originally described by Fiedler (1992) and augmented with data from other sources for this study (Table 1). Thermocline depth is defined as the depth of the 20°C isotherm. Thermocline thickness is defined as the difference in depth between the 20°C and 15°C isotherms.

Data were objectively gridded by seasons (December–February, March–May, June–August, September–November from 1975 through 1990) on a 2-degree latitude-longitude grid from lat. 20°S to 30°N latitude and from the coast out to long. 160°W. Decorrelation scales, the distances required for a substantial change in surface temperature or thermocline depth, have been estimated as 3 degrees latitude and 15 degrees longitude in this region (Sprintall and Meyers, 1991). At each grid point, means of at least 20 observations within up to 4 degrees latitude and 20 degrees longitude were calculated. The observations were weighted by the re-

Table 1

Numbers of bathythermograph profiles, after screening for errors and replicates, used to define habitat quality in yearly seasonal grids (1975–90) and in climatologies (1960–91). **NODC** = NOAA/NESDIS/National Oceanographic Data Center CD-ROM NODC-03: Global Ocean Temperature and Salinity Profiles, vol. 2, Pacific Ocean; **MOODS** = Navy Master Oceanographic Observations Data Set, including non-NODC observations through 1983 obtained from the Naval Oceanographic Office through NODC and 1985–90 observations obtained from Steve Pazan, Scripps Institution of Oceanography; **SOP** = French-American ship-of-opportunity observations obtained from NOAA/ERL/Pacific Marine Environmental Laboratory (Kessler, 1990); **FSFRL** = Japanese Far Seas Fisheries Research Laboratory MBT data obtained from PMEL and from NOS/Ocean Applications Branch (these data will be added to the NODC data set in the near future).

	1975–90	1960–91
NODC	61,486	127,365
MOODS	10,741	15,077
SOP	2,859	11,305
FSFRL	2,350	4,744
Total	77,436	158,491

ciprocal of the distance from the grid point. The range of observations around a grid point was increased in increments of 0.4 degrees latitude and 2 degrees longitude to obtain a minimum sample size of 20 for each grid point. Thus, local grid resolution decreases in data-poor regions, generally south of the equator where the maximum distance required was up to 20 degrees longitude. Within the MOPS area, sufficient observations were available within 2 degrees latitude and 10 degrees longitude of 71% of the gridpoints, and within 4 degrees latitude and 20 degrees longitude of 95% of the gridpoints. We converted observations to anomalies (deviations from the seasonal mean) before gridding to reduce the spatial variability of the observations. This minimized bias caused by interpolation over or extrapolation into large data gaps.

Relationships among abundances of dolphin species and environmental variables were analyzed by using CCA as described in Reilly and Fiedler (1994). Encounter rate, equal to number of schools sighted per unit of sighting effort (trackline distance), was used as a measure of relative abundance. The final abundance estimate also depends on school size and effective track width. However, Reilly and Fiedler (1994) found that weighting encounter rates by estimated school size in the CCA produced essentially the same species-environment patterns. Therefore, schools of all sizes occupied approximately the same habitats and school size variability within these habitats was not related to the environmental variables included in the analysis.

CCA was performed on MOPS sightings and environmental data as in Reilly and Fiedler (1994), except that mixed schools of spotted and spinner dolphins were counted as schools of both species rather than as an additional "species." Also, we used Hill's symmetric scaling of species and site scores (S=–3 in our implementation of CANOCO[2]). This alternative scaling of the ordination had no qualitative effect on species-environment patterns but seemed to give more reasonable results at the edges of the study area when scores were combined to quantify species habitat distributions.

Habitat quality for species i (H_i) at a gridpoint was calculated from the Gaussian responses fit to the two dominant canonical axes by CCA. The response to each environmental axis was calculated as a normal probability density function:

$$H_{ij} = t_{ij}^{-1} \exp\left(-0.5 * \left(\left(x_j - u_{ij}\right)/t_{ij}\right)^2\right),$$

where,

x_j = the site (gridpoint) score on environmental axis j,

u_{ij} = the species i score (optimum) on axis j,

t_{ij} = the tolerance (standard deviation) of species i on axis j.

Species scores and tolerances (u_{ij} and t_{ij}) were output by CANOCO as part of the CCA. Site scores (x_j) were calculated as linear combinations, defined by the output canonical axis coefficients, of normalized and gridded environmental observations. Habitat quality, H_i, was then calculated as the geometric mean of H_{ij}'s; each H_{ij} was scaled so that the mean value is 1.0 during 1975–90. Thus, H_i is equal to the abundance expected at a site, based on local environmental conditions, divided by the mean abundance in the study area during 1975–90.

Point estimates of annual abundance were provided by Anganuzzi[3] for pooled stocks: spotted dolphins include northern and southern offshore spotted dolphins, whitebelly spinner dolphins include northern and southern whitebelly spinner dolphins, and common dolphins include northern, central, and southern common dolphins. No estimates were made for striped dolphins, which were rarely set on by tuna vessels.

Results

The species-environment biplot (Fig. 1) summarizes the results of the CCA of five species and three environmental variables observed during 1986–90 MOPS research surveys. The eigenvalues of the three canonical axes were 0.296, 0.074, and 0.001. The first two axes explained 99.7% of the species-environment variance accounted for by all three axes. Therefore, the third axis was not used. The first two axes explained 20.5% of the total variance of species encounter rates (Table 2).

Positive scores on canonical axis 1 indicate cool surface temperature and a shallow, weak thermocline (Table 3). These are characteristics of the productive "cool upwelling" habitat that we identified with the first axis in the complete CCA (seven species and six environmental variables, Reilly and Fiedler, 1994). This habitat is found in the equatorial and eastern boundary current (Peru and Cali-

[2] Ter Braak, C. J. F. (1988). CANOCO—a FORTRAN program for canonical community ordination by [partial] [detrended] [canonical] correspondence analysis, principal components analysis and redundancy analysis (version 2.1). Tech. Rept. LWA-88-02, Groep Landbouwwiskunde, Postbus 100, 6700 AC Wageningen, The Netherlands.

[3] Anganuzzi, A. Inter-American Tropical Tuna Commission, 8604 La Jolla Shores Drive, La Jolla, CA 92038. Pers. commun. December 1991.

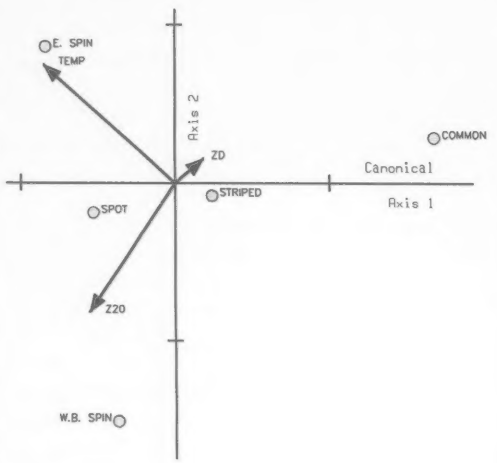

Figure 1

Ordination biplot of first two canonical axes from CCA of species-environment data from 1986–90 MOPS surveys of the ETP. Points represent species scores (optima) and vectors represent the regression relationships of environmental variables with the canonical axes. TEMP = surface temperature, Z20 = thermocline depth, ZD = thermocline thickness. SPOT = spotted dolphin (*Stenella attenuata*), COMMON = common dolphin (*Delphinus delphis*), E. SPIN = eastern spinner dolphin (*S. longirostris orientalis*), W. B. SPIN = whitebelly spinner dolphin (*S. longirostris*), STRIPED = striped dolphin (*S. coeruleoalba*).

Table 2

Fractions of individual and total species variances explained by canonical correspondence analysis (CCA). AX1 = canonical axis 1, AX2 = canonical axis 2. Dolphin species: spotted = *Stenella attenuata*, common = *Delphinus delphis*, eastern spinner = *S. longirostris orientalis*, whitebelly spinner = *S. longirostris*, striped = *S. coeruleoalba*.

	AX1	AX2	AX1+AX2
Spotted	0.191	0.000	0.191
Common	0.321	0.004	0.325
Eastern spinner	0.169	0.089	0.258
Whitebelly spinner	0.014	0.118	0.132
Striped	0.037	0.002	0.039
Total	0.164	0.041	0.205

fornia Currents) waters of the ETP and is also present seasonally in the region of the Costa Rica Dome at 10°N, 90°W (Fiedler, 1992). Positive scores on canonical axis 2 indicate warm surface temperature and a shallow thermocline (Table 3). These are characteristics of the "coastal tropical" habitat of Reilly and Fiedler (1994). This habitat is centered in the warmest tropical surface water of the ETP, along the coast of Mexico south of Baja California.

Species responses along the canonical axes (Fig. 2) showed some separation of species habitats, as in the complete CCA (Reilly and Fiedler, 1994). Axis 1 separated common dolphins from spotted and spinner dolphins, while axis 2 separated eastern and whitebelly spinner dolphins. The means (optima, Table 4) of a species distribution on the two canonical axes in Figure 2 are equal to the species scores plotted in the ordination biplot (Fig. 1).

The validity of the species/environment relationships calculated by CCA was confirmed in three ways. First, distributions of climatological H, derived from the CCA results and climatological values of environmental variables at each gridpoint in the MOPS area (Fiedler, 1992), were consistent with stock ranges indicated by the SOPS population boundaries, with the exception of whitebelly spinner dolphins (Fig. 3). Second, the distributions were similar to patterns in maps of tuna and research vessel sighting records (Perrin et al., 1985), although such maps can give only a rough indication of habitat distribution because the sighting or collection frequencies are not standardized by effort. Third, the distributions of H calculated for climatological September–November environmental conditions were significantly correlated with gridded fields of mean (August–November, 1986–90) MOPS encounter rates as follows: spotted dolphin $r = 0.52$, common dolphin $r = 0.45$, eastern spinner dolphin $r = 0.65$, whitebelly spinner dolphin $r = 0.36$, striped dolphin $r = 0.41$ ($P<0.01$ for all relationships).

Table 3

Regression/canonical coefficients for standardized environmental variables on two environmental axes (AX1 and AX2). TEMP = surface temperature, Z20 = thermocline (20°C isotherm) depth, ZD = thermocline thickness (difference between 20°C and 15°C isotherm depths).

	TEMP	Z20	ZD
AX1	–0.501	–0.326	+0.111
AX2	+0.439	–0.486	+0.088

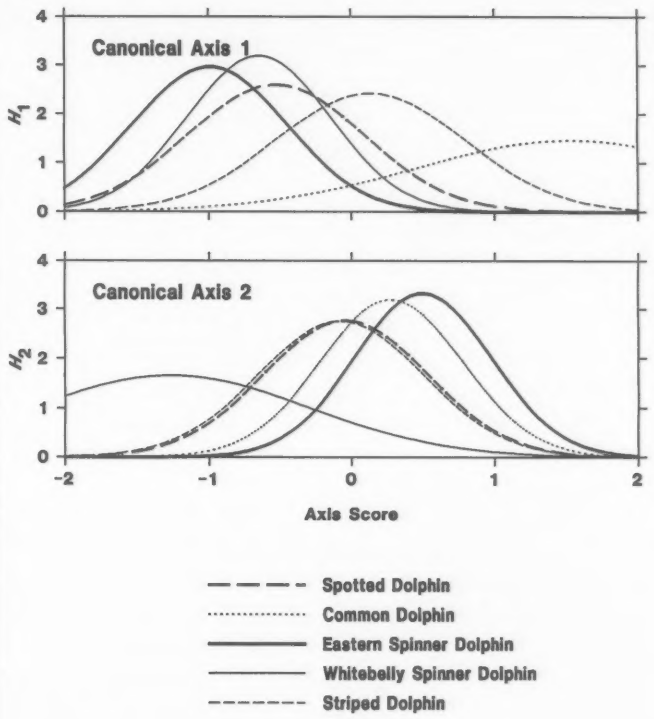

Figure 2

CCA-derived Gaussian distributions of dolphin species habitat quality, H (from MOPS 1986–90 encounter rates), along the first two canonical axes. The values are scaled so that the mean of H_{ij} is 1.0 over a range of ±2 units (standard deviations) on the canonical axis. Spotted dolphin = *Stenella attenuata*, common dolphin = *Delphinus delphis*, eastern spinner dolphin = *S. longirostris orientalis*, whitebelly spinner dolphin = *S. longirostris*, striped dolphin = *S. coeruleoalba*.

Spotted dolphin habitat was centered south and southwest of the southern coast of Mexico to about 3°N (Fig. 3). This corresponds to the warm, tropical surface water mass of Wyrtki (1966, see Fig. 1 in Reilly and Fiedler, 1994). The Costa Rica Dome (10°N, 90°W) was a notable gap in favorable spotted dolphin habitat.

Eastern spinner dolphins were even more closely associated with warm tropical surface water. Highest values of H for this stock were found off southern Mexico, in the center of the "coastal tropical" habitat defined by canonical axis 1 (Reilly and Fiedler, 1994). Whitebelly spinner dolphins were associated with subtropical surface water (Wyrtki, 1966) to the northwest and southwest of the tropical surface water in the core of the MOPS area.

Table 4

Dolphin species scores (standardized) ±tolerances on the first two canonical axes from canonical correspondence analysis (CCA). Dolphin species: spotted = *Stenella attenuata*, common = *Delphinus delphis*, eastern spinner = *S. longirostris orientalis*, whitebelly spinner = *S. longirostris*, striped = *S. coeruleoalba*.

	AX1	AX2
Spotted	−0.53 ± 0.57	0.19 ± 0.54
Common	1.68 ± 1.16	0.28 ± 0.48
Eastern spinner	−0.84 ± 0.49	0.86 ± 0.71
Whitebelly spinner	−0.37 ± 0.55	−1.51 ± 1.19
Striped	0.24 ± 0.69	−0.08 ± 0.55

Common dolphin habitat was centered in cool, upwelling-modified water in three regions: off Baja California, along 10°N with a maximum at the Costa Rica Dome, and in the equatorial surface water mass of Wyrtki (1966). These three habitat centers are occupied by the northern, central, and southern stocks of common dolphins (Perrin et al., 1985). The offshore H maximum along 10°N at 120–130°W does not correspond to high encounter rates in the MOPS data, but reflects a shoaling of the countercurrent thermocline ridge at that location (Fiedler, 1992).

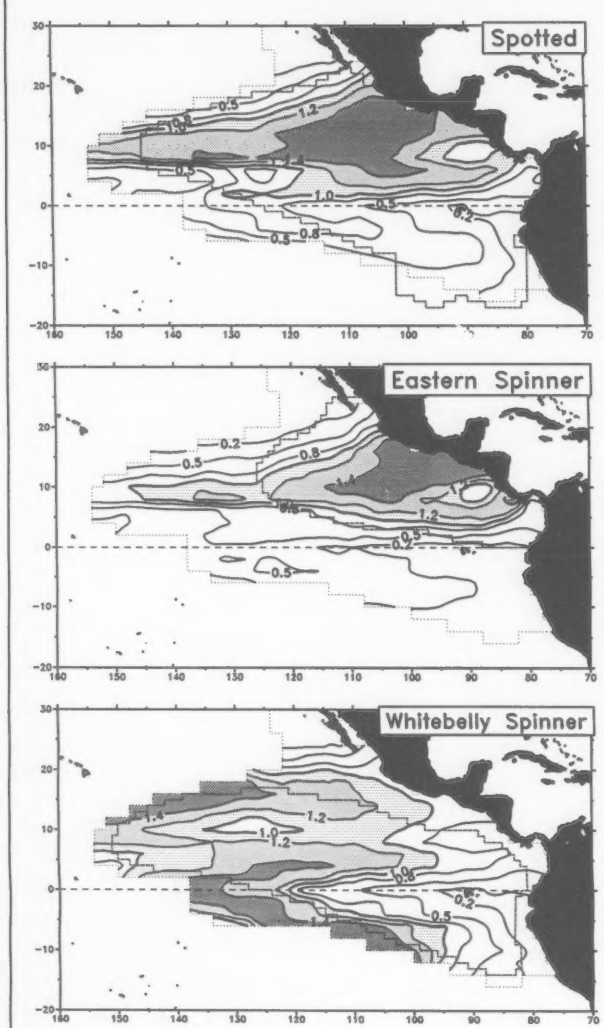

Figure 3

Mean habitat quality (H) for spotted (*Stenella attenuata*), eastern spinner (*S. longirostris orientalis*), whitebelly spinner (*S. longirostris*), common (*Delphinus delphis*), and striped (*S. coeruleoalba*) dolphins. H was calculated from climatological fields of surface temperature, thermocline depth, and thermocline thickness in the MOPS area. Heavy dashed lines delimit SOPS population areas used by Anganuzzi and Buckland (1989) and Anganuzzi et al. (1991) or, for striped dolphins, as defined by Au et al. (Footnote 1.)

Striped dolphins are the most widespread and abundant of the target species. The highest H values tended to be in regions between or offshore of the centers of spotted/eastern spinner dolphin habitat in tropical surface water near the coast of southern Mexico and northern, central, and southern common dolphin habitats off Baja California, near the Costa Rica Dome, and in equatorial water (see also Reilly, 1990).

Both seasonal and interannual variability were evident in time series of mean seasonal habitat quality, H (Fig. 4). The strongest interannual signal for all species can be attributed to the El Niño events of 1982–83 and 1986–87. During both events, H increased for spotted and spinner dolphins and decreased for common and striped dolphins. Seasonal variability, indicated by the deviations of the seasonal from the smoothed H values, was low for species with large geographic ranges (e.g. striped dolphin) and high for species with more restricted ranges (e.g. eastern spinner dolphin). Seasonal variability of H was as great as interannual variability for eastern spinner dolphins.

Annual dolphin abundance estimates, N_t, or interannnual change in abundance estimates, N_t–N_{t-1}, were related to changes in the environment, H, for spotted and eastern spinner dolphins. Annual spotted dolphin abundance was not significantly correlated with H, but interannual change in abundance was negatively correlated with H (Fig. 5, r=–0.65, P=0.01). Calculating year-to-year changes in abundance eliminates multi-year trends in the time series. Buckland et al. (1992) found significant trends in estimated spotted dolphin abundance which might complicate the relation between annual N and H values. An increase in H for spotted dolphins indicates an expansion of favorable habitat to the south of the SOPS population boundary west of 100°W (Fig. 6A).

Annual eastern spinner dolphin abundance was negatively correlated with H (r=–0.49, P=0.05). An increase in H for eastern spinner dolphins indicates an expansion of favorable habitat to the west and south of the SOPS population boundary (Fig. 6B).

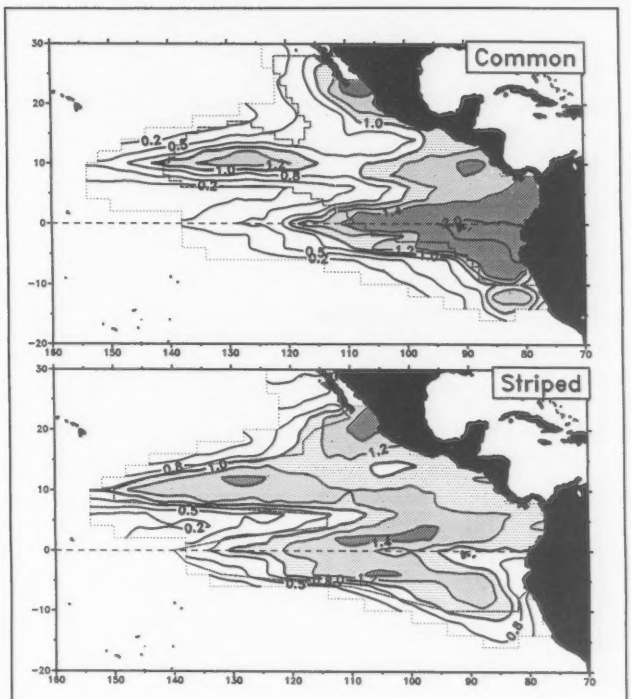

Figure 3 (Continued)

Common and whitebelly spinner dolphins did not show significant linear relationships between N and H (Fig. 7). For all four species, log-transformation of the abundance estimates or lagging N_t by up to four seasons did not change the significance levels of the linear relationships. However, common dolphin abundance appeared to be maximum at H near 1.0 and to decrease at lower or higher H values, except in 1983. Scatterplots of N_t vs. H_t for spotted and whitebelly spinner dolphins suggest similar nonlinear relationships. For common dolphins at low values of H, as in early 1983, very little high-quality or favorable habitat was available in the ETP (Fig. 6C). The only favorable habitat with $H>1$ was in equatorial water west of the Galapagos. Half of this favorable habitat was outside the SOPS boundary. At high values of H, as in early 1985, favorable habitat for the central and southern stocks (along 10°N and the equator, respectively) expanded. Favorable habitat along the equator extended beyond the SOPS boundary. At the same time, favorable habitat for the more abundant northern stock, off Baja California, was reduced.

Discussion

Estimated abundances of spotted and eastern spinner dolphins in the eastern tropical Pacific were correlated with changes in the environment, as described by the CCA-derived habitat quality index H. The time scale of the changes and the patterns of favorable habitat relative to nominal population boundaries (Fig. 6) suggest that the correlations resulted from a sampling effect, rather than a population effect. Thus, we have explained biases in annual population estimates that result in apparent population changes. For example, Anganuzzi and Buckland (1989) suggested that their low 1983 abundance estimate for spotted dolphins might be explained by dispersal of local concentrations of schools during the strong El Niño. Our results showed that spotted dolphin schools may have moved outside the nominal species range when the "coastal tropical" habitat expanded into equatorial water west of 100°W during this unusual event. Similarly, estimated eastern spinner dolphin abundance decreased slightly with increasing H because

of the dispersal of schools outside the nominal range used in calculating the abundance estimate. The center of distribution of spotted and eastern spinner dolphins is the warm tropical surface water in the core of the ETP. Therefore, the apparent responses of the two populations to environmental variability are similar.

The different effects of environmental variability on the habitats of the three stocks of common dolphins appear to complicate the response of the population as a whole. Data collected during surveys of the central and northern stocks of common dolphins in fall 1992 and 1993, respectively, will allow us to quantify stock-specific habitats and, perhaps, responses to environmental variability. We detected no effect of environmental variability on the abundance estimates of whitebelly spinner dolphins, but the CCA results inadequately define the geographical

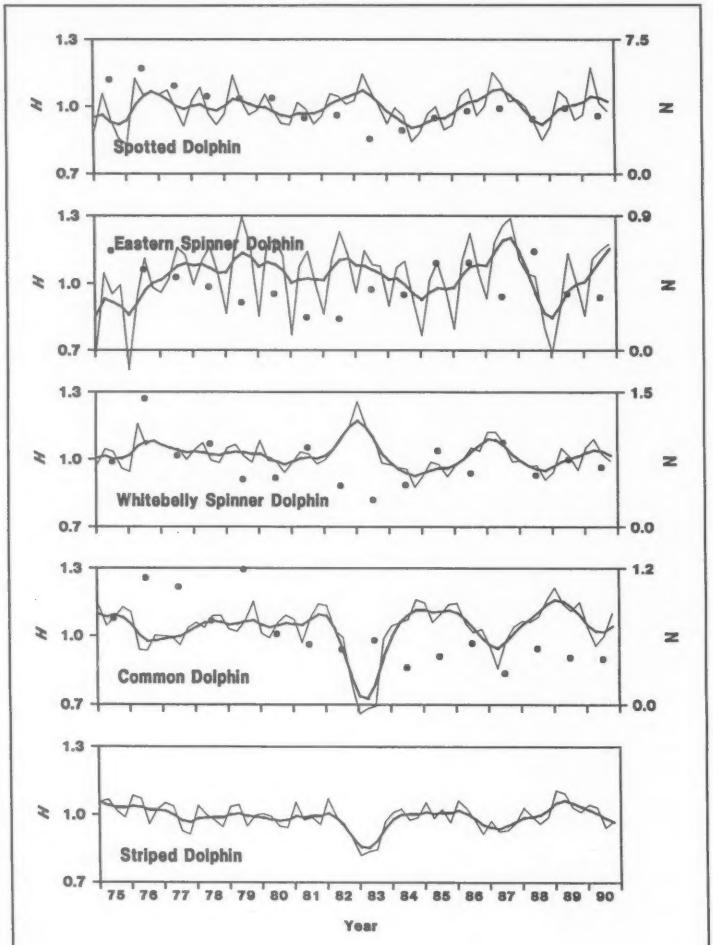

Figure 4

Mean SOPS area habitat quality (H) for five dolphin species: seasonal values (thin line) and smoothed values (five-season running mean, thick line). Dots are point estimates of species abundance ($N \times 10^{-6}$). Spotted dolphin = *Stenella attenuata*, common dolphin = *Delphinus delphis*, eastern spinner dolphin = *S. longirostris orientalis*, whitebelly spinner dolphin = *S. longirostris*, striped dolphin = *S. coeruleoalba*.

extent of the habitat of this stock (see Fig. 3). The apparent westward extension of the habitat outside the MOPS area is consistent with the recognition of the "whitebelly" form as a hybrid/intergrade between eastern and pantropical subspecies of spinner dolphins (Perrin, 1990). The partial separation of eastern and whitebelly spinner dolphin habitats defined by H is consistent with the management boundary between the two forms proposed by Perrin et al. (1991): eastern spinners north of 10°N and east of 125°W, and whitebelly spinners south of 10°N or west of 125°W.

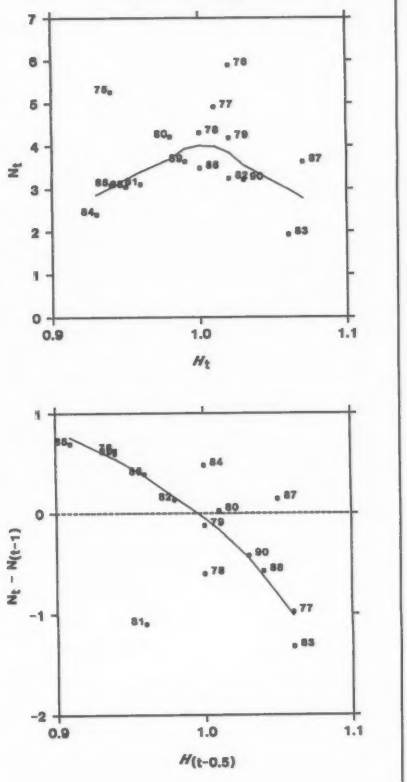

Figure 5

Abundance-environment relationships for spotted dolphins (*Stenella attenuata*) in the MOPS area: (**Top**) Annual abundance estimates ($N_t \times 10^{-6}$) vs. annual mean habitat quality (H_t). (**Bottom**) Interannual change in abundance estimates ($N_t - N_{t-1}, \times 10^{-6}$) vs. mean habitat quality from June of year ***t*-1** through May of year ***t*** ($H_{t-0.5}$). Solid line connects lowess-smoothed values (Wilkinson, 1990).

Reilly and Fiedler (1994) suggested that species habitats defined by axis scores from CCA could be used to improve the precision and accuracy of abundance estimates from research vessel surveys. Precision could be increased by post-stratifying the sighting data based on the spatial distribution of axis scores. Bias could be reduced by using axis scores to quantify the amount of habitat available within a survey area. The present results suggest that this approach could be extended by using species habitat distributions incorporating environmental variability along more than one canonical axis. For example, a large area of suitable spotted dolphin habitat existed in equatorial water beyond the SOPS population boundary during 1983, apparently causing a serious underestimate of abundance. Gerrodette et al.[4] suggested similar approaches for using fields of H to adjust abundance estimates from MOPS research vessel surveys.

We utilized the results of a multi-species CCA for this study. While this approach yields useful information about community structure, as in the separation of eastern and whitebelly spinner habitat, it does not retain the maximum amount of information about any single species for management applications. A similar type of analysis for each individual species or stock might explain more of the variability in abundance and improve the quantification of habitat quality defined by Gaussian responses along dominant environmental gradients. In addition, CCA could potentially be used to account for environmental effects on school size and effective trackline width that cause error in dolphin abundance estimates. However, preliminary results of a CCA incorporating school size (Reilly and Fiedler, 1994) showed no meaningful relation between school size and environmental variability. We have only begun to exploit CCA in our work and believe it is a powerful new technique with great potential for quantitative ecological studies of populations of marine mammals and other organisms. For example, environmental variability dominates variations in recruitment of many fish stocks (Longhurst, 1984; Hollowed et al., 1987). Although our time series was not long enough to address population change, this study demonstrates the potential of CCA to detect environmental effects in multi-stock fisheries studies.

[4] Gerrodette, T., P. C. Fiedler, and S. B. Reilly. 1991. Including habitat variability in line transect estimation of abundance and trends. NMFS/SWFSC Admin. Rep. No. LJ-91-37.

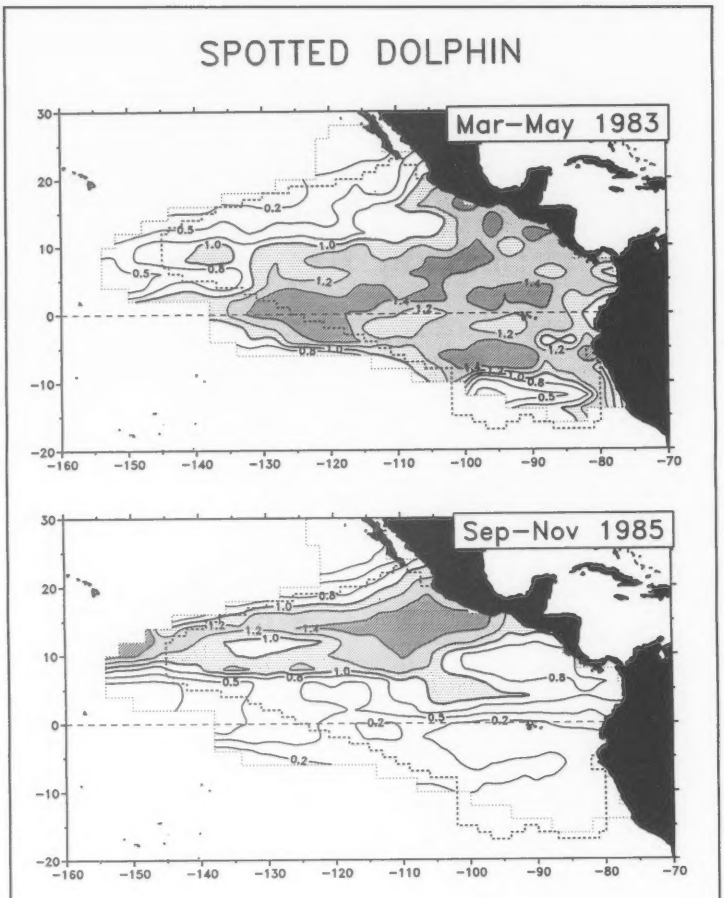

Figure 6A

Spotted dolphin (*Stenella attenuata*) habitat quality (*H*) calculated for extreme seasons: March–May 1983 and September–November 1985.

Acknowledgments

We thank the dedicated tuna vessel and research vessel observers, oceanographic technicians, and cooperative ship personnel who contributed to the collection of the sighting and environmental data. Robert Holland assisted in manipulating the large data sets for this study. Doug DeMaster provided continual support and encouragement.

Literature cited

Anganuzzi, A. A., and S. T. Buckland.
1989. Reducing bias in trends in dolphin relative abundance, estimated from tuna vessel data. Rep. Int. Whal. Comm. 39:323–334.

Buckland, S. T., K. L. Cattanach, and A. A. Anganuzzi.
1992. Estimating trends in abundance of dolphins associated with tuna in the eastern tropical Pacific Ocean, using sightings data collected on commercial tuna vessels. Fish. Bull. 90:1–12.

Fiedler, P. C.
1992. Seasonal climatologies and variability of eastern tropical Pacific surface waters. Dep. Commer., NOAA Tech. Rep. NMFS 109, 65 p.

Hollowed, A. B., K. M. Bailey, and W. S. Wooster.
1987. Patterns in recruitment of marine fishes in

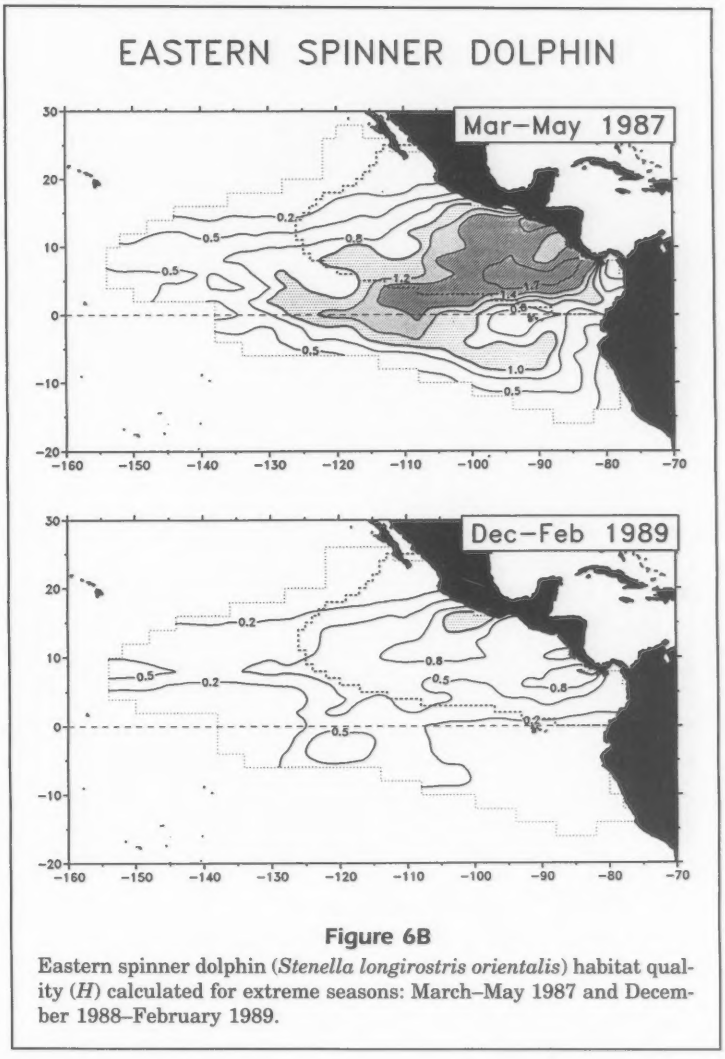

Figure 6B

Eastern spinner dolphin (*Stenella longirostris orientalis*) habitat quality (*H*) calculated for extreme seasons: March–May 1987 and December 1988–February 1989.

the northeast Pacific Ocean. Biol. Oceanogr. 5:99–131.

Holt, R. S., T. Gerrodette, and A. B. Cologne.
1987. Research vessel survey design for monitoring dolphin abundance in the eastern tropical Pacific. Fish. Bull. 85:435–446.

Kessler, W. S.
1990. Observations of long Rossby waves in the northern tropical Pacific. J. Geophys. Res. 95(C4):5183–5217.

Longhurst, A.
1984. Heterogeneity in the ocean - implications for fisheries. Rapp. P.-v. Réun. int. Explor. Mer, 185:268–282.

Perrin, W. F.
1969. Using porpoise to catch tuna. World Fish. 18(6):42–45.
1990. Subspecies of *Stenella longirostris* (Mammalia: Cetacea: Delphinidae). Proc. Biol. Soc. Wash. 103:453–463.

Perrin, W. F., M. D. Scott, G. J. Walker, and V. L. Cass.
1985. Review of geographical stocks of tropical dolphins (*Stenella* spp. and *Delphinus delphis*) in the eastern Pacific. Dep. Commer., NOAA Tech. Rep. NMFS 28, 28 p.

Perrin, W. F., P. A. Akin, and J. V. Kashiwada.
1991. Geographic variation in external morphology of the spinner dolphin *Stenella longirostris* in the eastern Pacific and implications for conservation. Fish. Bull. 89:411–428.

Reilly, S. B.
1990. Seasonal changes in distribution and habitat

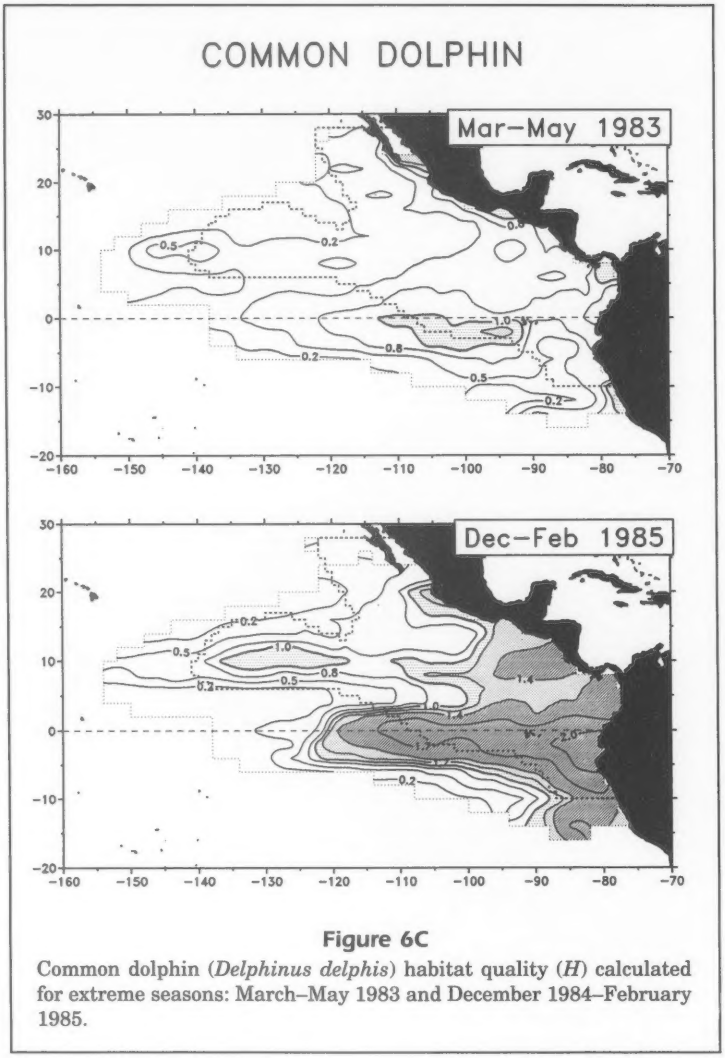

Figure 6C

Common dolphin (*Delphinus delphis*) habitat quality (*H*) calculated for extreme seasons: March–May 1983 and December 1984–February 1985.

differences among dolphins in the eastern tropical Pacific. Mar. Ecol. Prog. Ser. 66:1–11.

Reilly, S. B., and J. Barlow.
1986. Rates of increase in dolphin population size. Fish. Bull. 84:527–533.

Reilly, S. B., and P. C. Fiedler.
1994. Interannual variability of dolphin habitats in the eastern tropical Pacific. I: Research vessel surveys, 1986–1990. Fish. Bull. 92:434–450.

Smith, T. D.
1983. Changes in size of three dolphin (*Stenella* spp.) populations in the eastern tropical Pacific. Fish. Bull. 81:1–13.

Sprintall, J., and G. Meyers.
1991. An optimal XBT sampling network for the eastern Pacific Ocean. J. Geophys. Res. 96(C6): 10,539–10,552.

Ter Braak, C. J. F.
1986. Canonical correspondence analysis: a new eigenvector technique for multivariate direct gradient analysis. Ecology 67:1167–1179.

Wade, P. R., and T. Gerrodette.
1992. Estimates of dolphin abundance in the eastern tropical Pacific: preliminary analysis of five years of data. Rep. Int. Whal. Comm. 42:533–539.

Wilkinson, L.
1990. SYGRAPH: The system for graphics. SYSTAT, Inc., Evanston, IL.

Wyrtki, K.
1966. Oceanography of the eastern equatorial Pacific Ocean. Oceanogr. Mar. Biol. Ann. Rev. 4:33–68.

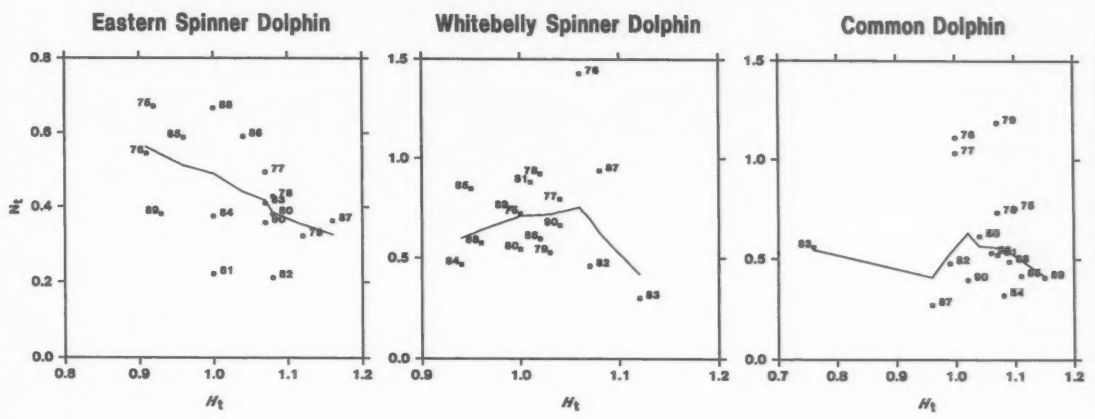

Figure 7

Abundance-environment relations for eastern spinner (*Stenella longirostris orientalis*), whitebelly spinner (*S. longirostris*), and common (*Delphinus delphis*) dolphins in the MOPS area, annual abundance estimates ($N_t \times 10^{-6}$) vs. annual mean habitat quality (H_t). Solid line connects lowess-smoothed values (Wilkinson, 1990).

Annual mass strandings of pelagic red crabs, *Pleuroncodes planipes* (Crustacea: Anomura: Galatheidae), in Bahia Magdalena, Baja California Sur, Mexico

David Aurioles-Gamboa
Centro de Investigationes Biologicas de Baja California Sur
Apartado Postal 128, LA Paz B. C. S., Mexico

Maria Isabel Castro-González
Instituto Nacional de la Nutrición "Salvador Zubirán"
Vasco de Quiroga #15, Col. y Del. Tlalpan. 14000, México D. F.

Ricardo Pérez-Flores
Centro de Investigaciones Biologicas de Baja California Sur Apartado Postal 128, La Paz B. C. S., México.

Pelagic red crabs (or langostilla in Spanish), *Pleuroncodes planipes*, are very abundant galatheid crustaceans off the west coast of Baja California. Some studies suggest that pelagic red crabs are the most abundant species in the microneckton, one of the most important consumers of phytoplankton, and the most common prey item for many marine vertebrates in the area (Boyd, 1962, 1967; Blackburn, 1969; Longhurst et al., 1967; Kato, 1974; Galván, 1988; Balart and Castro[1]).

Although widely used, the common name (pelagic red crab) describes only the planktonic period (about one year) in the life of the species. Larvae, juveniles, and young adults are planktonic. At about 17–20 mm standard carapace length (SCL), they become benthic, making occasional movements to the surface (mostly at night) in a circadian migration (Boyd, 1967). Once the animals reach 32–34 mm SCL, they are fully benthic as are other galatheid species (Boyd, 1967; Aurioles-Gamboa, 1992).

Pelagic red crabs breed from December through April; the peak of the reproductive season is in February (Boyd, 1962; Kato, 1974; Gómez, 1990). Females about 14–15 mm SCL, have been found carrying eggs, but most of the females start to breed when they are about 20 mm SCL (Boyd, 1962; Serrano, 1991).

The benthic population performs seasonal bathymetric movements, at least in the area from lat. 24° to 26° N, in which they disperse during winter and spring to occupy the benthos of the continental shelf (0–200 m depth). After the breeding season, the population moves to deeper waters (100–200 m), and probably invades the continental slope (Aurioles-Gamboa, 1992). Population withdrawal is associated with a rise in bottom temperature above 16°C, and pelagic red crabs remain from June through October in waters 100–200 m deep, where bottom temperature is in the range of 12–16°C (Aurioles-Gamboa, 1992).

One of the notable characteristics in pelagic red crab life history are mass strandings, which have been reported for Bahia Magdalena and the California Coast (Glynn, 1961; Boyd, 1962; Kato, 1974; Stewart et al., 1984). The main difference between strandings in California and Baja California is the frequency of ocurrence. Pelagic red crab beachings in California occur during El Niño events, which enable the population to move northward in warm water currents originating in the south. In contrast, pelagic red crab strandings in Bahia Magdalena are annual, and apparently recur on the same beaches and during the same season of year.

In Bahia Magdalena, pelagic red crabs were observed in the upper 50 cm of water of the surf zone before stranding. Onshore winds and receding tides hasten and intensify stranding (Boyd, 1962). Kato (1974) proposed that the presence of pelagic red crabs near shore is primarily due to winds, waves, and currents.

On 9 May 1991, one of us (D.A-G.) observed a mass stranding of pelagic red crabs on a beach of Magdalena Island close to the mouth of the Bahia Magdalena on the Pacific coast of Baja California (Fig. 1). About 1100 hours, a compact surface swarm of live crabs was seen 1–2 m from the beach. Small groups of crabs were thrown to the beach by waves, and were unable to return to the sea.

[1] Balart-Páez, E., and Castro-Aguirre, J. L. 1992. Habitos alimenticios de la merluza Bajacalifornia *Merluccius angustimanus*, en la costa occidental de Baja California Sur, México. Paper pres. at the IX International Symposium of Marine Biology, 1–5 June 1992, La Paz Baja California Sur, México.

Manuscript accepted 4 October 1993
Fishery Bulletin 92:464–470 (1994)

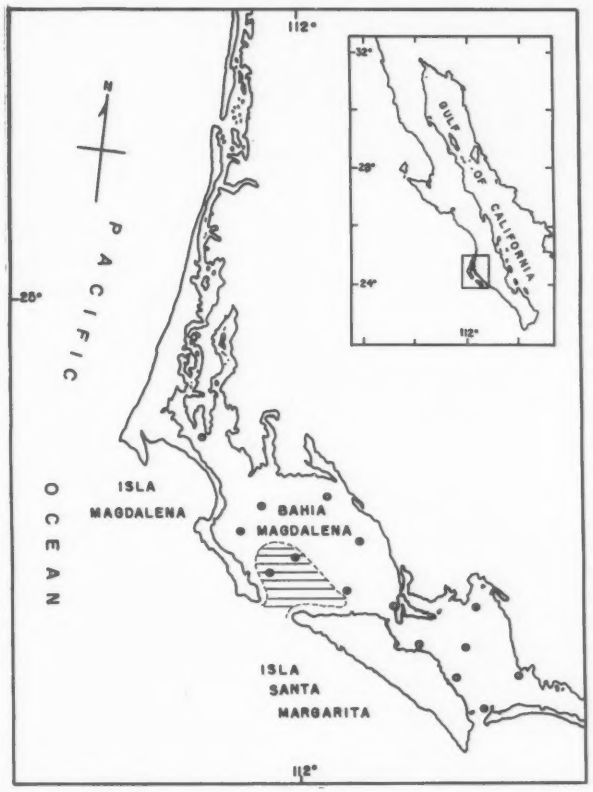

Figure 1

Study area on the west coast of Baja California Sur, México. Dots inside Bahia Magdalena indicate the location of stations sampled. The shaded area is the region where pelagic red crabs, *Pleuroncodes planipes*, were found as indicated by positive stations and visual observations (from Solís, 1991).

The general appearance of these pelagic red crabs (color and mobility) suggested that the crustaceans were healthy and that the stranding could be considered accidental (Boyd, 1962). We questioned local fishermen about crab strandings and determined that mass strandings 1) occur annually, usually in spring, from April through June, and 2) are common on Santa Margarita and Magdalena Islands but rarely seen on the peninsular coast.

Since strandings coincide with the end of the breeding season, we addressed the null hypothesis that stranded pelagic red crabs, particularly females, were in a weakened state because of energy expended in reproduction, as reported for many crustaceans (Hartnoll, 1985). It is known that pelagic red crabs are able to breed twice in a single breeding season and may produce, depending on body size, from 500 to 5000 eggs in each brood (Serrano, 1991). Based on this fact, debilitation caused by reproductive investment should be more evident in females. For that reason, the chemical composition of pelagic red crabs in Bahia Magdalena was determined for both sexes. We were aware that males were overrepresented in samples collected on the continental shelf (Boyd, 1962; Serrano, 1991); thus we also wished to determine if stranded animals were female-biased, as an explanation for the unbalanced sex ratio recorded on the continental shelf.

Materials and methods

To test whether the strandings were due to weakness caused by starvation or malnutrition, about 20 kg of live-stranded pelagic red crabs were collected as soon they were stranded. From this sample, a total of 1,150 individuals were sexed and measured for SCL to the nearest 1.0 mm. Sex was determined by the presence or absence of modified pleopods, which males use to fertilize the eggs (Boyd, 1962). Standard carapace length was measured from the antorbital notches of the rostrum to the midpoint of the posterior border of the carapace (Kato, 1974). This measurement is usually preferred over total length because it does not vary with shrinkage of the abdomen.

Stomach contents were analyzed in order to determine if 1) the animals had been feeding before stranding, and 2) the number of items and composition was similar to stomach contents of pelagic red crabs collected on the continental shelf (Pérez and Aurioles-Gamboa[2]). We examined the stomach contents from a subsample of nine individuals after fixing in formalin (4%), removing the cardiac-pyloric stomach from the animal, dissolving its contents in two drops of water and placing them on a smear slide. Pérez and Aurioles-Gamboa[2] determined that the average stomach composition in a swarm of crabs does not vary significantly after a sample of six crabs.

Food items were identified and counted under the microscope and relative abundance of major groups

[2] Pérez, F. R., and D. Aurioles-Gamboa. 1992. Cambios en la alimentación invierno-verano de la langostilla *Pleuroncodes planipes*, en la costa oeste de Baja California. Paper pres. at the IX International Symposium of Marine Biology, 1–5 June 1992. La Paz B. C. S. México.

of food items was determined. Following Pérez and Aurioles-Gamboa[2], we recorded some of the phyto and zooplankton components in four major groups: 1) phytoplankton, 2) zooplankton, 3) particulate organic matter (POM), and 4) inorganic matter (small grains of sand, clay or mud). The number of diatoms, crustacean parts, foraminifers, and other components, such as small agglomerations of POM, were counted and their numbers converted to relative frequency.

Proximate analyses was based on 200 g ♂ and 200 g ♀ of sun dried and milled pelagic red crabs (about 4 kgs of fresh crabs). The techniques used were those of the Association of Official Analytical Chemists (A.O.A.C., 1984): moisture (7.007), ash (7.009), crude fiber (7.006), crude protein (2.057), ether extract (7.060), carbohydrates (by difference from all other determinations at 100%). This methodology had been used previously to analyze pelagic red crabs sampled from the benthos of the continental shelf (Castro, 1993). Two-sample *t*-tests (Zar, 1984) were conducted to identify differences in food composition, proximate composition, and mean SCL between stranded pelagic red crabs in Bahia Magdalena and breeding pelagic red crabs collected on the continental shelf in March 1990. A chi-square test for determining a possible deviation of sex ratio was applied for the stranded pelagic red crabs (Zar, 1984).

Results

The stranded crabs formed a long brilliant red line of several kilometers on the interior coast of the northern part of Bahia Magdalena (Fig. 1). In addition, there were two lines of dried crabs separated by a few meters, higher on the beach and stranded during the previous days.

Behavior of pelagic red crabs during stranding

Two hours of observations on a surface swarm about 12 m long and 1 m wide were conducted after 1100 hours (11 May 1991) during the receding tide. The swarm was propelled to and from the beach by the waves and was unable to move offshore. When the swarm was pushed toward the beach by the wave action, some animals were thrown onto the sand and exposed as the water receded.

During sampling on the beach, the pelagic red crabs moved their legs and actively used their chelae as pincers. This behavior was typical of pelagic red crabs caught in trawls from the continental shelf. Pelagic red crabs had been caught from the shelf in all seasons, but only during mid-summer (when the bottom-surface temperature difference is as great as 17°C) did the crabs show signs of damage as they moved slowly and died rapidly on the deck (Aurioles-Gamboa, unpubl. data). In contrast, crabs were very active in the first minutes after stranding, and moved less frequently later. The crabs were brilliant red, which differentiated them from the lighter color of crabs collected on the continental shelf. Based on their vigorous activity, the pelagic red crabs stranded on Magdalena Island (Fig. 1) appeared to be in good health.

Stomach contents of stranded pelagic red crabs

The total number of items and relative frequency of the four major groups found in the stomachs is shown in Figure 2A. For comparison, the results of a typical sample taken on the continental shelf is provided in Figure 2B (Pérez, 1992). The minimum number of items counted was 457 and the maximum about 2,266. This range was greater than that found in crabs from the continental shelf (841–1,495 items). However, there was no significant difference in the mean number of items ($\bar{x}$=1,027 versus 1,100) between stomachs from the stranded crabs and those from the shelf (two sample *t*-test, $P>0.05$, df=9; $t=-0.3082$).

Food composition (particulate organic matter, zooplankton, and phytoplankton) was not different between crabs from the two regions. Inorganic matter (grains of sand, clay, etc.) was more abundant in the stomachs of the pelagic red crabs collected from the shelf ($\bar{x}$=365 versus 60; two sample *t*-test, $P<0.05$, df=9; $t=-0.0046$). This difference, however, does not account for a significant change in the feeding habits of crabs from the two samples.

Proximate composition of stranded red crabs

In stranded pelagic red crabs, the sexes were not different in protein and crude fiber (Table 1), however they differed significantly in lipids and ash contents (two sample *t*-test, $P<0.05$, df=9; $t=1.870$ and 10.012 respectively). Females had higher lipid and lower ash content than males, both by about 1.5%.

There were significant differences when the chemical composition of stranded crabs (sexes combined), were compared to crabs from the continental shelf (Table 1). Crabs from both areas were similar in their protein content, but differed in lipids and ash. The lipid content in Bahia Magdalena crabs was almost nine times higher than that in shelf crabs (*t*-test, $P<0.05$, df=16, $t=35.664$). Crabs from the continental shelf were higher in fiber and ash but lower in carbohydrate content.

It was also noted that during handling of stranded crabs an oily, orange film was left in the containers, a phenomenon not previously observed in crabs collected in more than 200 bottom trawls on the continental shelf (Aurioles-Gamboa, 1992). The substance probably contained carotenoids, which in this species have been identified as astaxanthins (Wilkie, 1972).

Size and sex of stranded pelagic red crabs

Pelagic red crabs collected in Bahia Magdalena were 12–28 mm SCL. Size distribution was similar for males and females (Fig. 3); mode and mean were 15.82 and 17.02 mm for females and 17.36 and 17.26 mm for males, respectively. Differences in mean size of males and females were statistically significant (two-sample t-test=2.057, $P<0.05$, df=1,147). In older organisms, slight sexual dimorphism is evident in males which are slightly larger and heavier with longer and wider chelae (Serrano and Aurioles-Gamboa, 1991).

Pelagic red crabs are about 14 mm SCL at the end of the first year of life (about February–March) and grow approximately 1 mm per month (Boyd, 1962). Because the crabs were about 17 mm SCL (mode), they should have been about 14–15 months old. Some individuals were about 24–28 mm SCL (Fig. 3), which according to Boyd (1962) were about 26–27 months old.

The number of females (605) in relation to the number of males (544), deviates significantly from the expected 1:1 proportion (chi-square $P<0.001$). In contrast, the sex ratio of crabs from the continental shelf is slightly male biased throughout the year (Serrano, 1991).

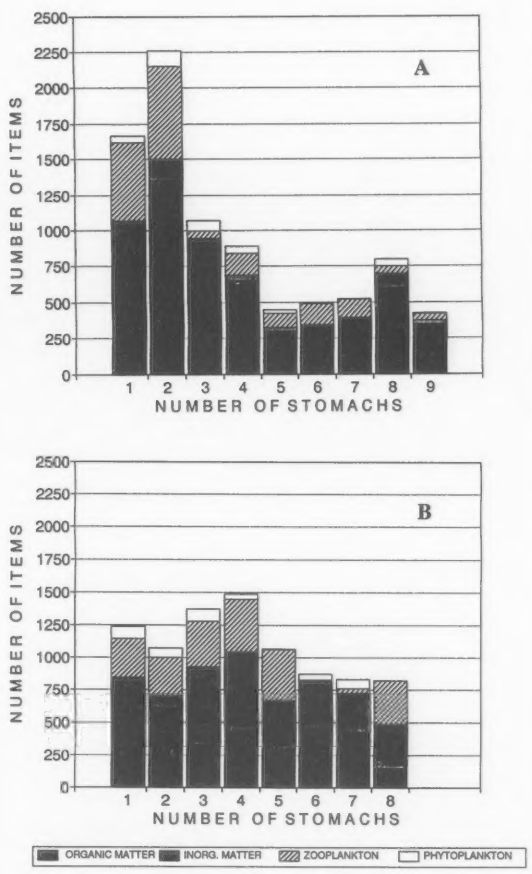

Figure 2

Total number of items and gross stomach composition from pelagic red crabs, *Pleuroncodes planipes*, collected in Bahía Magdalena (**A**), and organisms typically found on the benthos of the continental shelf off Baja California (**B**). POM = Particulate Organic Matter, IM = Inorganic Matter. Numbers below the x-axis indicate number of stomachs.

Discussion

Debilitated pelagic red crabs as explanation of strandings

We rejected the null hypothesis that stranded pelagic red crabs represent a debilitated fraction of the population because 1) the stranded crabs moved vigorously during and just after stranding, 2) the stomachs of crabs were full and the contents were similar to those collected on the continental shelf, which indicated they were feeding normally, 3) the chemical composition was generally similar to those collected on the continental shelf, and when different, did not suggest malnutrition, and 4) timing and area of strandings are better explained by physical phenomena (i.e. by accidental stranding due to funneling effect, wave action, and receding tide). Our observations support the observations made by Boyd (1962), that waves and receding tide play a major role after the animals enter the surf zone. Two available stranding reports (Boyd, 1962; Jorge Llinas[3]), indicated that beachings occurred during falling tides. According to local fishermen, the two higher lines of stranded crabs we found on the beach of Isla Magdalena on 9 May 1991, were stranded two mornings before our visit, also during receding tides.

[3] Llinas, J. Centro de Investigaciones Biologicas de Baja California Sur. Apdo. Postal 128. La Pax Baja California Sur, Mexico, personal commun. 1993.

Differences in pelagic red crab chemical composition

The lipid content of the younger stranded pelagic red crabs was different from that recorded in older specimens caught on the benthos of the continental shelf (Table 1). Differences in the proportion of chemical components between young and old individuals have been reported for many decapod species (Herring, 1973; Morris, 1973). The observed differences in lipid concentration and apparent pigmentation between young-adult and older-benthic pelagic red crabs cannot be considered abnormal or attributable to unhealthy specimens. There was no evidence to support the hypothesis of a debilitated fraction of pelagic red crabs, and strandings can be explained by mere accident.

The differences in lipid and ash content between male and female stranded crabs would be attributable to metabolic differences in which females require more lipid to invest in egg production (Hartnoll, 1985). Some females still had eggs attached on the pleopods as evidence of their reproductive condition; however, the low numbers of ovigerous females in the sample, suggested that we collected them at the end of the breeding season.

Table 1

Mean values for proximate chemical analyses of *Pleuroncodes planipes* samples from Bahia Magdalena and the Continental Shelf of Baja California.

	Bahia Magdalena				
	Males % n = 5		Females % n = 6		Significant difference 95% conf. *
Moisture	4.7	(0.28)	4.73	(0.23)	
Ash	29.79	(0.36)	28.21	(0.66)	+
Ether extract	12.79	(0.72)	15.46	(1.39)	+
Crude fiber	7.91	(0.99)	8.70	(0.65)	–
Crude protein	41.75	(0.14)	40.64	(0.07)	–
Carbohydrates	3.06		2.26		–
	Bahia Magdalena Both sexes % n = 11		Continental Shelf Both sexes % n = 12		
Moisture	4.71	(0.20)	4.12	(0.32)	
Ash	29.04	(0.24)	40.30	(0.03)	+
Ether extract	14.12	(1.98)	2.75	(0.007)	+
Crude fiber	8.30	(0.62)	12.83	(0.03)	+
Crude protein	41.19	(0.22)	38.61	(0.29)	–
Carbohydrates	2.64		1.39		–

* Two-sample *t*-test for means; + significant difference, – no difference (Alpha=0.05).

Size and sex of pelagic stranded red crabs

The stranded individuals we sampled were predominantly 13 to 20 mm SCL, although some larger crabs were also found (Fig. 3). Kato (1974) also reported individuals of these two size distributions in a mass stranding in Bahia Magdalena. Photos were available of a mass stranding in May of 1979, in which pelagic red crabs larger than 25 mm SCL (second year of life, Boyd 1962) were very abundant. Therefore, the over-representation of young adults in the 1991 stranding we sampled is not the rule, as both size and age groups were found.

The sex ratio (1:1.11) of our sample was significantly female biased ($P<0.05$, $\chi^2=22.97$, df=1,147). Benthic samples of crabs in Bahía Magdalena during 1990 (Solís, 1991), also

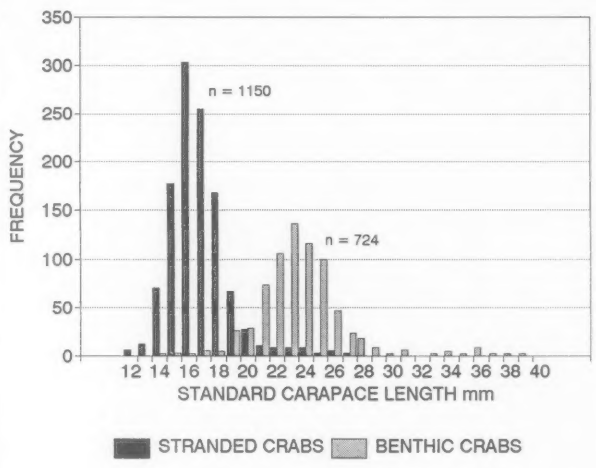

Figure 3

Size distribution of pelagic red crabs, *Pleuroncodes planipes*, stranded in Bahía Magdalena and the typical distribution of benthic crabs on the continental shelf off Baja California.

had an overrepresentation of females (1:1.23), suggesting that a higher abundance of females in stranded crabs would be a reflection of the sex ratio in the bay. Additional evidence for a female biased sex ratio in coastal waters comes from Serrano (1991), who reported higher frequency of females inshore during the breeding season. Similar findings were obtained by Escoto and Orellana (1981) for pelagic red crabs off the Nicaragua coast, and for a closely related species, *P. monodon*, from Chile (Arana and Culquichicón[4]). However, several authors have reported that the total sex ratio on the continental shelf is male biased (Boyd, 1962; Boyd and Johnson, 1963; Serrano, 1991). Boyd (1962), suggested that the sex-ratio differences on the continental shelf could be due to one or a combination of the following causes: 1) a deviation in primary sex ratio, 2) lower survival rate of females, or 3) the fact that plankton nets may not sample males and females with equal effectiveness.

The hypothesis that females die at a higher rate than males is supported by the present data, since females were more abundant where there was a natural cause of mass mortality. It has been mentioned that the breeding season of the species is synchronized to the time (winter-spring) when coastal upwelling is more intense. Pelagic red crabs may be more abundant in places where phytoplankton is more plentiful (Blackburn, 1969). Thus, it can be advantageous for pelagic red crab females to move to shore and release larvae in upwelled water. However, by doing so, females are more likely to enter Bahia Magdalena or other coastal lagoons and die in accidental strandings.

Literature cited

A. O. A. C.
1984. Official methods of analyses, 14th ed. Association of Analytical Chemists, Washington D.C.

Aurioles-Gamboa, D.
1992. Inshore-offshore movements of pelagic red crabs *Pleuroncodes planipes* (Decapoda, Anomura, Galatheidae) off the Pacific coast of Baja California Sur, México. Crustaceana 62(1):71–84.

Blackburn, M.
1969. Conditions related to upwelling which determine distribution of tropical tunas off western Baja California. U. S. Fish Wild. Serv. Fish. Bull. 68:147–176.

Boyd, C. M.
1962. The biology of a marine decapod crustacean, *Pleuroncodes planipes* Stimpson 1860. Ph.D. thesis, Univ. Calif. San Diego, 123 p.
1967. Benthic and pelagic habitats of the red crab *Pleuroncodes planipes*. Pacific Science 21:394–403.

Boyd, C. M., and M. W. Johnson.
1963. Variations in the larval stages of a decapod crustacean, *Pleuroncodes planipes*, Stimpson (Galatheidae). Biol. Bull.(Woods Hole) 124:142–152.

Castro, G. M. I.
1993. Procesos tecnologicos aplicados a la langostilla (*Pleuroncodes planipes* Stimpson) y cambios en su composición química a diferentes latitudes para su aprovechamiento en alimentación animal. Tésis de Maestría en producción animal, 82 p.

Escoto, R., and F. Orellana.
1981. Segundo crucero de evaluación del recurso langostino del Pacífico Nicaraguense. Boletín técnico del Instituto Nicaraguense de la Pesca (Diciembre 1980), 42 p.

Galván, M. F.
1988. Composición y análisis de la dieta del atún aleta amarilla *Thunnus albacares*, en el oceano Pacífico Mexicano durante el periodo 1984–1985. Tésis de Maestría en Ciencias, CICIMAR, 86 p.

Glynn, P. W.
1961. The first recorded mass strandings of pelagic red crabs, *Pleuroncodes planipes*, at Monterey Bay California since 1959, with notes on their biology. California Fish and Game 47 (1): 97–101.

Gómez, G. J.
1990. Variación de la distribución y abundancia de los estadios planctónicos de *Pleuroncodes planipes* (Crustacea: Galatheidae) en la costa occidental de Baja California Sur, México (1986). Tésis de Licenciatura en Biología Marina, Universidad Autonoma de Baja California Sur, México, 86 p.

Hartnoll, G. R.
1985. Growth, sexual maturity and reproductive output. *In* A. M. Wenner (ed.), Crustacean issues 3: factors in adult growth, p. 101–128. A. A. Balkema, Boston, and Rotterdam, Netherlands,

Herring, P. J.
1973. Depth distributions of the carotenoid pigments and lipids of some oceanic animals. 2: Decapod crustaceans. J. Mar. Biol. Assoc. U.K. 53:539–562.

Kato, S.
1974. Development of the pelagic red crab (Galatheidae, *Pleuroncodes planipes*) fishery in the eastern Pacific Ocean. Mar. Fish. Rev. 36 (10):1–9.

Longhurst, A. R., C. J. Lorenzen, and W. H. Thomas.
1967. The role of pelagic red crabs in the grazing of phytoplankton off Baja California. Ecology 48:190–200.

[4] Arana, E. P., and Z. M. Culquichicón. 1990. Estructura poblacional del langostino colorado (*Pleuroncodes monodon*) en la zona centro-sur de Chile. Estudios y Documentos. Final Rep. No. 7/89 to Universidad Católica de Valparaiso, Facultad de Recursos Naturales, Escuela de Ciencias del Mar, 56 p.

Morris, R. J.
1973. Relationships between the sex and degree of maturity of marine crustaceans and their lipid compositions. J. Mar. Biol. Assoc. U.K. 53:27–37.

Pérez, F. R.
1992. Alimentación de la langostilla *Pleuroncodes planipes* Stimpson, 1860, durante el periodo reproductivo (Marzo, 1990). Tésis de licenciatura en Biología, Universidad Nacional Autonoma de México, ENEP, Zaragoza, México, D. F., 53 p.

Serrano, P. V.
1991. Aspectos reproductivos de la langostilla *Pleuroncodes planipes* (Crustacea: Decapoda: Galatheidae). Tésis de Maestría en Ciencias Marinas, CICIMAR, 89 p, La Paz Baja California Sur, México.

Serrano, P. V., and D. Aurioles-Gamboa.
1991. Dimorfismo sexual en la langostilla, *Pleuroncodes planipes* Stimpson, 1860 (Crustacea: Decapoda: Galatheidae). Proc. of San Diego Society of Natural History 13:1–5.

Solís, F.
1991. Composición y distribución espacio-temporal de los macroinvertebrados bentónicos del complejo lagunar Magdalena-Almejas de la costa occidental de Baja California Sur. Tésis de licenciatura en Biología, Univ. Michoacana de San Nicolás de Hidalgo, México, 96 p.

Stewart, B. S, P. M. Yochem, and R. W. Schreiber.
1984. Pelagic red crabs as food for gulls: a possible benefit of El Niño. The Condor 86:341–342.

Wilkie, D. W.
1972. The carotenoid pigmentation of *Pleuroncodes planipes* Stimpson (Crustacea: Decapoda: Galatheidae). Comp. Biochem. Physiol. 42 (B):731–734.

Zar, J. H.
1984. Biostatistical analysis. Prentice-Hall, Englewood Cliffs, NJ, 716 p.

Mass marking coho salmon, *Oncorhynchus kisutch*, fry with lanthanum and cerium

Bridget C. Ennevor
Department of Fisheries and Oceans, 327–555 West Hastings Street
Vancouver, British Columbia, Canada V6B 5G3

Most current salmonid tagging programs identify small proportions of a population. However, under some circumstances it is desirable to mark entire populations. Chemical marking is a technique that can rapidly mark large numbers of fish without individual handling. Marking is accomplished by exposing the fish to biologically rare elements that are subsequently incorporated and retained in certain tissues in which they are not naturally found. Marking of entire hatchery populations could be valuable from a fisheries management perspective for stock identification (hatchery versus wild salmon), assessment of contribution to fisheries, and evaluation of current tagging and sampling techniques.

Ennevor and Beames (1993) have shown that some lanthanide elements (i.e. lanthanum and cerium) are suitable for mass marking juvenile coho salmon, *Oncorhynchus kisutch*. The lanthanide elements are not absorbed from the gastro-intestinal tract (Kyker, 1961; Ellis, 1968; Luckey and Venugopal, 1977), and therefore may be introduced through the fishes' rearing water. Because these are bone-seeking elements (Durbin et al., 1956; Jowsey et al., 1958), administered lanthanides are subsequently incorporated into the bony tissues of coho salmon fry and smolts (Ennevor, 1991; Ennevor and Beames, 1993). Analysis of the vertebral column, otoliths, and scales by inductively coupled plasma-mass spectrometry (ICP-MS) revealed that administered lanthanides are present in these bony tissues 10.5 months post-treatment (Ennevor, 1991; Ennevor and Beames, 1993). ICP-MS is capable of detection and quantification of the lanthanide elements at levels as low as 0.01 $\mu g \cdot g^{-1}$ (Longerich et al., 1987; Houk and Thompson, 1988).

Trials were performed to determine whether immersion into solutions of lanthanide elements would produce recognizable marks on juvenile salmon. These studies were designed 1) to investigate differences in toxicity and uptake between the chloride and acetate forms of lanthanum and cerium, and 2) to assess optimal concentrations and exposure times for marking coho salmon fry in the extremely soft and slightly acidic water at Capilano River Hatchery, British Columbia.

Materials and methods

In the following experiments, lanthanum and cerium were introduced into the rearing water of coho salmon fry at Capilano River Hatchery. The river water at this hatchery is slightly acidic and extremely soft (pH=6.5; hardness as $CaCO_3$=3.8). Concentrated lanthanide stock solutions were metered into the tanks at a rate of 1 $mL \cdot min^{-1}$ and the rearing water was set to flow in at a rate of 1 $L \cdot min^{-1}$. The lanthanide solutions and the rearing water were mixed prior to delivery to the tanks containing the fish.

Two experiments were conducted concurrently with coho salmon fry. One hundred fry, with an average initial weight of 3.2 g, were placed in each 35-L experimental tank. Experiment 1 had 4 treatment groups and a control tank where no lanthanide was administered. The lanthanide treatments and elemental concentrations were: 50 $\mu g \cdot L^{-1}$ of $LaCl_3$, $CeCl_3$, $La(C_2H_3O_2)_3$, or $Ce(C_2H_3O_2)_3$ continuously for 24 days. Experiment 2 involved 7 treatment groups: 50 $\mu g \cdot L^{-1}$ of $La(C_2H_3O_2)_3$ or $Ce(C_2H_3O_2)_3$ continuously for a total of 24 treatment days; 100 $\mu g \cdot L^{-1}$ of $La(C_2H_3O_2)_3$ or $Ce(C_2H_3O_2)_3$ on alternate days for a total of 12 treatment days over a 24-day period; 150 $\mu g \cdot L^{-1}$ of $La(C_2H_3O_2)_3$ or $Ce(C_2H_3O_2)_3$ every third day for a total of 8 treatment days over a 24-day period; and a control tank with no lanthanum or cerium. The treatment days consisted of 24 hours of exposure. Over the treatment period, equal amounts of lanthanum or cerium were administered to each treatment group of fry at the appropriate concentration and duration.

After completion of the lanthanide exposures, the fry were provided with untreated river water for 14 days prior to sampling. Ten fry were randomly sampled from each of the tanks, body weights recorded, and the vertebral columns were removed and prepared for ICP-MS analysis to determine lanthanide accumulation. The majority of flesh was dissected away from the bony tissue and any remaining traces of flesh were digested with a 6% sodium hypochlorite solution. The clean

Manuscript accepted 29 October 1993
Fishery Bulletin 92:471–473 (1994)

backbones were oven-dried at 70°C overnight, ground to a powder, and a 0.01 g subsample from each fish was used for analysis (Ennevor, 1991; Ennevor and Beames, 1993). The prepared samples were submitted to a commercial laboratory in North Vancouver, British Columbia for ICP-MS analyses.

Experiments 1 and 2 were analyzed by analysis of variance with SYSTAT statistical software (Wilkinson, 1989) and differences between means were tested at $P \leq 0.05$ with Tukey's multiple range test. The data were pooled by treatment groups with individual fish as experimental units.

Table 1

Percent mortalities during the 24-day treatment period, mean body weights of coho salmon, *Oncorhynchus kisutch*, fry at time of sampling, mean amounts (ng) ± 1 S.E.M. of lanthanum or cerium in vertebral columns of fry marked in Experiments 1 and 2. Within experiments, mean values sharing a similar superscript letter were not significantly different ($P \leq 0.05$) according to Tukey's Test.

	Treatment group[1]				
Element	Concentration ($\mu g \cdot L^{-1}$)	Duration (d)	Mortalities (%)	Mean fry weight[2] (g)	La or Ce (ng) ± S.E.M.
Experiment 1					
La*	50	24	2	3.7	$7.0^a \pm 1.2$
Ce*	50	24	2	4.2	$6.1^a \pm 0.9$
La	50	24	0	3.5	$5.6^a \pm 0.8$
Ce	50	24	0	4.1	$6.2^a \pm 0.8$
Control	0	24	1	3.7	$0.1^b \pm 0.0$
Experiment 2					
La	50	24	0	3.5	$5.6^a \pm 0.8$
Ce	50	24	0	4.1	$6.2^a \pm 0.8$
La	100	12	2	2.7	$4.6^{ab} \pm 0.5$
Ce	100	12	3	3.3	$4.4^{ab} \pm 0.3$
La	150	8	12	4.1	$4.0^b \pm 0.5$
Ce	150	8	1	3.7	$4.0^b \pm 0.0$
Control	0	24	1	3.7	$0.1^c \pm 0.0$

[1] La* or Ce* represents the chloride forms, $LaCl_3$ or $CeCl_3$, respectively; all other treatments used the acetate forms of $La(C_2H_3O_2)_3$ or $Ce(C_2H_3O_2)_3$.
[2] Mean weights of treatment groups after 24-day treatment period and 14-day rinse period completed.

Results

Experiment 1

Lanthanum and cerium administered at 50 $\mu g \cdot L^{-1}$ daily for 24 days had no apparent deleterious effect on the fry. They appeared to be healthy and fry weights between treated and non-treated groups did not differ after the 24-day treatments and 14-day rinse were completed. Few mortalities occurred in all groups (Table 1).

Analysis of the vertebral columns from the marked fry showed each of the lanthanides to be present in approximately equal amounts. Uptake did not differ between the treatment groups. The average concentration of lanthanide in the vertebral columns was 6.1 ng of lanthanum or 6.2 ng of cerium (Table 1).

Experiment 2

Throughout the treatments, mortalities were higher in tanks that contained the 150 $\mu g \cdot L^{-1}$ treatments of lanthanum or cerium (Table 1). Fewer mortalities were observed in the 100 $\mu g \cdot L^{-1}$ treatments; none in the 50 $\mu g \cdot L^{-1}$ treatments. However, after the 24-day treatment period and 14-day rinse period were completed, fry weights did not differ between groups treated with lanthanum or cerium and nontreated groups (Table 1).

Results of the analyses of the vertebral columns from the marked fry showed a trend of significantly ($P \leq 0.05$) decreased uptake of lanthanum and cerium with decreased exposure time regardless of concentration (Table 1). Groups treated with lanthanum or cerium at 50 $\mu g \cdot L^{-1}$ daily had the greatest accumulation, whereas the groups treated with 150 $\mu g \cdot L^{-1}$ every third day had the least. In the groups treated with either element, lanthanum and cerium were accumulated in approximately equal amounts.

Discussion

Coho salmon fry were successfully marked with lanthanum or cerium that was administered through the water supply. The lanthanides were detected in the vertebral columns of marked fry, which is consistent with previous findings (Ennevor, 1991; Ennevor and Beames, 1993) and with the bone-seeking characteristics of the lanthanide elements (Durbin et al., 1956; Jowsey et al., 1958). Ennevor and Beames (1993) have shown that lanthanides that are deposited in the vertebral column, otoliths, and scales remain in these tissues for at least 10.5 months after marking. Michibata (1981) also successfully marked medaka, *Oryzias latipes,* and goldfish, *Carassius auratus,* with samarium, another lanthanide, and these fishes retained detectable amounts of the element in their scales one year after marking.

Coho salmon fry exposed to 50 $\mu g \cdot L^{-1}$ of lanthanum or cerium daily resulted in higher levels of accumulation than fry exposed intermittently to concentrations of 100 $\mu g \cdot L^{-1}$ or 150 $\mu g \cdot L^{-1}$. In tanks with higher concentrations, number of mortalities increased as deposition of the elements in the vertebral column decreased. Therefore, toxicity and accumulation may be related to element concentration during treatments rather than accumulated exposure. A high concentration of lanthanides may impair gill function and prevent further uptake of lanthanides, as well as essential ions and oxygen (Behrens Yamada and Mulligan, 1990). Consequently, marking with a low concentration of lanthanide over an extended period is highly recommended.

A potential concern is the ability to detect the lanthanide mark in the bony tissues of returning adults. Because fish continually accumulate calcium in their bony tissues after marking, the relative amount of lanthanum or cerium will decline gradually as the fish grows (Behrens Yamada et al., 1979; Behrens Yamada and Mulligan, 1982). Marks laid down during freshwater growth stages will be concentrated in the center portion of bony tissues. A possible solution to this dilution problem is to analyze only the center where the element concentration would be about the same as when marked (Behrens Yamada and Mulligan, 1982). Scales of returning adults may be more suitable for sampling and analysis as they retain higher lanthanide concentrations (Ennevor and Beames, 1993). Also, scales are easier for sampling and can be removed for lanthanide determination without sacrificing the fish.

These studies demonstrate the successful marking of experimental groups of fry with lanthanum and cerium applied through the water supply. This technique can be adapted to mark large groups of juvenile salmon at hatchery stages quickly and efficiently without affecting growth or survival. Mass marking with lanthanides can mark large groups of fish for identification without apparent deleterious effects. In addition, the mark remains in the bony tissues for extended periods of time, and samples of bony tissues (i.e. scales and opercular punches) can be taken from marked fish, without sacrificing the fish, for identification by ICP-MS analyses.

Acknowledgments

I am grateful to K. R. Pitre, E. A. Perry, and F. K. Sandercock for their helpful comments on the manuscript. The assistance of staff and the facilities extended by Capilano Hatchery during the course of these experiments are appreciated. Thanks also go to R. Brown and his staff at Elemental Research Inc. who performed the ICP-MS analyses. Finally, I wish to acknowledge the continued financial support of the Department of Fisheries, Canada.

Literature cited

Behrens Yamada, S., and T. J. Mulligan.
1990. Screening of elements for the chemical marking of hatchery salmon. Am. Fish. Soc. Symposium 7:550–561.
1982. Strontium marking of hatchery-reared coho salmon, *Oncorhynchus kisutch* Walbaum, identification of adults. J. Fish. Biol. 20:5–9.

Behrens Yamada, S., T. J. Mulligan, and S. J. Fairchild.
1979. Stontium marking of hatchery-reared coho salmon (*Oncorhynchus kisutch* Walbaum). J. Fish. Biol. 14:267–275.

Durbin, P. W., M. H. Williams, M. Gee, R. H. Newman, and J. G. Hamilton.
1956. Metabolism of the lanthanons in the rat. Proc. Soc. Exp. Biol. Med. 91:78–85.

Ellis, W. C.
1968. Dysprosium as an indigestible marker and its determination by radio-activation analysis. J. Agric. Food Chem. 16:220–224.

Ennevor, B.C.
1991. The feasibility of using lanthanide elements to mass mark hatchery-production salmon. M.Sc. thesis, Univ. British Columbia, Vancouver, B.C., 182 p.

Ennevor, B. C., and R. M. Beames.
1993. The use of lanthanide elements to mass mark juvenile salmon. Can. J. Fish. Aquat. Sci. 50:1039–1044.

Houk, R. S., and J. J. Thompson.
1988. Inductively coupled plasma mass spectrometry. Mass Spectrom. Rev. 7:425–461.

Jowsey, J., R. E. Rowland, and J. H. Marshall.
1958. The deposition of rare earths in bone. Rad. Res. 8:490–501.

Kyker, G. C.
1961. Rare earths. *In* C. L. Comar and F. Bronner (eds.), Mineral metabolism, Vol. II, Part B, p. 499–529. Academic Press, New York.

Longerich, H. P., B. J. Fryer, D. F. Strong, and C. J. Kantipuly.
1987. Effects of operating conditions on the determination of the rare earth elements by inductively coupled plasma mass spectrometry (ICP-MS). Spectrochim. Acta 42B:75–92.

Luckey, T. D., and B. Venugopal.
1977. Lanthanides, the rare–earth metals. *In* T. D. Luckey and B. Venugopal (eds.), Metal toxicity in mammals, Vol. II. Plenum Press, New York.

Michibata, H.
1981. Labeling fish with an activable element through their diet. Can. J. Fish. Aquat. Sci. 38:1281–1282.

Wilkinson, L.
1989. SYSTAT: the system for statistics. Systat, Inc., Evanston, IL, 822 p.

Distribution and relative abundance of the blue shark, *Prionace glauca*, in the southwestern equatorial Atlantic Ocean

Fabio H. V. Hazin
Department of Marine Science and Technology
Tokyo University of Fisheries
5–7, Konan-4, Minato-ku, Tokyo 108, Japan
The Brazilian Research Council
CNPq (Conselho Nacional de Desenvolvimento Cientifico et Technologico)
Avenida W3 Norte, Quadra 511, Bloco A., Ed. Bittar II
Brasilia, D. F., CEP-75000-000, Brazil

Clara E. Boeckman
Elizabeth C. Leal
Universidade Federal Rural de Pernambuco, Rua Dom Manoel de Medeiros
s/n. Dois Irmaos, Recife-PE, Brazil

Rosangela P. T. Lessa
Brazilian Research Council, (CNPq)
Avenida W3 Norte, Quadra 511, Bloco A., Ed. Bittar II
Brasilia, D. F., CEP-75000-000, Brazil

Kohei Kihara
Kazuyuki Otsuka
Department of Marine Science and Technology
Tokyo University of Fisheries
5–7, Konan-4, Minato-ku, Tokyo 108, Japan

The blue shark, *Prionace glauca*, is one of the most abundant oceanic-epipelagic sharks and is probably the widest ranging chondrichthyian (Compagno, 1984). It is frequently caught by tuna longline fisheries in temperate, subtropical, and tropical waters of the world oceans (Pratt, 1979).

Hazin et al. (1990) investigated the distribution and abundance of pelagic sharks caught from 1983 until 1988 by Brazilian longliners in the southwestern equatorial Atlantic. Blue shark and sharks of the genus *Carcharhinus* were the dominant species, together representing nearly 95% of the shark catches (Hazin et al., 1990). They reported that blue shark abundance had a marked seasonal fluctuation with the highest catches taking place during the third and fourth quarters of the year and the lowest in the first quarter.

The objective of the present study is to further investigate the distribution and relative abundance of the blue shark, *Prionace glauca*, in the south-western equatorial Atlantic Ocean, including the following aspects: a) seasonal fluctuation of catch per unit of effort (CPUE) as related to sea surface temperature; b) sex, and size and age composition of blue shark catches; c) vertical distribution as related to the vertical temperature profile.

Material and methods

This study was based on shark catches during 50 fishing cruises by a commercial tuna longliner, FV *Argus*, from August to December 1987 and from February 1990 to December 1991. On 325 longline operations during these cruises, a total of 992 blue sharks were caught. The commercial longline consisted of 120 baskets, each with 7 branch lines. The bait was frozen Brazilian sardine, *Sardinella brasiliensis*. Average local time of set, retrieval, and mean soaking time of the longline is shown in Table 1. Further details of longline fishing gear and methods were described in Hazin (1986).

The fishing ground was located between lat. 2°S and 7°S and long. 32°W and 38°W. Fishing areas were divided into segments of 1° latitude × 1° longitude. The central positions of the 325 longline sets (Fig. 1) were calculated as the average latitude and longitude of the beginning and end of set and retrieval. Distribution of fishing effort by month is presented in Table 2. Blue shark relative abundance was expressed as average catch, in number of fish, per 100 hooks (CPUE). The mean CPUE was calculated as the total catch, in number of fish, divided by the total fishing effort, in 100 hooks. The distribution of blue shark mean CPUE by segments of 1° latitude × 1° longitude was observed and its relation to ocean depth analyzed. Ocean depths for each longline set were calculated as the weighted mean of the three closest values read from the nautical chart number 50, issued by the Brazilian Navy.

The monthly fluctuation of CPUE and sex ratio was analyzed and compared to sea surface temperature. An analysis of variance

Manuscript accepted 21 October 1993
Fishery Bulletin 92: 474–480 (1994)

(ANOVA) was performed to determine whether blue shark CPUEs were significantly different among months. The mean CPUE for each month was calculated and all monthly mean CPUEs were then compared by ANOVA, through one-way classification of data. The months were the only independent variable (Table 3). No CPUE data were available from October 1990 and from January and April 1991. Data on the sex of the specimens were not available from January to October 1991.

All lengths are reported as fork length (FL), which was measured from the tip of the snout to the fork of the tail. Blue sharks were always measured at the time of landing. Length data were available only for 1990 and 1991. To better understand seasonal variation in CPUE, CPUE data for the various age classes of male specimens from February through December 1990 were evaluated. Females were not included because they were present only from February to July. To calculate the age-CPUE distribution, male blue shark lengths were converted to age by Stevens' (1975) growth equation, as follows:

$$Lt = 423\ (1-e^{-0.11(t+1.035)})$$

Table 1

Average set, retrieval and soaking time (in decimals) with standard deviations, for longline operations of FV *Argus* from February to December 1990.

		Local time	Standard deviation
Set	Beginning	1.61	0.58
	End	4.00	0.53
Retrieval	Beginning	10.31	1.47
	End	17.52	1.68
Soaking time (hours)		11.11	1.54

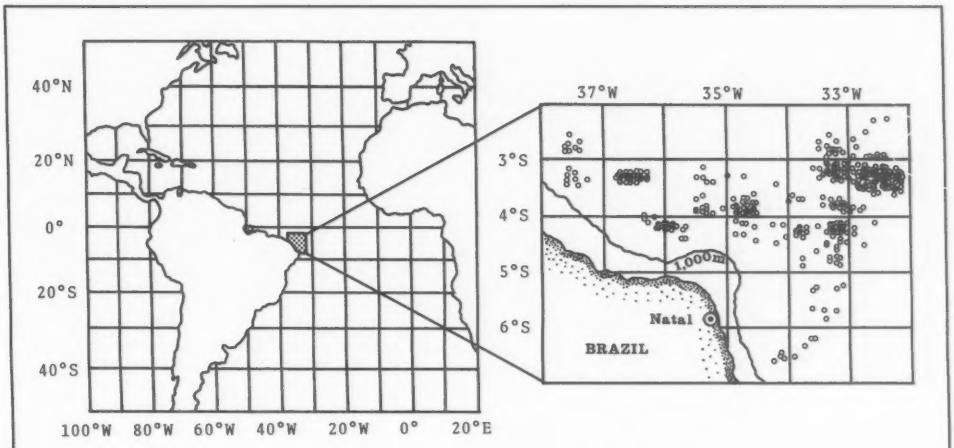

Figure 1

Location of the fishing ground (hatched area) and central positions of the longline sets made by the FV *Argus* from August to December 1987 and from February 1990 to December 1991, in the southwestern equatorial Atlantic Ocean.

Table 2

Distribution of fishing effort of FV *Argus* by months, from August to December 1987 and from February 1990 to December 1991, in the southwestern equatorial Atlantic Ocean.

	Jan.	Feb.	Mar.	Apr.	May	Jun.	Jul.	Aug.	Sep.	Oct.	Nov.	Dec.	Total
No. of sets	16	12	23	15	27	24	23	32	36	44	39	34	325
%	5	4	7	5	8	7	7	10	11	13	12	11	100

where Lt = total length, and t = age in years. Fork length data were converted to total length by the regression of Hazin et al. (1991):

$$FL = 11.27 + 0.78\ TL$$

where FL = fork length, and TL = total length.

Depths of longline hooks were estimated using the equations of Yoshihara (1952, 1954, a and b). Vertical distribution of males and females was studied through the relative distribution of mean catches on longline hooks, during February to June and July to December 1990. Differences in mean catch of males and females on longline hooks were evaluated by chi-square analysis (df=6). Sea water temperature from 0 to 300 m was surveyed in 35 DBT (digital bathythermograph) profiles: 6 in May 1990, 3 in May 1991, 5 in June 1991, 13 in November 1990, 2 in November 1991, and 6 in December 1990. From January to December 1990, sea surface temperature was measured by a mercury thermometer.

Results

From August to December 1987 and from February 1990 to December 1991, the blue shark mean CPUE by quadrates increased eastward, being particularly high east of long. 35°W (Fig. 2). Of the 325 sets, 260 (nearly 80%) were over bottom depths greater than 1,000 m. In these areas, the mean CPUE of blue shark was 0.50. The remaining 65 sets were in areas with depths shallower than 1,000 m, close to oceanic banks (Aracati, Sirius, and Guara banks), and west of 35°W. In these areas, the mean CPUE of blue shark was only 0.05.

The fluctuation of the monthly mean CPUE of blue shark in the area east of 35°W, over ocean depth of 1,000 m, for 1987, 1990 and 1991, were similar (Fig. 3). In 1990 and 1991 the CPUE was low until May, increased during June and July, decreased again in August, increased during September and October, and decreased once more in November and December. In 1987 the CPUE was low in August, increased in October and decreased during November and December. Differences in mean CPUE among months were significant (ANOVA; $P<0.0001$; Table 3).

The fluctuation of the monthly mean CPUE of male and female blue sharks was distinct (Fig. 4). CPUE for females was highest during March. From July to December, CPUE for females was low in this fishing ground. CPUE for males, however, was lowest during March, after which abundance increased and peaked during September and October. The sea surface temperature in 1990 was highest in May and lowest in September. During this year, in general, the CPUE of males tended to decrease with an increase in the sea surface temperature, whereas the CPUE of females tended to increase.

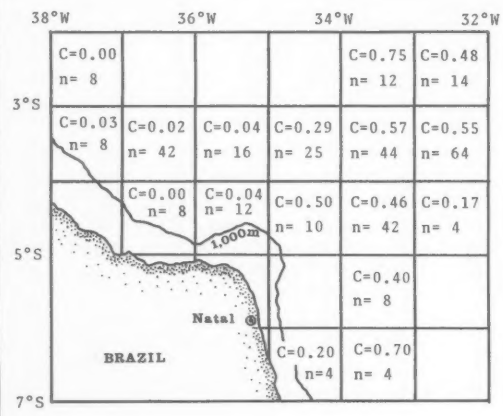

Figure 2

Mean catch per 100 hooks (CPUE) of blue shark, *Prionace glauca*, in the southwestern equatorial Atlantic Ocean, from August to December 1987 and from February 1990 to December 1991. C= CPUE; n= number of longline sets.

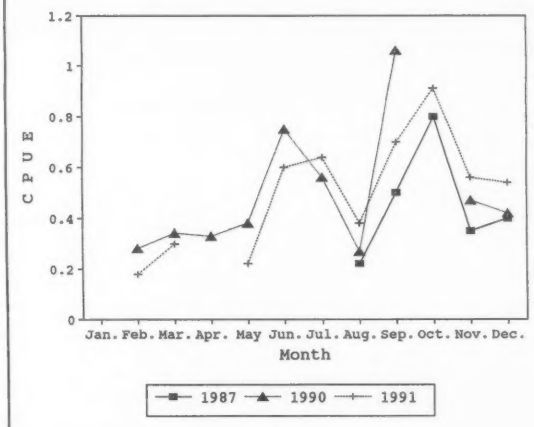

Figure 3

Monthly mean catch per 100 hooks (CPUE) of blue shark, *Prionace glauca*, in the southwestern equatorial Atlantic Ocean, in the area east of long. 35°W and with ocean depth over 1,000 m, from August to December 1987 and from February 1990 to December 1991.

Of 810 specimens, 652 (about 80%) were male and 158 were female (about 20%). Overall, the sex ratio (male/female) for the entire period was 4.12:1. The sex ratios for each month are given in Table 4.

Females ranged in size from 162 to 226 cm and males from 156 to 250 cm (Fig. 5). Seasonal fluctuation in male CPUE during 1990 was different among age groups (Fig. 6). From February to May, ages ranged from 4.5 to 8.5 years, with most (83%) individuals between 6 and 8.5 years old (83%). The CPUE rise in June–July was due to an increase in the same age classes as from February–May. Some older specimens from 9 to 10.5 years also appeared. The CPUE of fish younger than 7 years decreased markedly in August. During September–October the CPUE of ages 7.5 to 10 increased sharply. In November–December the CPUE of age classes from 7.5 to 8.5, and also 9.5, were reduced, whereas the CPUE of other age classes did not change much. From February to July, younger fish (4.5 to 7.5 years) were more abundant than from August to December, their CPUE being particularly high in June–July. From August to December, fish older than 7.5 years had a higher CPUE than in the previous months, with a peak in September–October.

The calculated depth of longline hooks during 137 longline fishing operations of 1990 ranged from 87 to 206 m (Table 5). The figures given in this table approximate the actual depths of longline hooks. The most striking feature of the DBT profiles is the pres-

Table 3

Analysis of variance (ANOVA) and expected mean squares for comparison of monthly mean CPUEs of blue sharks, *Prionace glauca*, caught by the FV *Argus*, during 325 longline sets, from August to December 1987 and from February 1990 to December 1991, in the southwestern equatorial Atlantic Ocean.

Source of variation	Degrees of freedom	Sum of squares	Mean squares	*F*	*P*
Month	24	11.41	0.48	4.65	<0.0001
Error	300	30.68	0.10	—	—
Total	324	42.09	—	—	—

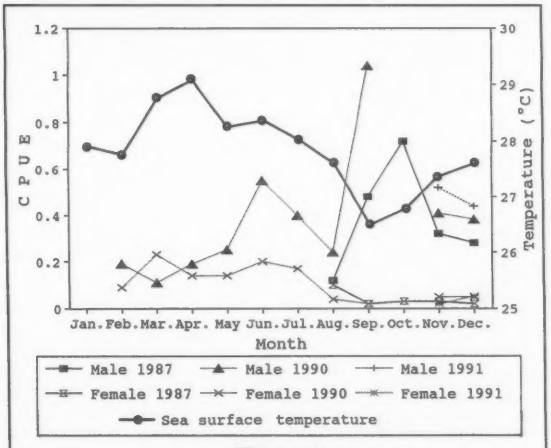

Figure 4

Monthly mean sea surface temperature in 1990 and monthly mean catch per 100 hooks (CPUE) of male and female blue shark, *Prionace glauca*, in the southwestern equatorial Atlantic Ocean, from August to December 1987 and from February 1990 to December 1991.

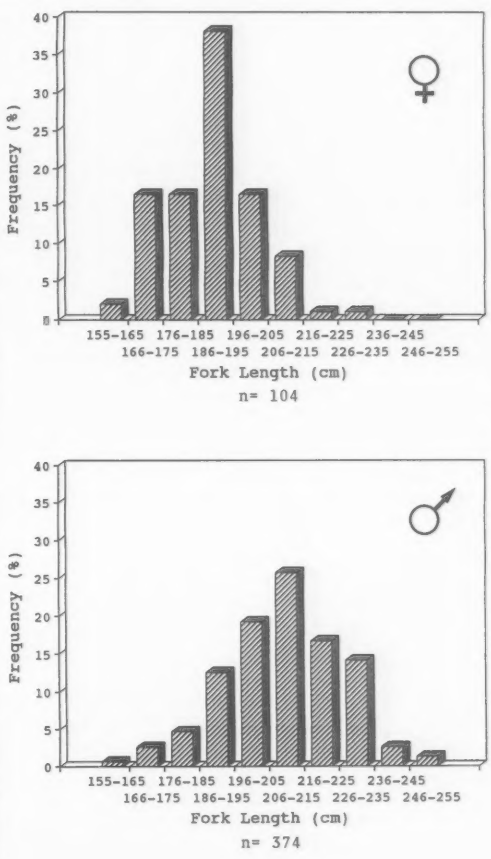

Figure 5

Length-frequency distribution of male and female blue shark, *Prionace glauca*, in the southwestern equatorial Atlantic Ocean, from February to December 1990 and November to December 1991. Males: n = 374; min. = 156 cm; max. = 250 cm. Females: n = 104; min. = 162 cm; max. = 226 cm.

ence of a steep thermocline during the entire year. The range and mean of sea water temperature at the calculated depths of longline hooks, and the mean depth and temperature at the top and bottom of the thermocline in May–June and November–December are shown in Table 6. All longline hooks were located in or below the thermocline (Fig. 7). During Nov.–Dec. the thermocline was about 30 m deeper than during May–June.

Male blue shark catches from February to June were concentrated among central, deeper hooks, whereas in the second half of the year they were more uniformly distributed (Fig. 8). Male catch was significantly different among hooks from February to June (chi-square; $P<0.005$), but not from July to December ($0.10 < P<0.25$). The difference of male catches, on hooks 3, 4, and 5 between February-June and July-December was significant ($0.05 < P<0.10$). The relative distribution of female blue shark catches along longline hooks from February to July (Fig. 8) was different from that of males; the highest catches took place on hooks 2 and 5. The difference between male and female catches among hooks during February to July was significant ($0.01 < P<0.05$). The distribution of male and female catch among hooks suggests that males were distributed in shallower waters between July and December than between February and June and that females from February to July had a shallower distribution than males.

From February to July, CPUE for females was highest in hooks 2 and 5 (130 to 165 m), and CPUE for males in hooks 3 and 4 (165 to 180 m) (Table 5). The corresponding range of sea water temperature was 13.8° to 20.4°C for females and 12.9° to 17.1°C for males (Table 6). Male catch among hooks from July to December, was much more uniform, suggesting a depth range for males from 90 to 180 m (Table 5), or from about 15° to 28°C (Table 6), up to the top of the thermocline (Fig. 7).

Table 4

Blue shark, *Prionace glauca*, monthly sex ratio (number of males per female), in the southwestern equatorial Atlantic Ocean.

Feb.	Mar.	Apr.	May	Jun.	Jul.	Aug.	Sep.	Oct.	Nov.	Dec.
2.08	0.48	1.29	1.79	2.71	2.35	6.00	54.00	25.00	16.00	8.50

Table 5

Mean and range of calculated depths (m) of longline hooks, during 137 longline operations, in the southwestern equatorial Atlantic Ocean, from February to December 1990.

Hook no.	Mean depth	Minimum	Maximum
1 and 7	92.66	87	96
2 and 6	131.56	120	140
3 and 5	164.19	145	181
4	179.20	154	206

Discussion

The results on horizontal distribution agree with those of Hazin et al. (1990), corroborating the oceanic character of blue shark (Fig. 2). Abundance was also clearly related to bottom depth. The mean CPUE of blue shark in areas of bottom depths greater than 1,000 m was 10 times higher than in shallower areas. The lower abundance of blue sharks west of 35°W

Table 6

Range and mean of sea water temperature (°C) at calculated depths (m) of longline hooks 1 to 7 and mean depth and temperature at the top and bottom of the thermocline, as inferred from 35 DBT (digital bathythermograph) surveys carried out in May–June and November–December 1990 and 1991, in the southwestern equatorial Atlantic Ocean.

	Hook number				Thermocline			
					Top		Bottom	
Month	1 and 7	2 and 6	3 and 5	4	Depth.	Temp.	Depth.	Temp.
May–June								
Temp. mean	22.6	16.3	14.8	13.2	55	28	120	13.5
Temp. range	18.5–25.7	13.8–20.4	13.1–17.1	12.9–13.3				
Nov.–Dec.								
Mean	27.6	17.0	15.4	14.9	85	27	130	15.5
Range	26.8–29.1	14.3–24.0	14.0–20.1	13.9–18.6				

(Fig. 2), therefore, is probably a consequence of ocean depth, because almost all sets performed in this fishing ground took place in shallow depths and in the vicinity of oceanic banks.

The monthly mean CPUEs of males and females (Fig. 4) show that the higher relative abundance of blue shark during the third and fourth quarters of the year (Hazin et al., 1990) is mostly comprised by males. These results indicate also that males and females are segregated and that their migratory movements are different. The different seasonal fluctuation of CPUE for different male age groups indicate that male specimens were also segregated by size. The use of Stevens' (1975) growth equation to calculate these ages from fork length may have limitations because it is based on data from the North Atlantic Ocean. Nevertheless, Amorim (1992) studied the growth of blue shark in the south-western Atlantic and found a value of k= 0.1126, which approximates Stevens' value of 0.11.

Differences in vertical distribution displayed by male and female blue sharks (Fig. 8) indicate that vertical sexual segregation likely occurred in the first half of the year. They also suggest that the depth range of male blue sharks may change seasonally.

Acknowledgments

We sincerely thank the Norte Pesca S/A, who provided all the data used in this research. We are particularly indebted to Alceu A. Couto and Anibal P. Souza for their valuable help in data collection. We also thank Francis G. Carey of the Woods Hole Oceanographic Institution who constructively criticized the manuscript, and Sakutaro Yamada for his technical assistance. Financial support was granted by the Ministry of Education of the Japanese Government through the Mombusho Scholarship Program and by the Brazilian Research Council (CNPq).

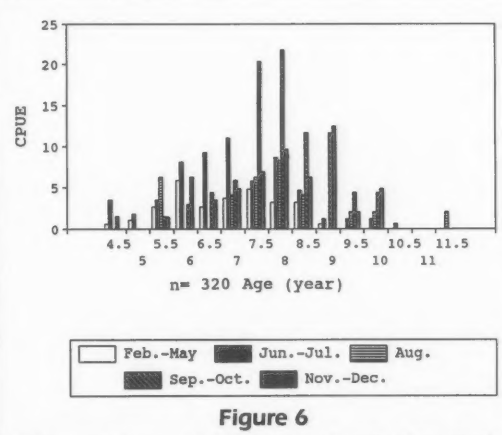

Figure 6

Mean catch per 10,000 hooks of male blue shark, *Prionace glauca*, by age classes, from February through December 1990, in the southwestern equatorial Atlantic Ocean. n = 320.

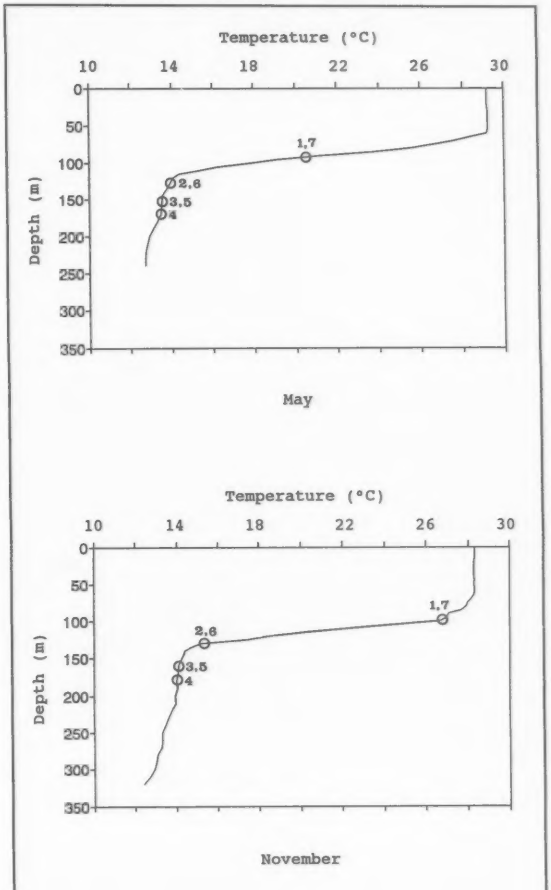

Figure 7

Typical temperature profiles for May and November, in the southwestern equatorial Atlantic Ocean, and the calculated mean depths of the hooks 1 to 7 of the longline of the FV *Argus*.

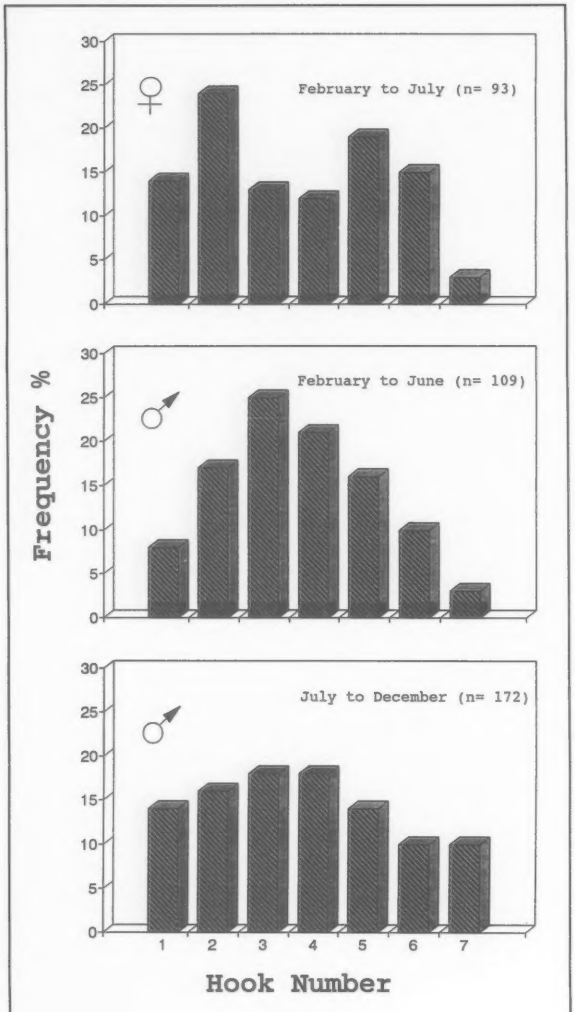

Figure 8

Male and female blue shark, *Prionace glauca*, catch-frequency distribution along the hooks of the longline, in the southwestern equatorial Atlantic Ocean, during February to June and July to December, 1990.

Literature cited

Amorim, A. F.

1992. Estudo da biologia, pesca e reprodução do cação azul, *Prionace glauca* L. 1758, capturado no sudeste e sul do Brasil. Ph.D. thesis, Universidade Estadual Paulista, Rio Claro, São Paulo, Brazil, 176 p.

Compagno, L. J. V.

1984. FAO species catalogue. Vol. 4, Parts 1 and 2: Sharks of the world: an annotated and illustrated catalogue of shark species known to date. FAO Fish. Synop. 125, 655 p.

Hazin, F. H. V.

1986. Pesca de atuns e afins com embarcação de pequeno porte no nordeste brasileiro. Graduation thesis, Universidade Federal Rural de Pernambuco, Recife, Brazil, 107 p.

Hazin, F. H. V., A. A. Couto, K. Kihara, K. Otsuka, and M. Ishino.

1990. Distribution and abundance of pelagic sharks in the south-western equatorial Atlantic. J. Tokyo Univ. Fish. 77(1):51–64.

Pratt, H. L., Jr.

1979. Reproduction of the blue shark, *Prionace glauca*. Fish. Bull. 77:445–470.

Stevens, J. D.

1975. Vertebral rings as a means of age determination in the blue shark (*Prionace glauca* L.). J. Mar. Biol. Assoc. U.K. 55:657–665.

Yoshihara, T.

1952. Distribution of catches of tuna longline. III: Swimming depth. [In Japanese.] Nippon Suisan Gakkaishi, 18(8):187–190.

1954a. Distribution of catches of tuna longline. IV: On the relation between K and psi with a table and a diagram. [In Japanese.] J. Tokyo Univ. Fish. 19(10):1012–1014.

1954b. On the distribution of catches by tuna longline. J. Tokyo Univ. Fish. 41(1):1–26.

Fishery Bulletin
Guide for Contributors

Preparation

Title page should include authors' full names and mailing addresses and the senior author's telephone and FAX number.

Abstract should not exceed one double-spaced typed page. It should state the main scope of the research but emphasize its conclusions and relevant findings. Because abstracts are circulated by abstracting agencies, it is important that they represent the research clearly and concisely.

Text must be typed double-spaced throughout. A brief introduction should portray the broad significance of the paper; the remainder of the paper should be divided into the following sections: **Materials and methods**, **Results**, **Discussion** (or **Conclusions**), and **Acknowledgments**. Headings within each section must be short, reflect a logical sequence, and follow the rules of multiple subdivision (i.e. there can be no subdivision without at least two items). The entire text should be intelligible to interdisciplinary readers; therefore, all acronyms, abbreviations, and technical terms should be spelled out the first time they are mentioned. The scientific names of species must be written out the first time they are mentioned; subsequent mention of scientific names may be abbreviated. Follow the *U.S. Government Printing Office Style Manual* (1984 ed.) and the *CBE Style Manual* (5th ed.) for editorial style, and the most current issue of the American Fisheries Society's *Common and Scientific Names of Fishes from the United States and Canada* for fish nomenclature. Dates should be written as follows: 11 November 1991. Measurements should be expressed in metric units, e.g., metric tons as (t); if other units of measurement are used, please make this fact explicit to the reader. The numeral one (1) should be typed as a one, not as a lower-case el (l).

Text footnotes should be numbered with Arabic numerals and typed on a separate sheet of paper. Footnote all personal communications, unpublished data, and unpublished manuscripts with full address of the communicator or author, or, as in the case of unpublished data, where the data are on file. Authors are advised to avoid references to nonstandard (gray) literature, such as internal, project, processed, or administrative reports, wherever possible. Where these references are used, please include whether they are available from NTIS (National Technical Information Service) or from some other public depository.

Literature cited comprises published works and those accepted for publication in peer-reviewed literature (in press). Follow the name and year system for citation format. In the text, cite Smith and Jones (1977) or (Smith and Jones, 1977). If there is a sequence of citations, list chronologically: Smith, 1932; Green, 1947; Smith and Jones, 1985. Abbreviations of serials should conform to abbreviations given in *Serial Sources for the BIOSIS Previews Database.*. Authors are responsible for the accuracy and completeness of all citations.

Tables should not be excessive in size and must be cited in numerical order in the text. Headings should be short but ample enough to allow the table to be intelligible on its own. All unusual symbols must be explained in the table heading. Other incidental comments may be footnoted with italic numerals. Use asterisks for probability in statistical data. Because tables are typeset, they need only be submitted typed and formatted, with double-spaced legends. Zeros should precede all decimal points for values less than one.

Figures include line illustrations and photographs (or slides) and must be cited in numerical order in the text. Unless photographs are submitted on glossy paper with good contrast, we cannot guarantee a good final printed copy. Figures are to be labeled with author's name and number of figure. Use Times Roman font (upper and lowercase letters) to label within figures. Avoid vertical lettering except for *y*-axis labels. Zeros should precede all decimal points for values less than one. Figures may be submitted as computer software files (along with laser-printed copies), as photomechanical transfers (PMTs), or as high quality photographic prints. Send only xerox copies of figures to the Scientific Editor; original figures will be requested later when the manuscript has been accepted for publication. Figure legends should explain all symbols and abbreviations and should be double-spaced on a separate page at the end of the manuscript.

Copyright law does not cover government publications; they fall within the public domain. If an author reproduces any part of a government publication in his work, reference to source is considered correct form.

Submission

Send printed copies (original and two copies) to the Scientific Editor:

Dr. Ronald Hardy, Scientific Editor
Northwest Fisheries Science Center,
F/NWC3
National Marine Fisheries Service, NOAA
2725 Montlake Boulevard East
Seattle, WA 98112-2097

Once the manuscript has been accepted for publication, you will be asked to submit a software copy of your manuscript to the Managing Editor. The software copy should be submitted in *WordPerfect* text format (or in standard ASCII text format if *WordPerfect* is unavailable) and should be placed on a 5.25-inch or 3.5-inch disk that is double-sided, double or high density, and that is compatible with either DOS or Apple Macintosh systems.

Copies of published articles and notes are available free of charge to the senior author (50 copies) and to his or her laboratory (50 copies). Additional copies may be purchased in lots of 100 when the author receives page proofs.